

**STRUCTURAL EFFECTS OF PHOSPHORYLATION AND  $\beta$ -*O*-GlcNAcylation  
ON  $\alpha$ -HELICES**

**AND**

**STRUCTURAL EFFECTS OF PHOSPHORYLATION AND R406W ON *tau*<sub>395-</sub>**

411

by

Michael Birch Elbaum

A thesis submitted to the Faculty of the University of Delaware in partial fulfillment of the requirements for the degree of Master of Science in Chemistry and Biochemistry

Summer 2014

© 2014 Michael Birch Elbaum  
All Rights Reserved

UMI Number: 1567802

All rights reserved

INFORMATION TO ALL USERS

The quality of this reproduction is dependent upon the quality of the copy submitted.

In the unlikely event that the author did not send a complete manuscript and there are missing pages, these will be noted. Also, if material had to be removed, a note will indicate the deletion.



UMI 1567802

Published by ProQuest LLC (2014). Copyright in the Dissertation held by the Author.

Microform Edition © ProQuest LLC.

All rights reserved. This work is protected against unauthorized copying under Title 17, United States Code



ProQuest LLC.  
789 East Eisenhower Parkway  
P.O. Box 1346  
Ann Arbor, MI 48106 - 1346

**STRUCTURAL EFFECTS OF PHOSPHORYLATION AND  $\beta$ -O-GlcNAcylation  
ON  $\alpha$ -HELICES**

**AND**

**STRUCTURAL EFFECTS OF PHOSPHORYLATION AND R406W ON *tau*<sub>395-</sub>**

**411**

by

Michael Birch Elbaum

Approved: \_\_\_\_\_  
Neal J. Zondlo, Ph.D.  
Professor in charge of thesis on behalf of the Advisory Committee

Approved: \_\_\_\_\_  
Murray Johnston, Ph.D.  
Chair of the Department of Chemistry and Biochemistry

Approved: \_\_\_\_\_  
George Watson, Ph.D.  
Dean of the College of Arts and Sciences

Approved: \_\_\_\_\_  
James G. Richards, Ph.D.  
Vice Provost for Graduate and Professional Education

## **ACKNOWLEDGMENTS**

First, I would like to thank my research advisor Neal Zondlo for his guidance. Over the past several years he has been constantly challenging me to improve myself, my knowledge, critical thinking, and lab skills. He has also created an environment in which I was able to explore science.

I would also like to thank other professors at the University of Delaware especially Dr. Douglass Taber, Dr. Sharon Rozovsky, Dr. Joe Fox, Dr. Donald Watson, Dr. Mary Watson, and Dr. Catherine Grimes for their knowledge and guidance.

I must also thank my team members and labmates for their support and guidance in the lab. I would like to especially thank Anil Pandey, Christina Forbes, Cay Tressler, Drew Urmev, and Himal Ganguly. They helped guide me in the lab and teach me skills necessary for success.

Finally, I would like to thank my family for supporting me throughout my graduate career. I thank my wife, Orly, for celebrating the good times and supporting me in the hard times. I would also like to thank my parents for their support and for always telling me to never give up on my dreams.

## TABLE OF CONTENTS

LIST OF TABLES .....	vi
LIST OF FIGURES .....	xii
ABSTRACT .....	xxi

### Chapter

1 STRUCTURAL EFFECTS OF PHOSPHORYLATION AND $\beta$ - <i>O</i> - GlcNAcylation ON $\alpha$ -HELICES AS A FUNCTION OF POSITION .....	1
Introduction .....	1
Results .....	5
Modifications on the N-terminal $\alpha$ -helical positions .....	7
Modifications on internal $\alpha$ -helical positions.....	21
Modifications on C-terminal $\alpha$ -helical positions .....	29
The dichotomy of phosphothreonine.....	33
Structural effects of post-translational modifications are analogous to proline.....	38
Phosphothreonine adopts a highly restricted conformation .....	41
Discussion.....	42
Experimental.....	55
Materials .....	55
Phosphorylation of serine/threonine on peptides on solid phase.....	56
Synthesis of Fmoc-Ser(Ac <sub>3</sub> O-GlcNAc)-OH and Fmoc-Thr(Ac <sub>3</sub> O- GlcNAc)-OH .....	57
Synthesis and characterization data for all peptides.....	58
Circular dichroism (CD) spectroscopy .....	61
NMR spectroscopy .....	85
REFERENCES .....	150
2 NEIGHBORING RESIDUE SIDE-CHAIN INTERACTIONS OF $\beta$ - OGlcNAc .....	155
Introduction .....	155

Results .....	158
Effects of Ser/Ser(OGlcNAc) and 4-I-Phe with an <i>i/i+2</i> relationship...	161
Effects of Ser/SerOGlcNAc and 4-I-Phe/4-B(OH) <sub>2</sub> -Phe with an <i>i/i+3</i> relationship .....	162
Neighboring side-chain interactions with an <i>i/i+4</i> relationship .....	164
Neighboring side-chain interactions with a relative <i>i/i+7</i> orientation ...	173
Discussion.....	178
Experimental.....	191
Materials .....	191
Phosphorylation of serine/threonine on peptides on solid phase.....	192
Synthesis of Fmoc-Ser(Ac <sub>3</sub> O-GlcNAc)-OH and Fmoc-Thr(Ac <sub>3</sub> O- GlcNAc)-OH .....	193
Solid-phase Aryl Borylation of peptides containing 4-I-Phe .....	194
Synthesis and characterization data for all peptides.....	195
Circular dichroism (CD) spectroscopy .....	198
NMR spectroscopy .....	211
REFERENCES .....	215
3 STRUCTURAL EFFECTS OF PHOSPHORYLATION AND R406W ON <i>tau</i> <sub>395-411</sub> .....	220
Introduction .....	220
Results .....	226
Analysis of Ac-TGPX-NH <sub>2</sub> peptides.....	228
Structural implications of pThr <sub>403</sub> /pSer <sub>404</sub> and R406W on <i>tau</i> peptides	234
Discussion.....	242
Experimental.....	252
Materials .....	252
Phosphorylation of serine/threonine on peptides on solid phase.....	253
Synthesis and characterization data for all peptides.....	254
NMR spectroscopy .....	257
REFERENCES.....	297

## LIST OF TABLES

<b>Table 1.1:</b>	Summary of CD data for peptides containing serine, serine modifications .....	9
<b>Table 1.2</b>	Summary of NMR data for peptides with serine and serine modifications at residue 1 .....	10
<b>Table 1.3:</b>	Summary of CD data for peptides with threonine and threonine modifications at residue 1 .....	12
<b>Table 1.4:</b>	Summary of NMR data for peptides with threonine and threonine modifications at residue 1 .....	14
<b>Table 1.5</b>	Summary of CD data for peptides containing modifications at residue 2 .....	17
<b>Table 1.6:</b>	Summary of NMR data for peptides containing threonine, phosphothreonine, serine, and phosphoserine at residue 2.....	19
<b>Table 1.7:</b>	Summary of CD data for peptides containing serine and serine modifications at residue 5.....	23
<b>Table 1.8:</b>	Summary of NMR data for peptides containing serine and serine modifications at residue 5.....	23
<b>Table 1.9:</b>	Summary of CD data for peptides containing threonine and threonine modifications at residue 5.....	25
<b>Table 1.10:</b>	Summary of NMR data for peptides containing threonine and threonine modifications at residue 5.....	26
<b>Table 1.11:</b>	Summary of CD data for peptides containing serine, phosphoserine, threonine, or phosphothreonine at residue 10.....	28
<b>Table 1.12</b>	Summary of NMR data for peptides containing serine, phosphoserine, threonine, or phosphothreonine at residue 10.....	29
<b>Table 1.13:</b>	Summary of CD data for peptides containing serine, serine modifications, threonine, and threonine modifications at residue 14.....	32

<b>Table 1.14:</b> Summary of NMR for peptides containing serine, serine modifications, threonine, and threonine modifications at residue 14.....	33
<b>Table 1.15:</b> Summary of CD data for peptides containing proline at residues 1, 2, 5, 10, or 14.....	40
<b>Table 1.16:</b> <sup>31</sup> P NMR of peptides containing phosphothreonine and phosphoserine at residue 2.....	42
<b>Table 1.17:</b> Purification procedure for synthetic peptides.....	59
<b>Table 1.18:</b> Characterization data for synthetic peptides.....	61
<b>Table 1.19:</b> Summary of CD data for all peptides.....	63
<b>Table 1.20:</b> Summary of CD data for all peptides.....	64
<b>Table 1.21:</b> Summary of <sup>1</sup> H NMR data for peptides with serine and Ser(OGlcNAc) at residue 1.....	88
<b>Table 1.22:</b> Summary of <sup>1</sup> H NMR data for peptides with phosphoserine at residue 1.....	89
<b>Table 1.23:</b> Summary of <sup>1</sup> H NMR data for peptides with threonine and Thr(OGlcNAc) at residue 1.....	91
<b>Table 1.24:</b> Summary of <sup>1</sup> H NMR data for peptides with phosphothreonine at residue 1.....	92
<b>Table 1.25:</b> Summary of <sup>1</sup> H NMR data for peptides with serine or phosphoserine at residue 2.....	94
<b>Table 1.26:</b> Summary of <sup>1</sup> H NMR data for peptide with phosphoserine at residue 2.....	95
<b>Table 1.27:</b> Summary of <sup>1</sup> H NMR data for peptides with threonine or phosphothreonine at residue 2.....	97
<b>Table 1.28:</b> Summary of <sup>1</sup> H NMR data for peptide with phosphothreonine at residue 2.....	98
<b>Table 1.29:</b> Summary of <sup>1</sup> H NMR data for peptides with serine and Ser(OGlcNAc) at residue 5.....	102

<b>Table 1.30:</b> Summary of $^1\text{H}$ NMR data for peptides with phosphoserine at residue 5	103
<b>Table 1.31:</b> Summary of $^1\text{H}$ NMR data for peptides with threonine and Thr(OGlcNAc) at residue 5	105
<b>Table 1.32:</b> Summary of $^1\text{H}$ NMR data for peptides with phosphothreonine at residue 5	106
<b>Table 1.33:</b> Summary of $^1\text{H}$ NMR data for peptides with serine or phosphoserine at residue 10	108
<b>Table 1.34:</b> Summary of $^1\text{H}$ NMR data for peptide with phosphoserine at residue 10	109
<b>Table 1.35:</b> Summary of $^1\text{H}$ NMR data for peptides with threonine or phosphothreonine at residue 10	111
<b>Table 1.36:</b> Summary of $^1\text{H}$ NMR data for peptide with phosphothreonine at residue 10	112
<b>Table 1.37:</b> Summary of $^1\text{H}$ NMR data for peptides with serine and Ser(OGlcNAc) at residue 14	114
<b>Table 1.38:</b> Summary of $^1\text{H}$ NMR data for peptides with phosphoserine at residue 14	115
<b>Table 1.39:</b> Summary of $^1\text{H}$ NMR data for peptides with threonine and Thr(OGlcNAc) at residue 14	117
<b>Table 1.40:</b> Summary of $^1\text{H}$ NMR data for peptides with phosphoserine at residue 14	118
<b>Table 1.41:</b> Summary of $^1\text{H}$ - $^{13}\text{C}$ HSQC and TOCSY NMR data at 278 K for peptides with Thr and pThr at residue 2	130
<b>Table 1.42:</b> Summary of $^1\text{H}$ - $^{13}\text{C}$ HSQC and TOCSY NMR data at 278 K for peptides with Thr and pThr at residue 10	132
<b>Table 1.43:</b> Amide proton chemical shifts of unmodified and modified serine residues	139
<b>Table 1.44:</b> Coupling constants between serine amide and alpha protons of unmodified and modified serine residues	139

<b>Table 1.45:</b> Alpha proton chemical shifts of unmodified and modified serine residues .....	140
<b>Table 1.46:</b> Beta proton chemical shifts of unmodified and modified serine residues .....	140
<b>Table 1.47:</b> Chemical shifts of acetyl protons on the N-terminus of peptides with unmodified and modified serine residues .....	141
<b>Table 1.48:</b> Chemical shifts of carboxamide protons on the C-terminus of peptides with unmodified and modified serine residues .....	141
<b>Table 1.49:</b> Mean chemical shifts of alanine amide protons on peptides with unmodified and modified serine residues .....	142
<b>Table 1.50:</b> Mean chemical shifts of alanine alpha protons on peptides with unmodified and modified serine residues .....	142
<b>Table 1.51:</b> Mean chemical shifts of alanine beta protons on peptides with unmodified and modified serine residues .....	143
<b>Table 1.53:</b> Coupling constants between threonine amide and alpha protons of unmodified and modified threonine residues .....	144
<b>Table 1.54:</b> Alpha proton chemical shifts of unmodified and modified threonine residues .....	144
<b>Table 1.55:</b> Beta proton chemical shifts of unmodified and modified threonine residues .....	145
<b>Table 1.56:</b> Gamma proton chemical shifts of unmodified and modified threonine residues .....	145
<b>Table 1.57:</b> Chemical shifts of acetyl protons on the N-terminus of peptides with modified and unmodified threonine residues .....	146
<b>Table 1.58:</b> Chemical shifts of carboxamide protons on the C-terminus on peptides with modified and unmodified threonine residues .....	146
<b>Table 1.59:</b> Mean chemical shifts of alanine amide protons on peptides with modified and unmodified threonine residues .....	147
<b>Table 1.60:</b> Mean chemical shifts of alanine alpha protons on peptides with modified and unmodified threonine residues .....	147

<b>Table 1.61:</b> Mean chemical shifts of alanine beta protons on peptides with modified and unmodified threonine residues .....	148
<b>Table 1.62:</b> Alpha and beta carbon chemical shifts of threonine on peptides with modified and unmodified threonine residues .....	148
<b>Table 1.63:</b> Mean alpha and beta carbon chemical shifts of alanine residues on peptides with modified and unmodified threonine residues .....	149
<b>Table 1.64:</b> Mean alpha carbon chemical shifts of lysine residues on peptides with modified and unmodified threonine residues .....	149
<b>Table 2.1:</b> Summary of CD data for peptides with <i>i/i+2</i> orientation .....	162
<b>Table 2.2:</b> Summary of CD data for peptides with <i>i/i+3</i> orientation .....	164
<b>Table 2.3:</b> Summary of CD data for peptides with <i>i/i+4</i> orientation .....	165
<b>Table 2.4:</b> Summary of CD data for peptides with <i>i/i-4</i> orientation .....	166
<b>Table 2.5:</b> Summary of CD data for peptides containing serine modifications at residue 1 and tryptophan at residue 5 of the $\alpha$ -helix .....	168
<b>Table 2.6:</b> Summary of NMR data for peptides containing serine modifications at residue 1 and tryptophan at residue 5 of the $\alpha$ -helix .....	169
<b>Table 2.7:</b> Summary of CD data for threonine and 4-I-Phe containing peptides ...	173
<b>Table 2.8:</b> Summary of CD data for peptides with a relative <i>i/i+4</i> orientation .....	175
<b>Table 2.9:</b> Summary of CD data in KF and NaCl.....	178
<b>Table 2.10:</b> Purification procedure for synthetic peptides.....	196
<b>Table 2.11:</b> Characterization data for synthetic peptides.....	197
<b>Table 2.12:</b> Summary of CD data for all peptides .....	199
<b>Table 2.13:</b> Summary of CD data for all peptides .....	200
<b>Table 2.14:</b> Summary of $^1\text{H}$ NMR data .....	213
<b>Table 2.15:</b> Summary of $^1\text{H}$ NMR data .....	214
<b>Table 3.1:</b> NMR-derived data for Ac-TGPX-NH <sub>2</sub> and Ac-TYPN-NH <sub>2</sub> peptides ..	230

<b>Table 3.2:</b>	NMR-derived data for <i>tau</i> <sub>403-406</sub> Ac-TSPX-NH <sub>2</sub> peptides.....	236
<b>Table 3.3:</b>	NMR-derived data for <i>tau</i> <sub>403-406</sub> Ac-TSPX-NH <sub>2</sub> peptides.....	239
<b>Table 3.4:</b>	NMR-derived Ser H $\alpha$ data for <i>tau</i> <sub>403-406</sub> Ac-TSPX-NH <sub>2</sub> and Gly H $\alpha$ data for Ac-TGPX-NH <sub>2</sub> peptides.....	241
<b>Table 3.5:</b>	NMR-derived data for <i>tau</i> <sub>395-411</sub> peptides.....	242
<b>Table 3.6:</b>	Purification procedure for synthetic peptides.....	256
<b>Table 3.7:</b>	Characterization data for synthetic peptides.....	257
<b>Table 3.8:</b>	Summary of <sup>1</sup> H NMR data for Ac-TGPX-NH <sub>2</sub> peptides.....	261
<b>Table 3.9:</b>	Summary of <sup>1</sup> H NMR data for Ac-TSPX-NH <sub>2</sub> peptides.....	263
<b>Table 3.10:</b>	Summary of <sup>1</sup> H NMR data for Ac-TpSPR-NH <sub>2</sub> peptide.....	265
<b>Table 3.11:</b>	Summary of <sup>1</sup> H NMR data for Ac-TpSPW-NH <sub>2</sub> peptide.....	266
<b>Table 3.12:</b>	Summary of <sup>1</sup> H NMR data for Ac-pTSPR-NH <sub>2</sub> peptide.....	268
<b>Table 3.13:</b>	Summary of <sup>1</sup> H NMR data for Ac-pTSPW-NH <sub>2</sub> peptide.....	269
<b>Table 3.14:</b>	Summary of <sup>1</sup> H NMR data for Ac-pTpSPR-NH <sub>2</sub> peptide.....	271
<b>Table 3.15:</b>	Summary of <sup>1</sup> H NMR data for Ac-pTpSPW-NH <sub>2</sub> peptide.....	272

## LIST of FIGURES

<b>Figure 1.1:</b> Phosphorylation and OGIcNAcylation are dynamic intracellular post-translational modifications of serine and threonine residues .....	2
<b>Figure 1.2:</b> Peptide sequences examined in this study.....	7
<b>Figure 1.3:</b> CD spectra of Ac-SKAAAKKAAAKAAGY-NH <sub>2</sub> peptides.....	8
<b>Figure 1.4:</b> Diagram of phi ( $\phi$ )torsion angles within a residue .....	10
<b>Figure 1.5:</b> CD spectra of Ac-TKAAAKKAAAKAAGY-NH <sub>2</sub> peptides .....	12
<b>Figure 1.6:</b> CD spectra of peptides containing modifications at residue 2 .....	16
<b>Figure 1.7:</b> Temperature-dependent <sup>1</sup> H NMR spectra (amide region) of Ac-AT(OPO <sub>3</sub> <sup>2-</sup> )AAAKKAAAKAAGY-NH <sub>2</sub> peptide.....	20
<b>Figure 1.8:</b> Diagram of Chi 1 ( $\chi_1$ ) torsion angle within a residue.....	21
<b>Figure 1.9:</b> CD spectra of Ac-AKAASAKAAAKAAGY-NH <sub>2</sub> peptides.....	22
<b>Figure 1.10:</b> CD spectra of Ac-AKAATAKAAAKAAGY-NH <sub>2</sub> peptides .....	24
<b>Figure 1.11:</b> CD spectra of Ac-AKAAAKAASAKAAGY-NH <sub>2</sub> peptides .....	27
<b>Figure 1.12:</b> CD spectra of Ac-YGAKAAAKKAAAKAS-NH <sub>2</sub> and Ac-YGAKAAAKKAAAKAT-NH <sub>2</sub> peptides.....	31
<b>Figure 1.13:</b> <sup>1</sup> H- <sup>13</sup> C HSQC spectra (H $\alpha$ -C $\alpha$ region) of peptides containing unmodified threonine and phosphothreonine at residue 2 and 10 .....	35
<b>Figure 1.14:</b> Dephosphorylation of peptides containing phosphothreonine at residue 2 or 10 of the $\alpha$ -helix by Antarctic phosphatase (CD spectra).....	37
<b>Figure 1.15:</b> Comparison of the effects of threonine modifications and proline as function of position.....	39
<b>Figure 1.16:</b> CD spectra of Ac-YGAKAAAKKAAAKAX-NH <sub>2</sub> peptides with proline and threonine modifications .....	40

<b>Figure 1.17:</b> Comparison of the effects of serine post-translational modifications as a function of position .....	45
<b>Figure 1.18:</b> Comparison of the effects of threonine post-translational modifications as a function of position .....	46
<b>Figure 1.19:</b> Summary of NMR data for peptides containing phosphothreonine .....	51
<b>Figure 1.20:</b> Crystal structure of the N-terminus of an $\alpha$ -helix on <i>B. subtilis</i> lipoteichoic acid synthase .....	53
<b>Figure 1.21:</b> Scheme for the chemical phosphorylation of peptides on resin and subsequent cleavage/deprotection .....	56
<b>Figure 1.22:</b> Synthesis of peracetylated 2-acetamido-2-deoxy- $\beta$ -D-glycosides of Fmoc-Thr-OH (R = CH <sub>3</sub> ) and Fmoc-Ser-OH.....	57
<b>Figure 1.22:</b> CD spectra of peptides with serine and serine modifications at residue 1. ....	65
<b>Figure 1.23:</b> CD spectra of peptides with threonine and threonine modifications at residue 1.....	66
<b>Figure 1.24:</b> CD spectra of peptides with serine and serine modifications at residue 2 .....	67
<b>Figure 1.25:</b> CD spectra of peptides with threonine and threonine modifications at residue 2.....	68
<b>Figure 1.26:</b> CD spectra of peptides with serine and serine modifications at residue 5 .....	69
<b>Figure 1.27:</b> CD spectra of peptides with threonine and threonine modifications at residue 5.....	70
<b>Figure 1.28:</b> CD spectra of peptides with serine and serine modifications at residue 10 .....	71
<b>Figure 1.29:</b> CD spectra of peptides with threonine and threonine modifications at residue 10.....	72
<b>Figure 1.30:</b> CD spectra of peptides with serine and serine modifications at residue 14 .....	73

<b>Figure 1.31:</b> CD spectra of peptides with threonine and threonine modifications at residue 14.....	74
<b>Figure 1.32:</b> CD spectra of peptides with proline at residue 1, 2, 5, 10.....	75
<b>Figure 1.33:</b> CD spectra of peptides proline at residue 14, alanine at residue 1 and 2, Aib at residue 2.....	76
<b>Figure 1.34:</b> CD spectra of peptides with phosphothreonine at residue 2 or 10 in 30% TFE.....	77
<b>Figure 1.35:</b> CD spectra of peptides in the absence and presence of MgCl <sub>2</sub> .....	78
<b>Figure 1.36:</b> Temperature-dependent CD of peptides containing serine and serine modifications.....	79
<b>Figure 1.37:</b> Temperature-dependent CD of peptides containing threonine and threonine modifications.....	80
<b>Figure 1.38:</b> Phosphatase assay for peptides containing phosphothreonine at residue 2 (CD spectra).....	81
<b>Figure 1.39:</b> HPLC analysis of dephosphorylation by phosphatase for phosphothreonine at residue 2.....	82
<b>Figure 1.40:</b> Phosphatase assay for peptides containing phosphothreonine at residue 10 (CD spectra).....	83
<b>Figure 1.41:</b> HPLC analysis of dephosphorylation by phosphatase for phosphothreonine at residue 10.....	84
<b>Figure 1.42:</b> <sup>1</sup> H NMR spectra (amide region) of Ac-SKAAAKKAAAKAAGY-NH <sub>2</sub> peptides with serine modifications.....	87
<b>Figure 1.43:</b> <sup>1</sup> H NMR spectra (amide region) of Ac-TKAAAKKAAAKAAGY-NH <sub>2</sub> peptides with threonine modifications.....	90
<b>Figure 1.44:</b> <sup>1</sup> H NMR spectra (amide region) of Ac-ASAAAKKAAAKAAGY-NH <sub>2</sub> peptides with serine modifications.....	93
<b>Figure 1.45:</b> <sup>1</sup> H NMR spectra (amide region) of Ac-ATAAAKAAAKAAGY-NH <sub>2</sub> peptides with threonine modifications.....	96
<b>Figure 1.46:</b> <sup>1</sup> H NMR spectra of Ac-AT(OPO <sub>3</sub> <sup>2-</sup> )AAAKKAAAKAAGY-NH <sub>2</sub> collected in D <sub>2</sub> O.....	99

<b>Figure 1.47:</b> Temperature-dependent $^1\text{H}$ NMR spectra (amide region) of Ac-AT(OPO <sub>3</sub> <sup>2-</sup> )AAAAKAAAAKAAGY-NH <sub>2</sub> peptide.....	100
<b>Figure 1.48:</b> $^1\text{H}$ NMR spectra (amide region) of Ac-AKAASAKAAAAKAAGY-NH <sub>2</sub> peptides with serine modifications .....	101
<b>Figure 1.48:</b> $^1\text{H}$ NMR spectra (amide region) of Ac-AKAATAKAAAAKAAGY-NH <sub>2</sub> peptides with threonine modifications.....	104
<b>Figure 1.49:</b> $^1\text{H}$ NMR spectra (amide region) of Ac-AKAAAAKAASAKAAGY-NH <sub>2</sub> peptides with serine modifications .....	107
<b>Figure 1.50:</b> $^1\text{H}$ NMR spectra (amide region) of Ac-AKAAAAKAATAKAAGY-NH <sub>2</sub> peptides with threonine modifications.....	110
<b>Figure 1.51:</b> $^1\text{H}$ NMR spectra (amide region) of Ac-YGAKAAAAKAAAAKAS-NH <sub>2</sub> peptides with serine modifications .....	113
<b>Figure 1.52:</b> $^1\text{H}$ NMR spectra (amide region) of Ac-YGAKAAAAKAAAAKAT-NH <sub>2</sub> peptides with threonine modifications.....	116
<b>Figure 1.53:</b> TOCSY spectra of Ac-SKAAAAKAAAAKAAGY-NH <sub>2</sub> peptides with serine modifications.....	119
<b>Figure 1.54:</b> TOCSY spectra of Ac-TKAAAAKAAAAKAAGY-NH <sub>2</sub> peptides with threonine modifications .....	120
<b>Figure 1.55:</b> TOCSY spectra of Ac-ASAAAAKAAAAKAAGY-NH <sub>2</sub> peptides with serine modifications.....	121
<b>Figure 1.56:</b> TOCSY spectra of Ac-ATAAAKAAAAKAAGY-NH <sub>2</sub> peptides with threonine modifications .....	122
<b>Figure 1.57:</b> TOCSY spectra of Ac-AKAASAKAAAAKAAGY-NH <sub>2</sub> peptides with serine modifications.....	123
<b>Figure 1.58:</b> TOCSY spectra of Ac-AKAATAKAAAAKAAGY-NH <sub>2</sub> peptides with threonine modifications .....	124
<b>Figure 1.59:</b> TOCSY spectra of Ac-AKAAAAKAASAKAAGY-NH <sub>2</sub> peptides with serine modifications.....	125
<b>Figure 1.60:</b> TOCSY spectra of Ac-AKAAAAKAATAKAAGY-NH <sub>2</sub> peptides with threonine modifications .....	126

<b>Figure 1.61:</b> TOCSY spectra of Ac-YGAKAAAKAAAKAS-NH <sub>2</sub> peptides with serine modifications.....	127
<b>Figure 1.62:</b> TOCSY spectra of Ac-YGAKAAAKAAAKAT-NH <sub>2</sub> peptides with threonine modifications .....	128
<b>Figure 1.63:</b> <sup>1</sup> H- <sup>13</sup> C HSQC spectra of Ac-ATAAAKAAAKAAGY-NH <sub>2</sub> peptides with unmodified Thr(free hydroxyl) and Thr(OPO <sub>3</sub> <sup>2-</sup> ).....	129
<b>Figure 1.64:</b> <sup>1</sup> H- <sup>13</sup> C HSQC spectra of Ac-AKAAAKAATAKAAGY-NH <sub>2</sub> peptides with unmodified Thr(free hydroxyl) and Thr(OPO <sub>3</sub> <sup>2-</sup> ).....	131
<b>Figure 1.65:</b> <sup>31</sup> P NMR spectra of peptide Ac-T(OPO <sub>3</sub> <sup>2-</sup> )KAAAKAAAKAAGY-NH <sub>2</sub> .....	133
<b>Figure 1.66:</b> <sup>31</sup> P NMR spectra of peptide Ac-AS(OPO <sub>3</sub> <sup>2-</sup> )AAAKAAAKAAGY-NH <sub>2</sub> .....	134
<b>Figure 1.67:</b> <sup>31</sup> P NMR spectra of peptide Ac-AT(OPO <sub>3</sub> <sup>2-</sup> )AAAKAAAKAAGY-NH <sub>2</sub> .....	135
<b>Figure 1.68:</b> <sup>31</sup> P NMR spectra of peptide Ac-AKAAT(OPO <sub>3</sub> <sup>2-</sup> )AKAAAKAAGY-NH <sub>2</sub> . 136	
<b>Figure 1.69:</b> <sup>31</sup> P NMR spectra of peptide Ac-AKAAAKAAT(OPO <sub>3</sub> <sup>2-</sup> )AKAAGY-NH <sub>2</sub> .....	137
<b>Figure 2.1:</b> Schematic representation of proposed intra- $\alpha$ -helical interaction between GlcNAc and 4-B(OH) <sub>2</sub> -Phe or 4-I-Phe .....	158
<b>Figure 2.2:</b> Peptide sequences examined in this study.....	159
<b>Figure 2.3:</b> Synthesis of peracetylated 2-acetamido-2-deoxy- $\beta$ -D-glycosides of Fmoc-Thr-OH (R = CH <sub>3</sub> ) and Fmoc-Ser-OH (R = H) .....	160
<b>Figure 2.4:</b> Synthetic scheme of solid-phase aryl borylation of peptides containing 4-I-Phe .....	161
<b>Figure 2.5:</b> Scheme for the chemical phosphorylation of peptides on resin and subsequent cleavage/deprotection .....	161
<b>Figure 2.6:</b> CD spectra of Ac-SK(4-I-Phe)AAAKAAAKAAGY-NH <sub>2</sub> peptides with unmodified Ser(free hydroxyl) and Ser(OGlcNAc) .....	162

<b>Figure 2.7:</b> CD spectra of Ac-SKA(4-X-Phe)AAKAAAKAAGY-NH <sub>2</sub> peptides with unmodified Ser(free hydroxyl) and Ser(OGlcNAc).....	163
<b>Figure 2.8:</b> CD spectra of Ac-SKAA(4-X-Phe)AKAAAKAAGY-NH <sub>2</sub> peptides with unmodified Ser(free hydroxyl) and Ser(OGlcNAc).....	165
<b>Figure 2.9:</b> CD spectra of Ac-(4-X-Phe)KAASAKAAAKAAGY-NH <sub>2</sub> peptides with serine unmodified Ser(free hydroxyl) and Ser(GlcNAc) .....	166
<b>Figure 2.10:</b> CD spectra of Ac-SKAAWAKAAAKAAGY-NH <sub>2</sub> peptides with unmodified Ser(free hydroxyl) and Ser(OGlcNAc) .....	168
<b>Figure 2.11:</b> Comparative TOCSY spectra of the amide region of peptides Ac-S(OGlcNAc)KAAAAKAAAKAAGY-NH <sub>2</sub> and Ac-S(OGlcNAc)KAAWAKAAAKAAGY-NH <sub>2</sub> .....	171
<b>Figure 2.12:</b> CD spectra of Ac-TKAA(4-I-Phe)AKAAAKAAGY-NH <sub>2</sub> peptides with threonine unmodified Thr(free hydroxyl) and Thr(GlcNAc).....	172
<b>Figure 2.13:</b> CD spectra of Ac-SKAAA(4-X-Phe)AAKAAGY-NH <sub>2</sub> peptides with serine unmodified Ser(free hydroxyl) and Ser(OGlcNAc) .....	175
<b>Figure 2.14:</b> CD spectra of Ac-SKAAA(4-X-Phe)AAKAAGY-NH <sub>2</sub> peptides in the presence and absence of $\beta$ -D-Fructose with serine unmodified Ser(free hydroxyl) and Ser(GlcNAc) .....	176
<b>Figure 2.15:</b> CD spectra of Ac-SKAAA(4-X-Phe)AAKAAGY-NH <sub>2</sub> peptides.....	177
<b>Figure 2.16:</b> CD comparison of 4-I-Phe and 4-B(OH) <sub>2</sub> -Phe as a function of position .....	184
<b>Figure 2.17:</b> Representative $\alpha$ -helix models with 4-B(OH) <sub>2</sub> -Phe.....	185
<b>Figure 2.18:</b> Partial scheme for the equilibrium of the boronic acid species in 192 mM aqueous phosphate buffer (pH 7.0) and 100 mM KF .....	186
<b>Figure 2.19:</b> Plausible equilibrium involved in stabilizing interactions observed between 4-B(OH) <sub>2</sub> -Phe and lysine .....	188
<b>Figure 2.20:</b> Plausible equilibrium involved in stabilizing interactions observed between 4-B(OH) <sub>2</sub> -Phe and lysine .....	190
<b>Figure 2.21:</b> Scheme for the chemical phosphorylation of peptides on resin and subsequent cleavage/deprotection .....	192

<b>Figure 2.22:</b> Synthesis of peracetylated 2-acetamido-2-deoxy- $\beta$ -D-glycosides of Fmoc-Thr-OH (R = CH <sub>3</sub> ) and Fmoc-Ser-OH (R = H) .....	193
<b>Figure 2.23:</b> Solid phase arylborlyation of peptides containing 4-Iodo-Phe .....	194
<b>Figure 2.24:</b> CD spectra of Ac-SK(4-I-Phe)AAKAAAANKAAGY-NH <sub>2</sub> and Ac-S(OGlcNAc)K(4-I-Phe)AAKAAAANKAAGY-NH <sub>2</sub> peptides .....	201
<b>Figure 2.25:</b> CD spectra of Ac-SKA(4-I-Phe)AAKAAAANKAAGY-NH <sub>2</sub> , Ac-SKA(4-B(OH) <sub>2</sub> -Phe)AAKAAAANKAAGY-NH <sub>2</sub> , Ac-S(OGlcNAc)KA(4-I-Phe)AAKAAAANKAAGY-NH <sub>2</sub> , and Ac-S(OGlcNAc)KA(4-B(OH) <sub>2</sub> -Phe)AAKAAAANKAAGY-NH <sub>2</sub> .....	202
<b>Figure 2.26:</b> CD spectra of Ac-SKAA(4-I-Phe)AKAAAANKAAGY-NH <sub>2</sub> , Ac-SKAA(4-B(OH) <sub>2</sub> -Phe)AKAAAANKAAGY-NH <sub>2</sub> , Ac-S(OGlcNAc)KAA(4-I-Phe)AKAAAANKAAGY-NH <sub>2</sub> , and Ac-S(OGlcNAc)KAA(4-B(OH) <sub>2</sub> -Phe)AKAAAANKAAGY-NH <sub>2</sub> .....	203
<b>Figure 2.27:</b> CD spectra of Ac-SKAAWAKAAAANKAAGY-NH <sub>2</sub> , Ac-S(OGlcNAc)KAAWAKAAAANKAAGY-NH <sub>2</sub> , and Ac-S(OPO <sub>3</sub> <sup>2-</sup> )KAAWAKAAAANKAAGY-NH <sub>2</sub> .....	204
<b>Figure 2.28:</b> CD spectra of Ac-TKAA(4-I-Phe)AKAAAANKAAGY-NH <sub>2</sub> and Ac-T(OGlcNAc)KAA(4-I-Phe)AKAAAANKAAGY-NH <sub>2</sub> .....	205
<b>Figure 2.29:</b> CD spectra of Ac- (4-I-Phe)KAASAKAAAANKAAGY-NH <sub>2</sub> , Ac- (4-I-Phe)KAAS(OGlcNAc)AKAAAANKAAGY-NH <sub>2</sub> , and Ac- (4-B(OH) <sub>2</sub> -Phe)KAAS(OGlcNAc)AKAAAANKAAGY-NH <sub>2</sub> .....	206
<b>Figure 2.30:</b> CD spectra of Ac-SKAAAANK(4-I-Phe)AAKKAAGY-NH <sub>2</sub> , Ac-SKAAAANK(4-B(OH) <sub>2</sub> -Phe)AAKKAAGY-NH <sub>2</sub> , Ac-S(OGlcNAc)KAAAANK(4-I-Phe)AAKKAAGY-NH <sub>2</sub> , and Ac-S(OGlcNAc)KAAAANK(4-B(OH) <sub>2</sub> -Phe)AAKKAAGY-NH <sub>2</sub> .....	207
<b>Figure 2.31:</b> CD spectra of peptides in the presence and absence of fructose .....	208
<b>Figure 2.32:</b> CD spectra of the peptides in the presence of 25 mM NaCl, 1M NaCl, and 1M KF .....	209
<b>Figure 2.33:</b> CD spectra of the peptides in the presence of 25 mM NaCl, 1M NaCl, and 1M KF .....	210
<b>Figure 2.34:</b> <sup>1</sup> H NMR spectra (amide region) of peptides with serine modifications: unmodified Ser(free hydroxyl), Ser(OGlcNAc), and Ser(OPO <sub>3</sub> <sup>2-</sup> ) .....	212

<b>Figure 3.1:</b> Local aromatic-proline interactions.....	224
<b>Figure 3.2:</b> Peptide sequences examined in this study.....	227
<b>Figure 3.3:</b> The <sup>1</sup> H NMR spectra of Ac-TGPY-NH <sub>2</sub> and Ac-TGPW-NH <sub>2</sub> . ....	232
<b>Figure 3.4:</b> The <sup>1</sup> H NMR spectra of H $\alpha$ region of Ac-TGPX-NH <sub>2</sub> .....	233
<b>Figure 3.5:</b> Schematic representation of the kinetic formation of paired helical filament formation promoted by both R406W mutation and phosphorylation of Ser <sub>404</sub> . ....	251
<b>Figure 3.6:</b> Scheme for the chemical phosphorylation of peptides on resin and subsequent cleavage/deprotection .....	253
<b>Figure 3.7:</b> <sup>1</sup> H NMR spectra (amide region) of Ac-TGPX-NH <sub>2</sub> peptides .....	258
<b>Figure 3.8:</b> <sup>1</sup> H NMR spectra (amide region) of Ac-TGPX-NH <sub>2</sub> peptides .....	259
<b>Figure 3.9:</b> <sup>1</sup> H NMR spectra (amide region) of Ac-TGPX-NH <sub>2</sub> peptides .....	260
<b>Figure 3.9:</b> <sup>1</sup> H NMR spectra (amide region) of Ac-TSPX-NH <sub>2</sub> peptides .....	262
<b>Figure 3.10:</b> <sup>1</sup> H NMR spectra (amide region) of Ac-TpSPX-NH <sub>2</sub> peptides .....	264
<b>Figure 3.11:</b> <sup>1</sup> H NMR spectra (amide region) of Ac-pTSPX-NH <sub>2</sub> peptides .....	267
<b>Figure 3.12:</b> <sup>1</sup> H NMR spectra (amide region) of Ac-pTpSPX-NH <sub>2</sub> peptides .....	270
<b>Figure 3.13:</b> <sup>1</sup> H NMR spectra (amide region) of <i>tau</i> <sub>395-411</sub> peptides .....	273
<b>Figure 3.14:</b> Full TOCSY spectra of Ac-TGPY-NH <sub>2</sub> (pH 4.0, 298 K).....	274
<b>Figure 3.15:</b> Full TOCSY spectra of Ac-TGPW-NH <sub>2</sub> (pH 4.0, 298 K).....	275
<b>Figure 3.16:</b> Full TOCSY spectra of Ac-TSPN-NH <sub>2</sub> (pH 4.0, 298 K) .....	276
<b>Figure 3.17:</b> Full TOCSY spectra of Ac-TSPR-NH <sub>2</sub> (pH 4.0, 298 K) .....	277
<b>Figure 3.18:</b> Full TOCSY spectra of Ac-TSPW-NH <sub>2</sub> (pH 4.0, 298 K) .....	278
<b>Figure 3.19:</b> Full TOCSY spectra of Ac-TpSPR-NH <sub>2</sub> (pH 6.5, 298 K) .....	279
<b>Figure 3.20:</b> Full TOCSY spectra of Ac-TpSPR-NH <sub>2</sub> (pH 7.2, 298 K) .....	280
<b>Figure 3.21:</b> Full TOCSY spectra of Ac-TpSPW-NH <sub>2</sub> (pH 6.5, 298 K) .....	281

<b>Figure 3.22:</b> Full TOCSY spectra of Ac-TpSPW-NH <sub>2</sub> (pH 7.2, 298 K) .....	282
<b>Figure 3.23:</b> Full TOCSY spectra of Ac-pTSPR-NH <sub>2</sub> (pH 6.5, 298 K) .....	283
<b>Figure 3.24:</b> Full TOCSY spectra of Ac-pTSPR-NH <sub>2</sub> (pH 7.2, 298 K) .....	284
<b>Figure 3.25:</b> Full TOCSY spectra of Ac-pTSPW-NH <sub>2</sub> (pH 6.5, 298 K) .....	285
<b>Figure 3.26:</b> Full TOCSY spectra of Ac-pTSPW-NH <sub>2</sub> (pH 7.2, 298 K) .....	286
<b>Figure 3.27:</b> Full TOCSY spectra of Ac-pTpSPR-NH <sub>2</sub> (pH 6.5, 298 K) .....	287
<b>Figure 3.28:</b> Full TOCSY spectra of Ac-pTpSPR-NH <sub>2</sub> (pH 7.2, 298 K) .....	288
<b>Figure 3.29:</b> Full TOCSY spectra of Ac-pTpSPW-NH <sub>2</sub> (pH 6.5, 298 K) .....	289
<b>Figure 3.30:</b> Full TOCSY spectra of Ac-pTpSPW-NH <sub>2</sub> (pH 7.2, 298 K) .....	290
<b>Figure 3.31:</b> Full TOCSY spectra of <i>tau</i> <sub>395-411</sub> (pH 6.5, 298 K) .....	291
<b>Figure 3.32:</b> Full TOCSY spectra of <i>tau</i> <sub>395-411</sub> R406W (pH 6.5, 298 K) .....	292
<b>Figure 3.33:</b> Full TOCSY spectra of <i>tau</i> <sub>395-411</sub> pSer <sub>404</sub> (pH 6.5, 298 K) .....	293
<b>Figure 3.34:</b> Full TOCSY spectra of <i>tau</i> <sub>395-411</sub> pSer <sub>404</sub> (pH 7.2, 298 K) .....	294
<b>Figure 3.35:</b> Full TOCSY spectra of <i>tau</i> <sub>395-411</sub> pSer <sub>404</sub> R406W (pH 6.5, 298 K) .....	295
<b>Figure 3.36:</b> Full TOCSY spectra of <i>tau</i> <sub>395-411</sub> pSer <sub>404</sub> R406W (pH 7.2, 298 K) .....	296

## ABSTRACT

The dynamic interplay between phosphorylation and  $\beta$ -*O*-GlcNAcylation (OGlcNAc) of serine and threonine plays critical roles in numerous intracellular processes. Changes in phosphorylation and OGlcNAcylation are linked to Alzheimer's disease, diabetes, and cancer. We have conducted a systematic study on a model  $\alpha$ -helix to determine the structural effects of phosphorylation and OGlcNAcylation of serine and threonine residues, on the N-terminus, C-terminus, and internal positions (Ac-XKAAXAKAAXAKAAGY-NH<sub>2</sub>, Ac-YGAKAAAANKAAAAX-NH<sub>2</sub>). We found that both phosphorylation and OGlcNAcylation on the N-terminus increase  $\alpha$ -helix stability, with phosphorylation exhibiting a greater increase in  $\alpha$ -helix stability than OGlcNAcylation. These stabilizing effects were found to be greater for threonine than serine, and for the dianionic phosphate over the monoanionic phosphate. In contrast, both phosphorylation and OGlcNAcylation reduced helix stability on internal and C-terminal positions relative to serine or threonine. These effects are not simply electrostatic interactions; we observe a unique cyclization of serine and threonine residues due to an intra-residue phosphate-amide hydrogen bond. Furthermore this interaction is greater for threonine than serine and for the dianionic phosphate over the monoanionic phosphate. On the N-terminus NMR data are consistent with an  $\alpha$ -helix capping mechanism in which the phosphate hydrogen bonds to its own amide, organizing and nucleating the first turn of the  $\alpha$ -helix through an induced  $n \rightarrow \pi^*$  interaction between the  $i-1$  carbonyl and the  $i$  (phosphorylated) carbonyl. On internal and C-terminal positions,  $\alpha$ -helix destabilization is due to this phosphate amide intra-

residue hydrogen bond disrupting the backbone hydrogen bonding network.

Interestingly, the overall effects of phosphorylation and OGlcNAcylation on an  $\alpha$ -helix are analogous to the effects observed for proline, with the effects of phosphothreonine greater than the effects of proline on the  $\alpha$ -helix at all positions.

To further understand the effects of serine GlcNAcylation on  $\alpha$ -helices, we sought to explore possible side-chain interactions with neighboring residues, such as hydrophobic, CH/ $\pi$ , or boronic acid/diol conjugates. A series of Baldwin model  $\alpha$ -helices (Ac-AKAAAKAAAKAAGY-NH<sub>2</sub>) were designed to explore  $i+2$ ,  $i+3$ ,  $i+4$ , and  $i+7$  interactions utilizing 4-iodo-phenylalanine (4-iodo-Phe) or 4-B(OH)<sub>2</sub>-phenylalanine (4-B(OH)<sub>2</sub>-Phe) as interacting residues. Although no interaction was found to exist between GlcNAc and either 4-iodo-Phe or 4-B(OH)<sub>2</sub>-Phe, an  $\alpha$ -helix stabilizing interaction was found involving lysine and boronic acid in a relative  $i / i+4$  relationship. The interaction between lysine and boronic acid exhibited an increase in  $\alpha$ -helix stability as the concentration of KF was increased, yet showed no increase in  $\alpha$ -helix stability when NaCl was used rather than KF. This observation is consistent with fluoride ions playing a crucial role in the  $\alpha$ -helix stabilizing interaction, as well as a mechanism involving more than a simple electrostatic model.

Phosphorylation is known to affect protein structure when there is no defined secondary structure such as an  $\alpha$ -helix. Many examples exist where phosphorylation sites have been identified in natively disordered proteins, such as the microtubule binding protein *tau*. Hyperphosphorylation of *tau* is associated with numerous neurodegenerative diseases, most notably Alzheimer's disease (AD). Within *tau*, phosphorylation of Ser<sub>404</sub> has shown to occur within patients with AD. Furthermore, elevated rates of AD onset have been observed due to a mutation of Arg<sub>406</sub> to Trp<sub>406</sub>.

Given the roles of both Ser<sub>404</sub> phosphorylation and R406W mutation in the onset of AD and other neurodegenerative disorders, I sought to determine the local structural effects of both phosphorylation and R406W mutation within *tau*. Due to the lack of organized secondary structure, one way to study regions of disordered proteins is to study small peptide fragments. Tetra-peptides of the sequence TSPX, representing residues 403-406 of *tau*, were synthesized, containing either or both phosphorylated Thr<sub>403</sub> and Ser<sub>404</sub> residues, containing either the native arginine or tryptophan mutation. We have found that phosphorylation of Ser<sub>404</sub> and R406W mutation both independently and dependently lead to a higher population of cis amide bonds. To validate the data obtained from tetra-peptides, larger *tau*<sub>395-411</sub> peptides with synthesized with both unmodified and phosphorylated Ser<sub>404</sub> and either Arg<sub>406</sub> or Trp<sub>406</sub>. The data herein are consistent with both phosphorylation of Ser<sub>404</sub> and R406W mutation leading to a higher population of cis amide bonds within *tau*. This increase in cis-Pro amide bond population may be directly correlated to the onset of AD.

## Chapter 1

# STRUCTURAL EFFECTS OF PHOSPHORYLATION AND $\beta$ -O-GlcNAcylation ON $\alpha$ -HELICES AS A FUNCTION OF POSITION

### Introduction

All living organisms exist in part due to highly regulated and complex networks of proteins. Post-translational modifications (PTMs) constitute the major mechanism in which proteins are regulated after transcription. The most common PTM is phosphorylation. Approximately 30% of all human proteins contain a covalently linked phosphate group, while the majority of intracellular proteins are phosphorylated.<sup>1</sup> Protein kinases, which are responsible for adding a covalently linked phosphate group to proteins, account for more than 2% of the human genome, with over 518 kinases identified.<sup>2,3</sup> In contrast to phosphorylation, the enzymatic process of adding  $\beta$ -D-N-acetylglucosamine (OGlcNAc) on serine or threonine (GlcNAcylation) is controlled by only one OGlcNAc transferase (OGT), whereas the removal is catalyzed by one OGlcNAcase (OGA) (Figure 1.1).<sup>3-7</sup> Currently, over 1000 proteins have been identified to be OGlcNAcyated across all organisms, making OGlcNAcylation one of the most common intracellular PTM. Interestingly, the cycling of OGlcNAc on proteins occurs on a timescale similar to phosphorylation.<sup>5,6</sup> Indeed, there often exists a dynamic interplay between phosphorylation and

OGlcNAcylation on the same threonine or serine residue, as is the case with c-Myc, estrogen receptor  $\beta$ , RNA polymerase II, and many other proteins.<sup>6, 8-11</sup> It is therefore critical to understand the induced structural effects of phosphorylation versus OGlcNAcylation on protein structure.

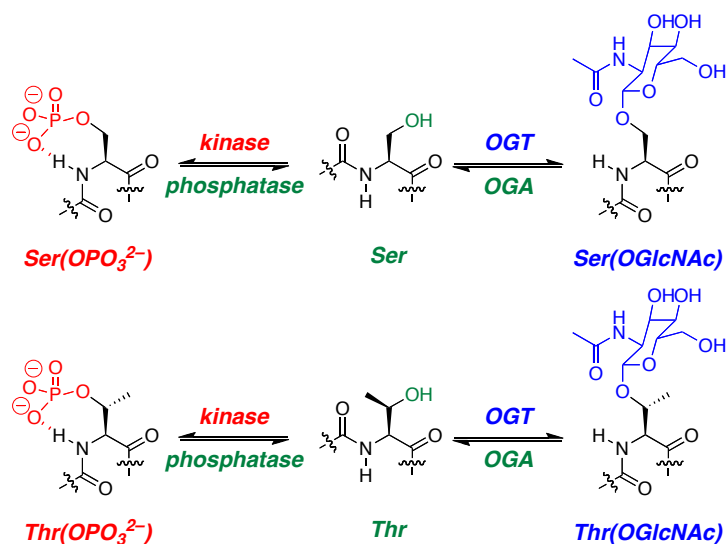


**Figure 1.1:** Phosphorylation and OGlcNAcylation are dynamic intracellular post-translational modifications of serine and threonine residues. OGT = O-GlcNAc transferase. OGA = O-GlcNAcase.

There have been studies performed to determine structural effects of phosphorylation versus OGlcNAcylation in a few specific contexts. Li studied these effects on a 17 residue model peptide from the N-terminus of murine estrogen receptor  $\beta$  (mER- $\beta$ ). They found that OGlcNAcylation of Ser<sup>16</sup> induced a type II  $\beta$ -turn-like formation, whereas phosphorylation opposes the turn, adopting a more extended conformation.<sup>9</sup> Wong examined the effects of Thr(OGlcNAc) on the C-terminal domain (CTD) of RNA polymerase II, which consists of highly conserved repeats of

the sequence (YSPTSPS)<sub>n</sub>. In model peptides of the sequence (YSPTSPS) they found that OGlcNAcylation led to a turn-like structure as well.<sup>10</sup>

The induced structural effects of phosphorylation and OGlcNAcylation have also been studied in more general contexts. Chan studied the structural effects of these PTMs on a designed  $\alpha$ -helix hairpin model with modifications in the loop region. They found minimal structural effects induced by both modifications.<sup>11</sup> More recently, our group studied the structural effects of phosphorylation versus OGlcNAcylation on the proline-rich domain of tau and proline-rich model peptides. It has been established that hyperphosphorylation of tau leads to the formation of neurofibrillary tangles (NFTs), the major component of neurodegenerative disorders such as Alzheimer's disease (AD), chronic traumatic encephalopathy (CTE), Down's syndrome, and other tauopathies.<sup>5, 12-14</sup> It has been shown that OGlcNAcylation regulates tau phosphorylation and acts to stabilize tau in the soluble form.<sup>15, 16</sup> Work performed by others in our group has demonstrated that within proline-rich sequences, phosphorylated serine and threonine (pSer, pThr) favor polyproline II structure, whereas GlcNAcyated serine and threonine (Ser(OGlcNAc), Thr(OGlcNAc)) oppose polyproline II. Greater structural effects were observed for modification on threonine over serine, and for phosphorylation over GlcNAcylation.<sup>16, 17</sup> Previously reported data suggest context dependence for the induced structural effects of phosphorylation and OGlcNAcylation. Therefore, I sought to determine the effects of these PTMs in the context of an  $\alpha$ -helix, the most common protein secondary structure.

Doig performed the first study on the effects of phosphorylation on monomeric  $\alpha$ -helices.<sup>19</sup> He found that pSer is stabilizing to  $\alpha$ -helix when on the first three residues, while on the N-terminus and destabilizing at residue 5 in the interior. The  $\alpha$ -helix stabilizing effects observed were attributed solely to electrostatics and

stabilization of the helix dipole, whereas helix disruption on internal positions was due to a desolvation penalty associated with the phosphate group. Doig later examined the effects of phosphoserine-lysine salt-bridges on  $\alpha$ -helix stability. He found that phosphoserine could be stabilizing at internal positions when in a relative  $i/i+4$  relationship to lysine.<sup>20</sup> DeGrado examined the effects of pSer in helix bundles and found that pSer at residue 2 had greater  $\alpha$ -helix stabilizing effects than at residue 1. Interestingly, computational models proposed a phosphate interaction with several amide protons.<sup>21</sup> Vinson found that pSer could be stabilizing at internal positions within an  $\alpha$ -helical coiled coil dimeric protein when adjacent to multiple arginines via inter-helical interactions.<sup>22</sup> He also found that pThr is destabilizing to a coiled coil. Again, these destabilizing effects were attributed to desolvation penalties involving the phosphate upon helix formation.<sup>23</sup> Although these initial studies laid the ground work for understanding structural effects of phosphorylation in the context of an  $\alpha$ -helix, they lack direct evidence to support their conclusions on the mechanism by which phosphorylation stabilizes an  $\alpha$ -helix at the N-terminus and destabilizes an  $\alpha$ -helix at internal positions. Furthermore, no direct comparisons have been made between pSer and pThr in the context of a model  $\alpha$ -helix.

In contrast to the effects of phosphorylation, substantially less work exists on the effects of OGlcNAcylation on  $\alpha$ -helices. Koksich and Hackenberger performed the only study examining the effects of phosphorylation versus glycosylation on  $\alpha$ -helix structure. They demonstrated that within the context of a coiled coil, both phosphorylation and glycosylation are destabilizing at internal solvent-exposed positions.<sup>24</sup> However, this study incorporated  $\beta$ -O-galactose, not  $\beta$ -OGlcNAc, for structural analysis. Previous work has demonstrated that the configuration of hydroxyls as well as the presence of an N-acetyl group can have a substantial impact

on structure.<sup>25</sup> In light of these issues, we sought to conduct a systematic study on a model  $\alpha$ -helix to determine the structural effects of phosphorylation and OGlcNAcylation of serine and threonine residues.

## Results

A series of peptides was synthesized based on Baldwin  $\alpha$ -helix model peptides (Ac-AKAAAKAAAKAAGY-NH<sub>2</sub> or Ac-YGAKAAAKAAAKA-NH<sub>2</sub>). Alanines were incorporated to ensure  $\alpha$ -helicity, while lysines were incorporated for solubility (Figure 1.1).<sup>26</sup> Tyrosine was incorporated for concentration determination on the C-terminus for peptides with N-terminal or internal modifications, and incorporated on the N-terminus for all peptides with C-terminal modifications, to avoid interactions with sites of modifications. Serine and threonine residues were incorporated on the N-terminus at residues 1 (N1) and 2 (N2) (Ac-XAKAAAKAAAKAAGY-NH<sub>2</sub> and N2 Ac-AXAAAKAAAKAAGY-NH<sub>2</sub>), at internal positions at residues 5 (N5) and 10 (N10) (Ac-AKAAAXAKAAAKAAGY-NH<sub>2</sub> and Ac-AKAAAKAAXAKAAGY-NH<sub>2</sub>), and on the C-terminus at residue 14 (N14) (Ac-YGAKAAAKAAAKAX-NH<sub>2</sub>). Peptides containing serine, phosphoserine, threonine, and phosphothreonine were incorporated using trityl/Fmoc-protected amino acids. Phosphorylation was conducted on solid-phase by selective trityl-deprotection, phosphitylation, oxidation, and cleavage/deprotection yielding a site selective phosphorylated residue.<sup>17,27</sup> OGlcNAcylated peptides were synthesized solid-phase incorporating Fmoc-Ser/Thr(Ac<sub>3</sub>OGlcNAc)-OH (synthesized solution-phase via a modified method of Arsequell) at the intended site of modification,

followed by initial purification, deesterification of the sugar hydroxyls, and final purification to obtain site specific incorporation of Ser/Thr(OGlcNAc).<sup>18, 28, 29</sup> All peptides were examined by circular dichroism (CD) at 0.5 °C (Table 1.15 and Table 1.16). Percent  $\alpha$ -helix was calculated by Baldwin's method, where % helix =  $100[(\phi)_{222} - [\phi]_C]/[\phi]_H - [\phi]_C$ , where  $[\phi]_C$  is the mean residue ellipticity (MRE) at 222 nm of 100% random coil, which equals  $2220 - 53T$ ,  $[\phi]_H$  is the MRE at 222 nm of 100%  $\alpha$ -helix, which equals  $(-44000 + 250T)/(1 - 3/n)$ , where  $T$  is the temperature in degrees Celsius (0.5) and  $n$  is the number of residues (16).<sup>30, 31</sup> All peptides containing serine or threonine were also analyzed by NMR at 278 K (Figures 1.42-1.52, Tables 1.21-1.40). Experiments on phosphorylated peptides were conducted at pH 4, where the phosphate is monoanionic, and pH 7.2, where the phosphate is mostly dianionic (typical pKa 5.5-6.0), to examine the effects of phosphate ionization state on structure. Peptides with unmodified serine or threonine, or OGlcNAcylated serine or threonine, were examined at pH 4.0.

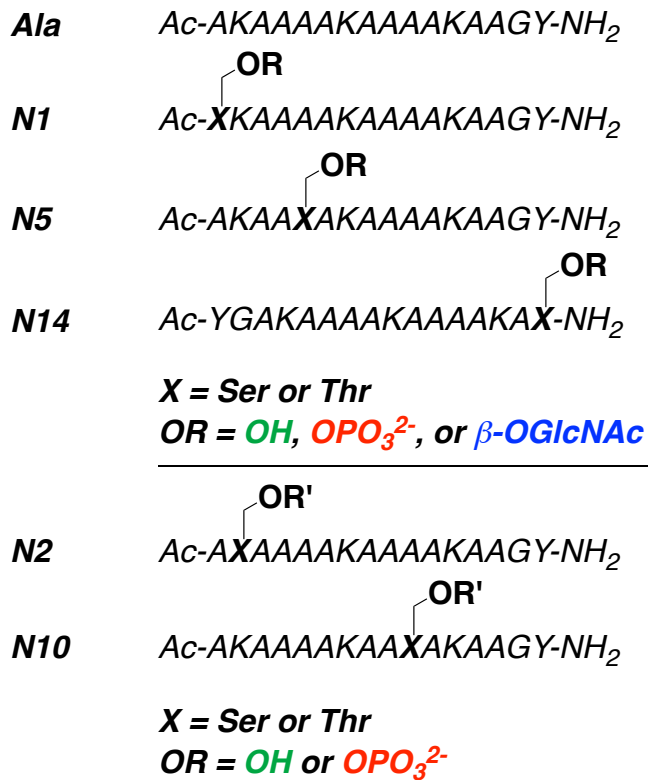


**Figure 1.2:** Peptide sequences examined in this study. Top: peptides with alanine substitution at all variable positions. Middle: peptides with modifications on the N-terminus at residue 1 (N1), at central residue 5 (N5), and on the C-terminus at residue 14 (N14). Bottom: peptides examining the effects of phosphorylation on the N-terminus at residue 2 (N2) and at central residue 10 (N10). Peptides were also synthesized with proline at positions N1, N2, N5, N10, N14, aminoisobutyric acid (Aib) at N2, and alanine at N2.

### Modifications on the N-terminal $\alpha$ -helical positions

All N1 serine peptide variants exhibited  $\alpha$ -helicity similar to that of the alanine peptide (Figure 1.3 and Table 1.1). Although alanine has a higher  $\alpha$ -helical propensity than serine, it is known that serine can function as an N-cap through a hydrogen bond between the lone pair of electrons on oxygen to the free N-terminal amide protons.<sup>26,</sup>

<sup>32-34</sup> Both phosphorylation (50.8% for the monoanionic phosphate 58.6% for the

dianionic phosphate) and OGlcNAcylation (50.6%) increase  $\alpha$ -helicity relative to unmodified serine (49.7%). As observed by Doig, the dianionic phosphoserine peptide exhibits the greatest  $\alpha$ -helicity. This observation is consistent with a favorable  $\alpha$ -helix dipole interaction, also observed for aspartate and glutamate, as well as possible N-terminal amide capping.<sup>19, 26, 33, 34</sup>

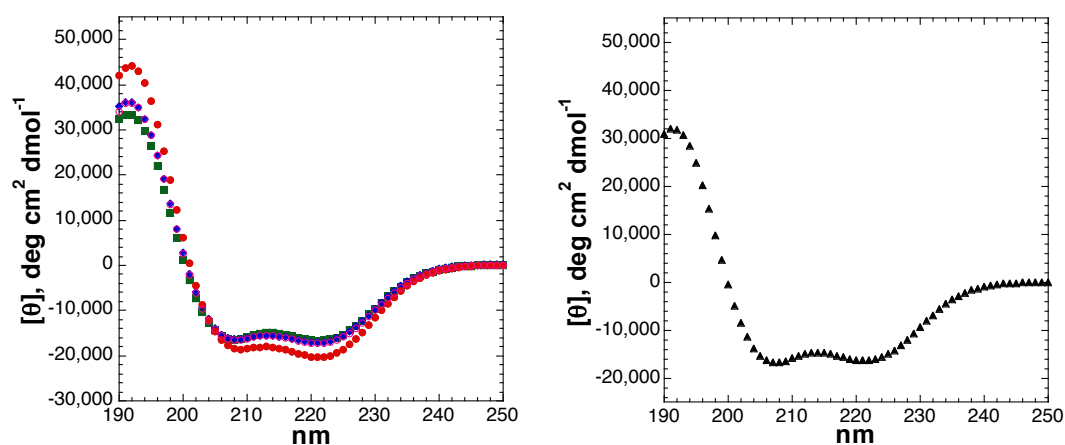


**Figure 1.3:** Left: CD spectra of Ac-SKAAAAKAAAAKAAGY-NH<sub>2</sub> peptides with serine modifications: unmodified Ser(free hydroxyl), Ser(OGlcNAc), Ser(OPO<sub>3</sub>H<sup>-</sup>), and Ser(OPO<sub>3</sub><sup>2-</sup>). Green squares: unmodified serine; blue diamonds: Ser(OGlcNAc); magenta circles: phosphorylated serine (pH 4.0); red circles: phosphorylated serine (pH 8.0). Right: CD spectra of Ac-AKAAAAKAAAAKAAGY-NH<sub>2</sub>. CD experiments were conducted in water with 10 mM phosphate (pH as indicated) and 25 mM KF at 0.5 °C.

Peptide	$[\theta]_{222}$	$[\theta]_{208}$	$[\theta]_{190}$	$\frac{[\theta]_{222}}{[\theta]_{208}}$	$-\frac{[\theta]_{190}}{[\theta]_{208}}$	% Helix
Ac- <b>Ser</b> KAAAAKAAAAKAAGY-NH <sub>2</sub>	-16621	-16434	32243	1.01	1.96	49.7
Ac- <b>Ser(OGlcNAc)</b> KAAAAKAAAAKAAGY-NH <sub>2</sub>	-16944	-16358	35272	1.04	2.16	50.6
Ac- <b>Ser(OPO<sub>3</sub>H)</b> KAAAAKAAAAKAAGY-NH <sub>2</sub>	-17030	-16635	33901	1.02	2.04	50.8
Ac- <b>Ser(OPO<sub>3</sub><sup>2-</sup>)</b> KAAAAKAAAAKAAGY-NH <sub>2</sub>	-19993	-18384	42092	1.09	2.29	58.6
Ac- <b>A</b> KAAAAKAAAAKAAGY-NH <sub>2</sub>	-16325	-16775	30780	0.97	1.83	48.9

**Table 1.1:** Summary of CD data for peptides containing serine, serine modifications, or alanine at residue 1. CD data were collected at 0.5 °C in 10 mM aqueous phosphate buffer (pH 4.0, 7.0, or 8.0) with 25 mM KF.

Peptides containing N-terminal serine and serine modifications were further examined by NMR. The NMR data reveal a decrease in  $^3J_{\alpha N}$ , which directly correlates to the  $\phi$  torsion angle and is consistent with serine adopting a more  $\alpha$ -helical conformation upon both phosphorylation and OGlcNAcylation (Figures 1.4 and Table 1.2). This observation is consistent with the CD data. Interestingly, SerOGlcNAc exhibited the smallest increase in  $\alpha$ -helicity of all serine post-translational modifications, yet the smallest  $^3J_{\alpha N}$  (3.3 Hz). This decrease upon OGlcNAcylation in  $^3J_{\alpha N}$  is consistent with SerOGlcNAc adopting a highly conformationally restricted structure on the N-terminus of the  $\alpha$ -helix. As observed by CD, the N-terminal dianionic phosphoserine peptide exhibits greater structural changes than the peptide with monoanionic phosphoserine. Both phosphorylated peptides exhibited a decrease in  $^3J_{\alpha N}$  compared to unmodified serine, with larger changes observed for the dianionic phosphoserine over the monoanionic ( $^3J_{\alpha N} = 4.4$  Hz and 3.6 Hz respectively). Interestingly, phosphoserine exhibits a large downfield chemical shift in the serine amide proton; the magnitude of this shift is greater for monoanionic phosphoserine (0.33 ppm) than dianionic phosphoserine (0.83 ppm). This downfield chemical shift is suggestive of a hydrogen bond interaction between the serine amide proton and the phosphate group, as observed by others.<sup>18, 35-37</sup> A small downfield shift of the N-

terminal acetyl protons was also observed due to phosphorylation, consistent with polarization of the acetyl carbonyl due to the phosphate amide hydrogen bond.

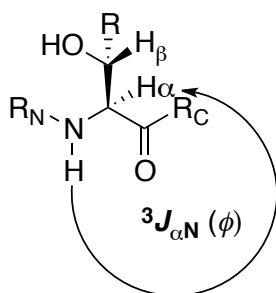


**Figure 1.4:** Phi ( $\phi$ ) torsion angle can be directly calculated from  ${}^3J_{\alpha N}$  values through a parametrized Karplus relationship. Values of  ${}^3J_{\alpha N} > 9$  Hz are indicative of an extended conformation of  $\phi$ , while values of  ${}^3J_{\alpha N} < 6$  Hz are indicative of a more compact conformation of  $\phi$ . Due to averaging of conformations,  ${}^3J_{\alpha N} = 6-8$  Hz are indicative of random coil.

Peptide	$\delta$ , H <sup>N</sup>	${}^3J_{\alpha N}$	$\delta$ , H $\alpha$	$\delta$ , H $\beta$	$\delta$ , H-Acetyl
Ac- <b>Ser</b> KAAAAKAAAAKAAGY-NH <sub>2</sub>	8.58	5.1	4.34	3.97, 3.90	2.10
Ac- <b>Ser(OGlcNAc)</b> KAAAAKAAAAKAAGY-NH <sub>2</sub>	8.62	3.3	4.33	4.11, 3.95	2.13, 2.07
Ac- <b>Ser(OPO<sub>3</sub>H)</b> KAAAAKAAAAKAAGY-NH <sub>2</sub>	8.91	4.4	4.40	4.20, 4.17	2.13
Ac- <b>Ser(OPO<sub>3</sub><sup>2-</sup>)</b> KAAAAKAAAAKAAGY-NH <sub>2</sub>	9.41	3.6	4.29	4.14, 4.08	2.15

**Table 1.2** Summary of NMR data for peptides with serine and serine modifications at residue 1. Chemical shifts ( $\delta$ ) of serine amide proton (H<sup>N</sup>), alpha proton (H $\alpha$ ), beta proton (H $\beta$ ), N-terminal acetyl protons (H-Acetyl), and coupling constants between serine alpha proton and amide proton ( ${}^3J_{\alpha N}$ ) are reported. Peptides were dissolved in 5 mM phosphate buffer (pH 4.0 or 7.2) containing 25 mM NaCl in 90% H<sub>2</sub>O/10% D<sub>2</sub>O. NMR experiments were performed at 5 °C.

To compare the effects of serine versus threonine post-translational modifications, peptides were synthesized and analyzed with threonine and threonine modifications at residue 1. Of peptides with serine or threonine derivatives at residue 1 in this series, unmodified threonine is the least  $\alpha$ -helical peptide (45.1%), consistent

with what others have observed for  $\alpha$ -helix propensity of amino acids (Figure 1.5 and Table 1.3).<sup>26, 32</sup> Again, both phosphorylation and OGlcNAcylation lead to an increase in  $\alpha$ -helicity. GlcNAcylation of threonine led to a substantial increase in  $\alpha$ -helical conformation (51.4%), greater than that observed for Ser(OGlcNAc). Even greater effects were observed for phosphorylation, with the dianionic phosphothreonine leading to 60.0%  $\alpha$ -helicity, while the monoanionic phosphothreonine led to 49.8%  $\alpha$ -helicity. Interestingly, the induced  $\alpha$ -helical conformation due to both phosphorylation and OGlcNAcylation are observed to be greater for threonine versus serine at residue 1. Although unmodified serine has greater  $\alpha$ -helical propensity than threonine, modified threonine induces more  $\alpha$ -helicity at residue 1 than modified serine.

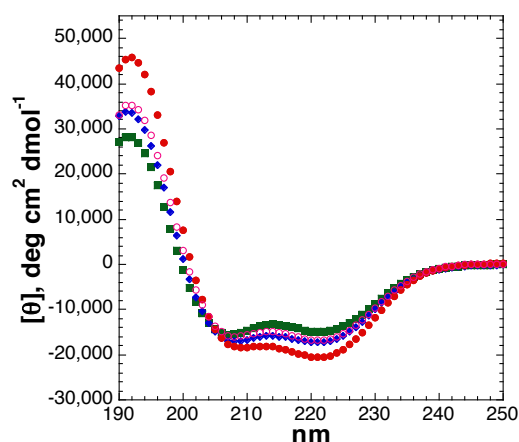


**Figure 1.5:** CD spectra of Ac-TKAAA KAAA KAAGY-NH<sub>2</sub> peptides with threonine modifications: unmodified Thr(free hydroxyl), Thr(OGlcNAc), Thr(OPO<sub>3</sub>H<sup>-</sup>), and Thr(OPO<sub>3</sub><sup>2-</sup>). Green squares: unmodified threonine; blue diamonds: Thr(OGlcNAc); magenta circles: phosphorylated threonine (pH 4.0); red circles: phosphorylated threonine (pH 8.0). CD experiments were conducted in water with 10 mM phosphate (pH as indicated) and 25 mM KF at 0.5 °C.

Peptide	[θ] <sub>222</sub>	[θ] <sub>208</sub>	[θ] <sub>190</sub>	[θ] <sub>222</sub> / [θ] <sub>208</sub>	-[θ] <sub>190</sub> /[θ] <sub>208</sub>	% Helix
Ac- <i>Thr</i> KAAA KAAA KAAGY-NH <sub>2</sub>	-14863	-15423	27161	0.96	1.76	45.1
Ac- <i>Thr(OGlcNAc)</i> KAAA KAAA KAAGY-NH <sub>2</sub>	-17267	-17120	32808	1.01	1.92	51.4
Ac- <i>Thr(OPO<sub>3</sub>H)</i> KAAA KAAA KAAGY-NH <sub>2</sub>	-16661	-15997	33161	1.04	2.07	49.8
Ac- <i>Thr(OPO<sub>3</sub><sup>2-</sup>)</i> KAAA KAAA KAAGY-NH <sub>2</sub>	-20495	-18290	43519	1.12	2.38	60.0

**Table 1.3:** Summary of CD data for peptides with threonine and threonine modifications at residue 1. CD data were collected at 0.5 °C in 10 mM aqueous phosphate buffer (pH 4.0, 7.0, or 8.0) with 25 mM KF.

The NMR data on threonine-containing peptides are consistent with the CD data (Table 1.4). The largest <sup>3</sup>J<sub>αN</sub> observed corresponds to the unmodified threonine peptide, which exhibited the least α-helicity of all peptides in this series. ThrOGlcNAc exhibited a <sup>3</sup>J<sub>αN</sub> of 5.1 Hz, consistent with the increased α-helicity observed by CD but indicative of less conformational restriction than had been

observed for SerOGlcNAc. Phosphorylation induces the largest structural changes by both CD and NMR. The decrease in  $^3J_{\alpha\text{N}}$  from unmodified to phosphorylated residue for both the monoanionic ( $\Delta^3J_{\alpha\text{N}} = 1.4$  Hz) and dianionic phosphothreonine ( $\Delta^3J_{\alpha\text{N}} = 2.7$  Hz) is greater overall than that observed for phosphoserine, suggesting greater conformational organization for threonine over serine due to phosphorylation. Similar to serine, threonine exhibits a substantial downfield chemical shift of the amide proton due to phosphorylation, suggesting an even stronger phosphate-amide interaction. Again, the downfield change in chemical shift is greater for the dianionic ( $\Delta^3J_{\alpha\text{N}} = 1.17$  ppm) than the monoanionic phosphothreonine ( $\Delta^3J_{\alpha\text{N}} = 0.40$  ppm), relative to unmodified threonine. Overall at residue 1, both phosphorylation and OGlcNAcylation increased  $\alpha$ -helicity for both serine and threonine; these effects are observed to be greater for threonine over serine, phosphorylation over OGlcNAcylation, and for the dianionic over the monoanionic phosphate, as also observed by others.<sup>18</sup>

Peptide	$\delta$ , H <sup>N</sup>	<sup>3</sup> J <sub>αN</sub>	$\delta$ , H $\alpha$	$\delta$ , H $\beta$	$\delta$ , H-Acetyl
Ac- <i>Thr</i> KAAAAKAAAAKAAGY-NH <sub>2</sub>	8.40	6.2	4.25	4.19	2.12
Ac- <i>Thr</i> ( <i>OGlcNAc</i> )KAAAAKAAAAKAAGY-NH <sub>2</sub>	8.34	5.1	4.18	4.26	2.15, 2.08
Ac- <i>Thr</i> ( <i>OPO<sub>3</sub>H</i> )KAAAAKAAAAKAAGY-NH <sub>2</sub>	8.80	4.8	4.23	4.64	2.16
Ac- <i>Thr</i> ( <i>OPO<sub>3</sub><sup>2-</sup></i> )KAAAAKAAAAKAAGY-NH <sub>2</sub>	9.57	3.5	4.04	4.47	2.16

**Table 1.4:** Summary of NMR data for peptides with threonine and threonine modifications at residue 1. Chemical shifts ( $\delta$ ) of threonine amide proton (H<sup>N</sup>), alpha proton (H $\alpha$ ), beta proton (H $\beta$ ), N-terminal acetyl protons (H-Acetyl), and coupling constants between threonine alpha proton and amide proton (<sup>3</sup>J<sub>αN</sub>) are reported. Peptides were dissolved in 5 mM phosphate buffer (pH 4.0 or 7.2) containing 25 mM NaCl in 90% H<sub>2</sub>O/10% D<sub>2</sub>O at 5 °C.

Doig and DeGrado independently observed that phosphoserine had greater  $\alpha$ -helix stabilizing effects at residue 2 on the N-terminus. To examine the effects at residue 2, peptides were synthesized replacing lysine with serine, serine modifications, threonine, threonine modifications, and alanine (Figure 1.6 and Table 1.5).<sup>19,21</sup> The peptide containing alanine at residue 2 exhibits an increase in  $\alpha$ -helicity due to the replacement of a lysine with alanine, consistent with alanine having a higher  $\alpha$ -helical propensity than lysine. Interestingly, the  $\alpha$ -helicity of peptides containing unmodified serine (49.8%) and threonine (46.1%) at residue 2 are identical to those containing unmodified serine and threonine at residue 1, indicating no inherent difference between either serine or threonine at residue 1 versus residue 2. Surprisingly, addition of an alanine residue at position 1 in peptides containing unmodified serine or threonine did not lead to an increase in  $\alpha$ -helicity, yet led to an increase in peptides with alanine at residues 1 and 2. These effects could possibly be due to a lower  $\alpha$ -helical propensity of unmodified serine or threonine at residue 2 compared to residue 1. In contrast to peptides containing unmodified serine and threonine at residues 1 versus 2, phosphorylation of serine at residue 2 led to an

increase in  $\alpha$ -helicity (56.4% for the monoanionic phosphoserine and 65.0% for dianionic phosphoserine) compared to phosphoserine at residue 1. Similar to phosphoserine, peptides with phosphothreonine at residue 2 (56.2% for the monoanionic phosphothreonine and 69.2% for dianionic phosphothreonine) were observed to have greater  $\alpha$ -helical conformation than those with phosphothreonine at residue 1. The peptide containing dianionic phosphothreonine at residue 2 had the highest  $\alpha$ -helical content over all peptides examined in this body of work.  $\alpha$ -Aminoisobutyric acid (Aib) has the highest  $\alpha$ -helix propensity of any amino acid in both proteins and designed  $\alpha$ -helices.<sup>38-40</sup> A peptide incorporating Aib at residue 2 was synthesized and analyzed via CD. The Aib-containing peptide yielded concentration-dependent CD data, indicating aggregation at higher concentrations. At 12.5  $\mu$ M peptide concentration, the peptide containing Aib at residue 2 had an  $\alpha$ -helical content of 63.1%, greater than that of alanine and both unmodified threonine and serine, yet less than that of both dianionic phosphorylated serine and threonine peptides.

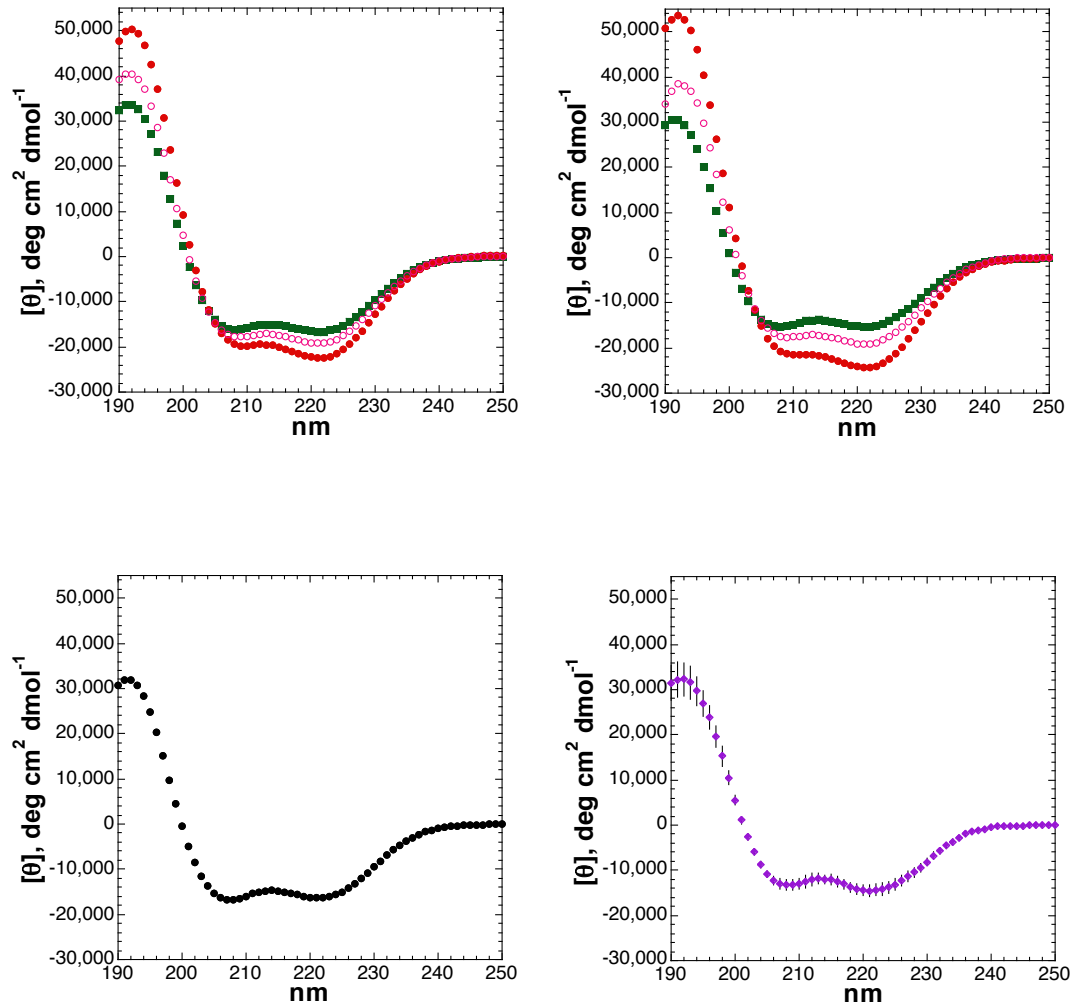


**Figure 1.6:** CD spectra of peptides containing modifications at residue 2. Top left: CD spectra of Ac-ASAAAAKAAAAKAAGY-NH<sub>2</sub> peptides with serine modifications: unmodified Ser(free hydroxyl), Ser(OPO<sub>3</sub>H<sup>-</sup>), and Ser(OPO<sub>3</sub><sup>2-</sup>). Green squares: unmodified serine; magenta circles: phosphorylated serine (pH 4.0); red circles: phosphorylated serine (pH 8.0). Top right: CD spectra of Ac-ATAAAKAAAAKAAGY-NH<sub>2</sub> peptides with threonine modifications: unmodified Thr(free hydroxyl), Thr(OPO<sub>3</sub>H<sup>-</sup>), and Thr(OPO<sub>3</sub><sup>2-</sup>). Green squares: unmodified threonine; magenta circles: phosphorylated threonine (pH 4.0); red circles: phosphorylated threonine (pH 8.0). Bottom left: CD spectra of Ac-AAAAAKAAAAKAAGY-NH<sub>2</sub> peptide. Bottom right: CD spectra of Ac-A(Aib)AAAAKAAAAKAAGY-NH<sub>2</sub> peptide at 12.5 μM concentration. CD experiments were conducted in water with 10 mM phosphate (pH as indicated) and 25 mM KF at 0.5 °C.

Peptide	$[\theta]_{222}$	$[\theta]_{208}$	$[\theta]_{190}$	$[\theta]_{222}/[\theta]_{208}$	$-[\theta]_{190}/[\theta]_{208}$	% Helix
Ac-A <b>Ser</b> AAAAKAAAAKAAGY-NH <sub>2</sub>	-16650	-16246	32311	1.02	1.99	49.8
Ac-A <b>Ser(OPO<sub>3</sub>H<sup>-</sup>)</b> AAAAKAAAAKAAGY-NH <sub>2</sub>	-19142	-17756	39137	1.08	2.20	56.4
Ac-A <b>Ser(OPO<sub>3</sub><sup>2-</sup>)</b> AAAAKAAAAKAAGY-NH <sub>2</sub>	-22401	-19376	47754	1.16	2.46	65.0
Ac-A <b>Thr</b> AAAAKAAAAKAAGY-NH <sub>2</sub>	-15248	-15328	29238	0.99	1.91	46.1
Ac-A <b>Thr(OPO<sub>3</sub>H<sup>-</sup>)</b> AAAAKAAAAKAAGY-NH <sub>2</sub>	-19076	-17383	34079	1.10	1.96	56.2
Ac-A <b>Thr(OPO<sub>3</sub><sup>2-</sup>)</b> AAAAKAAAAKAAGY-NH <sub>2</sub>	-23977	-20776	50682	1.15	2.44	69.2
Ac-A <b>A</b> AAAAKAAAAKAAGY-NH <sub>2</sub>	-21448	-19855	44597	1.08	2.25	62.5
Ac-A ( <b>Aib</b> )AAAAKAAAAKAAGY-NH <sub>2</sub> <sup>a</sup>	-21688	-20180	39844	1.07	1.97	63.1

**Table 1.5** Summary of CD data for peptides containing modifications at residue 2. CD data were collected at 0.5 °C with 80-100 μM peptide in 10 mM aqueous phosphate buffer (pH 4.0, 7.0, or 8.0) with 25 mM KF. <sup>a</sup> CD data for the peptide containing Aib at residue 2 were collected at 12.5 mM concentration due to aggregation at higher concentrations.

NMR experiments performed on peptides containing serine or threonine at residue 2 are consistent with the CD data (Table 1.6). Both serine and threonine residues exhibit a substantial decrease in  $^3J_{\alpha\text{N}}$  upon phosphorylation. Given that smaller values of  $^3J_{\alpha\text{N}}$  are indicative of a more restricted  $\phi$  torsion angle consistent with  $\alpha$ -helices; phosphorylation leads to a more structured  $\alpha$ -helical conformation of the serine and threonine  $\phi$  torsion angles. Interestingly, dianionic phosphothreonine exhibited unusual exchange dynamics (peak broadening and reduced peak size) and an extremely downfield amide chemical shift ( $\delta = 10.24$  ppm, with an overall change in chemical shift from unmodified to phosphorylated of 1.61 ppm) unlike any other amide observed in this study. These observations could be explained by proton exchange with the solvent or alternatively by the intra-residue phosphate amide hydrogen bond. Temperature-dependent NMR and CD experiments were performed to determine the nature of the exchange dynamics (Figure 1.7, Figure 1.37, and Figure 1.47). An increase in temperature led to a decrease in  $\alpha$ -helicity as observed by CD. NMR revealed an upfield chemical shift and a more resolved amide proton of

phosphothreonine with an increase in temperature. If the amide proton was exchanging with the solvent, I would have expected a decrease in the amide proton peak magnitude resolution with an increase in temperature due to increased exchange rates associated with an increase in temperature. These data are consistent with a strong phosphate-amide hydrogen bond which weakens as temperature increases and  $\alpha$ -helicity decreases.

Alpha protons in 90% H<sub>2</sub>O/D<sub>2</sub>O are coupled to both the amide proton and the beta proton, in order to obtain  $^3J_{H^a,H^b}$  NMR experiments were performed in D<sub>2</sub>O to exchange the amide protons with deuterium and eliminate the coupling with the alpha proton. These experiments revealed a  $^3J_{H^a,H^b}$  of 10.4 Hz, consistent with phosphothreonine at this position adopting a  $\chi_1$  torsion angle almost exclusively  $-60^\circ$  (Figure 1.46). Interestingly, the peptide containing dianionic phosphothreonine at residue 2 also has two of the most downfield alanine amide protons of any peptides examined and the second largest standard deviation of alanine amide protons ( $\delta_{Ala} = 8.97, 8.72; \sigma = 0.32$  ppm) (Table 1.59), suggesting formation of local structure involving phosphothreonine.

Peptide	$\delta$ , H <sup>N</sup>	<sup>3</sup> J <sub>αN</sub>	$\delta$ , H $\alpha$	$\delta$ , H $\beta$	$\delta$ , H-Acetyl
Ac-A <b>Ser</b> AAAAKAAAAKAAGY-NH <sub>2</sub>	8.62	5.7	4.41	4.02, 3.95	2.07
Ac-A <b>Ser(OPO<sub>3</sub>H)</b> AAAAKAAAAKAAGY-NH <sub>2</sub>	8.97	5.1	4.51	4.25, 4.20	2.09
Ac-A <b>Ser(OPO<sub>3</sub><sup>2-</sup>)</b> AAAAKAAAAKAAGY-NH <sub>2</sub>	9.57	4.3	4.41	4.10	2.13
Ac-A <b>Thr</b> AAAAKAAAAKAAGY-NH <sub>2</sub>	8.63	4.7	4.26	4.33	2.06
Ac-A <b>Thr(OPO<sub>3</sub>H)</b> AAAAKAAAAKAAGY-NH <sub>2</sub>	9.08	n.d.	4.16	4.22	2.11
Ac-A <b>Thr(OPO<sub>3</sub><sup>2-</sup>)</b> AAAAKAAAAKAAGY-NH <sub>2</sub>	10.24	3.7	4.02	4.51	2.15
285 K	10.15	4.0	4.02	4.50	2.14
298 K	9.94	4.0	4.04	4.48	2.13
305 K	9.81	4.9	4.05	4.48	2.12

**Table 1.6:** Summary of NMR data for peptides containing threonine, phosphothreonine, serine, and phosphoserine at residue 2. Chemical shifts ( $\delta$ ) of threonine amide proton (H<sup>N</sup>), alpha proton (H $\alpha$ ), beta proton (H $\beta$ ), N-terminal acetyl protons (H-Acetyl), and coupling constants between threonine alpha proton and amide proton (<sup>3</sup>J<sub>αN</sub>) are reported. Peptides were dissolved in 5 mM phosphate buffer (pH 4.0 or 7.2) containing 25 mM NaCl in 90% H<sub>2</sub>O/10% D<sub>2</sub>O at 5 °C or as indicated.

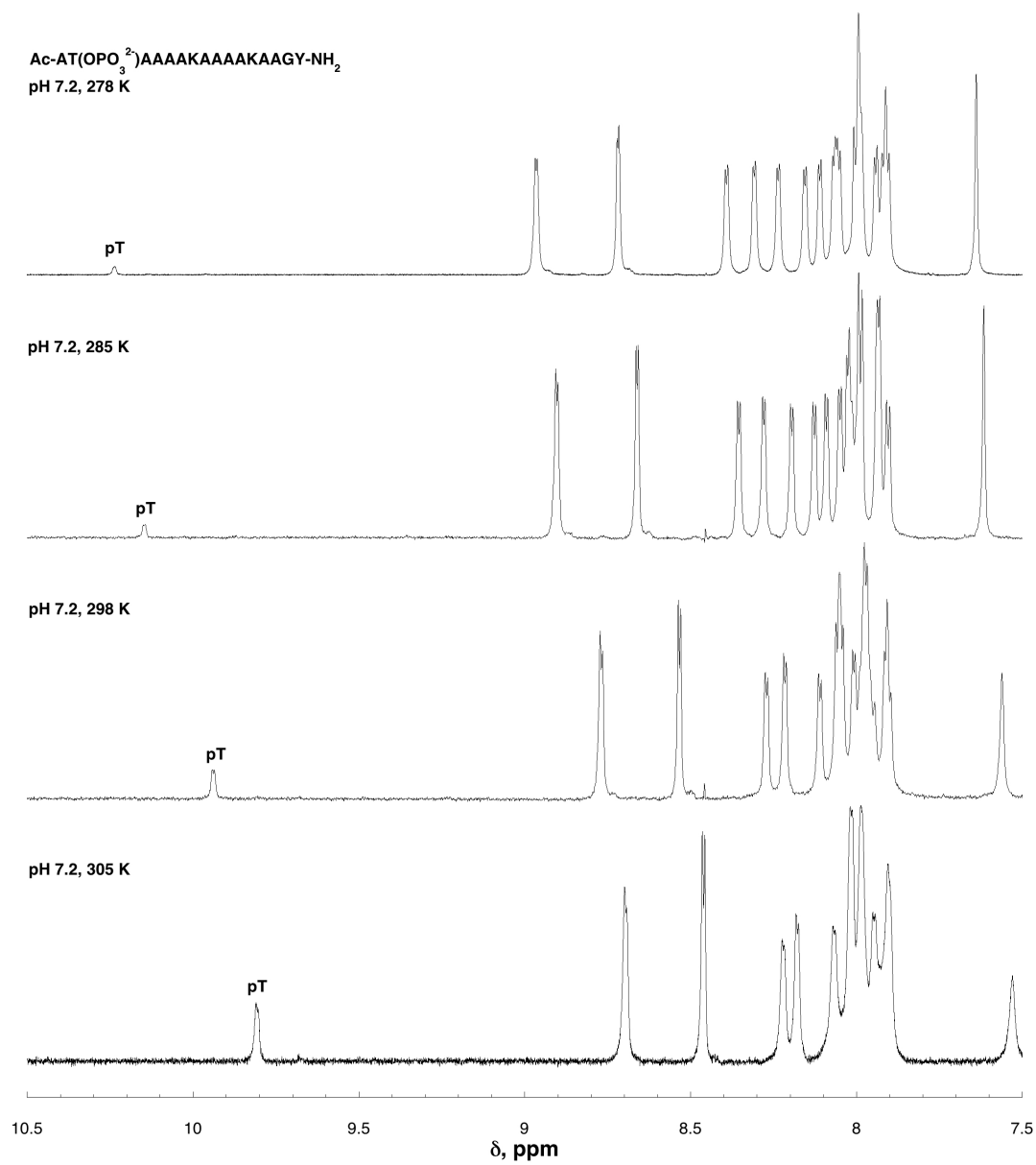


**Figure 1.7:** Temperature-dependent <sup>1</sup>H NMR spectra (amide region) of Ac-AT(OPO<sub>3</sub><sup>2-</sup>)AAAAKAAAAKAAGY-NH<sub>2</sub> peptide. The peptide was dissolved in 5 mM phosphate buffer (pH 7.2) containing 25 mM NaCl in 90% H<sub>2</sub>O/10% D<sub>2</sub>O.

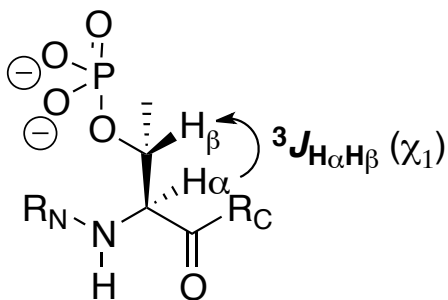


**Figure 1.8:** Chi 1 ( $\chi_1$ ) torsion angle can be directly calculated from  ${}^3J_{H_\alpha H_\beta}$  values through a parametrized Karplus relationship.

### Modifications on internal $\alpha$ -helical positions

To compare the effects of both post-translational modifications of serine and threonine at an  $\alpha$ -helical internal position, peptides were synthesized with both modifications of serine and threonine at residue 5 of the  $\alpha$ -helix. The peptide containing unmodified serine at residue 5 exhibited 30.9%  $\alpha$ -helicity, compared to 49.7% at residue 1 (Figure 1.9 and Table 1.7). These data highlight the preference for serine to be at the N-terminus within  $\alpha$ -helices. In contrast to N-terminal positions, serine, phosphoserine and SerOGlcNAc were all found to be disruptive to the  $\alpha$ -helix on internal positions relative to alanine. OGlcNAcylation also leads to a decrease in  $\alpha$ -helicity by 5.6 %, whereas phosphorylation leads to a larger decrease in  $\alpha$ -helicity, as was also observed by Doig at residue 5.<sup>19</sup> Unlike the effects at N-terminal positions, the  $\alpha$ -helicity of the monoanionic and dianionic phosphoserines are nearly identical, with the monoanionic phosphate exhibiting slightly greater structural effects. Interestingly, although the dianionic phosphoserine leads to a less  $\alpha$ -helical overall structure (as observed by CD), it also leads to greater conformational restriction, exhibiting a  ${}^3J_{\alpha N} = {}^3J_{\alpha N} = 4.5$  Hz compared to the monoanionic phosphoserine 5.7 Hz (Table 1.8). These data are consistent with greater induced structure for dianionic

phosphoserine over the monoanionic phosphoserine. Again, phosphoserine exhibits a large downfield chemical shift ( $\delta = 9.06$  ppm) compared to unmodified serine ( $\delta = 8.44$  ppm) consistent with the presence of the phosphate-amide interaction.

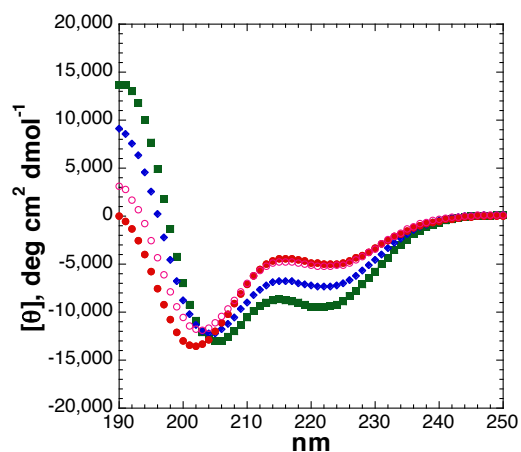


**Figure 1.9:** CD spectra of Ac-AKAASAKAAAKAAGY-NH<sub>2</sub> peptides with serine modifications: unmodified Ser(free hydroxyl), Ser(OGlcNAc), Ser(OPO<sub>3</sub>H<sup>-</sup>), and Ser(OPO<sub>3</sub><sup>2-</sup>). Green squares: unmodified serine; blue diamonds: Ser(OGlcNAc); magenta circles: phosphorylated serine (pH 4.0); red circles: phosphorylated serine (pH 8.0). CD experiments were conducted in water with 10 mM phosphate (pH as indicated) and 25 mM KF at 0.5 °C.

Peptide	$[\theta]_{222}$	$[\theta]_{208}$	$[\theta]_{190}$	$[\theta]_{222}/[\theta]_{208}$	$-[\theta]_{190}/[\theta]_{208}$	% Helix
Ac-AKAA <b>Ser</b> AKAAAAKAAGY-NH <sub>2</sub>	-9489	-12001	13623	0.79	1.14	30.9
Ac-AKAA <b>Ser(OGlcNAc)</b> AKAAAAKAAGY-NH <sub>2</sub>	-7362	-10510	9108	0.70	0.87	25.3
Ac-AKAA <b>Ser(OPO<sub>3</sub>H)</b> AKAAAAKAAGY-NH <sub>2</sub>	-5233	-8782	3170	0.60	0.36	19.6
Ac-AKAA <b>Ser(OPO<sub>3</sub><sup>2-</sup>)</b> AKAAAAKAAGY-NH <sub>2</sub>	-5019	-9115	25	0.55	0.00	19.1

**Table 1.7:** Summary of CD data for peptides containing serine and serine modifications at residue 5. CD data were collected at 0.5 °C with 80-100 μM peptide in 10 mM aqueous phosphate buffer (pH 4.0, 7.0, or 8.0) with 25 mM KF.

Peptide	$\delta, H^N$	$^3J_{\alpha N}$	$\delta, H\alpha$	$\delta, H\beta$	$\delta, H\text{-Acetyl}$
Ac-AKAA <b>Ser</b> AKAAAAKAAGY-NH <sub>2</sub>	8.44	n.d.	4.37	3.95	2.05
Ac-AKAA <b>Ser(OGlcNAc)</b> AKAAAAKAAGY-NH <sub>2</sub>	8.45	n.d.	4.46	4.09	2.04, 2.018
Ac-AKAA <b>Ser(OPO<sub>3</sub>H)</b> AKAAAAKAAGY-NH <sub>2</sub>	8.71	5.7	4.51	4.17	2.03
Ac-AKAA <b>Ser(OPO<sub>3</sub><sup>2-</sup>)</b> AKAAAAKAAGY-NH <sub>2</sub>	9.06	4.5	4.44	4.09	2.03

**Table 1.8:** Summary of NMR data for peptides containing serine and serine modifications at residue 5. Chemical shifts ( $\delta$ ) of serine amide proton ( $H^N$ ), alpha proton ( $H\alpha$ ), beta proton ( $H\beta$ ), N-terminal acetyl protons ( $H\text{-Acetyl}$ ), and coupling constants between serine alpha proton and amide proton ( $^3J_{\alpha N}$ ) are reported. Peptides were dissolved in 5 mM phosphate buffer (pH 4.0 or 7.2) containing 25 mM NaCl in 90% H<sub>2</sub>O/10% D<sub>2</sub>O at 5 °C.

To compare the effects of serine and threonine modifications, peptides were also synthesized and analyzed containing threonine and threonine modifications at residue 5 of the  $\alpha$ -helix. As was observed for the modifications in peptides with N-terminal modifications, greater structural effects were observed for all threonine peptides at residue 5 relative to modifications at serine, with all peptides exhibiting decreased  $\alpha$ -helicity (Figure 1.10 and Table 1.9). The peptide containing unmodified threonine at residue 5 exhibited 17.9%  $\alpha$ -helicity, compared to 45.1% at for threonine residue 1. These data are consistent with what others have observed for the  $\alpha$ -helical propensity of threonine based on the position within an  $\alpha$ -helix.  $\beta$ -branched amino

acid and are known to sterically disrupt formation of an  $\alpha$ -helix in favor of a more extended conformation, consistent with the observed results of threonine and threonine modifications.<sup>41-43</sup> In contrast to N-terminal positions, the greatest structural effects of threonine modifications observed were for Thr(OGlcNAc), which exhibited 6.2%  $\alpha$ -helicity, a far greater disruption of  $\alpha$ -helicity than that observed for Ser(OGlcNAc). The addition of a bulky GlcNAc unit increases the steric bulk of threonine, further disfavoring  $\alpha$ -helix formation. Surprisingly, and unlike any other phosphorylated peptide in this study, greater structural changes were observed for the monoanionic phosphothreonine (10.7%) than for the dianionic phosphothreonine (13.0%), with the monoanionic species leading to greater  $\alpha$ -helix disruption than the dianionic phosphate.

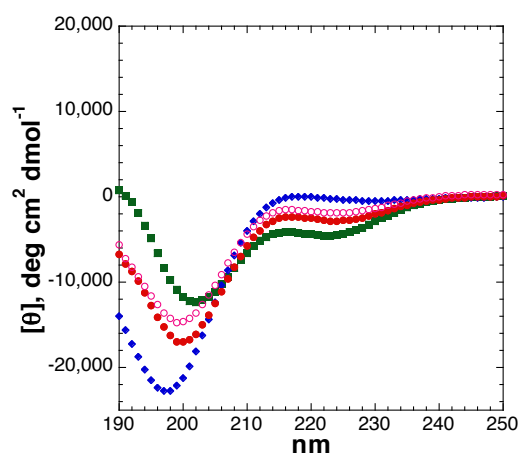


**Figure 1.10:** CD spectra of Ac-AKAATAKAAAKAAGY-NH<sub>2</sub> peptides with threonine modifications: unmodified Thr(free hydroxyl), Thr(OGlcNAc), Thr(OPO<sub>3</sub>H<sup>-</sup>), and Thr(OPO<sub>3</sub><sup>2-</sup>). Green squares: unmodified threonine; blue diamonds: Thr(OGlcNAc); magenta circles: phosphorylated threonine (pH 4.0); red circles: phosphorylated threonine (pH 8.0). CD experiments were conducted in water with 10 mM phosphate (pH as indicated) and 25 mM KF at 0.5 °C.

Peptide	$[\theta]_{222}$	$[\theta]_{208}$	$[\theta]_{190}$	$[\theta]_{222}/[\theta]_{208}$	$-[\theta]_{190}/[\theta]_{208}$	% Helix
Ac-AKAA <b>Thr</b> AKAAAAKAAGY-NH <sub>2</sub>	-4593	-8386	727	0.55	0.09	17.9
Ac-AKAA <b>Thr(OGlcNAc)</b> AKAAAAKAAGY-NH <sub>2</sub>	-145	-6835	-14035	0.02	-2.05	6.2
Ac-AKAA <b>Thr(OPO<sub>3</sub>H)</b> AKAAAAKAAGY-NH <sub>2</sub>	-1868	-6555	-5647	0.28	-0.86	10.7
Ac-AKAA <b>Thr(OPO<sub>3</sub><sup>2-</sup>)</b> AKAAAAKAAGY-NH <sub>2</sub>	-2742	-8292	-6777	0.33	-0.82	13.0

**Table 1.9:** Summary of CD data for peptides containing threonine and threonine modifications at residue 5. CD data were collected at 0.5 °C with 80-100 μM peptide in 10 mM aqueous phosphate buffer (pH 4.0, 7.0, or 8.0) with 25 mM KF.

Peptides containing threonine and threonine modifications at residue 5 were further examined by NMR (Table 1.10). Consistent with observed effects of threonine phosphorylation on the N-terminus, dianionic phosphothreonine at residue 5 exhibited a small  $^3J_{\alpha N}$  of 4.1 Hz and a large downfield chemical shift of the amide proton ( $\delta = 9.50$  ppm, compared to unmodified threonine  $\delta = 8.29$  ppm). The magnitude of the structural effects observed by NMR were greater for threonine phosphorylation than serine phosphorylation at residue 5 and for the dianionic phosphate over the monoanionic phosphate (Table 1.9). Interestingly, this is the only series in which the global structural effects and local structural effects are not consistent. Greater  $\alpha$ -helix disruption was observed for the monoanionic phosphate via CD, but greater locally induced structural effects were observed for the dianionic phosphate via NMR. I have previously observed the ability of dianionic phosphothreonine to strongly nucleate the  $\alpha$ -helix when on the N-terminus. The paradox of phosphothreonine at residue 5 could be due to disruption of the overall 14 residue  $\alpha$ -helix occurring in parallel to  $\alpha$ -helix nucleation of the remaining C-terminal 10 residues. This interpretation implies context dependence for threonine and serine phosphorylation throughout the  $\alpha$ -helix.

Peptide	$\delta$ , H <sup>N</sup>	<sup>3</sup> J <sub>αN</sub>	$\delta$ , H $\alpha$	$\delta$ , H $\beta$	$\delta$ , H-Acetyl
Ac-AKAA ThrAKAAAAKAAGY-NH <sub>2</sub>	8.29	n.d.	4.23	4.26	2.04
Ac-AKAA Thr(OGlcNAc)AKAAAAKAAGY-NH <sub>2</sub>	8.16	n.d.	4.34	4.24	2.06, 2.014
Ac-AKAA Thr(OPO <sub>3</sub> H <sup>-</sup> )AKAAAAKAAGY-NH <sub>2</sub>	8.57	n.d.	4.36	4.65	2.02
Ac-AKAA Thr(OPO <sub>3</sub> <sup>2-</sup> )AKAAAAKAAGY-NH <sub>2</sub>	9.50	4.1	4.11	4.39	2.01

**Table 1.10:** Summary of NMR data for peptides containing threonine and threonine modifications at residue 5. Chemical shifts ( $\delta$ ) of threonine amide proton (H<sup>N</sup>), alpha proton (H $\alpha$ ), beta proton (H $\beta$ ), N-terminal acetyl protons (H-Acetyl), and coupling constants between threonine alpha proton and amide proton (<sup>3</sup>J<sub>αN</sub>) are reported. Peptides were dissolved in 5 mM phosphate buffer (pH 4.0 or 7.2) containing 25 mM NaCl in 90% H<sub>2</sub>O/10% D<sub>2</sub>O at 5 °C.

To test this hypothesis, peptides were synthesized with serine, phosphoserine, threonine, and phosphothreonine at residue 10 of the  $\alpha$ -helix. Both peptides containing serine (26.6%) and threonine (21.7%) at residue 10 exhibit comparable  $\alpha$ -helicity to that observed at residue 5. These data indicate no inherent difference between serine or threonine residues at internal positions, consistent with what others have observed (Figure 1.11 and Table 1.11).<sup>44</sup> Interestingly, phosphorylation of both serine (13.6% for monoanionic phosphate and 6.9% for dianionic phosphate) and threonine (4.8% for monoanionic phosphate and 0.6% for dianionic phosphate) at residue 10 greatly reduced  $\alpha$ -helix stability relative to both phosphoserine and phosphothreonine at residue 5. In contrast to phosphoserine and phosphothreonine at residue 5, and consistent with observed results on the N-terminus, the observed structural effects were greater for threonine versus serine and for the dianionic phosphate versus the monoanionic phosphate. These data are consistent with context dependence for both phosphoserine and phosphothreonine in which overall  $\alpha$ -helix destabilization on internal positions are countered by nucleation effects on the remaining C-terminal portion. Positioning phosphothreonine towards the C-terminus

leaves only 4 residues available to participate in the  $\alpha$ -helix, forming an unstable  $\alpha$ -helix.<sup>32, 45</sup> This is evident in the observation that as the number of residues on the C-terminal portion of the  $\alpha$ -helix decreases,  $\alpha$ -helicity decreases.

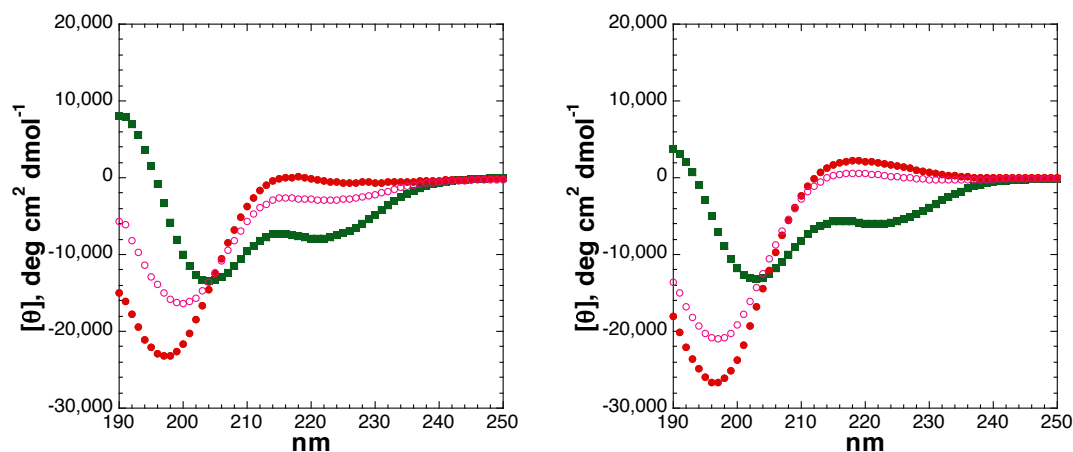


**Figure 1.11:** Left: CD spectra of Ac-AKAAAACAASAAGA-NH<sub>2</sub> peptides with serine modifications: unmodified Ser(free hydroxyl), Ser(OPO<sub>3</sub>H<sup>-</sup>), and Ser(OPO<sub>3</sub><sup>2-</sup>). Green squares: unmodified serine; magenta circles: phosphorylated serine (pH 4.0); red circles: phosphorylated serine (pH 8.0). Right: CD spectra of Ac-AKAAAACAATAAGA-NH<sub>2</sub> peptides with threonine modifications: unmodified Thr(free hydroxyl), Thr(OPO<sub>3</sub>H<sup>-</sup>), and Thr(OPO<sub>3</sub><sup>2-</sup>). Green squares: unmodified threonine; magenta circles: phosphorylated threonine (pH 4.0); red circles: phosphorylated threonine (pH 8.0). CD experiments were conducted in water with 10 mM phosphate (pH as indicated) and 25 mM KF at 0.5 °C.

Peptide	$[\theta]_{222}$	$[\theta]_{208}$	$[\theta]_{190}$	$[\theta]_{222}/[\theta]_{208}$	$-[\theta]_{190}/[\theta]_{208}$	% Helix
Ac-AKAAAKAA <b>Ser</b> AKAAGY-NH <sub>2</sub>	-7883	-11530	8113	0.68	0.70	26.6
Ac-AKAAAKAA <b>Ser(OPO<sub>3</sub>H)</b> AKAAGY-NH <sub>2</sub>	-2936	-8145	-5752	0.36	-0.71	13.6
Ac-AKAAAKAA <b>Ser(OPO<sub>3</sub><sup>2-</sup>)</b> AKAAGY-NH <sub>2</sub>	-431	-6789	-14930	0.06	-2.20	6.9
Ac-AKAAAKAA <b>Thr</b> AKAAGY-NH <sub>2</sub>	-6020	-10003	3732	0.60	0.37	21.7
Ac-AKAAAKAA <b>Thr(OPO<sub>3</sub>H)</b> AKAAGY-NH <sub>2</sub>	382	-5396	-13528	-0.07	-2.51	4.8
Ac-AKAAAKAA <b>Thr(OPO<sub>3</sub><sup>2-</sup>)</b> AKAAGY-NH <sub>2</sub>	1967	-5542	-18077	-0.35	-3.26	0.6

**Table 1.11:** Summary of CD data for peptides containing serine, phosphoserine, threonine, or phosphothreonine at residue 10. CD data were collected at 0.5 °C in 10 mM aqueous phosphate buffer (pH 4.0, 7.0, or 8.0) with 25 mM KF.

Peptides containing serine, phosphoserine, threonine, and phosphothreonine at residue 10 were further analyzed by NMR (Table 1.12). Consistent with phosphorylation at all other positions, a large downfield chemical shift was observed for both dianionic phosphoserine ( $\delta = 9.01$ ) and dianionic phosphothreonine ( $\delta = 9.41$ ), with larger shifts observed for the dianionic phosphate over the monoanionic, and for threonine modification over serine modification. Surprisingly, phosphoserine (3.3 Hz, the smallest  $^3J_{\alpha N}$  of any phosphorylated residue in this study) and phosphothreonine (4.1 Hz) both exhibit small  $^3J_{\alpha N}$  coupling constants, indicating a highly restricted and  $\alpha$ -helical  $\phi$  torsion angle while the peptides remain in a globally random coil state as observed by CD. Interestingly, dianionic phosphothreonine exhibits the largest dispersion of alanine amide protons of any peptide in this study ( $\sigma = 0.43$  ppm) (Table 1.59), with alanine amide protons at 8.80 ppm and 8.61 ppm, suggestive of formation of local structure while remaining globally unstructured as observed via CD.

Peptide	$\delta$ , H <sup>N</sup>	<sup>3</sup> J <sub>αN</sub>	$\delta$ , H $\alpha$	$\delta$ , H $\beta$	$\delta$ , H-Acetyl
Ac-AKAAAAKAA <b>Ser</b> AKAAGY-NH <sub>2</sub>	8.30	n.d.	4.37	3.92, 3.90	2.06
Ac-AKAAAAKAA <b>Ser(OPO<sub>3</sub>H)</b> AKAAGY-NH <sub>2</sub>	8.54	n.d.	4.50	4.18, 4.14	2.03
Ac-AKAAAAKAA <b>Ser(OPO<sub>3</sub><sup>2-</sup>)</b> AKAAGY-NH <sub>2</sub>	9.01	3.3	4.42	4.05	2.03
Ac-AKAAAAKAA <b>Thr</b> AKAAGY-NH <sub>2</sub>	8.19	6.8	4.25	4.21	2.06
Ac-AKAAAAKAA <b>Thr(OPO<sub>3</sub>H)</b> AKAAGY-NH <sub>2</sub>	8.44	n.d.	4.40	4.62	2.02
Ac-AKAAAAKAA <b>Thr(OPO<sub>3</sub><sup>2-</sup>)</b> AKAAGY-NH <sub>2</sub>	9.41	4.5	4.09	4.34	2.03

**Table 1.12** Summary of NMR data for peptides containing serine, phosphoserine, threonine, or phosphothreonine at residue 10. Chemical shifts ( $\delta$ ) of threonine amide proton (H<sup>N</sup>), alpha proton (H $\alpha$ ), beta proton (H $\beta$ ), N-terminal acetyl protons (H-Acetyl), and coupling constants between threonine alpha proton and amide proton (<sup>3</sup>J<sub>αN</sub>) are reported. Peptides were dissolved in 5 mM phosphate buffer (pH 4.0 or 7.2) containing 25 mM NaCl in 90% H<sub>2</sub>O/10% D<sub>2</sub>O at 5 °C.

### Modifications on C-terminal $\alpha$ -helical positions

No previous studies on the effects of phosphorylation or GlcNAcylation of serine or threonine residues on the C-terminus of a model  $\alpha$ -helix have been performed. To determine the effects of these modifications on the C-terminus, peptides containing serine, serine modifications, threonine, and threonine modifications were synthesized and analyzed via CD and NMR (Figure 1.12 and Tables 1.13). Both serine (35.9%) and threonine (30.1%) exhibited lower  $\alpha$ -helicity than at N-terminal positions, but greater  $\alpha$ -helicity than at internal positions. These results are consistent with the ability of both serine and threonine to function as C-terminal  $\alpha$ -helix caps via their hydrogen bond acceptors.<sup>26, 32, 46</sup> In contrast to effects at N-terminal positions, GlcNAcylation of both serine and threonine led to a decrease in  $\alpha$ -helicity relative to unmodified peptides. Interestingly, the peptide containing Ser(OGlcNAc) (28.2%) at residue 14 had similar  $\alpha$ -helicity to Ser(OGlcNAc) at residue 5 (25.3%). In contrast to serine, Thr(OGlcNAc) (23.5%) had far greater  $\alpha$ -helicity relative to Thr(OGlcNAc) at residue 5 (6.2%). Placing a  $\beta$ -branched amino

acid on the C-terminus is inherently more stable than at internal positions due to sterics, consistent with the observed effects of threonine GlcNAcylation.<sup>26</sup> Effects of phosphorylation on the C-terminus of an  $\alpha$ -helix have never before been examined. Doig noted based on calculations that a C-terminal phosphoserine may be destabilizing, and to a greater extent than at internal positions.<sup>19</sup> As expected, phosphorylation of both serine (20.7% for monoanionic phosphate and 15.7% for dianionic phosphate) and threonine (19.0% for monoanionic phosphate and 14.8% for dianionic phosphate) led to a decrease in  $\alpha$ -helicity relative to unmodified residues. Interestingly, the effects of both phosphoserine and phosphothreonine on  $\alpha$ -helicity are similar on the C-terminus relative to residue 5. These data suggest that the local effects of phosphorylation in disrupting the  $\alpha$ -helix hydrogen bonding backbone lead to greater helix destabilization than positioning a negatively charged phosphate on the negatively charged C-terminus of the  $\alpha$ -helix macro-dipole.

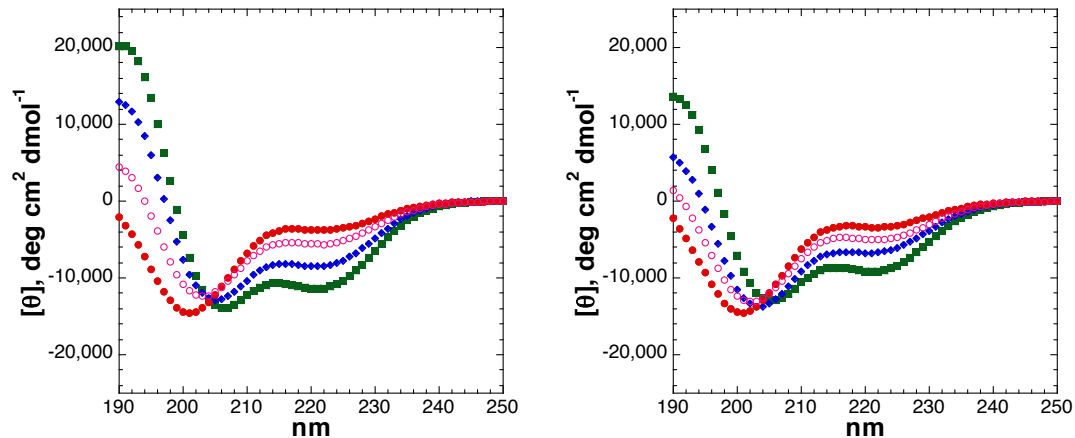


**Figure 1.12:** Left: CD spectra of Ac-YGAKAAAANKAAAAS-NH<sub>2</sub> peptides with serine modifications: unmodified Ser(free hydroxyl), Ser(OGlcNAc), Ser(OPO<sub>3</sub>H<sup>-</sup>), and Ser(OPO<sub>3</sub><sup>2-</sup>). Green squares: unmodified serine; blue diamonds: Ser(OGlcNAc); magenta circles: phosphorylated serine (pH 4.0); red circles: phosphorylated serine (pH 8.0). Right: CD spectra of Ac-YGAKAAAANKAAAAT-NH<sub>2</sub> peptides with threonine modifications: unmodified Thr(free hydroxyl), Thr(OGlcNAc), Thr(OPO<sub>3</sub>H<sup>-</sup>), and Thr(OPO<sub>3</sub><sup>2-</sup>). Green squares: unmodified threonine; blue diamonds: Thr(OGlcNAc); magenta circles: phosphorylated threonine (pH 4.0); red circles: phosphorylated threonine (pH 8.0). CD experiments were conducted in water with 10 mM phosphate (pH as indicated) and 25 mM KF at 0.5 °C.

Peptide	$[\theta]_{222}$	$[\theta]_{208}$	$[\theta]_{190}$	$[\theta]_{222}/[\theta]_{208}$	$-[\theta]_{190}/[\theta]_{208}$	% Helix
Ac-YGAKAAAAKAAAAKA <b>Ser</b> -NH <sub>2</sub>	-11375	-13477	20103	0.84	1.49	35.9
Ac-YGAKAAAAKAAAAKA <b>Ser(OGlcNAc)</b> -NH <sub>2</sub>	-8461	-11840	12910	0.71	1.09	28.2
Ac-YGAKAAAAKAAAAKA <b>Ser(OPO<sub>3</sub>H<sup>-</sup>)</b> -NH <sub>2</sub>	-5630	-9603	4445	0.59	0.46	20.7
Ac-YGAKAAAAKAAAAKA <b>Ser(OPO<sub>3</sub><sup>2-</sup>)</b> -NH <sub>2</sub>	-3734	-8814	-2015	0.42	-0.23	15.7
Ac-YGAKAAAAKAAAAKA <b>Thr</b> -NH <sub>2</sub>	-9190	-12024	13630	0.76	1.13	30.1
Ac-YGAKAAAAKAAAAKA <b>Thr(OGlcNAc)</b> -NH <sub>2</sub>	-6685	-11064	5746	0.60	0.52	23.5
Ac-YGAKAAAAKAAAAKA <b>Thr(OPO<sub>3</sub>H<sup>-</sup>)</b> -NH <sub>2</sub>	-4984	-9420	1437	0.53	0.15	19.0
Ac-YGAKAAAAKAAAAKA <b>Thr(OPO<sub>3</sub><sup>2-</sup>)</b> -NH <sub>2</sub>	-3417	-8524	-2248	0.40	-0.26	14.8

**Table 1.13:** Summary of CD data for peptides containing serine, serine modifications, threonine, and threonine modifications at residue 14. CD data were collected at 0.5 °C in 10 mM aqueous phosphate buffer (pH 4.0, 7.0, or 8.0) with 25 mM KF.

Peptides containing serine, phosphoserine, threonine, and phosphothreonine at the C-terminus were further analyzed by NMR (Table 1.14). Interestingly, both dianionic phosphoserine ( $^3J_{\alpha\text{N}} = 6.3$  Hz) and dianionic phosphothreonine ( $^3J_{\alpha\text{N}} = 6.2$  Hz) exhibit larger  $^3J_{\alpha\text{N}}$  values than at any other positions in peptides in this study, along with an upfield chemical shift of the amide protons relative to other positions. These data are consistent with both phosphorylated serine and threonine residues possessing  $\phi$  torsion angles divergent from those in  $\alpha$ -helices. Indeed tyrosine, which does not participate in the  $\alpha$ -helix, displays  $^3J_{\alpha\text{N}}$  values of 6.4-6.6 Hz, similar to that of both phosphorylated residues at the C-terminus. These results suggest a weakening of the phosphate-amide interaction for phosphorylated residues on the C-terminus, leading to a more extended conformation of both serine and threonine residues. Also observed was an upfield chemical shift in one of the carboxamide amide protons of dianionic phosphothreonine ( $\delta = 7.89$  ppm; all other peptides exhibited carboxamide peaks in the range of  $\delta = 7.59$ -7.71 ppm), consistent with weakening of the hydrogen bond between the carboxamide and the *i*-4 carbonyl. The data are also consistent with

the phosphate interacting with the C-terminal carboxamide. In contrast to phosphorylation on the N-terminus, placing a negatively charged phosphate on the negatively charged end of the  $\alpha$ -helix macro-dipole would be destabilizing to both the overall  $\alpha$ -helix as well as the phosphate-amide interaction. Data herein as well as work performed by others on the effects of positive and negatively charged residues on the C-terminus of  $\alpha$ -helices support this observation.<sup>26, 47, 48</sup> Again, observed effects are greater for phosphorylation over OGlcNAcylation, for threonine over serine, and for the dianionic phosphate over the monoanionic phosphate.

Peptide	$\delta$ , H <sup>N</sup>	<sup>3</sup> J <sub><math>\alpha</math>N</sub>	$\delta$ , H $\alpha$	$\delta$ , H $\beta$	$\delta$ , H-Acetyl
Ac-YGAKAAAAKAAAAKA <b>Ser</b> -NH <sub>2</sub>	8.22	n.d.	4.37	3.93, 3.91	1.99
Ac-YGAKAAAAKAAAAKA <b>Ser(OGlcNAc)</b> -NH <sub>2</sub>	8.30	n.d.	4.48	4.11, 3.89	2.03, 1.981
Ac-YGAKAAAAKAAAAKA <b>Ser(OPO<sub>3</sub>H)</b> -NH <sub>2</sub>	8.57	6.8	4.50	4.18, 4.09	1.97
Ac-YGAKAAAAKAAAAKA <b>Ser(OPO<sub>3</sub><sup>2-</sup>)</b> -NH <sub>2</sub>	9.02	6.3	4.42	4.06	1.98
Ac-YGAKAAAAKAAAAKA <b>Thr</b> -NH <sub>2</sub>	8.18	7.9	4.29	4.29	1.98
Ac-YGAKAAAAKAAAAKA <b>Thr(OGlcNAc)</b> -NH <sub>2</sub>	8.18	8.0	4.42	4.34	2.05, 1.975
Ac-YGAKAAAAKAAAAKA <b>Thr(OPO<sub>3</sub>H)</b> -NH <sub>2</sub>	8.42	7.9	4.39	4.64	1.98
Ac-YGAKAAAAKAAAAKA <b>Thr(OPO<sub>3</sub><sup>2-</sup>)</b> -NH <sub>2</sub>	8.93	6.2	4.26	4.46	1.99

**Table 1.14:** Summary of NMR for peptides containing serine, serine modifications, threonine, and threonine modifications at residue 14. Chemical shifts ( $\delta$ ) of threonine amide proton (H<sup>N</sup>), alpha proton (H $\alpha$ ), beta proton (H $\beta$ ), N-terminal acetyl protons (H-Acetyl), and coupling constants between threonine alpha proton and amide proton (<sup>3</sup>J <sub>$\alpha$ N) are reported. Peptides were dissolved in 5 mM phosphate buffer (pH 4.0 or 7.2) containing 25 mM NaCl in 90% H<sub>2</sub>O/10% D<sub>2</sub>O at 5 °C.</sub>

### The dichotomy of phosphothreonine

Of all the peptides examined in this study, phosphothreonine at residue 2 exhibited the greatest  $\alpha$ -helicity, while phosphothreonine at residue 10 exhibited a complete random coil structure. Heteronuclear NMR spectroscopy was conducted using <sup>1</sup>H-<sup>13</sup>C HSQC experiments to determine the residue-specific effects of threonine

phosphorylation at both of these positions via chemical shift index analysis (Figure 1.13). An upfield shift in  $H\alpha$ , a downfield shift in  $C\alpha$ , and an upfield shift in  $C\beta$  are indicative of increased  $\alpha$ -helical content.<sup>49-51</sup> Phosphothreonine at residue 2 causes a global upfield shift in  $H\alpha$  ( $\Delta\delta = 0.24$  ppm) and downfield shift in  $C\alpha$  ( $\Delta\delta = -3.41$  ppm) in all residues that participate in the  $\alpha$ -helix compared to data on unmodified threonine here. The average chemical shift of alanine and lysine amide protons in peptides containing unmodified threonine is 50.7 ppm (alanine) and 54.9 ppm (lysine), while the peptide containing phosphothreonine at residue 2 exhibits average amide proton chemical shifts of 51.4 ppm (alanine) and 55.6 ppm (lysine) (Table 1.63 and Table 1.64). Phosphorylation induces the largest structural changes in threonine, leading to a dramatic 3.41 ppm downfield shift in threonine  $C\alpha$  and a 0.24 ppm upfield shift in  $H\alpha$ .

Although threonine at residue 2 (46.1%  $\alpha$ -helicity) and threonine at residue 10 (21.7%) exhibit very different  $\alpha$ -helical content, the threonine chemical shifts of both  $H\alpha$  (4.26 ppm for residue 2 and 4.25 ppm for residue 10) and  $C\alpha$  (59.81 ppm for residue 2 and 59.72 ppm for residue 10) for both peptides are almost identical. In contrast to the results for threonine at residue 2, phosphothreonine at residue 10 causes a downfield shift in  $H\alpha$  ( $\Delta\delta = 0.23$  ppm) and an upfield shift in  $C\alpha$  ( $\Delta\delta = -0.61$  ppm) in all alanine and lysine residues, consistent with a decrease in  $\alpha$ -helicity. The average chemical shift of alanine and lysine for unmodified threonine is 50.1 ppm and 53.9 ppm, respectively, while the phosphorylated peptide exhibits averages of 49.3 ppm and 52.9 ppm. Interestingly, unlike all other residues, phosphothreonine exhibits a downfield shift in  $C\alpha$  and an upfield shift in  $H\alpha$ . These data are consistent with CD data, in which phosphorylation induces structural changes in all alanine and lysine

residues causing them to become more  $\alpha$ -helical with phosphorylation at residue 2, or less  $\alpha$ -helical with phosphothreonine at residue 10.

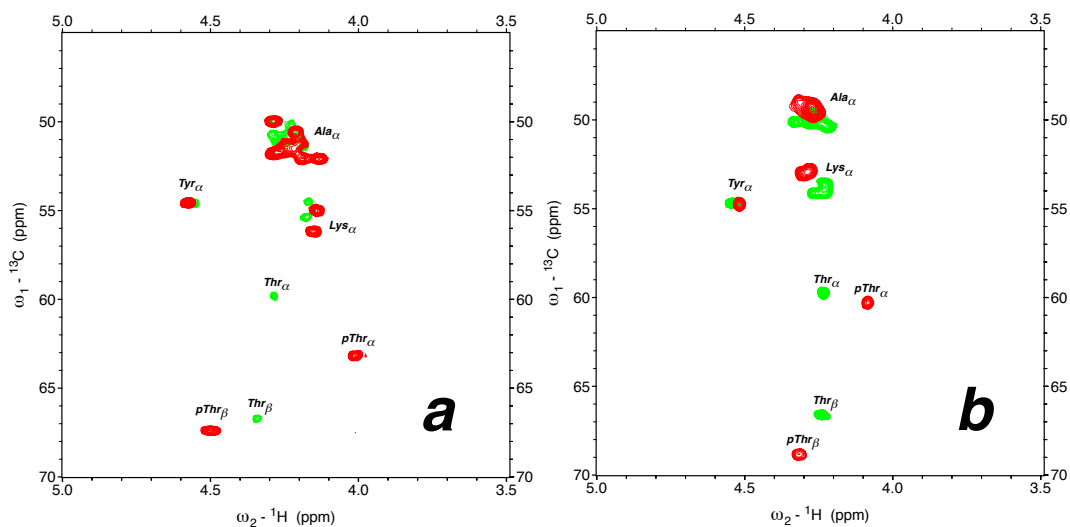


**Figure 1.13:**  ${}^1\text{H}$ - ${}^{13}\text{C}$  HSQC spectra ( $\text{H}\alpha$ - $\text{C}\alpha$  region) of peptides containing unmodified threonine (green) and phosphothreonine (red). (a) Peptides containing threonine or phosphothreonine at residue 2. (b) Peptides containing threonine or phosphothreonine at residue 10. Data were collected at 5  $^{\circ}\text{C}$  in  $\text{D}_2\text{O}$  containing 5 mM phosphate (pH 4.0 for unmodified peptides and pH 8.0 for phosphorylated peptides) and 25 mM NaCl.

In order to identify the ability of phosphorylation to act as an inducible switch for  $\alpha$ -helicity, peptides with phosphothreonine at residue 2 and phosphothreonine at residue 10 were incubated with Antarctic phosphatase, a non-specific phosphatase (Figure 1.14). The effects of dephosphorylation on structure were monitored via CD. The peptide with phosphothreonine at residue 2 exhibited a decrease in  $\alpha$ -helicity upon incubation with phosphatase; after 240 min of incubation, dephosphorylation had progressed to 76% completion (as determined by HPLC) (Figure 1.39). At this point the peptide exhibited  $\alpha$ -helicity similar to that of the

peptide containing unmodified threonine at residue 2. In contrast, the peptide with phosphothreonine at residue 10 exhibited an increase in  $\alpha$ -helicity upon incubation with phosphatase; after 480 min of incubation, dephosphorylation had progressed to 90% completion as determined by HPLC (Figure 1.41). Phosphatases generally prefer to dephosphorylate proteins and peptides that are in a random coil state, which lack secondary and tertiary structure. Interestingly, the activity of the phosphatase was lower for the peptide containing phosphothreonine at residue 10, which exhibits a random coil conformation. This decrease in phosphatase activity, along with NMR data, suggests the formation of a local structure around phosphothreonine, despite the random coil signature by CD. These data, combined with NMR data, are suggestive of interactions between the phosphate, and the amides of both threonine and two alanines. In all, these results demonstrate the ability of phosphatases and kinases to turn off or on secondary structure, and the ability of phosphorylation to act as inducible structural switches.

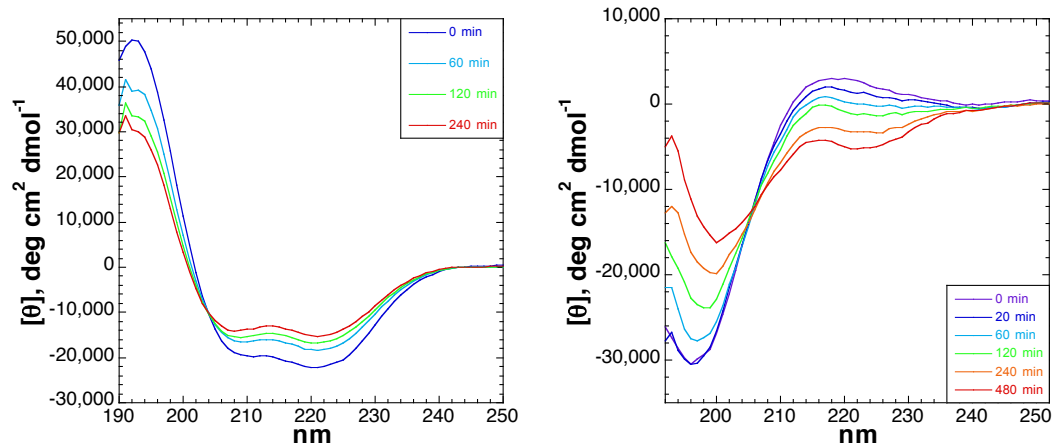


**Figure 1.14:** Left: CD spectra of a solution containing 25  $\mu\text{M}$  peptide Ac-AT( $\text{OPO}_3^{2-}$ )AAAAKAAAKAAGY-NH<sub>2</sub> in buffer (40 mM Tris-HCl (pH 8.0), 25 mM KF, 1 mM MgCl<sub>2</sub>, and 100  $\mu\text{M}$  ZnCl<sub>2</sub>) at 0.5 °C as a function of time of incubation with phosphatase. Data were collected at initial time (dark blue). To this solution were added 10 units (2  $\mu\text{L}$ ) of Antarctic phosphatase and the solution incubated in a 37 °C water bath. The total duration of incubation was 240 min. CD spectra were collected at time points of 60 min (light blue), 120 min (green), and 240 min (red). Right: CD spectra of a solution containing 25  $\mu\text{M}$  peptide Ac-AKAAAKAAT( $\text{OPO}_3^{2-}$ )AKAAGY-NH<sub>2</sub> in buffer (40 mM Tris-HCl (pH 8.0), 25 mM KF, 1 mM MgCl<sub>2</sub>, and 100  $\mu\text{M}$  ZnCl<sub>2</sub>) at 0.5 °C as a function of time of incubation with phosphatase. Data were collected at initial time (purple). To this solution were added 40 units (8  $\mu\text{L}$ ) of Antarctic phosphatase and the solution incubated in a 37 °C water bath. The total duration of incubation was 480 min. CD spectra were collected at time points of 20 min (dark blue), 60 min (light blue), 120 min (green), 240 min (orange), and 480 min (red). At each time point, the sample was cooled to 0.5 °C for 5 min and data were collected. The sample was then placed back in the water bath until the next time point.

## Structural effects of post-translational modifications are analogous to proline

We have observed that both phosphorylation and OGlcNAcylation of serine and threonine stabilize an  $\alpha$ -helix on the N-terminus, with greater stabilization observed for phosphorylation versus GlcNAcylation, and for threonine versus serine. In contrast, both phosphorylation and OGlcNAcylation of serine and threonine destabilize an  $\alpha$ -helix on internal positions, with greater destabilization observed for threonine modifications. Proline behaves in a similar manner to serine and threonine modifications. Proline on the N-terminus acts to cap the helix through a favorable interaction between its carbonyl and  $i+4$  amide proton, while on internal and C-terminal positions destabilizes the  $\alpha$ -helix via disruption of the amide backbone hydrogen bonding network due to the absence of an amide proton, as well as unfavorable sterics with the prior residue.<sup>41, 52-55</sup> To directly compare the effects of proline with serine and threonine modifications, a series of proline peptides was synthesized and analyzed incorporating proline at residues 1, 2, 5, 10, and 14.

As expected, proline on the N-terminus exhibits significant  $\alpha$ -helicity, consistent with what others have observed, though to a far lesser extent than phosphothreonine (Figure 1.15, Figure 1.16, and Table 1.15). In contrast to both phosphothreonine and phosphoserine, proline exhibits lesser helicity when at residue 2 (33.4%) than at residue 1 (37.6%).<sup>44, 52, 56</sup> Proline at residues 5 (2.8%) and 10 (2.5%) substantially destabilized the  $\alpha$ -helix, comparable to the effects Thr(OGlcNAc) at residue 5 and phosphothreonine at residues 10. Unlike phosphothreonine, the relative internal position of proline did not have an impact on  $\alpha$ -helicity; proline at residue 5 and 10 both had the same CD signature, consistent with results DeGrado obtained studying the natural propensity of amino acids occurring within  $\alpha$ -helices of

proteins.<sup>44</sup> Proline at residue 14 on the C-terminus was destabilizing as well, but to a lesser extent than at internal positions. Proline exhibited a modest decrease in  $\alpha$ -helical content on the C-terminus similar to ThrOGlcNAc. Overall, proline exhibited a wide range of  $\alpha$ -helix modulation, as expected. The  $\alpha$ -helical content of proline is similar to that of threonine modifications at internal and C-terminal positions, yet induced less of an  $\alpha$ -helix on the N-terminus relative to threonine modifications.

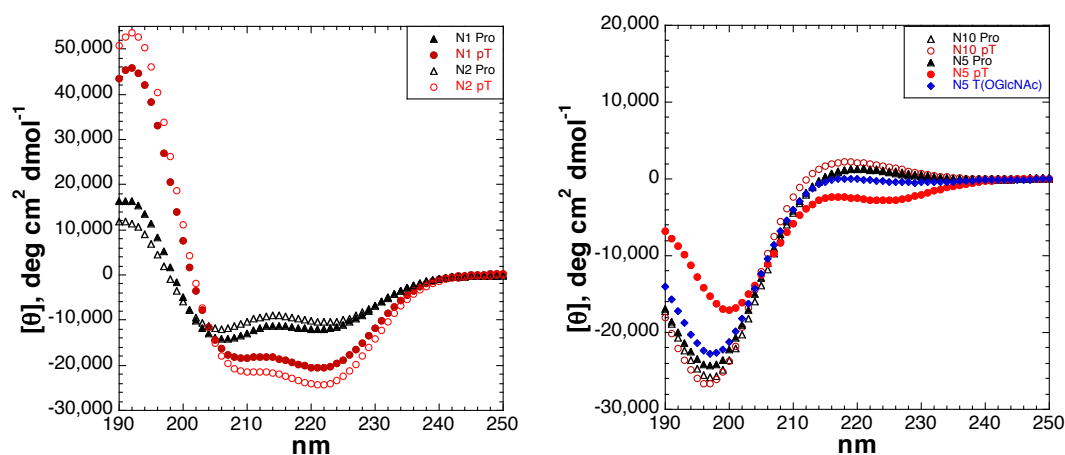


**Figure 1.15:** Comparison of the effects of threonine modifications and proline as function of position. Left: Proline (black triangles) and dianionic phosphothreonine (red circles) on the N-terminus at residue 1 (closed triangles and circles) and at residue 2 (open triangles and circles). Right: Proline (black triangles), ThrOGlcNAc (blue diamonds), and dianionic phosphothreonine (red circles) on internal positions at residue 5 (closed triangles, diamonds, and circles) and residue 10 (open triangles, and circles).

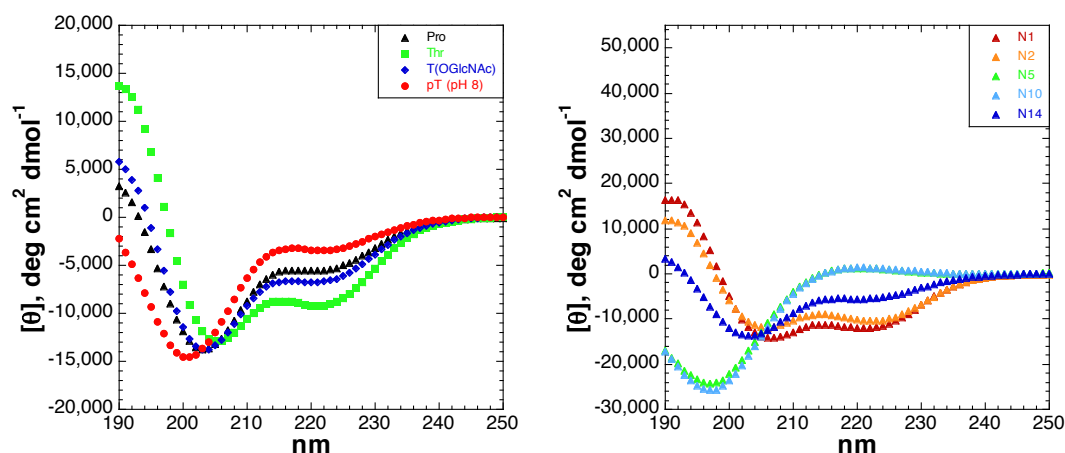


**Figure 1.16:** Left: CD spectra of Ac-YGAKAAAAKAAAAKAX-NH<sub>2</sub> peptides with proline and threonine modifications: unmodified Thr (free hydroxyl), Thr(OGlcNAc), Thr(OPO<sub>3</sub>H<sup>-</sup>), and Thr(OPO<sub>3</sub><sup>2-</sup>). Black triangles: proline; green squares: unmodified threonine; blue diamonds: Thr(OGlcNAc); magenta circles: phosphorylated threonine (pH 4.0); red circles: phosphorylated threonine (pH 8.0). Right: Peptides with proline as a function of position. Red: residue 1; orange: residue 2; green: residue 5; light blue: residue 10; dark blue: residue 14.

Peptide	[θ] <sub>222</sub>	[θ] <sub>208</sub>	[θ] <sub>190</sub>	[θ] <sub>222</sub> / [θ] <sub>208</sub>	-[θ] <sub>190</sub> /[θ] <sub>208</sub>	% Helix
Ac- <b>Pro</b> KAAAAKAAAAKAAGY-NH <sub>2</sub>	-12026	-13891	16191	0.87	1.17	37.6
Ac-A <b>Pro</b> AAAAKAAAAKAAGY-NH <sub>2</sub>	-10462	-11395	11687	0.92	1.03	33.4
Ac-AKAA <b>Pro</b> AKAAAAKAAGY-NH <sub>2</sub>	1147	-7230	-16913	-0.16	-2.34	2.8
Ac-AKAAAAKAA <b>Pro</b> AKAAGY-NH <sub>2</sub>	1261	-7756	-17185	-0.16	-2.22	2.5
Ac-YGAKAAAAKAAAAKA <b>Pro</b> -NH <sub>2</sub>	-5527	-10737	3261	0.51	0.30	20.4

**Table 1.15:** Summary of CD data for peptides containing proline at residues 1, 2, 5, 10, and 14. CD data were collected at 0.5 °C with 80-100 μM peptide in 10 mM aqueous phosphate buffer (pH 4.0, 7.0, or 8.0) with 25 mM KF.

### Phosphothreonine adopts a highly restricted conformation

Throughout this study, we have observed through  $^3J_{\alpha\text{N}}$  coupling constants that dianionic phosphothreonine adopts a highly restricted conformation. The  $\chi_2$  torsion angle for phosphoserine and phosphothreonine, which defines the angle between the beta-carbon and gamma-phosphorous atoms, was determined using coupled  $^{31}\text{P}$  NMR at pH 8.0 (Table 1.16). Brister et al. reported findings that phosphothreonine may adopt a conformation in which the  $\text{C}_\beta\text{-H}_\beta$  is in a near-eclipsed conformation relative to the  $\text{O}_\gamma\text{-P}$  bond.<sup>18</sup>  $^3J_{\text{PH}_\beta}$  in an eclipsed conformation would be approximately 10.4 Hz based on a parametrized Karplus equation.<sup>57</sup> The  $^3J_{\text{PH}_\beta}$  of peptides was examined as a function of peptide identity and  $\alpha$ -helical content. In general, conditions that favored  $\alpha$ -helicity (such as low temperature and trifluoroethanol (TFE)) exhibited larger  $^3J_{\text{PH}_\beta}$  (Table 1.16). This eclipsing conformation correlates with the presence of a phosphate-amide hydrogen bond. As such we would expect larger  $^3J_{\text{PH}_\beta}$  for peptides with the strongest phosphate-amide hydrogen bond and smaller  $^3J_{\text{PH}_\beta}$  for peptides with weaker hydrogen bonds. Dianionic phosphothreonine at residue 2 in 30% TFE exhibited the largest  $^3J_{\text{PH}_\beta}$  of 9.6 Hz. Along with  $^1\text{H}$  NMR data, these results are consistent with the phosphate-amide hydrogen bond being strongest at this position. In contrast, phosphothreonine at residue 14 on the C-terminus exhibited the smallest  $^3J_{\text{PH}_\beta}$  of 7.8 Hz. Along with  $^1\text{H}$  NMR data, these results suggest a weakening of the phosphate-amide hydrogen bond. Interestingly, all values of  $^3J_{\text{PH}_\beta}$  for phosphothreonine were greater than that of the second most  $\alpha$ -helical peptide in this study, with phosphoserine at residue 2 (7.4 Hz at 278 K, consistent with what others have observed for phosphoserine).<sup>58</sup> This finding emphasizes the greater conformational restriction of phosphothreonine over phosphoserine.

Peptide	$^3J_{\text{PH}_\alpha}$
Ac- <b>Thr</b> ( $\text{OPO}_3^{2-}$ )KAAAAKAAAAKAAGY-NH <sub>2</sub>	
278 K	8.6
298 K	7.9
Ac-A <b>Ser</b> ( $\text{OPO}_3^{2-}$ )AAAAKAAAAKAAGY-NH <sub>2</sub>	
278 K	6.7
298 K	7.4
Ac-A <b>Thr</b> ( $\text{OPO}_3^{2-}$ )AAAAKAAAAKAAGY-NH <sub>2</sub>	
278 K (30% TFE)	9.6
278 K	9.5
298 K	9.0
310 K	8.3
323 K	7.5
Ac-AKAA <b>Thr</b> ( $\text{OPO}_3^{2-}$ )AKAAAAKAAGY-NH <sub>2</sub>	
278 K	8.9
298 K	8.8
Ac-AKAAAAKAA <b>Thr</b> ( $\text{OPO}_3^{2-}$ )AKAAGY-NH <sub>2</sub>	
278 K	8.5
298 K	8.4
310 K	8.3
323 K	8.3
338 K	8.1
Ac-YGAKAAAAKAAAAKA <b>Thr</b> ( $\text{OPO}_3^{2-}$ )-NH <sub>2</sub>	
278 K	7.8
298 K	7.8

**Table 1.16:**  $^{31}\text{P}$  NMR of peptides containing phosphothreonine and phosphoserine at residue 2 in 5 mM phosphate buffer pH 8.0 with 25 mM NaCl in D<sub>2</sub>O.

## Discussion

This body of work is the first to describe the global and local structural effects of both phosphorylation and OGlcNAcylation of both serine and threonine residues on N-terminal, internal, and C-terminal positions of an  $\alpha$ -helix. I found that the global effects of phosphorylation and OGlcNAcylation were similar in direction at all positions, with both modifications stabilizing the  $\alpha$ -helix on the N-terminus and destabilizing the  $\alpha$ -helix on internal and C-terminal positions. In general, both phosphorylation and OGlcNAcylation had greater global and local structural effects on threonine than serine, with greater structural effects observed for the dianionic phosphate over the monoanionic. Peptides containing threonine were found to be less  $\alpha$ -helical than those containing serine at the N-terminus, yet peptides containing both

modifications on threonine were found to be more  $\alpha$ -helical than serine peptides with these modifications. Serine and threonine on the N-terminus had a greater  $\alpha$ -helical propensity than alanine at the same position.

In contrast, both modifications led to a substantial decrease in  $\alpha$ -helicity on internal positions, leading to almost a complete random coil in some cases. Increased destabilization that was observed at residue 10 over residue 5 for phosphorylated peptides highlights the dichotomy of both phosphoserine and phosphothreonine, with the ability to nucleate as well as disrupt  $\alpha$ -helicity. These results emphasize the context dependence of phosphorylation. Others have observed the stabilizing effects of phosphoserine on the N-terminus and the disrupting effects of both phosphoserine and phosphothreonine on internal positions, yet none have identified either the dramatic effects of phosphothreonine on the N-terminus or the dichotomy of both phosphoserine and phosphothreonine on internal positions.<sup>19-21, 23</sup>

The data herein highlight the context dependence of both phosphorylation and OGlcnAcylation on positions within  $\alpha$ -helices. On a model  $\alpha$ -helix, both OGlcnAcylation and phosphorylation stabilize the helix on the N-terminus and destabilize the helix on internal and C-terminal positions. Together, these PTMs can magnify the natural  $\alpha$ -helix propensities of both serine and threonine (Figure 1.17 and Figure 1.18). Often,  $\alpha$ -helices in proteins are short in length and stabilized by capping boxes comprised of motifs that add extra stability not only to the  $\alpha$ -helix but also to the overall tertiary structure of a protein.<sup>59, 60</sup> Overall, the  $\alpha$ -helical population of peptides containing unmodified serine varied between 49.7% (residue 1) to 26.6% (residue 10) indicating an overall range of  $\alpha$ -helicity of 23.1% based on position. Phosphoserine varied from 65.0% (residue 2) to 6.9% (residue 10), indicating an overall range of 58.1%. Ser(OGlcnAc) varied from 50.6% (residue 1) to 25.3%

(residue 5) indicating an overall range of  $\alpha$ -helicity of 25.3%. All effects of these PTMs were observed to be greater for threonine than serine, particularly for GlcNAcylated peptides. The  $\alpha$ -helical population of peptides containing unmodified threonine varied between 46.1% (residue 1) to 17.9% (residue 5), indicating an overall range of 28.2 %  $\alpha$ -helicity whereas Thr(OGlcNAc) and phosphothreonine exhibited ranges of 45.2% and 68.6%, respectively. Given that phosphorylation and OGlcNAcylation are involved in regulating transcriptional activity and the role of  $\alpha$ -helix recognition leading to transcriptional activity, these data suggest that these post-translational modifications may play a large role in regulating transcriptional elements via induction or disruption of  $\alpha$ -helices, especially those which are marginally stable.<sup>6</sup>

9, 62-66

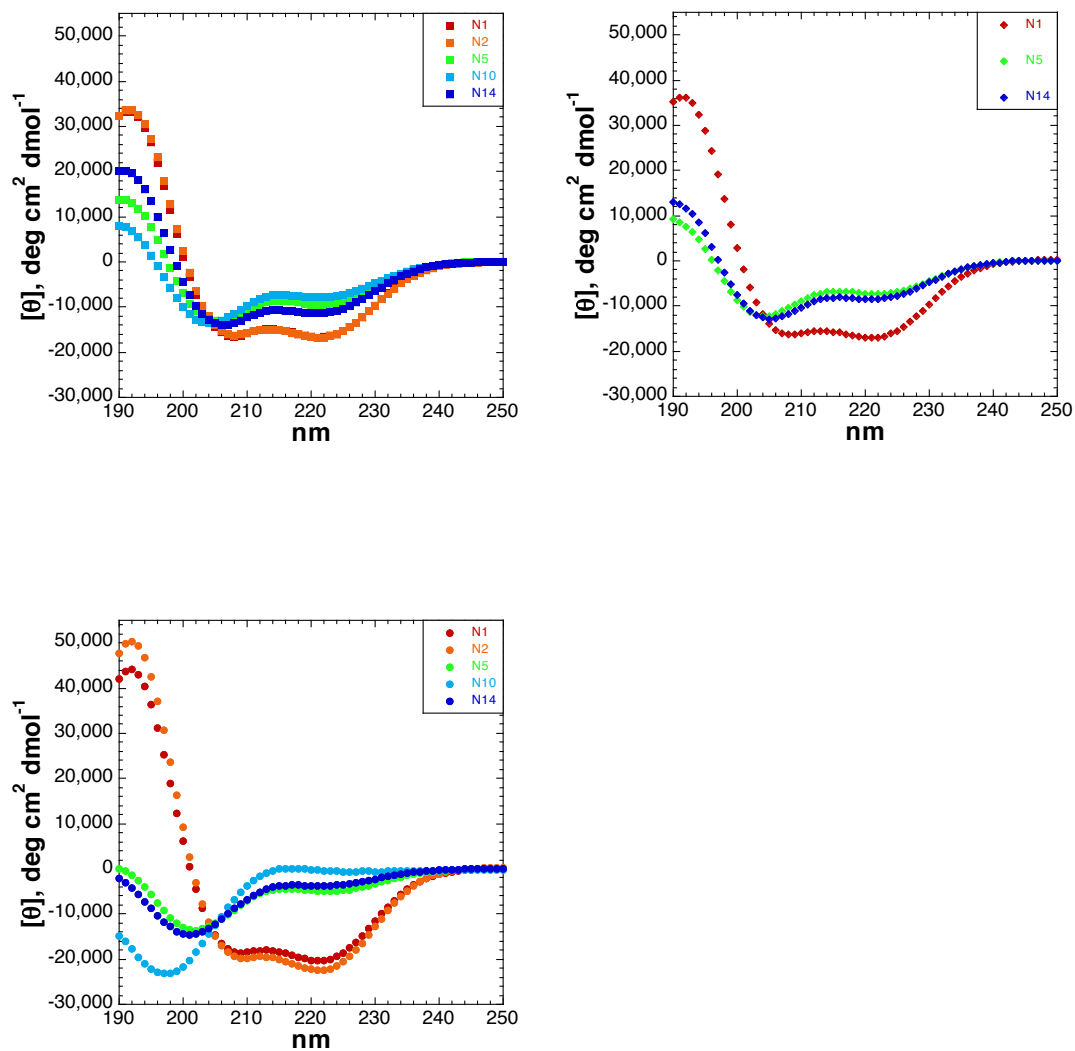


**Figure 1.17:** Comparison of the effects of serine post-translational modifications as a function of position: (top left) unmodified serine; (top right) SerOGlcNAc; (bottom) phosphoserine (pH 8.0). Red: modifications at residue 1; orange: residue 2; green: residue 5; cyan: residue 10; blue: residue 14.

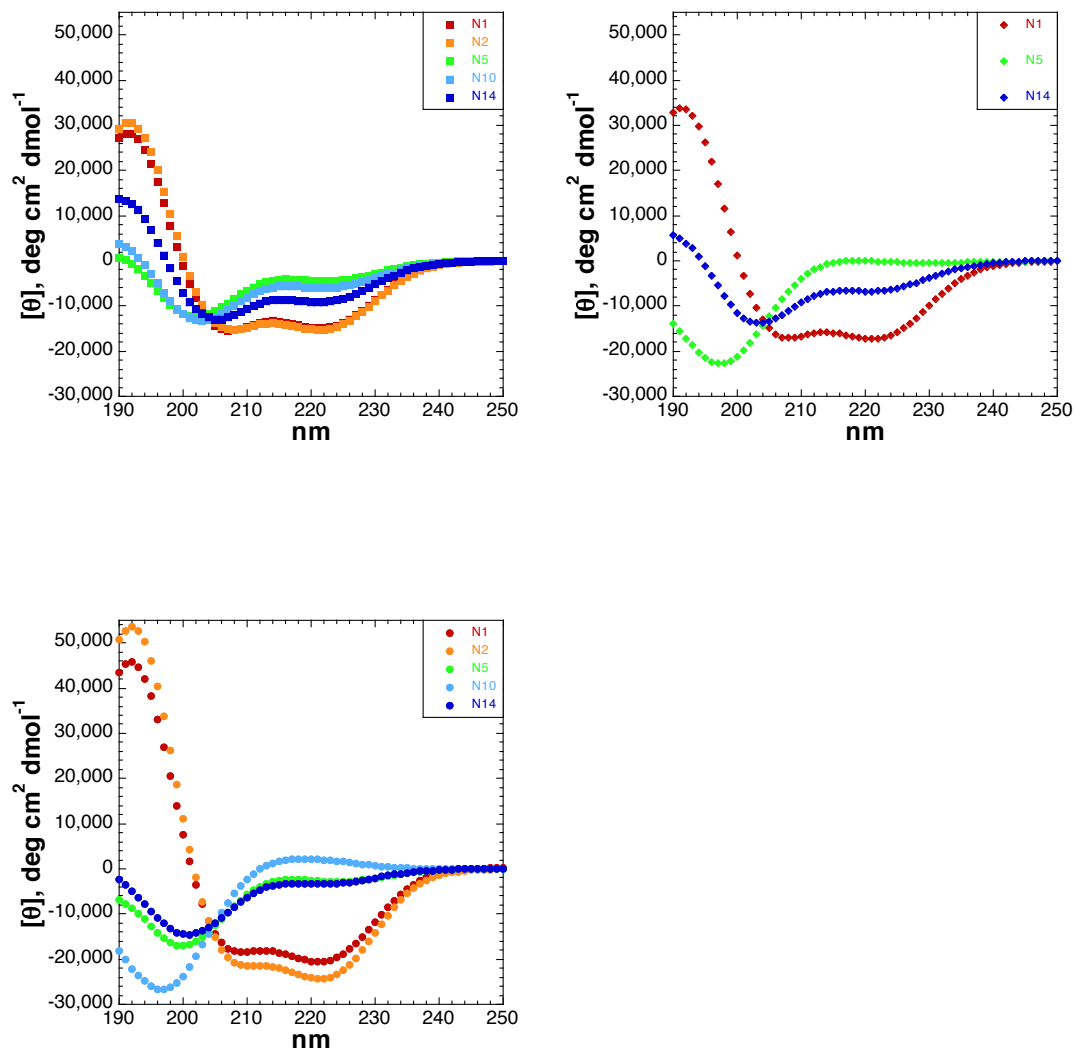


**Figure 1.18:** Comparison of the effects of threonine PTMs as a function of position: (top left) unmodified threonine; (top right) ThrOGlcNAc; (bottom) phosphothreonine (pH 8.0). Red: modifications at residue 1; orange: residue 2; green: residue 5; cyan: residue 10; blue: residue 14.

The overall effects observed for both phosphorylation and GlcNAcylation are comparable to those observed for proline. On the N-terminus, proline stabilizes the  $\alpha$ -helix through a favorable capping interaction between its carbonyl and the  $i+4$  amide

proton, while lacking a free amide proton of its own.<sup>41</sup> On internal positions, proline is highly disruptive to the  $\alpha$ -helix through both a steric clash with the  $i-1$  residue as well as termination of the amide backbone hydrogen bonding network due to lacking an amide proton.<sup>52-55</sup> Interestingly, proline does not differentiate between internal positions at residue 5 and 10, consistent with what others have observed.<sup>44</sup> The discrepancy which phosphoserine and particularly phosphothreonine exhibits on  $\alpha$ -helicity based on position originates from the ability of both phosphorylated residues to strongly nucleate  $\alpha$ -helices at their N-terminus. Proline does not strongly nucleate  $\alpha$ -helices in a similar manner to phosphorylated serine and threonine residue. These differences lead to similar internal propensities of proline throughout the helix. Proline is also destabilizing on the C-terminal position due to lacking an amide hydrogen suitable for capping a free  $i-4$  carbonyl. Together, these results suggest that both phosphorylation and GlcNAcylation can act similar to proline, but as inducible start and stop signals in  $\alpha$ -helices.

The observed similar structural effects of phosphorylation and OGlcNAcylation on  $\alpha$ -helices stands in contrast to results from our group and others. Li found that on the N-terminus of mER- $\beta$ , OGlcNAcylation of Ser<sup>16</sup> led to a type II  $\beta$ -turn-like structure, whereas phosphorylation opposed this structure adopting a more extended conformation.<sup>9</sup> Wong also found that OGlcNAcylation of threonine on the CTD of RNA polymerase II induced a turn-like structure in model peptides (YSPTSPS).<sup>10</sup> Others in our group found in the context of a polyproline helix that phosphorylation and OGlcNAcylation have opposing structural effects as well; phosphorylation favors polyproline helix, while OGlcNAcylation opposes it.<sup>18</sup> The context dependence of both OGlcNAcylation and phosphorylation on secondary structure may be interpreted through their general mode of action. The stabilizing

effects of OGlcNAcylation on the N-terminus could be due to free amide proton capping interactions between the multiple alcohols on the sugar and amide hydrogen. Alternatively, stabilization of the  $\alpha$ -helix could be due to a decrease in entropic penalties associated with  $\alpha$ -helix formation from the induced conformational restriction caused by the GlcNAc unit on serine or threonine, as observed in the decrease in  $^3J_{\alpha N}$  upon the addition of GlcNAc. On internal and C-terminal positions, OGlcNAcylation is destabilizing to  $\alpha$ -helix formation, most likely due to the sterics caused by addition of a bulky sugar group.  $\alpha$ -helices form a compact structure in which sterically demanding residues are destabilizing due to steric clashes with adjacent residues. Previous work performed in the context of polyproline helices demonstrated that GlcNAcylation reinforced the inherent propensity of threonine and serine in disfavoring polyproline helices (PPII).<sup>17, 18, 61</sup> On the N-terminus where GlcNAcylation was stabilizing to  $\alpha$ -helix, GlcNAcylation led to a decrease in  $^3J_{\alpha N}$  values, indicative of conformational restriction of the  $\phi$  torsion angle. On all other positions, GlcNAcylation was observed to be destabilizing. Although  $^3J_{\alpha N}$  values on all destabilizing positions were not obtained, ThrOGlcNAc on residue 14 was observed to have a  $^3J_{\alpha N}$  of 8.0 Hz, consistent with a more extended conformation here. These data suggest that an increase in  $^3J_{\alpha N}$  should also be observed for positions that disfavor  $\alpha$ -helix formation. The observation that GlcNAcylation disfavors both  $\alpha$ -helicity and PPII suggests that the role of GlcNAc is significantly steric in nature and can favor more extended conformations.

In contrast to GlcNAcylation, the primary mechanism of phosphorylation appears to be dictated by stereoelectronic effects associated with the phosphate amide hydrogen bond. Every phosphorylated residue in this study was observed to have a dramatic downfield chemical shift of its amide proton, consistent with an intra-residue

phosphate-amide hydrogen bond, also observed by others.<sup>18, 67-70</sup> The formation of this hydrogen bond dictates that serine and particularly threonine adopt a highly conformationally restricted structures. In every position, phosphorylation decreased the  $^3J_{\alpha\text{N}}$  of the serine or threonine residue (Table 1.44 and Table 1.53). In the context of  $\alpha$ -helices and polyproline structures ( $\phi$  in ideal structures are  $-57^\circ$  and  $-75^\circ$ , respectively, for  $\alpha$ -helix and PPII), the induction of conformational restriction and a more compact  $\phi$  would be favorable. However, as observed within  $\alpha$ -helices, internal phosphoserine and phosphothreonine are highly disruptive to  $\alpha$ -helix, despite maintaining  $\alpha$ -helical values of  $\phi$ , due to the disruption of the hydrogen bonding of the helix backbone. In contrast to  $\alpha$ -helices, internal positions of polyproline helices do not have these issues, as the amide hydrogens do not participate in secondary structure stabilization. Conformational restriction, occupancy of the amide proton, and electronic effects all must be considered when understanding the effects of phosphoserine and phosphothreonine on secondary structure.

Interestingly,  $^3J_{\alpha\text{N}}$  (ordering of structure), the amide hydrogen chemical shift, and the  $\text{H}\alpha$  chemical shift of phosphorylated residues followed no consistent trend relating to  $\alpha$ -helicity (Figure 1.19).  $^3J_{\alpha\text{N}}$  directly correlates to the  $\phi$  torsion angle. A decrease in  $^3J_{\alpha\text{N}}$  is indicative of conformational restriction and ordering. Both phosphoserine and phosphothreonine exhibit  $^3J_{\alpha\text{N}}$  values that increase when  $\alpha$ -helicity decreases, as expected. A dramatic increase in  $^3J_{\alpha\text{N}}$  is observed for C-terminal phosphorylated residues. For unknown reasons, the major outlier in this series is phosphoserine at residue 10, which exhibits a particularly small  $^3J_{\alpha\text{N}}$ . Interestingly, phosphoserine and phosphothreonine are divergent in the alpha proton chemical shift at residue 2, with the serine alpha proton exhibiting a downfield chemical shift and threonine exhibiting an upfield chemical shift. These data provide further evidence

that the NMR data do not necessarily follow  $\alpha$ -helical trends, and are strongly associated with the significant local interactions of the phosphorylated residue.

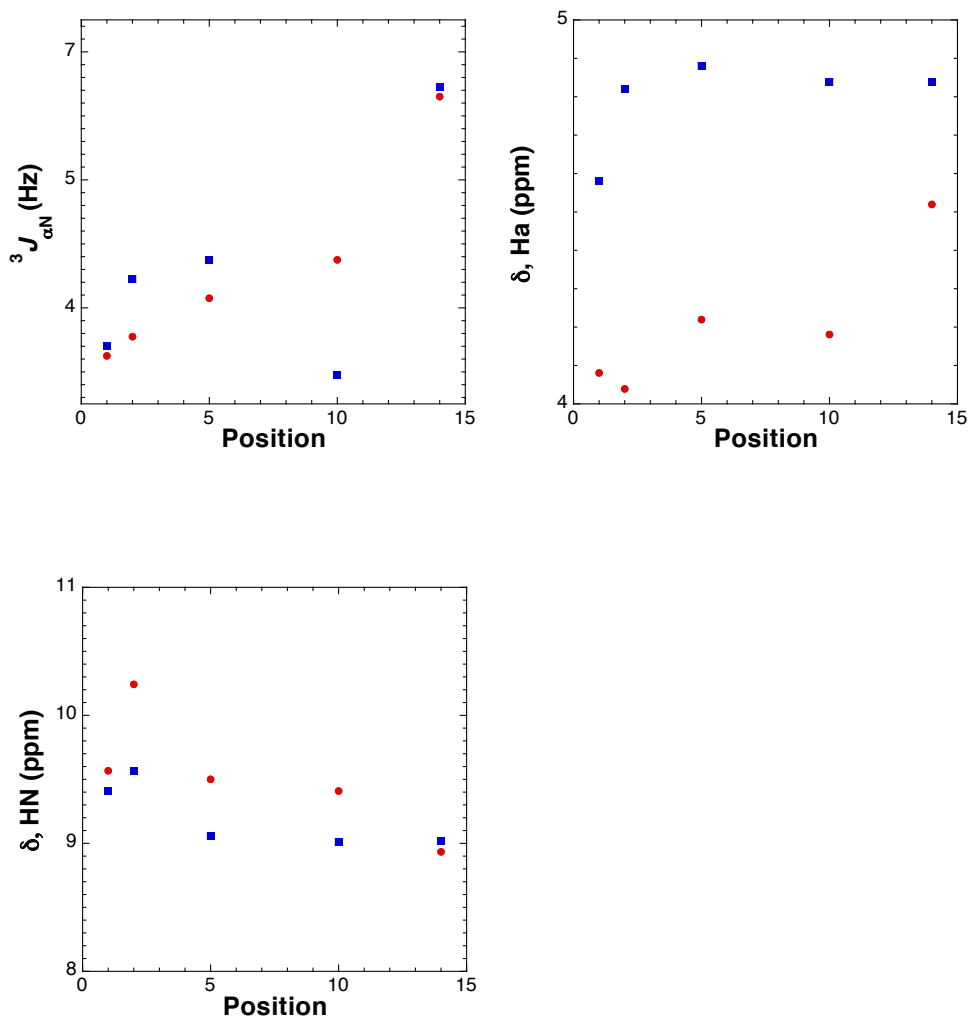


**Figure 1.19:** Summary of NMR data for peptides containing phosphothreonine (red circles) and phosphoserine (blue squares). Top left:  ${}^3J_{\alpha N}$  coupling constant as a function of  $\alpha$ -helical position. Top right: chemical shift of the threonine/serine alpha proton as a function of  $\alpha$ -helical position. Bottom: chemical shift of threonine/serine amide hydrogen as a function of  $\alpha$ -helical position.

Phosphorylated residues on the N-terminus strongly stabilize the  $\alpha$ -helix. Greater stabilization was observed for phosphothreonine over phosphoserine and for phosphorylation at residue 2 over residue 1. Indeed, within  $\alpha$ -helices phosphoserine and phosphothreonine most commonly occur on the N-terminus as observed within high-resolution crystal structures in the Protein Data Bank (PDB) (pSer: 1h4x, 2fwn, 3mk1, 3q16, 2w5w, 2bik, 3f3z, 1mki, 3qic; pThr: 3ot9, 4iza, 2ga3, 2jfl, 2w8d, 2wtv, 3u02). Although Doig suggested electrostatics as the primary mechanism of  $\alpha$ -helix stabilization by phosphorylation at the N-terminus, these structures suggest a common  $\alpha$ -helix capping motif based on multiple non-covalent interactions (Figure 1.20).<sup>19</sup> The phosphate participates in an intra-residue hydrogen bond with the amide proton on the phosphorylated residue, forming a seven-member ring. This phosphate-amide intra-residue hydrogen bond caps its own amide and polarizes the  $i-1$  amide carbonyl, which is conjugated to the  $i$  residue phosphorylated amide hydrogen. This polarization has two effects: it strengthens the backbone hydrogen bond between the  $i-1$  carbonyl and the  $i+3$  amide hydrogen while also inducing an  $n \rightarrow \pi^*$  interaction between the oxygen's lone pair electrons and the LUMO of the  $i$  (phosphorylated residue) carbonyl.<sup>18, 73-78</sup> This  $n \rightarrow \pi^*$  interaction polarizes the  $i$  (phosphorylated residue) carbonyl, strengthening the backbone hydrogen bond between the  $i$  carbonyl and the  $i+4$  amide proton. This structural model is also consistent with the observed downfield acetyl chemical shifts (Table 1.57). The greatest position for  $\alpha$ -helix stabilization upon phosphorylation was observed to be at residue 2.<sup>19, 21</sup> We have demonstrated that phosphorylation induces a restricted conformation of the phosphorylated residue, creating a more  $\alpha$ -helical conformation of  $\phi$  torsion angle. This conformational restriction could act to organize the  $i-1$  residue, decreasing the entropic penalty of  $\alpha$ -helix formation. Alternatively, it may

align the  $i-1$  residue act more favorably in hydrogen bonding with an  $i+2$  or  $i+3$  amide hydrogen.

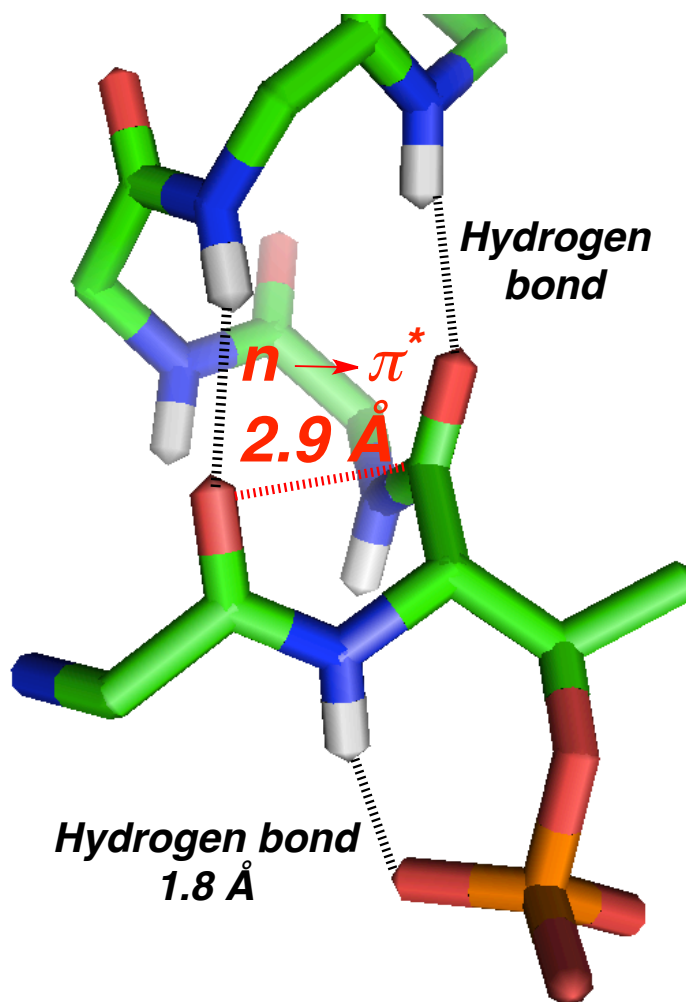


**Figure 1.20:** Crystal structure of the N-terminus of an  $\alpha$ -helix on *B. subtilis* lipoteichoic acid synthase, 2.35 Å resolution, residues 296-301 (pdb 2w8d). Phosphate-amide hydrogen bonds indicated with black dashed lines; the  $n \rightarrow \pi^*$  interaction is indicated with a red dashed line.

Herein, I have conducted a rigorous examination of the effects of phosphorylation and OGlcNAcylation of threonine and serine on the stability and structure of  $\alpha$ -helices. In general, I have found that the structural effects are qualitatively similar, with both phosphorylation and OGlcNAcylation stabilizing the  $\alpha$ -helix on N-terminal positions, while destabilizing the  $\alpha$ -helix on internal and C-terminal positions. Greater structural effects were observed for modifications on threonine over serine, for phosphorylation over OGlcNAcylation, and for the dianionic phosphate over the monoanionic phosphate. These data indicates that both phosphorylation and OGlcNAcylation can act as inducible start and stop signals in  $\alpha$ -helices. Across all peptides, phosphorylation induced a large downfield chemical shift of the amide proton, consistent with an intra-residue phosphate-amide hydrogen bond. This hydrogen bond may be the proper context in which to interpret the effects of phosphorylation of serine and threonine residues on secondary structure.

## Experimental

### Materials

Fmoc-L-amino acids were purchased from Chem-Impex (Wood Dale, IL) or Novabiochem (San Diego, CA). O-(1H-Benzotriazol-1-yl)-1,1,3,3-tetramethyluronium hexafluorophosphate (HBTU), O-(7-azabenzotriazol-1-yl)-1,1,3,3-tetramethyluronium hexafluorophosphate (HATU), Rink amide resin (loading capacity of 0.37 mmol/g), and diisopropylethylamine (DIPEA) were purchased from Chem-Impex. 1,2-Ethanedithiol (EDT) was purchased from TCI America (Portland, OR). Trifluoroacetic acid (TFA), triethylsilane (TES), phenol, thioanisole, *N,N'*-diisopropylcarbodiimide (DIC), and tetrazole were purchased from Acros. Boron trifluoride diethyl etherate ( $\text{BF}_3 \cdot \text{OEt}_2$ ) and piperidine were purchased from Aldrich. Acetonitrile (MeCN), methylene chloride ( $\text{CH}_2\text{Cl}_2$ ), methanol (MeOH), chloroform ( $\text{CHCl}_3$ ), tetrahydrofuran (THF), dimethylformamide (DMF), pyridine, diethyl ether ( $\text{Et}_2\text{O}$ ), sodium chloride, acetic acid, and acetic anhydride were purchased from Fischer.  $\beta$ -D-Glucosamine pentaacetate ( $\text{Ac}_3\text{O-GlcNAc}$ ), 2,2,2-trifluoroethanol (TFE), and *O,O'*-dibenzyl-*N,N'*-diisopropylphosphoramidite was purchased from Alfa Aesar. Antarctic phosphatase was purchased from New England BioLabs (Ipswich, MA). Deionized water was purified by a Milipore Synergy 185 water purification system with a Simpapak2 cartridge.

### Phosphorylation of serine/threonine on peptides on solid phase

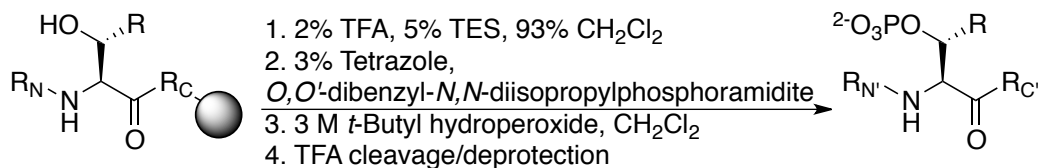


**Figure 1.21:** Scheme for the chemical phosphorylation of peptides on resin and subsequent cleavage/deprotection. R = CH<sub>3</sub> (Thr) or R = H (Ser).

Trityl-protected serine/threonine residues were incorporated at intended sites of chemical phosphorylation to allow for selective modification of the peptides on resin. The resin was swelled in CH<sub>2</sub>Cl in a fritted reaction vessel for 45 minutes. Trityl deprotection was effected using a solution of 2% TFA, 5% TES, and 93% CH<sub>2</sub>Cl<sub>2</sub> (3×3 mL, 1 minute each), followed by washing of the resin with CH<sub>2</sub>Cl<sub>2</sub>. To the resin was added 3 mL of 3% tetrazole solution in MeCN (1.35 mmol) and 500 μL of *O,O'*-dibenzyl-*N,N*-diisopropylphosphoramidite (1.52 mmol). The phosphorylation reaction was allowed to mix for 6 hours. The resin was then washed with DMF (3×3 mL) and CH<sub>2</sub>Cl<sub>2</sub> (3×3 mL). The resin was then treated with 4 mL of 3 M *tert*-butyl hydroperoxide in CH<sub>2</sub>Cl<sub>2</sub> for 1 hour, after which it was washed with DMF (3×3 mL), MeOH (3×3 mL), and CH<sub>2</sub>Cl<sub>2</sub> (3×3 mL). The resin was dried after washing with diethyl ether. The phosphorylated peptide was then subjected to cleavage from the resin and deprotection using reagent K (84% TFA and 4% each of H<sub>2</sub>O/phenol/thioanisole/ethanedithiol) or 92.5% TFA/5% TES/2.5% H<sub>2</sub>O for 3 hours.

## Synthesis of Fmoc-Ser(Ac<sub>3</sub>O-GlcNAc)-OH and Fmoc-Thr(Ac<sub>3</sub>O-GlcNAc)-OH

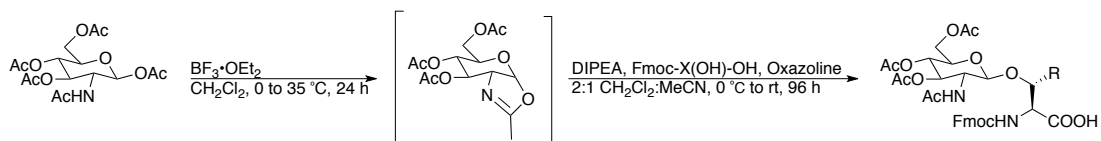


**Figure 1.22:** Synthesis of peracetylated 2-acetamido-2-deoxy- $\beta$ -D-glycosides of Fmoc-Thr-OH (R = CH<sub>3</sub>) and Fmoc-Ser-OH (R = H).

To a vacuum-dried mixture of  $\beta$ -D-Glucosamine pentaacetate (1.92 g, 2.5 mmol) and 4 Å molecular sieves was added CH<sub>2</sub>Cl<sub>2</sub> (32 mL). At 0 °C, BF<sub>3</sub>·OEt<sub>2</sub> (1.6 mL, 15.3 mmol) was added dropwise. The solution was then heated at 35 °C for 24 hours with the reaction monitored by TLC (10% MeOH/CHCl<sub>3</sub>) and visualized using cerium molybdate. When formation of the oxazoline was complete, the reaction was cooled to 0 °C and DIPEA (800  $\mu$ L, 4.6 mmol) was added dropwise over 5 minutes. The solution was then warmed to room temperature and was allowed to react for an additional 10 minutes. Fmoc-L-Thr(OH)-OH (1.73 g, 5.08 mmol) or Fmoc-L-Ser(OH)-OH (1.66 g, 5.08 mmol) was dissolved in 18 mL of 2:1 CH<sub>2</sub>Cl<sub>2</sub>:MeCN and added to the solution. After 24 hours, a second batch of the oxazoline was added to the solution and the combined solution allowed to react for an additional 72 hours. The solution was then diluted with 80 mL CH<sub>2</sub>Cl<sub>2</sub> and filtered through Celite. The solution was washed with saturated Na<sub>2</sub>CO<sub>3</sub> (100 mL) and brine (100 mL). The aqueous layers were combined and extracted with CH<sub>2</sub>Cl<sub>2</sub> (3×50 mL). The organic layers were combined, dried over sodium sulfate, and the solvent removed under reduced pressure.<sup>71</sup> The crude mixture was then purified via flash column chromatography (SiO<sub>2</sub>; 100% EtOAc, followed by a series of mixtures composed of

EtOAc/MeCN/MeOH/H<sub>2</sub>O with relative volumes of 70/2.5/1.25/1.25, followed by 70/5/2.5/2.5, then 70/10/5/5).<sup>73</sup> Isolated products were dried over sodium sulfate and concentrated under reduced pressure. Fmoc-L-Thr(Ac<sub>3</sub>O-GlcNAc)-OH was obtained as a white solid (1.10 g) in 32% isolated yield. Fmoc-L-Ser(Ac<sub>3</sub>O-GlcNAc)-OH was obtained as a white solid (1.36 g) in 40% isolated yield. Product identity was confirmed via comparison to previously reported NMR data.<sup>70</sup>

### **Synthesis and characterization data for all peptides**

Peptides were synthesized on a Rainin PS3 peptide synthesizer on Rink amide resin via standard Fmoc solid phase peptide synthesis, using HBTU as a coupling reagent for all canonical amino acids, and using HATU for all glycosylated amino acids. 60 minute couplings were performed with 4 equivalents of canonical amino acids. Glycosylated amino acids were coupled twice for 3 hours each using 1.5 equivalents of amino acid. All non-glycosylated peptides were acetylated on the N-terminus using 5% acetic anhydride in pyridine. Glycosylated peptides were acetylated using 1:1 0.5 M DIC:acetic acid in THF for 1 hour. All peptides contain a C-terminal amide.

Non-glycosylated peptides were subjected to cleavage from resin and deprotection for 3 hours using reagent K (84% TFA and 4% each of H<sub>2</sub>O/phenol/thioanisole/ethanedithiol) or a solution of 92.5% TFA, 5% TES, and 2.5% H<sub>2</sub>O. Glycosylated peptides were subjected to cleavage from resin and deprotection for 90 minutes using a solution of 92.5% TFA, 5% TES, and 2.5% H<sub>2</sub>O. TFA was removed by evaporation. Peptides were precipitated with cold ether and the precipitate was dried. The peptides were dissolved in water, then filtered through a 0.45 μm

syringe filter. The peptides were purified using reverse phase HPLC on a Vydac C18 semi-preparative column (250 × 10 mm, 5-10 μm particle, 300 Å pore) or on a Varian Microsorb MV C18 analytical column (250 × 4.6 mm, 3-5 μm particle, 100 Å pore) using a linear gradient of buffer B (20% water, 80% MeCN, and 0.05% TFA) in buffer A (98% water, 2% MeCN, and 0.06% TFA). Dried Acylated O-GlcNAcylated peptides were subjected to deesterification by adding 1.4 mL of a solution of 25 mM NaOMe in methanol and allowed to react for 2 hours. The solutions were then neutralized with 35 μL of 1 M AcOH, lyophilized, and purified on HPLC. Peptide purity was verified via the observation of a single peak upon reinjection on an analytical HPLC column. Peptides were characterized by ESI-MS (positive ion mode) on an LCQ Advantage (Finnigan) or Shimadzu mass spectrometer.

**Table 1.17:** Purification procedure for synthetic peptides.

Peptide sequence	Peptide purification	$t_R$
Ac- <i>Ser</i> KAAAAKAAAAKAAGY-NH <sub>2</sub>	0-25% buffer B in buffer A over 60 minutes	44.3 min
Ac- <i>Ser</i> (Ac <sub>3</sub> O <i>GlcNAc</i> )KAAAAKAAAAKAAGY-NH <sub>2</sub>	0-30% buffer B in buffer A over 60 minutes	49.6 min
Ac- <i>Ser</i> (O <i>GlcNAc</i> )KAAAAKAAAAKAAGY-NH <sub>2</sub>	0-25% buffer B in buffer A over 60 minutes	48.4 min
Ac- <i>Ser</i> (OPO <sub>3</sub> <sup>2-</sup> )KAAAAKAAAAKAAGY-NH <sub>2</sub>	0-25% buffer B in buffer A over 60 minutes	48.4 min
Ac- <i>Thr</i> KAAAAKAAAAKAAGY-NH <sub>2</sub>	0-25% buffer B in buffer A over 60 minutes	48.1 min
Ac- <i>Thr</i> (Ac <sub>3</sub> O <i>GlcNAc</i> )KAAAAKAAAAKAAGY-NH <sub>2</sub>	0-30% buffer B in buffer A over 60 minutes	51.0 min
Ac- <i>Thr</i> (O <i>GlcNAc</i> )KAAAAKAAAAKAAGY-NH <sub>2</sub>	0-25% buffer B in buffer A over 60 minutes	50.5 min
Ac- <i>Thr</i> (OPO <sub>3</sub> <sup>2-</sup> )KAAAAKAAAAKAAGY-NH <sub>2</sub>	0-25% buffer B in buffer A over 60 minutes	51.5 min
Ac-A <i>Ser</i> AAAAKAAAAKAAGY-NH <sub>2</sub>	0-25% buffer B in buffer A over 60 minutes	57.1 min
Ac-A <i>Ser</i> (OPO <sub>3</sub> <sup>2-</sup> )AAAAKAAAAKAAGY-NH <sub>2</sub>	0-25% buffer B in buffer A over 60 minutes	51.7 min
Ac-A <i>Thr</i> AAAAKAAAAKAAGY-NH <sub>2</sub>	0-30% buffer B in buffer A over 60 minutes	50.2 min
Ac-A <i>Thr</i> (OPO <sub>3</sub> <sup>2-</sup> )AAAAKAAAAKAAGY-NH <sub>2</sub>	0-25% buffer B in buffer A over 60 minutes	54.9 min
Ac-AKAA <i>Ser</i> AkAAAAKAAGY-NH <sub>2</sub>	0-20% buffer B in buffer A over 60 minutes	53.1 min

Ac-AKAA <b>Ser</b> (Ac <sub>3</sub> <b>OGlcNAc</b> )AKAAAAKAAGY-NH <sub>2</sub>	0-25% buffer B in buffer A over 60 minutes	55.5 min
Ac-AKAA <b>Ser</b> ( <b>OGlcNAc</b> )AKAAAAKAAGY-NH <sub>2</sub>	0-20% buffer B in buffer A over 60 minutes	54.1 min
Ac-AKAA <b>Ser</b> ( <b>OPO<sub>3</sub><sup>2-</sup></b> )AKAAAAKAAGY-NH <sub>2</sub>	0-20% buffer B in buffer A over 60 minutes	49.1 min
Ac-AKAA <b>Thr</b> AKAAAAKAAGY-NH <sub>2</sub>	0-20% buffer B in buffer A over 60 minutes	55.8 min
Ac-AKAA <b>Thr</b> (Ac <sub>3</sub> <b>OGlcNAc</b> )AKAAAAKAAGY-NH <sub>2</sub>	0-25% buffer B in buffer A over 60 minutes	54.8 min
Ac-AKAA <b>Thr</b> ( <b>OGlcNAc</b> )AKAAAAKAAGY-NH <sub>2</sub>	0-20% buffer B in buffer A over 60 minutes	46.6 min
Ac-AKAA <b>Thr</b> ( <b>OPO<sub>3</sub><sup>2-</sup></b> )AKAAAAKAAGY-NH <sub>2</sub>	0-20% buffer B in buffer A over 60 minutes	53.2 min
Ac-AKAAAAKAA <b>Ser</b> AKAAGY-NH <sub>2</sub>	0-20% buffer B in buffer A over 60 minutes	52.1 min
Ac-AKAAAAKAA <b>Ser</b> ( <b>OPO<sub>3</sub><sup>2-</sup></b> )AKAAGY-NH <sub>2</sub>	Isocratic 100% buffer A over 10 minutes followed by a linear gradient of 0-20% buffer B in buffer A over an additional 50 minutes	50.6 min
Ac-AKAAAAKAA <b>Thr</b> AKAAGY-NH <sub>2</sub>	Isocratic 100% buffer A over 10 minutes followed by a linear gradient of 0-20% buffer B in buffer A over an additional 50 minutes	49.2 min
Ac-AKAAAAKAA <b>Thr</b> ( <b>OPO<sub>3</sub><sup>2-</sup></b> )AKAAGY-NH <sub>2</sub>	Isocratic 100% buffer A over 10 minutes followed by a linear gradient of 0-20% buffer B in buffer A over an additional 50 minutes	47.7 min
Ac-YGAKAAAAKAAAAKA <b>Ser</b> -NH <sub>2</sub>	0-20% buffer B in buffer A over 60 minutes	53.6 min
Ac-YGAKAAAAKAAAAKA <b>Ser</b> (Ac <sub>3</sub> <b>OGlcNAc</b> )-NH <sub>2</sub>	0-30% buffer B in buffer A over 60 minutes	48.8 min
Ac-YGAKAAAAKAAAAKA <b>Ser</b> ( <b>OGlcNAc</b> )-NH <sub>2</sub>	0-20% buffer B in buffer A over 60 minutes	52.3 min
Ac-YGAKAAAAKAAAAKA <b>Ser</b> ( <b>OPO<sub>3</sub><sup>2-</sup></b> )-NH <sub>2</sub>	Isocratic 100% buffer A over 10 minutes followed by a linear gradient of 0-20% buffer B in buffer A over an additional 50 minutes	51.9 min
Ac-YGAKAAAAKAAAAKA <b>Thr</b> -NH <sub>2</sub>	0-20% buffer B in buffer A over 60 minutes	59.6 min
Ac-YGAKAAAAKAAAAKA <b>Thr</b> (Ac <sub>3</sub> <b>OGlcNAc</b> )-NH <sub>2</sub>	0-25% buffer B in buffer A over 60 minutes	55.3 min
Ac-YGAKAAAAKAAAAKA <b>Thr</b> ( <b>OGlcNAc</b> )-NH <sub>2</sub>	0-20% buffer B in buffer A over 60 minutes	54.4 min
Ac-YGAKAAAAKAAAAKA <b>Thr</b> ( <b>OPO<sub>3</sub><sup>2-</sup></b> )-NH <sub>2</sub>	0-20% buffer B in buffer A over 60 minutes	50.9 min
Ac- <b>Pro</b> KAAAAKAAAAKAAGY-NH <sub>2</sub>	0-25% buffer B in buffer A over 60 minutes	51.3 min
Ac-A <b>Pro</b> AAAAKAAAAKAAGY-NH <sub>2</sub>	0-30% buffer B in buffer A over 60 minutes	52.5 min
Ac-AKAA <b>Pro</b> AKAAAAKAAGY-NH <sub>2</sub>	Isocratic 100% buffer A over 20 minutes followed by a linear gradient of 0-20% buffer B in buffer A over an additional 40 minutes	57.3 min
Ac-AKAAAAKAA <b>Pro</b> AKAAGY-NH <sub>2</sub>	Isocratic 100% buffer A over 20 minutes followed by a linear gradient of 0-20% buffer B in buffer A over an additional 40 minutes	50.3 min
Ac-YGAKAAAAKAAAAKA <b>Pro</b> -NH <sub>2</sub>	0-20% buffer B in buffer A over 60 minutes	54.2 min
Ac-AKAAAAKAAAAKAAGY-NH <sub>2</sub>	0-20% buffer B in buffer A over 60 minutes	59.5 min
Ac-AKAAAAKAAAAKAAGY-NH <sub>2</sub>	0-30% buffer B in buffer A over 60 minutes	54.1 min
Ac-A( <b>Aib</b> )AAAAKAAAAKAAGY-NH <sub>2</sub>	0-35% buffer B in buffer A over 60 minutes	51.5 min

**Table 1.18:** Characterization data for synthetic peptides.

Peptide sequence	Calculated mass	Observed mass
Ac- <b>Ser</b> KAAAAKAAAAKAAGY-NH <sub>2</sub>	1460.8	731.6 (M+2H) <sup>2+</sup>
Ac- <b>Ser</b> (Ac <sub>3</sub> <b>OGlcNAc</b> )KAAAAKAAAAKAAGY-NH <sub>2</sub>	1788.9	896.1 (M+2H) <sup>2+</sup>
Ac- <b>Ser</b> ( <b>OGlcNAc</b> )KAAAAKAAAAKAAGY-NH <sub>2</sub>	1662.9	832.9 (M+2H) <sup>2+</sup>
Ac- <b>Ser</b> ( <b>OPO</b> <sub>3</sub> <sup>2-</sup> )KAAAAKAAAAKAAGY-NH <sub>2</sub>	1540.6	771.6 (M+2H) <sup>2+</sup>
Ac- <b>Thr</b> KAAAAKAAAAKAAGY-NH <sub>2</sub>	1474.8	738.6 (M+2H) <sup>2+</sup>
Ac- <b>Thr</b> (Ac <sub>3</sub> <b>OGlcNAc</b> )KAAAAKAAAAKAAGY-NH <sub>2</sub>	1803.9	903.1 (M+2H) <sup>2+</sup>
Ac- <b>Thr</b> ( <b>OGlcNAc</b> )KAAAAKAAAAKAAGY-NH <sub>2</sub>	1677.9	840.0 (M+2H) <sup>2+</sup>
Ac- <b>Thr</b> ( <b>OPO</b> <sub>3</sub> <sup>2-</sup> )KAAAAKAAAAKAAGY-NH <sub>2</sub>	1554.7	778.6 (M+2H) <sup>2+</sup>
Ac- <b>ASer</b> AAAAKAAAAKAAGY-NH <sub>2</sub>	1403.8	703.2 (M+2H) <sup>2+</sup>
Ac- <b>ASer</b> ( <b>OPO</b> <sub>3</sub> <sup>2-</sup> )AAAAKAAAAKAAGY-NH <sub>2</sub>	1483.7	743.1 (M+2H) <sup>2+</sup>
Ac- <b>AThr</b> AAAAKAAAAKAAGY-NH <sub>2</sub>	1417.8	710.2 (M+2H) <sup>2+</sup>
Ac- <b>AThr</b> ( <b>OPO</b> <sub>3</sub> <sup>2-</sup> )AAAAKAAAAKAAGY-NH <sub>2</sub>	1497.3	750.1 (M+2H) <sup>2+</sup>
Ac-AKAA <b>Ser</b> KAAAAKAAGY-NH <sub>2</sub>	1460.8	731.6 (M+2H) <sup>2+</sup>
Ac-AKAA <b>Ser</b> (Ac <sub>3</sub> <b>OGlcNAc</b> )KAAAAKAAGY-NH <sub>2</sub>	1788.9	896.2 (M+2H) <sup>2+</sup>
Ac-AKAA <b>Ser</b> ( <b>OGlcNAc</b> )KAAAAKAAGY-NH <sub>2</sub>	1662.9	833.2 (M+2H) <sup>2+</sup>
Ac-AKAA <b>Ser</b> ( <b>OPO</b> <sub>3</sub> <sup>2-</sup> )KAAAAKAAGY-NH <sub>2</sub>	1540.6	771.6 (M+2H) <sup>2+</sup>
Ac-AKAA <b>Thr</b> KAAAAKAAGY-NH <sub>2</sub>	1474.8	738.7 (M+2H) <sup>2+</sup>
Ac-AKAA <b>Thr</b> (Ac <sub>3</sub> <b>OGlcNAc</b> )KAAAAKAAGY-NH <sub>2</sub>	1803.9	903.4 (M+2H) <sup>2+</sup>
Ac-AKAA <b>Thr</b> ( <b>OGlcNAc</b> )KAAAAKAAGY-NH <sub>2</sub>	1677.9	840.2 (M+2H) <sup>2+</sup>
Ac-AKAA <b>Thr</b> ( <b>OPO</b> <sub>3</sub> <sup>2-</sup> )KAAAAKAAGY-NH <sub>2</sub>	1554.8	778.7 (M+2H) <sup>2+</sup>
Ac-AKAAAAKAA <b>Ser</b> KAAGY-NH <sub>2</sub>	1460.8	731.7 (M+2H) <sup>2+</sup>
Ac-AKAAAAKAA <b>Ser</b> ( <b>OPO</b> <sub>3</sub> <sup>2-</sup> )KAAGY-NH <sub>2</sub>	1540.6	771.5 (M+2H) <sup>2+</sup>
Ac-AKAAAAKAA <b>Thr</b> KAAGY-NH <sub>2</sub>	1474.8	738.6 (M+2H) <sup>2+</sup>
Ac-AKAAAAKAA <b>Thr</b> ( <b>OPO</b> <sub>3</sub> <sup>2-</sup> )KAAGY-NH <sub>2</sub>	1554.8	778.7 (M+2H) <sup>2+</sup>
Ac-YGAKAAAAKAAAAKA <b>Ser</b> -NH <sub>2</sub>	1460.8	731.7 (M+2H) <sup>2+</sup>
Ac-YGAKAAAAKAAAAKA <b>Ser</b> (Ac <sub>3</sub> <b>OGlcNAc</b> )-NH <sub>2</sub>	1788.9	896.3 (M+2H) <sup>2+</sup>
Ac-YGAKAAAAKAAAAKA <b>Ser</b> ( <b>OGlcNAc</b> )-NH <sub>2</sub>	1662.9	833.1 (M+2H) <sup>2+</sup>
Ac-YGAKAAAAKAAAAKA <b>Ser</b> ( <b>OPO</b> <sub>3</sub> <sup>2-</sup> )-NH <sub>2</sub>	1540.6	771.7 (M+2H) <sup>2+</sup>
Ac-YGAKAAAAKAAAAKA <b>Thr</b> -NH <sub>2</sub>	1475.7	738.7 (M+2H) <sup>2+</sup>
Ac-YGAKAAAAKAAAAKA <b>Thr</b> (Ac <sub>3</sub> <b>OGlcNAc</b> )-NH <sub>2</sub>	1803.9	903.3 (M+2H) <sup>2+</sup>
Ac-YGAKAAAAKAAAAKA <b>Thr</b> ( <b>OGlcNAc</b> )-NH <sub>2</sub>	1677.9	840.1 (M+2H) <sup>2+</sup>
Ac-YGAKAAAAKAAAAKA <b>Thr</b> ( <b>OPO</b> <sub>3</sub> <sup>2-</sup> )-NH <sub>2</sub>	1554.8	778.7 (M+2H) <sup>2+</sup>
Ac- <b>Pro</b> KAAAAKAAAAKAAGY-NH <sub>2</sub>	1470.8	736.7 (M+2H) <sup>2+</sup>
Ac- <b>APro</b> AAAAKAAAAKAAGY-NH <sub>2</sub>	1414.7	708.2 (M+2H) <sup>2+</sup>
Ac-AKAA <b>Pro</b> KAAAAKAAGY-NH <sub>2</sub>	1493.8	736.7 (M+2H) <sup>2+</sup>
Ac-AKAAAAKAA <b>Pro</b> KAAGY-NH <sub>2</sub>	1493.9	736.6 (M+2H) <sup>2+</sup>
Ac-YGAKAAAAKAAAAKA <b>Pro</b> -NH <sub>2</sub>	1470.8	736.7 (M+2H) <sup>2+</sup>
Ac-AKAAAAKAAAAKAAGY-NH <sub>2</sub>	1444.8	723.8 (M+2H) <sup>2+</sup>
Ac-AAAAAKAAAAKAAGY-NH <sub>2</sub>	1387.8	695.1 (M+2H) <sup>2+</sup>
Ac-A( <b>Aib</b> )AAAAKAAAAKAAGY-NH <sub>2</sub>	1401.8	702.2 (M+2H) <sup>2+</sup>

### Circular dichroism (CD) spectroscopy

CD spectra were collected on a Jasco J-810 Spectropolarimeter in a 1 mm cell at 0.5 °C unless otherwise indicated. The concentrations of the peptides were determined by UV absorption using  $\epsilon_{280} = 1280 \text{ M}^{-1}\text{cm}^{-1}$  for tyrosine. Peptide

concentrations were 80 to 100  $\mu\text{M}$  in in 10 mM aqueous phosphate buffer (pH 4.0, 7.0 or 8.0) with 25 mM KF. The pH of each individual solution was recorded and adjusted to the indicated pH using dilute HCl or NaOH as necessary. Individual scans were made at 1 nm intervals with 2 nm bandwidth and an averaging time of 4 s. Data are the average of at least three independent trials. Data were background corrected but were not smoothed. Error bars indicate standard error. Percent  $\alpha$ -helix was calculated using a method from Baldwin where  $\% \text{Helix} = 100 * (([\theta]_{222} - [\theta]_C) / ([\theta]_H - [\theta]_C))$ , where  $[\theta]_C$  = mean residue ellipticity at 222 nm of 100% random coil =  $2220 - 53T$ ,  $[\theta]_H$  = mean residue ellipticity at 222 nm of 100%  $\alpha$ -helix =  $(-44000 + 250T) / (1 - 3/n)$ ,  $T$  = temperature in  $^{\circ}\text{C}$  (0.5), and  $n$  = number of residues (16).

Peptide	$[\theta]_{222}$	$[\theta]_{208}$	$[\theta]_{190}$	$[\theta]_{222}/[\theta]_{208}$	$-[\theta]_{190}/[\theta]_{208}$	% Helix
Ac- <b>Ser</b> KAAAAKAAAAKAAGY-NH <sub>2</sub>	-16621	-16434	32243	1.01	1.96	49.7
Ac- <b>Ser(OGlcNAc)</b> KAAAAKAAAAKAAGY-NH <sub>2</sub>	-16944	-16358	35272	1.04	2.16	50.6
Ac- <b>Ser(OPO<sub>3</sub>H)</b> KAAAAKAAAAKAAGY-NH <sub>2</sub>	-17030	-16635	33901	1.02	2.04	50.8
Ac- <b>Ser(OPO<sub>3</sub><sup>2-</sup>)</b> KAAAAKAAAAKAAGY-NH <sub>2</sub>	-19993	-18384	42092	1.09	2.29	58.6
Ac- <b>Thr</b> KAAAAKAAAAKAAGY-NH <sub>2</sub>	-14863	-15423	27161	0.96	1.76	45.1
Ac- <b>Thr(OGlcNAc)</b> KAAAAKAAAAKAAGY-NH <sub>2</sub>	-17267	-17120	32808	1.01	1.92	51.4
Ac- <b>Thr(OPO<sub>3</sub>H)</b> KAAAAKAAAAKAAGY-NH <sub>2</sub>	-16661	-15997	33161	1.04	2.07	49.8
Ac- <b>Thr(OPO<sub>3</sub><sup>2-</sup>)</b> KAAAAKAAAAKAAGY-NH <sub>2</sub>	-20495	-18290	43519	1.12	2.38	60.0
Ac-A <b>Ser</b> AAAAKAAAAKAAGY-NH <sub>2</sub>	-16650	-16246	32311	1.02	1.99	49.8
Ac-A <b>Ser(OPO<sub>3</sub>H)</b> AAAAKAAAAKAAGY-NH <sub>2</sub>	-19142	-17756	39137	1.08	2.20	56.4
Ac-A <b>Ser(OPO<sub>3</sub><sup>2-</sup>)</b> AAAAKAAAAKAAGY-NH <sub>2</sub>	-22401	-19376	47754	1.16	2.46	65.0
Ac-A <b>Thr</b> AAAAKAAAAKAAGY-NH <sub>2</sub>	-15248	-15328	29238	0.99	1.91	46.1
Ac-A <b>Thr(OPO<sub>3</sub>H)</b> AAAAKAAAAKAAGY-NH <sub>2</sub>	-19076	-17383	34079	1.10	1.96	56.2
Ac-A <b>Thr(OPO<sub>3</sub><sup>2-</sup>)</b> AAAAKAAAAKAAGY-NH <sub>2</sub>	-23977	-20776	50682	1.15	2.44	69.2
Ac-AKAA <b>Ser</b> KAAAAKAAGY-NH <sub>2</sub>	-9489	-12001	13623	0.79	1.14	30.9
Ac-AKAA <b>Ser(OGlcNAc)</b> KAAAAKAAGY-NH <sub>2</sub>	-7362	-10510	9108	0.70	0.87	25.3
Ac-AKAA <b>Ser(OPO<sub>3</sub>H)</b> KAAAAKAAGY-NH <sub>2</sub>	-5233	-8782	3170	0.60	0.36	19.6
Ac-AKAA <b>Ser(OPO<sub>3</sub><sup>2-</sup>)</b> KAAAAKAAGY-NH <sub>2</sub>	-5019	-9115	25	0.55	0.00	19.1
Ac-AKAA <b>Thr</b> KAAAAKAAGY-NH <sub>2</sub>	-4593	-8386	727	0.55	0.09	17.9
Ac-AKAA <b>Thr(OGlcNAc)</b> KAAAAKAAGY-NH <sub>2</sub>	-145	-6835	-14035	0.02	-2.05	6.2
Ac-AKAA <b>Thr(OPO<sub>3</sub>H)</b> KAAAAKAAGY-NH <sub>2</sub>	-1868	-6555	-5647	0.28	-0.86	10.7
Ac-AKAA <b>Thr(OPO<sub>3</sub><sup>2-</sup>)</b> KAAAAKAAGY-NH <sub>2</sub>	-2742	-8292	-6777	0.33	-0.82	13.0
Ac-AKAAAAKAA <b>Ser</b> KAAGY-NH <sub>2</sub>	-7883	-11530	8113	0.68	0.70	26.6
Ac-AKAAAAKAA <b>Ser(OPO<sub>3</sub>H)</b> KAAGY-NH <sub>2</sub>	-2936	-8145	-5752	0.36	-0.71	13.6
Ac-AKAAAAKAA <b>Ser(OPO<sub>3</sub><sup>2-</sup>)</b> KAAGY-NH <sub>2</sub>	-431	-6789	-14930	0.06	-2.20	6.9

Ac-AKAAAAKAA <i>Thr</i> AKAAGY-NH <sub>2</sub>	-6020	-10003	3732	0.60	0.37	21.7
Ac-AKAAAAKAA <i>Thr(OPO<sub>3</sub>H)</i> AKAAGY-NH <sub>2</sub>	382	-5396	-13528	-0.07	-2.51	4.8
Ac-AKAAAAKAA <i>Thr(OPO<sub>3</sub><sup>2-</sup>)</i> AKAAGY-NH <sub>2</sub>	1967	-5542	-18077	-0.35	-3.26	0.6
Ac-YGAKAAAAKAAAAKA <i>Ser</i> -NH <sub>2</sub>	-11375	-13477	20103	0.84	1.49	35.9
Ac-YGAKAAAAKAAAAKA <i>Ser(OGlcNAc)</i> -NH <sub>2</sub>	-8461	-11840	12910	0.71	1.09	28.2
Ac-YGAKAAAAKAAAAKA <i>Ser(OPO<sub>3</sub>H)</i> -NH <sub>2</sub>	-5630	-9603	4445	0.59	0.46	20.7
Ac-YGAKAAAAKAAAAKA <i>Ser(OPO<sub>3</sub><sup>2-</sup>)</i> -NH <sub>2</sub>	-3734	-8814	-2015	0.42	-0.23	15.7
Ac-YGAKAAAAKAAAAKA <i>Thr</i> -NH <sub>2</sub>	-9190	-12024	13630	0.76	1.13	30.1
Ac-YGAKAAAAKAAAAKA <i>Thr(OGlcNAc)</i> -NH <sub>2</sub>	-6685	-11064	5746	0.60	0.52	23.5
Ac-YGAKAAAAKAAAAKA <i>Thr(OPO<sub>3</sub>H)</i> -NH <sub>2</sub>	-4984	-9420	1437	0.53	0.15	19.0
Ac-YGAKAAAAKAAAAKA <i>Thr(OPO<sub>3</sub><sup>2-</sup>)</i> -NH <sub>2</sub>	-3417	-8524	-2248	0.40	-0.26	14.8
Ac-AKAAAAKAAAAKAAGY-NH <sub>2</sub>	-16325	-16775	30780	0.97	1.83	48.9
Ac-AKAAAAKAAAAKAAGY-NH <sub>2</sub>	-21448	-19855	44597	1.08	2.25	62.5
Ac-A(Aib)AKAAAAKAAAAKAAGY-NH <sub>2</sub>	-21688	-20180	39844	1.07	1.97	63.1
Ac- <i>Pro</i> KAAAAKAAAAKAAGY-NH <sub>2</sub>	-12026	-13891	16191	0.87	1.17	37.6
Ac-A <i>Pro</i> KAAAAKAAAAKAAGY-NH <sub>2</sub>	-10462	-11395	11687	0.92	1.03	33.4
Ac-AKAA <i>Pro</i> KAAAAKAAAAKAAGY-NH <sub>2</sub>	1147	-7230	-16913	-0.16	-2.34	2.8
Ac-AKAAAAKAA <i>Pro</i> AKAAGY-NH <sub>2</sub>	1261	-7756	-17185	-0.16	-2.22	2.5
Ac-YGAKAAAAKAAAAKA <i>Pro</i> -NH <sub>2</sub>	-5527	-10737	3261	0.51	0.30	20.4
<b>30 % TFE</b>						
Ac-A <i>Thr(OPO<sub>3</sub><sup>2-</sup>)</i> AKAAAAKAAAAKAAGY-NH <sub>2</sub>	-25994	-23478	54742	1.11	2.33	74.5
Ac-AKAAAAKAA <i>Thr(OPO<sub>3</sub><sup>2-</sup>)</i> AKAAGY-NH <sub>2</sub>	-2346	-7823	-3311	0.30	-0.42	12.0

**Table 1.19:** Summary of CD data for all peptides. CD data were collected at 0.5 °C with 80-100 μM peptide in 10 mM aqueous phosphate buffer (pH 4.0, 7.0, or 8.0) with 25 mM KF. <sup>a</sup> n.a. = no local maximum or minimum was observed.

Peptide	λ at local [θ] <sub>min</sub> , nm	[θ] <sub>min</sub> , deg cm <sup>2</sup> dmol <sup>-1</sup>	λ at local [θ] <sub>min</sub> , nm	[θ] <sub>min</sub> , deg cm <sup>2</sup> dmol <sup>-1</sup>	λ at local [θ] <sub>max</sub> , nm	local [θ] <sub>max</sub> , deg cm <sup>2</sup> dmol <sup>-1</sup>
Ac- <i>Ser</i> KAAAAKAAAAKAAGY-NH <sub>2</sub>	221	-16668	208	-16230	192	33258
Ac- <i>Ser(OGlcNAc)</i> KAAAAKAAAAKAAGY-NH <sub>2</sub>	221	-17047	209	-16377	191	36196
Ac- <i>Ser(OPO<sub>3</sub>H)</i> KAAAAKAAAAKAAGY-NH <sub>2</sub>	221	-17335	208	-16635	192	35986
Ac- <i>Ser(OPO<sub>3</sub><sup>2-</sup>)</i> KAAAAKAAAAKAAGY-NH <sub>2</sub>	221	-20480	209	-18582	192	44154
Ac- <i>Thr</i> KAAAAKAAAAKAAGY-NH <sub>2</sub>	221	-14891	207	-15474	191	28123
Ac- <i>Thr(OGlcNAc)</i> KAAAAKAAAAKAAGY-NH <sub>2</sub>	221	-17328	208	-17120	191	33681
Ac- <i>Thr(OPO<sub>3</sub>H)</i> KAAAAKAAAAKAAGY-NH <sub>2</sub>	221	-16741	208	-15997	192	35156
Ac- <i>Thr(OPO<sub>3</sub><sup>2-</sup>)</i> KAAAAKAAAAKAAGY-NH <sub>2</sub>	221	-20571	209	-18538	192	45696
Ac-A <i>Ser</i> KAAAAKAAAAKAAGY-NH <sub>2</sub>	221	-16684	208	-16246	192	33618
Ac-A <i>Ser(OPO<sub>3</sub>H)</i> KAAAAKAAAAKAAGY-NH <sub>2</sub>	221	-19112	209	-17823	191	40473
Ac-A <i>Ser(OPO<sub>3</sub><sup>2-</sup>)</i> KAAAAKAAAAKAAGY-NH <sub>2</sub>	221	-22466	210	-19731	192	50364
Ac-A <i>Thr</i> KAAAAKAAAAKAAGY-NH <sub>2</sub>	221	-15313	208	-15328	191	30423
Ac-A <i>Thr(OPO<sub>3</sub>H)</i> KAAAAKAAAAKAAGY-NH <sub>2</sub>	221	-19143	209	-17595	192	38407
Ac-A <i>Thr(OPO<sub>3</sub><sup>2-</sup>)</i> KAAAAKAAAAKAAGY-NH <sub>2</sub>	221	-24362	210	-21449	192	53581
Ac-AKAA <i>Ser</i> KAAAAKAAAAKAAGY-NH <sub>2</sub>	222	-9489	205	-13024	191	13649

Ac-AKAA <i>Ser</i> ( <i>OGlcNAc</i> )AKAAAAKAAGY-NH <sub>2</sub>	222	-7362	205	-12242	190	9108
Ac-AKAA <i>Ser</i> ( <i>OPO<sub>3</sub>H</i> )AKAAAAKAAGY-NH <sub>2</sub>	222	-5233	199	-14689	n.a.	n.a.
Ac-AKAA <i>Ser</i> ( <i>OPO<sub>3</sub><sup>2-</sup></i> )AKAAAAKAAGY-NH <sub>2</sub>	223	-5023	199	-16939	n.a.	n.a.
Ac-AKAA <i>Thr</i> AKAAAAKAAGY-NH <sub>2</sub>	222	-4593	202	-12425	190	727
Ac-AKAA <i>Thr</i> ( <i>OGlcNAc</i> )AKAAAAKAAGY-NH <sub>2</sub>	n.a.	n.a.	197	-22764	218	25
Ac-AKAA <i>Thr</i> ( <i>OPO<sub>3</sub>H</i> )AKAAAAKAAGY-NH <sub>2</sub>	223	-1914	199	-14689	n.a.	n.a.
Ac-AKAA <i>Thr</i> ( <i>OPO<sub>3</sub><sup>2-</sup></i> )AKAAAAKAAGY-NH <sub>2</sub>	224	-2837	200	-17019	n.a.	n.a.
Ac-AKAAAAKAA <i>Ser</i> AKAAGY-NH <sub>2</sub>	221	-7895	204	-13506	n.a.	n.a.
Ac-AKAAAAKAA <i>Ser</i> ( <i>OPO<sub>3</sub>H</i> )AKAAGY-NH <sub>2</sub>	224	-2921	200	-16446	216	-2611
Ac-AKAAAAKAA <i>Ser</i> ( <i>OPO<sub>3</sub><sup>2-</sup></i> )AKAAGY-NH <sub>2</sub>	231	-643	198	-23248	218	95
Ac-AKAAAAKAA <i>Thr</i> AKAAGY-NH <sub>2</sub>	222	-6020	203	-13174	190	3732
Ac-AKAAAAKAA <i>Thr</i> ( <i>OPO<sub>3</sub>H</i> )AKAAGY-NH <sub>2</sub>	n.a.	n.a.	197	-21024	218	612
Ac-AKAAAAKAA <i>Thr</i> ( <i>OPO<sub>3</sub><sup>2-</sup></i> )AKAAGY-NH <sub>2</sub>	n.a.	n.a.	197	-26722	219	2161
Ac-YGAKAAAAKAAAAKA <i>Ser</i> -NH <sub>2</sub>	221	-11435	208	-13477	191	20119
Ac-YGAKAAAAKAAAAKA <i>Ser</i> ( <i>OGlcNAc</i> )-NH <sub>2</sub>	221	-8533	205	-12940	190	12910
Ac-YGAKAAAAKAAAAKA <i>Ser</i> ( <i>OPO<sub>3</sub>H</i> )-NH <sub>2</sub>	222	-5630	203	-12376	190	4445
Ac-YGAKAAAAKAAAAKA <i>Ser</i> ( <i>OPO<sub>3</sub><sup>2-</sup></i> )-NH <sub>2</sub>	222	-3734	201	-14623	n.a.	n.a.
Ac-YGAKAAAAKAAAAKA <i>Thr</i> -NH <sub>2</sub>	221	-9211	205	-12930	190	13630
Ac-YGAKAAAAKAAAAKA <i>Thr</i> ( <i>OGlcNAc</i> )-NH <sub>2</sub>	220	-6770	203	-13784	190	5746
Ac-YGAKAAAAKAAAAKA <i>Thr</i> ( <i>OPO<sub>3</sub>H</i> )-NH <sub>2</sub>	222	-4984	202	-13082	190	1437
Ac-YGAKAAAAKAAAAKA <i>Thr</i> ( <i>OPO<sub>3</sub><sup>2-</sup></i> )-NH <sub>2</sub>	222	-3417	201	-14553	n.a.	n.a.
Ac-AKAAAAKAAAAKAAGY-NH <sub>2</sub>	221	-16343	207	-16778	191	31845
Ac-AKAAAAKAAAAKAAGY-NH <sub>2</sub>	221	-16343	207	-16778	191	31845
Ac-A(Aib)AAAAKAAAAKAAGY-NH <sub>2</sub>	221	-14528	209	-13279	193	31550
Ac- <i>Pro</i> KAAAAKAAAAKAAGY-NH <sub>2</sub>	221	-12072	206	-14191	191	16379
Ac-A <i>Pro</i> AAAAKAAAAKAAGY-NH <sub>2</sub>	222	-10463	206	-11951	191	11706
Ac-AKAA <i>Pro</i> KAAAAKAAGY-NH <sub>2</sub>	n.a.	n.a.	197	-24321	220	1264
Ac-AKAAAAKAA <i>Pro</i> AKAAGY-NH <sub>2</sub>	n.a.	n.a.	197	-25830	221	1329
Ac-YGAKAAAAKAAAAKA <i>Pro</i> -NH <sub>2</sub>	221	-5596	203	-13728	217	-5501
<b>30 % TFE</b>						
Ac-A <i>Thr</i> ( <i>OPO<sub>3</sub><sup>2-</sup></i> )AAAAKAAAAKAAGY-NH <sub>2</sub>	221	-26121	210	-24309	193	58778
Ac-AKAAAAKAA <i>Thr</i> ( <i>OPO<sub>3</sub><sup>2-</sup></i> )AKAAGY-NH <sub>2</sub>	200	-14491	n.a.	n.a.	190	-3311

**Table 1.20:** Summary of CD data for all peptides. CD data were collected at 0.5 °C with 80-100 μM peptide in 10 mM aqueous phosphate buffer (pH 4.0, 7.0, or 8.0) with 25 mM KF. <sup>a</sup> n.a. = no local maximum or minimum was observed.

## CD spectroscopy under standard conditions

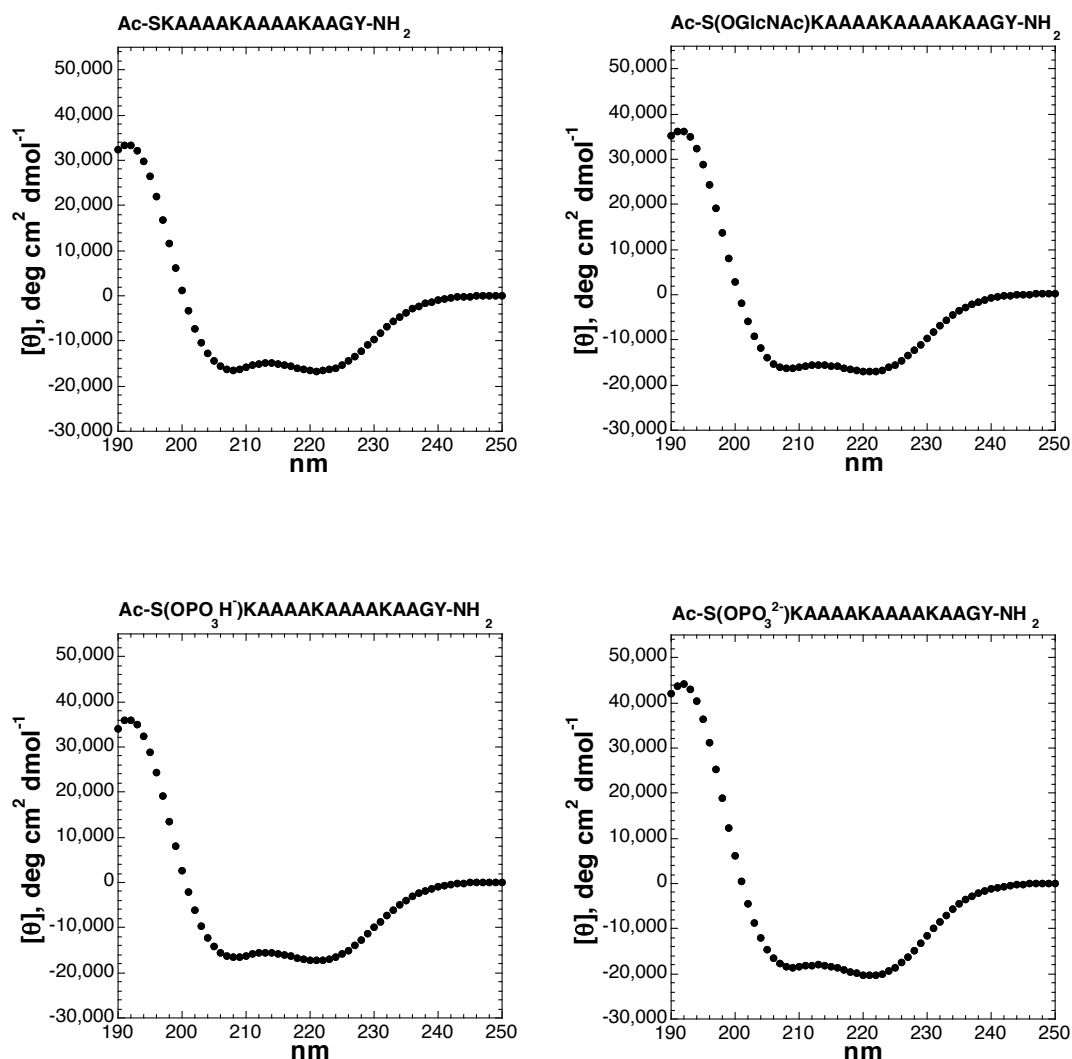


**Figure 1.22:** CD spectra of peptides with serine and serine modifications at residue 1. Top: CD spectra of  $\text{Ac-SKAAAAKAAAAKAAGY-NH}_2$  (left) and  $\text{Ac-S(OGlcNAc)KAAAAKAAAAKAAGY-NH}_2$  (right); peptides were dissolved in 10 mM phosphate buffer (pH 7.0) containing 25 mM KF. Bottom left: CD spectrum of  $\text{Ac-S(OPO}_3\text{H}^-)\text{KAAAAKAAAAKAAGY-NH}_2$  in 10 mM phosphate buffer (pH 4.0) containing 25 mM KF. Bottom right: CD spectrum of  $\text{Ac-S(OPO}_3^{2-})\text{KAAAAKAAAAKAAGY-NH}_2$  in 10 mM phosphate buffer (pH 8.0) containing 25 mM KF.

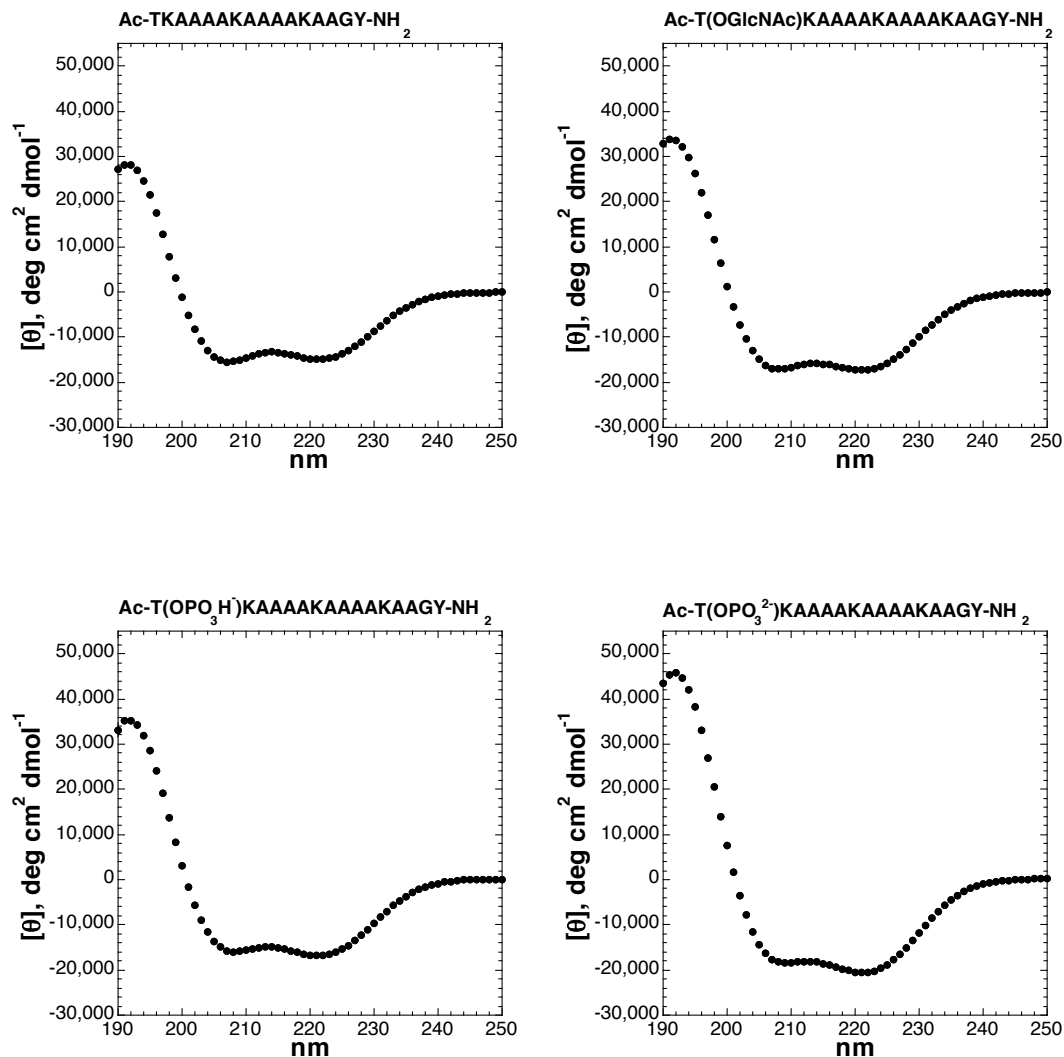


**Figure 1.23:** CD spectra of peptides with threonine and threonine modifications at residue 1. Top: CD spectra of **Ac-TKAAAAKAAAAKAAGY-NH<sub>2</sub>** (left) and **Ac-T(OGlcNAc)KAAAAKAAAAKAAGY-NH<sub>2</sub>** (right); peptides were dissolved in 10 mM phosphate buffer (pH 7.0) containing 25 mM KF. Bottom left: CD spectrum of **Ac-T(OPO<sub>3</sub>H<sup>-</sup>)KAAAAKAAAAKAAGY-NH<sub>2</sub>** in 10 mM phosphate buffer (pH 4.0) containing 25 mM KF. Bottom right: CD spectrum of **Ac-T(OPO<sub>3</sub><sup>2-</sup>)KAAAAKAAAAKAAGY-NH<sub>2</sub>** in 10 mM phosphate buffer (pH 8.0) containing 25 mM KF.

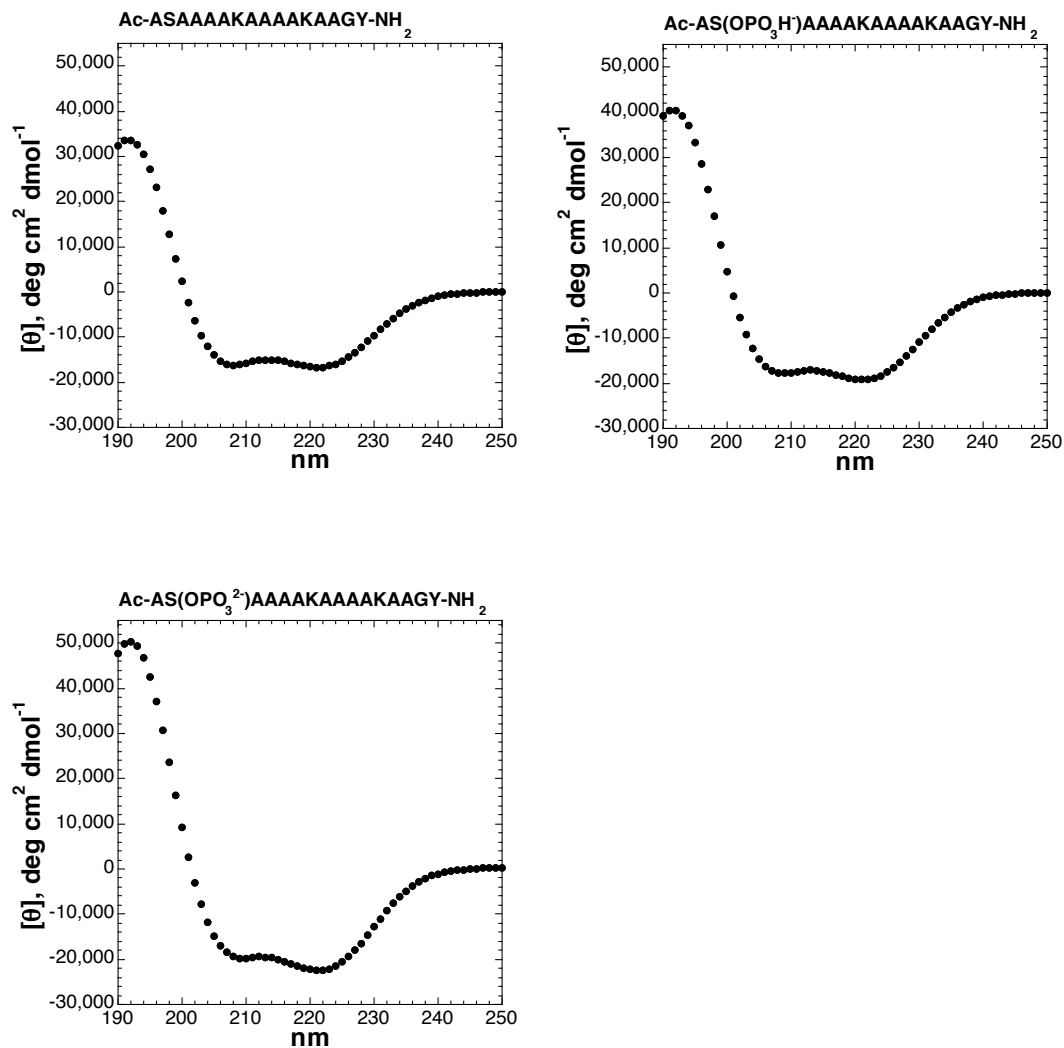


**Figure 1.24:** CD spectra of peptides with serine and serine modifications at residue 2. Top left: CD spectrum of  $\text{Ac-ASAAAAKAAAAKAAGY-NH}_2$  in 10 mM phosphate buffer (pH 7.0) containing 25 mM KF. Top right: CD spectrum of  $\text{Ac-AS(OPO}_3\text{H)AAAAKAAAAKAAGY-NH}_2$  in 10 mM phosphate buffer (pH 4.0) containing 25 mM KF. Bottom middle: CD spectrum of  $\text{Ac-AS(OPO}_3^{2-})AAAAKAAAAKAAGY-NH}_2$  in 10 mM phosphate buffer (pH 8.0) containing 25 mM KF.

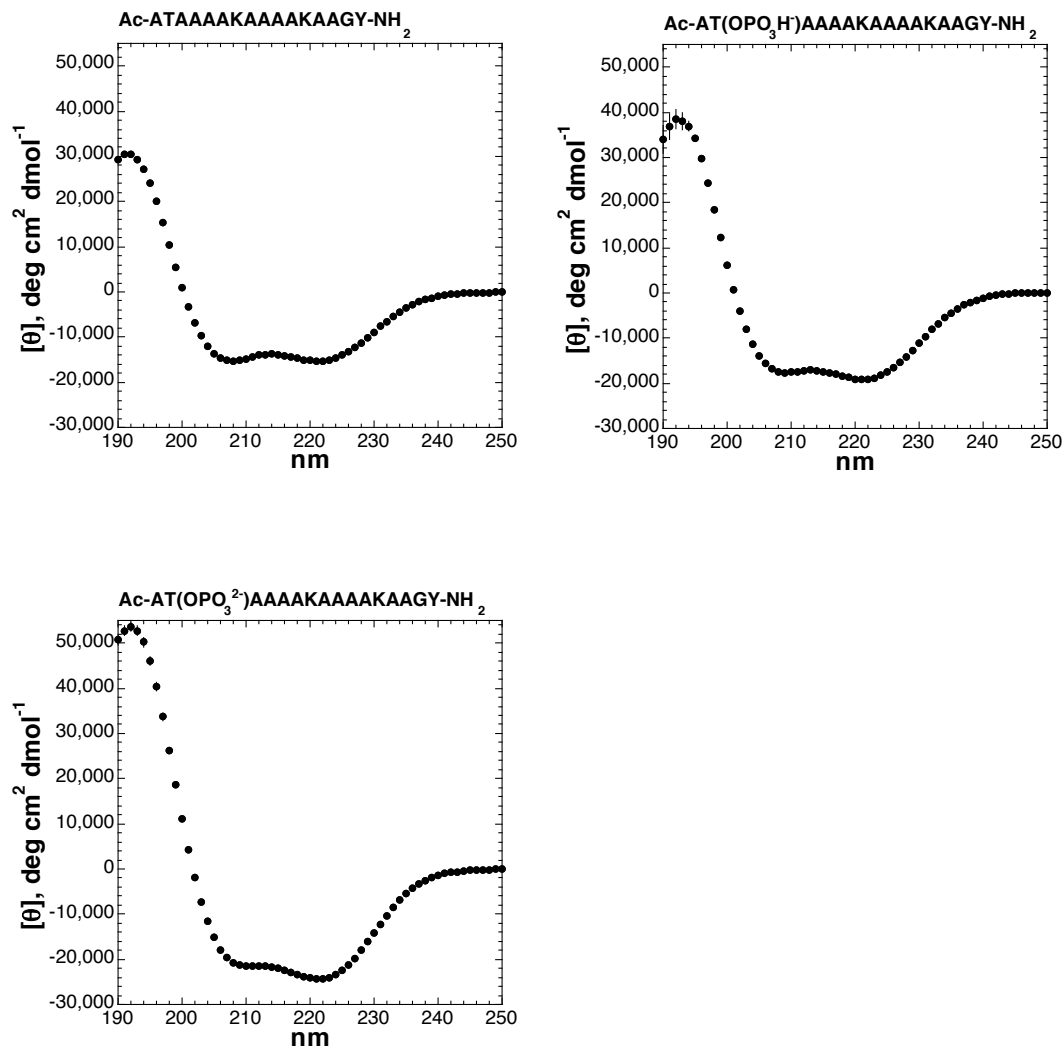


**Figure 1.25:** CD spectra of peptides with threonine and threonine modifications at residue 2. Top left: CD spectrum of  $\text{Ac-ATAAAKAAAAKAAGY-NH}_2$  in 10 mM phosphate buffer (pH 7.0) containing 25 mM KF. Top right: CD spectrum of  $\text{Ac-AT(OPO}_3\text{H}^-)\text{AAAAKAAAAKAAGY-NH}_2$  in 10 mM phosphate buffer (pH 4.0) containing 25 mM KF. Bottom left: CD spectrum of  $\text{Ac-AT(OPO}_3^{2-})\text{AAAAKAAAAKAAGY-NH}_2$  in 10 mM phosphate buffer (pH 8.0) containing 25 mM KF.

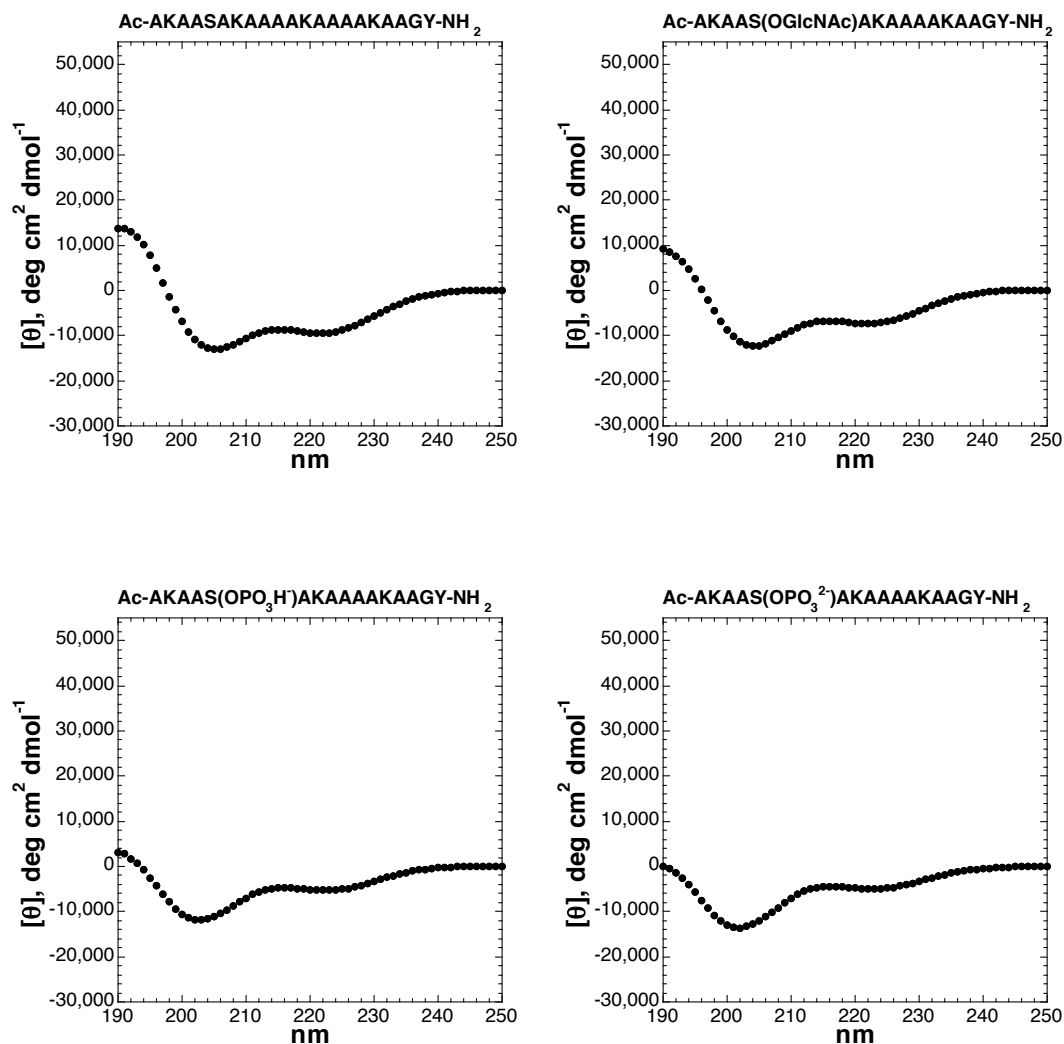


**Figure 1.26:** CD spectra of peptides with serine and serine modifications at residue 5. Top: CD spectra of **Ac-AKAASAKAAAAKAAGY-NH<sub>2</sub>** (left) and **Ac-AKAAS(OGlcNAc)AKAAAAKAAGY-NH<sub>2</sub>** (right); peptides were dissolved in 10 mM phosphate buffer (pH 7.0) containing 25 mM KF. Bottom left: CD spectrum of **Ac-AKAAS(OPO<sub>3</sub>H<sup>-</sup>)AKAAAAKAAGY-NH<sub>2</sub>** in 10 mM phosphate buffer (pH 4.0) containing 25 mM KF. Bottom right: CD spectrum of **Ac-AKAAS(OPO<sub>3</sub><sup>2-</sup>)AKAAAAKAAGY-NH<sub>2</sub>** in 10 mM phosphate buffer (pH 8.0) containing 25 mM KF.

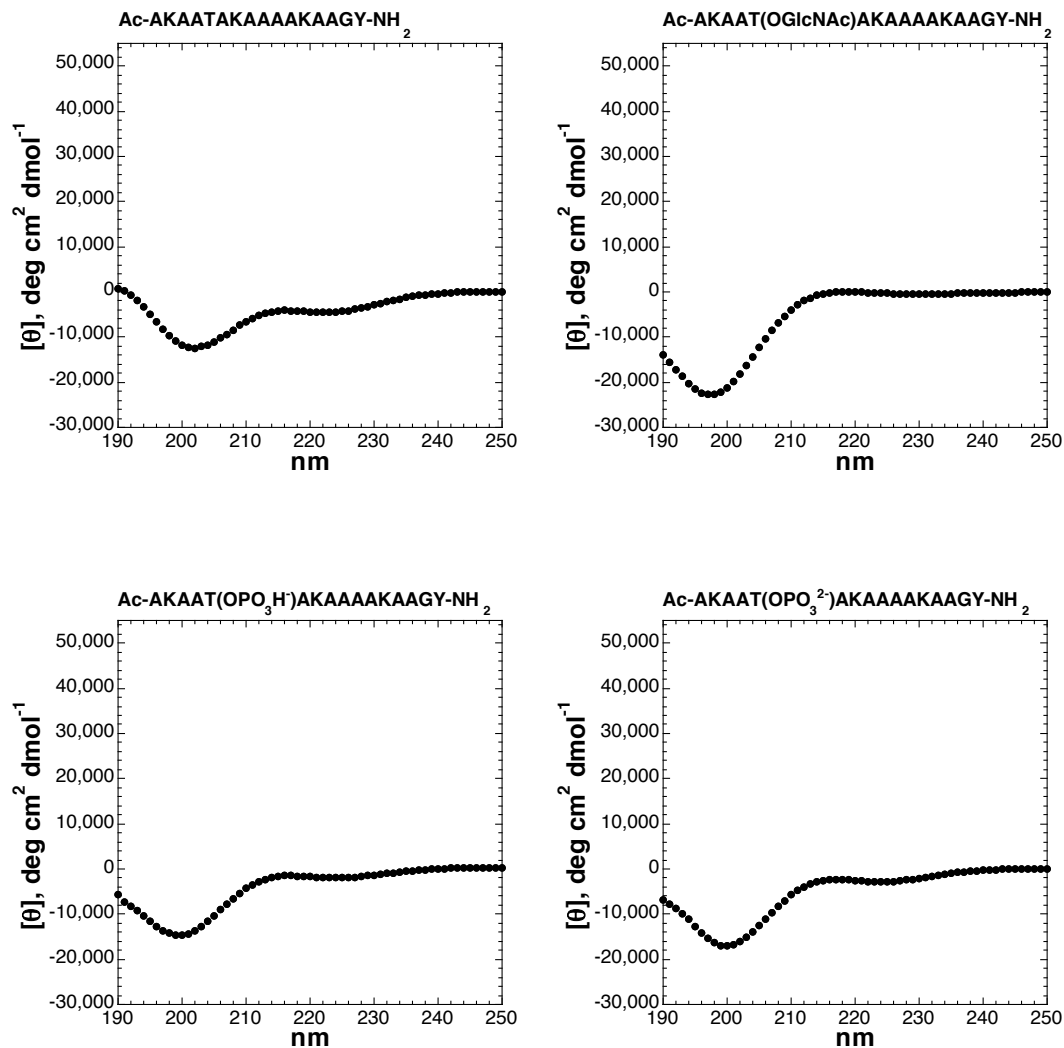


**Figure 1.27:** CD spectra of peptides with threonine and threonine modifications at residue 5. Top: CD spectra of **Ac-AKAATAKAAAAKAAGY-NH<sub>2</sub>** (left) and **Ac-AKAAT(OGlcNAc)AKAAAAKAAGY-NH<sub>2</sub>** (right); peptides were dissolved in 10 mM phosphate buffer (pH 7.0) containing 25 mM KF. Bottom left: CD spectrum of **Ac-AKAAT(OPO<sub>3</sub>H<sup>-</sup>)AKAAAAKAAGY-NH<sub>2</sub>** in 10 mM phosphate buffer (pH 4.0) containing 25 mM KF. Bottom right: CD spectrum of **Ac-AKAAT(OPO<sub>3</sub><sup>2-</sup>)AKAAAAKAAGY-NH<sub>2</sub>** in 10 mM phosphate buffer (pH 8.0) containing 25 mM KF.

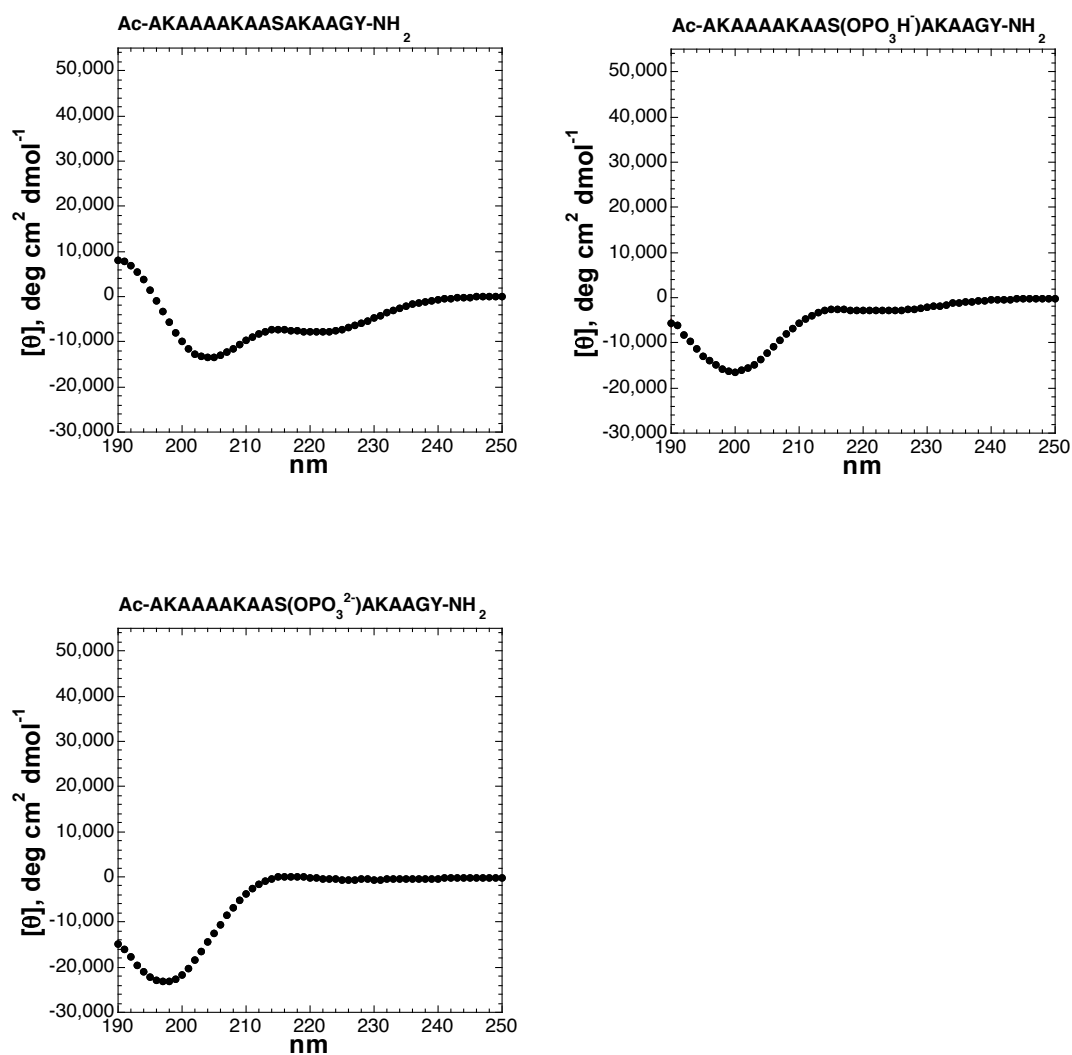


**Figure 1.28:** CD spectra of peptides with serine and serine modifications at residue 10. Top left: CD spectrum of **Ac-AKAAAAKAASAKAAGY-NH<sub>2</sub>** in 10 mM phosphate buffer (pH 7.0) containing 25 mM KF. Top right: CD spectrum of **Ac-AKAAAAKAAS(OPO<sub>3</sub>H<sup>-</sup>)AKAAGY-NH<sub>2</sub>** in 10 mM phosphate buffer (pH 4.0) containing 25 mM KF. Bottom middle: CD spectrum of **Ac-AKAAAAKAAS(OPO<sub>3</sub><sup>2-</sup>)AKAAGY-NH<sub>2</sub>** in 10 mM phosphate buffer (pH 8.0) containing 25 mM KF.

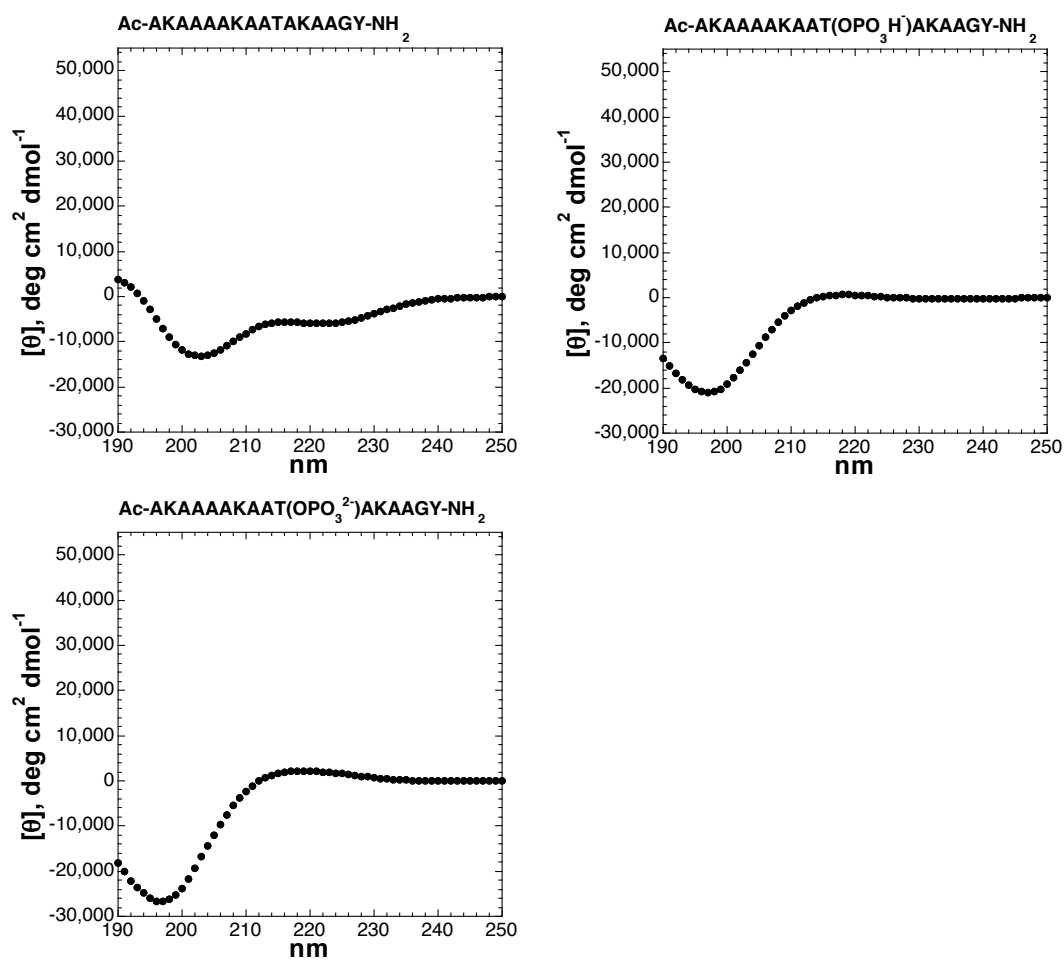


**Figure 1.29:** CD spectra of peptides with threonine and threonine modifications at residue 10. Top left: CD spectrum of **Ac-AKAAAAKAATAKAAGY-NH<sub>2</sub>** in 10 mM phosphate buffer (pH 7.0) containing 25 mM KF. Top right: CD spectrum of **Ac-AKAAAAKAAT(OPO<sub>3</sub>H)AKAAGY-NH<sub>2</sub>** in 10 mM phosphate buffer (pH 4.0) containing 25 mM KF. Bottom middle: CD spectrum of **Ac-AKAAAAKAAT(OPO<sub>3</sub><sup>2-</sup>)AKAAGY-NH<sub>2</sub>** in 10 mM phosphate buffer (pH 8.0) containing 25 mM KF.

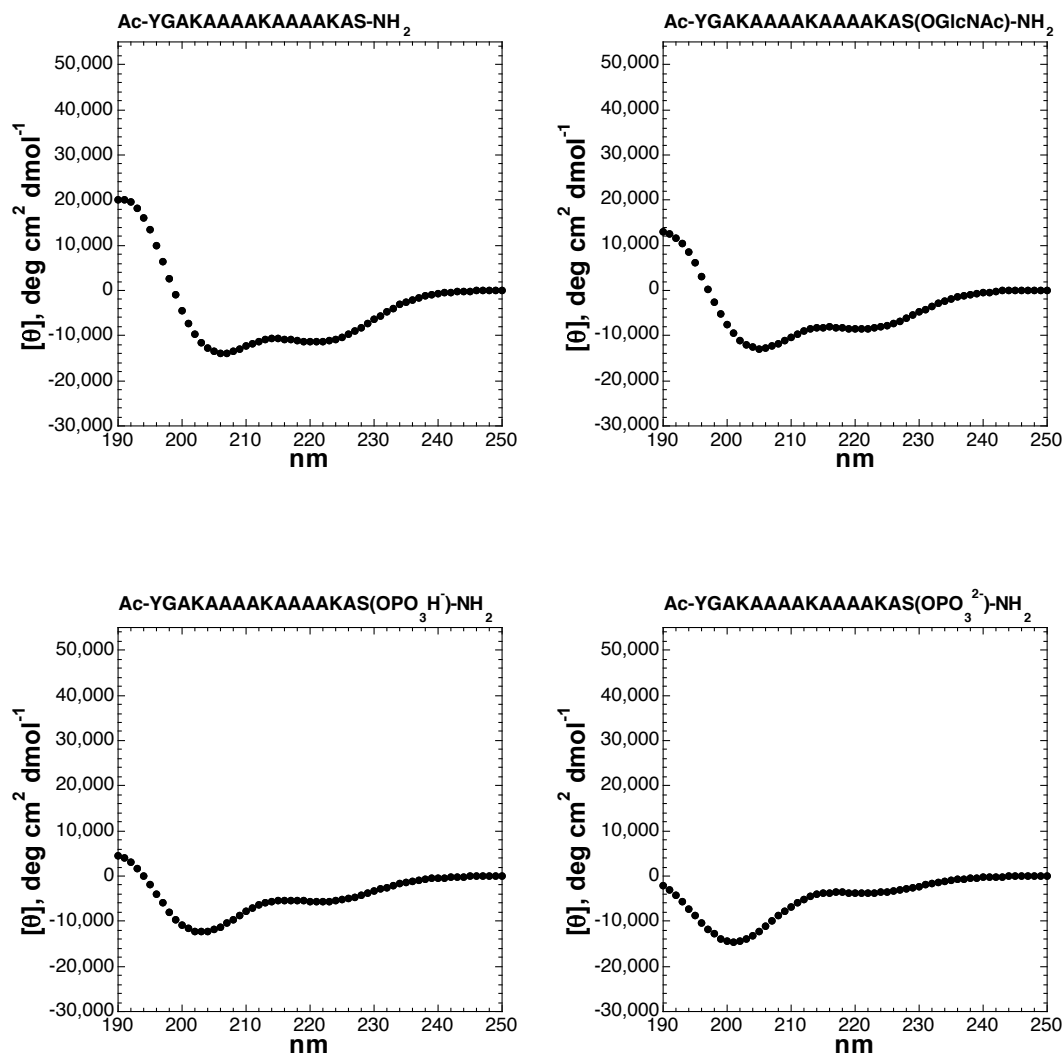


**Figure 1.30:** CD spectra of peptides with serine and serine modifications at residue 14. Top: CD spectra of  $\text{Ac-YGAKAAAAKAAAAKAS-NH}_2$  (left) and  $\text{Ac-YGAKAAAAKAAAAKAS(OGlcNAc)-NH}_2$  (right); peptides were dissolved in 10 mM phosphate buffer (pH 7.0) containing 25 mM KF. Bottom left: CD spectrum of  $\text{Ac-YGAKAAAAKAAAAKAS(OPO}_3\text{H}^-)\text{-NH}_2$  in 10 mM phosphate buffer (pH 4.0) containing 25 mM KF. Bottom right: CD spectrum of  $\text{Ac-YGAKAAAAKAAAAKAS(OPO}_3^{2-})\text{-NH}_2$  in 10 mM phosphate buffer (pH 8.0) containing 25 mM KF.

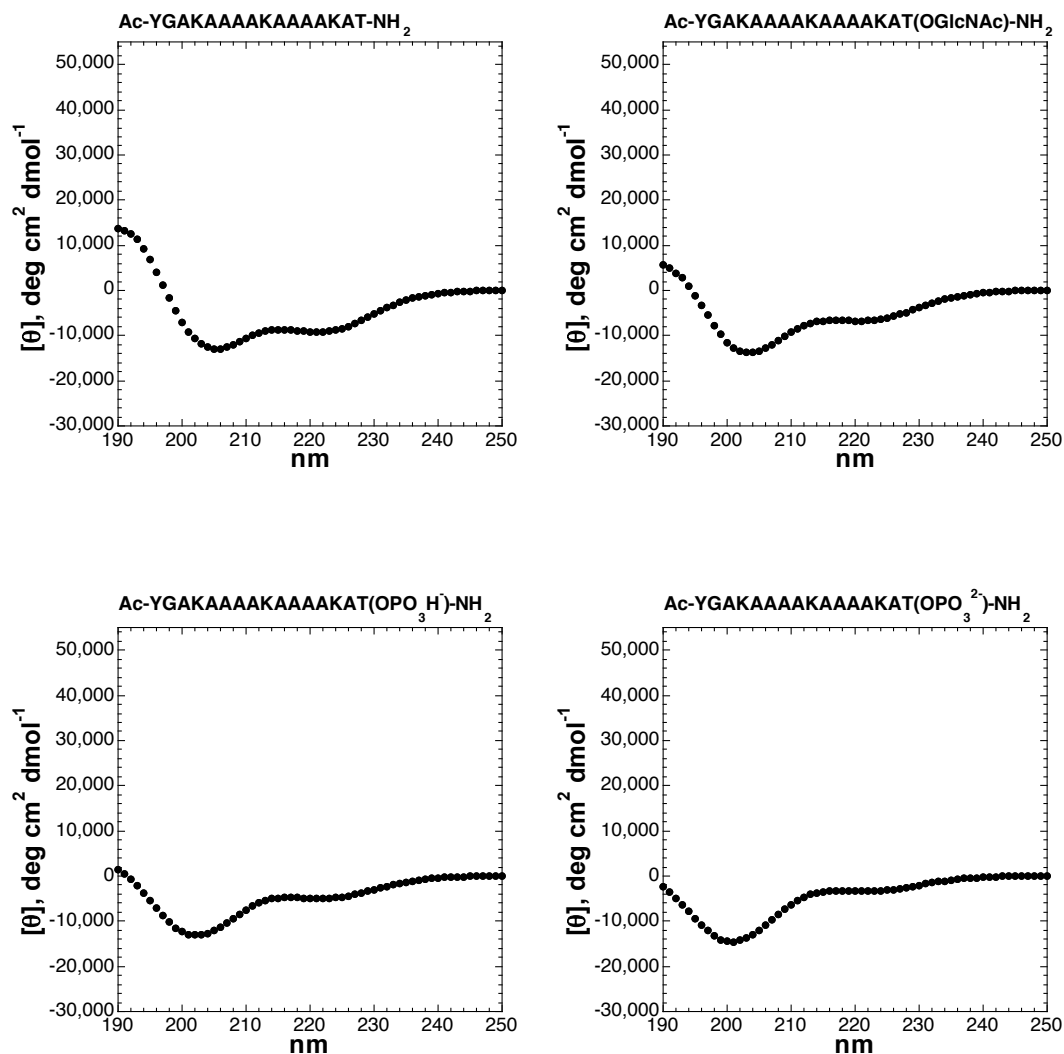


**Figure 1.31:** CD spectra of peptides with threonine and threonine modifications at residue 14. Top: CD spectra of **Ac-YGAKAAAAKAAAAKAT-NH<sub>2</sub>** (left) and **Ac-YGAKAAAAKAAAAKAT(OGlcNAc)-NH<sub>2</sub>** (right); peptides were dissolved in 10 mM phosphate buffer (pH 7.0) containing 25 mM KF. Bottom left: CD spectrum of **Ac-YGAKAAAAKAAAAKAT(OPO<sub>3</sub>H<sup>-</sup>)-NH<sub>2</sub>** in 10 mM phosphate buffer (pH 4.0) containing 25 mM KF. Bottom right: CD spectrum of **Ac-YGAKAAAAKAAAAKAT(OPO<sub>3</sub><sup>2-</sup>)-NH<sub>2</sub>** in 10 mM phosphate buffer (pH 8.0) containing 25 mM KF.

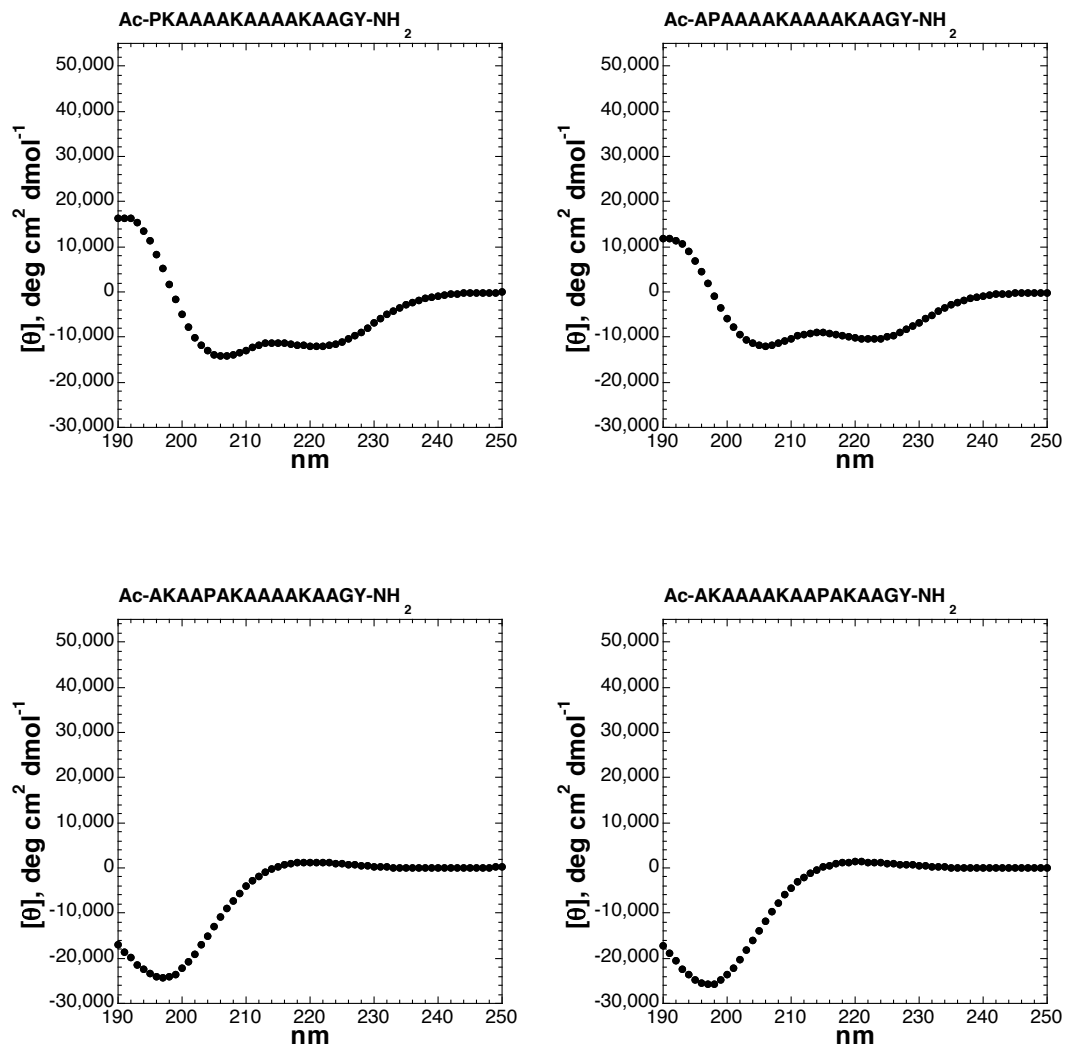


**Figure 1.32:** CD spectra of peptides with proline at residue 1, 2, 5, 10. Top left: CD spectrum of **Ac-PKAAAAKAAAAKAAGY-NH<sub>2</sub>**; top right: CD spectrum of **Ac-APAAAAKAAAAKAAGY-NH<sub>2</sub>**; bottom left: CD spectrum of **Ac-AKAAPAKAAAAKAAGY-NH<sub>2</sub>**; bottom right: CD spectrum of **Ac-AKAAAAKAAPAKAAGY-NH<sub>2</sub>**; peptides were dissolved in 10 mM phosphate buffer (pH 7.0) containing 25 mM KF.

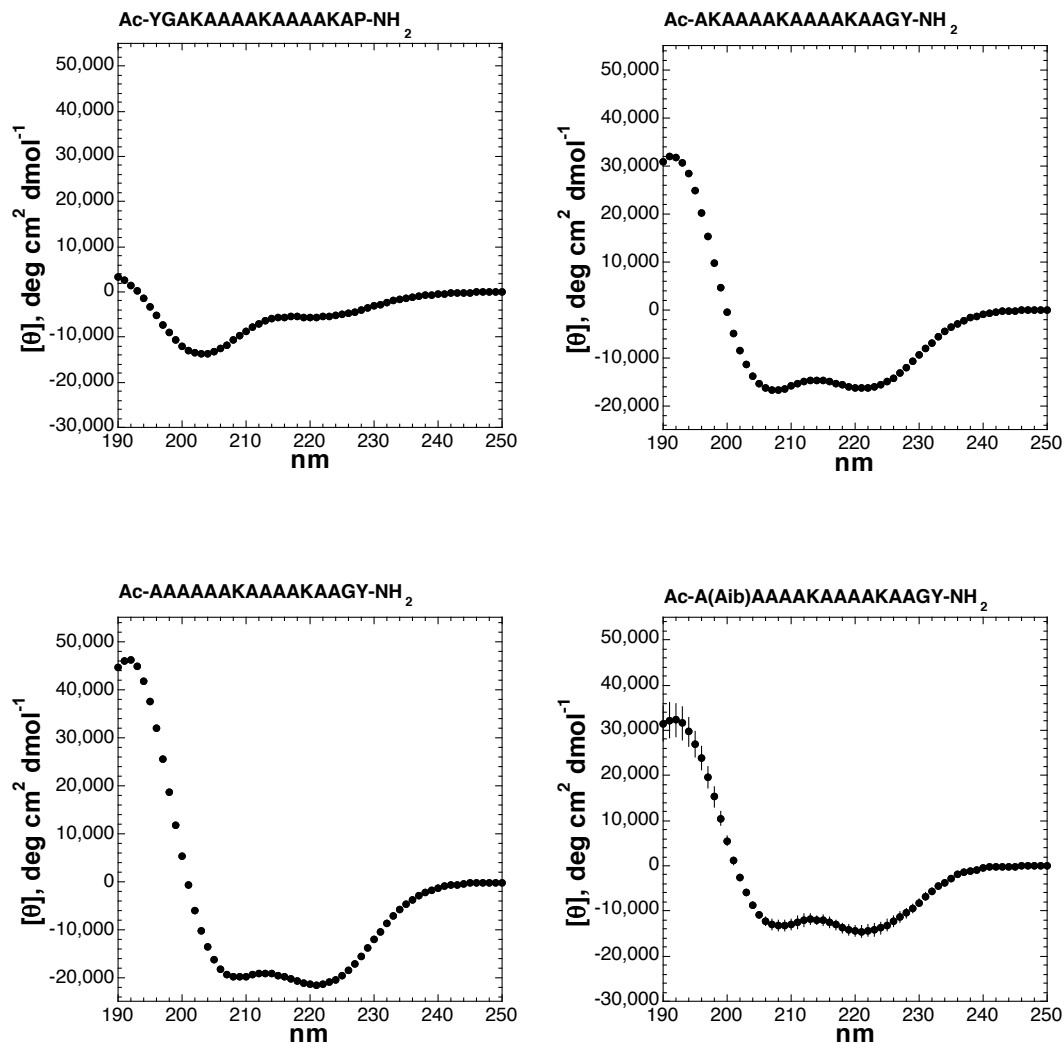


**Figure 1.33:** CD spectra of peptides proline at residue 14; alanine at residue 1, and 2; Aib at residue 2. Top left: CD spectrum of Ac-YGAKAAAAKAAAAKAP-NH<sub>2</sub>; top right: CD spectrum of AKAAAAKAAAAKAAGY-NH<sub>2</sub>; bottom left: CD spectrum of Ac-AAAAAKAAAAKAAGY-NH<sub>2</sub>; bottom right: CD spectrum of Ac-A(Aib)AAAAKAAAAKAAGY-NH<sub>2</sub> (12.5 mM); peptides were dissolved in 10 mM phosphate buffer (pH 7.0) containing 25 mM KF.

### CD spectra in 30% TFE/H<sub>2</sub>O

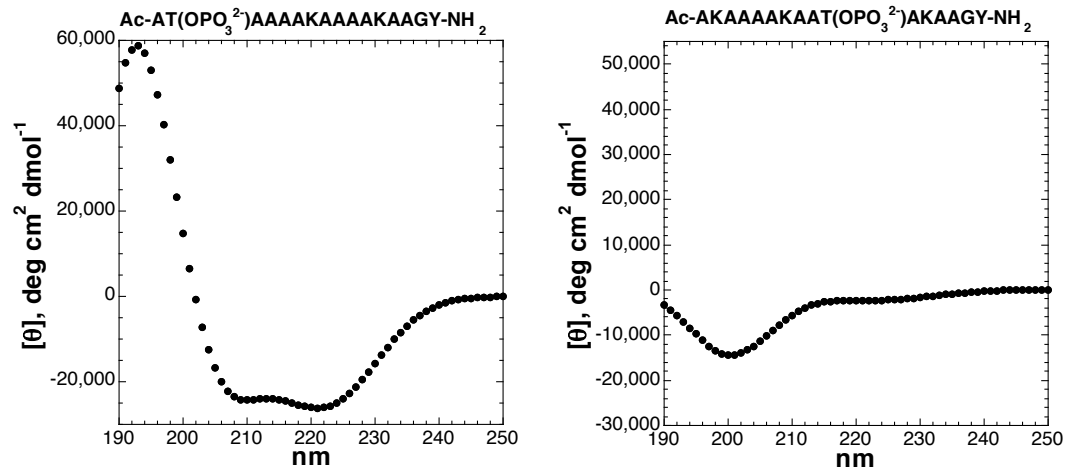


**Figure 1.34:** CD spectra of peptides with phosphothreonine at residue 2 or 10 in 30% TFE. Left: CD spectrum of Ac-AT(OPO<sub>3</sub><sup>2-</sup>)AAAAKAAAKAAGY-NH<sub>2</sub>; right: CD spectrum of AKAAAAKAAT(OPO<sub>3</sub><sup>2-</sup>)AKAAGY-NH<sub>2</sub>; peptides were dissolved in 10 mM phosphate buffer (pH 8.0) containing 25 mM KF and 30% TFE.

### CD spectra in the absence and presence of MgCl<sub>2</sub>

All experiments herein were conducted in the absence of MgCl<sub>2</sub> except those involving phosphatase. CD experiments were conducted in the absence and presence of MgCl<sub>2</sub> to determine the effects of Mg<sup>2+</sup> on the structure of peptides containing a phosphorylated threonine residue. The data indicate that there are no apparent effects of Mg<sup>2+</sup> on the structure of a peptide containing a phosphorylated threonine residue.

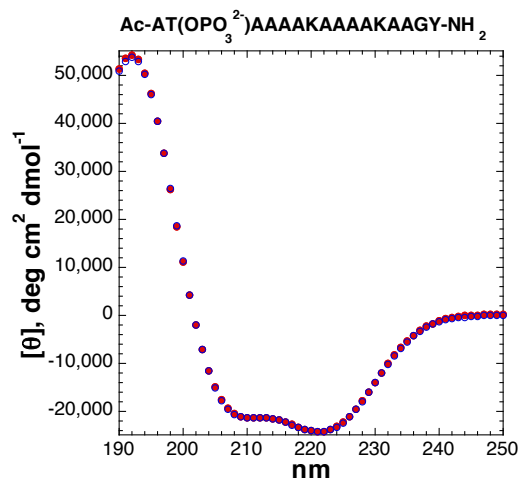


**Figure 1.35:** CD spectra of peptides in the absence and presence of MgCl<sub>2</sub>. CD spectra of Ac-AT(OPO<sub>3</sub><sup>2-</sup>)AAAAKAAAAKAAGY-NH<sub>2</sub>: red circles: 0 mM MgCl<sub>2</sub>; blue circles: 2 mM MgCl<sub>2</sub>. Peptides were dissolved in 10 mM aqueous phosphate buffer (pH 8.0) containing 25 mM KF.

## Temperature-dependent CD spectra

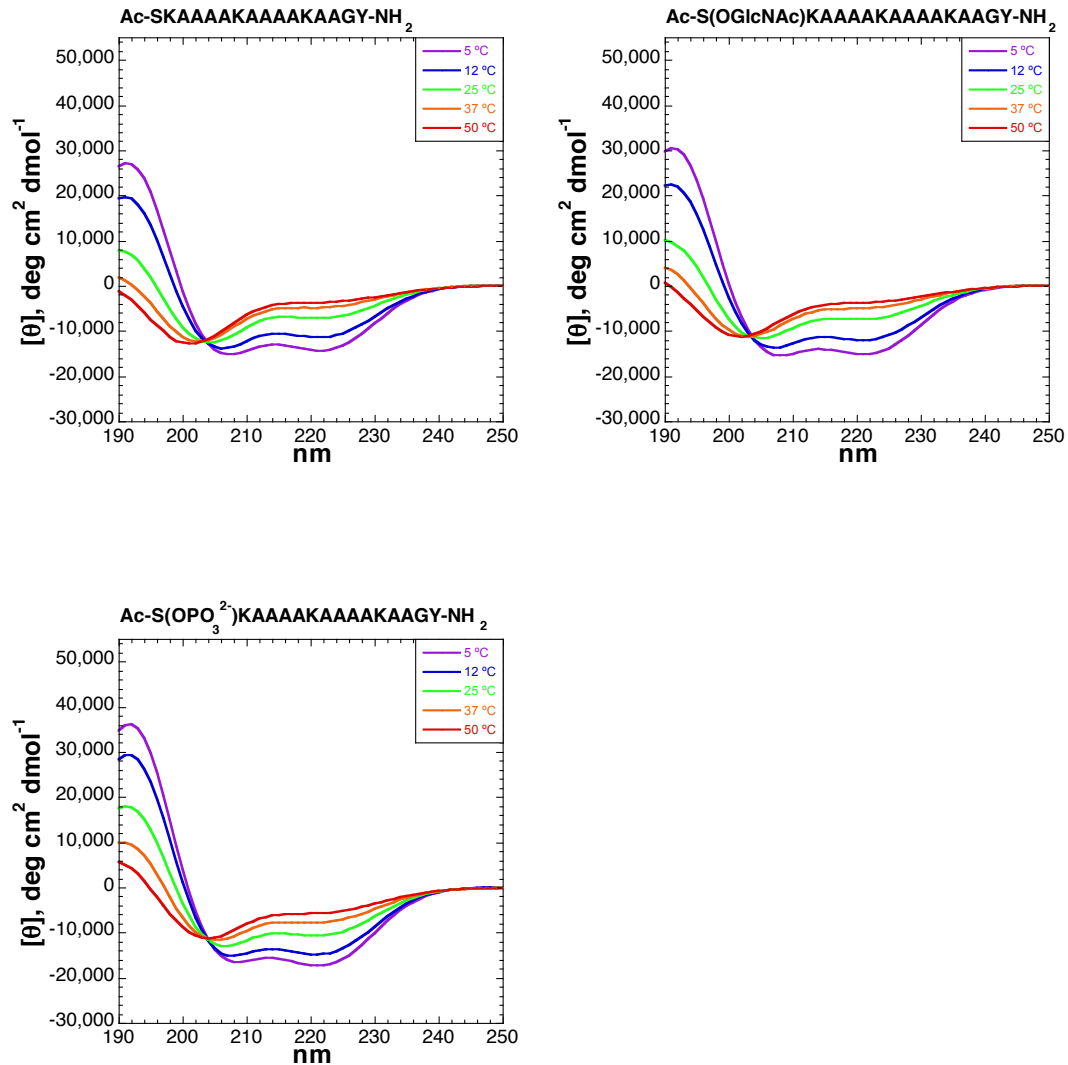


**Figure 1.36:** Temperature-dependent CD of peptides containing serine and serine modifications. Top: CD spectra of  $\text{Ac-SKAAAAKAAAAKAAGY-NH}_2$  (left) and  $\text{Ac-S(OGlcNAc)KAAAAKAAAAKAAGY-NH}_2$  (right); peptides were dissolved in 10 mM aqueous phosphate buffer (pH 7.0) containing 25 mM KF. Bottom: CD spectrum of  $\text{Ac-S(OPO}_3^{2-})\text{KAAAAKAAAAKAAGY-NH}_2$  in 10 mM aqueous phosphate buffer (pH 8.0) containing 25 mM KF. All peptides exhibit an isodichroic point at 204 nm.

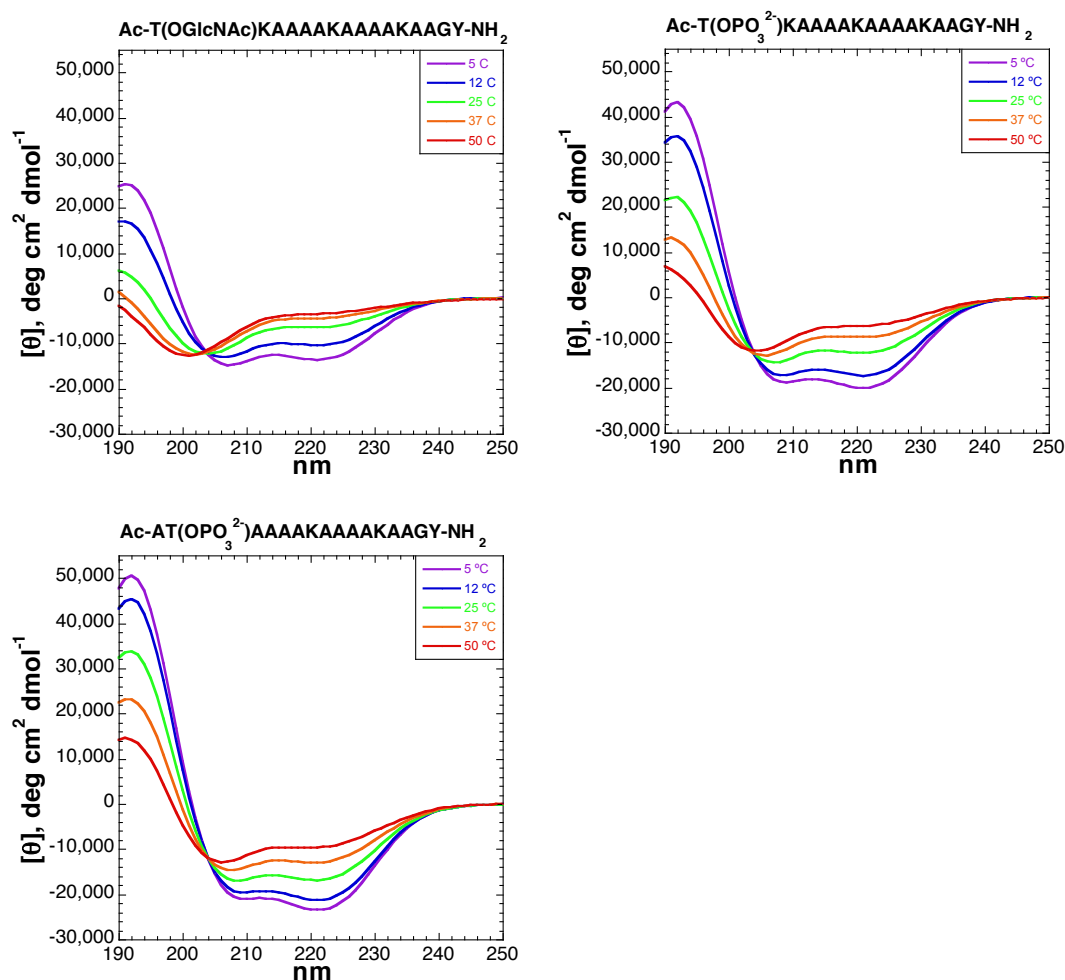


**Figure 1.37:** Temperature-dependent CD of peptides containing threonine and threonine modifications. Top left: CD spectrum of **Ac-T(OGlcNAc)KAAAAKAAAAKAAGY-NH<sub>2</sub>** in 10 mM aqueous phosphate buffer (pH 7.0) containing 25 mM KF. Top right: CD spectrum of **Ac-T(OPO<sub>3</sub><sup>2-</sup>)KAAAAKAAAAKAAGY-NH<sub>2</sub>**; bottom left: CD spectrum of **Ac-AT(OPO<sub>3</sub><sup>2-</sup>)AAAAKAAAAKAAGY-NH<sub>2</sub>**; peptides were dissolved in 10 mM aqueous phosphate buffer (pH 8.0) containing 25 mM KF. All peptides exhibit an isodichroic point at 204 nm.

## Dephosphorylation of the peptide Ac-AT(OPO<sub>3</sub><sup>2-</sup>)AAAAKAAAAKAAGY-NH<sub>2</sub> by Antarctic phosphatase: CD spectra

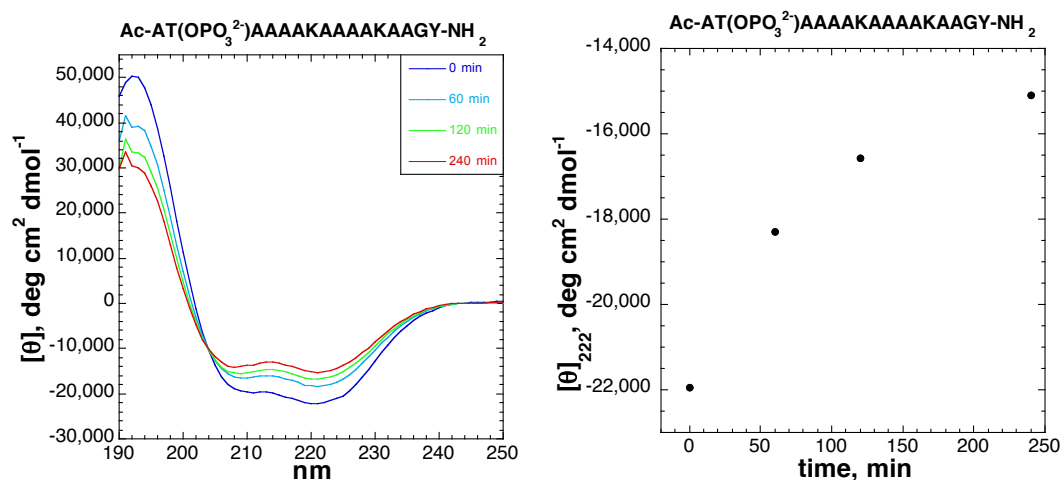


**Figure 1.38:** Phosphatase assay for peptides containing phosphothreonine at residue 2. Top: CD spectra of a solution containing 25  $\mu$ M peptide Ac-AT(OPO<sub>3</sub><sup>2-</sup>)AAAAKAAAAKAAGY-NH<sub>2</sub> in buffer (40 mM Tris-HCl (pH 8.0), 25 mM KF, 1 mM MgCl<sub>2</sub>, and 100  $\mu$ M ZnCl<sub>2</sub>) at 0.5 °C as a function of time of incubation with phosphatase. Data were collected at initial time (dark blue). To this solution were added 10 units (2  $\mu$ L) of Antarctic phosphatase and the solution incubated in a 37 °C water bath. The total duration of incubation was 240 min. CD spectra were collected at time points of 60 min (light blue), 120 min (green), and 240 min (red). At each time point, the sample was cooled to 0.5 °C for 5 min and data were collected. The sample was then placed back in the water bath until the next time point. Bottom: Mean residue ellipticity at 222 nm as a function of time incubated with phosphatase.

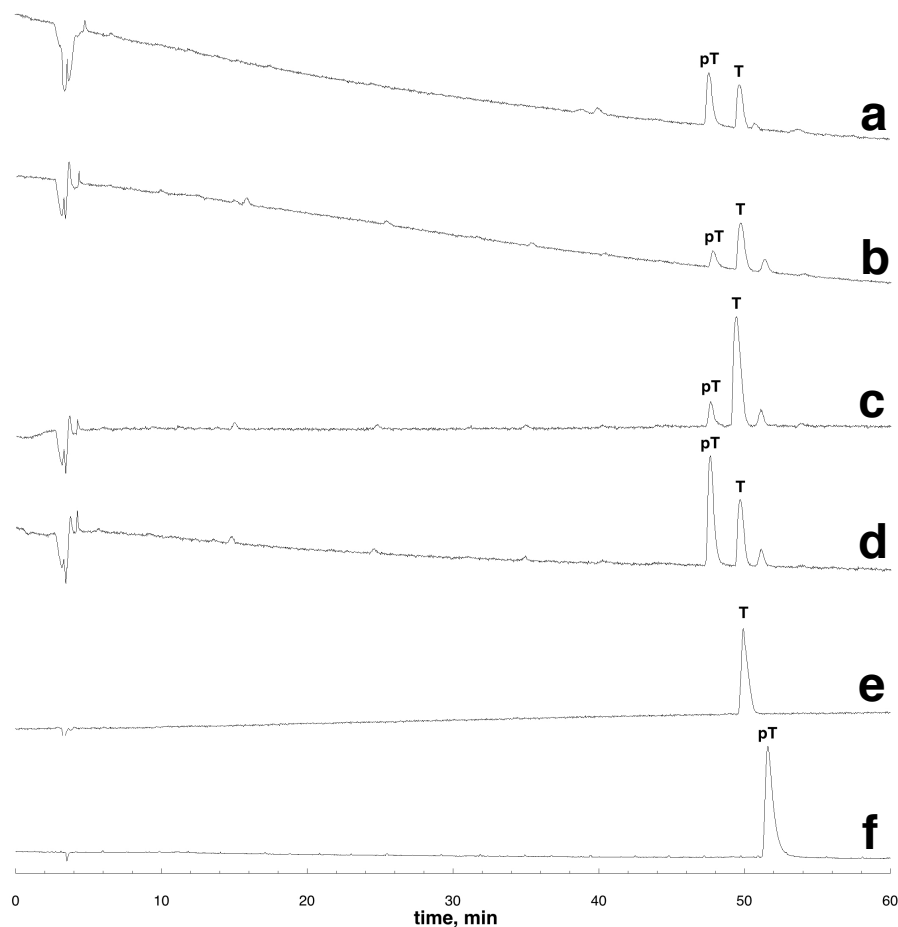


**Figure 1.39:** HPLC analysis of dephosphorylation by phosphatase for phosphothreonine at residue 2. pT indicates phosphorylated peptide, T indicates unmodified peptide. **(a)** Peptide was incubated at 37 °C with 10 units of Antarctic phosphatase for 60 min; pT (56%), T (44%). **(b)** Peptide was incubated at 37 °C with 10 units of Antarctic phosphatase for 240 min; pT (24%), T (76%). **(c)** Coinjection of **(b)** with Ac-ATAAAKAAAAKAAGY-NH<sub>2</sub>. **(d)** Coinjection of **(b)** with Ac-AT(OPO<sub>3</sub><sup>2-</sup>)AAAAKAAAAKAAGY-NH<sub>2</sub>. **(e)** Reinjection of Ac-ATAAAKAAAAKAAGY-NH<sub>2</sub>. HPLC experiments in **(a)**-**(e)** were conducted using a linear gradient of 0-35% buffer B in buffer A over 60 minutes. **(f)** Reinjection of Ac-AT(OPO<sub>3</sub><sup>2-</sup>)AAAAKAAAAKAAGY-NH<sub>2</sub> using a linear gradient of 0-30% buffer B in buffer A over 60 minutes.

## Dephosphorylation of the peptide Ac-AKAAAAKAAT(OPO<sub>3</sub><sup>2-</sup>)AKAAGY-NH<sub>2</sub> by Antarctic phosphatase: CD spectra

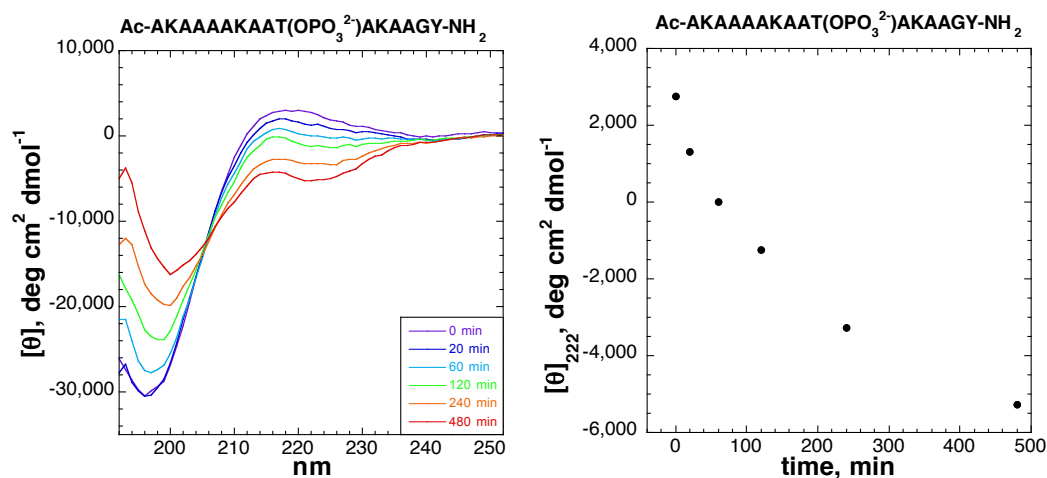


**Figure 1.40:** Phosphatase assay for peptides containing phosphothreonine at residue 10. Top: CD spectra of a solution containing 25  $\mu\text{M}$  peptide Ac-AKAAAAKAAT(OPO<sub>3</sub><sup>2-</sup>)AKAAGY-NH<sub>2</sub> in buffer (40 mM Tris-HCl (pH 8.0), 25 mM KF, 1 mM MgCl<sub>2</sub>, and 100  $\mu\text{M}$  ZnCl<sub>2</sub>) at 0.5 °C as a function of time of incubation with phosphatase. Data were collected at initial time (purple). To this solution were added 40 units (8  $\mu\text{L}$ ) of Antarctic phosphatase and the solution incubated in a 37 °C water bath. The total duration of incubation was 480 min. CD spectra were collected at time points of 20 min (dark blue), 60 min (light blue), 120 min (green), 240 min (orange), and 480 min (red). At each time point, the sample was cooled to 0.5 °C for 5 min and data were collected. The sample was then placed back in the water bath until the next time point. Bottom: Mean residue ellipticity at 222 nm as a function of time incubated with phosphatase.

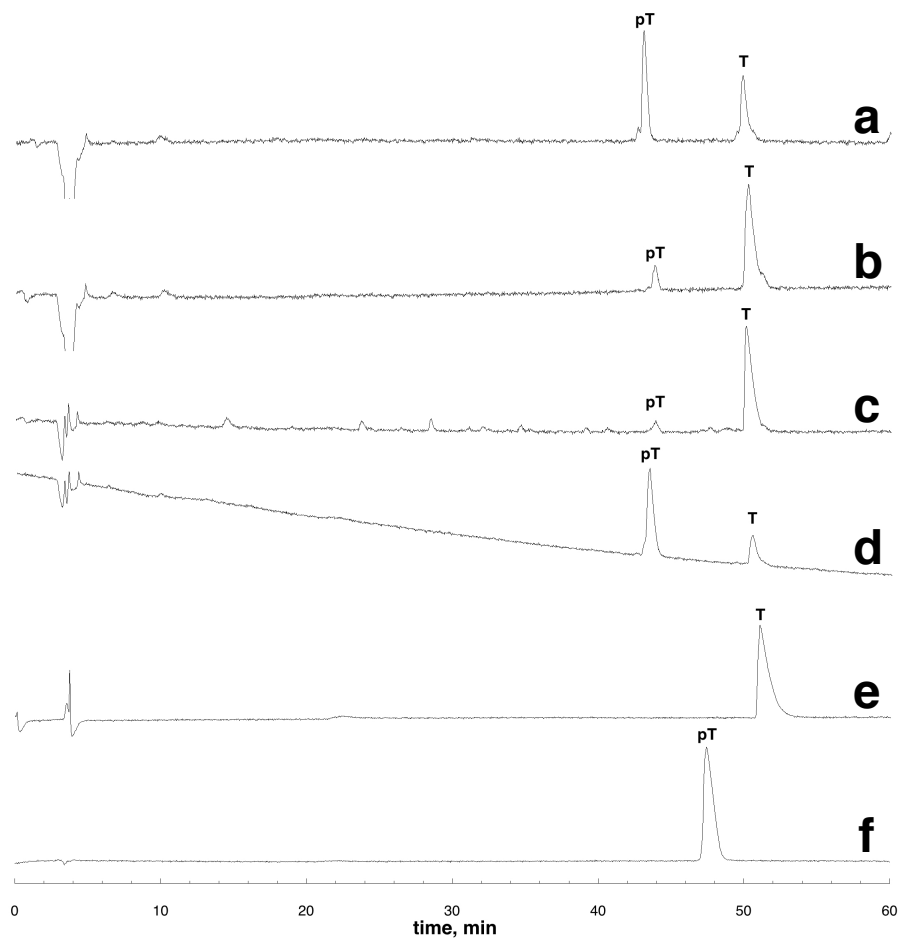


**Figure 1.41:** HPLC analysis of dephosphorylation by phosphatase for phosphothreonine at residue 10. HPLC analysis of dephosphorylation by phosphatase. pT indicates phosphorylated peptide, T indicates unmodified peptide. (a) Peptide was incubated at 37 °C with 40 units of Antarctic phosphatase for 120 min; pT (57%), T (43%). (b) Peptide was incubated at 37 °C with 40 units of Antarctic phosphatase for 480 min; pT (10%), T (90%). (c) Co-injection of (b) with **Ac-AKAAAAKAATAKAAGY-NH<sub>2</sub>**. (d) Co-injection of (b) with **Ac-AKAAAAKAAT(OPO<sub>3</sub><sup>2-</sup>)AKAAGY-NH<sub>2</sub>**. (e) Reinjection of **Ac-AKAAAAKAATAKAAGY-NH<sub>2</sub>**. HPLC experiments in (a)-(e) were conducted using isocratic 100% buffer A over 10 minutes followed by a linear gradient of 0-30% buffer B in buffer A over an additional 50 minutes. (f) Reinjection of **Ac-AKAAAAKAAT(OPO<sub>3</sub><sup>2-</sup>)AKAAGY-NH<sub>2</sub>** using isocratic 100% buffer A over 10 minutes followed by a linear gradient of 0-25% buffer B in buffer A over an additional 50 minutes.

## NMR spectroscopy

NMR spectra of peptides were collected at 278 K or 298 K on a Brüker AVC 600 MHz NMR spectrometer equipped with a triple resonance cryoprobe or a TXI probe. Peptides were dissolved in a solution containing 5 mM phosphate buffer (pH 4.0, 7.2, or 8.0) and 25 mM NaCl in 90% H<sub>2</sub>O/10% D<sub>2</sub>O. The pH of each individual sample was recorded and adjusted as necessary using dilute HCl or NaOH. All NMR spectra were internally referenced with 100  $\mu$ M TSP. 1-D NMR spectra were collected with a Watergate pulse sequence and a relaxation delay of 3 s. Coupling constants between the amide and  $\alpha$ -protons ( $^3J_{\alpha N}$ ) were determined directly from the 1-D spectra. Errors in  $^3J_{\alpha N}$  are estimated to be  $\leq 0.2$  Hz. TOCSY NMR spectra were collected with a Watergate TOCSY pulse sequence, sweep widths of 6009 Hz in  $t_1$  and  $t_2$ ,  $400 \times 2048$  complex data points, 8 scans per  $t_1$  increment, a relaxation delay of 1.5 s, and a TOCSY mixing time of 60 ms.

$^1\text{H}$ - $^{13}\text{C}$  HSQC (heteronuclear single quantum coherence) spectra were recorded for both phosphorylated and unmodified peptides **Ac-ATAAAKAAA KAAGY-NH<sub>2</sub>** and **Ac-AKAAA KAATAKAAGY-NH<sub>2</sub>**. The peptides were dissolved in 5 mM phosphate buffer (pH 8.0 for phosphorylated peptides or pH 4.0 for unmodified peptides) in D<sub>2</sub>O with 25 mM NaCl and 100  $\mu$ M TSP. NMR spectra were acquired on samples with natural abundance  $^{13}\text{C}$ , using sweep widths of 20833 and 5388 Hz in  $t_1$  and  $t_2$ , respectively,  $400 \times 2048$  complex data points, 24 scans per  $t_1$  increment, and a relaxation delay of 2.0 s.

$^{31}\text{P}$  NMR spectroscopy was performed on a Brüker DRX 400 MHz NMR spectrometer equipped with a BBO probe. The peptides were dissolved in 5 mM phosphate buffer (pH 8.0) with 25 mM NaCl in D<sub>2</sub>O or 30% TFE/D<sub>2</sub>O.  $^{31}\text{P}$  spectra were collected with 65536 data points and a relaxation delay of 2 or 5 seconds. An

exponential multiplication with 1 Hz of line broadening was applied prior to Fourier transform. The NMR spectra were externally referenced by placing a capillary filled with  $\text{H}_3\text{PO}_4$  in an NMR tube containing phosphate buffer and referencing the  $\text{H}_3\text{PO}_4$  peak to 0 ppm.

## $^1\text{H}$ NMR spectra of all peptides (amide region (stacked spectra))

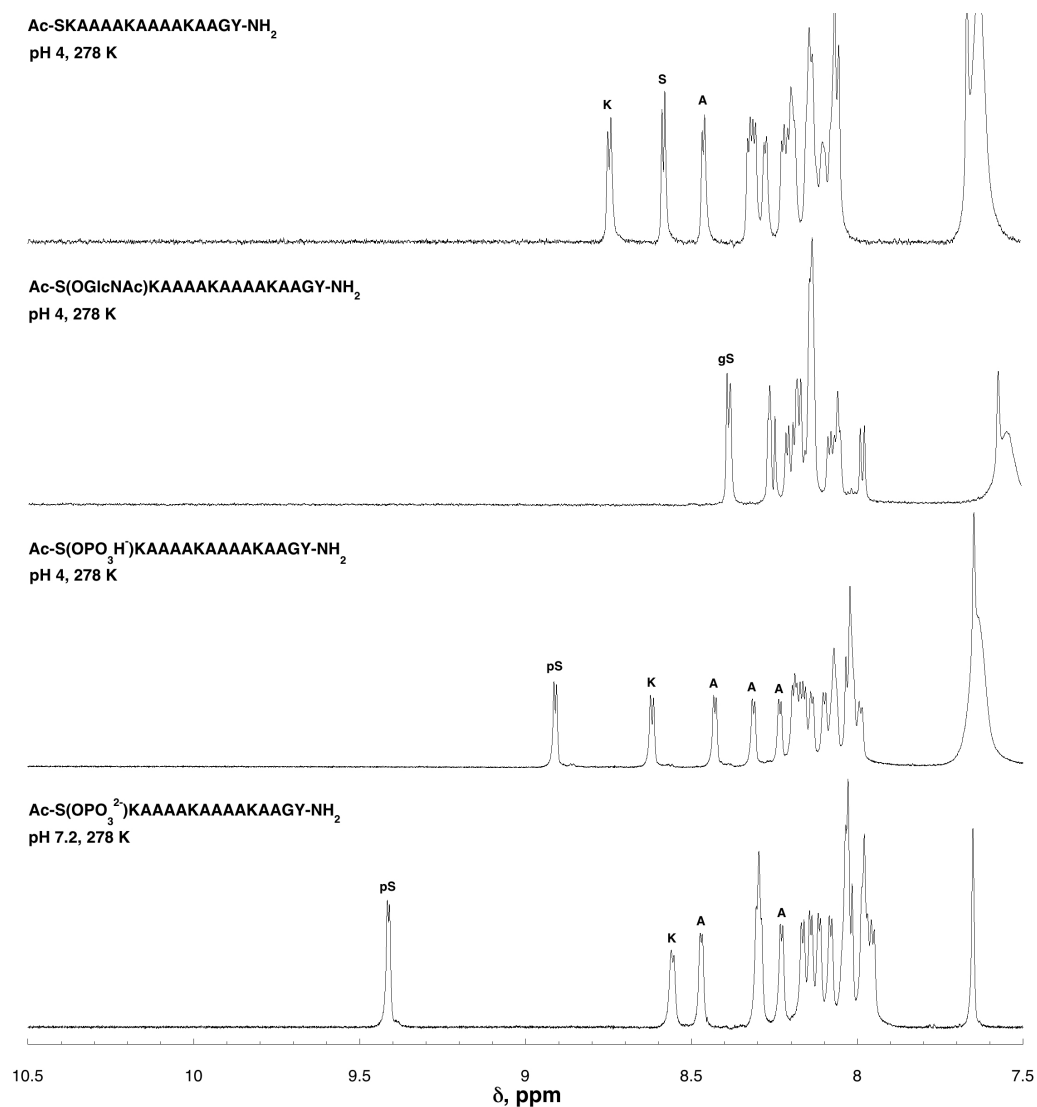


**Figure 1.42:**  $^1\text{H}$  NMR spectra (amide region) of Ac-SKAAAAKAAAAKAAGY-NH<sub>2</sub> peptides with serine modifications: unmodified Ser(free hydroxyl), Ser(OGlcNAc), Ser(OPO<sub>3</sub>H<sup>-</sup>), and Ser(OPO<sub>3</sub><sup>2-</sup>). pS indicates phosphorylated serine residue. gS indicates Ser(OGlcNAc) residue. Peptides were dissolved in 5 mM phosphate buffer (pH 4.0 or 7.2) containing 25 mM NaCl in 90% H<sub>2</sub>O/10% D<sub>2</sub>O. Data were collected at 278 K.

Peptide	$\delta$ , H <sup>N</sup>	<sup>3</sup> J $\alpha$ <sub>N</sub>	$\delta$ , H $\alpha$	$\delta$ , H $\beta$
Ac- <b>Ser</b> KAAAAKAAAAKAAGY-NH <sub>2</sub>				
Ser	8.58	5.1	4.34	3.97, 3.90
Lys	8.74	5.7	4.24	1.82
	8.20	n.d. <sup>a</sup>	4.15	1.85
	8.06	n.d.	4.15	1.82
Ala	8.46	4.2	4.22	1.39
	8.32	n.d.	4.17	1.43
	8.30	n.d.	4.24	1.46
	8.27	4.4	4.20	1.46
	8.22	n.d.	4.25	1.46
	8.19	n.d.	4.24	1.43
	8.14	n.d.	4.22	1.43
	8.10	n.d.	4.26	1.40
	8.07	n.d.	4.15	1.40
	8.05	n.d.	4.18	1.43
Gly	8.13	n.d.	3.93, 3.84	n.a. <sup>b</sup>
Tyr	8.06	n.d.	4.54	3.09, 2.93
Ac- <b>Ser(OGlcNAc)</b> KAAAAKAAAAKAAGY-NH <sub>2</sub>				
GlcNAc	8.43	9.8	n.a.	n.a.
Ser	8.62	3.3	4.33	4.11, 3.95
Lys	8.54	5.1	4.21	1.86
	8.19	n.d.	4.16	1.90
	8.03	n.d.	4.16	1.86
Ala	8.47	4.0	4.24	1.43
	8.29	n.d.	4.23	1.47
	8.29	n.d.	4.23	1.47
	8.26	4.0	4.20	1.47
	8.21	n.d.	4.25	1.47
	8.16	n.d.	4.24	1.46
	8.13	n.d.	4.23	1.46
	8.12	n.d.	4.22	1.45
	8.07	n.d.	4.26	1.42
	8.05	n.d.	4.20	1.49
Gly	8.11	n.d.	3.94, 3.85	n.a.
Tyr	8.05	n.d.	4.54	3.10, 2.96

**Table 1.21:** Summary of <sup>1</sup>H NMR data for peptides with serine and Ser(OGlcNAc) at residue 1. Data were collected in 5 mM phosphate buffer (pH 4.0) containing 25 mM NaCl. <sup>a</sup> n.d. = not determined due to spectral overlap. <sup>b</sup> n.a. = not applicable.

Peptide	$\delta$ , H <sup>N</sup>	<sup>3</sup> J $\alpha_N$	$\delta$ , H $\alpha$	$\delta$ , H $\beta$
Ac- <i>Ser(OPO<sub>3</sub>H)</i> KAAAAKAAAAKAAGY-NH <sub>2</sub>				
Ser	8.91	4.4	4.40	4.20, 4.17
Lys	8.62	5.5	4.26	1.85
	8.18	n.d. <sup>a</sup>	4.15	1.90
	7.99	n.d.	4.13	1.86
Ala	8.43	4.4	4.25	1.44
	8.31	4.6	4.23	1.49
	8.23	4.7	4.19	1.48
	8.19	n.d.	4.16	1.47
	8.16	n.d.	4.24	1.49
	8.13	n.d.	4.23	1.48
	8.10	n.d.	4.22	1.48
	8.07	n.d.	4.20	1.44
	8.02	n.d.	4.27	1.41
	8.01	n.d.	4.18	1.44
Gly	8.07	n.d.	3.93, 3.86	n.a. <sup>b</sup>
Tyr	8.02	n.d.	4.54	3.11, 2.95
Ac- <i>Ser(OPO<sub>3</sub><sup>2-</sup>)</i> KAAAAKAAAAKAAGY-NH <sub>2</sub>				
Ser	9.41	3.6	4.29	4.14, 4.08
Lys	8.56	5.4	4.26	1.88
	8.16	n.d.	4.13	1.92
	7.95	n.d.	4.13	1.89
Ala	8.47	4.2	4.24	1.46
	8.30	n.d.	4.24	1.50
	8.29	n.d.	4.17	1.48
	8.23	4.3	4.20	1.49
	8.14	4.7	4.26	1.50
	8.11	4.7	4.24	1.49
	8.08	4.3	4.23	1.49
	8.03	4.5	4.20	1.48
	7.98	n.d.	4.19	1.47
	7.97	n.d.	4.28	1.44
Gly	8.03	n.d.	3.95, 3.86	n.a.
Tyr	8.02	n.d.	4.55	3.11, 2.96

**Table 1.22:** Summary of <sup>1</sup>H NMR data for peptides with phosphoserine at residue 1. Data were collected in 5 mM phosphate buffer (pH 4.0 or 7.2) containing 25 mM NaCl. <sup>a</sup>n.d. = not determined due to spectral overlap. <sup>b</sup>n.a. = not applicable.

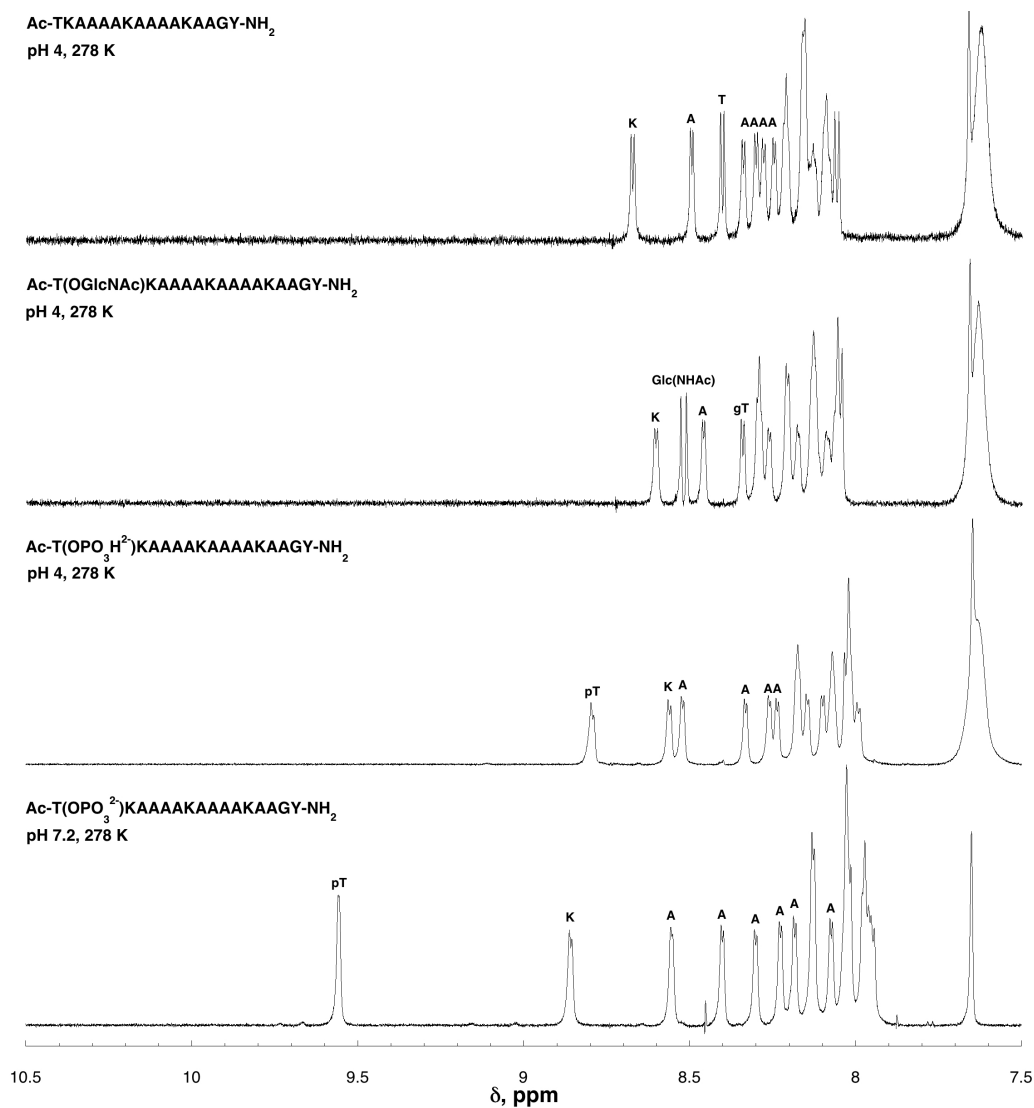


**Figure 1.43:** <sup>1</sup>H NMR spectra (amide region) of Ac-TKAAAKAAAAKAAGY-NH<sub>2</sub> peptides with threonine modifications: unmodified Thr(free hydroxyl), Thr(OGlcNAc), Thr(OPO<sub>3</sub>H<sup>-</sup>), and Thr(OPO<sub>3</sub><sup>2-</sup>). pT indicates phosphorylated threonine residue. gT indicates Thr(OGlcNAc) residue. Peptides were dissolved in 5 mM phosphate buffer (pH 4.0 or 7.2) containing 25 mM NaCl in 90% H<sub>2</sub>O/10% D<sub>2</sub>O. Data were collected at 278 K.

Peptide	$\delta$ , H <sup>N</sup>	<sup>3</sup> J $\alpha_N$	$\delta$ , H $\alpha$	$\delta$ , H $\beta$
Ac- <i>Thr</i> KAAAAKAAAAKAAGY-NH <sub>2</sub>				
Thr	8.40	6.2	4.25	4.19
Lys	8.68	5.6	4.22	1.83
	8.22	4.2	4.15	1.86
	8.08	n.d. <sup>a</sup>	4.15	1.83
Ala	8.50	4.3	4.23	1.40
	8.34	5.1	4.18	1.43
	8.30	5.0	4.24	1.46
	8.28	4.6	4.20	1.44
	8.25	n.d.	4.24	1.46
	8.21	n.d.	4.23	1.45
	8.16	n.d.	4.21	1.43
	8.16	n.d.	4.21	1.43
	8.13	n.d.	4.25	1.41
	8.09	n.d.	4.19	1.43
Gly	8.16	n.d.	3.92, 3.85	n.a. <sup>b</sup>
Tyr	8.06	n.d.	4.53	3.10, 2.95
Ac- <i>Thr(OGlcNAc)</i> KAAAAKAAAAKAAGY-NH <sub>2</sub>				
GlcNAc	8.52	9.9	n.a.	n.a.
Thr	8.34	5.1	4.18	4.26
Lys	8.60	5.1	4.20	1.84
	8.21	n.d.	4.16	1.89
	8.05	n.d.	4.16	1.85
Ala	8.47	4.2	4.22	1.42
	8.30	n.d.	4.26	1.48
	8.29	n.d.	4.18	1.46
	8.26	4.5	4.20	1.47
	8.21	n.d.	4.24	1.48
	8.18	n.d.	4.24	1.47
	8.13	n.d.	4.22	1.45
	8.12	n.d.	4.21	1.42
	8.09	n.d.	4.27	1.41
	8.07	n.d.	4.20	1.44
Gly	8.12	n.d.	3.94, 3.86	n.a.
Tyr	8.05	n.d.	4.53	3.11, 2.97

**Table 1.23:** Summary of <sup>1</sup>H NMR data for peptides with threonine and Thr(OGlcNAc) at residue 1. Data were collected in 5 mM phosphate buffer (pH 4.0) containing 25 mM NaCl. <sup>a</sup> n.d. = not determined due to spectral overlap. <sup>b</sup> n.a. = not applicable.

Peptide	$\delta$ , H <sup>N</sup>	<sup>3</sup> J $\alpha_N$	$\delta$ , H $\alpha$	$\delta$ , H $\beta$
Ac- <i>Thr(OPO<sub>3</sub>H)</i> KAAAAKAAAAKAAGY-NH <sub>2</sub>				
Thr	8.80	4.8	4.23	4.64
Lys	8.56	5.2	4.21	1.85
	8.18	n.d. <sup>a</sup>	4.15	1.90
	7.99	n.d.	4.14	1.87
Ala	8.53	4.5	4.23	1.44
	8.34	4.5	4.23	1.49
	8.26	3.9	4.16	1.46
	8.24	4.4	4.19	1.47
	8.17	n.d.	4.24	1.50
	8.15	n.d.	4.23	1.47
	8.10	n.d.	4.23	1.46
	8.07	n.d.	4.19	1.44
	8.02	n.d.	4.26	1.42
	8.02	n.d.	4.18	1.44
Gly	8.07	n.d.	3.93, 3.85	n.a. <sup>b</sup>
Tyr	8.03	n.d.	4.53	3.10, 2.95
Ac- <i>Thr(OPO<sub>3</sub><sup>2-</sup>)</i> KAAAAKAAAAKAAGY-NH <sub>2</sub>				
Thr	9.57	3.5	4.04	4.47
Lys	8.87	4.5	4.20	n.d.
	8.14	n.d.	4.15	1.94
	7.95	n.d.	4.14	1.89
Ala	8.56	3.8	4.23	1.45
	8.41	4.4	4.18	1.50
	8.31	4.2	4.27	1.51
	8.24	4.4	4.20	1.50
	8.19	4.6	4.27	1.51
	8.14	n.d.	4.26	1.50
	8.08	n.d.	4.22	1.50
	8.03	n.d.	4.20	1.47
	7.98	n.d.	4.18	1.47
	7.94	n.d.	4.28	1.44
Gly	8.04	n.d.	3.95, 3.86	n.a.
Tyr	8.03	n.d.	4.56	3.12, 2.97

**Table 1.24:** Summary of <sup>1</sup>H NMR data for peptides with phosphothreonine at residue 1. Data were collected in 5 mM phosphate buffer (pH 4.0 or 7.2) containing 25 mM NaCl. <sup>a</sup>n.d. = not determined due to spectral overlap. <sup>b</sup>n.a. = not applicable.

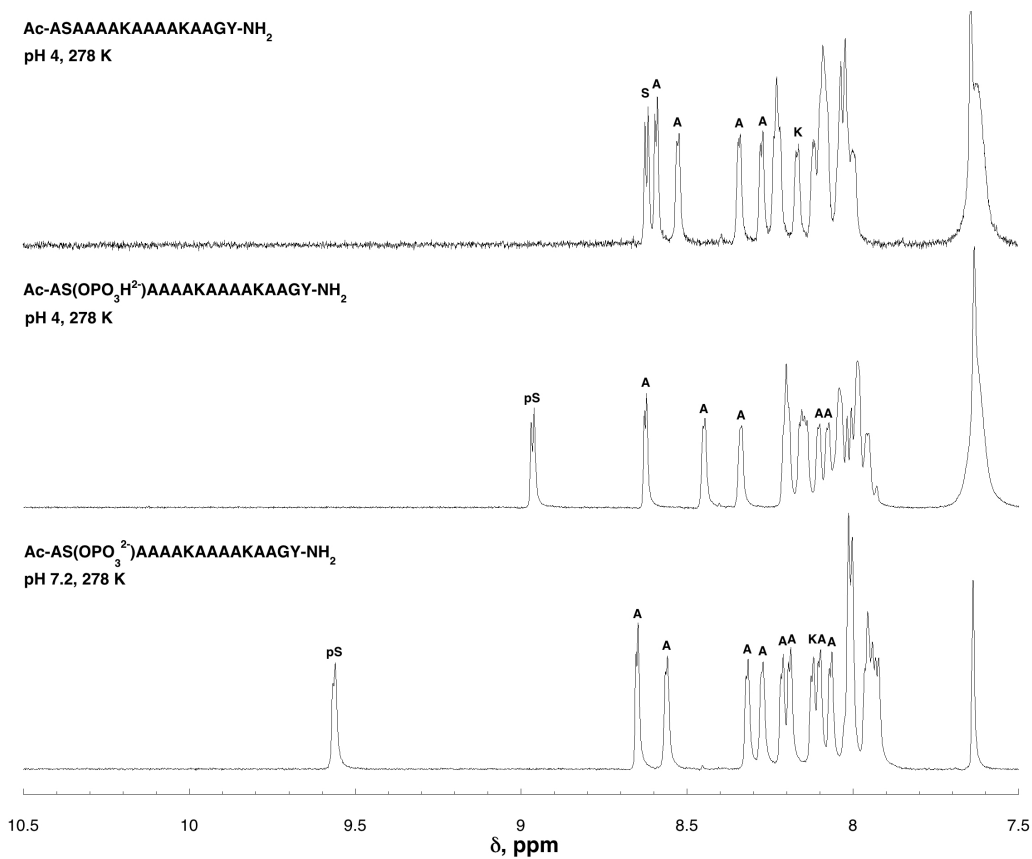


**Figure 1.44:** <sup>1</sup>H NMR spectra (amide region) of Ac-ASAAAAKAAAAKAAGY-NH<sub>2</sub> peptides with serine modifications: unmodified Ser(free hydroxyl), Ser(OPO<sub>3</sub>H<sup>-</sup>), and Ser(OPO<sub>3</sub><sup>2-</sup>). pS indicates phosphorylated serine residue. Peptides were dissolved in 5 mM phosphate buffer (pH 4.0 or 7.2) containing 25 mM NaCl in 90% H<sub>2</sub>O/10% D<sub>2</sub>O. Data were collected at 278 K.

Peptide	$\delta$ , H <sup>N</sup>	<sup>3</sup> J $\alpha$ <sub>N</sub>	$\delta$ , H $\alpha$	$\delta$ , H $\beta$
Ac-A <b>Ser</b> AAAAKAAAAKAAGY-NH <sub>2</sub>				
Ser	8.62	5.7	4.41	4.02, 3.95
Lys	8.17	5.0	4.16	1.90
	8.00	n.d. <sup>a</sup>	4.16	1.87
Ala	8.59	4.5	4.24	1.43
	8.53	3.9	4.28	1.46
	8.35	4.0	4.18	1.46
	8.28	4.3	4.24	1.49
	8.24	n.d.	4.25	1.49
	8.23	n.d.	4.21	1.48
	8.12	n.d.	4.25	1.48
	8.11	n.d.	4.24	1.48
	8.09	n.d.	4.25	1.46
	8.05	n.d.	4.27	1.43
	8.02	n.d.	4.19	1.46
Gly	8.09	n.d.	3.95, 3.87	n.a. <sup>b</sup>
Tyr	8.04	n.d.	4.55	3.12, 2.97
Ac-A <b>Ser(OPO<sub>3</sub>H)</b> AAAAKAAAAKAAGY-NH <sub>2</sub>				
Ser	8.97	5.1	4.51	4.25, 4.20
Lys	8.14	n.d.	4.15	1.92
	7.96	n.d.	4.15	1.88
Ala	8.63	4.0	4.23	1.45
	8.45	3.8	4.28	1.48
	8.34	n.d.	4.18	1.49
	8.21	n.d.	4.22	1.50
	8.20	n.d.	4.24	1.50
	8.16	n.d.	4.24	1.51
	8.11	n.d.	4.24	1.49
	8.08	n.d.	4.23	1.50
	8.04	n.d.	4.21	1.46
	8.00	n.d.	4.28	1.45
	7.99	n.d.	4.19	1.45
Gly	8.05	n.d.	3.96, 3.85	n.a.
Tyr	8.02	n.d.	4.57	3.13, 2.97

**Table 1.25:** Summary of <sup>1</sup>H NMR data for peptides with serine or phosphoserine at residue 2. Data were collected in 5 mM phosphate buffer (pH 4.0) containing 25 mM NaCl. <sup>a</sup> n.d. = not determined due to spectral overlap or peak broadening. <sup>b</sup> n.a. = not applicable.

Peptide	$\delta$ , H <sup>N</sup>	<sup>3</sup> J $\alpha$ <sub>N</sub>	$\delta$ , H $\alpha$	$\delta$ , H $\beta$
Ac-A <b>Ser</b> (OPO <sub>3</sub> <sup>2-</sup> )AAAAKAAAAKAAGY-NH <sub>2</sub>				
Ser	9.57	4.3	4.41	4.10
Lys	8.13	4.9	4.16	1.93
	7.93	n.d. <sup>a</sup>	4.15	1.90
Ala	8.65	4.0	4.22	1.48
	8.57	3.9	4.30	1.47
	8.32	4.1	4.26	1.53
	8.28	4.5	4.18	1.51
	8.22	4.5	4.23	1.51
	8.19	4.1	4.27	1.51
	8.10	n.d.	4.26	1.51
	8.07	n.d.	4.25	1.51
	8.01	n.d.	4.20	1.47
	7.97	n.d.	4.20	1.47
	7.95	n.d.	4.29	1.46
Gly	8.02	n.d.	3.94, 3.89	n.a. <sup>b</sup>
Tyr	8.01	n.d.	4.57	3.13, 2.98

**Table 1.26:** Summary of <sup>1</sup>H NMR data for peptide with phosphoserine at residue 2. Data were collected in 5 mM phosphate buffer (pH 4.0) containing 25 mM NaCl. <sup>a</sup> n.d. = not determined due to spectral overlap or peak broadening. <sup>b</sup> n.a. = not applicable.

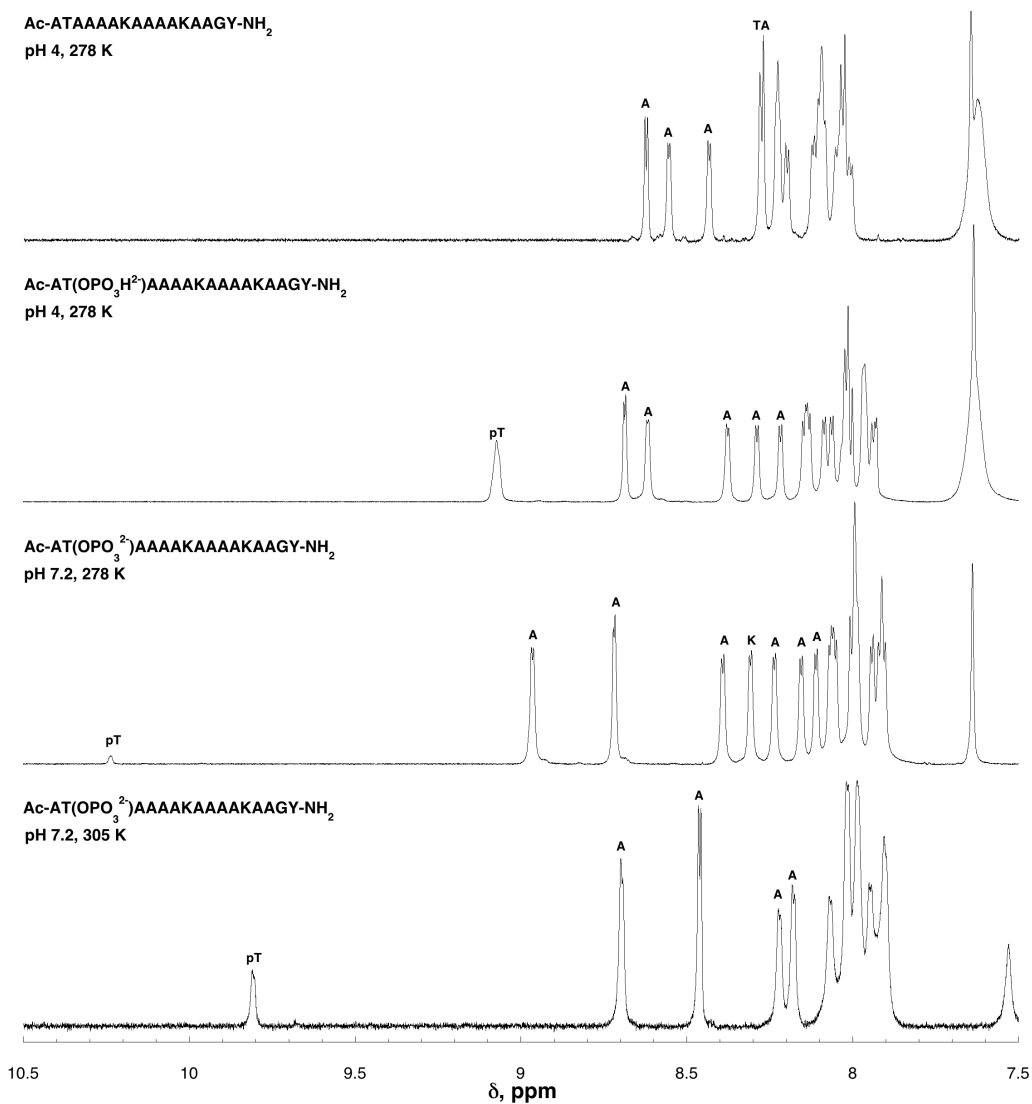


**Figure 1.45:** <sup>1</sup>H NMR spectra (amide region) of Ac-ATAAAAKAAAAKAAGY-NH<sub>2</sub> peptides with threonine modifications: unmodified Thr(free hydroxyl), Thr(OPO<sub>3</sub>H<sup>-</sup>), and Thr(OPO<sub>3</sub><sup>2-</sup>). pT indicates phosphorylated threonine residue. Peptides were dissolved in 5 mM phosphate buffer (pH 4.0 or 7.2) containing 25 mM NaCl in 90% H<sub>2</sub>O/10% D<sub>2</sub>O. Data were collected at 278 K or 305 K.

Peptide	$\delta$ , H <sup>N</sup>	<sup>3</sup> J $\alpha_N$	$\delta$ , H $\alpha$	$\delta$ , H $\beta$
Ac-A <i>Thr</i> AAAAKAAAAKAAGY-NH <sub>2</sub>				
Thr	8.63	4.7	4.26	4.33
Lys	8.20	n.d. <sup>a</sup>	4.15	1.89
	8.01	n.d.	4.15	1.86
Ala	8.56	3.8	4.27	1.45
	8.44	4.2	4.25	1.43
	8.28	n.d.	4.16	1.49
	8.28	n.d.	4.23	1.49
	8.23	n.d.	4.24	1.48
	8.23	n.d.	4.21	1.48
	8.12	n.d.	4.23	1.47
	8.10	n.d.	4.22	1.47
	8.09	n.d.	4.21	1.44
	8.05	n.d.	4.26	1.41
	8.03	n.d.	4.19	1.44
Gly	8.10	n.d.	3.92,3.86	n.a. <sup>b</sup>
Tyr	8.03	n.d.	4.54	3.11,2.95
Ac-A <i>Thr(OPO<sub>3</sub>H)</i> AAAAKAAAAKAAGY-NH <sub>2</sub>				
Thr	9.08	n.d.	4.21	4.62
Lys	8.15	n.d.	4.15	1.92
	7.94	n.d.	4.12	1.88
Ala	8.69	3.5	4.19	1.45
	8.62	3.3	4.24	1.44
	8.38	3.9	4.15	1.48
	8.29	4.5	4.25	1.51
	8.22	4.5	4.19	1.49
	8.13	n.d.	4.25	1.50
	8.09	n.d.	4.24	1.49
	8.06	n.d.	4.22	1.49
	8.02	n.d.	4.19	1.45
	7.97	n.d.	4.19	1.45
	7.96	n.d.	4.28	1.45
Gly	8.02	n.d.	3.94,3.85	n.a.
Tyr	8.01	n.d.	4.55	3.12,2.97

**Table 1.27:** Summary of <sup>1</sup>H NMR data for peptides with threonine or phosphothreonine at residue 2. Data were collected in 5 mM phosphate buffer (pH 4.0) containing 25 mM NaCl. <sup>a</sup> n.d. = not determined due to spectral overlap or peak broadening. <sup>b</sup> n.a. = not applicable.

Peptide	$\delta$ , H <sup>N</sup>	$^3J_{\alpha_N}$	$\delta$ , H $\alpha$	$\delta$ , H $\beta$
Ac-A Thr(OPO <sub>3</sub> <sup>2-</sup> )AAAAKAAAAKAAGY-NH <sub>2</sub>				
Thr	10.24	3.7 <sup>c</sup>	4.02	4.51
Lys	8.16	4.3	4.14	1.94
	7.91	n.d. <sup>a</sup>	4.13	1.91
Ala	8.97	3.7	4.26	1.44
	8.72	3.2	4.12	1.49
	8.40	4.4	4.27	1.56
	8.31	4.1	4.16	1.51
	8.24	4.3	4.19	1.52
	8.12	4.3	4.27	1.53
	8.08	n.d.	4.25	1.52
	8.06	n.d.	4.23	1.51
	7.99	n.d.	4.19	1.48
	7.95	n.d.	4.18	1.48
	7.92	n.d.	4.28	1.44
Gly	7.99	n.d.	3.97, 3.86	n.a. <sup>b</sup>
Tyr	8.01	n.d.	4.57	3.13, 2.97
Ac-A Thr(OPO <sub>3</sub> <sup>2-</sup> )AAAAKAAAAKAAGY-NH <sub>2</sub>				
Thr	9.81	4.9 <sup>c</sup>	4.05	4.48
Lys	8.02	n.d.	4.25	1.93
	7.90	n.d.	4.20	1.89
Ala	8.71	3.4	4.25	1.48
	8.47	4.3	4.20	1.47
	8.22	n.d.	4.24	1.52
	8.18	n.d.	4.17	1.49
	8.07	n.d.	4.20	1.49
	8.01	n.d.	4.27	1.50
	7.98	n.d.	4.27	1.49
	7.98	n.d.	4.27	1.43
	7.98	n.d.	4.27	1.43
	7.94	n.d.	4.24	1.50
	7.90	n.d.	4.20	1.46
Gly	8.07	n.d.	3.94, 3.85	n.a.
Tyr	7.93	n.d.	4.57	3.12, 2.97

**Table 1.28:** Summary of <sup>1</sup>H NMR data for peptide with phosphothreonine at residue 2. Data were collected at 278 K (top) or 305 K (bottom) in 5 mM phosphate buffer (pH 7.2) containing 25 mM NaCl. <sup>a</sup> n.d. = not determined due to spectral overlap. <sup>b</sup> n.a. = not applicable. <sup>c</sup> Coupling constant was determined using exponential (-4.2 Hz) and Gaussian smoothing (2.4 Hz).

**$^1\text{H}$  NMR spectrum of Ac-AT(OPO<sub>3</sub><sup>2-</sup>)AAAAKAAAAKAAGY-NH<sub>2</sub> in D<sub>2</sub>O**

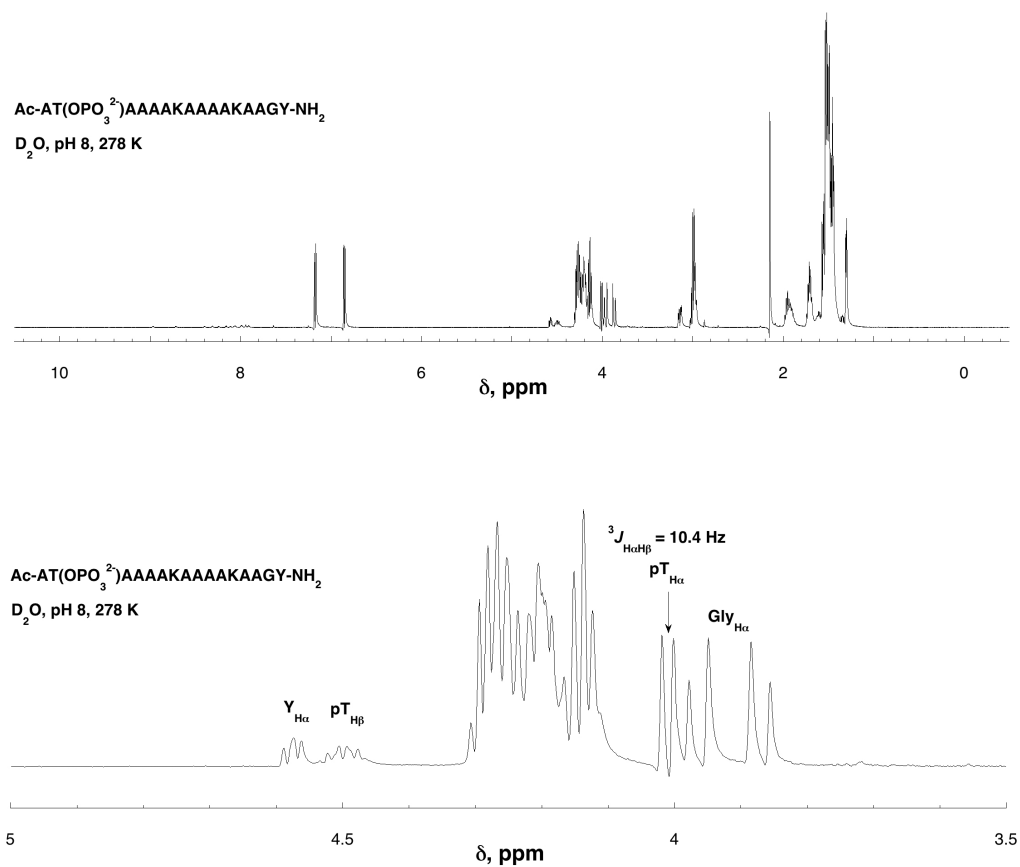


**Figure 1.46:** The  $^1\text{H}$  NMR spectra of Ac-AT(OPO<sub>3</sub><sup>2-</sup>)AAAAKAAAAKAAGY-NH<sub>2</sub> was collected in D<sub>2</sub>O to eliminate coupling between threonine alpha and amide protons, in order to determine the coupling constant between Thr(OPO<sub>3</sub><sup>2-</sup>) H $\alpha$  and H $\beta$ . Peptide was dissolved in buffer containing 5 mM phosphate buffer (pH 8.0) containing 25 mM NaCl in D<sub>2</sub>O. The  $^3J_{\text{H}\alpha\text{H}\beta}$  coupling constant for Thr(OPO<sub>3</sub><sup>2-</sup>) is indicated (10.4 Hz).

**Temperature-dependent NMR spectra (amide region) for  
Ac-AT(OPO<sub>3</sub><sup>2-</sup>)AAAAKAAAAKAAGY-NH<sub>2</sub>**

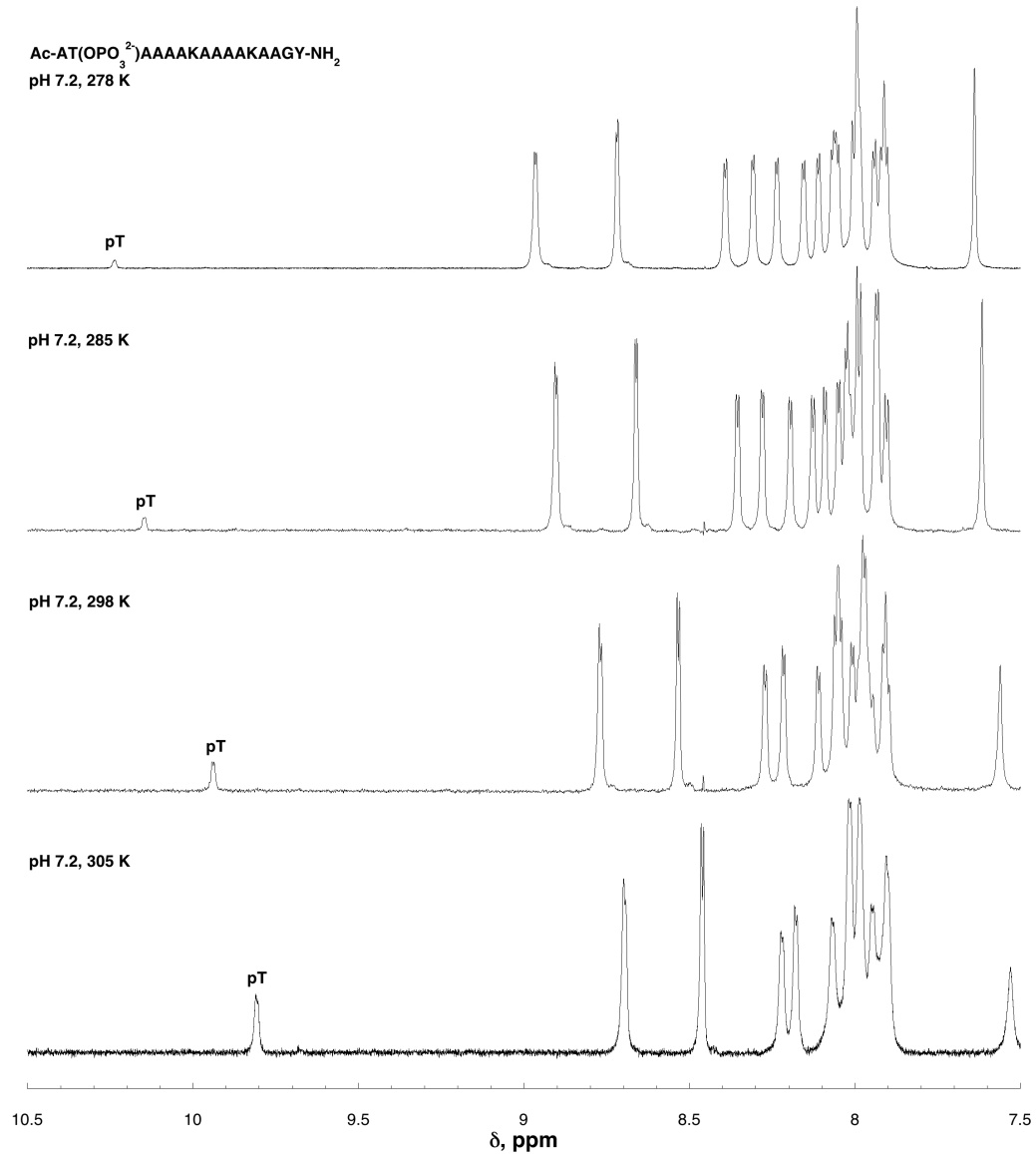


**Figure 1.47:** Temperature-dependent <sup>1</sup>H NMR spectra (amide region) of Ac-AT(OPO<sub>3</sub><sup>2-</sup>)AAAAKAAAAKAAGY-NH<sub>2</sub> peptide. The peptide was dissolved in 5 mM phosphate buffer (pH 7.2) containing 25 mM NaCl in 90% H<sub>2</sub>O/10% D<sub>2</sub>O.

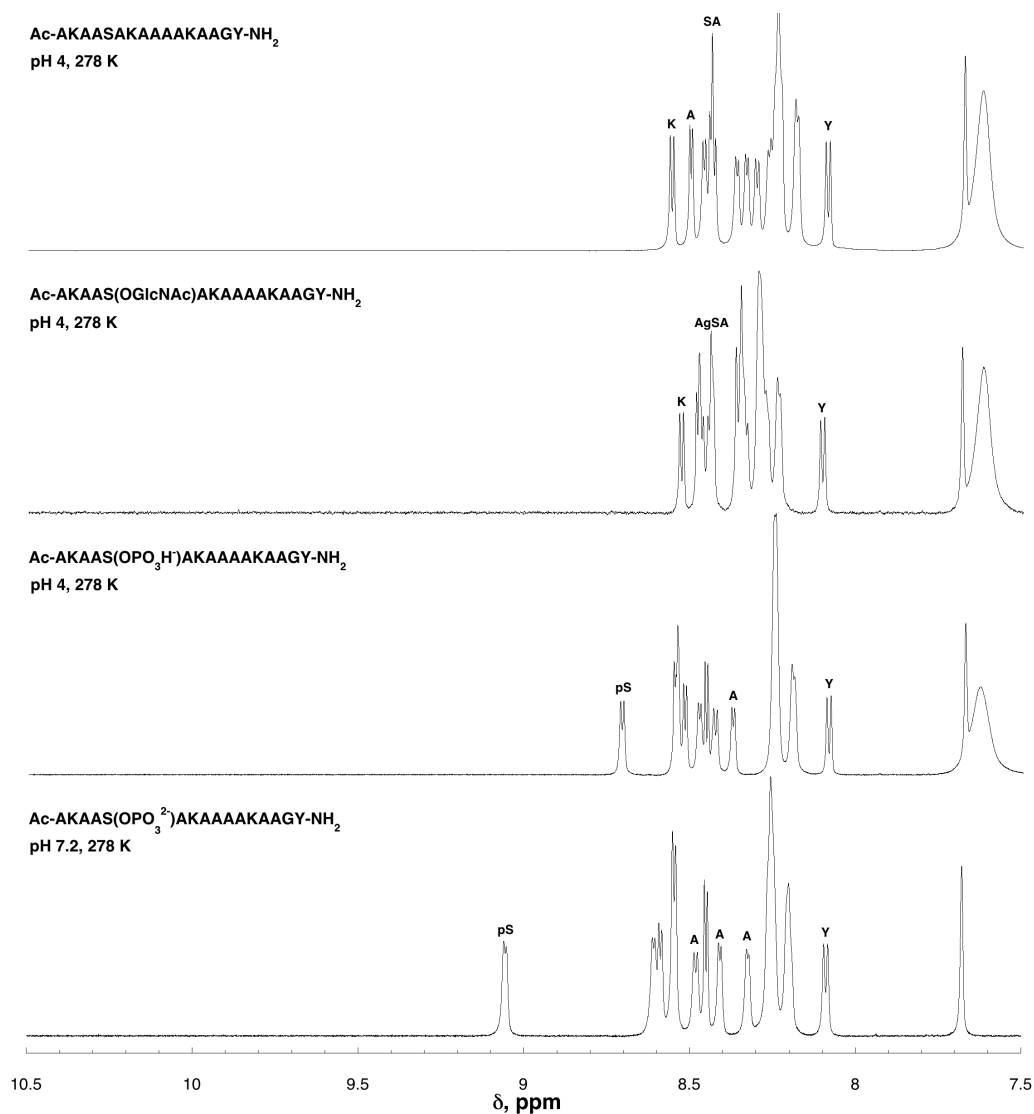


**Figure 1.48:** <sup>1</sup>H NMR spectra (amide region) of Ac-AKAASAKAAAAKAAGY-NH<sub>2</sub> peptides with serine modifications: unmodified Ser(free hydroxyl), Ser(OGlcNAc), Ser(OPO<sub>3</sub>H<sup>-</sup>), and Ser(OPO<sub>3</sub><sup>2-</sup>). pS indicates phosphorylated serine residue. gS indicates Ser(OGlcNAc) residue. Peptides were dissolved in 5 mM phosphate buffer (pH 4.0 or 7.2) containing 25 mM NaCl in 90% H<sub>2</sub>O/10% D<sub>2</sub>O. Data were collected at 278 K.

Peptide	$\delta$ , H <sup>N</sup>	<sup>3</sup> J $\alpha$ <sub>N</sub>	$\delta$ , H $\alpha$	$\delta$ , H $\beta$
Ac-AKAA <b>Ser</b> AKAAAAKAAGY-NH <sub>2</sub>				
Ser	8.44	n.d. <sup>a</sup>	4.37	3.95
Lys	8.56	6.4	4.25	1.81
	8.31	5.8	4.19	1.83
	8.19	n.d.	4.20	1.82
Ala	8.51	4.6	4.20	1.39
	8.47	5.0	4.26	1.44
	8.45	n.d.	4.25	1.42
	8.37	5.0	4.29	1.46
	8.34	4.9	4.21	1.44
	8.27	n.d.	4.25	1.45
	8.25	n.d.	4.23	1.42
	8.24	n.d.	4.25	1.43
	8.23	n.d.	4.25	1.44
	8.18	n.d.	4.20	1.42
Gly	8.24	n.d.	3.93, 3.86	n.a. <sup>b</sup>
Tyr	8.09	7.4	4.53	3.11, 2.96
Ac-AKAA <b>Ser(OGlcNAc)</b> AKAAAAKAAGY-NH <sub>2</sub>				
GlcNAc	8.36	n.d.	n.a.	n.a.
Ser	8.45	n.d.	4.46	4.09
Lys	8.53	6.6	4.27	1.77
	8.36	n.d.	4.22	1.84
	8.24	n.d.	4.20	1.79
Ala	8.49	n.d.	4.20	1.38
	8.47	n.d.	4.25	1.43
	9.47	n.d.	4.25	1.44
	8.44	n.d.	4.26	1.41
	8.35	n.d.	4.22	1.43
	8.34	n.d.	4.26	1.43
	8.30	n.d.	4.25	1.42
	8.30	n.d.	4.25	1.42
	8.27	n.d.	4.24	1.42
	8.24	n.d.	4.20	1.41
Gly	8.28	n.d.	3.94, 3.87	n.a.
Tyr	8.11	7.4	4.52	3.11, 2.97

**Table 1.29:** Summary of <sup>1</sup>H NMR data for peptides with serine and Ser(OGlcNAc) at residue 5. Data were collected in 5 mM phosphate buffer (pH 4.0) containing 25 mM NaCl. <sup>a</sup> n.d. = not determined due to spectral overlap. <sup>b</sup> n.a. = not applicable.

Peptide	$\delta$ , H <sup>N</sup>	<sup>3</sup> J $\alpha$ <sub>N</sub>	$\delta$ , H $\alpha$	$\delta$ , H $\beta$
Ac-AKAA <b>Ser</b> (OPO <sub>3</sub> H)AKAAAAKAAGY-NH <sub>2</sub>				
Ser	8.71	5.7	4.51	4.17
Lys	8.55	n.d. <sup>a</sup>	4.29	1.79
	8.43	6.2	4.21	1.85
	8.19	n.d.	4.20	1.81
Ala	8.55	n.d.	4.30	1.43
	8.52	5.1	4.26	1.42
	8.48	4.7	4.28	1.44
	8.46	5.3	4.23	1.32
	8.38	5.0	4.20	1.43
	8.25	n.d.	4.24	1.43
	8.25	n.d.	4.24	1.43
	8.25	n.d.	4.24	1.43
	8.25	n.d.	4.24	1.43
	8.20	n.d.	4.19	1.42
Gly	8.25	n.d.	3.93, 3.85	n.a. <sup>b</sup>
Tyr	8.09	7.4	4.52	3.11, 2.96
Ac-AKAA <b>Ser</b> (OPO <sub>3</sub> <sup>2-</sup> )AKAAAAKAAGY-NH <sub>2</sub>				
Ser	9.06	4.5	4.44	4.09
Lys	8.55	n.d.	4.29	1.81
	8.49	6.3	4.25	1.87
	8.20	n.d.	4.19	1.82
Ala	8.62	4.6	4.28	1.43
	8.60	5.2	4.28	1.42
	8.55	n.d.	4.29	1.44
	8.46	5.3	4.25	1.37
	8.41	4.8	4.21	1.44
	8.33	4.5	4.25	1.45
	8.27	n.d.	4.25	1.43
	8.25	n.d.	4.26	1.42
	8.25	n.d.	4.26	1.42
	9.25	n.d.	4.26	1.42
Gly	8.26	n.d.	3.94, 3.86	n.a.
Tyr	8.09	7.5	4.54	3.11, 2.96

**Table 1.30:** Summary of <sup>1</sup>H NMR data for peptides with phosphoserine at residue 5. Data were collected in 5 mM phosphate buffer (pH 4.0 or 7.2) containing 25 mM NaCl. <sup>a</sup> n.d. = not determined due to spectral overlap. <sup>b</sup> n.a. = not applicable.

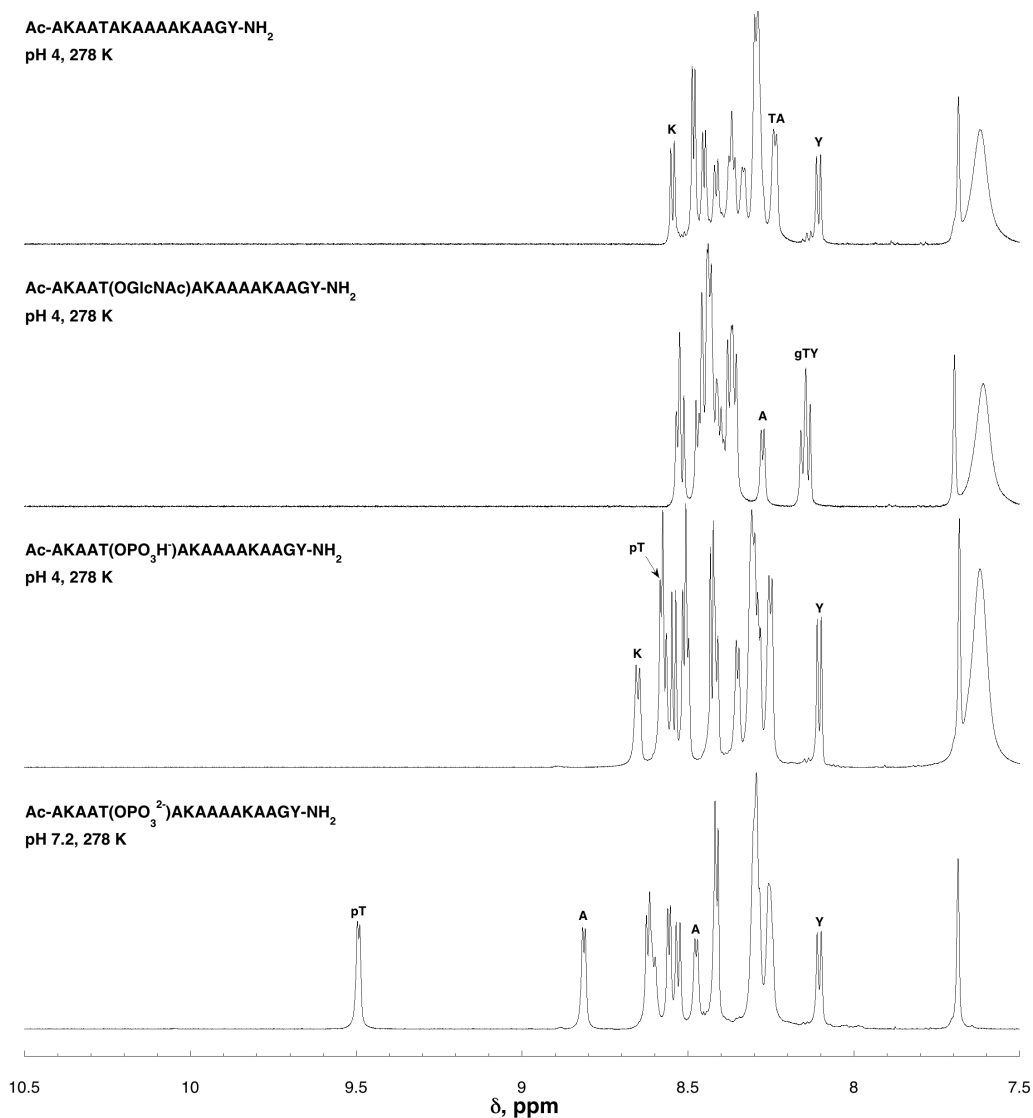


**Figure 1.48:** <sup>1</sup>H NMR spectra (amide region) of Ac-AKAATAKAAAAKAAGY-NH<sub>2</sub> peptides with threonine modifications: unmodified Thr(free hydroxyl), Thr(OGlcNAc), Thr(OPO<sub>3</sub>H<sup>-</sup>), and Thr(OPO<sub>3</sub><sup>2-</sup>). pT indicates phosphorylated threonine residue. gT indicates Thr(OGlcNAc) residue. Peptides were dissolved in 5 mM phosphate buffer (pH 4.0 or 7.2) containing 25 mM NaCl in 90% H<sub>2</sub>O/10% D<sub>2</sub>O. Data were collected at 278 K.

Peptide	$\delta$ , H <sup>N</sup>	<sup>3</sup> J $\alpha_N$	$\delta$ , H $\alpha$	$\delta$ , H $\beta$
Ac-AKAA <b>Thr</b> AKAAAAKAAGY-NH <sub>2</sub>				
Thr	8.29	n.d. <sup>a</sup>	4.23	4.26
Lys	8.55	6.4	4.35	1.84, 1.78
	8.42	6.0	4.21	1.82
	8.24	n.d.	4.22	1.83, 1.79
Ala	8.48	n.d.	4.32	1.45
	8.48	n.d.	4.22	1.38
	8.45	n.d.	4.27	1.41
	8.38	n.d.	4.27	1.43
	8.36	n.d.	4.23	1.43
	8.34	n.d.	4.26	1.42
	8.30	n.d.	4.25	1.42
	8.30	n.d.	4.23	1.42
	8.29	n.d.	4.23	1.42
	8.24	n.d.	4.21	1.42
Gly	8.29	n.d.	3.95, 3.87	n.a. <sup>b</sup>
Tyr	8.11	7.5	4.53	3.11, 2.97
Ac-AKAA <b>Thr(OGlcNAc)</b> AKAAAAKAAGY-NH <sub>2</sub>				
GlcNAc	8.47	n.d.	n.a.	n.a.
Thr	8.16	n.d.	4.34	4.24
Lys	8.52	n.d.	4.31	1.83, 1.73
	8.45	n.d.	4.23	1.83, 1.76
	8.36	n.d.	4.22	1.79, 1.76
Ala	8.53	n.d.	4.31	1.42
	8.46	n.d.	4.25	1.40
	8.44	n.d.	4.23	1.38
	8.44	n.d.	4.23	1.38
	8.44	n.d.	4.23	1.38
	8.44	n.d.	4.23	1.38
	8.42	n.d.	4.25	1.38
	8.41	n.d.	4.25	1.39
	8.38	n.d.	4.24	1.39
	8.28	5.2	4.30	1.40
Gly	8.39	n.d.	3.92, 3.85	n.a.
Tyr	8.14	n.d.	4.51	3.09, 2.96

**Table 1.31:** Summary of <sup>1</sup>H NMR data for peptides with threonine and Thr(OGlcNAc) at residue 5. Data were collected in 5 mM phosphate buffer (pH 4.0) containing 25 mM NaCl. <sup>a</sup> n.d. = not determined due to spectral overlap. <sup>b</sup> n.a. = not applicable.

Peptide	$\delta$ , H <sup>N</sup>	<sup>3</sup> J $\alpha_N$	$\delta$ , H $\alpha$	$\delta$ , H $\beta$
Ac-AKAAThr(OPO <sub>3</sub> H)AKAAAAKAAGY-NH <sub>2</sub>				
Thr	8.57	n.d. <sup>a</sup>	4.36	4.65
Lys	8.65	6.3	4.24	1.84
	8.54	7.0	4.32	1.82, 1.77
	8.25	n.d.	4.19	1.82, 1.79
Ala	8.58	n.d.	4.34	1.43
	8.51	n.d.	4.26	1.41
	8.51	n.d.	4.26	1.41
	8.43	n.d.	4.23	1.35
	8.42	n.d.	4.22	1.40
	8.42	n.d.	4.21	1.41
	8.35	4.9	4.24	1.42
	8.31	n.d.	4.24	1.41
	8.29	n.d.	4.23	1.42
	8.25	n.d.	4.23	1.40
Gly	8.30	n.d.	3.93, 3.86	n.a. <sup>b</sup>
Tyr	8.10	7.4	4.52	3.10, 2.96
Ac-AKAAThr(OPO <sub>3</sub> <sup>2-</sup> )AKAAAAKAAGY-NH <sub>2</sub>				
Thr	9.50	4.1	4.11	4.39
Lys	8.61	n.d.	4.23	1.85
	8.53	6.8	4.30	1.80
	8.25	n.d.	4.21	1.83, 1.80
Ala	8.82	4.7	4.28	1.42
	8.63	n.d.	4.30	1.40
	8.56	4.9	4.26	1.43
	8.48	4.8	4.24	1.43
	8.42	n.d.	4.23	1.42
	8.41	n.d.	4.24	1.35
	8.30	n.d.	4.27	1.41
	8.30	n.d.	4.24	1.40
	8.29	n.d.	4.23	1.42
	8.26	n.d.	4.22	1.41
Gly	8.30	n.d.	3.92, 3.86	n.a.
Tyr	8.10	7.3	4.53	3.11, 2.97

**Table 1.32:** Summary of <sup>1</sup>H NMR data for peptides with phosphothreonine at residue 5. Data were collected in 5 mM phosphate buffer (pH 4.0 or 7.2) containing 25 mM NaCl. <sup>a</sup> n.d. = not determined due to spectral overlap. <sup>b</sup> n.a. = not applicable.

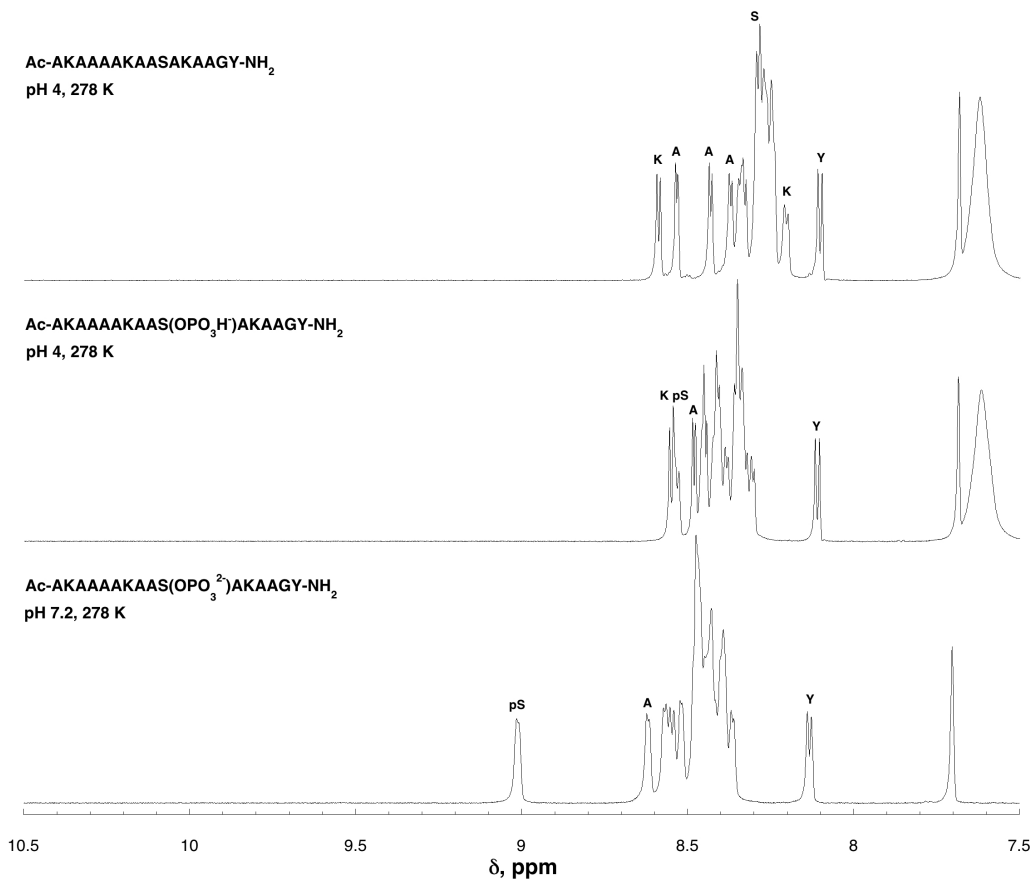


**Figure 1.49:** <sup>1</sup>H NMR spectra (amide region) of Ac-AKAAAAKAASAKAAGY-NH<sub>2</sub> peptides with serine modifications: unmodified Ser(free hydroxyl), Ser(OPO<sub>3</sub>H<sup>-</sup>), and Ser(OPO<sub>3</sub><sup>2-</sup>). pS indicates phosphorylated serine residue. Peptides were dissolved in 5 mM phosphate buffer (pH 4.0 or 7.2) containing 25 mM NaCl in 90% H<sub>2</sub>O/10% D<sub>2</sub>O. Data were collected at 278 K.

Peptide	$\delta$ , H <sup>N</sup>	<sup>3</sup> J $\alpha$ <sub>N</sub>	$\delta$ , H $\alpha$	$\delta$ , H $\beta$
Ac-AKAAAKAA <i>Ser</i> AKAAGY-NH <sub>2</sub>				
Ser	8.30	n.d. <sup>a</sup>	4.37	3.92, 3.90
Lys	8.59	6.1	4.22	1.81
	8.26	n.d.	4.19	1.84
Ala	8.21	6.1	4.20	1.84, 1.79
	8.54	4.2	4.18	1.39
	8.44	4.9	4.24	1.41
	8.38	4.9	4.20	1.42
	8.35	n.d.	4.26	1.46
	8.34	n.d.	4.24	1.45
	8.29	n.d.	4.25	1.40
	8.29	n.d.	4.25	1.43
	8.28	n.d.	4.24	1.42
	8.27	n.d.	4.22	1.42
Gly	8.25	n.d.	4.26	1.43
Tyr	8.29	n.d.	3.92, 3.86	n.a. <sup>b</sup>
Tyr	8.11	7.4	4.52	3.10, 2.95
Ac-AKAAAKAA <i>Ser(OPO<sub>3</sub>H)</i> AKAAGY-NH <sub>2</sub>				
Ser	8.54	n.d.	4.50	4.18, 4.14
Lys	8.56	n.d.	4.25	1.82, 1.77
	8.36	n.d.	8.35	1.80
	8.35	n.d.	8.35	1.80
Ala	8.49	4.9	4.20	1.37
	8.47	n.d.	4.27	1.43
	8.46	n.d.	4.25	1.39
	8.44	n.d.	4.25	1.41
	8.43	n.d.	4.25	1.41
	8.42	n.d.	4.23	1.40
	8.40	n.d.	4.24	1.38
	8.35	n.d.	4.25	1.40
	8.33	n.d.	4.24	1.40
	8.32	n.d.	4.25	1.40
Gly	8.36	n.d.	3.91, 3.85	n.a.
Tyr	8.12	7.3	4.49	3.09, 2.96

**Table 1.33:** Summary of <sup>1</sup>H NMR data for peptides with serine or phosphoserine at residue 10. Data were collected in 5 mM phosphate buffer (pH 4.0) containing 25 mM NaCl. <sup>a</sup> n.d. = not determined due to spectral overlap. <sup>b</sup> n.a. = not applicable.

Peptide	$\delta$ , H <sup>N</sup>	$^3J_{\alpha N}$	$\delta$ , H $\alpha$	$\delta$ , H $\beta$
Ac-AKAAAKAA <i>Ser</i> (OPO <sub>3</sub> <sup>2-</sup> )AKAAGY-NH <sub>2</sub>				
Ser	9.01	3.3	4.42	4.05
Lys	8.55	n.d.	4.28	1.83, 1.76
	8.43	n.d.	4.27	1.78
	8.39	n.d.	4.27	1.79
Ala	8.62	3.9	4.26	1.39
	8.56	n.d.	4.29	1.41
	8.52	n.d.	4.28	1.43
	8.47	n.d.	4.26	1.39
	8.47	n.d.	4.24	1.38
	8.47	n.d.	4.23	1.37
	8.43	n.d.	4.27	1.41
	8.42	n.d.	4.27	1.41
	8.39	n.d.	4.27	1.40
	8.37	4.6	4.27	1.39
Gly	8.41	n.d.	3.92, 3.86	n.a.
Tyr	8.13	7.3	4.51	3.10, 2.98

**Table 1.34:** Summary of <sup>1</sup>H NMR data for peptide with phosphoserine at residue 10. Data were collected in 5 mM phosphate buffer (pH 7.2) containing 25 mM NaCl. <sup>a</sup> n.d. = not determined due to spectral overlap. <sup>b</sup> n.a. = not applicable.

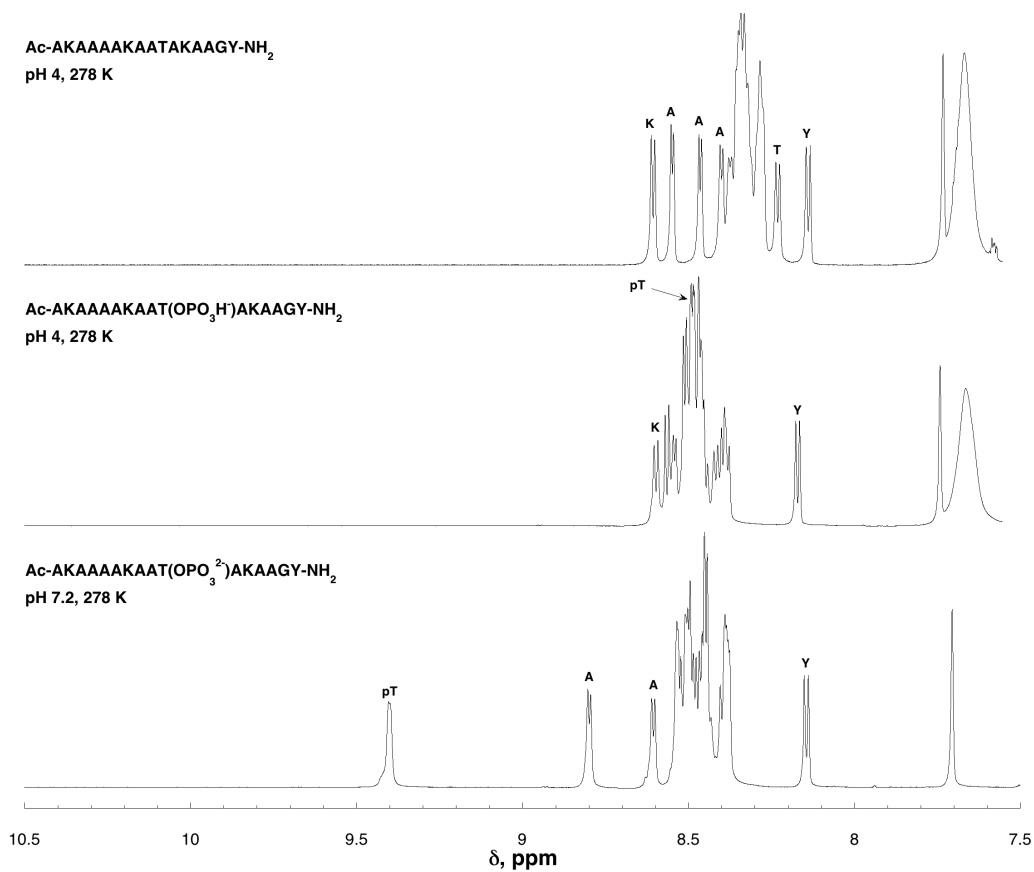


**Figure 1.50:** <sup>1</sup>H NMR spectra (amide region) of Ac-AKAAAAKAATAKAAGY-NH<sub>2</sub> peptides with threonine modifications: unmodified Thr(free hydroxyl), Thr(OPO<sub>3</sub>H<sup>-</sup>), and Thr(OPO<sub>3</sub><sup>2-</sup>). pT indicates phosphorylated threonine residue. Peptides were dissolved in 5 mM phosphate buffer (pH 4.0 or 7.2) containing 25 mM NaCl in 90% H<sub>2</sub>O/10% D<sub>2</sub>O. Data were collected at 278 K.

Peptide	$\delta, H^N$	$^3J_{\alpha N}$	$\delta, H\alpha$	$\delta, H\beta$
<b>Ac-AKAAAAKAAThrAKAAGY-NH<sub>2</sub></b>				
Thr	8.19	6.8	4.25	4.21
Lys	8.57	6.3	4.25	1.83
	8.31	n.d. <sup>a</sup>	4.25	1.82
Ala	8.24	n.d.	4.24	1.89
	8.52	4.4	4.21	1.41
	8.36	5.0	4.23	1.45
	8.34	5.0	4.33	1.49
	8.31	n.d.	4.26	1.46
	8.31	n.d.	4.26	1.46
	8.29	n.d.	4.27	1.41
	8.28	n.d.	4.27	1.46
	8.27	n.d.	4.27	1.46
	8.24	n.d.	4.27	1.42
Gly	8.24	n.d.	4.27	1.42
Gly	8.29	n.d.	3.95, 3.85	n.a. <sup>b</sup>
Tyr	8.10	7.4	4.52	3.13, 2.97
<b>Ac-AKAAAAKAAThr(OPO<sub>3</sub>H)AKAAGY-NH<sub>2</sub></b>				
Thr	8.44	n.d.	4.40	4.62
Lys	8.56	6.9	4.27	1.79
	8.53	n.d.	4.27	1.81, 1.75
Ala	8.38	n.d.	4.27	1.80, 1.77
	8.50	n.d.	4.35	1.42
	8.48	n.d.	4.25	1.38
	8.47	n.d.	4.24	1.39
	8.46	n.d.	4.24	1.38
	8.45	n.d.	4.24	1.38
	8.45	n.d.	4.24	1.38
	8.44	n.d.	4.24	1.38
	8.43	n.d.	4.24	1.38
	8.36	n.d.	4.26	1.39
8.35	n.d.	4.26	1.39	
Gly	8.41	n.d.	3.90, 3.85	n.a.
Tyr	8.13	7.3	4.50	3.08, 2.96

**Table 1.35:** Summary of <sup>1</sup>H NMR data for peptides with threonine or phosphothreonine at residue 10. Data were collected in 5 mM phosphate buffer (pH 4.0) containing 25 mM NaCl. <sup>a</sup> n.d. = not determined due to spectral overlap. <sup>b</sup> n.a. = not applicable.

Peptide	$\delta$ , H <sup>N</sup>	<sup>3</sup> J $\alpha$ <sub>N</sub>	$\delta$ , H $\alpha$	$\delta$ , H $\beta$
Ac-AKAAAAKAA <i>Thr</i> (OPO <sub>3</sub> <sup>2-</sup> )AKAAGY-NH <sub>2</sub>				
Thr	9.41	4.5	4.09	4.34
Lys	8.53	n.d. <sup>a</sup>	4.28	1.82, 1.76
	8.50	n.d.	4.26	1.77
	8.40	n.d.	4.28	1.80
Ala	8.80	5.2	4.26	1.38
	8.61	5.7	4.32	1.38
	8.53	n.d.	4.26	1.40
	8.50	n.d.	4.26	1.38
	8.50	n.d.	4.26	1.38
	8.48	n.d.	4.26	1.40
	8.45	n.d.	4.25	1.39
	8.45	n.d.	4.25	1.39
	8.39	n.d.	4.27	1.39
	8.38	n.d.	4.26	1.39
Gly	8.44	n.d.	3.91, 3.86	n.a. <sup>b</sup>
Tyr	8.15	7.3	4.51	3.10, 2.98

**Table 1.36:** Summary of <sup>1</sup>H NMR data for peptide with phosphothreonine at residue 10. Data were collected in 5 mM phosphate buffer (pH 7.2) containing 25 mM NaCl. <sup>a</sup>n.d. = not determined due to spectral overlap. <sup>b</sup>n.a. = not applicable.

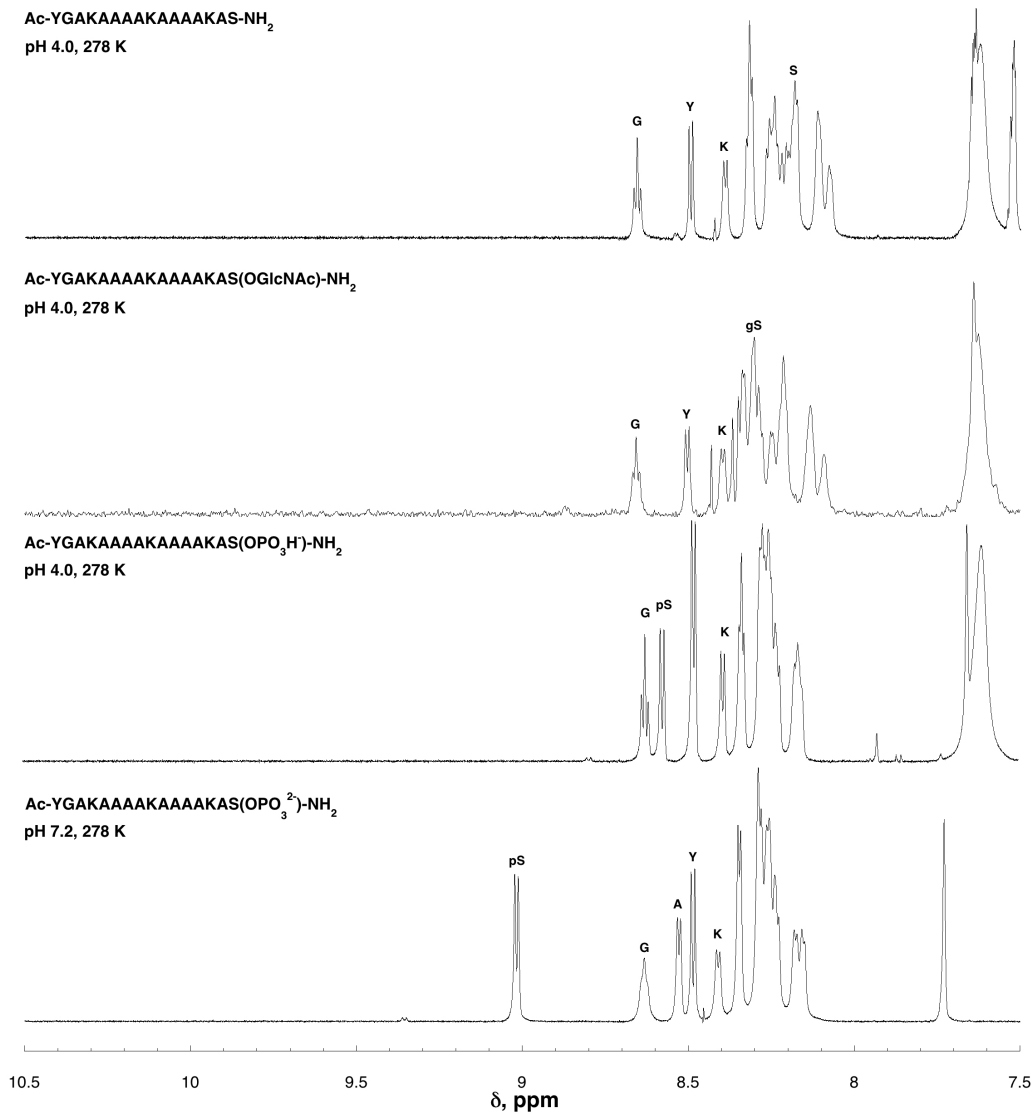


**Figure 1.51:** <sup>1</sup>H NMR spectra (amide region) of Ac-YGAKAAAKAAAKAS-NH<sub>2</sub> peptides with serine modifications: unmodified Ser(free hydroxyl), Ser(OGlcNAc), Ser(OPO<sub>3</sub>H<sup>-</sup>), and Ser(OPO<sub>3</sub><sup>2-</sup>). pS indicates phosphorylated serine residue. gS indicates Ser(OGlcNAc) residue. Peptides were dissolved in 5 mM phosphate buffer (pH 4.0 or 7.2) containing 25 mM NaCl in 90% H<sub>2</sub>O/10% D<sub>2</sub>O. Data were collected at 278 K.

Peptide	$\delta$ , H <sup>N</sup>	<sup>3</sup> J $\alpha$ <sub>N</sub>	$\delta$ , H $\alpha$	$\delta$ , H $\beta$
Ac-YGAKAAAAKAAAAKASer-NH <sub>2</sub>				
Ser	8.22	n.a.	4.37	3.93, 3.91
Lys	8.39	5.1 <sup>a</sup>	4.18	1.85
	8.19	n.d.	4.17	1.87
	8.11	n.d.	4.23	1.87, 1.84
Ala	8.33	n.d.	4.20	1.39
	8.32	n.d.	4.19	1.44
	8.31	n.d.	4.19	1.44
	8.27	n.d.	4.24	1.47
	8.25	n.d.	4.30	1.45
	8.24	n.d.	4.22	1.45
	8.18	n.d.	4.24	1.45
	8.18	n.d.	4.25	1.45
	8.11	n.d.	4.23	1.45
	8.07	n.d.	4.25	1.44
Gly	8.65	5.9	3.93, 3.86	n.a. <sup>b</sup>
Tyr	8.50	6.5	4.45	3.05, 2.95
Ac-YGAKAAAAKAAAAKASer(OGlcNAc)-NH <sub>2</sub>				
GlcNAc	8.36	n.d.	n.a.	n.a.
Ser	8.30	n.d.	4.48	4.11, 3.89
Lys	8.40	6.0	4.20	1.84
	8.22	n.d.	4.20	1.85
	8.14	n.d.	4.25	1.87, 1.80
Ala	8.33	n.d.	4.21	1.43
	8.32	n.d.	4.28	1.42
	8.31	n.d.	4.28	1.42
	8.29	n.d.	4.24	1.43
	8.29	n.d.	4.24	1.42
	8.28	n.d.	4.24	1.42
	8.24	n.d.	4.15	1.45
	8.19	n.d.	4.27	1.45
	8.14	n.d.	4.25	1.45
	8.09	n.d.	4.26	1.44
Gly	8.65	6.0	3.92, 3.86	n.a.
Tyr	8.49	6.4	4.45	3.06, 2.95

**Table 1.37:** Summary of <sup>1</sup>H NMR data for peptides with serine and Ser(OGlcNAc) at residue 14. Data were collected in 5 mM phosphate buffer (pH 4.0) containing 25 mM NaCl. <sup>a</sup> n.d. = not determined due to spectral overlap. <sup>b</sup> n.a. = not applicable.

Peptide	$\delta$ , H <sup>N</sup>	<sup>3</sup> J $\alpha_N$	$\delta$ , H $\alpha$	$\delta$ , H $\beta$
Ac-YGAKAAAAKAAAAKASer(OPO <sub>3</sub> H)-NH <sub>2</sub>				
Ser	8.57	6.8	4.50	4.18, 4.09
Lys	8.39	6.2	4.20	1.82
	8.26	n.d. <sup>a</sup>	4.24	1.82
Ala	8.24	n.d.	4.22	1.82
	8.48	n.d.	4.32	1.43
	8.28	n.d.	4.23	1.42
	8.27	n.d.	4.25	1.43
	8.27	n.d.	4.25	1.43
	8.25	n.d.	4.26	1.42
	8.25	n.d.	4.26	1.42
	8.24	n.d.	4.26	1.42
	8.22	n.d.	4.23	1.43
	8.17	n.d.	4.27	1.41
Gly	8.16	n.d.	4.26	1.42
Tyr	8.62	6.1	3.89, 3.85	n.a. <sup>b</sup>
Tyr	8.48	n.d.	4.45	3.05, 2.96
Ac-YGAKAAAAKAAAAKASer(OPO <sub>3</sub> <sup>2-</sup> )-NH <sub>2</sub>				
Ser	9.02	6.3	4.42	4.06
Lys	8.42	6.0	4.22	1.83
	8.29	n.d.	4.25	1.88, 1.79
Ala	8.25	n.d.	4.24	1.84
	8.53	5.4	4.35	1.46
	8.42	n.d.	4.23	1.42
	8.42	n.d.	4.23	1.42
	8.29	n.d.	4.32	1.44
	8.29	n.d.	4.32	1.44
	8.27	n.d.	4.24	1.44
	8.27	n.d.	4.24	1.44
	8.23	n.d.	4.25	1.43
	8.18	n.d.	4.28	1.42
Gly	8.16	n.d.	4.28	1.43
Gly	8.64	n.d.	3.92, 3.86	n.a.
Tyr	8.49	6.6	4.47	3.07, 2.95

**Table 1.38:** Summary of <sup>1</sup>H NMR data for peptides with phosphoserine at residue 14. Data were collected in 5 mM phosphate buffer (pH 4.0 or 7.2) containing 25 mM NaCl. <sup>a</sup> n.d. = not determined due to spectral overlap. <sup>b</sup> n.a. = not applicable.

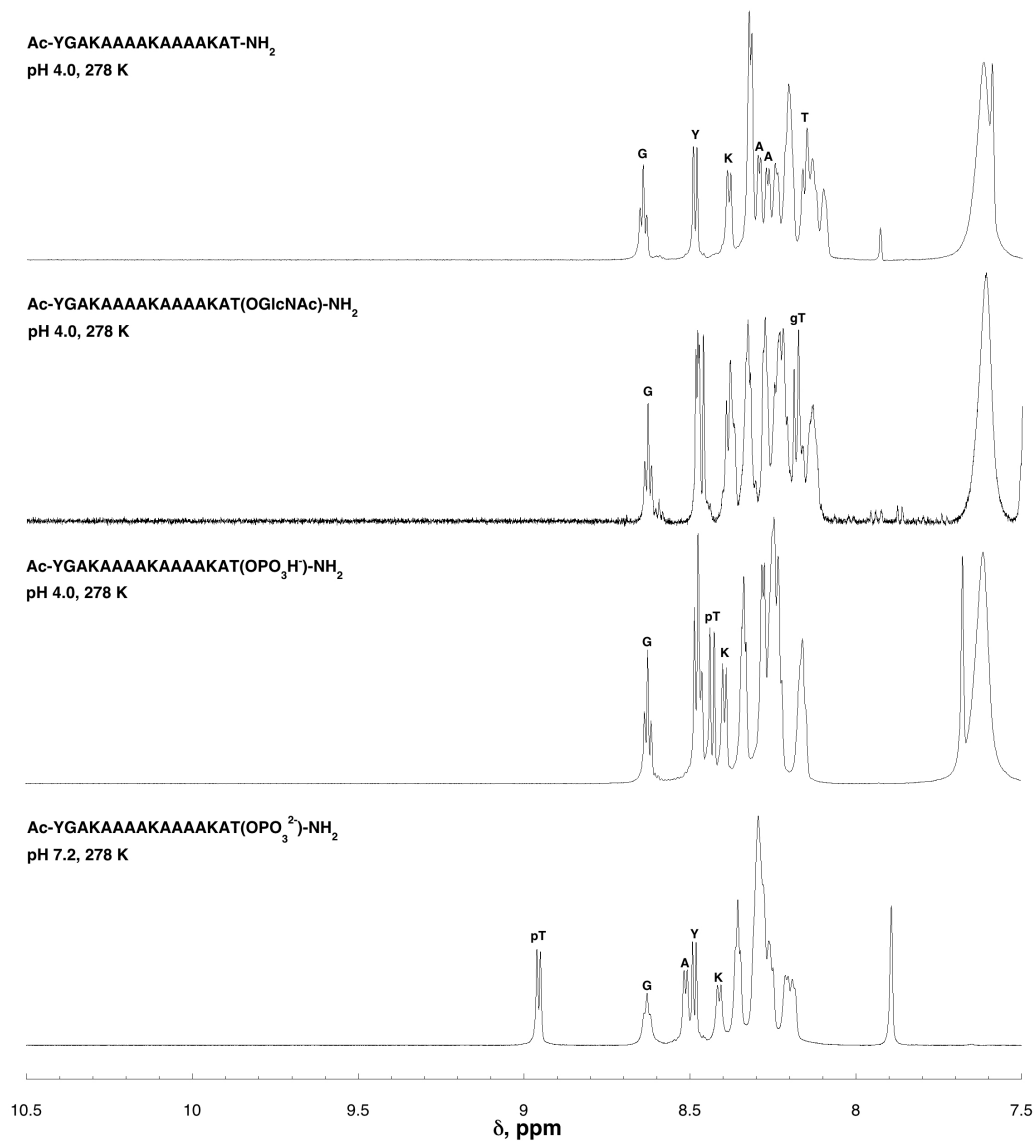


**Figure 1.52:** <sup>1</sup>H NMR spectra (amide region) of Ac-YGAKAAAAKAAAAKAT-NH<sub>2</sub> peptides with threonine modifications: unmodified Thr(free hydroxyl), Thr(OGlcNAc), Thr(OPO<sub>3</sub>H<sup>-</sup>), and Thr(OPO<sub>3</sub><sup>2-</sup>). pT indicates phosphorylated threonine residue, gT indicates Thr(OGlcNAc) residue. Peptides were dissolved in 5 mM phosphate buffer (pH 4.0 or 7.2) containing 25 mM NaCl in 90% H<sub>2</sub>O/10% D<sub>2</sub>O. Data were collected at 278 K.

Peptide	$\delta$ , H <sup>N</sup>	<sup>3</sup> J $\alpha$ <sub>N</sub>	$\delta$ , H $\alpha$	$\delta$ , H $\beta$
Ac-YGAKAAAAKAAAAKA $Thr$ -NH <sub>2</sub>				
Thr	8.18	7.9	4.29	4.29
Lys	8.39	6.0	4.20	1.84
	8.22	n.d. <sup>a</sup>	4.18	1.86
	8.14	n.d.	4.25	1.87, 1.81
Ala	8.33	n.d.	4.20	1.43
	8.32	n.d.	4.36	1.44
	8.30	n.d.	4.23	1.42
	8.28	4.3	4.24	1.43
	8.25	4.8	4.23	1.44
	8.21	n.d.	4.25	1.47
	8.20	n.d.	4.24	1.47
	8.14	n.d.	4.25	1.44
	8.13	n.d.	4.25	1.44
	8.10	n.d.	4.26	1.43
Gly	8.65	6.0	3.92, 3.85	n.a. <sup>b</sup>
Tyr	8.50	6.4	4.46	3.06, 2.97
Ac-YGAKAAAAKAAAAKA $Thr(OGlcNAc)$ -NH <sub>2</sub>				
GlcNAc	8.47	n.d.	n.a.	n.a.
Thr	8.18	8.0	4.42	4.34
Lys	8.39	n.d.	4.21	1.82
	8.23	n.d.	4.21	1.82
	8.17	n.d.	4.27	1.86, 1.76
Ala	8.37	n.d.	4.35	1.44
	8.33	n.d.	4.23	1.40
	8.33	n.d.	4.23	1.40
	8.27	n.d.	4.23	1.43
	8.27	n.d.	4.23	1.43
	8.24	n.d.	4.22	1.43
	8.23	n.d.	4.21	1.43
	8.21	n.d.	4.23	1.43
	8.13	n.d.	4.25	1.42
	8.13	n.d.	4.25	1.42
Gly	8.63	6.0	3.90, 3.85	n.a.
Tyr	8.48	n.d.	4.46	3.05, 2.94

**Table 1.39:** Summary of <sup>1</sup>H NMR data for peptides with threonine and Thr(OGlcNAc) at residue 14. Data were collected in 5 mM phosphate buffer (pH 4.0) containing 25 mM NaCl. <sup>a</sup> n.d. = not determined due to spectral overlap. <sup>b</sup> n.a. = not applicable.

Peptide	$\delta$ , H <sup>N</sup>	$^3J_{\alpha_N}$	$\delta$ , H $\alpha$	$\delta$ , H $\beta$
Ac-YGAKAAAAKAAAACA Thr( <i>OPO<sub>3</sub>H</i> )-NH <sub>2</sub>				
Thr	8.42	7.9	4.39	4.64
Lys	8.39	6.3	4.21	1.82
	8.23	n.d. <sup>a</sup>	4.25	1.83, 1.80
	8.23	n.d.	4.25	1.83, 1.80
Ala	8.46	n.d.	4.40	1.44
	8.33	n.d.	4.20	1.40
	8.33	n.d.	4.20	1.40
	8.27	n.d.	4.24	1.38
	8.27	n.d.	4.24	1.38
	8.24	n.d.	4.23	1.41
	8.23	n.d.	4.23	1.41
	8.22	n.d.	4.23	1.41
	8.16	n.d.	4.26	1.41
	8.15	n.d.	4.26	1.41
Gly	8.62	6.0	3.90, 3.83	n.a. <sup>b</sup>
Tyr	8.47	n.d.	4.45	3.03, 2.94
Ac-YGAKAAAAKAAAACA Thr( <i>OPO<sub>3</sub><sup>2-</sup></i> )-NH <sub>2</sub>				
Thr	8.93	6.2	4.26	4.46
Lys	8.41	6.1	4.23	1.82
	8.30	n.d.	4.29	1.84, 1.80
	8.27	n.d.	4.23	1.83
Ala	8.51	5.7	4.38	1.44
	8.35	n.d.	4.23	1.41
	8.35	n.d.	4.23	1.41
	8.30	n.d.	4.30	1.44
	8.29	n.d.	4.26	1.44
	8.28	n.d.	4.25	1.44
	8.26	n.d.	4.25	1.44
	8.25	n.d.	4.24	1.44
	8.21	n.d.	4.27	1.42
	8.19	n.d.	4.28	1.42
Gly	8.63	5.4	3.91, 3.84	n.a.
Tyr	8.48	6.6	4.48	3.06, 2.96

**Table 1.40:** Summary of <sup>1</sup>H NMR data for peptides with phosphoserine at residue 14. Data were collected in 5 mM phosphate buffer (pH 4.0 or 7.2) containing 25 mM NaCl. <sup>a</sup> n.d. = not determined due to spectral overlap. <sup>b</sup> n.a. = not applicable.

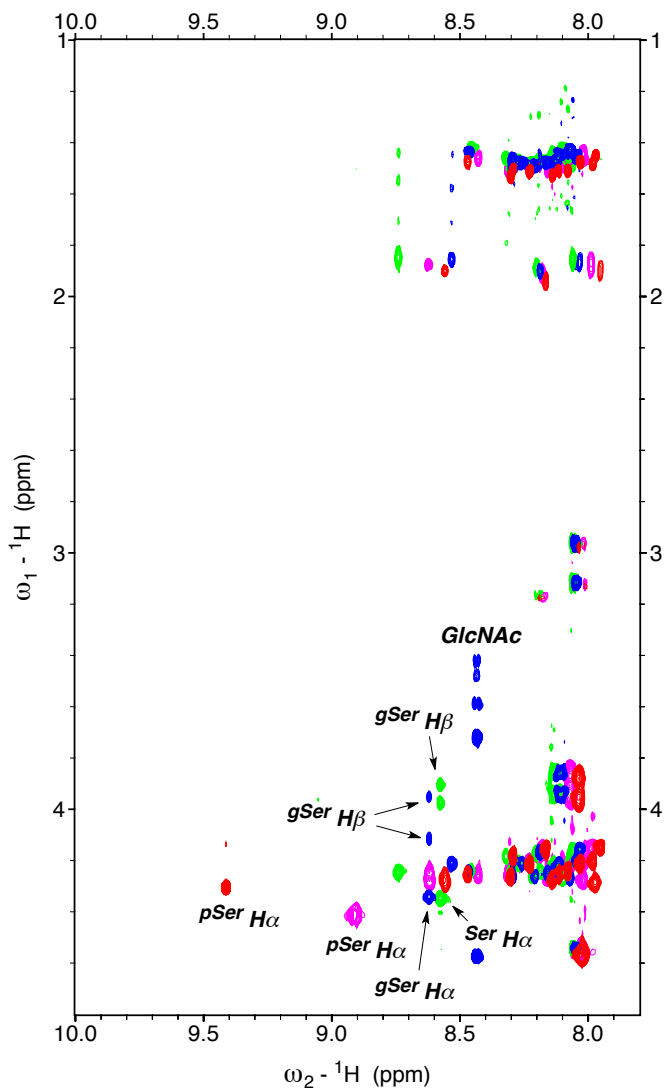


**Figure 1.53:** TOCSY spectra of Ac-SKAAAAKAAAAKAAGY-NH<sub>2</sub> peptides with serine modifications: unmodified Ser(free hydroxyl), Ser(OGlcNAc), Ser(OPO<sub>3</sub>H<sup>-</sup>), and Ser(OPO<sub>3</sub><sup>2-</sup>). pSer indicates phosphorylated serine residue; gSer indicates Ser(OGlcNAc) residue. Green: unmodified serine; blue: Ser(OGlcNAc); magenta: phosphorylated serine (pH 4.0); red: phosphorylated serine (pH 7.2). Peptides were dissolved in 5 mM phosphate buffer (pH 4.0 or 7.2) containing 25 mM NaCl in 90% H<sub>2</sub>O/10% D<sub>2</sub>O. Data were collected at 278 K.

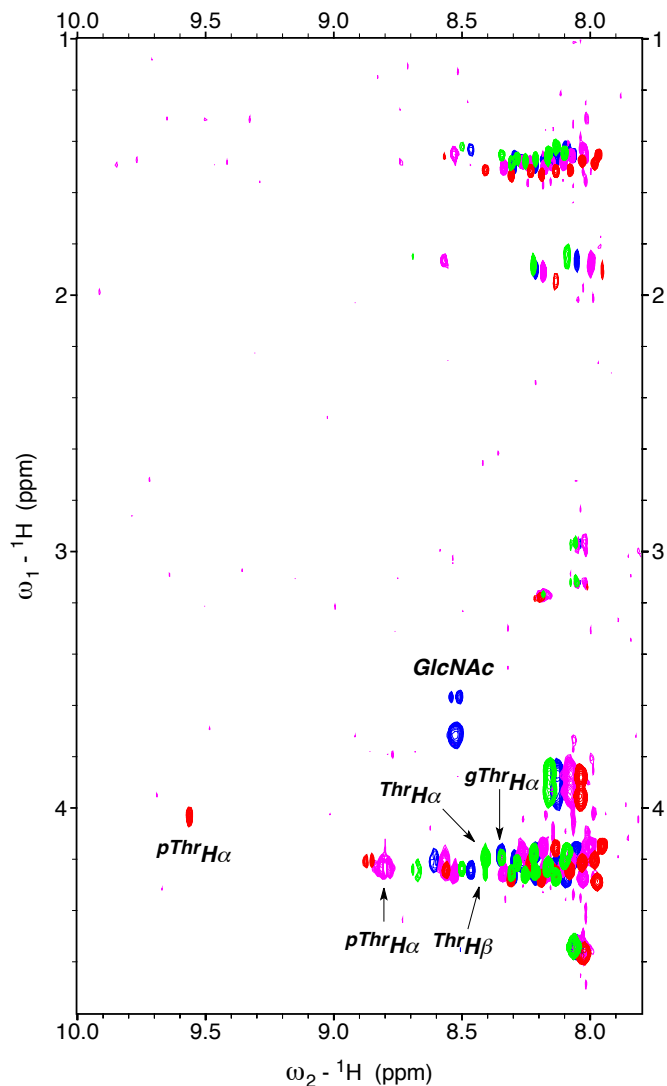


**Figure 1.54:** TOCSY spectra of Ac-TKAAAAKAAAAKAAGY-NH<sub>2</sub> peptides with threonine modifications: unmodified Thr(free hydroxyl), Thr(OGlcNAc), Thr(OPO<sub>3</sub>H<sup>-</sup>), and Thr(OPO<sub>3</sub><sup>2-</sup>). pThr indicates phosphorylated threonine residue; gThr indicates Thr(OGlcNAc) residue. Green: unmodified threonine; blue: Thr(OGlcNAc); magenta: phosphorylated threonine (pH 4.0); red: phosphorylated threonine (pH 7.2). Peptides were dissolved in 5 mM phosphate buffer (pH 4.0 or 7.2) containing 25 mM NaCl in 90% H<sub>2</sub>O/10% D<sub>2</sub>O. Data were collected at 278 K.

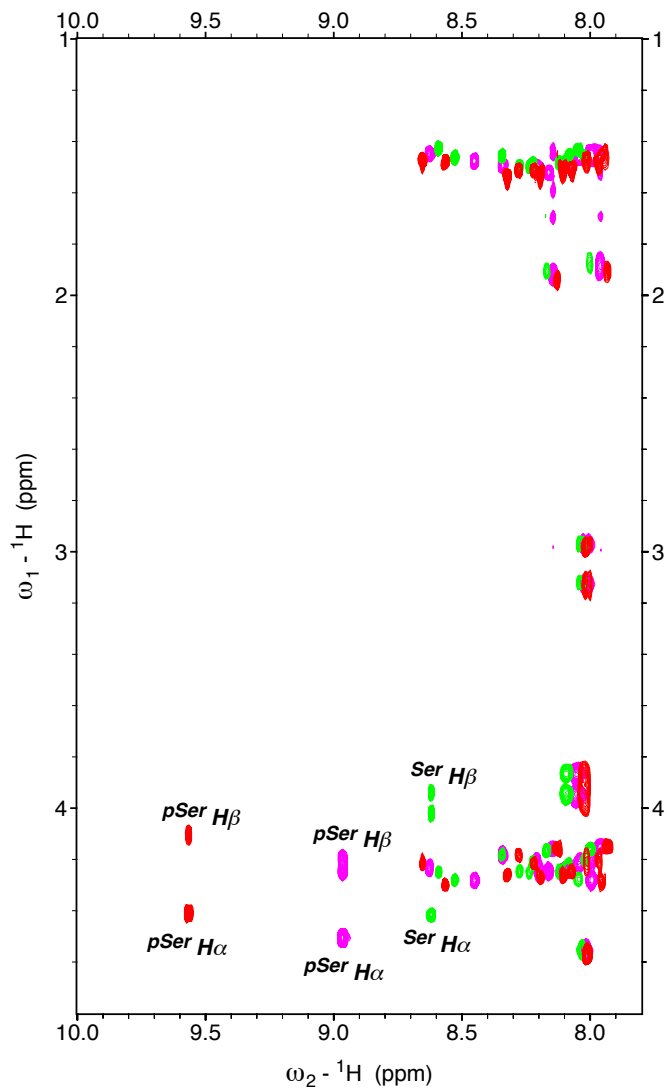


**Figure 1.55:** TOCSY spectra of Ac-ASAAAAKAAAAKAAGY-NH<sub>2</sub> peptides with serine modifications: unmodified Ser(free hydroxyl), Ser(OPO<sub>3</sub>H<sup>-</sup>), and Ser(OPO<sub>3</sub><sup>2-</sup>). pSer indicates phosphorylated serine residue. Green: unmodified serine; magenta: phosphorylated serine (pH 4.0); red: phosphorylated serine (pH 7.2). Peptides were dissolved in 5 mM phosphate buffer (pH 4.0 or 7.2) containing 25 mM NaCl in 90% H<sub>2</sub>O/10% D<sub>2</sub>O. Data were collected at 278 K.

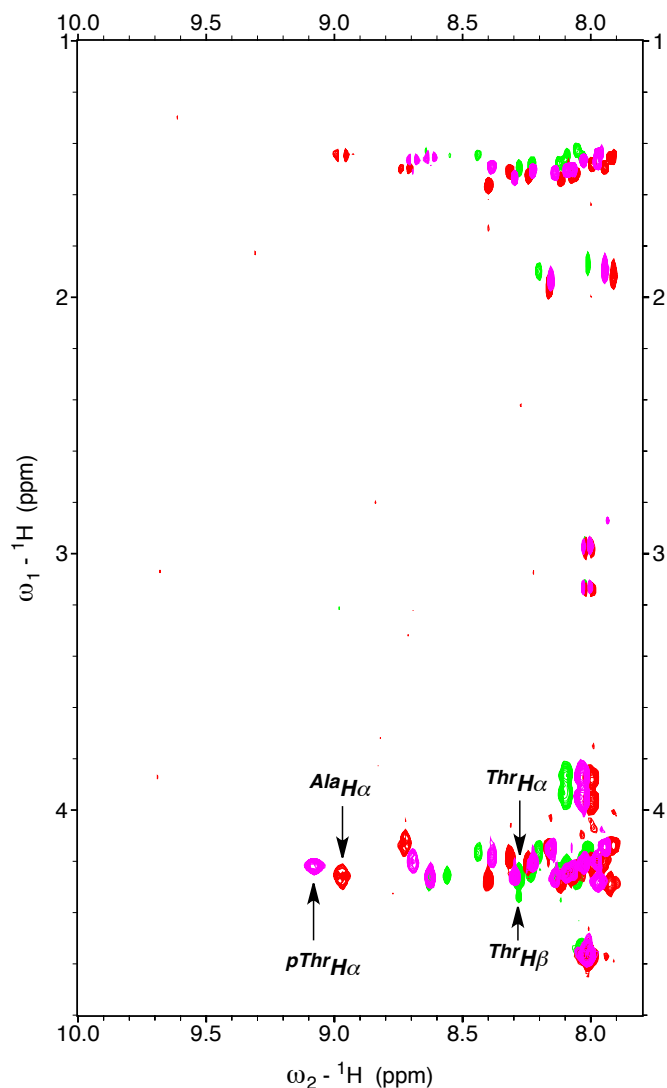


**Figure 1.56:** TOCSY spectra of Ac-ATAAAKAAAKAAGY-NH<sub>2</sub> peptides with threonine modifications: unmodified Thr(free hydroxyl), Thr(OPO<sub>3</sub>H<sup>-</sup>), and Thr(OPO<sub>3</sub><sup>2-</sup>). pThr indicates phosphorylated threonine residue. Green: unmodified threonine; magenta: phosphorylated threonine (pH 4.0); red: phosphorylated threonine (pH 7.2). Peptides were dissolved in 5 mM phosphate buffer (pH 4.0 or 7.2) containing 25 mM NaCl in 90% H<sub>2</sub>O/10% D<sub>2</sub>O. Data were collected at 278 K. The phosphorylated threonine amide proton ( $\delta = 10.24$  ppm) is not observed in the TOCSY spectrum at pH 7.2 and 298 K due to exchange dynamics. The peak at 10.24 ppm was assigned based on temperature-dependent NMR spectroscopy (Figure S25). At pH 7.2 at 305 K, this phosphothreonine is readily observed ( $\delta = 9.81$  ppm) in the TOCSY spectrum.

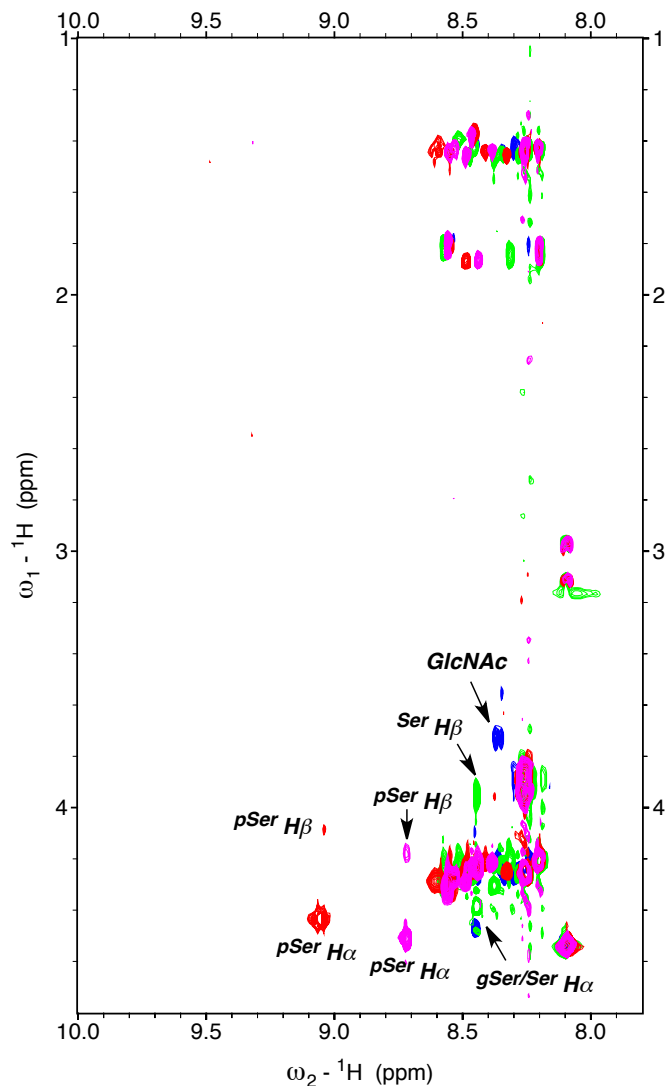


**Figure 1.57:** TOCSY spectra of Ac-AKAASAKAAAAKAAGY-NH<sub>2</sub> peptides with serine modifications: unmodified Ser(free hydroxyl), Ser(OGlcNAc), Ser(OPO<sub>3</sub>H<sup>-</sup>), and Ser(OPO<sub>3</sub><sup>2-</sup>). pSer indicates phosphorylated serine residue; gSer indicates Ser(OGlcNAc) residue. Green: unmodified serine; blue: Ser(OGlcNAc); magenta: phosphorylated serine (pH 4.0); red: phosphorylated serine (pH 7.2). Peptides were dissolved in 5 mM phosphate buffer (pH 4.0 or 7.2) containing 25 mM NaCl in 90% H<sub>2</sub>O/10% D<sub>2</sub>O. Data were collected at 278 K.

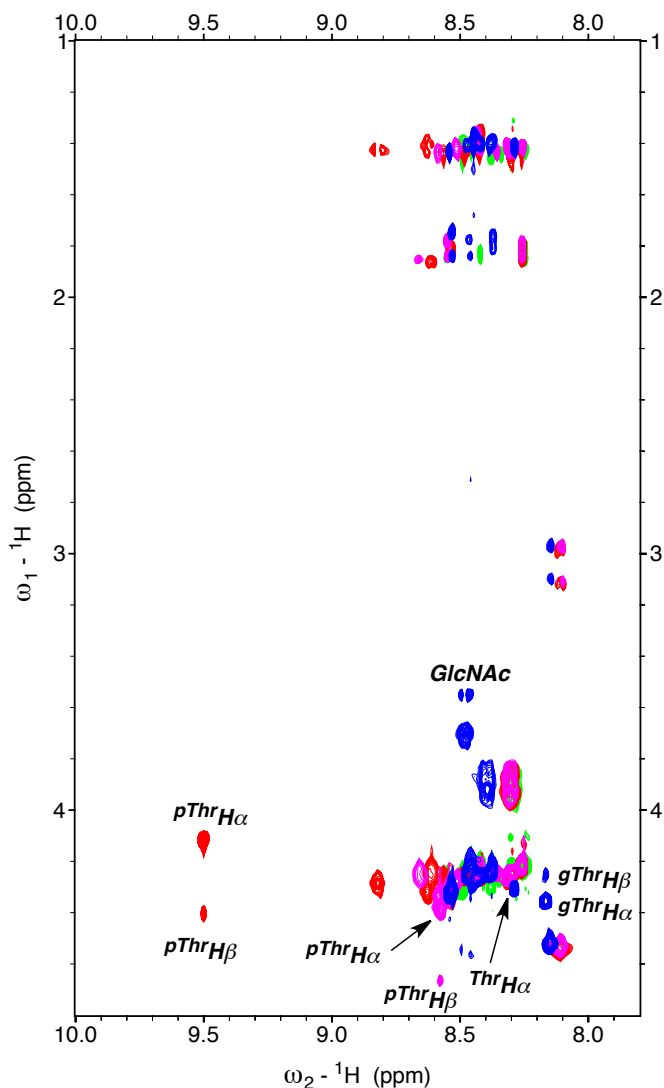


**Figure 1.58:** TOCSY spectra of Ac-AKAATAKAAA KAAGY-NH<sub>2</sub> peptides with threonine modifications: unmodified Thr(free hydroxyl), Thr(OGlcNAc), Thr(OPO<sub>3</sub>H<sup>-</sup>), and Thr(OPO<sub>3</sub><sup>2-</sup>). pThr indicates phosphorylated threonine residue; gThr indicates Thr(OGlcNAc) residue. Green: unmodified threonine; blue: Thr(OGlcNAc); magenta: phosphorylated threonine (pH 4.0); red: phosphorylated threonine (pH 7.2). Peptides were dissolved in 5 mM phosphate buffer (pH 4.0 or 7.2) containing 25 mM NaCl in 90% H<sub>2</sub>O/10% D<sub>2</sub>O. Data were collected at 278 K.

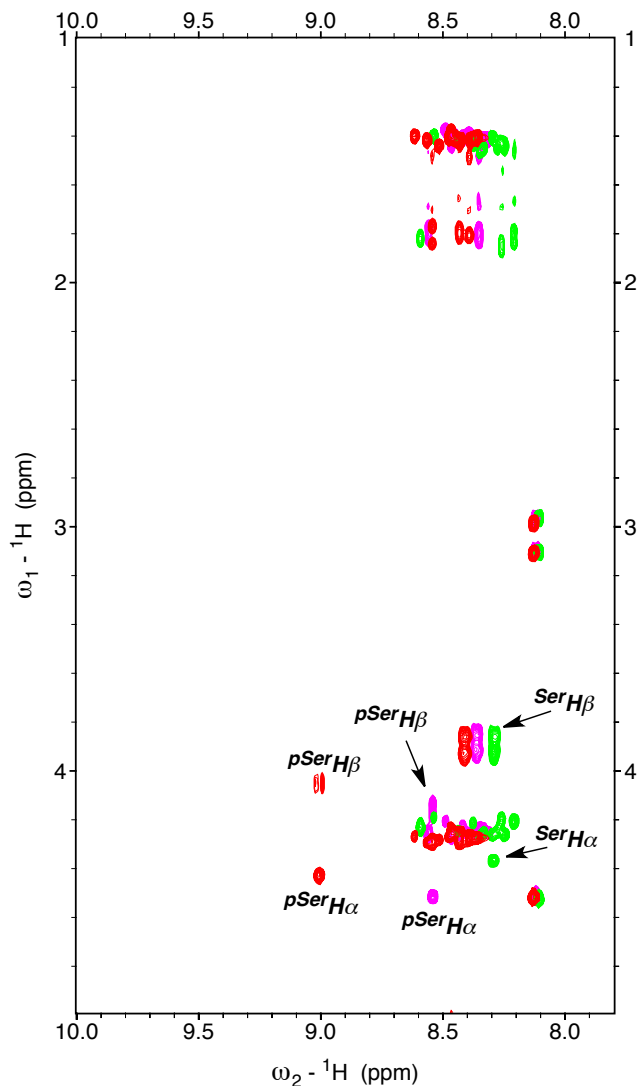


**Figure 1.59:** TOCSY spectra of Ac-AKAAAAKAASAKAAGY-NH<sub>2</sub> peptides with serine modifications: unmodified Ser(free hydroxyl), Ser(OPO<sub>3</sub>H<sup>-</sup>), and Ser(OPO<sub>3</sub><sup>2-</sup>). pSer indicates phosphorylated serine residue. Green: unmodified serine; magenta: phosphorylated serine (pH 4.0); red: phosphorylated serine (pH 7.2). Peptides were dissolved in 5 mM phosphate buffer (pH 4.0 or 7.2) containing 25 mM NaCl in 90% H<sub>2</sub>O/10% D<sub>2</sub>O. Data were collected at 278 K.

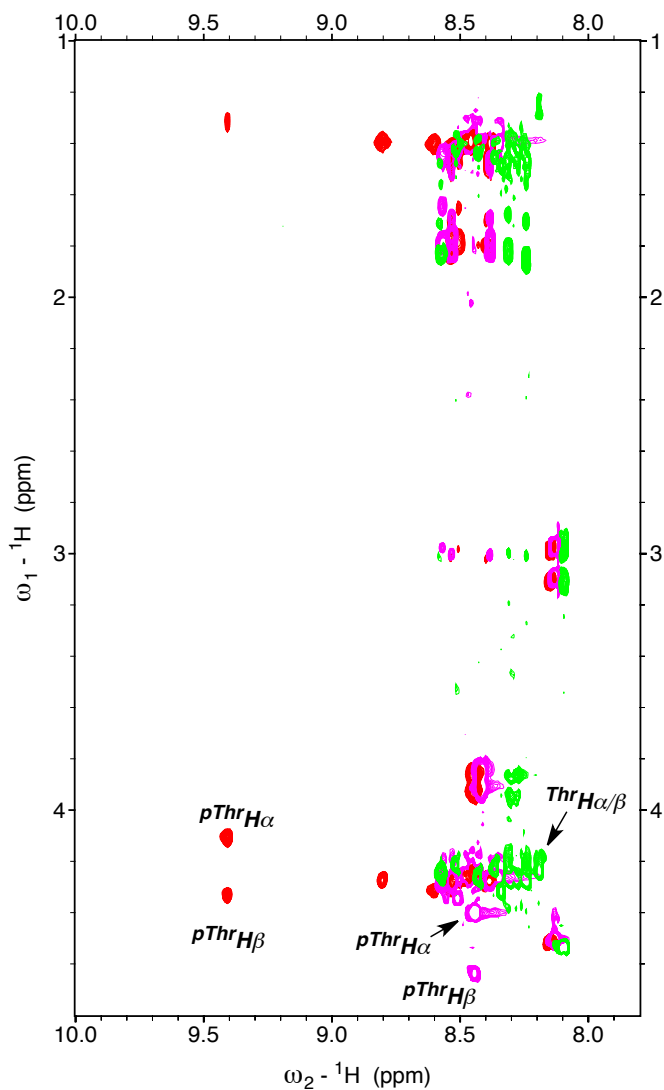


**Figure 1.60:** TOCSY spectra of Ac-AKAAAAKAATAKAAGY-NH<sub>2</sub> peptides with threonine modifications: unmodified Thr(free hydroxyl), Thr(OPO<sub>3</sub>H<sup>-</sup>), and Thr(OPO<sub>3</sub><sup>2-</sup>). pThr indicates phosphorylated threonine residue. Green: unmodified threonine; magenta: phosphorylated threonine (pH 4.0); red: phosphorylated threonine (pH 7.2). Peptides were dissolved in 5 mM phosphate buffer (pH 4.0 or 7.2) containing 25 mM NaCl in 90% H<sub>2</sub>O/10% D<sub>2</sub>O. Data were collected at 278 K.

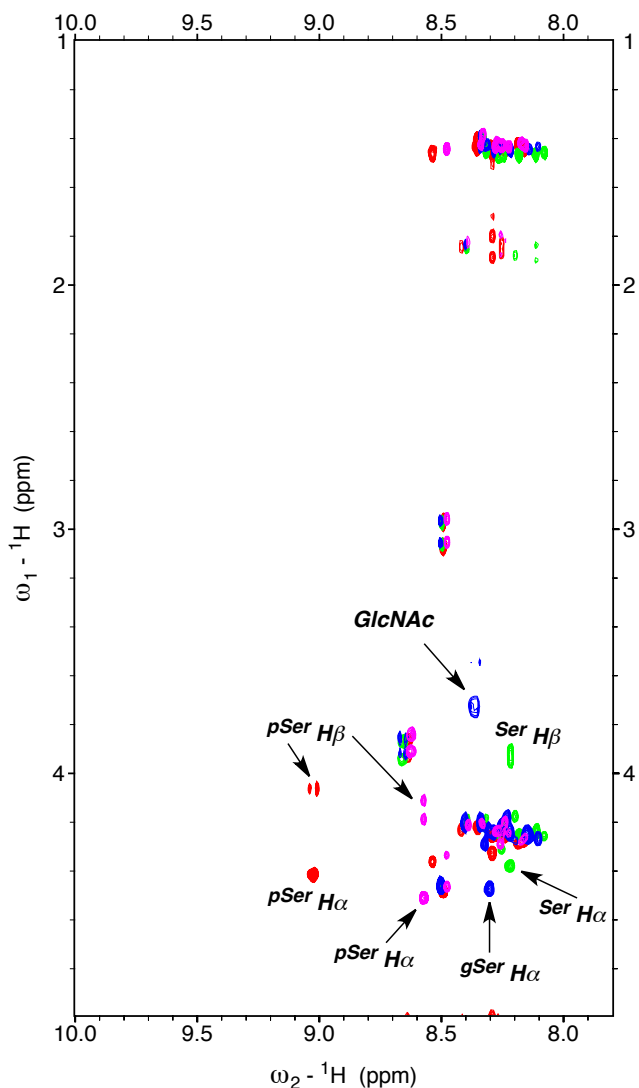


**Figure 1.61:** TOCSY spectra of Ac-YGAKAAAANKAAAAS-NH<sub>2</sub> peptides with serine modifications: unmodified Ser(free hydroxyl), Ser(OGlcNAc), Ser(OPO<sub>3</sub>H<sup>-</sup>), and Ser(OPO<sub>3</sub><sup>2-</sup>). pSer indicates phosphorylated serine residue; gSer indicates Ser(OGlcNAc) residue. Green: unmodified serine; blue: Ser(OGlcNAc); magenta: phosphorylated serine (pH 4.0); red: phosphorylated serine (pH 7.2). Peptides were dissolved in 5 mM phosphate buffer (pH 4.0 or 7.2) containing 25 mM NaCl in 90% H<sub>2</sub>O/10% D<sub>2</sub>O. Data were collected at 278 K.

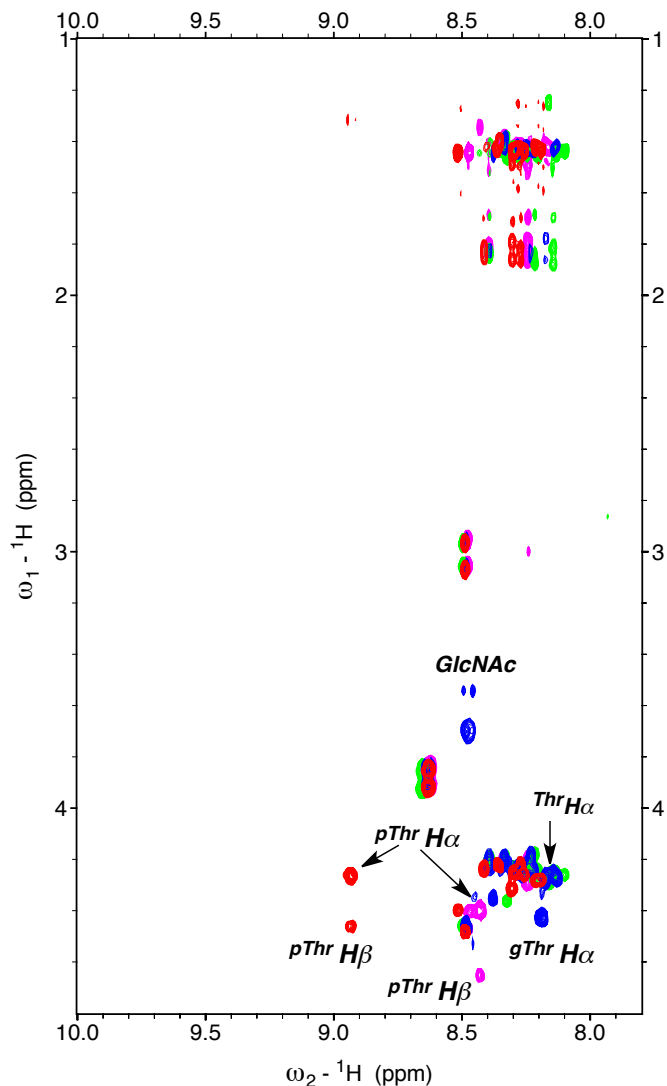


**Figure 1.62:** TOCSY spectra of Ac-YGAKAAAAKAAAAKAT-NH<sub>2</sub> peptides with threonine modifications: unmodified Thr(free hydroxyl), Thr(OGlcNAc), Thr(OPO<sub>3</sub>H<sup>-</sup>), and Thr(OPO<sub>3</sub><sup>2-</sup>). pThr indicates phosphorylated threonine residue; gThr indicates Thr(OGlcNAc) residue. Green: unmodified threonine; blue: Thr(OGlcNAc); magenta: phosphorylated threonine (pH 4.0); red: phosphorylated threonine (pH 7.2). Peptides were dissolved in 5 mM phosphate buffer (pH 4.0 or 7.2) containing 25 mM NaCl in 90% H<sub>2</sub>O/10% D<sub>2</sub>O. Data were collected at 278 K.

**$^1\text{H}$ - $^{13}\text{C}$  HSQC spectra of phosphorylated and unmodified Ac-AKAAAKAATAKAAGY-NH<sub>2</sub>**

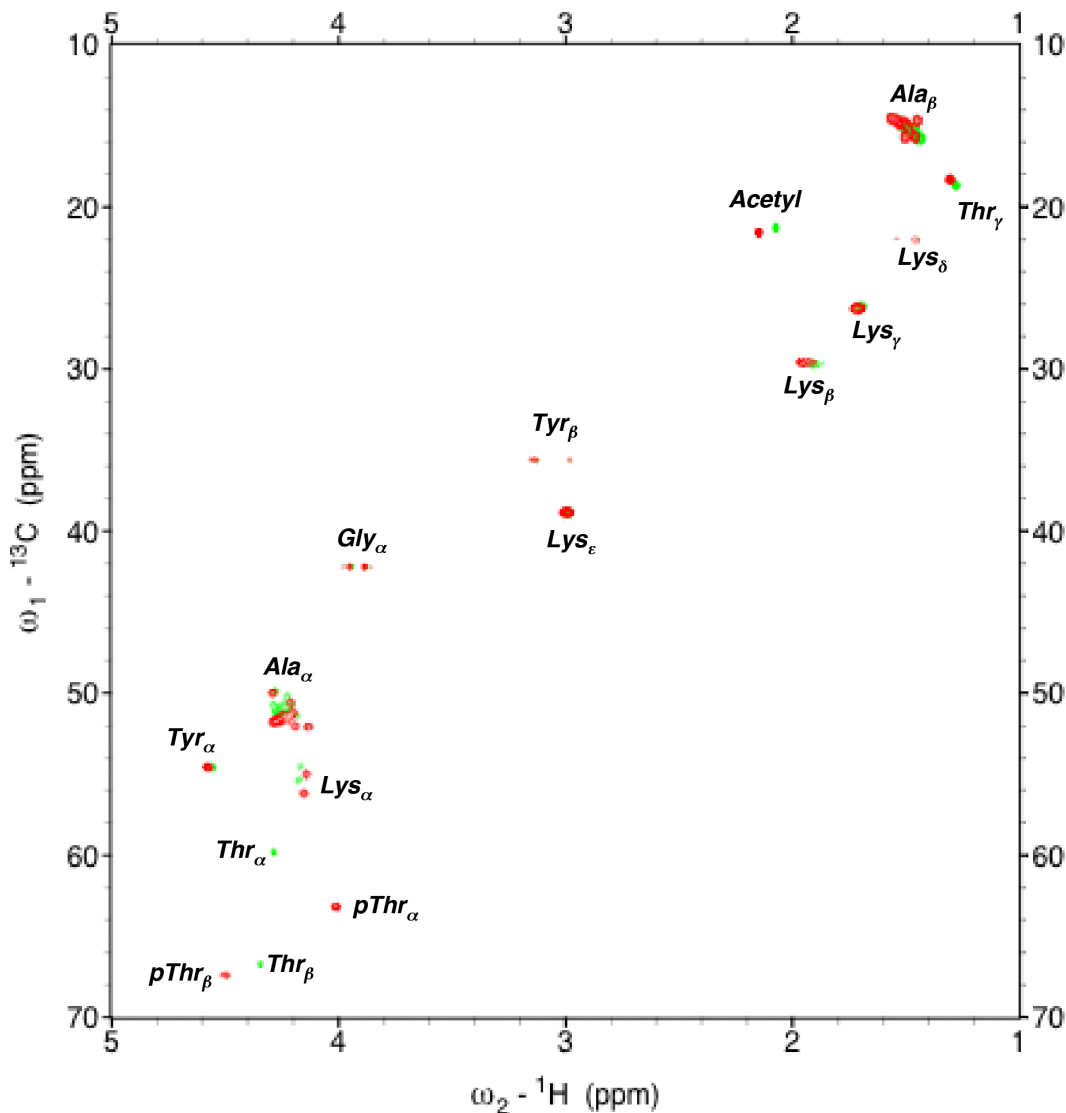


**Figure 1.63:**  $^1\text{H}$ - $^{13}\text{C}$  HSQC spectra of Ac-ATAAAKAATAKAAGY-NH<sub>2</sub> peptides with unmodified Thr(free hydroxyl) and Thr(OPO<sub>3</sub><sup>2-</sup>). pThr indicates phosphorylated threonine. Green: unmodified threonine; red: phosphorylated threonine (pH 8.0). Peptides were dissolved in 5 mM phosphate buffer (pH 4.0 or 8.0) containing 25 mM NaCl in D<sub>2</sub>O (278 K).

Peptide	$\delta, H^N$	$\delta, H\alpha$	$\delta, C\alpha$	$\delta, C\beta$
Ac-A <i>Thr</i> AAAAKAAAAKAAGY-NH <sub>2</sub>				
Thr	8.63	4.26	59.81	66.72
Lys	8.20	4.15	55.36	29.70
	8.01	4.15	54.49	29.70
Ala	8.56	4.27	50.73	15.14
	8.44	4.25	50.71	15.03
	8.28	4.16	49.91	15.18
	8.28	4.23	51.12	15.19
	8.23	4.24	51.09	15.22
	8.23	4.21	50.94	15.30
	8.12	4.23	50.27	15.64
	8.10	4.22	50.30	15.70
	8.09	4.21	50.91	15.76
	8.05	4.26	50.73	15.76
	8.03	4.19	51.39	15.83
Gly	8.10	3.92, 3.86	42.20	n.a.
Tyr	8.03	4.54	54.60	35.69
Acetyl	n.a.	2.06	21.27	n.a.
Ac-A <i>Thr</i> ( <i>OPO</i> <sub>3</sub> <sup>2-</sup> )AAAAKAAAAKAAGY-NH <sub>2</sub>				
Thr	10.24	4.02	63.22	67.42
Lys	8.16	4.14	56.17	29.59
	7.91	4.13	54.97	29.59
Ala	8.97	4.26	49.93	14.52
	8.72	4.12	51.76	14.68
	8.40	4.27	51.70	14.82
	8.31	4.16	51.44	15.09
	8.24	4.19	51.57	15.67
	8.12	4.27	51.44	15.27
	8.08	4.25	50.62	15.09
	8.06	4.23	51.20	15.36
	7.99	4.19	51.44	15.36
	7.95	4.18	52.07	15.69
	7.92	4.28	52.07	14.68
Gly	7.99	3.97, 3.86	42.19	n.a.
Tyr	8.01	4.57	54.59	35.59
Acetyl	n.a.	2.15	21.57	n.a.

**Table 1.41:** Summary of <sup>1</sup>H-<sup>13</sup>C HSQC and TOCSY NMR data at 278 K of peptides with Thr and pThr at residue 2. <sup>1</sup>H-<sup>13</sup>C HSQC spectra were collected at pH 4.0 for unmodified threonine and at pH 8.0 for phosphorylated threonine. Data were collected in 5 mM phosphate buffer containing 25 mM NaCl in D<sub>2</sub>O. TOCSY data were collected at pH 4.0 for unmodified threonine and at pH 7.2 for phosphorylated threonine. Data were collected in 5 mM phosphate buffer containing 25 mM NaCl in 90% H<sub>2</sub>O/D<sub>2</sub>O.

**$^1\text{H}$ - $^{13}\text{C}$  HSQC spectra of phosphorylated and unmodified Ac-AKAAAAKAATAKAAGY-NH<sub>2</sub>**

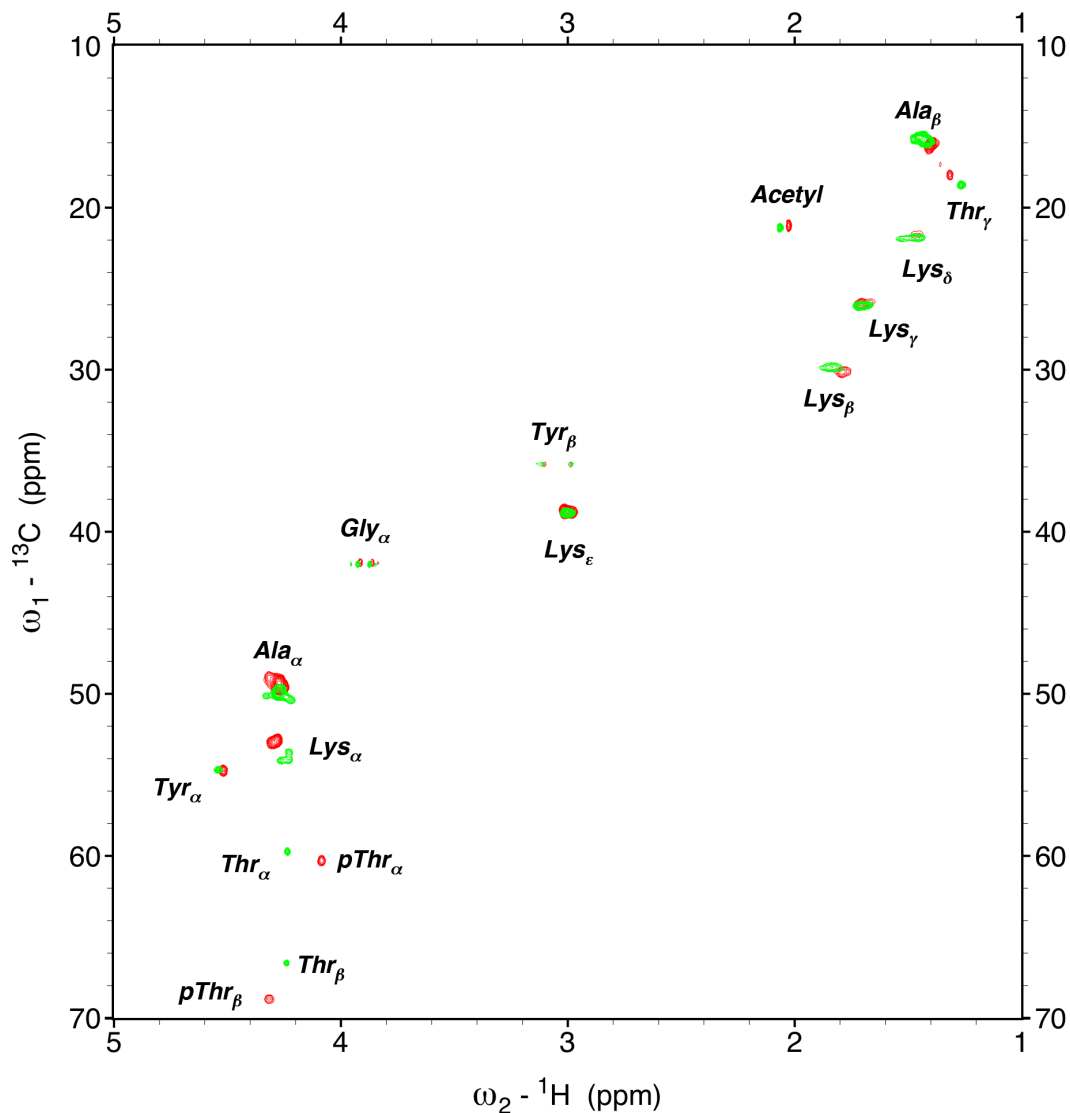


**Figure 1.64:**  $^1\text{H}$ - $^{13}\text{C}$  HSQC spectra of Ac-AKAAAAKAATAKAAGY-NH<sub>2</sub> peptides with unmodified Thr(free hydroxyl) and Thr(OPO<sub>3</sub><sup>2-</sup>). pThr indicates phosphorylated threonine. Green: unmodified threonine; red: phosphorylated threonine (pH 8.0). Peptides were dissolved in 5 mM phosphate buffer (pH 4.0 or 8.0) containing 25 mM NaCl in D<sub>2</sub>O (278 K).

Peptide	$\delta, H^N$	$\delta, H\alpha$	$\delta, C\alpha$	$\delta, C\beta$
Ac-AKAAAAKAA <i>Thr</i> AKAAGY-NH <sub>2</sub>				
Thr	8.19	4.25	59.72	66.61
Lys	8.57	4.25	54.13	29.88
	8.31	4.25	54.06	29.88
	8.24	4.24	53.64	29.88
Ala	8.52	4.21	50.12	15.75
	8.36	4.23	50.02	15.71
	8.34	4.33	49.75	15.69
	8.31	4.26	49.99	15.73
	8.31	4.26	50.07	15.77
	8.29	4.27	50.04	15.80
	8.28	4.27	50.04	15.83
	8.27	4.27	50.07	15.85
	8.24	4.27	50.21	15.87
	8.24	4.27	50.38	15.89
Gly	8.29	3.95, 3.85	42.04	n.a.
Tyr	8.10	4.52	54.67	35.85
Acetyl	n.a.	2.06	21.22	n.a.
Ac-AKAAAAKAA <i>Thr(OPO<sub>3</sub><sup>2-</sup>)</i> AKAAGY-NH <sub>2</sub>				
Thr	9.41	4.09	60.33	68.85
Lys	8.53	4.28	53.01	30.05
	8.50	4.26	52.96	30.13
	8.40	4.28	52.87	30.13
Ala	8.80	4.26	49.15	16.14
	8.61	4.32	49.04	16.14
	8.53	4.26	49.31	16.08
	8.50	4.26	49.31	16.08
	8.50	4.26	49.33	16.08
	8.48	4.26	49.33	16.07
	8.45	4.25	49.33	16.06
	8.45	4.25	49.43	16.06
	8.39	4.27	49.54	16.06
	8.38	4.26	49.55	16.06
Gly	8.44	3.91, 3.86	41.89	n.a.
Tyr	8.15	4.51	54.73	35.82
Acetyl	n.a.	2.02	21.11	n.a.

**Table 1.42:** Summary of <sup>1</sup>H-<sup>13</sup>C HSQC and TOCSY NMR data at 278 K of peptides with Thr and pThr at residue 10. <sup>1</sup>H-<sup>13</sup>C HSQC spectra were collected at pH 4.0 for unmodified threonine and at pH 8.0 for phosphorylated threonine. Data were collected in 5 mM phosphate buffer containing 25 mM NaCl in D<sub>2</sub>O. TOCSY data were collected at pH 4.0 for unmodified threonine and at pH 7.2 for phosphorylated threonine. Data were collected in 5 mM phosphate buffer containing 25 mM NaCl in 90% H<sub>2</sub>O/D<sub>2</sub>O.

### $^{31}\text{P}$ spectra of phosphorylated peptides.

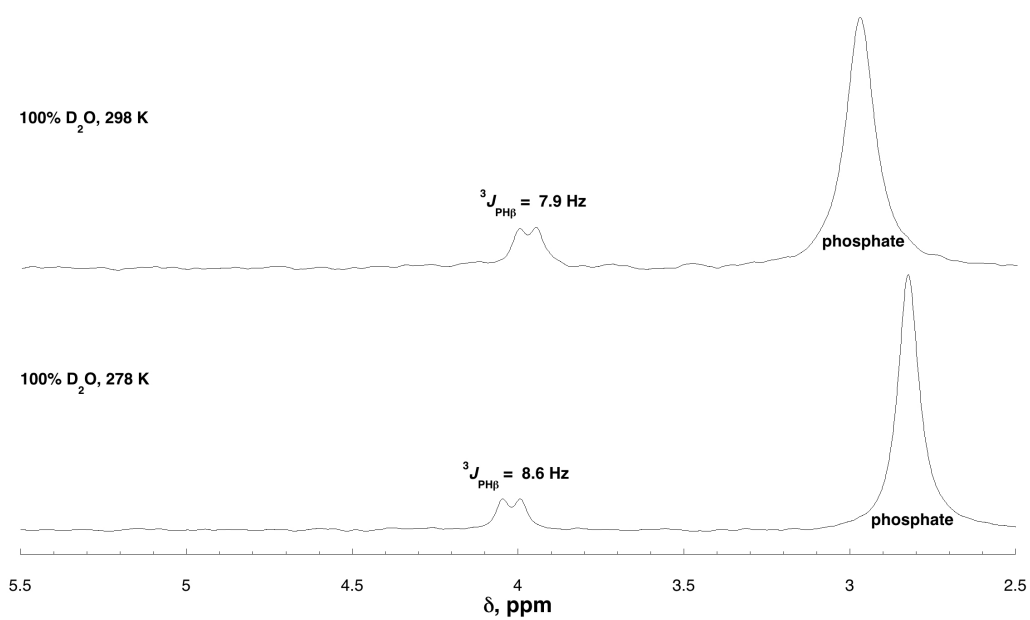


**Figure 1.65:**  $^{31}\text{P}$  NMR spectra of peptide Ac-T(OPO<sub>3</sub><sup>2-</sup>)KAAAKAATAAGY-NH<sub>2</sub> in 5 mM phosphate buffer (pH 8.0) containing 25 mM NaCl in D<sub>2</sub>O.

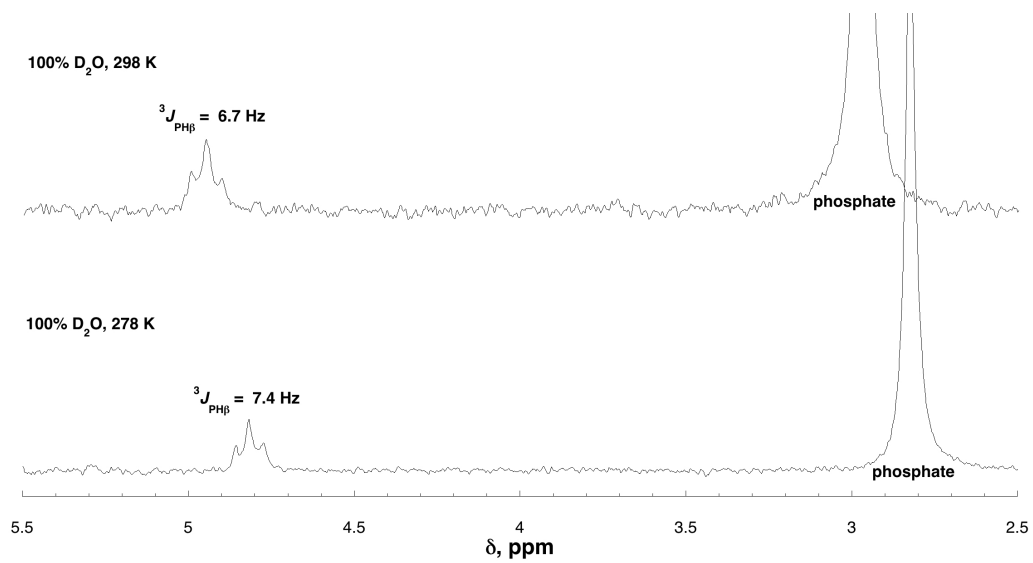


**Figure 1.66:**  $^{31}\text{P}$  NMR spectra of peptide Ac-AS(OPO<sub>3</sub><sup>2-</sup>)AAAAA KAAGY-NH<sub>2</sub> in 5 mM phosphate buffer (pH 8.0) containing 25 mM NaCl in D<sub>2</sub>O.

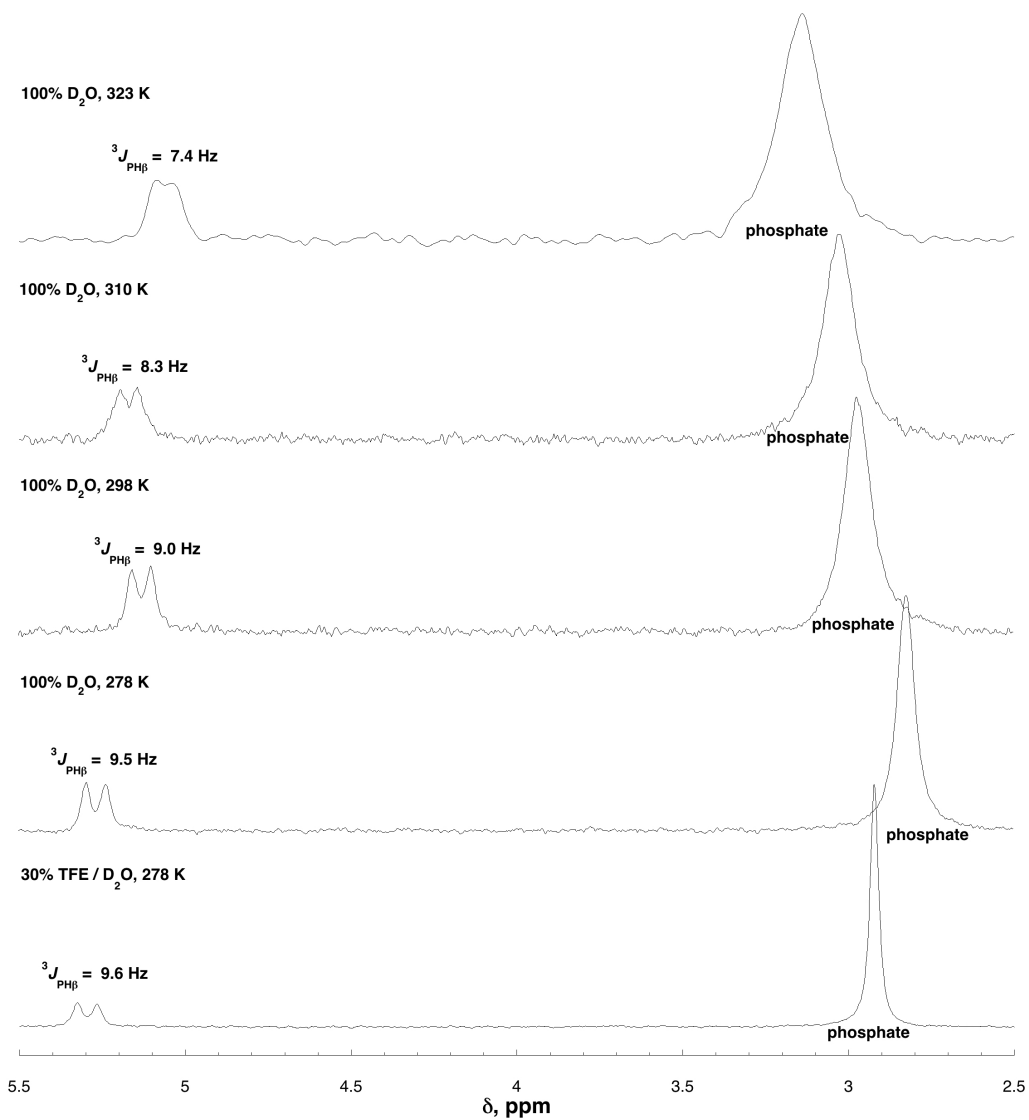


**Figure 1.67:**  $^{31}\text{P}$  NMR spectra of peptide  $\text{Ac-AT}(\text{OPO}_3^{2-})\text{AAAKAAA KAAGY-NH}_2$  in 5 mM phosphate buffer (pH 8.0) containing 25 mM NaCl in  $\text{D}_2\text{O}$  or 30% TFE/ $\text{D}_2\text{O}$ .

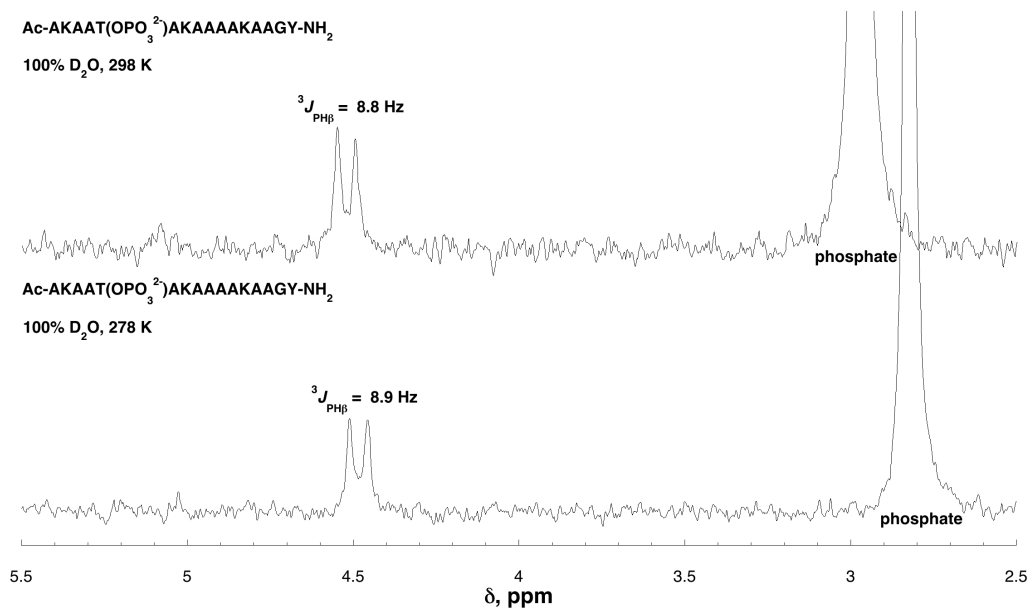


**Figure 1.68:** <sup>31</sup>P NMR spectra of peptide Ac-AKAAT(OPO<sub>3</sub><sup>2-</sup>)AKAAAAKAAGY-NH<sub>2</sub> in 5 mM phosphate buffer (pH 8.0) containing 25 mM NaCl in D<sub>2</sub>O.

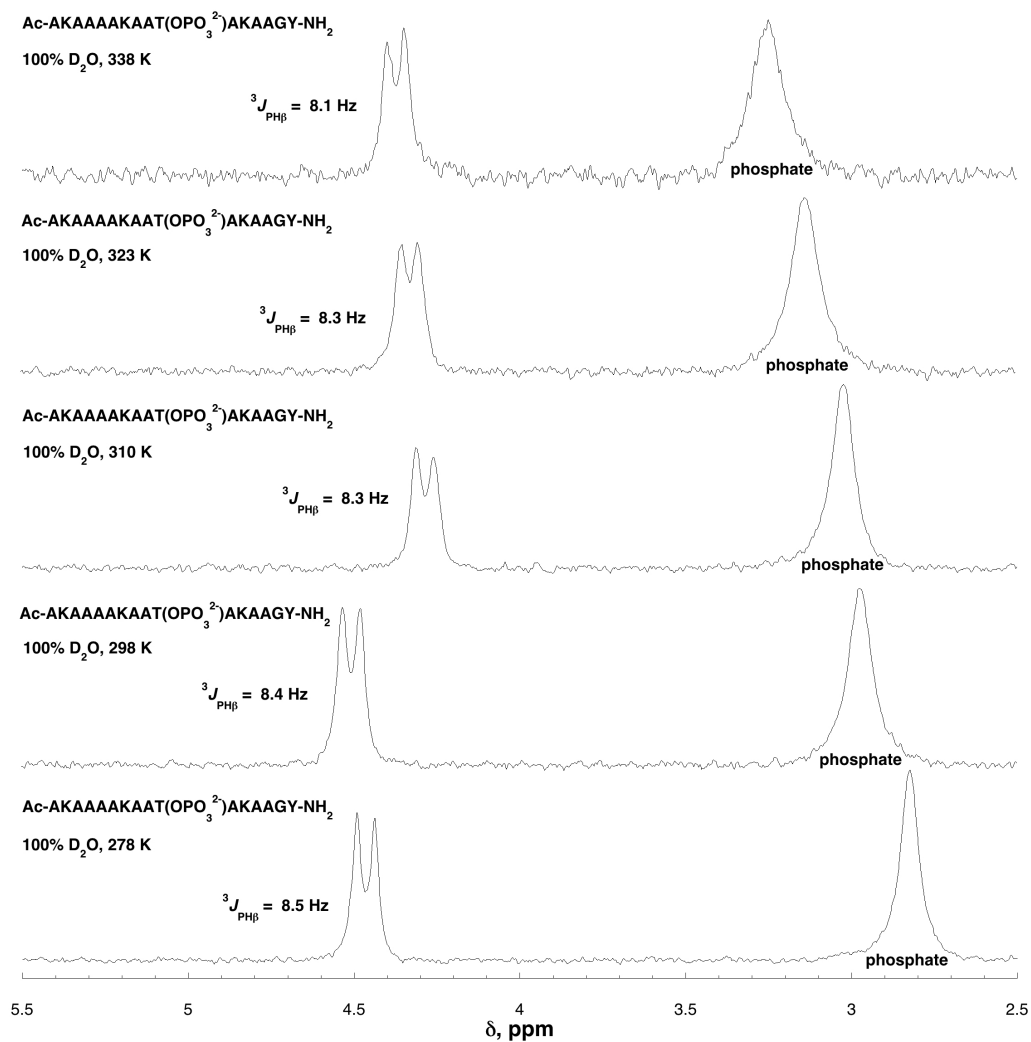


**Figure 1.69:**  $^{31}\text{P}$  NMR spectra of peptide Ac-AKAAAAKAAT(OPO<sub>3</sub><sup>2-</sup>)AKAAGY-NH<sub>2</sub> in 5 mM phosphate buffer (pH 8.0) containing 25 mM NaCl in D<sub>2</sub>O.

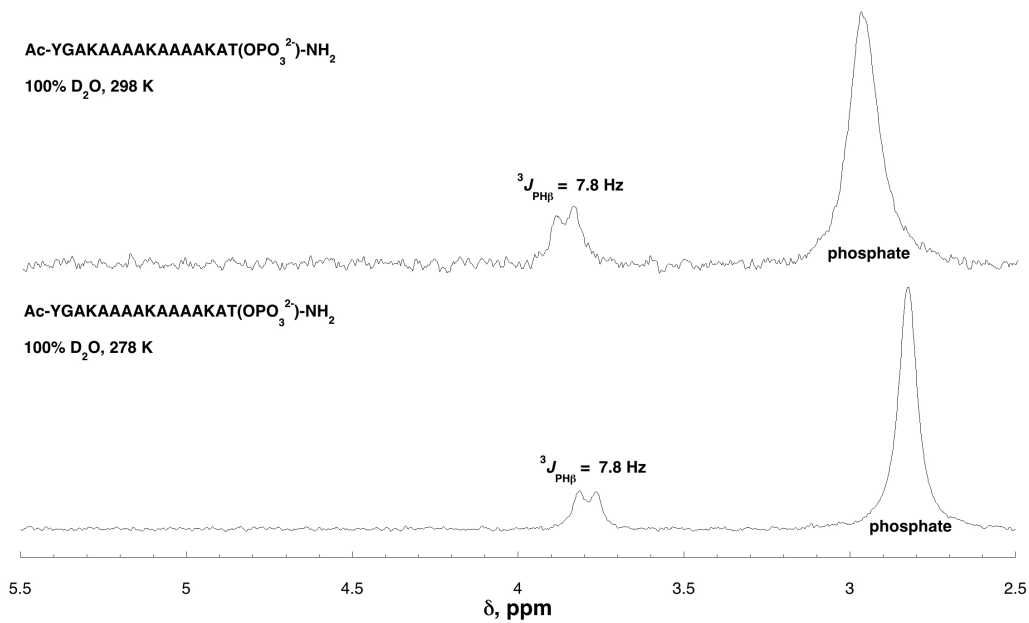


**Figure 1.70:**  $^{31}\text{P}$  NMR spectra of peptide Ac-YGAKAAAKAAAKAT(OPO<sub>3</sub><sup>2-</sup>)-NH<sub>2</sub> in 5 mM phosphate buffer (pH 8.0) containing 25 mM NaCl in D<sub>2</sub>O.

## Quantitative analysis of NMR data

$\delta, \text{H}^{\text{N}}$	<i>Ser(OH)</i>	<i>Ser(OGlcNAc)</i>	<i>Ser(OPO<sub>3</sub>H<sup>-</sup>)</i>	<i>Ser(OPO<sub>3</sub><sup>2-</sup>)</i>
<b>N1</b>	8.58	8.62	8.91	9.41
<b>N2</b>	8.62	n.a.	8.97	9.57
<b>N5</b>	8.44	8.45	8.71	9.06
<b>N10</b>	8.30	n.a.	8.54	9.01
<b>N14</b>	8.22	8.30	8.57	9.02

**Table 1.43:** Amide proton chemical shifts of unmodified and modified serine residues on peptides with unmodified Ser(free hydroxyl), Ser(OGlcNAc), Ser(OPO<sub>3</sub>H<sup>-</sup>) at pH 4.0, and Ser(OPO<sub>3</sub><sup>2-</sup>) at pH 7.2. The positions of modified and unmodified serine residues are indicated: residue 1 (N1), residue 2 (N2), residue 5 (N5), residue 10 (N10), and residue 14 (N14).

<sup>3</sup> $J_{\alpha\text{N}}$	<i>Ser(OH)</i>	<i>Ser(OGlcNAc)</i>	<i>Ser(OPO<sub>3</sub>H<sup>-</sup>)</i>	<i>Ser(OPO<sub>3</sub><sup>2-</sup>)</i>
<b>N1</b>	5.1	3.3	4.4	3.6
<b>N2</b>	5.7	n.a.	5.1	4.3
<b>N5</b>	n.d.	n.d.	5.7	4.5
<b>N10</b>	n.d.	n.a.	n.a.	3.3
<b>N14</b>	n.d.	n.d.	6.8	6.3

**Table 1.44:** Coupling constants between serine amide and alpha protons of unmodified and modified serine residues on peptides with unmodified Ser(free hydroxyl), Ser(OGlcNAc), Ser(OPO<sub>3</sub>H<sup>-</sup>) at pH 4.0, and Ser(OPO<sub>3</sub><sup>2-</sup>) at pH 7.2. The positions of modified and unmodified serine residues are indicated: residue 1 (N1), residue 2 (N2), residue 5 (N5), residue 10 (N10), and residue 14 (N14).

$\delta, H\alpha$	<i>Ser(OH)</i>	<i>Ser(OGlcNAc)</i>	<i>Ser(OPO<sub>3</sub>H<sup>-</sup>)</i>	<i>Ser(OPO<sub>3</sub><sup>2-</sup>)</i>
<b>N1</b>	4.34	4.35	4.40	4.29
<b>N2</b>	4.41	n.a.	4.51	4.41
<b>N5</b>	4.37	4.46	4.51	4.44
<b>N10</b>	4.37	n.a.	4.50	4.42
<b>N14</b>	4.37	4.48	4.50	4.42

**Table 1.45:** Alpha proton chemical shifts of unmodified and modified serine residues on peptides with unmodified Ser(free hydroxyl), Ser(OGlcNAc), Ser(OPO<sub>3</sub>H<sup>-</sup>) at pH 4.0, and Ser(OPO<sub>3</sub><sup>2-</sup>) at pH 7.2. The positions of modified and unmodified serine residues are indicated: residue 1 (N1), residue 2 (N2), residue 5 (N5), residue 10 (N10), and residue 14 (N14).

$\delta, H\beta$	<i>Ser(OH)</i>	<i>Ser(OGlcNAc)</i>	<i>Ser(OPO<sub>3</sub>H<sup>-</sup>)</i>	<i>Ser(OPO<sub>3</sub><sup>2-</sup>)</i>
<b>N1</b>	3.97, 3.90	4.11, 3.95	4.20, 4.17	4.14, 4.08
<b>N2</b>	4.02, 3.95	n.a.	4.25, 4.20	4.10
<b>N5</b>	3.95	4.09	4.17	4.09
<b>N10</b>	3.92, 3.90	n.a.	4.18, 4.14	4.05
<b>N14</b>	3.93, 3.91	4.11, 3.89	4.18, 4.09	4.06

**Table 1.46:** Beta proton chemical shifts of unmodified and modified serine residues on peptides with unmodified Ser(free hydroxyl), Ser(OGlcNAc), Ser(OPO<sub>3</sub>H<sup>-</sup>) at pH 4.0, and Ser(OPO<sub>3</sub><sup>2-</sup>) at pH 7.2. The positions of modified and unmodified serine residues are indicated: residue 1 (N1), residue 2 (N2), residue 5 (N5), residue 10 (N10), and residue 14 (N14).

$\delta$ , H-Acetyl	<i>Ser(OH)</i>	<i>Ser(OGlcNAc)</i>	<i>Ser(OPO<sub>3</sub>H<sup>-</sup>)</i>	<i>Ser(OPO<sub>3</sub><sup>2-</sup>)</i>
<b>N1</b>	2.097	2.127, 2.068	2.133	2.154
<b>N2</b>	2.069	n.a.	2.090	2.127
<b>N5</b>	2.049	2.040, 2.018	2.029	2.026
<b>N10</b>	2.059	n.a.	2.033	2.033
<b>N14</b>	1.989	2.029, 1.981	1.974	1.983

**Table 1.47:** Chemical shifts of acetyl protons on the N-terminus of peptides with unmodified Ser(free hydroxyl), Ser(OGlcNAc), Ser(OPO<sub>3</sub>H<sup>-</sup>) at pH 4.0, and Ser(OPO<sub>3</sub><sup>2-</sup>) at pH 7.2. Chemical shifts of acetyl protons on GlcNAc are also reported for peptides containing Ser(OGlcNAc). The positions of modified and unmodified serine residues are indicated: residue 1 (N1), residue 2 (N2), residue 5 (N5), residue 10 (N10), and residue 14 (N14).

$\delta$ , Carboxamide (-CONH <sub>2</sub> )	<i>Ser(OH)</i>	<i>Ser(OGlcNAc)</i>	<i>Ser(OPO<sub>3</sub>H<sup>-</sup>)</i>	<i>Ser(OPO<sub>3</sub><sup>2-</sup>)</i>
<b>N1</b>	7.66, 7.24	7.66, 7.24	7.65, 7.24	7.65, 7.25
<b>N2</b>	7.64, 7.23	n.a.	7.64, 7.24	7.63, 7.23
<b>N5</b>	7.68, 7.22	7.69, 7.22	7.67, 7.22	7.68, 7.23
<b>N10</b>	7.68, 7.22	n.a.	7.69, 7.22	7.70, 7.23
<b>N14</b>	7.64, 7.34	7.64, 7.38	7.65, 7.35	7.73, 7.30

**Table 1.48:** Chemical shifts of carboxamide protons on the C-terminus of peptides with unmodified Ser(free hydroxyl), Ser(OGlcNAc), Ser(OPO<sub>3</sub>H<sup>-</sup>) at pH 4.0, and Ser(OPO<sub>3</sub><sup>2-</sup>) at pH 7.2. The positions of modified and unmodified serine residues are indicated: residue 1 (N1), residue 2 (N2), residue 5 (N5), residue 10 (N10), and residue 14 (N14).

Mean $\delta$ , $H^N_{Ala}$	<i>Ser(OH)</i>	<i>Ser(OGlcNAc)</i>	<i>Ser(OPO<sub>3</sub>H<sup>-</sup>)</i>	<i>Ser(OPO<sub>3</sub><sup>2-</sup>)</i>
<b>N1</b>	8.21 ± 0.12	8.21 ± 0.12	8.17 ± 0.12	8.16 ± 0.15
<b>N2</b>	8.24 ± 0.18	n.a.	8.22 ± 0.19	8.21 ± 0.22
<b>N5</b>	8.33 ± 0.11	8.47 ± 0.34	8.36 ± 0.13	8.50 ± 0.28
<b>N10</b>	8.34 ± 0.09	n.a.	8.41 ± 0.06	8.47 ± 0.07
<b>N14</b>	8.23 ± 0.08	8.25 ± 0.08	8.26 ± 0.08	8.31 ± 0.11

**Table 1.49:** Mean chemical shifts of alanine amide protons on peptides with unmodified Ser(free hydroxyl), Ser(OGlcNAc), Ser(OPO<sub>3</sub>H<sup>-</sup>) at pH 4.0, and Ser(OPO<sub>3</sub><sup>2-</sup>) at pH 7.2. The positions of modified and unmodified serine residues are indicated: residue 1 (N1), residue 2 (N2), residue 5 (N5), residue 10 (N10), and residue 14 (N14). Standard deviations of the mean values are indicated.

Mean $\delta$ , $H^\alpha_{Ala}$	<i>Ser(OH)</i>	<i>Ser(OGlcNAc)</i>	<i>Ser(OPO<sub>3</sub>H<sup>-</sup>)</i>	<i>Ser(OPO<sub>3</sub><sup>2-</sup>)</i>
<b>N1</b>	4.21 ± 0.03	4.23 ± 0.02	4.22 ± 0.03	4.23 ± 0.03
<b>N2</b>	4.24 ± 0.03	n.a.	4.23 ± 0.03	4.24 ± 0.02
<b>N5</b>	4.24 ± 0.03	4.24 ± 0.02	4.24 ± 0.03	4.26 ± 0.02
<b>N10</b>	4.23 ± 0.02	n.a.	4.24 ± 0.02	4.26 ± 0.02
<b>N14</b>	4.23 ± 0.03	4.24 ± 0.04	4.26 ± 0.02	4.27 ± 0.04

**Table 1.50:** Mean chemical shifts of alanine alpha protons on peptides with unmodified Ser(free hydroxyl), Ser(OGlcNAc), Ser(OPO<sub>3</sub>H<sup>-</sup>) at pH 4.0, and Ser(OPO<sub>3</sub><sup>2-</sup>) at pH 7.2. The positions of modified and unmodified serine residues are indicated: residue 1 (N1), residue 2 (N2), residue 5 (N5), residue 10 (N10), and residue 14 (N14). Standard deviations of the mean values are indicated.

Mean $\delta$ , $H^{\beta}_{Ala}$	<i>Ser(OH)</i>	<i>Ser(OGlcNAc)</i>	<i>Ser(OPO<sub>3</sub>H<sup>-</sup>)</i>	<i>Ser(OPO<sub>3</sub><sup>2-</sup>)</i>
<b>N1</b>	1.43 ± 0.02	1.46 ± 0.02	1.46 ± 0.03	1.48 ± 0.02
<b>N2</b>	1.47 ± 0.02	n.a.	1.48 ± 0.02	1.49 ± 0.02
<b>N5</b>	1.43 ± 0.02	1.42 ± 0.02	1.42 ± 0.03	1.42 ± 0.02
<b>N10</b>	1.42 ± 0.02	n.a.	1.40 ± 0.02	1.40 ± 0.02
<b>N14</b>	1.44 ± 0.02	1.42 ± 0.01	1.41 ± 0.01	1.43 ± 0.01

**Table 1.51:** Mean chemical shifts of alanine beta protons on peptides with unmodified Ser(free hydroxyl), Ser(OGlcNAc), Ser(OPO<sub>3</sub>H<sup>-</sup>) at pH 4.0, and Ser(OPO<sub>3</sub><sup>2-</sup>) at pH 7.2. The positions of modified and unmodified serine residues are indicated: residue 1 (N1), residue 2 (N2), residue 5 (N5), residue 10 (N10), and residue 14 (N14). Standard deviations of the mean values are indicated.

### Quantitative analysis of NMR data: peptides containing threonine and modified threonine residues

$\delta$ , $H^N$	<i>Thr(OH)</i>	<i>Thr(OGlcNAc)</i>	<i>Thr(OPO<sub>3</sub>H<sup>-</sup>)</i>	<i>Thr(OPO<sub>3</sub><sup>2-</sup>)</i>
<b>N1</b>	8.40	8.34	8.80	9.57
<b>N2</b>	8.63	n.a.	9.08	10.24
<b>N5</b>	8.29	8.16	8.57	9.50
<b>N10</b>	8.19	n.a.	8.44	9.41
<b>N14</b>	8.18	8.18	8.42	8.93

**Table 1.52:** Amide proton chemical shifts of unmodified and modified threonine residues on peptides containing unmodified Thr(free hydroxyl), Thr(OGlcNAc), Thr(OPO<sub>3</sub>H<sup>-</sup>) at pH 4.0, and Thr(OPO<sub>3</sub><sup>2-</sup>) at pH 7.2. The positions of modified and unmodified threonine residues are indicated: residue 1 (N1), residue 2 (N2), residue 5 (N5), residue 10 (N10), and residue 14 (N14).

$^3 J_{\alpha N}$	<i>Thr(OH)</i>	<i>Thr(OGlcNAc)</i>	<i>Thr(OPO<sub>3</sub>H<sup>-</sup>)</i>	<i>Thr(OPO<sub>3</sub><sup>2-</sup>)</i>
<b>N1</b>	6.2	5.1	4.8	3.5
<b>N2</b>	4.7	n.a.	n.d.	3.7
<b>N5</b>	n.d.	n.d.	n.d.	4.1
<b>N10</b>	6.8	n.a.	n.d.	4.5
<b>N14</b>	7.9	8.0	7.9	6.2

**Table 1.53:** Coupling constants between threonine amide and alpha protons of unmodified and modified threonine residues on peptides containing unmodified Thr(free hydroxyl), Thr(OGlcNAc), Thr(OPO<sub>3</sub>H<sup>-</sup>) at pH 4.0, and Thr(OPO<sub>3</sub><sup>2-</sup>) at pH 7.2. The positions of modified and unmodified threonine residues are indicated: residue 1 (N1), residue 2 (N2), residue 5 (N5), residue 10 (N10), and residue 14 (N14).

$\delta, H_{\alpha}$	<i>Thr(OH)</i>	<i>Thr(OGlcNAc)</i>	<i>Thr(OPO<sub>3</sub>H<sup>-</sup>)</i>	<i>Thr(OPO<sub>3</sub><sup>2-</sup>)</i>
<b>N1</b>	4.25	4.18	4.23	4.04
<b>N2</b>	4.26	n.a.	4.21	4.02
<b>N5</b>	4.23	4.34	4.36	4.11
<b>N10</b>	4.25	n.a.	4.40	4.09
<b>N14</b>	4.29	4.42	4.39	4.26

**Table 1.54:** Alpha proton chemical shifts of unmodified and modified threonine residues on peptides containing unmodified Thr(free hydroxyl), Thr(OGlcNAc), Thr(OPO<sub>3</sub>H<sup>-</sup>) at pH 4.0, and Thr(OPO<sub>3</sub><sup>2-</sup>) at pH 7.2. The positions of modified and unmodified threonine residues are indicated: residue 1 (N1), residue 2 (N2), residue 5 (N5), residue 10 (N10), and residue 14 (N14).

$\delta, \text{H}\beta$	<i>Thr(OH)</i>	<i>Thr(OGlcNAc)</i>	<i>Thr(OPO<sub>3</sub>H<sup>-</sup>)</i>	<i>Thr(OPO<sub>3</sub><sup>2-</sup>)</i>
<b>N1</b>	4.19	4.26	4.64	4.47
<b>N2</b>	4.33	n.a.	4.62	4.51
<b>N5</b>	4.26	4.24	4.65	4.39
<b>N10</b>	4.21	n.a.	4.62	4.34
<b>N14</b>	4.29	4.34	4.64	4.46

**Table 1.55:** Beta proton chemical shifts of unmodified and modified threonine residues on peptides containing unmodified Thr(free hydroxyl), Thr(OGlcNAc), Thr(OPO<sub>3</sub>H<sup>-</sup>) at pH 4.0, and Thr(OPO<sub>3</sub><sup>2-</sup>) at pH 7.2. The positions of modified and unmodified threonine residues are indicated: residue 1 (N1), residue 2 (N2), residue 5 (N5), residue 10 (N10), and residue 14 (N14).

$\text{Thr, H}\gamma$	<i>Thr(OH)</i>	<i>Thr(OGlcNAc)</i>	<i>Thr(OPO<sub>3</sub>H<sup>-</sup>)</i>	<i>Thr(OPO<sub>3</sub><sup>2-</sup>)</i>
<b>N1</b>	1.27	1.23	1.40	1.32
<b>N2</b>	1.27	n.a.	1.35	1.30
<b>N5</b>	1.26	1.20	1.36	1.32
<b>N10</b>	1.25	n.a.	1.33	1.31
<b>N14</b>	1.25	1.18	1.34	1.31

**Table 1.56:** Gamma proton chemical shifts of unmodified and modified threonine residues on peptides containing unmodified Thr(free hydroxyl), Thr(OGlcNAc), Thr(OPO<sub>3</sub>H<sup>-</sup>) at pH 4.0, and Thr(OPO<sub>3</sub><sup>2-</sup>) at pH 7.2. The positions of modified and unmodified threonine residues are indicated: residue 1 (N1), residue 2 (N2), residue 5 (N5), residue 10 (N10), and residue 14 (N14).

$\delta$ , Acetyl	<i>Thr(OH)</i>	<i>Thr(OGlcNAc)</i>	<i>Thr(OPO<sub>3</sub>H<sup>-</sup>)</i>	<i>Thr(OPO<sub>3</sub><sup>2-</sup>)</i>
<b>N1</b>	2.123	2.148, 2.080	2.162	2.154
<b>N2</b>	2.060	n.a.	2.108	2.147
<b>N5</b>	2.038	2.059, 2.014	2.016	2.013
<b>N10</b>	2.059	n.a.	2.019	2.025
<b>N14</b>	1.981	2.054, 1.975	1.975	1.985

**Table 1.57:** Chemical shifts of acetyl protons on the N-terminus of peptides containing unmodified Thr(free hydroxyl), Thr(OGlcNAc), Thr(OPO<sub>3</sub>H<sup>-</sup>) at pH 4.0, and Thr(OPO<sub>3</sub><sup>2-</sup>) at pH 7.2). Chemical shifts of acetyl protons on GlcNAc are also reported for peptides containing Thr(OGlcNAc). The positions of modified and unmodified threonine residues are indicated: residue 1 (N1), residue 2 (N2), residue 5 (N5), residue 10 (N10), and residue 14 (N14).

$\delta$ , Carboxamide (-CONH <sub>2</sub> )	<i>Thr(OH)</i>	<i>Thr(OGlcNAc)</i>	<i>Thr(OPO<sub>3</sub>H<sup>-</sup>)</i>	<i>Thr(OPO<sub>3</sub><sup>2-</sup>)</i>
<b>N1</b>	7.66, 7.23	7.66, 7.23	7.65, 7.25	7.65, 7.24
<b>N2</b>	7.65, 7.23	n.a.	7.63, 7.23	7.64, 7.25
<b>N5</b>	7.68, 7.22	7.70, 7.22	7.68, 7.22	7.69, 7.23
<b>N10</b>	7.68, 7.22	n.a.	7.69, 7.21	7.71, 7.22
<b>N14</b>	7.59, 7.32	7.50, 7.39	7.67, 7.30	7.89, 7.25

**Table 1.58:** Chemical shifts of carboxamide protons on the C-terminus on peptides with unmodified Thr(free hydroxyl), Thr(OGlcNAc), Thr(OPO<sub>3</sub>H<sup>-</sup>) at pH 4.0, and Thr(OPO<sub>3</sub><sup>2-</sup>) at pH 7.2). The positions of modified and unmodified threonine residues are indicated: residue 1 (N1), residue 2 (N2), residue 5 (N5), residue 10 (N10), and residue 14 (N14).

Mean $\delta$ , $H^N_{Ala}$	<i>Thr(OH)</i>	<i>Thr(OGlcNAc)</i>	<i>Thr(OPO<sub>3</sub>H<sup>-</sup>)</i>	<i>Thr(OPO<sub>3</sub><sup>2-</sup>)</i>
<b>N1</b>	8.24 ± 0.11	8.21 ± 0.12	8.19 ± 0.15	8.19 ± 0.19
<b>N2</b>	8.22 ± 0.16	n.a.	8.22 ± 0.24	8.25 ± 0.32
<b>N5</b>	8.36 ± 0.08	8.42 ± 0.06	8.41 ± 0.10	8.45 ± 0.17
<b>N10</b>	8.32 ± 0.08	n.a.	8.44 ± 0.05	8.31 ± 0.43
<b>N14</b>	8.23 ± 0.08	8.25 ± 0.08	8.27 ± 0.09	8.30 ± 0.09

**Table 1.59:** Mean chemical shifts of alanine amide protons on peptides with unmodified Thr(free hydroxyl), Thr(OGlcNAc), Thr(OPO<sub>3</sub>H<sup>-</sup>) at pH 4.0, and Thr(OPO<sub>3</sub><sup>2-</sup>) at pH 7.2. The positions of modified and unmodified threonine residues are indicated: residue 1 (N1), residue 2 (N2), residue 5 (N5), residue 10 (N10), and residue 14 (N14). Standard deviations of the mean values are indicated.

Mean $\delta$ , $H^\alpha_{Ala}$	<i>Thr(OH)</i>	<i>Thr(OGlcNAc)</i>	<i>Thr(OPO<sub>3</sub>H<sup>-</sup>)</i>	<i>Thr(OPO<sub>3</sub><sup>2-</sup>)</i>
<b>N1</b>	4.22 ± 0.02	4.22 ± 0.03	4.21 ± 0.03	4.23 ± 0.04
<b>N2</b>	4.23 ± 0.04	n.a.	4.22 ± 0.04	4.22 ± 0.05
<b>N5</b>	4.25 ± 0.03	4.25 ± 0.03	4.25 ± 0.03	4.25 ± 0.02
<b>N10</b>	4.26 ± 0.03	n.a.	4.26 ± 0.02	4.27 ± 0.02
<b>N14</b>	4.25 ± 0.04	4.24 ± 0.04	4.25 ± 0.05	4.27 ± 0.04

**Table 1.60:** Mean chemical shifts of alanine alpha protons on peptides with unmodified Thr(free hydroxyl), Thr(OGlcNAc), Thr(OPO<sub>3</sub>H<sup>-</sup>) at pH 4.0, and Thr(OPO<sub>3</sub><sup>2-</sup>) at pH 7.2. The positions of modified and unmodified threonine residues are indicated: residue 1 (N1), residue 2 (N2), residue 5 (N5), residue 10 (N10), and residue 14 (N14). Standard deviations of the mean values are indicated.

Mean $\delta$ , $H^{\beta}_{Ala}$	<i>Thr(OH)</i>	<i>Thr(OGlcNAc)</i>	<i>Thr(OPO<sub>3</sub>H<sup>-</sup>)</i>	<i>Thr(OPO<sub>3</sub><sup>2-</sup>)</i>
<b>N1</b>	1.43 ± 0.02	1.45 ± 0.02	1.46 ± 0.02	1.49 ± 0.02
<b>N2</b>	1.46 ± 0.03	n.a.	1.47 ± 0.02	1.50 ± 0.04
<b>N5</b>	1.42 ± 0.02	1.39 ± 0.01	1.41 ± 0.02	1.41 ± 0.02
<b>N10</b>	1.44 ± 0.03	n.a.	1.39 ± 0.01	1.39 ± 0.01
<b>N14</b>	1.44 ± 0.02	1.42 ± 0.01	1.41 ± 0.02	1.43 ± 0.01

**Table 1.61:** Mean chemical shifts of alanine beta protons on peptides with unmodified Thr(free hydroxyl), Thr(OGlcNAc), Thr(OPO<sub>3</sub>H<sup>-</sup>) at pH 4.0, and Thr(OPO<sub>3</sub><sup>2-</sup>) at pH 7.2. The positions of modified and unmodified threonine residues are indicated: residue 1 (N1), residue 2 (N2), residue 5 (N5), residue 10 (N10), and residue 14 (N14). Standard deviations of the mean values are indicated.

	<i>Thr(OH)</i>	<i>Thr(OPO<sub>3</sub><sup>2-</sup>)</i>	$\Delta\delta$
$\delta$ , $C^{\alpha}$			
<b>N2</b>	59.81	63.22	+3.41
<b>N10</b>	59.72	60.33	+0.61
$\delta$ , $C^{\beta}$			
<b>N2</b>	66.72	67.42	+0.70
<b>N10</b>	66.61	68.85	+2.24

**Table 1.62:** Alpha and beta carbon chemical shifts of threonine on peptides containing unmodified Thr(free hydroxyl) and Thr(OPO<sub>3</sub><sup>2-</sup>) at pH 8.0. The change in chemical shifts from unmodified to phosphorylated threonine is indicated.

	<i>Thr(OH)</i> Mean $\delta$	<i>Thr(OPO<sub>3</sub><sup>2-</sup>)</i> Mean $\delta$	$\Delta\delta$
<b>C<sup><math>\alpha</math></sup><sub>Ala</sub></b>			
<b>N2</b>	50.74 $\pm$ 0.41	51.39 $\pm$ 0.60	+0.65
<b>N10</b>	50.07 $\pm$ 0.16	49.33 $\pm$ 0.16	-0.74
<b>C<sup><math>\beta</math></sup><sub>Ala</sub></b>			
<b>N2</b>	15.43 $\pm$ 0.29	15.11 $\pm$ 0.38	-0.32
<b>N10</b>	15.79 $\pm$ 0.07	16.08 $\pm$ 0.03	+0.29

**Table 1.63:** Mean alpha and beta carbon chemical shifts of alanine residues on peptides containing unmodified Thr(free hydroxyl) and Thr(OPO<sub>3</sub><sup>2-</sup>) at pH 8.0. Standard deviations of mean values are indicated. The change in mean chemical shift of alanine between the peptides indicated.

	<i>Thr(OH)</i> Mean $\delta$	<i>Thr(OPO<sub>3</sub><sup>2-</sup>)</i> Mean $\delta$	$\Delta\delta$
<b>Lys, C<math>\gamma</math></b>			
<b>N2</b>	54.94	55.60	+0.66
<b>N10</b>	53.93	52.95	-0.98

**Table 1.64:** Mean alpha carbon chemical shifts of lysine residues on peptides containing unmodified Thr(free hydroxyl) and Thr(OPO<sub>3</sub><sup>2-</sup>) at pH 8.0. The change in mean chemical shift of lysine between the peptides is indicated.

## REFERENCES

1. Cohen, P. *Eur J Biochem* **2001**, 268, 5001-5010.
2. Manning, G., Whyte, D. B., Martinez, and R., Hunter, T., and Sudarsanam, S. *Science* **2002**, 298, 1912-1934.
3. Wang, Z., Gucek, M., and Hart, G. W. *Proc. Natl. Acad. Sci.* **2008**, 105, 13793-13798.
4. Hu, P., Shimoji, S., and Hart, G. W. *FEBS Lett* **2010**, 584, 2526-2538.
5. Hart, G. W., Housley, M. P., and Slawson. *Nature* **2007**, 446, 1017-1022.
6. Hart, G. W., Slawson, C., Ramirez-Correa, G., and Lagerlof, O. *Ann Rev Biochem* **2011**, 80, 825-858.
7. Comer, F. I., Hart G. W. *J. Biol. Chem.* **2000**, 275, 29179-29182.
8. Kamemura, K., Hayes, B. K., Comer, F. I., and Hart, G. W. *J Biol Chem* **2002**, 277, 19229-19235.
9. Chen, Y.-X., Du, J.-T., Zhou, L.-X., Liu, X.-H., Zhao, Y.-F., Nakanishi, H., and Li, Y.-M. *Chem. Biol.* **2006**, 13, 937-944.
10. Simanek, E. E., Huang, D.-H., Pasternack, L., Machajewski, T. D., Seitz, O., Millar, D. S., Dyson, H. J., and Wong, C.-H. *J. Am. Chem. Soc.* **1998**, 120, 11567-11575.
11. Liang, F.-C., Chen, R. P.-Y., Lin, C.-C., Huang, K.-T., and Chan, S. I. *Biochem. Biophys. Res. Commun.* **2006**, 342, 482-488.
12. Alonso, A. D. C., Grundke-Iqbal, I., and Iqbal, K. *Nat. Med.* **1996**, 2, 783-787.
13. Buee, L., Bussiere, T., Buee-Scherrer, V., Delacourte, A., Hof, P. R., *Brain. Res. Rev.* **2000**, 33, 95-130
14. Avila, J., Lucas, J. J., Perez, M., Hernandez, F. *Physiol. Rev.* **2004**, 84, 361-384.

15. Liu, Fei., Iqbal, Khalid., Grundke-Iqbal, I., Hart, G. W., and Gong, C.-X. *Proc. Natl. Acad. Sci.* **2004**, *101*, 10804-10809.
16. Yuzwa, S. A., Shan, X., Macauley, M. S., Clark, T., Skorobogatko, Y., Vosseller, K., and Vocadlo, D. J. *Nat. Chem. Biol.* **2012**, *8*, 393-399.
17. Bielska, A. A., and Zondlo, N. J. *Biochemistry.* **2006**, *45*, 5527-5537.
18. Brister, M. A., Pandey, A. K., Bielska, A. A., and Zondlo, N. J. *J. Am. Chem. Soc.* **2014**, *136*, 3803-3816.
19. Andrew, C. D., Warwicker, J., Jones, G. R., Doig, A. J. *Biochemistry*, **2002**, *41*, 1897-1905.
20. Errington, N., Doig, A. J., *Biochemistry*, **2005**, *44*, 7553-7558.
21. Signarvic, R. S., DeGrado, W. F. *J. Mol. Biol.* **2003**, *334*, 1-12.
22. Szilak, L., Moitra, J., and Vinson, C. *Protein. Science.* **1997**, *6*, 1273-1283.
23. Szilak, L., Moitra, J., Krylov, D., and Vinson, C. *Nat. Struct. Biol.* **1997**, *4*, 112-114.
24. Broncel, M., Falenski, J. A., Wagner, S. C., Hackenberger, C. P. R., Kocsch, B. *Chem. Eur. J.* **2010**, *16*, 7881-7888.
25. Tachibana, Y., Fletcher, G. L., Fujitani, S. T., Monde, K., Nishimura, S.-I. *Angew. Chem. Int. Ed.* **2004**, *43*, 856-862.
26. Doig, A. J., Baldwin, R. L. *Protein Sci.* **1995**, *4*, 1325-1336.
27. Balakrishnan, S., Zondlo, N. J. *J. Am. Chem. Soc.* **2006**, *128*, 5590-5591.
28. Arsequell, G., Krippner, L., Dwek, R. A. *J. Chem. Soc., Chem. Commun.* **1994**, 2383-2384.
29. Sjölin, P., Elofsson, M., Kihlberg, J. *J. Org. Chem.* **1996**, *61*, 560-565.
30. Luo, P. Z., Baldwin, R. L. *Biochemistry*, **1997**, *36*, 8413-8421.
31. Rohl, C. A., Baldwin, R. L. *Biochemistry*, **1997**, *36*, 8435-8422
32. Chakrabarty, A., Doig, A. J., Baldwin, R. L. *Proc. Natl. Acad. Sci.* **1993**, *90*, 11332-11336.
33. Cochran, D. A. E., Penel, S., Doig, A. J. *Protein Sci.* **2001**, *10*, 463-470.

34. Stapley, B. J., Doig, A. J. *J. Mol. Biol.* **1997**, *272*, 456-464.
35. Tholey, A., Lindemann, A., Kinzel, V., Reed, J. *Biophysical J.* **1999**, *76*, 76-87.
36. Bienkiewicz, E. A., Lumb, K. J. *J. Biomol. NMR.* **1999**, *15*, 203-206.
37. Landrieu, I., Lacosse, L., Leroy, A., Wieruszkeski, J.-M., Trivelli, X., Sillen, A., Sibille, N., Schwalbe, H., Saxena, K., Langer, T., Lippens, G. *J. Am. Chem. Soc.* **2006**, *128*, 3575-3583.
38. Marshall, G. R., Hodkin, E. E., Langs, D. A., Smith, G. D., Zabrocki, J., Leplawy, M. R. *Proc. Natl. Acad. Sci.* **1990**, *87*, 487-491.
39. Banerjee, R., Basu, G. *ChemBioChem.* **2002**, *12*, 1263-1266
40. Venkataraman, J., Shankaramma, S. C., Balaram, P. *Chem. Rev.* **2001**, *101*, 3131-3152.
41. Chakrabarty, A., Kortemme, T., Baldwin, R. L. *Protein Sci.* **1994**, *3*, 843-852.
42. Lyu, P. C., Liff, M. I., Marky, L. A., Kallenbach, N. R. *Science.* **1990**, *250*, 669-673.
43. O'Neil, K. T., DeGrado, W. F. *Science.* **1990**, *250*, 646-651.
44. Engel, D. E., DeGrado, W. F. *J. Mol. Biol.* **2004**, *337*, 1195-1205.
45. Shepherd, N. E., Hoang, H. N., Abbenante, G., Fairlie, D. P. *J. Am. Chem. Soc.* *127*, 2974-2983.
46. Serrano, L., Fersht, A. R. *Nature.* **1989**, *342*, 296-299.
47. Shoemaker, K. R., Kim, P. S., York, E. J., Stewart, J. M., Baldwin, R. L. *Nature.* **1987**, *326*, 563-567.
48. Schneider, J. P., DeGrado, W. F. *J. Am. Chem. Soc.* **1998**, *120*, 2764-2767.
49. Wishart, D. S., Sykes, B. D., Richards, F. M. *Biochemistry*, **1992**, *31*, 1647-1651
50. Wishart, D. S., Sykes, B. D. *J. Biomol. NMR.* **1994**, *4*, 171-180

51. Zondlo, S. C., Lee, A. E., Zondlo, N. J. *Biochemistry*, **2006**, *45*, 11945-11957.
52. Richardson, J. S., Richardson, D. C. *Science*, **1988**, *240*, 1648-1652.
53. Presta, L. G., Rose, G. D. *Science*, **1988**, *240*, 1632-1641.
54. Barlow, D. J., Thornton, J. M. *J. Mol. Biol.* **1988**, *201*, 601-619.
55. Gunasekaran, K., Nagarajaram, H. A., Ramakrishnan, C., Balaram, P. *J. Mol. Biol.* **1998**, *275*, 917-932.
56. Penel, S., Hughes, E., Doig, A. J. *J. Mol. Biol.* **1999**, *287*, 127-143.
57. Lankhorst, P. P., Haasnoot, C. A. G., Erkelens, C., Altona, C. *J. Biomol. Struct. Dynam.* **1984**, *1*, 1387-1405.
58. Vogel, H. J., Bridger, W. A. *Biochemistry*. **1982**, *21*, 5825-5831.
59. Zhou, H. X., Lyu, P., Wemmer, D. E., Kallenbach, N. R. *Proteins*, **1994**, *18*, 1-7.
60. Lu, M., Shu, W., Ji, H., Spek, E., Wang, L., Kallenbach, N. R. *J. Mol. Biol.* **1999**, *288*, 743-752.
61. Brown, A. M., Zondlo, N. J. *Biochemistry*. **2012**, *51*, 5041-5051.
62. Slawson, C., Hart, G. W. *Nat. Rev. Cancer*. **2011**, *11*, 678-684.
63. Guarracino, D. A., Bullock, B. N., Arora, P. S. *Biopolymers*, **2010**, *95*, 1-7.
64. Iakoucheva, L. M., Radivojac, P., Brown, C. J., O'Conner, T. R., Sikes, J. G., Obradovic, Z., Dunker, A. K. *Nucleic Acid Res.* **2004**, *32*, 1037-1049.
65. Schlummer, S., Vetter, R., Kuder, N., Henkel, A., Chen, Y.-X., Li, Y. M., Kuhlmann, J., Waldmann, H. *ChemBioChem*. **2006**, *7*, 88-97.
66. Lee, C. W., Ferreon, J. C., Ferreon, A. C. M., Aral, M., Wright, P. E. *Proc. Natl. Acad. Sci.* **2010**, *107*, 19290-19295.
67. Ramelot, T. A., Nicholson, L. K. *J. Mol. Biol.* **2001**, *307*, 871-884.
68. Du, J.-T., Li, Y.-M., Wei, W., Wu, G.-S., Zhao, Y.-F., Kanazawa, K., Nemoto, T., Nakanishi, H. *J. Am. Chem. Soc.* **2005**, *127*, 16350-16351.

69. Lee, K.-K., Kim, E., Joo, C., Song, J., Han, H., Cho, M. *J. Phys. Chem. B.* **2008**, *112*, 16782-16787.
70. Kim, S.-Y., Jung, Y., Hwang, G.-S., Han, H., Cho, M. *Proteins*, **2011**, *79*, 3155-3165.
71. Arsequell, G., Krippner, L., Dwek, R. A., Wong, S. Y. C. *J. Chem. Soc., Chem. Commun.* **1994**, 2383-2384.
72. Vaddypally, S., Xu, C., Zhao, S., Fan, Y., Schafmeister, C. E., Zdilla, M. J. *Inorg. Chem.* **2013**, *52*, 6457-6463.
73. Hinderaker, M. P., Raines, R. T. *Protein Sci.* **2003**, *12*, 1188-1194.
74. Hodges, J. A., Raines, R. T. *Org. Lett.* **2006**, *8*, 4695-4697.
75. Choudhary, A., Gandla, D., Krow, G. R., Raines, R. T. *J. Am. Chem. Soc.* **2009**, *131*, 7244-7246.
76. Bartlett, G. J., Choudhary, A., Raines, R. T., Woolfson, D. N. *Nat. Chem. Biol.* **2010**, *6*, 615-620.
77. Newberry, R. W., VanVeller, B., Guzei, I. A., Raines, R. T. *J. Am. Chem. Soc.* **2013**, *135*, 7843-7846.
78. Bartlett, G. J., Newberry, R. W., VanVeller, B., Raines, R. T., Woolfson, D. N. *J. Am. Chem. Soc.* **2013**, *135*, 18682-18688.

## Chapter 2

### NEIGHBORING RESIDUE SIDE-CHAIN INTERACTIONS OF $\beta$ -OGlcNAc

#### Introduction

I previously examined the effects of OGlcNAcylation of an isolated serine or threonine residue on the structure of an  $\alpha$ -helix. I found that both Ser(OGlcNAc) and Thr(OGlcNAc) stabilize an  $\alpha$ -helix when located at the N-terminus while both destabilize the  $\alpha$ -helix when located at internal and C-terminal positions. However, in nature the contexts in which OGlcNAcylation functions are far more complex than isolated  $\alpha$ -helical peptides. In biological systems, recognition of carbohydrates can occur through CH- $\pi$  interactions where the  $\alpha$ -face of the carbohydrate interacts with the face of an aromatic side chain, as is commonly found with lectin recognition of saccharides as it relates to immune system functions.<sup>1-9</sup> Alternatively, carbohydrates are also known to form covalent complexes with boronic acids through diol exchange, common in synthetically designed recognition motifs.<sup>10-14</sup> Within these two contexts, I sought to develop carbohydrate recognition motifs using peptides containing aromatic and/or boronic acid functional groups.

There are several different methods for studying the effects of carbohydrate/aromatic interactions using model systems, two of which involve small molecules and peptides. Cuevas found through NMR and theoretical calculations that fucose and benzene in an aqueous environment have a stabilizing interaction of approximately 3.0 kcal/mol. This experiment was modeled after a galactose/tyrosine interaction occurring between the influenza virus hemagglutinin and 2,3-

sialyllactose.<sup>15, 16</sup> Bernardi synthesized a series of small molecules containing a phenylalanine with an N-terminal ether linkage to four different monosaccharides (glucose, galactose, *N*-acetyl-glucosamine (GlcNAc), and *N*-acetyl-galactosamine). Using a combination of NMR and computational studies, she found the strength of the carbohydrate/aromatic interaction to be between 1.2-4.4 kcal/mol, consistent with results obtained by Cuevas and others.<sup>17,18</sup> Using a combinatorial approach, Asensio was able to determine how structural variations in the carbohydrate structure can affect the energy of CH/ $\pi$  interactions by 0.7 kcal/mol in his model system.<sup>19</sup> In several systems CH/ $\pi$  interactions have been used to design host-guest sugar sensors based on synthetic lectins.<sup>7, 9, 20</sup>

Relatively fewer model systems exist for studying the effects of carbohydrate/ $\pi$  interactions in isolated peptide systems. Kelly and coworkers have found that sequences of F-X-N-X-T and F-N-X-T (for type I  $\beta$ -turn) and F-Y-Z-N-X-T (for type II  $\beta$ -turn) in the WW domain of human Pin1 protein exhibit enhanced (0.7-2.0 kcal/mol) stability when Asn(NGlcNAc) is present due to a CH/ $\pi$  interaction (X = any residue, Z = any residue except Pro).<sup>21 22</sup> More recently, they studied the contribution of the CH/ $\pi$  interaction in residues 6-39 of Pin1 WW domain for both 5 and 6 residue sequons (sequence of consecutive amino acids serving as an attachment site for saccharides), finding that both hydrophobic and CH/ $\pi$  interactions contribute significantly to the overall interaction.<sup>23</sup> Waters has utilized a  $\beta$ -hairpin model to examine the effects of Ser(OGlcNAc) interactions with a cross-strand tryptophan residue, finding a stabilization of 0.5 kcal/mol due to the GlcNAc/Trp interaction. Interestingly, she found different NOE signatures between GlcNAc and other sugars examined, although the data remain consistent with an interaction between the face of

Trp and the  $\alpha$ -face of GlcNAc.<sup>24</sup> To date, no model peptide systems have been designed utilizing  $\alpha$ -helices to explore carbohydrate/ $\pi$  interactions.

Aryl boronic acids have been widely utilized in saccharide recognition for a variety of different applications such as oligosaccharide sensors, selective membrane fusion systems, and microbicides.<sup>25-33</sup> Designed boronic acid-containing peptides have been developed in limited numbers for the detection of free saccharides in an aqueous environment.<sup>32, 34</sup> Currently, there are no designed sensors for the specific detection of glycosylation of proteins utilizing boronic acids; all current designs are based on the detection of free saccharides. Having found the ability of Ser(OGlcNAc) to serve as inducible start and stop signals in  $\alpha$ -helices, I sought to explore intra-helical interactions between Ser(OGlcNAc) and neighboring side chains containing aromatic and aryl boronic acid residues (Figure 2.1). To examine both CH/ $\pi$  and GlcNAc/boronic acid interactions, peptides were synthesized using 4-Iodo-phenylalanine (4-I-Phe) as the aromatic amino to explore CH/ $\pi$  interactions. 4-I-Phe was readily converted to 4-B(OH)<sub>2</sub>-Phe via aryl borylation producing the aryl boronic acid to explore GlcNAc/boronic acid interactions.

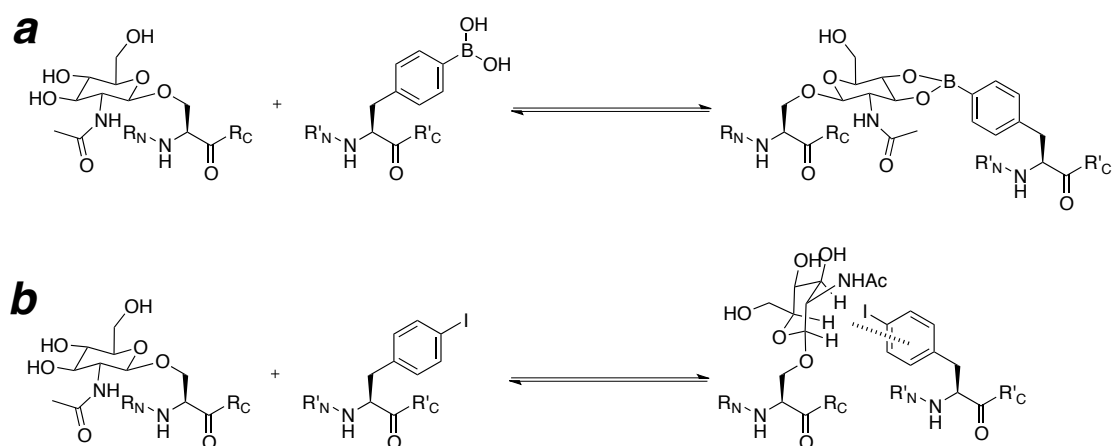


**Figure 2.1:** Schematic representation of proposed intra- $\alpha$ -helical interaction between GlcNAc and 4-B(OH)<sub>2</sub>-Phe or 4-I-Phe. Diols of the GlcNAc unit could form a conjugate with 4-B(OH)<sub>2</sub>-Phe (**a**). Axial protons of the GlcNAc unit could form a CH/ $\pi$  interaction with the aromatic face of 4-I-Phe (**b**).

## Results

A series of peptides was synthesized based on our previous Baldwin  $\alpha$ -helix model peptides (Ac-AKAAA(AKAAA)KAAGY-NH<sub>2</sub>), to allow direct comparison to peptides previously analyzed. Work performed by others has established both covalent and non-covalent interactions of natural and unnatural side-chains within  $\alpha$ -helices to be stabilizing in relative  $i/i+3$ ,  $i/i+4$ , and  $i/i+7$  relationship along one  $\alpha$ -helical face with one interacting partner at position  $i$  and the other at position  $i+3$ ,  $i+4$ , or  $i+7$  (3, 4, or 7 residues respectively, subsequent in the sequence).<sup>35-42</sup> The series of peptides herein are designed to explore interactions between positions  $i+3$ ,  $i+4$ ,  $i-4$ , and  $i+7$  all relative to serine at residue 1 or at residue 5 (for  $i-4$  interactions) of the  $\alpha$ -helix (Figure 2.2). Serine or Ser(OGlcNAc) is denoted by position  $i$ , while 4-I-Phe varies in position (Figure 2.1 (a)). A peptide containing Ser(OGlcNAc) at residue 1 and 4-I-Phe at residue 3 was also synthesized to explore possible CH/ $\pi$  interactions in a relative  $i+2$  position. Given the observation that greater structural effects were observed for

Thr(OGlcNAc) than Ser(OGlcNAc), peptides were also synthesized containing Thr or Thr(OGlcNAc) at residue 1 and 4-I-Phe at residue 5. Phosphorylation and OGlcNAcylation are dynamic competing intracellular processes. To better understand the biological contexts of these PTMs regarding neighboring aromatic residues; peptides were also synthesized with phosphoserine or Ser(OGlcNAc) at residue 1 and Trp at residue 5 (Figure 2.2 (c)).

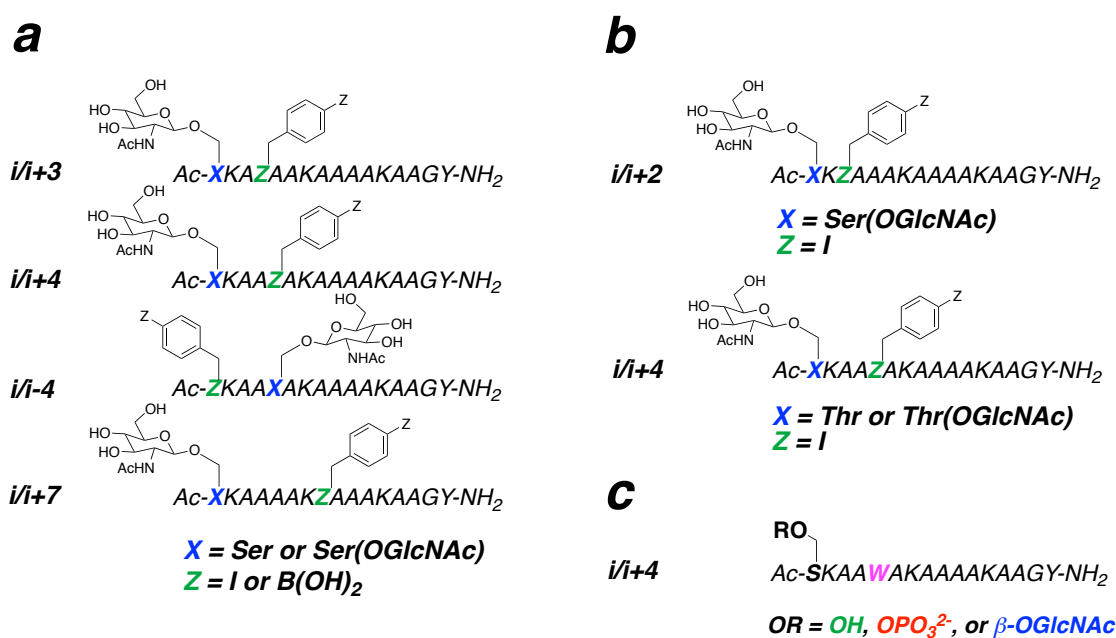


**Figure 2.2:** Peptide sequences examined in this study. **(a)** Peptides synthesized to examine the effects of Ser or Ser(OGlcNAc) (residue 1 or 5) interactions in a relative  $i+3$ ,  $i+4$ ,  $i-4$ , and  $i+7$  relationship to Ser or Ser(OGlcNAc). **(b)** Peptides exploring the effects of Ser(OGlcNAc) and 4-I-Phe in an  $i/i+2$  relationship and Thr/Thr(OGlcNAc) and 4-I-Phe in an  $i/i+4$  relationship. **(c)** Peptides containing Ser, phosphoserine, and Ser(OGlcNAc) in an  $i/i+4$  relationship to Trp.

OGlcNAcylated peptides were synthesized on solid-phase support incorporating Fmoc-Ser/Thr(Ac<sub>3</sub>OGlcNAc)-OH (synthesized in solution phase via a modified method of Arsequell) at the intended site of modification, followed by initial purification, deesterification of the sugar hydroxyls, and final purification to obtain site-specific incorporation of Ser/Thr(OGlcNAc) (Figure 2.3).<sup>45</sup> Peptides containing 4-I-Phe were readily converted to 4-B(OH)<sub>2</sub>-Phe via solid-phase aryl borylation (Figure 2.4).<sup>46</sup> Peptides containing phosphoserine were incorporated using Fmoc-S(trityl)-OH. Phosphorylation was conducted on solid-phase by selective trityl-deprotection, phosphitylation, oxidation, and cleavage/deprotection yielding a site-selective phosphorylated serine residue (Figure 2.5). All peptides were analyzed by circular dichroism (CD) at 0.5 °C.

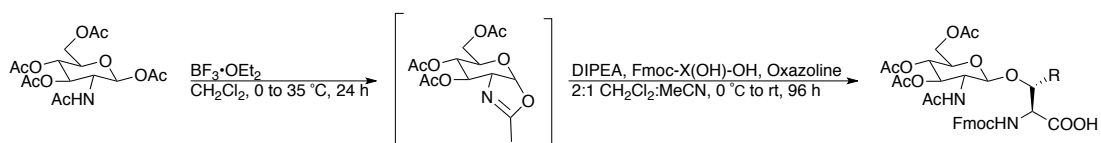


**Figure 2.3:** Synthesis of peracetylated 2-acetamido-2-deoxy- $\beta$ -D-glycosides of Fmoc-Thr-OH (R = CH<sub>3</sub>) and Fmoc-Ser-OH (R = H).



**Figure 2.4:** Synthetic scheme of solid-phase aryl borylation of peptides containing 4-I-Phe. R<sub>N</sub>/R'<sub>N</sub> = N-terminal portion of the peptide containing Ser(OAc<sub>3</sub>GlcNAc) at residue 1. R<sub>C</sub> = C-terminal portion of the peptide on solid support containing protected amino acids. R'<sub>C</sub> = C-terminal portion of the peptide deprotected and cleaved from solid support.

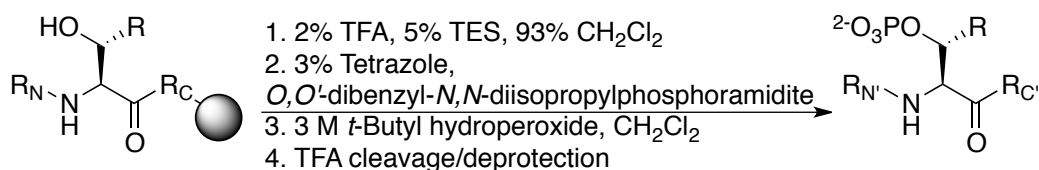


**Figure 2.5:** Scheme for the chemical phosphorylation of peptides on resin and subsequent cleavage/deprotection. R = CH<sub>3</sub> (Thr) or R = H (Ser).

### Effects of Ser/Ser(OGlcNAc) and 4-I-Phe with an *i/i+2* relationship

The first positions examined for possible hydrophobic or CH/ $\pi$  interactions between sugars and aromatic amino acids are the relative *i/i+2* positions of the  $\alpha$ -helix, with both Ser and Ser(OGlcNAc) at residue 1 and 4-I-Phe at residue 3 (Figure 2.6 and Table 2.1). GlcNAcylation of serine at this position led to a small increase in  $\alpha$ -helicity from 27.9% (Ser) to 31.7% (Ser(OGlcNAc)). Our previous work on the isolated effects of Ser and Ser(OGlcNAc) suggest that this small increase in  $\alpha$ -helicity is due to the isolated effects of the GlcNAc sugar on the N-terminus rather than any interaction with 4-I-Phe, consistent with no interaction between GlcNAc and 4-I-Phe in this sequence relationship.

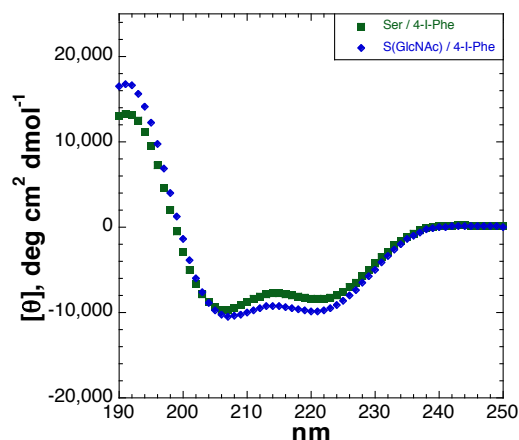


**Figure 2.6:** CD spectra of Ac-SK(4-I-Phe)AAAKAAAAKAAGY-NH<sub>2</sub> peptides with unmodified Ser(free hydroxyl) and Ser(OGlcNAc). Green squares: unmodified serine; blue diamonds: Ser(OGlcNAc). CD experiments were conducted in water with 10 mM phosphate (pH 7.0) and 25 mM KF at 0.5 °C.

Peptide	[θ] <sub>222</sub>	[θ] <sub>208</sub>	[θ] <sub>190</sub>	[θ] <sub>222</sub> /[θ] <sub>208</sub>	-[θ] <sub>190</sub> /[θ] <sub>208</sub>	% Helix
Ac-SK(4-I-Phe)AAAKAAAAKAAGY-NH <sub>2</sub>	-8352	-9487	13055	0.88	1.38	27.9
Ac-S(GlcNAc)K(4-I-Phe)AAAKAAAAKAAGY-NH <sub>2</sub>	-9791	-10412	16521	0.94	1.59	31.7

**Table 2.1:** Summary of CD data for peptides with *i/i+2* orientation. CD data were collected at 0.5 °C in 10 mM aqueous phosphate buffer pH 7.0 with 25 mM KF.

### Effects of Ser/SerOGlcNAc and 4-I-Phe/4-B(OH)<sub>2</sub>-Phe with an *i/i+3* relationship

Side chain-side chain interactions in a relative *i/i+3* position have been shown to exist with both electrostatic interactions and stapled peptides, although the interacting geometry provides less residue overlap than with the relative *i/i+4* orientation. Peptides with Ser/Ser(OGlcNAc) at residue 1 and 4-I-Phe or 4-B(OH)<sub>2</sub>-Phe at residue 4 demonstrated moderate variations in  $\alpha$ -helicity (Figure 2.7 and Table 2.2). In contrast to every other peptide in this body of work, **Ser<sub>*i*</sub>/4-I-Phe<sub>*i+3*</sub>** showed greater  $\alpha$ -helicity than **Ser(OGlcNAc)<sub>*i*</sub>/4-I-Phe<sub>*i+3*</sub>**, despite the observation that

OGlcNAcylation of serine leads to an increase in  $\alpha$ -helicity while on the N-terminus. This observation is consistent with no favorable interactions being present between GlcNAc and 4-I-Phe when in an  $i/i+3$  relationship. **Ser(OGlcNAc)/4-B(OH)<sub>2</sub>-Phe<sub>*i*+3</sub>** exhibited greater  $\alpha$ -helicity than the peptides with the unmodified serine. These data are consistent with the observed isolated effects of GlcNAcylation of serine on the N-terminus and not with an interaction between GlcNAc and the boronic acid.

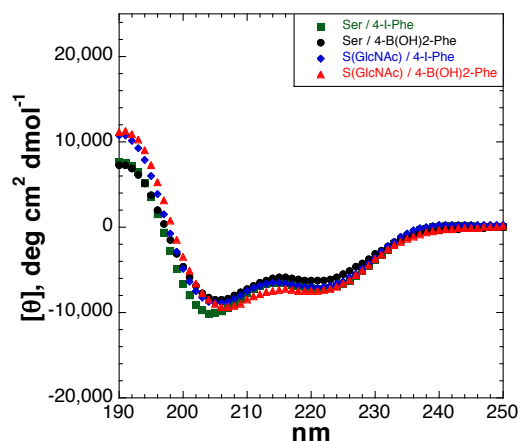


**Figure 2.7:** CD spectra of Ac-SKA(4-X-Phe)AAKAAA KAAGY-NH<sub>2</sub> peptides with unmodified Ser(free hydroxyl) and Ser(OGlcNAc). Green squares: unmodified serine/4-I-Phe; black circles: unmodified serine/4-B(OH)<sub>2</sub>; blue diamonds: Ser(OGlcNAc)/4-I-Phe; red triangles: Ser(OGlcNAc)/4-B(OH)<sub>2</sub>-Phe. CD experiments were conducted in water with 10 mM phosphate (pH 7.0) and 25 mM KF at 0.5 °C.

Peptide	$[\theta]_{222}$	$[\theta]_{208}$	$[\theta]_{190}$	$[\theta]_{222}/[\theta]_{208}$	$-[\theta]_{190}/[\theta]_{208}$	% Helix
Ac-SKA(4-I-Phe)AAKAAAAKAAGY-NH <sub>2</sub>	-7186	-8941	7597	0.80	0.85	24.8
Ac-SKA(4-B(OH) <sub>2</sub> -Phe)AAKAAAAKAAGY-NH <sub>2</sub>	-6222	-8056	7259	0.77	0.90	22.2
Ac-S(GlcNAc)KA(4-I-Phe)AAKAAAAKAAGY-NH <sub>2</sub>	-7006	-8366	10753	0.84	1.29	24.3
Ac-S(GlcNAc)KA(4-B(OH) <sub>2</sub> -Phe)AAKAAAAKAAGY-NH <sub>2</sub>	-7403	-9217	11143	0.80	1.21	25.4

**Table 2.2:** Summary of CD data for peptides with *i/i+3* orientation. CD data were collected at 0.5 °C with 80-100 μM peptide in 10 mM aqueous phosphate buffer pH 7.0 with 25 mM KF.

### Neighboring side-chain interactions with an *i/i+4* relationship

The most geometrically favorable interaction of side-chains on an  $\alpha$ -helix face occurs with an *i/i+4* relationship. Peptides were synthesized and analyzed with Ser/Ser(OGlcNAc) at residue 1 with 4-I-Phe or 4-B(OH)<sub>2</sub>-Phe at residue 5. In addition, peptides were synthesized with a reversed polarity orientation, to determine the dependence of interactions on  $\alpha$ -helical position (N-terminal versus internal) (Figure 2.8 and Table 2.3). For peptides with Ser at residue 1, a modest increase in  $\alpha$ -helicity was observed due to GlcNAcylation, consistent with previous results on peptides lacking an aromatic residue. None of the peptides exhibited any substantial changes in  $\alpha$ -helicity due to the presence of either 4-I-Phe or 4-B(OH)<sub>2</sub>-Phe, consistent with no interaction between GlcNAc and either the boronic acid or aromatic group with a relative *i/i+4* relationship.

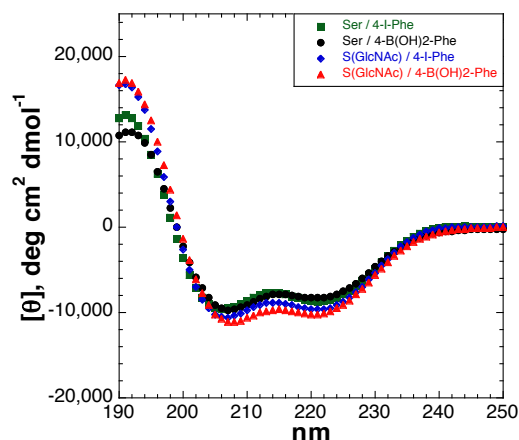


**Figure 2.8:** CD spectra of Ac-SKAA(4-X-Phe)AKAAAAKAAGY-NH<sub>2</sub> peptides with unmodified Ser(free hydroxyl) and Ser(OGlcNAc). Green squares: unmodified serine/4-I-Phe; black circles: unmodified serine/4-B(OH)<sub>2</sub>; blue diamonds: Ser(OGlcNAc)/4-I-Phe; red triangles: Ser(OGlcNAc)/4-B(OH)<sub>2</sub>-Phe. CD experiments were conducted in water with 10 mM phosphate (pH 7.0) and 25 mM KF at 0.5 °C.

Peptide	[θ] <sub>222</sub>	[θ] <sub>208</sub>	[θ] <sub>190</sub>	[θ] <sub>222</sub> /[θ] <sub>208</sub>	-[θ] <sub>190</sub> /[θ] <sub>208</sub>	% Helix
Ac-SKAA(4-I-Phe)AKAAAAKAAGY-NH <sub>2</sub>	-8670	-9327	12733	0.93	1.37	28.7
Ac-SKAA(4-B(OH) <sub>2</sub> -Phe)AKAAAAKAAGY-NH <sub>2</sub>	-8241	-9658	10702	0.85	1.11	27.6
Ac-S(GlcNAc)KAA(4-I-Phe)AKAAAAKAAGY-NH <sub>2</sub>	-9607	-10413	16572	0.92	1.59	31.2
Ac-S(GlcNAc)KAA(4-B(OH) <sub>2</sub> -Phe)AKAAAAKAAGY-NH <sub>2</sub>	-10083	-11121	16837	0.91	1.51	32.4

**Table 2.3:** Summary of CD data for peptides with *i/i+4* orientation. CD data were collected at 0.5 °C in 10 mM aqueous phosphate buffer pH 7.0 with 25 mM KF.

Previous work has demonstrated that both Ser and Ser(OGlcNAc) are both destabilizing to the α-helix on internal positions, with Ser(OGlcNAc) decreasing α-helix stability by 0.12 kcal/mol relative to Ser. The CD signatures of peptides with both 4-I-Phe and 4-B(OH)<sub>2</sub>-Phe at residue 1 and Ser(OGlcNAc) at residue 5 are almost identical, indicating no inherent difference between the two aromatic residues on the N-terminus (Figure 2.9 and Table 2.4). Ser(OGlcNAc) at residue 5 with either aromatic at residue 1 exhibits a decrease in helix stability by 0.12 kcal/mol, consistent

with the observed isolated effects of GlcNAcylation on an  $\alpha$ -helical interior position. Taken together, these results indicate that there is no significant interaction between GlcNAc and either the 4-I-Phe or 4-B(OH)<sub>2</sub>-Phe with an *i/i-4* relative orientation.

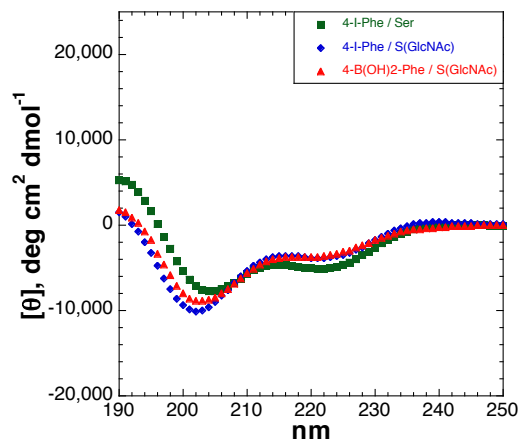


**Figure 2.9:** CD spectra of Ac-(4-X-Phe)KAASAKAAAAKAAGY-NH<sub>2</sub> peptides with serine unmodified Ser(free hydroxyl) and Ser(GlcNAc). Green squares: unmodified 4-I-Phe/serine; blue diamonds: 4-I-Phe/Ser(GlcNAc); red triangles: 4-B(OH)<sub>2</sub>-Phe/Ser(GlcNAc). CD experiments were conducted in water with 10 mM phosphate (pH 7.0) and 25 mM KF at 0.5 °C.

Peptide	[ $\theta$ ] <sub>222</sub>	[ $\theta$ ] <sub>208</sub>	[ $\theta$ ] <sub>190</sub>	[ $\theta$ ] <sub>222</sub> /[ $\theta$ ] <sub>208</sub>	-[ $\theta$ ] <sub>190</sub> /[ $\theta$ ] <sub>208</sub>	% Helix
Ac-(4-I-Phe)KAASAKAAAAKAAGY-NH <sub>2</sub>	-5058	-6711	5300	0.75	0.79	19.2
Ac-(4-I-Phe)KAAS(GlcNAc)AKAAAAKAAGY-NH <sub>2</sub>	-3840	-6794	1566	0.57	0.23	15.9
Ac-(4-B(OH) <sub>2</sub> -Phe)KAAS(GlcNAc)AKAAAAKAAGY-NH <sub>2</sub>	-3637	-6929	1701	0.52	0.25	15.4

**Table 2.4:** Summary of CD data for peptides with *i/i-4* orientation. CD data were collected at 0.5 °C in 10 mM aqueous phosphate buffer pH 7.0 with 25 mM KF.

Although no significant interactions were found with  $i/i+4$  relationships between Ser(OGlcNAc) and 4-I-Phe or 4-B(OH)<sub>2</sub>-Phe, it is plausible that a larger, more electron-rich natural amino-acid such as tryptophan could interact with GlcNAc in this relative geometry. It is also known that anion/ $\pi$  interactions are repulsive, suggesting that GlcNAc/aromatic interactions may stabilize the  $\alpha$ -helix while phosphate/aromatic interactions may destabilize the  $\alpha$ -helix, acting as a molecular switch for secondary structure. Such a mechanism would be similar to work performed by Waters involving  $\beta$ -hairpin peptides.<sup>47, 48</sup> To determine the context dependence of phosphorylation and GlcNAcylation in proximity to Trp, peptides were synthesized containing serine, phosphoserine, or Ser(OGlcNAc) at residue 1 and Trp at residue 5 with a relative  $i/i+4$  relationship (Figure 2.10 and Table 2.5). Interestingly, the addition of Trp alone leads to an increase in  $\alpha$ -helicity of approximately 14% relative to 4-I-Phe and 4-B(OH)<sub>2</sub>-Phe. Previous studies have demonstrated that the effects of different hydrophobic aromatic residues (Trp, Tyr, and Phe) at internal positions of  $\alpha$ -helices are negligible.<sup>49, 50</sup> Trp at residue 5 is in a relative  $i/i+3$  relationship to lysine, potentially suggestive of a stabilizing cation/ $\pi$  interaction, observed by others in a relative  $i/i+4$  orientation on  $\alpha$ -helices.<sup>44, 51</sup>

Both Ser(OGlcNAc) and phosphoserine led to an overall increase in  $\alpha$ -helicity relative to serine at the N-terminus of an  $\alpha$ -helix. The peptide with Ser(OGlcNAc) exhibited a small increase in  $\alpha$ -helicity, consistent with the observed isolated effects of GlcNAcylation in model peptides. These data suggest that there is no significant interaction of the sugar with the Trp residue. Phosphorylation led to a large increase in  $\alpha$ -helicity and stabilized the  $\alpha$ -helix by 0.23 kcal/mol, comparable to the 0.20 kcal/mol stabilization observed with the isolated effects of serine phosphorylation.

Taken together, these results suggest no observable interaction between either the phosphate or GlcNAc with Trp.

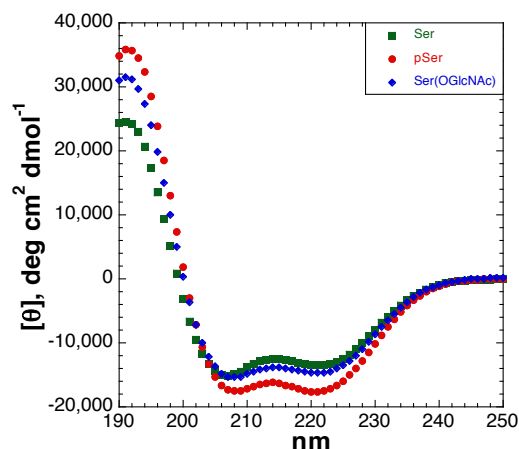


**Figure 2.10:** CD spectra of Ac-SKAAWAKAAAAKAAGY-NH<sub>2</sub> peptides with unmodified Ser(free hydroxyl) and Ser(OGlcNAc). Green squares: unmodified serine; red circles: phosphorylated serine (pH 8); blue diamonds: Ser(OGlcNAc). CD experiments were conducted in water with 10 mM phosphate (pH 7.0 or 8.0) and 25 mM KF at 0.5 °C.

Peptide	[θ] <sub>222</sub>	[θ] <sub>208</sub>	[θ] <sub>190</sub>	[θ] <sub>222</sub> /[θ] <sub>208</sub>	-[θ] <sub>190</sub> /[θ] <sub>208</sub>	% Helix
Ac-SKAAWAKAAAAKAAGY-NH <sub>2</sub>	-13508	-14847	24321	0.91	1.64	41.5
Ac-S(GlcNAc)KAAWAKAAAAKAAGY-NH <sub>2</sub>	-14677	-15379	31017	0.95	2.02	44.6
Ac-Ser(OPO <sub>3</sub> <sup>2-</sup> )KAAWAKAAAAKAAGY-NH <sub>2</sub>	-17504	-17555	34788	1.00	1.98	52.1

**Table 2.5:** Summary of CD data for peptides containing serine modifications at residue 1 and tryptophan at residue 5 of the α-helix. CD data were collected at 0.5 °C with 80-100 μM peptide in 10 mM aqueous phosphate buffer pH 7.0 with 25 mM KF.

To further explore the nature of these interactions, 1-D <sup>1</sup>H and TOCSY NMR experiments were performed on peptides containing phosphoserine or Ser(OGlcNAc) in a relative *i/i+4* relationship to Trp (Table 2.6). As was observed for the isolated peptides containing only these post-translational modifications, Ser(OGlcNAc) at

residue 1 led to greater conformational restriction than phosphorylation, as evident by the small decrease in  $^3J_{\alpha N}$  comparing phosphorylation to GlcNAcylation (5.0 Hz for Ser(OGlcNAc) and 5.2 Hz for Ser(OPO<sub>3</sub><sup>2-</sup>). The magnitude of the conformational restriction due to both modifications is overall smaller than that observed in peptides without Trp, most likely due to the decrease in overall  $\alpha$ -helicity that results from substitution of Trp for Ala. Alternatively, interactions between the Trp residue and phosphoserine or Ser(OGlcNAc) residues could affect the  $\phi$  torsion angle of serine. Again, a downfield chemical shift of phosphoserine amide proton is observed, yet to a smaller extent than for isolated peptides.

Peptide	$\delta$ , H <sup>N</sup>	$^3J_{\alpha N}$	$\delta$ , H $\alpha$	$\delta$ , H $\beta$
Ac- <b>Ser(GlcNAc)</b> KAAWAKAAAAKAAGY-NH <sub>2</sub>	8.50	5.0	4.32	3.98, 3.80
Ac- <b>Ser(OPO<sub>3</sub><sup>2-</sup>)</b> KAAWAKAAAAKAAGY-NH <sub>2</sub>	8.77	5.2	4.39	4.16, 4.11

**Table 2.6:** Summary of NMR data for peptides containing serine modifications at residue 1 and tryptophan at residue 5 of the  $\alpha$ -helix. Chemical shifts ( $\delta$ ) of serine amide proton (H<sup>N</sup>), alpha proton (H $\alpha$ ), beta proton (H $\beta$ ), and coupling constants between serine alpha proton and amide proton ( $^3J_{\alpha N}$ ) are reported. Peptides were dissolved in 5 mM phosphate buffer (pH 4.0 or 6.5) containing 25 mM NaCl in 90% H<sub>2</sub>O/10% D<sub>2</sub>O at 5 °C.

NMR spectroscopy reveals a small downfield chemical shift of all GlcNAc protons of approximately 0.06 ppm in changing  $i/i+4$  alanine to tryptophan substitution, consistent with a weak interaction between the hydrogen and the ring current of the aromatic (Figure 2.11).<sup>24, 52</sup> This trend could alternatively be explained by effects of  $\alpha$ -helicity on the chemical shift of GlcNAc protons. However, the extent of peptide  $\alpha$ -helicity had no observed effects on the chemical shift of GlcNAc protons

for isolated Ser(OGlcNAc) or Thr(OGlcNAc) peptides without Trp. As was observed for peptides with alanine at residue 5, phosphorylation of serine induces a downfield shift of the serine amide proton. The  $\alpha$ -helicity of phosphoserine  $i/i+4$  to Trp was determined to be 52.1% at pH 8.0 via CD. I had previously determined the  $\alpha$ -helicity of phosphoserine at residue 1  $i/i+4$  alanine to be 50.8 % helicity at pH 4.0 and 58.6% helicity at pH 8.0. The observed effects of the phosphorylation-induced downfield chemical shift originates from the hydrogen bond between the phosphate and the phosphorylated residue amide hydrogen; position, temperature, and pH all have had effects on the extent of downfield shift. The phosphoserine at residue 1 in an  $i/i+4$  to Trp, demonstrates the least downfield amide proton at 8.77 ppm (compared to phosphoserine at residue 1  $i/i+4$  to alanine 8.91 ppm (pH 4.0) and 9.41 (pH 7.2)) and the largest  $^3J_{\alpha N}$  (5.2 Hz) (compared to phosphoserine at residue 1  $i/i+4$  to alanine 4.4 Hz (pH 4.0) and 3.6 Hz (pH 7.2)). These data suggest a weakening of the phosphate-amide hydrogen bond, even though the  $\alpha$ -helicity is in between that of phosphoserine at residue 1 in an  $i/i+4$  orientation to alanine (pH 4-8). This finding suggests the presence of other  $\alpha$ -helix stabilizing interactions within the Trp-containing peptide that are not present in other peptides, such as a possible  $i/i+3$  Lys/Trp cation/ $\pi$  interaction.

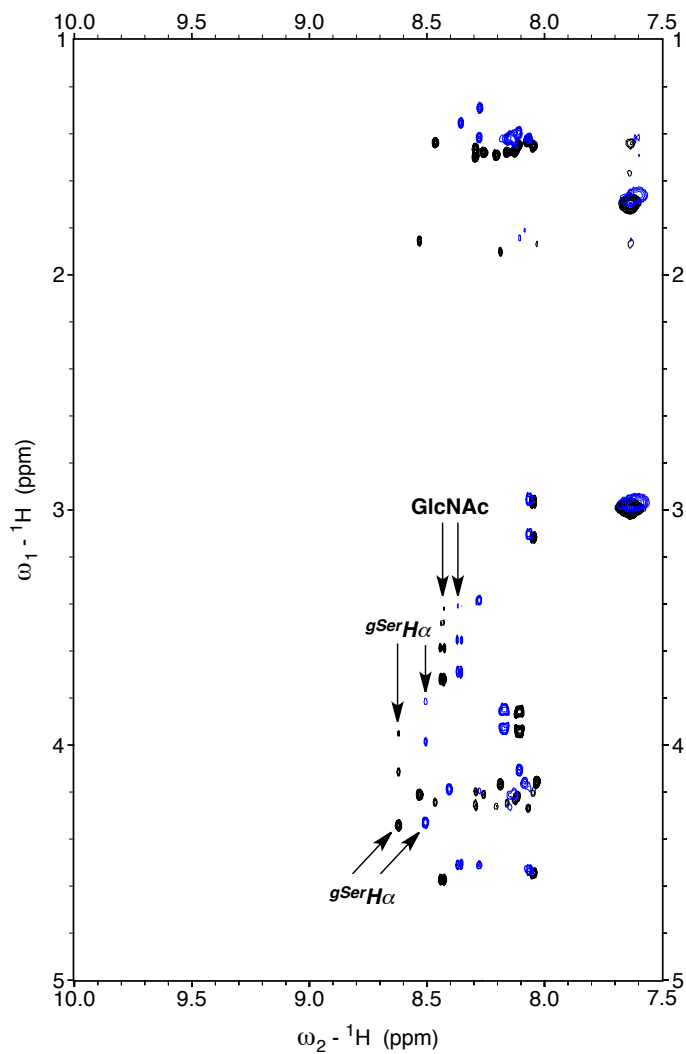


**Figure 2.11:** Comparative TOCSY spectra of the amide region of peptides **Ac-S(OGlcNAc)KAAAKKAAAKAAGY-NH<sub>2</sub>** (black) and **Ac-S(OGlcNAc)KAAWAKAAAKAAGY-NH<sub>2</sub>** (blue). gSer indicates Ser(OGlcNAc). Peptides were dissolved in 5 mM phosphate buffer (pH 4.0) containing 25 mM NaCl in 90% H<sub>2</sub>O/10% D<sub>2</sub>O. Data were collected at 278 K.

Previously, I had demonstrated that greater structural effects were generally observed for modifications on threonine than for modifications on serine. To explore the possibility of CH/ $\pi$  interactions of Thr(OGlcNAc), peptides were synthesized with Thr or Thr(OGlcNAc) at residue 1 and 4-I-Phe at residue 5. The peptides were analyzed via CD (Figure 2.12, Table 2.7). GlcNAcylation of threonine in an *i/i+4* relationship to 4-I-Phe led to a small increase in  $\alpha$ -helicity by 5%, consistent with the observed effects of GlcNAcylation of threonine in stabilizing an  $\alpha$ -helix on the N-terminus and not consistent with any significant interaction between the GlcNAc unit and the aromatic ring of 4-I-Phe. These results are consistent with the results obtained for Ser(OGlcNAc) with aromatic residues in the same relative orientation.

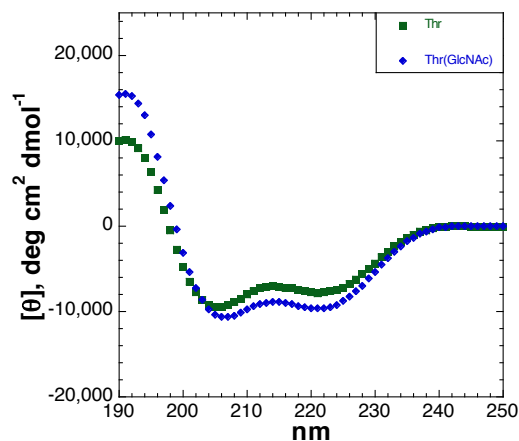


**Figure 2.12:** CD spectra of Ac-TKAA(4-I-Phe)AKAAA KAAGY-NH<sub>2</sub> peptides with threonine unmodified Thr(free hydroxyl) and Thr(GlcNAc). Green squares: unmodified threonine; blue diamonds: Thr(GlcNAc). CD experiments were conducted in water with 10 mM phosphate (pH 7.0) and 25 mM KF at 0.5 °C.

Peptide	$[\theta]_{222}$	$[\theta]_{208}$	$[\theta]_{190}$	$[\theta]_{222}/[\theta]_{208}$	$-[\theta]_{190}/[\theta]_{208}$	% Helix
Ac-7KAA(4-I-Phe)AKAAAAKAAGY-NH <sub>2</sub>	-7777	-8892	9998	0.87	1.12	26.3
Ac-7(GlcNAc)KAA(4-I-Phe)AKAAAAKAAGY-NH <sub>2</sub>	-9614	-10458	15407	0.92	1.47	31.2

**Table 2.7:** Summary of CD data for threonine and 4-I-Phe containing peptides. CD data were collected at 0.5 °C with 80-100 μM peptide in 10 mM aqueous phosphate buffer pH 7.0 with 25 mM KF.

### Neighboring side-chain interactions with a relative *i/i+7* orientation

Another common orientation of interactions involved in intra- $\alpha$ -helical side-chain interactions occurs with residues with a relative *i/i+7* relationship. To explore the possible interactions with this geometry, peptides were synthesized with Ser or Ser(OGlcNAc) at residue 1 and 4-I-Phe or 4-B(OH)<sub>2</sub>-Phe at residue 8 of the  $\alpha$ -helix. Overall, the largest changes in  $\alpha$ -helicity in peptides in this chapter occurs with Ser or Ser(OGlcNAc) at residue 1 and 4-I-Phe or 4-B(OH)<sub>2</sub>-Phe at residue 8 in an *i/i+7* orientation; demonstrating an overall range of approximately 10% helicity (Figure 2.13, Table 2.8). The data suggest that the presence 4-B(OH)<sub>2</sub>-Phe at residue 8 and GlcNAc at residue 1 are independently responsible for  $\alpha$ -helix stabilization. Both peptides containing 4-B(OH)<sub>2</sub>-Phe had comparable CD signatures, which overall exhibited greater  $\alpha$ -helical population than the peptides containing 4-I-Phe. Within peptides containing 4-B(OH)<sub>2</sub>-Phe or with 4-I-Phe, the peptide with Ser(OGlcNAc) demonstrated greater  $\alpha$ -helical conformation than the peptide with serine, consistent with the observed stabilizing effects of GlcNAc on the N-terminus of  $\alpha$ -helices. In contrast to every other series in this study, the two most  $\alpha$ -helical peptides in this series contained 4-B(OH)<sub>2</sub>-Phe, while the least  $\alpha$ -helical peptides contained 4-I-Phe. This observation is consistent with the presence of an additional stabilizing interaction

involving the presence of the boronic acid independent of the presence of the GlcNAc unit, suggesting no interaction between GlcNAc and either 4-I-Phe or 4-B(OH)<sub>2</sub>-Phe.

To confirm that this stabilizing interaction does not involve an interaction between GlcNAc and the boronic acid, CD experiments were performed on peptides containing Ser or Ser(OGlcNAc) at residue 1 and 4-B(OH)<sub>2</sub>-Phe at residue 8, in the absence or presence of 12.5 mM  $\beta$ -D-fructose.  $\beta$ -D-fructose is known to have a high association constant with boronic acids ( $K_{eq} = 160 \text{ M}^{-1}$  with phenylboronic acid in 100 mM phosphate buffer (pH 7.4)) and could potentially favor association of fructose over any interaction with GlcNAc (Figure 2.14).<sup>9, 53, 54</sup> The presence of  $\beta$ -D-fructose only affected peptides containing 4-B(OH)<sub>2</sub>-Phe, regardless of the presence of GlcNAc, confirming that this interaction is due solely to the boronic acid and not the presence of GlcNAc. Surprisingly, the addition of fructose slightly increased the  $\alpha$ -helicity of boronic acid-containing peptides. Interestingly, both peptides containing 4-B(OH)<sub>2</sub>-Phe are in a relative  $i/i+4$  position to lysine and demonstrate increased  $\alpha$ -helical character, with an average helix stabilization energy of 0.14 kcal/mol. Binding of fructose to the boronic acid could induce the  $sp^3$  hybridized anion of boron. This anionic species could possibly have a favorable electrostatic interaction with lysine, forming an  $i/i+4$  salt-bridge, which is also observed in other contexts.<sup>35, 39, 41</sup> Alternatively, fructose adds several hydrogen bonding donors that could also potentially interact favorably with lysine.

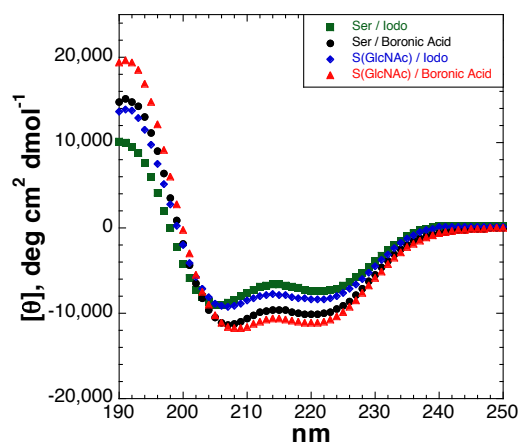


**Figure 2.13:** CD spectra of Ac-SKAAAAK(4-X-Phe)AAAKAAGY-NH<sub>2</sub> peptides with serine unmodified Ser(free hydroxyl) and Ser(OGlcNAc). Green squares: unmodified serine/4-I-Phe; black circles: unmodified serine/4-B(OH)<sub>2</sub>; blue diamonds: Ser(OGlcNAc)/4-I-Phe; red triangles: Ser(OGlcNAc)/4-B(OH)<sub>2</sub>-Phe. CD experiments were conducted in water with 10 mM phosphate (pH 7.0) and 25 mM KF at 0.5 °C.

Peptide	[θ] <sub>222</sub>	[θ] <sub>208</sub>	[θ] <sub>190</sub>	[θ] <sub>222</sub> /[θ] <sub>208</sub>	-[θ] <sub>190</sub> /[θ] <sub>208</sub>	% Helix
Ac-SKAAAAK(4-I-Phe)AAAKAAGY-NH <sub>2</sub>	-7382	-8468	10101	0.87	1.19	25.3
Ac-SKAAAAK(4-B(OH) <sub>2</sub> -Phe)AAAKAAGY-NH <sub>2</sub>	-10037	-11269	14697	0.89	1.30	32.3
Ac-S(GlcNAc)KAAAAK(4-I-Phe)AAAKAAGY-NH <sub>2</sub>	-8338	-9149	13675	0.91	1.49	27.8
Ac-S(GlcNAc)KAAAAK(4-B(OH) <sub>2</sub> -Phe)AAAKAAGY-NH <sub>2</sub>	-10982	-11783	19349	0.93	1.64	34.8

**Table 2.8:** Summary of CD data for peptides with a relative *i/i+4* orientation. CD data were collected at 0.5 °C with 80-100 μM peptide in 10 mM aqueous phosphate buffer pH 7.0 with 25 mM KF.

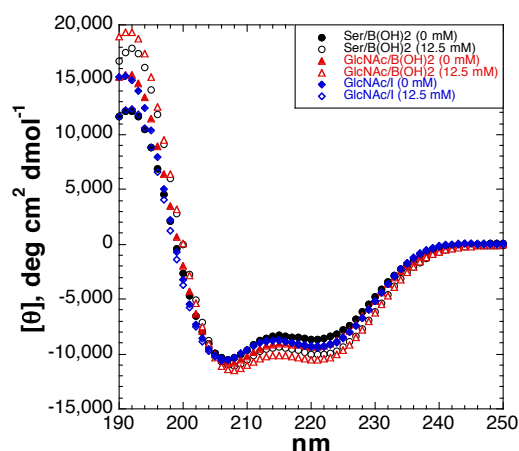


**Figure 2.14:** CD spectra of Ac-SKAAAAK(4-X-Phe)AAAKAAGY-NH<sub>2</sub> peptides in the presence and absence of β-D-Fructose with serine unmodified Ser(free hydroxyl) and Ser(GlcNAc). Black circles: unmodified serine/4-B(OH)<sub>2</sub>; red triangles: Ser(GlcNAc)/4-B(OH)<sub>2</sub>-Phe; blue diamonds: Ser(GlcNAc)/4-I-Phe. CD experiments were conducted in water with 10 mM phosphate (pH 7.0), 25 mM KF, and 12.5 mM β-D-Fructose (open shapes) at 0.5 °C.

The α-helix stabilization proposed between lysine and 4-B(OH)<sub>2</sub>-Phe could be due to cation/π interactions or electrostatics. In order to determine the nature of this interaction, CD experiments were performed on peptides containing serine at residue 1 and 4-I-Phe or 4-B(OH)<sub>2</sub>-Phe at residue 8 in 1 M KF, 25 mM NaCl, and 1 M NaCl (Figure 2.15 and Table 2.9). The peptides containing 4-I-Phe exhibited similar α-helicity in both NaCl and KF, with the CD spectra at 1 M NaCl and 1 M KF identical. The boronic acid-containing peptides exhibited similar α-helicity in both 25 mM NaCl and 25 mM KF. In contrast to 4-I-Phe, the boronic acid-containing peptides exhibited a substantial increase in α-helicity in 1 M KF relative to 1 M NaCl, suggesting dependence on the presence of the fluoride anions. The data herein suggest that this stabilizing interaction cannot be ascribed to simple electrostatics. <sup>19</sup>F and <sup>11</sup>B NMR

were performed to potentially identify an interaction directly. However, no NMR resonances were detected for either experiment.

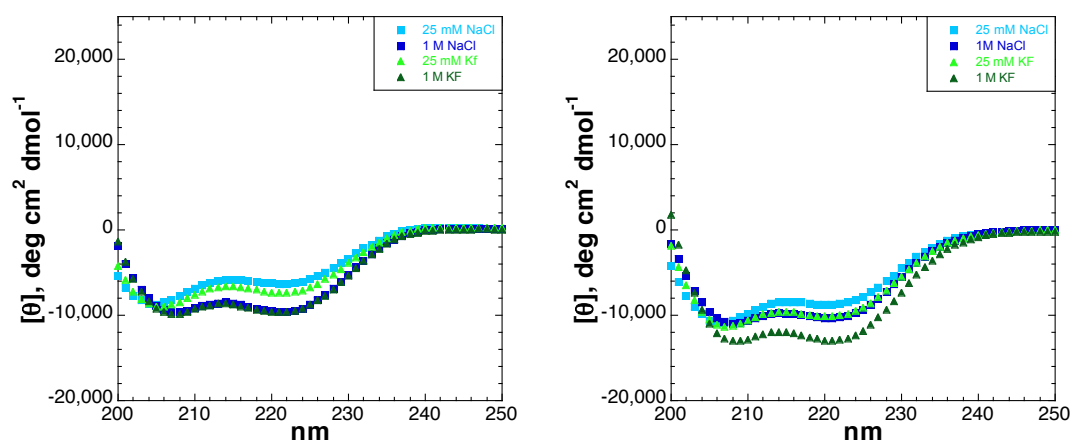


**Figure 2.15:** CD spectra of Ac-SKAAAAK(4-X-Phe)AAAKAAGY-NH<sub>2</sub> peptides. (Left) peptides containing serine at residue 1 and 4-I-Phe at residue 8. (Right) peptides containing serine at residue 1 and 4-B(OH)<sub>2</sub>-Phe at residue 8. CD experiments were conducted in water with 10 mM phosphate (pH 7.0) and 25 mM KF (light blue squares), 1 M KF (dark blue squares), 25 mM NaCl (light green triangles), or 1 M NaCl (dark green triangles) at 0.5 °C.

Peptide	$[\theta]_{222}$	$[\theta]_{208}$	$[\theta]_{190}$	$[\theta]_{222}/[\theta]_{208}$	$-[\theta]_{190}/[\theta]_{208}$	% Helix
Ac-SKAAAAK(4-I-Phe)AAAKAAGY-NH <sub>2</sub>						
25 mM NaCl	-6321	-7766	n.a.	0.81	n.a.	22.5
1 M NaCl	-9572	-9620	n.a.	1.00	n.a.	31.1
25 mM KF	-7382	-8468	10101	0.87	1.19	25.3
1 M KF	-9616	-9823	15285	0.98	1.56	31.2
Ac-SKAAAAK(4-B(OH) <sub>2</sub> -Phe)AAAKAAGY-NH <sub>2</sub>						
25 mM NaCl	-8668	-10666	n.a.	0.81	n.a.	28.7
1 M NaCl	-10282	-10972	n.a.	0.94	n.a.	33.0
25 mM KF	-10037	-11269	14697	0.89	1.30	32.3
1 M KF	-12898	-13051	22100	0.99	1.69	39.9

**Table 2.9:** Summary of CD data in KF and NaCl. CD experiments were conducted in water with 10 mM phosphate (pH 7.0) and KF or NaCl (at indicated concentrations) at 0.5 °C.

## Discussion

Herein, I have conducted a rigorous examination to determine potential neighboring side chain interactions between Ser(OGlcNAc) and either 4-I-Phe or 4-B(OH)<sub>2</sub>-Phe at relative  $i/i+3$ ,  $i/i+4$ ,  $i/i-4$ , and  $i/i+7$  positions within an  $\alpha$ -helical context. Peptides containing serine, phosphoserine, Ser(OGlcNAc), Thr, and Thr(OGlcNAc) at residue 1 and Trp at residue 5 were also examined to determine potential interactions involving a larger, more electron-rich natural amino acid. I have found no data to support any significant interaction between GlcNAc and either an aromatic ring or an aryl boronic acid within an  $\alpha$ -helix. The data herein suggest that the major role of Ser/Thr(OGlcNAc) in isolated  $\alpha$ -helical peptides, is predominantly steric in nature and has no significant interactions with neighboring aromatic side-chains. Within an  $\alpha$ -helix, hydrogen-bonding interactions may be possible between the GlcNAc unit and neighboring residues, although not explored in this study. Indeed, several structural studies exist demonstrating that the major role of Ser/Thr(OGlcNAc) is to direct backbone conformation through conformational restriction and/or sterics, not through stabilizing side-chain interactions, although there is a dearth of work in

this area.<sup>55-58</sup> Previous work by Doig has demonstrated that residues containing larger and bulkier side-chains at residue 1 on  $\alpha$ -helices exist almost exclusively with a  $\chi_1$  of  $g^+$  or  $g^-$ .<sup>59, 60</sup> Although many of these residues have been shown to participate in  $i/i+4$  interactions, Ser/Thr(OGlcNAc) may have greater steric restrictions than canonical amino acids, with the sugar moiety extending out from the N-terminus away from  $i+4$  aromatic side chains. In such a conformation, it would not be possible for a CH/ $\pi$  or boronic acid/diol interaction to occur on one face of an  $\alpha$ -helix, as consistent with observations herein.

Peptides were also examined to explore the effects of serine modifications in a relative  $i/i+4$  relationship to Trp. The presence of Trp had no appreciable stabilizing or destabilizing effects on  $\alpha$ -helicity relative to either serine or modified serine. However, both serine and Ser(OGlcNAc) demonstrated greater  $\alpha$ -helicity with Trp at residue 5 compared to similar peptides containing 4-I-Phe or 4-B(OH)<sub>2</sub>-Phe at the same relative position as Trp. In contrast to our observations, Baldwin and DeGrado both found that the differences between hydrophobic aromatic residues at internal positions of  $\alpha$ -helices have a negligible impact on  $\alpha$ -helix stability, suggestive of additional helix stabilizing interactions existing only in peptides containing Trp at residue 5.<sup>49, 50</sup> Compared to alanine-rich peptides, substitution of alanine at residue 5 with Trp led to peptides with a similar extent of  $\alpha$ -helical population, with differences of only 6-8%  $\alpha$ -helicity from Trp to Ala substitution. This finding is not consistent with previously established  $\alpha$ -helical propensities of Trp and Ala in alanine-rich peptides.<sup>49</sup> In the same study, Chakrabarty and Baldwin found that tyrosine had a slightly higher  $\alpha$ -helical propensity than tryptophan when both residues were in a relative  $i/i+3$  relationship with lysine, although in this case lysine was C-terminal to the aromatic residues. In our study and in contrast to similar studies, Ac-

SKAAXAKAAAKAAGY-NH<sub>2</sub> exhibited higher  $\alpha$ -helical content when lysine was *i*+4 to Trp (41.5%), versus 4-I-Phe (28.7%) or 4-B(OH)<sub>2</sub>-Phe (27.6%). Similar results were obtained for Ac-S(OGlcNAc)KAAXAKAAAKAAGY-NH<sub>2</sub>. GlcNAcylation and phosphorylation are dynamic intracellular processes. Thus peptides containing phosphoserine at residue 1 and tryptophan at residue 5 were also analyzed to determine potential intra- $\alpha$ -helical electrostatic interactions between tryptophan and the phosphate.

To determine the electrostatic effects of serine phosphorylation in a relative *i*/*i*+4 relationship to tryptophan, I synthesized and analyzed by NMR Ac-S(OPO<sub>3</sub><sup>2-</sup>)KAAWAKAAAKAAGY-NH<sub>2</sub>. Previous data, as well as work performed by others, have found a dramatic downfield chemical shift of phosphorylated serine and threonine amide hydrogens relative to unmodified serine and threonine residues.<sup>58, 61-64</sup> I have previously demonstrated that within model  $\alpha$ -helices, the strength of this phosphate-amide hydrogen bond can be qualitatively viewed through both the extent of the downfield chemical shift as well as the increase in conformational restriction of the peptide via <sup>3</sup>J<sub>aN</sub>. NMR spectroscopy was performed at pH 6.5 on the Trp-containing peptide, leading to a mixed protonation state of the phosphate group. Interestingly, the peptide containing pSer *i*/*i*+4 to Trp at pH 8.0 has an  $\alpha$ -helical population (via CD) between that of the peptide containing pSer *i*/*i*+4 to Ala at pH 4.0 (monoanionic phosphate) and 8.0 (dianionic phosphate). Furthermore, the peptide containing pSer *i*/*i*+4 to Trp exhibited a more upfield chemical shift of the phosphoserine amide proton (8.77 ppm for Trp at pH 6.5) than for the peptide containing pSer *i*/*i*+4 to Ala (8.91 ppm for Ala at pH 4.0, and 9.41 ppm for Ala at pH 9.41) as well as an increase in <sup>3</sup>J<sub>aN</sub> (5.2 Hz for pSer *i*/*i*+4 to Trp at pH 6.5, 4.4 Hz for pSer *i*/*i*+4 to Ala at pH 4.0, and 3.6 Hz for pSer *i*/*i*+4 to Ala at pH 7.2). These data are

consistent with a weakening of the phosphate-amide hydrogen bond due to substitution of Ala for Trp. The data herein suggest an additional  $\alpha$ -helix stabilizing interaction unique to peptides containing Trp at residue 5. The origin of this added stabilization most likely comes from an interaction with lysine at residue 2 engaging in a favorable  $i/i+3$  cation/ $\pi$  interaction with Trp.<sup>44, 51</sup> Previous work has demonstrated the overall preference for Trp to participate in such interactions over other aromatic amino acids due to increased electron density and surface area of the aromatic ring, providing insight into why this interaction was not observed for 4-I-Phe or 4-B(OH)<sub>2</sub>-Phe.<sup>65, 66</sup> Alternatively, the increased stability could also be due to increased hydrophobicity of Trp over other 4-I-Phe or 4-B(OH)<sub>2</sub>-Phe.

Although no appreciable effects were observed by CD, analysis of peptides containing Ser(OGlcNAc) at residue 1 and Trp at residue 5 revealed a small upfield chemical shift of all protons on the sugar's ring system relative to that of peptides with alanine at residue 5. The  $\alpha$ -hydrogen of GlcNAc exhibited the largest upfield shift (0.06 ppm) of all GlcNAc hydrogens. Work performed on the isolated effects of GlcNAcylation revealed no chemical shift differences among the protons on the sugar's ring system as a function of  $\alpha$ -helicity, although changes in the N-acetyl amide proton chemical shift were observed. Given the expected conformation of Ser(OGlcNAc) at residue 1, and given that chemical shift changes were observed for all hydrogens on the GlcNAc ring system and not solely on one face, it would seem unlikely that these effects are due to specific CH/ $\pi$  interactions within the  $\alpha$ -helix involving Trp.

Although no evidence of interactions was detected between the GlcNAc and either 4-I-Phe or 4-B(OH)<sub>2</sub>-Phe by CD, a stabilizing interaction was detected within peptides containing the boronic acid at specific residues (Figure 2.10). CD analysis of

peptides as a function of aromatic positions revealed that 4-I-Phe maintains a constant  $\alpha$ -helical population throughout the peptide, consistent with similar aromatic residues such as tyrosine and phenylalanine.<sup>50</sup> In contrast to 4-I-Phe, 4-B(OH)<sub>2</sub>-Phe demonstrates specific  $\alpha$ -helical conformational preferences within the peptide. These preferences are generally not dependent on the presence of the GlcNAc, indicating interactions within the peptide other than those involving GlcNAc. As there would be no precedence for an interaction with alanine, the most likely residue would be lysine.

The  $\alpha$ -helical trend in stabilization observed in peptides containing the boronic acid is as follows as a function of 4-B(OH)<sub>2</sub>-Phe position (Figure 2.16): residue 8 (**c**) > residue 5 (**b**) > residue 4 (**c**). Doig has previously determined the preferred  $\chi_1$  of phenylalanine (67% *t* and 32% *g*<sup>+</sup>), tyrosine (66% *t* and 33% *g*<sup>+</sup>), and lysine (46% *t* and 52% *g*<sup>+</sup>) at internal positions of  $\alpha$ -helices (Figure 2.17).<sup>60</sup> These models suggest that the boronic acid is interacting with lysine in relative *i/i*+3 and *i/i*+4 positions. The peptide exhibiting the most  $\alpha$ -helicity contains 4-B(OH)<sub>2</sub>-Phe in a relative *i/i*+4 position to lysine, leading to favorable geometric overlap for interactions of side-chain residues. There also exists the possibility of a cation/ $\pi$  interaction between the positively charged amine and the aromatic face of the aryl boronic acid, which could help to coordinate the amine into proximity of the boronic acid and/or contribute to the overall stabilizing effects. The stabilizing effects of 4-B(OH)<sub>2</sub>-Phe at residue 5 is more likely due to an *i/i*+7 interaction with lysine, over a relative *i/i*-3 interaction, based on both the preferred conformation of lysine and 4-B(OH)<sub>2</sub>-Phe, as well as favorable geometry of the amine and aryl boronic acid while in preferred rotamers. No effects were observed for the boronic acid at residue 4, likely due to 4-B(OH)<sub>2</sub>-Phe needing to adopt a  $\chi_1$  of *g*<sup>-</sup> for an interaction in a relative *i/i*+3 relationship to lysine at residue 7

(both phenylalanine and tyrosine rarely adopt a  $\chi_1$  of  $g^-$  while at internal positions of  $\alpha$ -helices).

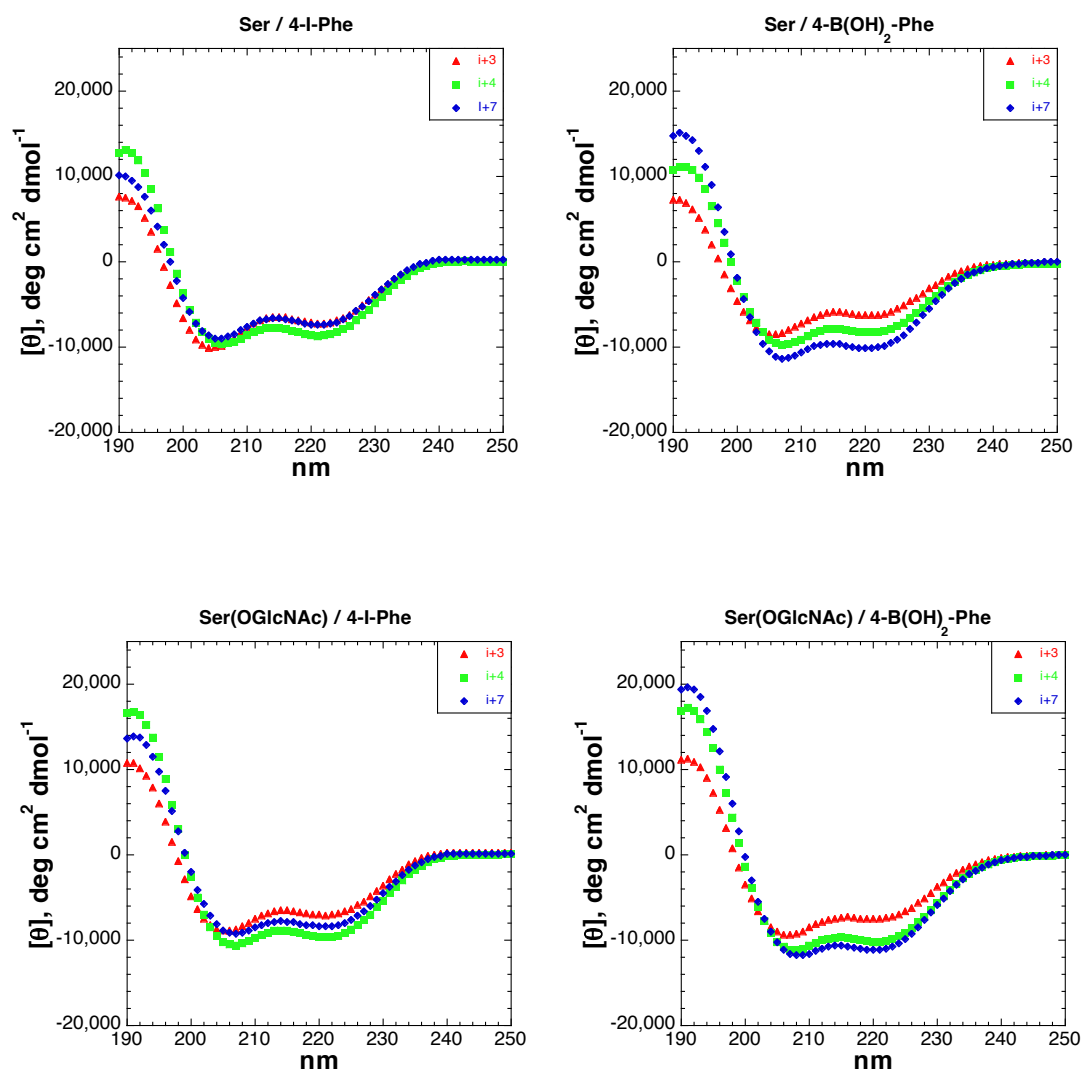


**Figure 2.16:** CD comparison of 4-I-Phe and 4-B(OH)<sub>2</sub>-Phe as a function of position. (Top left) CD spectra of peptides containing serine at residue 1 and 4-I-Phe. (Top right) CD spectra of peptides containing serine at residue 1 and 4-B(OH)<sub>2</sub>-Phe. (Bottom left) CD spectra of peptides containing Ser(OGlcNAc) at residue 1 and 4-I-Phe. (Bottom right) CD spectra of peptides containing Ser(OGlcNAc) at residue 1 and 4-B(OH)<sub>2</sub>-Phe. Peptides containing 4-I-Phe or 4-B(OH)<sub>2</sub>-Phe at relative positions to serine: (red triangles) *i*+3, (green squares) *i*+4, and (blue diamonds) *i*+7. CD experiments were conducted in water with 10 mM phosphate (pH 7.0), 25 mM KF at 0.5 °C.

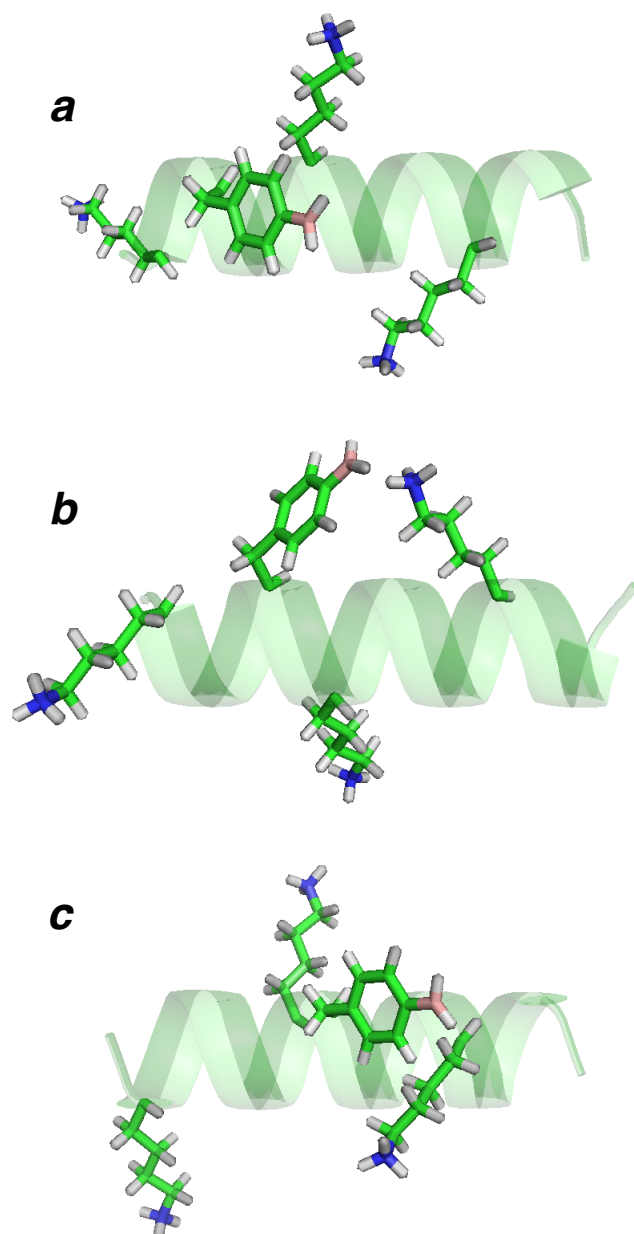


**Figure 2.17:** Representative  $\alpha$ -helix models with 4-B(OH)<sub>2</sub>-Phe at residue 4 (**a**), residue 5 (**b**), and residue 8 (**c**). Models were created using MacPyMOL version 1.3 and Chimera version 1.6.1.  $\chi_1$  was chosen based on the most common rotamer for internal lysine ( $\chi_1 = +60^\circ$ ), while 4-B(OH)<sub>2</sub>-Phe ( $\chi_1 = +180^\circ$ ) was based on phenylalanine and tyrosine at internal positions of  $\alpha$ -helices.<sup>60</sup>

Although the data are consistent with an interaction between lysine and the aryl boronic acid, the exact nature of the interaction is more obscure. Aryl boronates are known to exchange with hard anions in aqueous environments, leading to a complex equilibrium in the presence of aqueous KF. Work performed by Perrin has demonstrated that the addition of  $\text{ArBF}_3$  to an aqueous solution containing 192 mM phosphate buffer (pH 7.0) and 100 mM KF leads exclusively to species **6** (Figure 2.18)<sup>67</sup> He expanded on his study by incorporating both electron-donating groups (EDG) and electron-withdrawing groups (EWG) para to the aryltrifluoroboronate. No boron-fluoride species were found to be stable within the aqueous environment, suggesting that fluoride should play no mechanistic role other than electrostatic within the interaction between 4-B(OH)<sub>2</sub>-Phe and lysine. In other studies performed under aqueous conditions, no boron-fluoride species were detected at pH > 7.<sup>68, 69</sup>

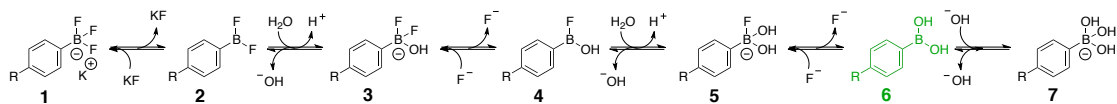


**Figure 2.18:** Partial scheme for the equilibrium of the boronic acid species in 192 mM aqueous phosphate buffer (pH 7.0) and 100 mM KF at pH 7.0 (R = EWG or EDG). Green denotes the only stable species observed (**6**).<sup>68</sup>

However, James has demonstrated that the aryl boronate-fluoride species can be stabilized in the presence of an amine in 50% H<sub>2</sub>O/MeOH (pH 5.5).<sup>70</sup> He found that aryl-B(OH)<sub>2</sub>F was stabilized by a proposed intramolecular H-F hydrogen bond with an adjacent protonated tertiary amine, which could alternatively be interpreted as an electrostatic interaction between the boronate and the protonated amine, both consistent with <sup>11</sup>B and <sup>19</sup>F NMR data obtained. A similar mechanism could explain

the observed 4-B(OH)<sub>2</sub>-Phe / lysine interaction, and explain why this interaction strengthens in high concentrations of KF (Figure 2.19). One could envision two separate, yet similar pathways where one equilibrium involves coordination via cation/ $\pi$  interaction **1**. In either case, the presence of the adjacent amine may create a localized basic environment around the boronic acid, facilitating the formation of **2a** and **2b**, which would be enhanced by the localization of the amine due to a cation/ $\pi$  interaction.<sup>71</sup> Furthermore, the formation of **2b** would increase the electron density in the aromatic ring which is known to occur when arylborates change their hybridization from sp<sup>2</sup> to sp<sup>3</sup>, further increasing the magnitude of the cation/ $\pi$  interaction. The positively charged amine could also stabilize the negatively charged boronate after the addition of the fluoride creating a stabilizing *i/i+4* salt bridge. Alternatively, release of the hydroxide anion would form species **3a** and **3b**. The presence of a hydrogen bond between fluoride and the amine proton could exist in either species **2** or **3**, although this is unlikely as fluorines are poor hydrogen bond acceptors. The equilibrium of this interaction would dictate that elevated concentrations of KF could push the equilibrium towards either species **2** or **3**.

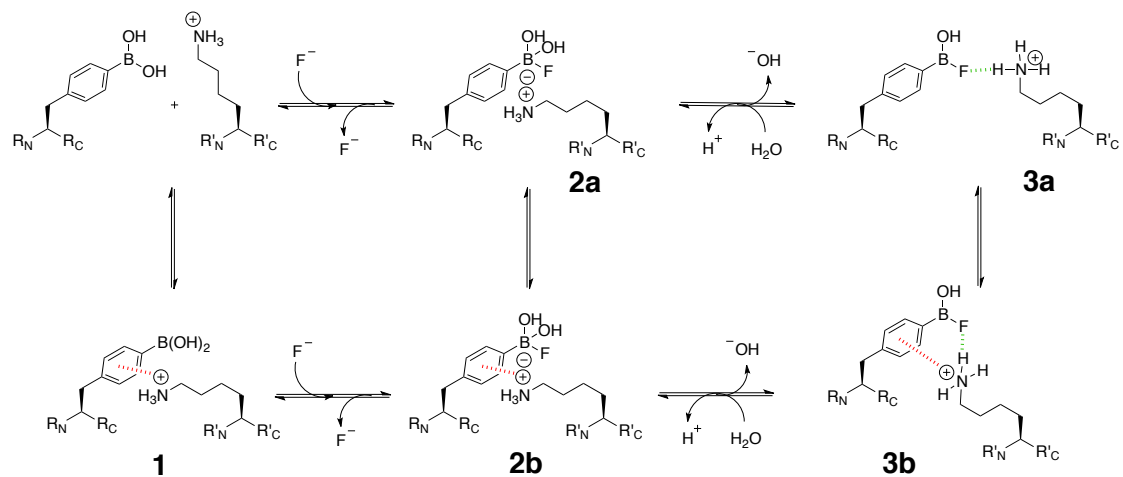


**Figure 2.19:** Plausible equilibrium involved in stabilizing interactions observed between 4-B(OH)<sub>2</sub>-Phe and lysine in a relative *i/i+4* relationship in the presence of KF.

An alternate equilibrium involving lysine and 4-B(OH)<sub>2</sub>-Phe may be involved in stabilizing the  $\alpha$ -helix, rationalized through a direct interaction between boron and the lysine nitrogen. Commonly known as an activated boronic acid, positioning an amine or oxygen adjacent to boronic acids (typically  $\delta$  to boron forming a 5 membered ring) forms the tetrahedral boron species through donation of the lone pair electrons into boron's empty p-orbital (Figure 2.20 (2)).<sup>8, 9, 30, 33, 71-74</sup> This preforms the aryl-boronate, which is enthalpically costly to form from the trigonal species. The positively charge lysine may further stabilize the negatively charged boronate species. Furthermore, hard anions such as fluoride are known to exchange with other species on aryl boronic acids and preformation of the boronate makes exchange more enthalpically favorable. This kinetic equilibrium may explain why elevated concentrations of fluoride and fructose led to increased  $\alpha$ -helicity. Alternatively, the observed stabilization could be a mixed equilibrium between schemes 2.3 and 2.4 and/or involving intermediates not pictured. Alternatively, the small increase in  $\alpha$ -helicity observed due to this interaction could have been caused by a small population of peptides exhibiting a large increase in  $\alpha$ -helicity, such as stapled peptides. However, further characterization would be necessary to determine the nature of such interactions. One such experiment would be to analyze the peptide Ac-(4-B(OH)<sub>2</sub>-Phe)-AAAKAAAKAAAAGY-NH<sub>2</sub> to confirm the optimal orientation of the lysine to the boronic acid. These peptides may also be further studied in helix-bundles.<sup>79</sup> Such molecules could have applications in medicinal chemistry, as drug delivery systems, encodable sensors for lysine acetylation, sugar sensors, and fluoride sensors.

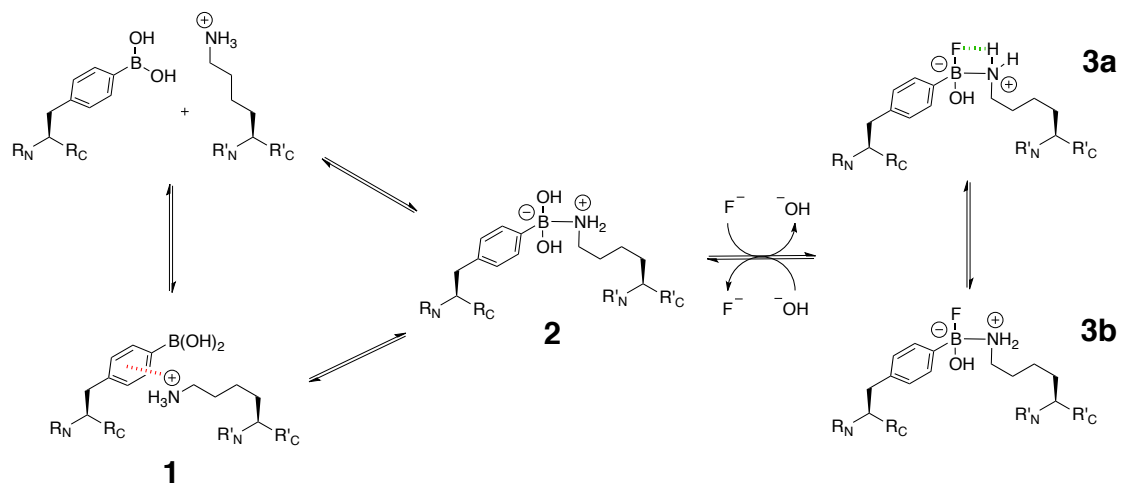


**Figure 2.20:** Plausible equilibrium involved in stabilizing interactions observed between 4-B(OH)<sub>2</sub>-Phe and lysine in a relative *i/i+4* relationship in the presence of KF.

## Experimental

### Materials

Fmoc-L-amino acids were purchased from Chem-Impex (Wood Dale, IL) or Novabiochem (San Diego, CA). O-(1H-Benzotriazol-1-yl)-1,1,3,3-tetramethyluronium hexafluorophosphate (HBTU), O-(7-azabenzotriazol-1-yl)-1,1,3,3-tetramethyluronium hexafluorophosphate (HATU), Rink amide resin (loading capacity of 0.37 mmol/g), and diisopropylethylamine (DIPEA) were purchased from Chem-Impex. 1,2-Ethanedithiol (EDT) was purchased from TCI America (Portland, OR). Trifluoroacetic acid (TFA), triethylsilane (TES), phenol, thioanisole, N,N'-diisopropylcarbodiimide (DIC), and tetrazole were purchased from Acros. Boron trifluoride diethyl etherate (BF<sub>3</sub>•OEt<sub>2</sub>), 1,1'-Bis(diphenylphosphino)ferrocene (dppf), palladium (II) chloride, bis(pinacolato) diboron, dimethylsulfoxide, and piperidine were purchased from Aldrich. Acetonitrile (MeCN), methylene chloride (CH<sub>2</sub>Cl<sub>2</sub>), methanol (MeOH), chloroform (CHCl<sub>3</sub>), tetrahydrofuran (THF), dimethylformamide (DMF), pyridine, diethyl ether (Et<sub>2</sub>O), sodium chloride, acetic acid, and acetic anhydride were purchased from Fischer. β-D-Glucosamine pentaacetate (Ac<sub>3</sub>O-GlcNAc), 2,2,2-trifluoroethanol (TFE), and O,O'-dibenzyl-N,N-diisopropylphosphoramidite was purchased from Alfa Aesar. Antarctic phosphatase was purchased from New England BioLabs (Ipswich, MA). Deionized water was purified by a Milipore Synergy 185 water purification system with a Simpapak2 cartridge.

## Phosphorylation of serine/threonine on peptides on solid phase

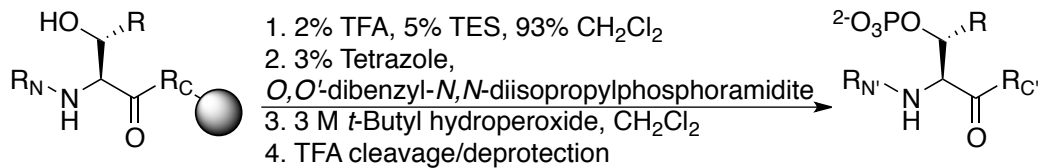


**Figure 2.21:** Scheme for the chemical phosphorylation of peptides on resin and subsequent cleavage/deprotection. R = CH<sub>3</sub> (Thr) or R = H (Ser).

Trityl-protected serine/threonine residues were incorporated at intended sites of chemical phosphorylation to allow for selective modification of the peptides on resin. The resin was swelled in CH<sub>2</sub>Cl in a fritted reaction vessel for 45 minutes. Trityl deprotection was effected using a solution of 2% TFA, 5% TES, and 93% CH<sub>2</sub>Cl<sub>2</sub> (3×3 mL, 1 minute each), followed by washing of the resin with CH<sub>2</sub>Cl<sub>2</sub>. To the resin was added 3 mL of 3% tetrazole solution in MeCN (1.35 mmol) and 500 μL of *O,O'*-dibenzyl-*N,N*-diisopropylphosphoramidite (1.52 mmol). The phosphitylation reaction was allowed to mix for 6 hours. The resin was then washed with DMF (3×3 mL) and CH<sub>2</sub>Cl<sub>2</sub> (3×3 mL). The resin was then treated with 4 mL of 3 M *tert*-butyl hydroperoxide in CH<sub>2</sub>Cl<sub>2</sub> for 1 hour, after which it was washed with DMF (3×3 mL), MeOH (3×3 mL), and CH<sub>2</sub>Cl<sub>2</sub> (3×3 mL). The resin was dried after washing with diethyl ether. The phosphorylated peptide was then subjected to cleavage from the resin and deprotection using reagent K (84% TFA and 4% each of H<sub>2</sub>O/phenol/thioanisole/ethanedithiol) or 92.5% TFA/5% TES/2.5% H<sub>2</sub>O for 3 hours.

## Synthesis of Fmoc-Ser(Ac<sub>3</sub>O-GlcNAc)-OH and Fmoc-Thr(Ac<sub>3</sub>O-GlcNAc)-OH

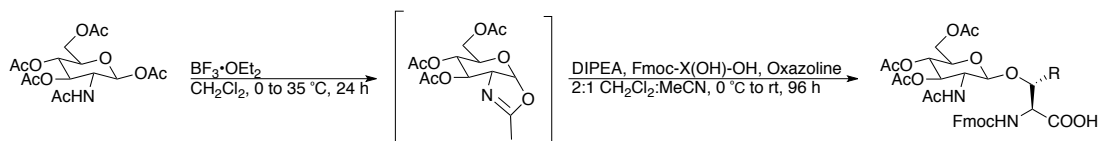


**Figure 2.22:** Synthesis of peracetylated 2-acetamido-2-deoxy- $\beta$ -D-glycosides of Fmoc-Thr-OH (R = CH<sub>3</sub>) and Fmoc-Ser-OH (R = H).

To a vacuum-dried mixture of  $\beta$ -D-Glucosamine pentaacetate (1.92 g, 2.5 mmol) and 4 Å molecular sieves was added CH<sub>2</sub>Cl<sub>2</sub> (32 mL). At 0 °C, BF<sub>3</sub>·OEt<sub>2</sub> (1.6 mL, 15.3 mmol) was added dropwise. The solution was then heated at 35 °C for 24 hours with the reaction monitored by TLC (10% MeOH/CHCl<sub>3</sub>) and visualized using cerium molybdate. When formation of the oxazoline was complete, the reaction was cooled to 0 °C and DIPEA (800  $\mu$ L, 4.6 mmol) was added dropwise over 5 minutes. The solution was then warmed to room temperature and was allowed to react for an additional 10 minutes. Fmoc-L-Thr(OH)-OH (1.73 g, 5.08 mmol) or Fmoc-L-Ser(OH)-OH (1.66 g, 5.08 mmol) was dissolved in 18 mL of 2:1 CH<sub>2</sub>Cl<sub>2</sub>:MeCN and added to the solution. After 24 hours, a second batch of the oxazoline was added to the solution and the combined solution allowed to react for an additional 72 hours. The solution was then diluted with 80 mL CH<sub>2</sub>Cl<sub>2</sub> and filtered through Celite. The solution was washed with saturated Na<sub>2</sub>CO<sub>3</sub> (100 mL) and brine (100 mL). The aqueous layers were combined and extracted with CH<sub>2</sub>Cl<sub>2</sub> (3×50 mL). The organic layers were combined, dried over sodium sulfate, and the solvent removed under reduced pressure.<sup>75</sup> The crude mixture was then purified via flash column chromatography (SiO<sub>2</sub>; 100% EtOAc, followed by a series of mixtures composed of

EtOAc/MeCN/MeOH/H<sub>2</sub>O with relative volumes of 70/2.5/1.25/1.25, followed by 70/5/2.5/2.5, then 70/10/5/5).<sup>76</sup> Isolated products were dried over sodium sulfate and concentrated under reduced pressure. Fmoc-L-Thr(Ac<sub>3</sub>O-GlcNAc)-OH was obtained as a white solid (1.10 g) in 32% isolated yield. Fmoc-L-Ser(Ac<sub>3</sub>O-GlcNAc)-OH was obtained as a white solid (1.36 g) in 40% isolated yield. Product identity was confirmed via comparison to previously reported NMR data.

### Solid-phase Aryl Borylation of peptides containing 4-I-Phe



**Figure 2.23:** Solid phase arylborlyation of peptides containing 4-Iodo-Phe.

To a 2 mL vial containing 30 mg of resin with the 4-iodophenylalanine-containing peptide (1.0 mM), potassium acetate (7.7 mg, 78 μM), PdCl<sub>2</sub>(dppf) (1.7 mg, 2.3 μM), dppf (1.1 mg, 1.3 μM), and bis(pinacolato) diboron (13.2 mg, 52 μM) was added DMSO (470 μL). The vial was sparged with nitrogen gas and then capped. The mixture was then stirred in an oil bath set to 80 °C for 24 h. The resin was then washed with DMF (3 × 4 mL), CH<sub>2</sub>Cl<sub>2</sub> (3 × 4 mL), and then dried with ether. The peptide was then cleaved (2.5% H<sub>2</sub>O, 5% TES, and 92.5% TFA) and purified via HPLC.<sup>77,78</sup>

## Synthesis and characterization data for all peptides

Peptides were synthesized on a Rainin PS3 peptide synthesizer on Rink amide resin via standard Fmoc solid phase peptide synthesis, using HBTU as a coupling reagent for all canonical amino acids, and using HATU for all glycosylated amino acids. 60 minute couplings were performed with 4 equivalents of canonical amino acids. Glycosylated amino acids were coupled twice for 3 hours each using 1.5 equivalents of amino acid. All non-glycosylated peptides were acetylated on the N-terminus using 5% acetic anhydride in pyridine. Glycosylated peptides were acetylated using 1:1 0.5 M DIC:acetic acid in THF for 1 hour. All peptides contain a C-terminal amide.

Non-glycosylated peptides were subjected to cleavage from resin and deprotection for 3 hours using reagent K (84% TFA and 4% each of H<sub>2</sub>O/phenol/thioanisole/ethanedithiol) or a solution of 92.5% TFA, 5% TES, and 2.5% H<sub>2</sub>O. Glycosylated peptides were subjected to cleavage from resin and deprotection for 90 minutes using a solution of 92.5% TFA, 5% TES, and 2.5% H<sub>2</sub>O. TFA was removed by evaporation. Peptides were precipitated with cold ether and the precipitate was dried. The peptides were dissolved in water, then filtered through a 0.45  $\mu$ m syringe filter. The peptides were purified using reverse phase HPLC on a Vydac C18 semi-preparative column (250  $\times$  10 mm, 5-10  $\mu$ m particle, 300 Å pore) or on a Varian Microsorb MV C18 analytical column (250  $\times$  4.6 mm, 3-5  $\mu$ m particle, 100 Å pore) using a linear gradient of buffer B (20% water, 80% MeCN, and 0.05% TFA) in buffer A (98% water, 2% MeCN, and 0.06% TFA). Dried Acylated O-GlcNAcylated peptides were subjected to deesterification by adding 1.4 mL of a solution of 25 mM NaOMe in methanol and allowed to react for 2 hours. The solutions were then

neutralized with 35  $\mu$ L of 1 M AcOH, lyophilized, and purified on HPLC. Peptide purity was verified via the observation of a single peak upon reinjection on an analytical HPLC column. Peptides were characterized by ESI-MS (positive ion mode) on an LCQ Advantage (Finnigan) or Shimadzu mass spectrometer.

**Table 2.10:** Purification procedure for synthetic peptides.

Peptide sequence	Peptide purification	$t_R$
Ac-SK(4-I-Phe)AAAKAAAAKAAGY-NH <sub>2</sub>	0-35% buffer B in buffer A over 60 minutes	51.1 min
Ac-S(Ac <sub>3</sub> OGlcNAc)K(4-I-Phe)AAAKAAAAKAAGY-NH <sub>2</sub>	0-40% buffer B in buffer A over 60 minutes	50.9 min
Ac-S(OGlcNAc)K(4-I-Phe)AAAKAAAAKAAGY-NH <sub>2</sub>	0-35% buffer B in buffer A over 60 minutes	53.3 min
Ac-SKA(4-I-Phe)AAAKAAAAKAAGY-NH <sub>2</sub>	0-30% buffer B in buffer A over 60 minutes	51.5 min
Ac-S(Ac <sub>3</sub> OGlcNAc)KA(4-I-Phe)AAKAAAAKAAGY-NH <sub>2</sub>	0-40% buffer B in buffer A over 60 minutes	50.5 min
Ac-S(OGlcNAc)KA(4-I-Phe)AAKAAAAKAAGY-NH <sub>2</sub>	0-30% buffer B in buffer A over 60 minutes	56.0 min
Ac-SKA(4-B(OH) <sub>2</sub> -Phe)AAKAAAAKAAGY-NH <sub>2</sub>	0-25% buffer B in buffer A over 60 minutes	49.2 min
Ac-S(Ac <sub>3</sub> OGlcNAc)KA(4-B(OH) <sub>2</sub> -Phe)AAKAAAAKAAGY-NH <sub>2</sub>	0-35% buffer B in buffer A over 60 minutes	43.6 min
Ac-S(GlcNAc)KA(4-B(OH) <sub>2</sub> -Phe)AAKAAAAKAAGY-NH <sub>2</sub>	0-20% buffer B in buffer A over 60 minutes	59.1 min
Ac-SKAA(4-I-Phe)AAKAAAAKAAGY-NH <sub>2</sub>	0-35% buffer B in buffer A over 60 minutes	47.9 min
Ac-S(Ac <sub>3</sub> OGlcNAc)KAA(4-I-Phe)AKAAAAKAAGY-NH <sub>2</sub>	0-45% buffer B in buffer A over 60 minutes	45.8 min
Ac-S(OGlcNAc)KAA(4-I-Phe)AKAAAAKAAGY-NH <sub>2</sub>	0-35% buffer B in buffer A over 60 minutes	47.7 min
Ac-SKAA(4-B(OH) <sub>2</sub> -Phe)AKAAAAKAAGY-NH <sub>2</sub>	0-25% buffer B in buffer A over 60 minutes	50.1 min
Ac-S(Ac <sub>3</sub> OGlcNAc)KAA(4-B(OH) <sub>2</sub> -Phe)AKAAAAKAAGY-NH <sub>2</sub>	0-30% buffer B in buffer A over 60 minutes	50.6 min
Ac-S(GlcNAc)KAA(4-B(OH) <sub>2</sub> -Phe)AKAAAAKAAGY-NH <sub>2</sub>	0-25% buffer B in buffer A over 60 minutes	49.2 min
Ac-SKAAWAAKAAAAKAAGY-NH <sub>2</sub>	0-30% buffer B in buffer A over 60 minutes	53.1 min
Ac-S(Ac <sub>3</sub> OGlcNAc)KAAWAKAAAAKAAGY-NH <sub>2</sub>	0-35% buffer B in buffer A over 60 minutes	52.4 min
Ac-S(OGlcNAc)KAAWAKAAAAKAAGY-NH <sub>2</sub>	0-30% buffer B in buffer A over 60 minutes	52.3 min
Ac-S(OPO <sub>3</sub> <sup>2-</sup> )KAAWAKAAAAKAAGY-NH <sub>2</sub>	0-30% buffer B in buffer A over 60 minutes	55.3 min
Ac-TKAA(4-I-Phe)AAKAAAAKAAGY-NH <sub>2</sub>	0-35% buffer B in buffer A over 60 minutes	50.7 min
Ac-T(Ac <sub>3</sub> OGlcNAc)KAA(4-I-Phe)AKAAAAKAAGY-NH <sub>2</sub>	0-40% buffer B in buffer A over 60 minutes	50.2 min
Ac-T(OGlcNAc)KAA(4-I-Phe)AKAAAAKAAGY-NH <sub>2</sub>	0-30% buffer B in buffer A over 60	57.1 min

	minutes	
Ac-(4-I-Phe)KAASAKAAAAKAAGY-NH <sub>2</sub>	0-40% buffer B in buffer A over 60 minutes	47.4 min
Ac-(4-I-Phe)KAAS(Ac <sub>3</sub> OGlcNAc)AKAAAAKAAGY-NH <sub>2</sub>	0-40% buffer B in buffer A over 60 minutes	55.0 min
Ac-(4-I-Phe)KAAS(OGlcNAc)AKAAAAKAAGY-NH <sub>2</sub>	0-35% buffer B in buffer A over 60 minutes	49.1 min
Ac-(4-B(OH) <sub>2</sub> -Phe)KAAS(Ac <sub>3</sub> OGlcNAc)AKAAAAKAAGY-NH <sub>2</sub>	0-20% buffer B in buffer A over 120 minutes	101.8 min
Ac-(4-B(OH) <sub>2</sub> -Phe)KAAS(OGlcNAc)AKAAAAKAAGY-NH <sub>2</sub>	0-20% buffer B in buffer A over 60 minutes	48.5 min
Ac-SKAAAAK(4-I-Phe)AAAAKAAGY-NH <sub>2</sub>	0-30% buffer B in buffer A over 60 minutes	53.5 min
Ac-S(Ac <sub>3</sub> OGlcNAc)KAAAAK(4-I-Phe)AAAAKAAGY-NH <sub>2</sub>	0-50% buffer B in buffer A over 60 minutes	51.0 min
Ac-S(OGlcNAc)KAAAAK(4-I-Phe)AAAAKAAGY-NH <sub>2</sub>	0-30% buffer B in buffer A over 60 minutes	53.3 min
Ac-SKAAAAK(4-B(OH) <sub>2</sub> -Phe)AAAAKAAGY-NH <sub>2</sub>	0-20% buffer B in buffer A over 60 minutes	58.7 min
Ac-S(Ac <sub>3</sub> OGlcNAc)KAAAAK(4-B(OH) <sub>2</sub> -Phe)AAAAKAAGY-NH <sub>2</sub>	0-30% buffer B in buffer A over 120 minutes	101.2 min
Ac-S(OGlcNAc)KAAAAK(4-B(OH) <sub>2</sub> -Phe)AAAAKAAGY-NH <sub>2</sub>	0-25% buffer B in buffer A over 120 minutes	107.3 min

**Table 2.11:** Characterization data for synthetic peptides.

Peptide sequence	Calculated mass	Observed mass
Ac-SK(4-I-Phe)AAAAAAAAKAAGY-NH <sub>2</sub>	1663.7 (M+H)	832.5 (M+2H)
Ac-S(Ac <sub>3</sub> OGlcNAc)K(4-I-Phe)AAAAAAAAKAAGY-NH <sub>2</sub>	1991.9 (M+H)	997.1 (M+2H)
Ac-S(OGlcNAc)K(4-I-Phe)AAAAAAAAKAAGY-NH <sub>2</sub>	1865.8 (M+H)	933.9 (M+2H)
Ac-SKA(4-I-Phe)AAAAAAAAKAAGY-NH <sub>2</sub>	1663.7 (M+H)	832.5 (M+2H)
Ac-S(Ac <sub>3</sub> OGlcNAc)KA(4-I-Phe)AAAAAAAAKAAGY-NH <sub>2</sub>	1991.9 (M+H)	997.2 (M+2H)
Ac-S(OGlcNAc)KA(4-I-Phe)AAAAAAAAKAAGY-NH <sub>2</sub>	1865.8 (M+H)	934 (M+2H)
Ac-SKA(4-B(OH) <sub>2</sub> -Phe)AAAAAAAAKAAGY-NH <sub>2</sub>	1580.8 (M+H)	791.4 (M+2H)
Ac-S(Ac <sub>3</sub> OGlcNAc)KA(4-B(OH) <sub>2</sub> -Phe)AAAAAAAAKAAGY-NH <sub>2</sub>	1910.0 (M+H)	997.2 (M+2H)
Ac-S(GlcNAc)KA(4-B(OH) <sub>2</sub> -Phe)AAAAAAAAKAAGY-NH <sub>2</sub>	1783.9 (M+H)	956.3 (M+2H)
Ac-SKAA(4-I-Phe)AAAAAAAAKAAGY-NH <sub>2</sub>	1663.7 (M+H)	833 (M+2H)
Ac-S(Ac <sub>3</sub> OGlcNAc)KAA(4-I-Phe)AKAAAAKAAGY-NH <sub>2</sub>	1991.9 (M+H)	997.2 (M+2H)
Ac-S(OGlcNAc)KAA(4-I-Phe)AKAAAAKAAGY-NH <sub>2</sub>	1865.8 (M+H)	934 (M+2H)
Ac-SKAA(4-B(OH) <sub>2</sub> -Phe)AKAAAAKAAGY-NH <sub>2</sub>	1580.8 (M+H)	792 (M+2H)
Ac-S(Ac <sub>3</sub> OGlcNAc)KAA(4-B(OH) <sub>2</sub> -Phe)AKAAAAKAAGY-NH <sub>2</sub>	1910.0 (M+H)	638 (M+3H)
Ac-S(GlcNAc)KAA(4-B(OH) <sub>2</sub> -Phe)AKAAAAKAAGY-NH <sub>2</sub>	1783.9 (M+H)	893 (M+2H)
Ac-SKAAWAKAAAAKAAGY-NH <sub>2</sub>	1575.8 (M+H)	789.2 (M+2H)
Ac-S(Ac <sub>3</sub> OGlcNAc)KAAWAKAAAAKAAGY-NH <sub>2</sub>	1905.0 (M+H)	953.7 (M+2H)
Ac-S(OGlcNAc)KAAWAKAAAAKAAGY-NH <sub>2</sub>	1778.9 (M+H)	890.7 (M+2H)
Ac-S(OPO <sub>3</sub> <sup>2-</sup> )KAAWAKAAAAKAAGY-NH <sub>2</sub>	1655.8 (M+H)	829.1 (M+2H)
Ac-TKAA(4-I-Phe)AAAAAAAAKAAGY-NH <sub>2</sub>	1676.7 (M+H)	840.2 (M+2H)
Ac-T(Ac <sub>3</sub> OGlcNAc)KAA(4-I-Phe)AKAAAAKAAGY-NH <sub>2</sub>	2005.9 (M+H)	1004.2 (M+2H)
Ac-T(OGlcNAc)KAA(4-I-Phe)AKAAAAKAAGY-NH <sub>2</sub>	1879.8 (M+H)	941.1 (M+2H)

Ac-(4-I-Phe)KAASAKAAAAKAAGY-NH <sub>2</sub>	1663.7 (M+H)	832.3 (M+2H)
Ac-(4-I-Phe)KAAS(Ac <sub>3</sub> OGlcNAc)AKAAAAKAAGY-NH <sub>2</sub>	1991.9 (M+H)	997.2 (M+2H)
Ac-(4-I-Phe)KAAS(OGlcNAc)AKAAAAKAAGY-NH <sub>2</sub>	1865.8 (M+H)	623 (M+3H)
Ac-(4-B(OH) <sub>2</sub> -Phe)KAAS(Ac <sub>3</sub> OGlcNAc)AKAAAAKAAGY-NH <sub>2</sub>	1910.0 (M+H)	956 (M+2H)
Ac-(4-B(OH) <sub>2</sub> -Phe)KAAS(OGlcNAc)AKAAAAKAAGY-NH <sub>2</sub>	1783.9 (M+H)	596 (M+3H)
Ac-SKAAAAK(4-I-Phe)AAAAKAAGY-NH <sub>2</sub>	1663.7 (M+H)	832.6 (M+2H)
Ac-S(Ac <sub>3</sub> OGlcNAc)KAAAAK(4-I-Phe)AAAAKAAGY-NH <sub>2</sub>	1991.9 (M+H)	997.1 (M+2H)
Ac-S(OGlcNAc)KAAAAK(4-I-Phe)AAAAKAAGY-NH <sub>2</sub>	1865.8 (M+H)	934 (M+2H)
Ac-SKAAAAK(4-B(OH) <sub>2</sub> -Phe)AAAAKAAGY-NH <sub>2</sub>	1580.8 (M+H)	791.5 (M+2H)
Ac-S(Ac <sub>3</sub> OGlcNAc)KAAAAK(4-B(OH) <sub>2</sub> -Phe)AAAAKAAGY-NH <sub>2</sub>	1910.0 (M+H)	956.1 (M+2H)
Ac-S(OGlcNAc)KAAAAK(4-B(OH) <sub>2</sub> -Phe)AAAAKAAGY-NH <sub>2</sub>	1783.9 (M+H)	596 (M+3H)

### Circular dichroism (CD) spectroscopy

CD spectra were collected on a Jasco J-810 Spectropolarimeter in a 1 mm cell at 0.5 °C unless otherwise indicated. The concentrations of the peptides were determined by UV absorption using  $\epsilon_{280}$ : 1569 M<sup>-1</sup>cm<sup>-1</sup> for peptides containing tyrosine and 4-I-Phe (280 M<sup>-1</sup>cm<sup>-1</sup>), 1508 M<sup>-1</sup>cm<sup>-1</sup> for peptides containing tyrosine and 4-B(OH)<sub>2</sub>-Phe (228 M<sup>-1</sup>cm<sup>-1</sup>), or 6970 M<sup>-1</sup>cm<sup>-1</sup> for peptides containing tyrosine and Trp (5690 M<sup>-1</sup>cm<sup>-1</sup>). Peptide concentrations were 80 to 100  $\mu$ M in 10 mM aqueous phosphate buffer (pH 4.0, 7.0 or 8.0) with 25 mM KF. The pH of each individual solution was recorded and adjusted to the indicated pH using dilute HCl or NaOH as necessary. Individual scans were made at 1 nm intervals with 2 nm bandwidth and an averaging time of 4 s. Data are the average of at least three independent trials. Data were background corrected but were not smoothed. Error bars indicate standard error. Percent  $\alpha$ -helix was calculated using a method from Baldwin where %Helix =  $100 * (([\theta]_{222} - [\theta]_C) / ([\theta]_H - [\theta]_C))$ , where  $[\theta]_C$  = mean residue ellipticity at 222 nm of 100% random coil =  $2220 - 53T$ ,  $[\theta]_H$  = mean residue ellipticity at 222 nm of 100%  $\alpha$ -helix =  $(-44000 + 250T) / (1 - 3/n)$ ,  $T$  = temperature in °C (0.5), and  $n$  = number of residues (16).

## Summary of CD data

Peptide	$[\theta]_{222}$	$[\theta]_{208}$	$[\theta]_{190}$	$[\theta]_{222}/[\theta]_{208}$	$-[\theta]_{190}/[\theta]_{208}$	% Helix
Ac-SK(4-I-Phe)AAKAAAAKAAGY-NH <sub>2</sub>	-8352	-9487	13055	0.88	1.38	27.9
Ac-S(GlcNAc)K(4-I-Phe)AAKAAAAKAAGY-NH <sub>2</sub>	-9791	-10412	16521	0.94	1.59	31.7
Ac-SKA(4-I-Phe)AAKAAAAKAAGY-NH <sub>2</sub>	-7186	-8941	7597	0.80	0.85	24.8
Ac-SKA(4-B(OH) <sub>2</sub> -Phe)AAKAAAAKAAGY-NH <sub>2</sub>	-6222	-8056	7259	0.77	0.90	22.2
Ac-S(GlcNAc)KA(4-I-Phe)AAKAAAAKAAGY-NH <sub>2</sub>	-7006	-8366	10753	0.84	1.29	24.3
Ac-S(GlcNAc)KA(4-B(OH) <sub>2</sub> -Phe)AAKAAAAKAAGY-NH <sub>2</sub>	-7403	-9217	11143	0.80	1.21	25.4
Ac-SKAA(4-I-Phe)AKAAAAKAAGY-NH <sub>2</sub>	-8670	-9327	12733	0.93	1.37	28.7
Ac-SKAA(4-B(OH) <sub>2</sub> -Phe)AKAAAAKAAGY-NH <sub>2</sub>	-8241	-9658	10702	0.85	1.11	27.6
Ac-S(GlcNAc)KAA(4-I-Phe)AKAAAAKAAGY-NH <sub>2</sub>	-9607	-10413	16572	0.92	1.59	31.2
Ac-S(GlcNAc)KAA(4-B(OH) <sub>2</sub> -Phe)AKAAAAKAAGY-NH <sub>2</sub>	-10083	-11121	16837	0.91	1.51	32.4
Ac-SKAAWAKAAAAKAAGY-NH <sub>2</sub>	-13508	-14847	24321	0.91	1.64	41.5
Ac-S(GlcNAc)KAAWAKAAAAKAAGY-NH <sub>2</sub>	-14677	-15379	31017	0.95	2.02	44.6
Ac-Ser(OPO <sub>3</sub> <sup>2-</sup> )KAAWAKAAAAKAAGY-NH <sub>2</sub>	-17504	-17555	34788	1.00	1.98	52.1
Ac-TKAA(4-I-Phe)AKAAAAKAAGY-NH <sub>2</sub>	-7777	-8892	9998	0.87	1.12	26.3
Ac-T(GlcNAc)KAA(4-I-Phe)AKAAAAKAAGY-NH <sub>2</sub>	-9614	-10458	15407	0.92	1.47	31.2
Ac-(4-I-Phe)KAAAKAAAAKAAGY-NH <sub>2</sub>	-5058	-6711	5300	0.75	0.79	19.2
Ac-(4-I-Phe)KAA S(GlcNAc)AKAAAAKAAGY-NH <sub>2</sub>	-3840	-6794	1566	0.57	0.23	15.9
Ac-(4-B(OH) <sub>2</sub> -Phe)KAA S(GlcNAc)AKAAAAKAAGY-NH <sub>2</sub>	-3637	-6929	1701	0.52	0.25	15.4
Ac-SKAAAK(4-I-Phe)AAKAAAGY-NH <sub>2</sub>	-7382	-8468	10101	0.87	1.19	25.3
Ac-SKAAAK(4-B(OH) <sub>2</sub> -Phe)AAKAAAGY-NH <sub>2</sub>	-10037	-11269	14697	0.89	1.30	32.3
Ac-S(GlcNAc)KAAAK(4-I-Phe)AAKAAAGY-NH <sub>2</sub>	-8338	-9149	13675	0.91	1.49	27.8
Ac-S(GlcNAc)KAAAK(4-B(OH) <sub>2</sub> -Phe)AAKAAAGY-NH <sub>2</sub>	-10982	-11783	19349	0.93	1.64	34.8

**Table 2.12:** Summary of CD data for all peptides. CD data were collected at 0.5 °C with 80-100 μM peptide in 10 mM aqueous phosphate buffer (pH 4.0, 7.0, or 8.0) with 25 mM KF.

Peptide	$\lambda$ at local [ $\theta$ ] <sub>min</sub> , nm	[ $\theta$ ] <sub>min</sub> , deg cm <sup>2</sup> dmol <sup>-1</sup>	$\lambda$ at local [ $\theta$ ] <sub>min</sub> , nm	[ $\theta$ ] <sub>min</sub> , deg cm <sup>2</sup> dmol <sup>-1</sup>	$\lambda$ at local [ $\theta$ ] <sub>max</sub> , nm	local [ $\theta$ ] <sub>max</sub> , deg cm <sup>2</sup> dmol <sup>-1</sup>
Ac-SK(4- <i>I-Phe</i> )AAKAAAAKAAGY-NH <sub>2</sub>	221	-8377	207	-9707	191	13201
Ac-S(GlcNAc)K(4- <i>I-Phe</i> )AAKAAAAKAAGY-NH <sub>2</sub>	221	-9892	207	-10516	191	16706
Ac-SKA(4- <i>I-Phe</i> )AAKAAAAKAAGY-NH <sub>2</sub>	222	-7186	204	-10069	190	7597
Ac-SKA(4- <i>B(OH)</i> <sub>2</sub> - <i>Phe</i> )AAKAAAAKAAGY-NH <sub>2</sub>	221	-6257	206	-8500	191	7297
Ac-S(GlcNAc)KA(4- <i>I-Phe</i> )AAKAAAAKAAGY-NH <sub>2</sub>	221	-7061	206	-8926	190	10753
Ac-S(GlcNAc)KA(4- <i>B(OH)</i> <sub>2</sub> - <i>Phe</i> )AAKAAAAKAAGY-NH <sub>2</sub>	219	-7544	207	-9351	191	11236
Ac-SKAA(4- <i>I-Phe</i> )AKAAAAKAAGY-NH <sub>2</sub>	221	-8683	206	-9648	191	13139
Ac-SKAA(4- <i>B(OH)</i> <sub>2</sub> - <i>Phe</i> )AKAAAAKAAGY-NH <sub>2</sub>	221	-8292	207	-9723	191	11103
Ac-S(GlcNAc)KAA(4- <i>I-Phe</i> )AKAAAAKAAGY-NH <sub>2</sub>	221	-9637	207	-10594	191	16736
Ac-S(GlcNAc)KAA(4- <i>B(OH)</i> <sub>2</sub> - <i>Phe</i> )AKAAAAKAAGY-NH <sub>2</sub>	220	-10200	208	-11121	191	17249
Ac-SKAAWAKAAAAKAAGY-NH <sub>2</sub>	221	-13539	207	-15101	191	24516
Ac-S(GlcNAc)KAAWAKAAAAKAAGY-NH <sub>2</sub>	221	-14715	208	-15379	191	31554
Ac-Ser(OPO <sub>3</sub> <sup>2-</sup> )KAAWAKAAAAKAAGY-NH <sub>2</sub>	221	-17602	208	-17555	191	35774
Ac-TKAA(4- <i>I-Phe</i> )AKAAAAKAAGY-NH <sub>2</sub>	221	-7815	206	-9546	191	10119
Ac-T(GlcNAc)KAA(4- <i>I-Phe</i> )AKAAAAKAAGY-NH <sub>2</sub>	221	-9646	207	-10640	191	15503
Ac-(4- <i>I-Phe</i> )KAAAKAAAAKAAGY-NH <sub>2</sub>	221	-5098	204	-7754	190	5300
Ac-(4- <i>I-Phe</i> )KAA(S(GlcNAc))AKAAAAKAAGY-NH <sub>2</sub>	221	-3860	202	-10166	190	1566
Ac-(4- <i>B(OH)</i> <sub>2</sub> - <i>Phe</i> )KAAS(GlcNAc)AKAAAAKAAGY-NH <sub>2</sub>	219	-3795	203	-8841	190	1701
Ac-SKAAAK(4- <i>I-Phe</i> )AAKAAAGY-NH <sub>2</sub>	221	-7403	206	-9001	190	10101
Ac-SKAAAK(4- <i>B(OH)</i> <sub>2</sub> - <i>Phe</i> )AAKAAAGY-NH <sub>2</sub>	221	-10110	207	-11325	191	15174
Ac-S(GlcNAc)KAAAK(4- <i>I-Phe</i> )AAKAAAGY-NH <sub>2</sub>	221	-8422	207	-9278	191	13928
Ac-S(GlcNAc)KAAAK(4- <i>B(OH)</i> <sub>2</sub> - <i>Phe</i> )AAKAAAGY-NH <sub>2</sub>	220	-11170	208	-11783	191	19681

**Table 2.13:** Summary of CD data for all peptides. CD data were collected at 0.5 °C with 80-100 μM peptide in 10 mM aqueous phosphate buffer (pH 4.0, 7.0, or 8.0) with 25 mM KF.

## CD spectroscopy under standard conditions

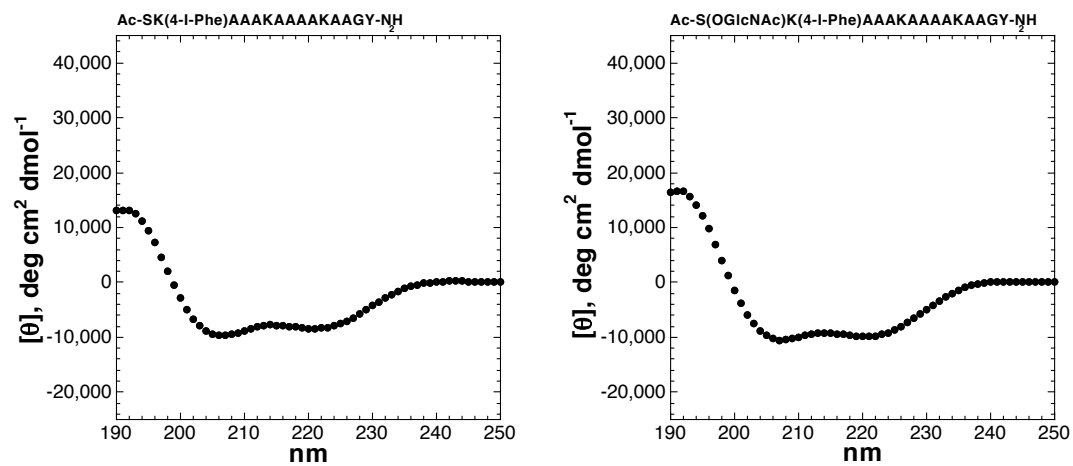


**Figure 2.24:** CD spectra of Ac-SK(4-I-Phe)AAAKAAAKAAGY-NH<sub>2</sub> (left) and Ac-S(OGlcNAc)K(4-I-Phe)AAAKAAAKAAGY-NH<sub>2</sub> (right); peptides were dissolved in 10 mM phosphate buffer (pH 7.0) containing 25 mM KF at 0.5 °C.

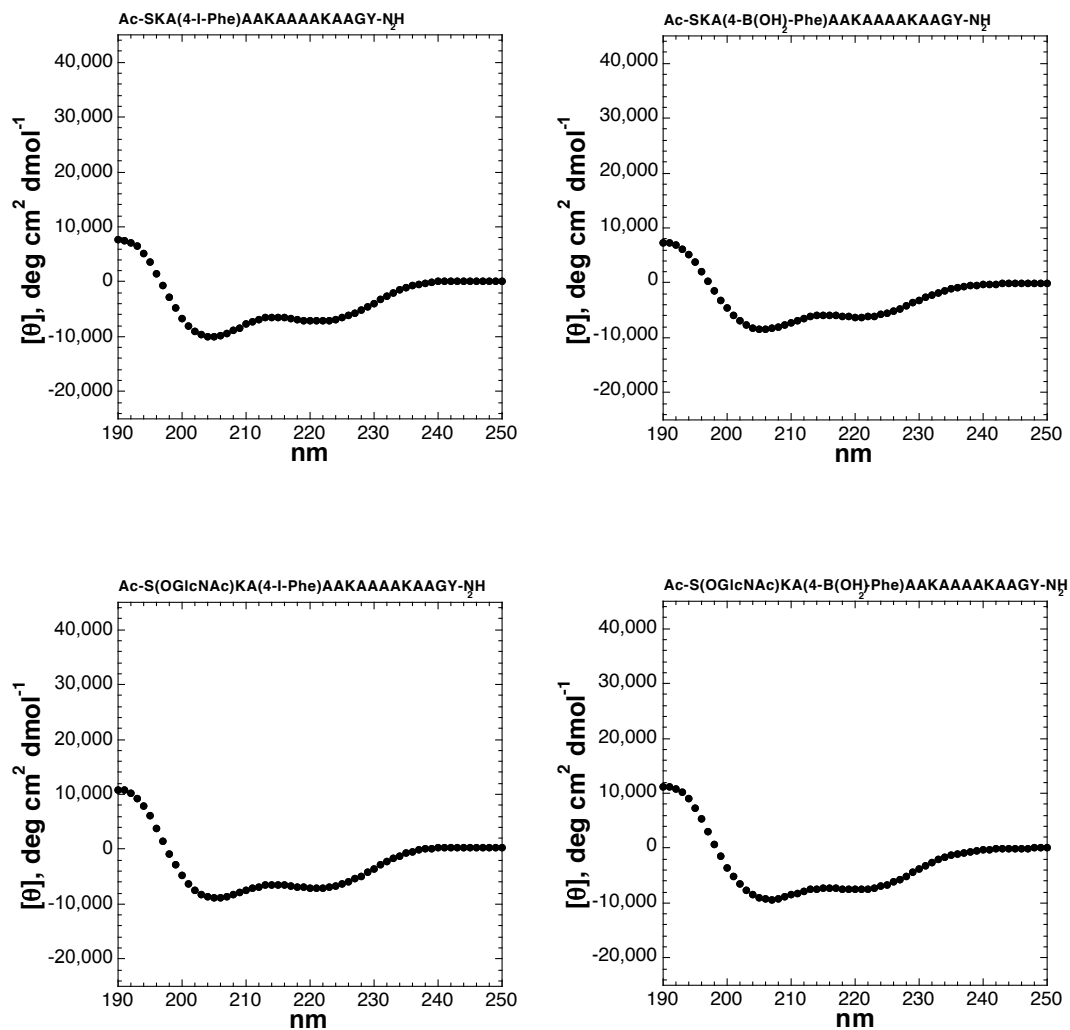


**Figure 2.25:** CD spectra of Ac-SKA(4-I-Phe)AAKAAA KAAGY-NH<sub>2</sub> (top left), Ac-SKA(4-B(OH)<sub>2</sub>-Phe)AAKAAA KAAGY-NH<sub>2</sub> (top right), Ac-S(OGlcNAc)KA(4-I-Phe)AAKAAA KAAGY-NH<sub>2</sub> (bottom left), and Ac-S(OGlcNAc)KA(4-B(OH)<sub>2</sub>-Phe)AAKAAA KAAGY-NH<sub>2</sub> (bottom right); peptides were dissolved in 10 mM phosphate buffer (pH 7.0) containing 25 mM KF at 0.5 °C.

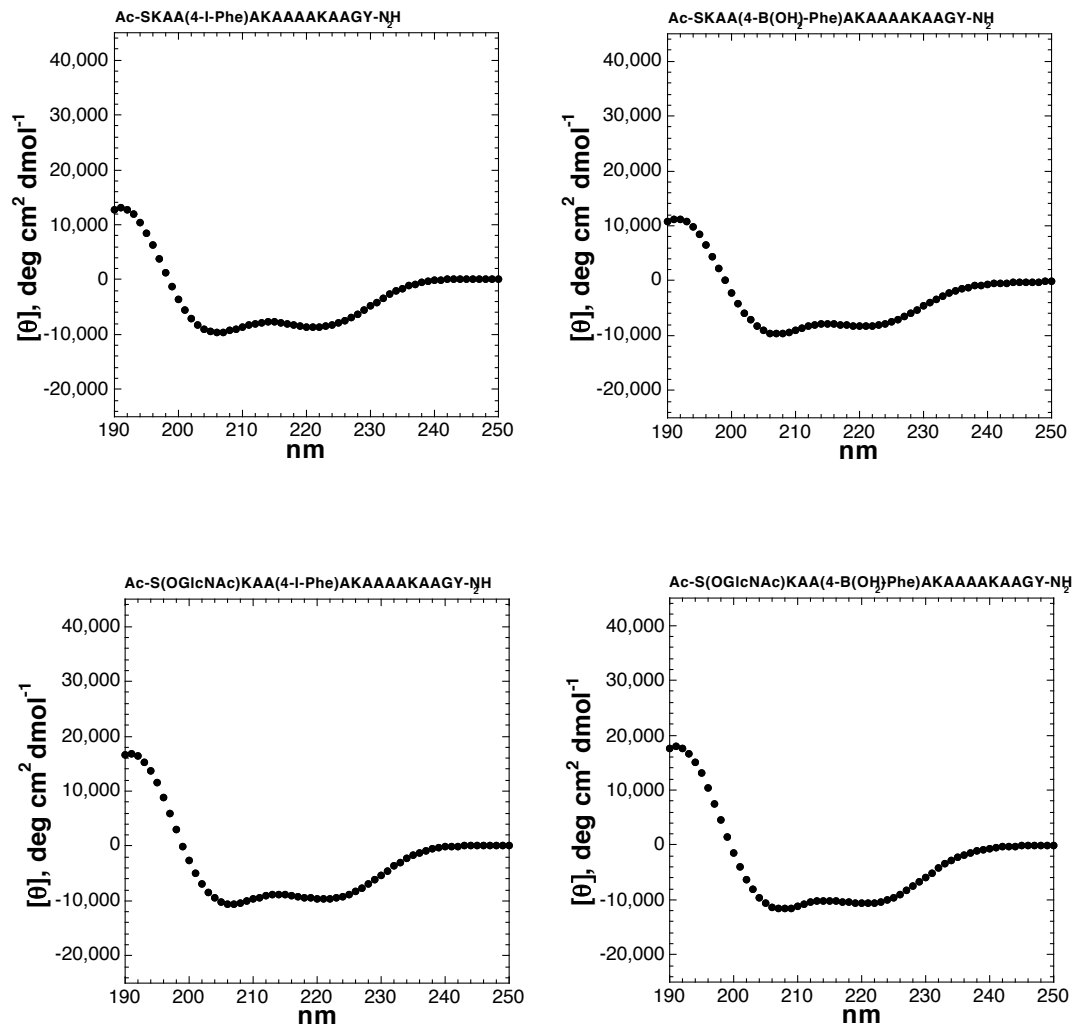


**Figure 2.26:** CD spectra of Ac-SKAA(4-I-Phe)AKAAAAKAAGY-NH<sub>2</sub> (top left), Ac-SKAA(4-B(OH)<sub>2</sub>-Phe)AKAAAAKAAGY-NH<sub>2</sub> (top right), Ac-S(OGlcNAc)KAA(4-I-Phe)AKAAAAKAAGY-NH<sub>2</sub> (bottom left), and Ac-S(OGlcNAc)KAA(4-B(OH)<sub>2</sub>-Phe)AKAAAAKAAGY-NH<sub>2</sub> (bottom right); peptides were dissolved in 10 mM phosphate buffer (pH 7.0) containing 25 mM KF at 0.5 °C.

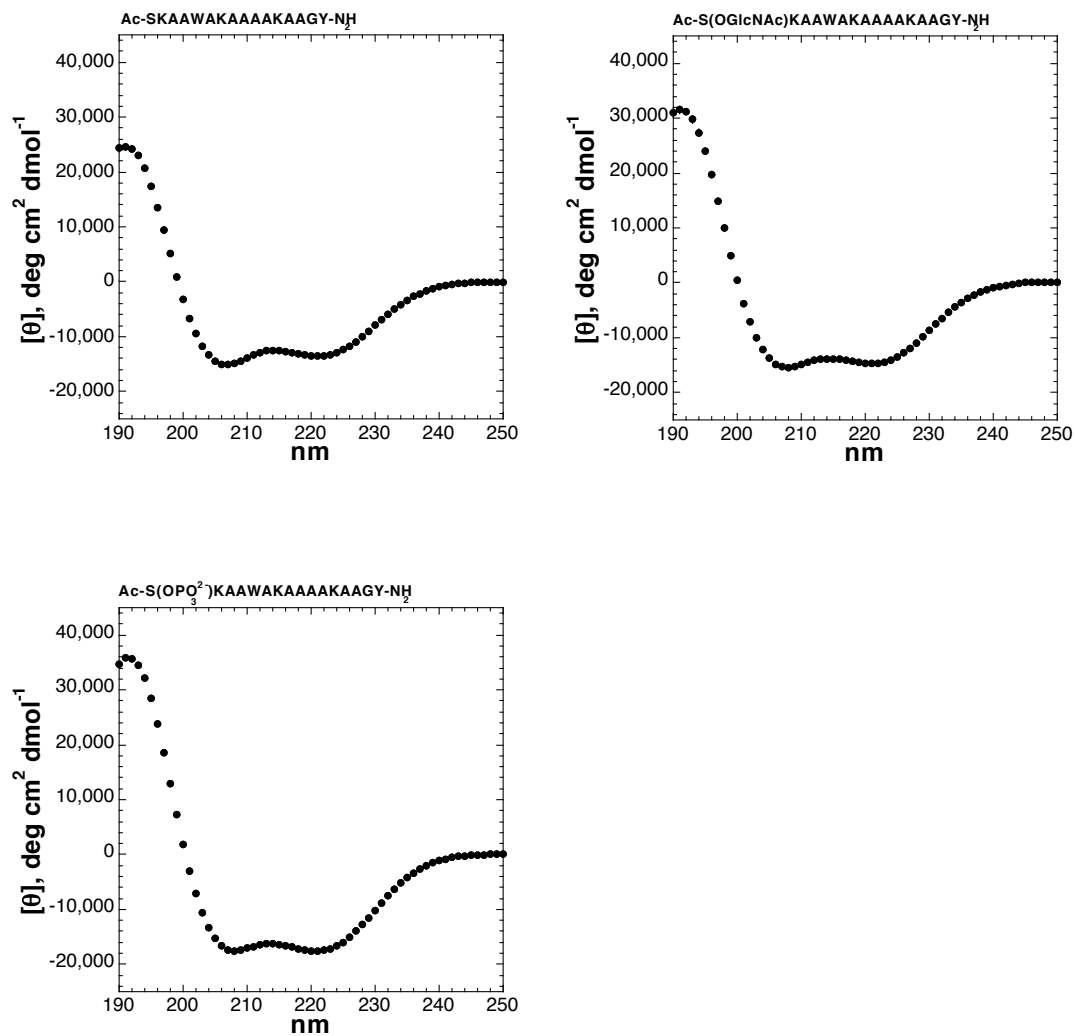


**Figure 2.27:** CD spectra of Ac-SKAAWAKAAAAKAAGY-NH<sub>2</sub> (top left), Ac-S(OGlcNAc)KAAWAKAAAAKAAGY-NH<sub>2</sub> (top right); peptides were dissolved in 10 mM phosphate buffer (pH 7.0) containing 25 mM KF. Bottom left: CD spectra of Ac-S(OPO<sub>3</sub><sup>2-</sup>)KAAWAKAAAAKAAGY-NH<sub>2</sub> in 10 mM phosphate buffer (pH 8.0) containing 25 mM KF at 0.5 °C.

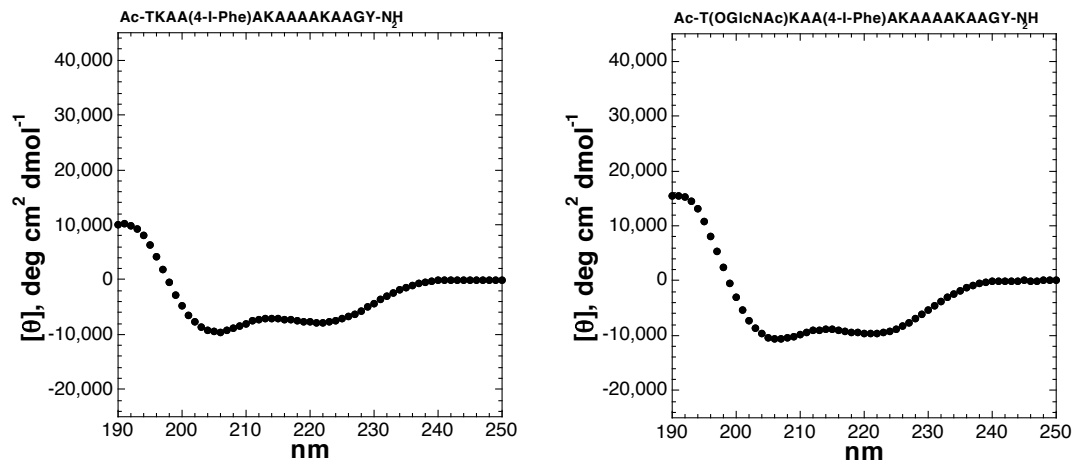


**Figure 2.28:** CD spectra of Ac-TKAA(4-I-Phe)AKAAAAKAAGY-NH<sub>2</sub> (left) and Ac-T(OGlcNAc)KAA(4-I-Phe)AKAAAAKAAGY-NH<sub>2</sub> (right); peptides were dissolved in 10 mM phosphate buffer (pH 7.0) containing 25 mM KF at 0.5 °C.

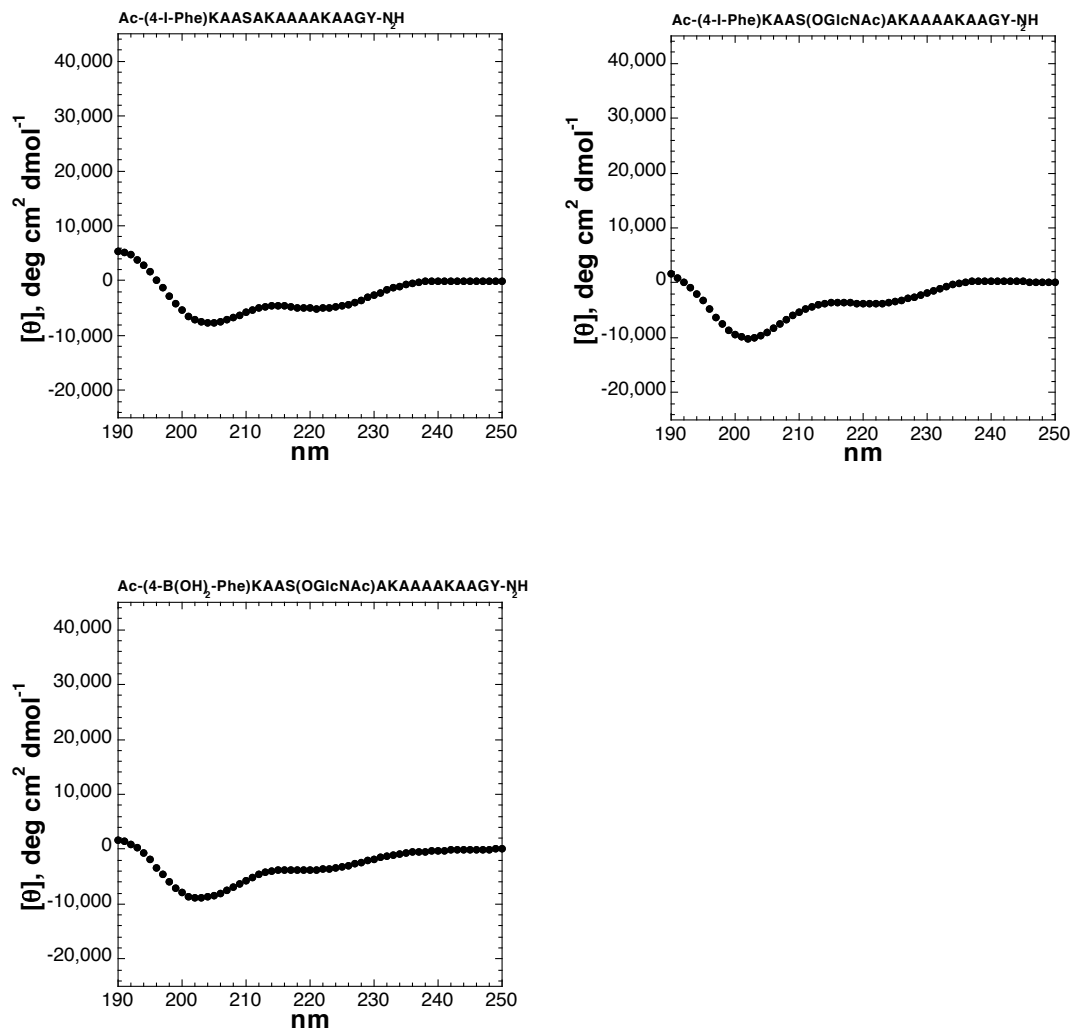


**Figure 2.29:** CD spectra of Ac- (4-I-Phe)KAASAKAAAAKAAGY-NH<sub>2</sub> (top left), Ac- (4-I-Phe)KAAS(OGlcNAc)AKAAAAKAAGY-NH<sub>2</sub> (top right), and Ac- (4-B(OH)<sub>2</sub>-Phe)KAAS(OGlcNAc)AKAAAAKAAGY-NH<sub>2</sub> (bottom left); peptides were dissolved in 10 mM phosphate buffer (pH 7.0) containing 25 mM KF at 0.5 °C.

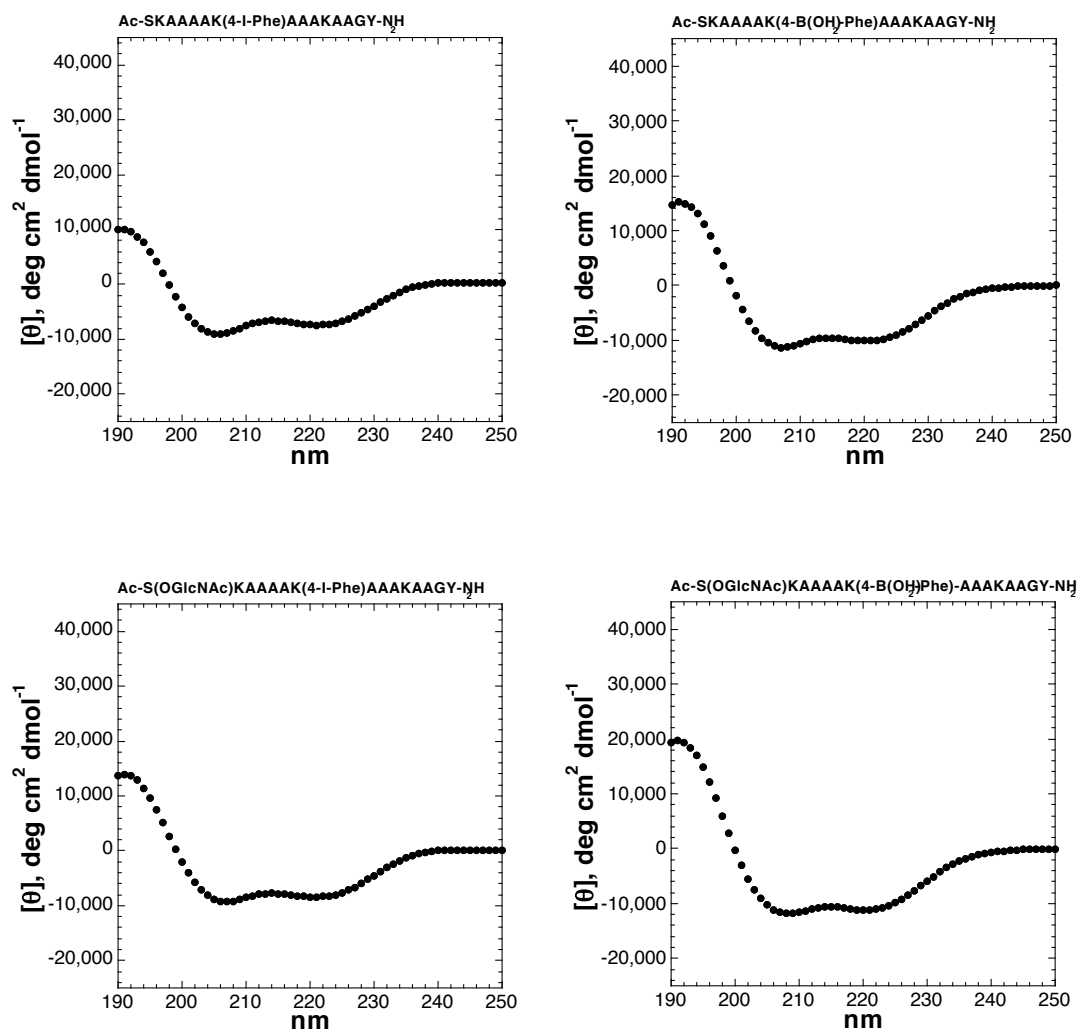


**Figure 2.30:** CD spectra of Ac-SKAAAAK(4-I-Phe)AAAKAAGY-NH<sub>2</sub> (top left), Ac-SKAAAAK(4-B(OH)<sub>2</sub>-Phe)AAAKAAGY-NH<sub>2</sub> (top right), Ac-S(OGlcNAc)KAAAAK(4-I-Phe)AAAKAAGY-NH<sub>2</sub> (bottom left), and Ac-S(OGlcNAc)KAAAAK(4-B(OH)<sub>2</sub>-Phe)AAAKAAGY-NH<sub>2</sub> (bottom right); peptides were dissolved in 10 mM phosphate buffer (pH 7.0) containing 25 mM KF at 0.5 °C.

## CD spectroscopy in the presence and absence of $\beta$ -D-Fructose

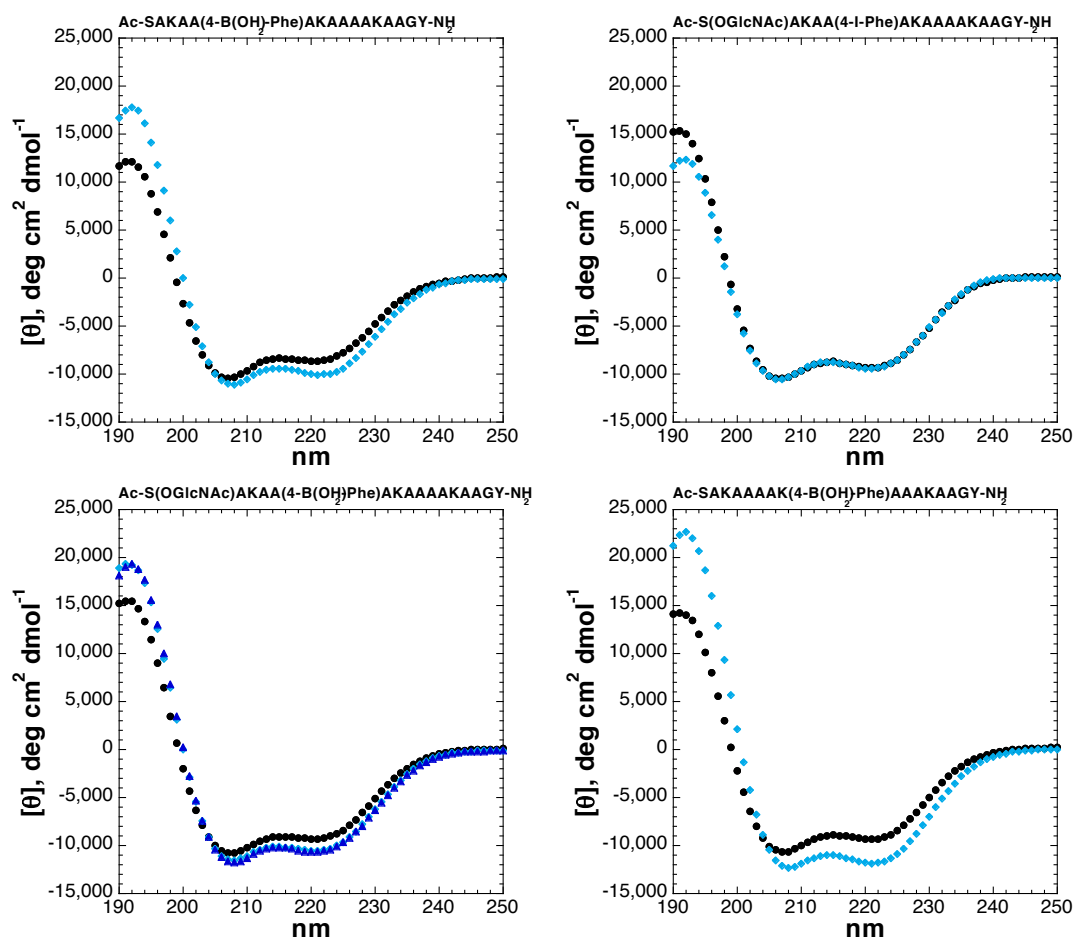


**Figure 2.31:** CD spectra of peptides in the presence and absence of fructose. CD spectra of Ac-SKAA(4-B(OH)<sub>2</sub>)AKAAA KAAGY-NH<sub>2</sub> (top left), Ac-S(OGlcNAc)KAA(4-I-Phe)AKAAA KAAGY-NH<sub>2</sub> (top right), Ac-S(OGlcNAc)KAA(4-B(OH)<sub>2</sub>-Phe)AKAAA KAAGY-NH<sub>2</sub> (bottom left), and Ac-SKAAA AK(4-B(OH)<sub>2</sub>-Phe)AAKAAGY-NH<sub>2</sub> (bottom right); peptides were dissolved in 10 mM phosphate buffer (pH 7.0) containing 25 mM KF at 0.5 °C. Black circles: 0 mM fructose; light blue diamonds: 12.5 mM fructose; dark blue triangles: 25 mM fructose. No differences were observed between 12.5 mM and 25 mM fructose.

## CD spectroscopy in the presence of 25 mM NaCl, 1M NaCl, and 1M KF

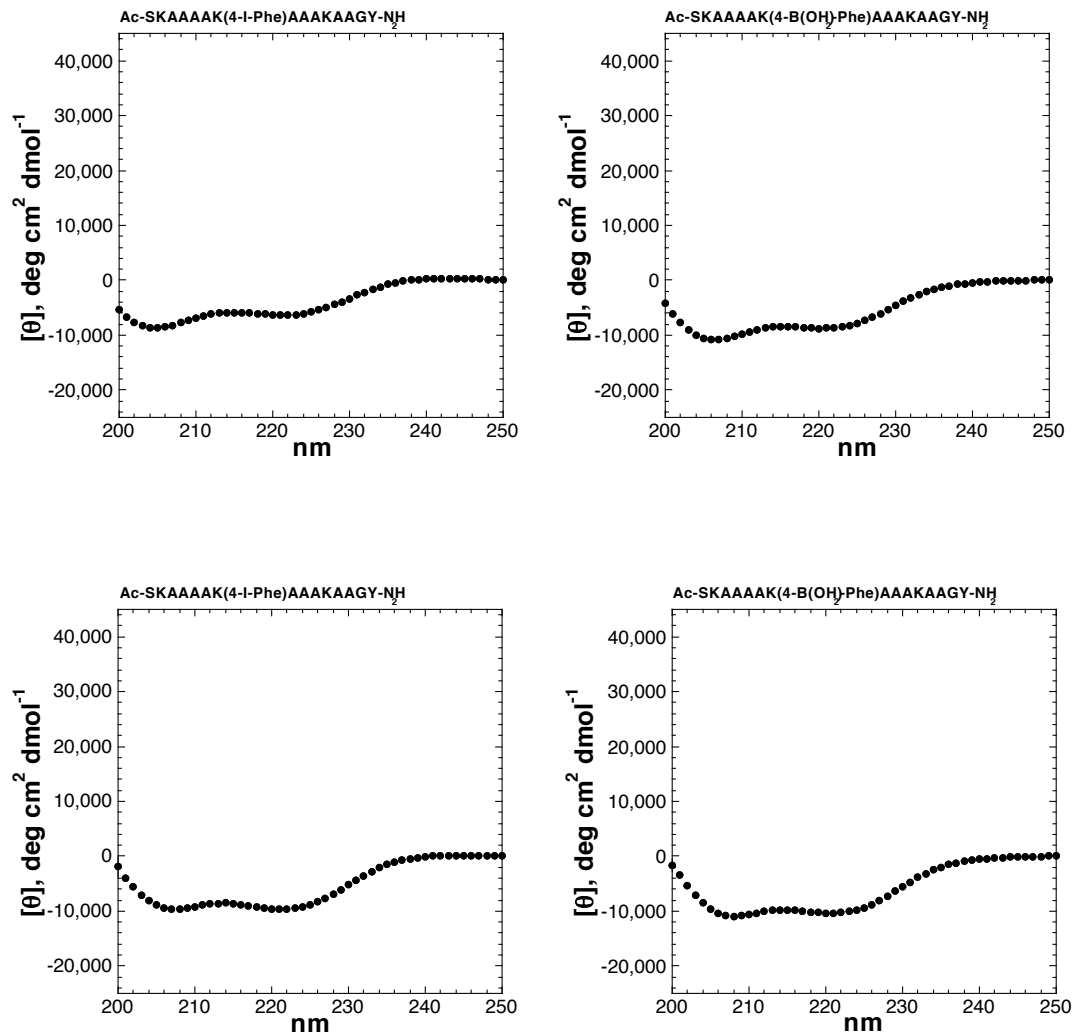


**Figure 2.32:** CD spectra of the peptides in the presence of 25 mM NaCl, 1M NaCl, and 1M KF. Top: CD spectra of Ac-SKAAAAK(4-I-Phe)AAAKAAGY-NH<sub>2</sub> (left) and Ac-SKAAAAK(4-B(OH)<sub>2</sub>-Phe)AAAKAAGY-NH<sub>2</sub> (right) in 10 mM phosphate buffer (pH 7.0) containing 25 mM NaCl at 0.5 °C. Bottom: CD spectra of Ac-SKAAAAK(4-I-Phe)AAAKAAGY-NH<sub>2</sub> (left) and Ac-SKAAAAK(4-B(OH)<sub>2</sub>-Phe)AAAKAAGY-NH<sub>2</sub> (right) in 10 mM phosphate buffer (pH 7.0) containing 1 M NaCl at 0.5 °C.

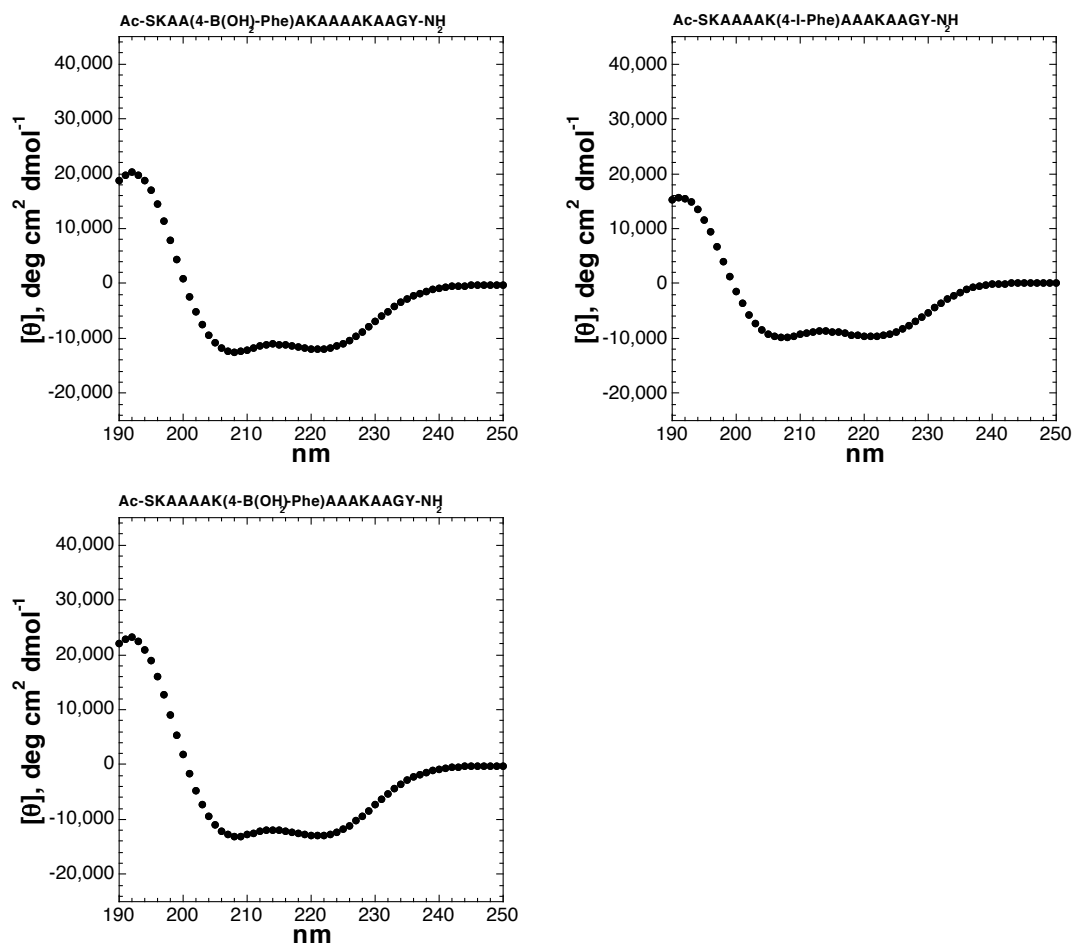


**Figure 2.33:** CD spectra of the peptides in the presence of 25 mM NaCl, 1M NaCl, and 1M KF. CD spectra of Ac-SKAA(4-B(OH)<sub>2</sub>-Phe)AKAAAAKAAGY-NH<sub>2</sub> (top left), Ac-SKAAAAK(4-I-Phe)AAAKAAGY-NH<sub>2</sub> (top right), and Ac-SKAAAAK(4-B(OH)<sub>2</sub>-Phe)AAAKAAGY-NH<sub>2</sub> (bottom left); peptides were dissolved in 10 mM phosphate buffer (pH 7.0) containing 1 M KF at 0.5 °C.

## NMR spectroscopy

NMR spectra of peptides were collected at 278 K or 298 K on a Bruker AVX 600 MHz NMR spectrometer equipped with a triple resonance cryoprobe or a TXI probe. Peptides were dissolved in a solution containing 5 mM phosphate buffer (pH 4.0, 7.2, 8.0, or 8.5) and 25 mM NaCl in 90% H<sub>2</sub>O/10% D<sub>2</sub>O. The pH of each individual sample was recorded and adjusted as necessary using dilute HCl or NaOH. All NMR spectra were internally referenced with 100  $\mu$ M TSP. 1-D NMR spectra were collected with a Watergate pulse sequence and a relaxation delay of 3 s. Coupling constants between the amide and  $\alpha$ -protons ( $^3J_{\alpha N}$ ) were determined directly from the 1-D spectra. Errors in  $^3J_{\alpha N}$  are estimated to be  $\leq 0.2$  Hz. TOCSY NMR spectra were collected with a Watergate TOCSY pulse sequence, sweep widths of 6009 Hz in t<sub>1</sub> (7200 Hz for Trp containing peptides) and t<sub>2</sub>, 400  $\times$  2048 complex data points, 8 scans per t<sub>1</sub> increment, a relaxation delay of 1.5 s, and a TOCSY mixing time of 60 ms.

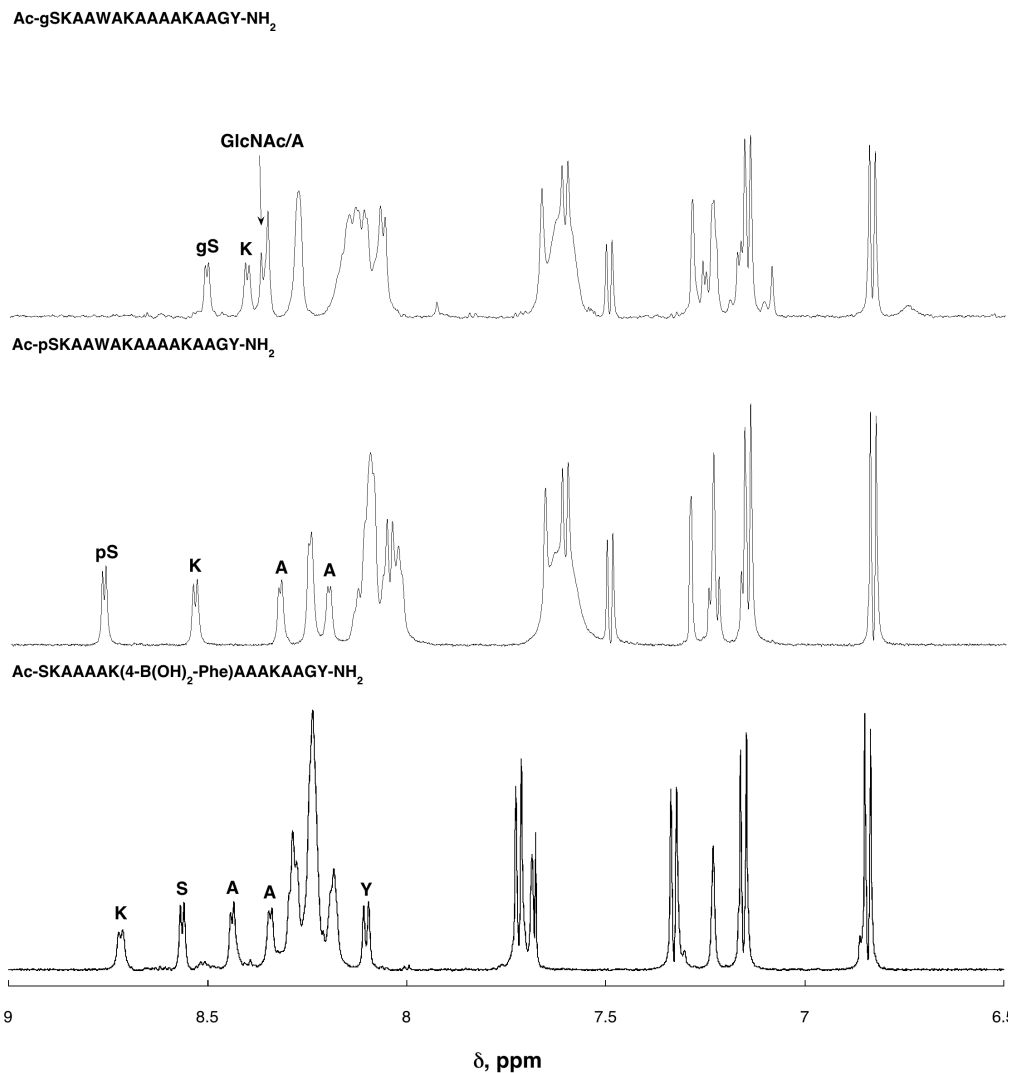


**Figure 2.34:** <sup>1</sup>H NMR spectra (amide region) of peptides with serine modifications: unmodified Ser(free hydroxyl), Ser(OGlcNAc), and Ser(OPO<sub>3</sub><sup>2-</sup>). pS indicates phosphorylated serine residue. gS indicates Ser(OGlcNAc) residue. Peptides were dissolved in 5 mM phosphate buffer (pH 4.0, 7.0, or 7.2) containing 25 mM NaCl in 90% H<sub>2</sub>O/10% D<sub>2</sub>O. Data were collected at 278 K.

Peptide	$\delta$ , H <sup>N</sup>	<sup>3</sup> J <sub>αN</sub>	$\delta$ , H <sub>α</sub>	$\delta$ , H <sub>β</sub>
<b>Ac-Ser(OPO<sub>3</sub><sup>2-</sup>)KAAWAKAAAAKAAGY-NH<sub>2</sub></b>				
Ser	8.77	5.2	4.39	4.16, 4.11
Lys	8.54	5.7	4.23	1.83, 1.81
	8.12	n.d.	4.20	1.85
Trp	8.03	n.d.	4.14	1.82
	8.25	n.d.	4.48	3.4
Ala	8.32	4.5	4.22	1.37
	8.25	n.d.	4.09	1.28
	8.20	4.2	4.16	1.42
	8.10	n.d.	4.19	1.42
	8.10	n.d.	4.25	1.42
	8.09	n.d.	4.19	1.42
	8.06	n.d.	4.09	1.39
	8.03	n.d.	4.14	1.42
Gly	8.02	n.d.	4.16	1.42
Tyr	8.13	n.d.	3.93, 3.84	n.a.
Tyr	8.05	n.d.	4.52	3.10, 2.94
<b>Ac-Ser(GlcNAc)KAAWAKAAAAKAAGY-NH<sub>2</sub></b>				
GlcNAc	8.36	n.d.	n.a.	n.a.
Ser	8.50	5.0	4.32	3.98, 3.80
Lys	8.40	n.d.	4.18	1.77
	8.11	n.d.	4.09	1.82
Trp	8.08	n.d.	4.16	1.80
	8.28	n.d.	4.50	3.38
Ala	8.35	5.3	4.21	1.34
	8.28	n.d.	4.19	1.41
	8.27	n.d.	4.09	1.27
	8.15	n.d.	4.21	1.41
	8.14	n.d.	4.24	1.42
	8.13	n.d.	4.20	1.41
	8.09	n.d.	4.16	1.41
	8.08	n.d.	4.16	1.42
Gly	8.07	n.d.	4.17	1.41
Gly	8.17	n.d.	3.93, 3.84	n.a.
Tyr	8.06	n.d.	4.53	3.09, 2.95

**Table 2.14:** Summary of <sup>1</sup>H NMR data. Data were collected in 5 mM phosphate buffer (pH 4.0 or 7.2) containing 25 mM NaCl. <sup>a</sup> n.d. = not determined due to spectral overlap. <sup>b</sup> n.a. = not applicable.

Peptide	$\delta$ , H <sup>N</sup>	<sup>3</sup> J <sub>αN</sub>	$\delta$ , H $\alpha$	$\delta$ , H $\beta$
Ac- <b>Ser</b> ( <i>GlcNAc</i> )KAAAAK(4-B(OH) <sub>2</sub> -Phe)AAAAKAAGY-NH <sub>2</sub>				
Ser	8.56	5.5	4.36	3.95, 3.88
Lys	8.72	6.1	4.28	1.85, 1.80
	8.23	n.d.	4.13	1.79, 1.68
	8.19	n.d.	4.17	1.76, 1.63
4-B(OH) <sub>2</sub> -Phe	8.28	n.d.	4.57	3.22, 3.13
Ala	8.43	4.8	4.23	1.4
	8.34	4.7	4.19	1.41
	8.29	n.d.	4.24	1.45
	8.28	n.d.	4.16	1.42
	8.23	n.d.	4.22	1.41
	8.23	n.d.	4.22	1.41
	8.23	n.d.	4.22	1.41
	8.23	n.d.	4.12	1.4
	8.18	n.d.	4.17	1.4
Gly	8.25	n.d.	3.92, 3.84	n.a.
Tyr	8.10	7.5	4.52	3.10, 2.94

**Table 2.15:** Summary of <sup>1</sup>H NMR data. Data were collected in 5 mM phosphate buffer (pH 7.0) containing 25 mM NaCl. <sup>a</sup> n.d. = not determined due to spectral overlap. <sup>b</sup> n.a. = not applicable.

## REFERENCES

1. Phillips, D. C. *Proc. Nat. Acad. Sci.* **1967**, *57*, 483-495.
2. Quioco, F. A., *Ann. Rev. Biochem.* **1986**, *55*, 287-315.
3. Vyas, N. K., Vyas, M. N. Quioco, F. A. *Science.* **1988**, *242*, 1290-1295.
4. Sujatha, M. S., Sasidhar, Y. U., Balaji, P. V. *Biochemistry*, **2005**, *44*, 8554-8562.
5. Asensio, J. L., Arda, A., Canada, F. J., Jimenez-Barbero, J. *Acc. Chem. Res.* **2013**, *46*, 946-954.
6. Bernardi, A., Arosio, D., Potenza, D., Sanchez-Medina, I., Mari, S., Canada, F. J., Jimenez-Barbero, J. *Chem. Eur. J.* **2004**, *10*, 4395-4406.
7. Barwell, N. P., Davis, A. P. *J. Org. Chem.* **2011**, *76*, 6548-6557.
8. van Kooyk, Y., Rabinovich, G. A. *Nat. Immunol.* **2009**, *9*, 593-601.
9. Arnaud, J., Audfray, A., Imberty, A. *Chem. Soc. Rev.* **2013**, *42*, 4798-4813.
10. Wulff, G. Krieger, S. Kuhneweg, B., Steigel, A. *J. Am. Chem. Soc.* **1994**, *116*, 409-410.
11. Deng, G., James, T. D., Shinkai, S. *J. Am. Chem. Soc.* **1994**, *116*, 4567-4572.
12. Mikami, M., Shinkai, S. *J. Chem. Soc., Chem. Commun.* **1995**, 153-154.
13. Bosch, L. I., Fyles, T. M., James, T. D. *Tetrahedron*, **2004**, *60*, 11175-11190.
14. Dowlut, M., Hall, D. G. *J. Am. Chem. Soc.* **2006**, *128*, 4226-4227.
15. Fernando-Alonso, M. C., Canada, F. J., Jimenez-Barbero, J., Cuevas, G. J. *Am. Chem. Soc.* **2005**, *127*, 7379-7386.

16. Vandenbussche, S. Diaz, D., Fernandez-Alonso, M. C., Pan, W., Vincent, S. P., Cuevas, G., Canada, F. J., Jimenez-Barbero, J., Bartik, K. *Chem. Eur. J.* **2008**, *14*, 7570-7578.
17. Terraneo, G., Potenza, D., Canales, A., Jimenez-Barbero, J., Baldrige, K. K., Bernardi, A. *J. Am. Chem. Soc.* **2007**, *129*, 2890-2900.
18. Morales, J. C., Reina, J. J., Diaz, I., Avino, A., Nieto, P. M., Eritja, R. *Chem. Eur. J.* **2008**, *14*, 7828-7835.
19. Santana, A. G., Jimenez-Moreno, E., Gomez, A. M., Cozana, F., Gonzalez, C., Jimenez-Oses, G., Jimenez-Barbero, J., Asensio, J. L. *J. Am. Chem. Soc.* **2013**, *135*, 3347-3350.
20. Ke, C., Destecroix, H., Crump, M. P., Davis, A. P. *Nat. Chem.* **2012**, *4*, 718-723.
21. Culyba, E. K., Price, J. L., Hanson, S. R., Dhar, A., Wong, C.-H., Gruebele, M., Power, E. T., Kelly, J. W. *Science*. **2011**, *331*, 571-575.
22. Price, J. L., Powers, D. L., Powers, E. T., Kelly, J. W. *Proc. Natl. Acad. Sci.* **2011**, *108*, 14127-14132.
23. Chen, W., Enck, S., Price, J. L., Powers, D. L., Powers, E. T., Wong, C.-H., Dyson, H. J., Kelly, J. W. *J. Am. Chem. Soc.* **2013**, *135*, 9877-9884.
24. Laughrey, Z. R., Kiehna, S. E., Riemen, A. J., Waters, M. L. *J. Am. Chem. Soc.* **2008**, *130*, 14625-14633.
25. James, T. D., Sandanayake, K. R. A. S., Shinkai, S. *Angew. Chem. Int. Ed. Engl.* **1996**, *35*, 1910-1922.
26. Sugasaki, A., Sugiyasu, K., Ikeda, M., Takeuchi, M., Shinkai, S. *J. Am. Chem. Soc.* **2001**, *123*, 10239-10244.
27. Asher, S. A., Alexeev, V. L., Goponenko, A. V., Sharma, A. C., Lednev, I. K., Wilcox, C. S., Finegold, D. N. *J. Am. Chem. Soc.* **2003**, *125*, 3322-3329.
28. Zhang, T., Anslyn, E. V. *Org. Lett.* **2006**, *8*, 1649-1652.
29. Kashiwada, A., Tsuboi, M., Matsuda, K. *Chem. Commun.* **2009**, 695-697.
30. Kashiwada, A., Yamane, I., Tsuboi, M., Ando, S., Matsuda, K. *Langmuir*. **2011**, *28*, 2299-2305.

31. Edwards, N. Y., Sager, T. W., McDevitt, J. T., Anslyn, E. V. *J. Am. Chem. Soc.* **2007**, *129*, 13575-13583.
32. Pal, A., Berube, M., Hall, D. G. *Angew. Chem. Int. Ed.* **2010**, *49*, 1492-1495.
33. Jay, J. I., Lai, B. E., Myszka, D. G., Mahalingam, A., Langheinrich, K., Katz, D. F., Kiser, P. F. *Mol. Pharm.* **2010**, *7*, 116-129.
34. Edwards, N. Y., Sager, T. W., McDevitt, J. T., Anslyn, E. V. *J. Am. Chem. Soc.* **2007**, *129*, 13575-13583.
35. Chorev, M., Roubini, E., McKee, R. L., Gibbons, S. W., Goldman, M. E., Caulfield, M. P., Rosenblatt, M. *Biochemistry*, **1991**, *30*, 5968-5974.
36. Blackwell, H. E., Grubbs, R. H. *Angew. Chem. Int. Ed.* **1998**, *37*, 3281-3284.
37. Schafmeister, C. E. Po, J., Verdine, G. L. *J. Am. Chem. Soc.* **2000**, *122*, 5891-5892.
38. Sia, S. K., Carr, P. A., Cochran, A. G., Malashkevich, V. N., Kim, P. S. *Proc. Natl. Acad. Sci.* **2002**, *99*, 14664-14669.
39. Errington, N., Doig, A. J. *Biochemistry*, **2005**, *44*, 7553-7558.
40. Leduc, A.-M., Trent, J. O., Wittliff, J. L., Bramlett, K. S., Briggs, S. L., Chirgadze, N. Y., Wang, Y., Burris, T. P., Spatola, A. F. *Proc. Natl. Acad. Sci.* **2003**, *100*, 11273-11278.
41. Harrison, R. S., Shepherd, N. E., Hoang, H. N., Ruiz-Gomez, G., Hill, T. A., Driver, R. W., Desai, V. S., Young, P. R., Abbenante, G., Fairlie, D. P. *Proc. Natl. Acad. Sci.* **2010**, *107*, 11686-11691.
42. Azzarito, V., Long, K., Murphy, N. S., Wilson, A. J. *Nat. Chem.* **2013**, *5*, 161-173.
43. Butterfield, S. M., Patel, P. R., Waters, M. L. *J. Am. Chem. Soc.* **2002**, *124*, 9751-9755.
44. Tsou, L. K., Tatko, C. D., Waters, M. L. *J. Am. Chem. Soc.* **2002**, *124*, 14917-14921.
45. Arsequell, G., Krippner, L., Dwek, R. A., Wong, S. Y. C. *J. Chem. Soc., Chem. Commun.* **1994**, 2383-2384.

46. Afonso, A., Roses, C., Planas, M., Feliu, L. *Eur. J. Org. Chem.* **2010**, 1461-1468.
47. Riemen, A. J., Waters, M. L. *J. Am. Chem. Soc.* **2009**, *131*, 14081-14087.
48. Riemen, A. J., Waters, M. L. *J. Am. Chem. Soc.* **2010**, *132*, 9007-9013.
49. Chakrabartty, A., Kortemme, T., Baldwin, R. L. *Protein. Sci.* **1994**, *3*, 843-852.
50. Engel, D. E., DeGrado, W. F. *J. Mol. Biol.* **2004**, *337*, 1195-1205.
51. Shi, Z., Olson, C. A., Kallenbach, N. R. *J. Am. Chem. Soc.* **2002**, *124*, 3284-3291.
52. Pople, J. A. *J. Chem. Phys.* **1956**, *24*, 1111.
53. Norrild, J. C., Eggert, H. *J. Chem. Soc., Perkin Trans 2.* **1996**, 2583-2588.
54. Springsteen, G., Wang, B. *Tetrahedron*, **2002**, *58*, 5291-5300.
55. Simanek, E. E., Huang, D.-H., Pasternack, L., Machajewski, T. D., Seitz, O., Millar, D. S., Dyson, H. J., and Wong, C.-H. *J. Am. Chem. Soc.* **1998**, *120*, 11567-11575.
56. Liang, F.-C., Chen, R. P.-Y., Lin, C.-C., Huang, K.-T., and Chan, S. I. *Biochem. Biophys. Res. Commun.* **2006**, *342*, 482-488.
57. Chen, Y.-X., Du, J.-T., Zhou, L.-X., Liu, X.-H., Zhao, Y.-F., Nakanishi, H., and Li, Y.-M. *Chem. Biol.* **2006**, *13*, 937-944.
58. Brister, M. A., Pandey, A. K., Bielska, A. A., and Zondlo, N. J. *J. Am. Chem. Soc.* **2014**, *136*, 3803-3816.
59. Stapley, B. J., Doig, A. J. *J. Mol. Biol.* **1997**, *272*, 456-464.
60. Penel, S., Hughes, E., Doig, A. J. *J. Mol. Biol.* **1999**, *287*, 127-143.
61. Ramelot, T. A., Nicholson, L. K. *J. Mol. Biol.* **2001**, *307*, 871-884.
62. Du, J.-T., Li, Y.-M., Wei, W., Wu, G.-S., Zhao, Y.-F., Kanazawa, K., Nemoto, T., Nakanishi, H. *J. Am. Chem. Soc.* **2005**, *127*, 16350-16351.
63. Lee, K.-K., Kim, E., Joo, C., Song, J., Han, H., Cho, M. *J. Phys. Chem. B.* **2008**, *112*, 16782-16787.

64. Kim, S.-Y., Jung, Y., Hwang, G.-S., Han, H., Cho, M. *Proteins*, **2011**, *79*, 3155-3165.
65. Gallivan, J. P., Dougherty, D. A. *Proc. Natl. Acad. Sci. USA*. **1999**, *96*, 9459-9464.
66. Dougherty, D. A. *Science*, **1996**, *271*, 163-168.
67. Ting, R., Harwig, C. W., Lo, J., Li, Y., Adam, M. J., Ruth, T. J., Perrin, D. M. *J. Org. Chem.* **2008**, *73*, 4662-4670.
68. Yuchi, Akio., Sakurai, J., Tatebe, A., Hattori, H., Wada, H. *Anal. Chim. Acta*. **1999**, *387*, 189-195.
69. Ting, R., Harwig, C., Keller, U., McCormick, S., Austin, P., Overall, C. M., Adam, M. J., Ruth, T. J., Perrin, D. M. *J. Am. Chem. Soc.* **2008**, *130*, 12045-12055.
70. Cooper, C. R., Spencer, N., James, T. D. *Chem. Commun.* **1998**, 1365-1366.
71. James, T. D., Sandanayake, K. R. A. S., Shinkai, S. *Angew. Chem. Int. Ed. Engl.* **1996**, *35*, 1910-1922.
72. Dowlut, M., Hall, D. G. *J. Am. Chem. Soc.* **2006**, *128*, 4226-4227.
73. Edwards, N. Y., Sager, T. W., McDevitt, J. T., Anslyn, E. V. *J. Am. Chem. Soc.* **2007**, *129*, 13575-13583.
74. Cal, P. M. S. D., Vicente, J. B., Pires, E., Coelho, A. V., Veiros, L. F., Cordeiro, C., Gois, M. P. *J. Am. Chem. Soc.* **2012**, *134*, 10299-10305.
75. Arsequell, G., Krippner, L., Dwek, R. A., Wong, S. Y. C., *J. Chem. Soc., Chem. Commun.* **1994**, 2383-2384.
76. Vaddypally, S., Xu, C., Zhao, S., Fan, Y., Schafmeister, C. E., Zdilla, M. J. *Inorg. Chem.* **2013**, *52*, 6457-6463.
77. Nataro, C., Fosbenner, S. *J. Chem. Educ.* **2009**, *86*, 1412-1415.
78. Afonso, A., Roses, C., Planas, M., Feliu, L. *Eur. J. Org. Chem.* **2010**, 1461-1468.
79. Melicher, M. S., Chu, J., Walker, A. S., Miller, S. J., Baxter, R. H. G., Schepartz, A. *Org. Lett.* **2013**, *15*, 5048-5051.

## Chapter 3

### STRUCTURAL EFFECTS OF PHOSPHORYLATION AND R406W ON *tau*<sub>395</sub>

411

#### Introduction

Alzheimer's disease (AD) is a common form of dementia, with over 5 million cases of AD in the United States.<sup>1</sup> These numbers are expected to drastically increase as the baby-boomer population continues to age. Thus, determining the causes of AD onset continues to be a major goal. Development of AD has been associated with the formation of both extracellular neural plaques and intracellular neurofibrillary tangles (NFTs) in the brain, as described originally by Alzheimer in 1906. Extracellular plaques observed in AD brains, composed of  $\beta$ -amyloid fibers formed by A $\beta$  peptide aggregation, are associated with neuritic degradation and signaling defects.<sup>2-6</sup> Intracellular NFTs are composed of mostly paired helical filaments (PHFs) which aggregate and lead to neurodegeneration.<sup>7</sup> The major protein components of PHFs are hyperphosphorylated variants of the microtubule-associated protein (MAP) *tau*.<sup>8-11</sup> Tau in its native state is natively disordered and highly soluble.<sup>12-17</sup> Structurally, *tau* is subdivided into several domains; a N-terminal domain, central proline rich domain (PRD) followed by a tubulin binding domain (TBD) consisting of sequence repeats, and a carboxyl-terminal region.<sup>18-21</sup> Mandelkow has suggested, based on detailed FRET experiments, a global hairpin or "paper clip" model for *tau* stabilization in which the C-terminal tail is layered between the TBD and N-terminus.<sup>22</sup> Interestingly, protease-resistant segments of *tau* repeats have been discovered within AD brains.<sup>23, 24</sup>

Furthermore, others have observed that the repeat domain of *tau* more effectively aggregates in vitro than full-length *tau*.<sup>13, 25</sup> These findings suggest that apoptotic caspase cleavage of *tau* at the N-terminal and/or C-terminal ends may lead to aggregation in vivo.<sup>22</sup> Furthermore, others have demonstrated that truncation of *tau* on the C-terminus leads to an increase in polymerization rate when in the presence of polyanions.<sup>26-30</sup> Others have suggested that the C-terminal portion of *tau* interacts with the repeat domain, functioning to prevent polymerization.<sup>31, 32</sup> Current models suggest that phosphorylation of Ser<sub>396/404</sub> on the C-terminal tail of *tau* causes disassociation of the C-terminus with the repeat region, leading to aggregation through *tau-tau* interactions.<sup>33, 34</sup> Consistent with this model, Ser<sub>396/404</sub> are known to be phosphorylated within AD brains.<sup>35-38</sup> Both Ser<sub>396</sub> and Ser<sub>404</sub> precede a proline residue, requiring proline-directed kinases for phosphorylation. Two main kinases responsible for phosphorylation of serine residues are cyclin dependent protein kinase-5 (cdk5) and glycogen synthase kinase-3 $\beta$  (GSK-3 $\beta$ ).<sup>39-41</sup> Importantly, phosphorylation of Ser<sub>404</sub> by cdk5 promotes subsequent phosphorylation of both Ser<sub>396</sub> and Ser<sub>400</sub> by GSK-3 $\beta$ .<sup>37, 42</sup> In addition to the role of hyperphosphorylation of *tau* in the onset of AD, within animal models, R406W mutation of *tau* leads to filament formation and associative memory deficit identical to that found within AD.<sup>43-45</sup> Tau mutation R406W has also been associated with Parkinson's disease and frontotemporal dementia within humans. Given that phosphorylation of Ser<sub>404</sub> is observed in patients with AD, and R406W mutation is observed to lead to increased rates of AD formation within animal models, we sought to elucidate the mechanism by which both events structurally modify *tau*.

From a structural biologist's perspective, it is interesting that R/W<sub>406</sub> follows Pro<sub>405</sub>, due to proline's unique ability to facilitate *cis* amide bonds in Pro-aromatic sequence motifs. Amino acids within peptides and proteins are linked through amide

bonds *via* the carboxylate carbon and the amine nitrogen. The partial double bond character of the amide bond restricts rotation and leads to two energetically preferred conformations (*trans* and *cis*) with a rotational barrier of approximately 20 kcal/mol.<sup>46</sup> Within the context of all amino-acids within proteins, the *trans* amide bond has been demonstrated to be the most energetically favorable, with *cis* bonds composing 0.5-1.5% of all bonds.<sup>47, 48</sup> Proline exhibits a higher propensity for *cis* amide bonds, with Xxx-Pro amide bonds exhibiting 5-6% *cis* bonds, but those amides without proline containing approximately 0.05% *cis* bonds.<sup>46, 49-52</sup> In model peptides and proteins found within the PDB, aromatic-proline and proline-aromatic sequences exhibit the highest propensity for *cis* amide bonds, suggestive of *cis* bond stabilization due to the presence of the aromatic residue (Figure 3.1).<sup>46, 49, 52-62</sup> While studying the structure of bovine pancreatic trypsin inhibitor (BPTI), Creighton observed that residues 1-15 of BTI exhibited 20% *cis* amide bonds when tyrosine was present and 5% in the absence of tyrosine following Pro<sub>8</sub>-Pro<sub>9</sub>. He suggested the increase in *cis* population was due to a stabilizing interaction between the aromatic side-chain and the side-chain of proline.<sup>53</sup> Studying the structure of type VI  $\beta$ -turns, Dyson and Wright found that SYPYDV and SYPFDV (charged termini) sequences revealed NOE connectivities between the proline and aromatic ring protons, suggestive of hydrophobic stacking.<sup>54, 55</sup> Raleigh later demonstrated that these interactions are more general and were observed to stabilize the *cis* conformation in Ac-GXPG-NH<sub>2</sub> systems containing only one aromatic residue preceding proline.<sup>58</sup> These interactions were shown to exist in Ac-AXPAL-NH<sub>2</sub> (aromatic-*cis*-Pro) and Ac-PPF-NH<sub>2</sub> (*cis*-Pro-aromatic) models, and formed pseudo-turns within proteins, demonstrating that these interactions persisted outside of sequences prone to  $\beta$ -turns and peptides with neutral termini.<sup>52, 57, 63</sup> Interestingly, the observed aromatic-proline interaction in GXPG and Ac-AXPAL-

NH<sub>2</sub> peptides were found to have an aryl electronic component, with greater *cis* population observed for Aromatic-Pro sequences containing more electron-rich aromatics. These observations are not fully rationalized by hydrophobic interactions proposed by Dyson and Wright.<sup>57, 58</sup> They are, however, consistent with a CH/ $\pi$  interaction between the aromatic face and the proline side chain (H $\alpha$ , H $\beta$ , and/or H $\delta$ ) (Figure 3.1).<sup>62, 64-71</sup> Within our own lab, the Ac-TXPN-NH<sub>2</sub> model system has been utilized extensively to demonstrate control of *cis/trans* isomerism by electronic control of both the aromatic and/or proline residues via natural/unnatural amino acids and solid-phase chemical modifications.<sup>62, 71-77</sup>

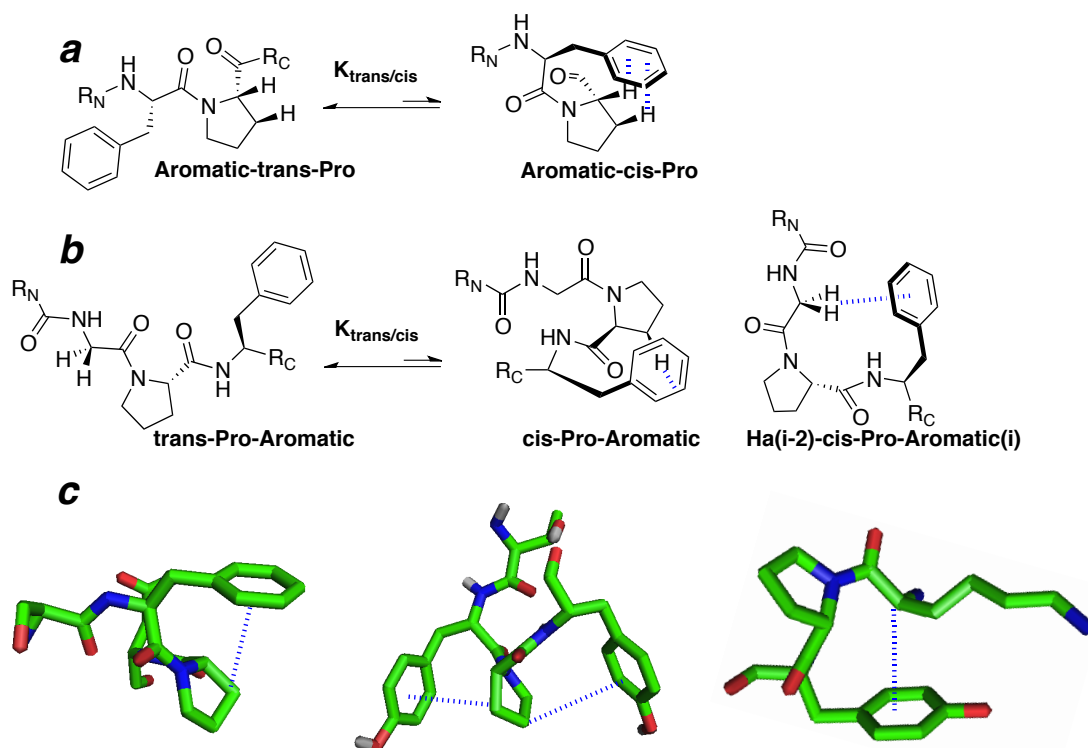


**Figure 3.1:** Local aromatic-proline interactions. (a) cis-trans isomerism of an aromatic-Pro amide bond. The cis conformation is stabilized by CH/π interactions between H $\alpha$  and H $\beta$  of proline and the aromatic face (blue dashed lines). (b) cis-trans isomerism of a Pro-aromatic amide bond. The cis conformation is stabilized by CH/π interactions between either the side chain of proline and the aromatic face (left, center) or H $\alpha$  of the *i*-2 residue and the aromatic (*i*) face (blue dashed lines). (c) (left) An aromatic-cis-Pro interaction in the sequence SFPN (PDB 1H4I). (c) (center) An Aromatic-cis-Pro and cis-Pro-Aromatic interaction in the sequence TYPY (PDB 1ADE). (c) (right) A Ha(*i*-2)-cis-Pro-aromatic(*i*) interaction in the sequence KPY (PDB 2DUR). The cis conformation is stabilized by CH/π interactions between the side chain of proline and the aromatic face (left, center) or H $\alpha$  of the *i*-2 residue and the aromatic (*i*) face (right) (blue dashed lines).

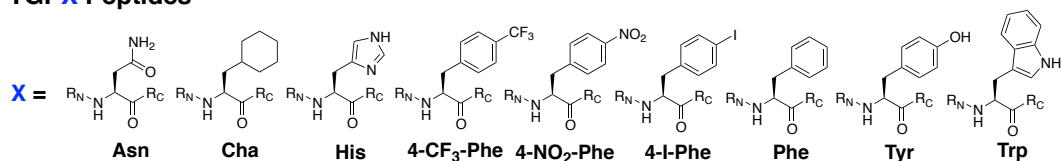
Stabilizing CH/ $\pi$  interactions observed in Xxx-cis-Pro-aromatic sequences also occur through interactions between the aromatic (*i*) face and the alpha protons of the *i*-2 residue (Figure X).<sup>59, 62, 63, 78</sup> Recently, Basu confirmed in tripeptides (Ac-PPX-NH<sub>2</sub> and Ac-XPY-NH<sub>2</sub>) the presence of a *cis* stabilizing H $\alpha$ (*i*-2)-cis-Pro-aromatic(*i*) CH/ $\pi$  interaction.<sup>79, 80</sup> Furthermore, it was demonstrated on Ac-XPY-NH<sub>2</sub> peptides that all canonical amino acids (except for asparagine) exhibited increased populations of *cis* amide bonds relative to Ac-XPA-NH<sub>2</sub> peptides. Interestingly, R406W mutation leads to the sequence SPW within *tau*, analogous to the Ac-PPW-NH<sub>2</sub> peptides found to have a H $\alpha$ (*i*-2)-cis-Pro-aromatic(*i*) CH/ $\pi$  interaction, suggesting R406W may play a role in *cis*-*trans* isomerism within *tau*. Protein phosphatase 2 (PP2A), the major Pro-directed phosphatase, is responsible for dephosphorylating exclusively *trans* pSer/pThr-Pro motifs.<sup>81, 82</sup> PP2A is assisted by Pin1, a peptidyl-prolyl isomerase, responsible for catalyzing the *cis*-*trans* isomerization of the peptide bond between pSer/pThr-Pro amide bonds. Interestingly, Pin1 is found to be down regulated and/or inhibited by oxidation in patients with AD, leading higher *cis* bond populations.<sup>83-85</sup>

In light of these findings, we hypothesized that both phosphorylation of Ser<sub>404</sub> and increased *cis* amide bond via R406W *cis*-Pro-aromatic interactions may play a critical role in *cis/trans* isomerism within *tau* leading to higher *cis* populations. To identify the possibility and strength of H $\alpha$ (*i*-2)-cis-Pro-aromatic(*i*) CH/ $\pi$  interactions in an analogous system to *tau*<sub>403-406</sub>, Ac-TGPX-NH<sub>2</sub> peptides were examined where X = natural and non-natural aromatic amino acids containing both electron-donating and electron-withdrawing groups at position 4 of the aromatic ring. Tau-derived peptides Ac-TSPR-NH<sub>2</sub> and Ac-TSPW-NH<sub>2</sub> were examined to identify the possibility and strength of H $\alpha$ (*i*-2)-cis-Pro-aromatic(*i*) CH/ $\pi$  interactions within *tau*. Both *tau*<sub>403-406</sub> analogues were further examined to determine the effects of serine and/or threonine

phosphorylation. To our knowledge, the effects of phosphorylation on aromatic-proline interactions have not been established.

## Results

To improve our understanding of proline-aromatic sequences, a series of peptides was synthesized of the sequence Ac-TGPX-NH<sub>2</sub>, where X= electron-rich, electron-neutral, or electron-deficient aromatic residues (Figure 3.2). As a control, peptides were also synthesized containing Asn or cyclohexylalanine (Cha) at residue 4. Threonine was chosen to maintain homology between *tau*<sub>403-406</sub> sequences (TSPR/W) and our TGPX model. Given that a proposed interaction involves the alpha protons at residue 2 and the aromatic ring of residue 4, glycine was chosen at residue 2 due to greater CH/ $\pi$  interactions of glycine H $\alpha$  over other canonical amino acids (Glycine lacks of conformational and steric restrictions observed with other amino acids (entropic penalties associated with  $\chi_1$  restriction)).<sup>62, 78</sup> To elucidate the local structural effects of phosphorylation and R406W on *tau*<sub>403-406</sub>, a series of tetrapeptides was synthesized of the sequence TSPR/W. Serine and threonine amino acids were incorporated using trityl/Fmoc-protected amino acids. Phosphorylation was conducted on solid-phase by selective trityl-deprotection, phosphitylation, oxidation, and cleavage/deprotection yielding a site selective phosphorylated residue. To confirm the observed results in *tau*<sub>403-406</sub> are consistent with larger *tau* segments, *tau*<sub>395-411</sub> peptides were synthesized containing Arg<sub>406</sub> and Ser/pSer<sub>404</sub> or Trp<sub>406</sub> and Ser/pSer<sub>404</sub>. All peptides were analyzed by NMR at 298 K.

**a****TGPX Peptides****b*****tau* Peptides**

<i>tau</i> <sub>403-406</sub>	TSPR    TpSPR    pTSPR    pTpSPR
<i>tau</i> <sub>403-406</sub> R <sub>406</sub> W	TSPW    TpSPW    pTSPW    pTpSPW
<i>tau</i> <sub>395-411</sub>	K <sub>395</sub> SPVVS <sup>G</sup> DTSP <sup>R</sup> HLSNV <sub>411</sub>
<i>tau</i> <sub>395-411</sub> pS <sub>404</sub>	K <sub>395</sub> SPVVS <sup>G</sup> DTpSP <sup>R</sup> HLSNV <sub>411</sub>
<i>tau</i> <sub>395-411</sub> R <sub>406</sub> W	K <sub>395</sub> SPVVS <sup>G</sup> DTSP <sup>W</sup> HLSNV <sub>411</sub>
<i>tau</i> <sub>395-411</sub> R <sub>406</sub> W pS <sub>404</sub>	K <sub>395</sub> SPVVS <sup>G</sup> DTpSP <sup>W</sup> HLSNV <sub>411</sub>

**Figure 3.2:** Peptide sequences examined in this study. **(a)** Tetra-peptides of the sequence Ac-TGPX-NH<sub>2</sub> were examined with residue 4 containing amino acids with aromatic side-chains containing electron-rich, electron-neutral, or electron-deficient aromatic amino acids. Peptides were also synthesized containing asparagine or cyclohexylalanine (Cha) as controls. **(b)** Sequences of *tau*-derived peptides examined in this study. Tetra-peptides of *tau*<sub>403-406</sub> were initially studied containing either Arg<sub>406</sub> or Trp<sub>406</sub> with unmodified Thr and Ser, phosphorylated Ser or Thr, and phosphorylated Ser and Thr residues. Larger *tau*<sub>395-411</sub> peptides were studied containing either phosphorylated or unmodified Ser<sub>404</sub> and Arg<sub>406</sub> or Trp<sub>406</sub>. All peptides in this study were acylated on the N-terminus and contained a C-terminal carboxamide.

### Analysis of Ac-TGPX-NH<sub>2</sub> peptides

The primary goal of these experiments is to identify the electronic component of an H $\alpha$ (*i*-2)-cis-Pro-aromatic interaction. Such an interaction within Ac-TGPX-NH<sub>2</sub> would that the the same interaction might be important in *tau* due to R406W. Peptides Ac-TGPX-NH<sub>2</sub> were synthesized and analyzed by NMR to identify the possibility and strength of an H $\alpha$ (*i*-2)-cis-Pro-aromatic interaction leading to increases in the population of cis-Pro amide bond ( $K_{trans/cis}$ ) (Figure 3.1).  $K_{trans/cis}$  describes an equilibrium expression determined by NMR; the ratio of the concentration of peptide with a trans amide bond to the concentration of peptide with a cis amide bond. Given that  $K_{trans/cis}$  is an equilibrium expression between two states, the free energy ( $\Delta G$ ) differences between the two states may be calculated ( $\Delta G = -RT \ln K_{trans/cis}$ ). The residue cyclohexyl-alanine was also examined as a control, due to similar size as aromatic residues without the aromatic component. All peptides containing aromatic residues (except TGPH(H<sup>+</sup>) at pH 4.0) favored the cis conformation relative to the control peptides TGPN ( $K_{trans/cis} = 7.4$ ) or TGPCha ( $K_{trans/cis} = 4.5$ ) (Table 1). Notably, in previous studies on this model sequence, peptides with asparagine at the same position was observed to have the highest population of cis-Pro amide bonds of all nonaromatic/nonproline residues.<sup>60, 62</sup> Previously reported data on TYPN exhibiting a  $K_{trans/cis}$  of 2.7 is consistent with Tyr stabilizing the *cis* state by -0.60 kcal/mol due to stabilization of Tyr-cis-Pro CH/ $\pi$  interactions.<sup>60, 62, 70</sup> Surprisingly, there was no overall common trend of cis population among the aromatic residues relative to the electronics of the aromatic ring in  $K_{trans/cis}$ . The peptide with tyrosine was observed to have a  $K_{trans/cis}$  of 3.0, exhibiting a higher population of cis than that of the peptide with the more electron-rich tryptophan ( $K_{trans/cis} = 3.7$ ). Peptides containing electron-neutral phenylalanine and weakly electron-withdrawing 4-I-Phe were observed to have

the highest content of cis bond population ( $K_{trans/cis} = 2.5$ ). These deviations may be rationalized by the entropic penalty associated with the conformational restraint in the *cis* state competing with the favorable enthalpy associated with the CH/ $\pi$  interaction.<sup>80</sup> Among the electron-deficient aromatic amino acids, a clear trend was observed in  $K_{trans/cis}$  relating to the electronics of the aromatic amino acid: 4-I-Phe > 4-CF<sub>3</sub>-Phe > 4-NO<sub>2</sub>-Phe > His, with His at pH 4.0 exhibiting the greatest population of trans ( $K_{trans/cis} = 10.0$ ). Interestingly, the control peptide containing Cha was also observed to have a high population of the cis isomer, in contrast to Ac-TXPN-NH<sub>2</sub> peptides with aromatic-Pro sequences.<sup>58, 62</sup> The observed increase in cis-Pro amide bonds could possibly be explained by hydrophobic effects, where the hydrophobic face of the cyclohexyl ring associates with the hydrophobic surface of the aliphatic proline ring. Overall, cis-trans isomerism of TGPX was modulated by 0.82 kcal mol<sup>-1</sup>. To determine the nature of the observed higher  $K_{trans/cis}$  for Tyr over Trp, additional NMR experiments were performed on TGPW and TGPY peptides.

TGPX, X=	$K_{trans/cis}$	$\Delta G_{trans/cis}$ kcal mol <sup>-1</sup>
TGPH (pH 4)	10	-1.36
TGPH (pH 8.5)	4	-0.82
TGPW	3.7	-0.77
TGP(4-NO <sub>2</sub> -Phe)	3.6	-0.76
TGP(4-CF <sub>3</sub> -Phe)	3.5	-0.74
TGPY	3	-0.65
TGPF	2.5	-0.54
TGP(4-I-Phe)	2.5	-0.54
TGPCha	4.5	-0.89
TGPN	7.4	-1.18
TYPN	2.7	-0.58

**Table 3.1:** NMR-derived data for Ac-TGPX-NH<sub>2</sub> and Ac-TYPN-NH<sub>2</sub><sup>(60)</sup> model peptides.  $\Delta G = -RT \ln K_{trans/cis}$ . Peptides were dissolved in 5 mM phosphate buffer (pH 4.0 or 8.5) containing 25 mM NaCl in 90% H<sub>2</sub>O/10% D<sub>2</sub>O. Data were collected at 298 K.

In order to identify the glycine alpha protons of Ac-TGPY-NH<sub>2</sub> and Ac-TGPW-NH<sub>2</sub> in both trans and cis states, TOCSY NMR experiments were performed. These experiments revealed a large upfield chemical shift of the glycine alpha protons for cis isomers for peptides containing aromatic amino acids (Figure 3.3 and Figure 3.4). These observations are consistent with a CH/ $\pi$  interaction between the aromatic face and the glycine alpha hydrogens due to ring current effects of the aromatic face on the alpha hydrogens.<sup>83, 84</sup> Interestingly, the magnitude of the chemical shifts were not the same for both glycine alpha hydrogens within each cis isomer. The glycine hydrogens for TGPY cis isomer were found to have chemical shifts of 3.59 ppm and 2.94 ppm, where the same hydrogens in the trans state exhibited a chemical

shift of 4.01 ppm. The glycine hydrogens for TGPW cis isomer were found to have chemical shifts of 3.19 ppm and 2.48 ppm, where the same protons in the trans state exhibited chemical shifts of 4.00 ppm and 3.90 ppm. Overall, a greater upfield chemical shift was observed for TGPW glycine alpha hydrogens for the cis isomers over that of TPGY, consistent with a stronger CH/ $\pi$  interaction involving the aromatic face of the indole over tyrosine; expected for the more electron-rich indole ring. Although unconfirmed by TOCSY NMR, shifts in Gly H $\alpha$  protons were observed for all peptides of the TGPX series (Figure X) when *i*-2 to the aromatic residue. Notably, no upfield shift was observed for the Gly alpha hydrogen in the peptide containing Cha, as expected for a non-aromatic interaction. Surprisingly, the observed CH/ $\pi$  interaction does not have the expected correlation with the observed  $K_{trans/cis}$ , suggestive of other factors, such as entropy contributions to the overall  $K_{trans/cis}$ .

Collectively, these data are consistent with H $\alpha$ (*i*-2)-cis-Pro-aromatic interactions occurring within Ac-TGPX-NH<sub>2</sub> peptides in the presence of an aromatic residue. Furthermore, these data suggest that these interactions may be common, occurring within peptides and proteins containing XP-aromatic sequences. These CH/ $\pi$  interactions exist in both TGP-aromatic, GP-aromatic, and PP-aromatic sequences, suggesting their presence in *tau*<sub>403-406</sub> TSP-aromatic sequences.<sup>79, 80</sup> Single point substitution of serine for glycine allows for direct correlation between Ac-TGPX-NH<sub>2</sub> peptides and Ac-TSPX-NH<sub>2</sub> *tau*<sub>403-406</sub> derived peptides.

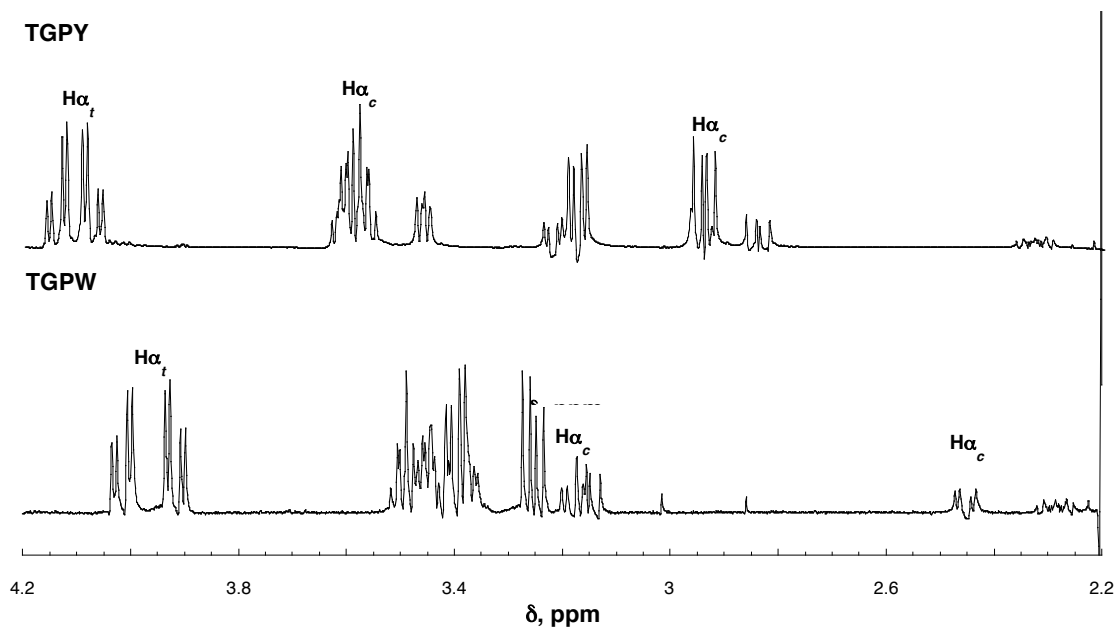


**Figure 3.3:** The <sup>1</sup>H NMR spectra of (top) **Ac-TGPY-NH<sub>2</sub>** and (bottom) **Ac-TGPW-NH<sub>2</sub>**. Peptides were dissolved in 5 mM phosphate buffer (pH 4.0) containing 25 mM NaCl in 90% H<sub>2</sub>O/10% D<sub>2</sub>O. Data were collected at 298 K. Glycine alpha protons are labeled for both the trans (Hα<sub>t</sub>) and cis (Hα<sub>c</sub>) isomers.

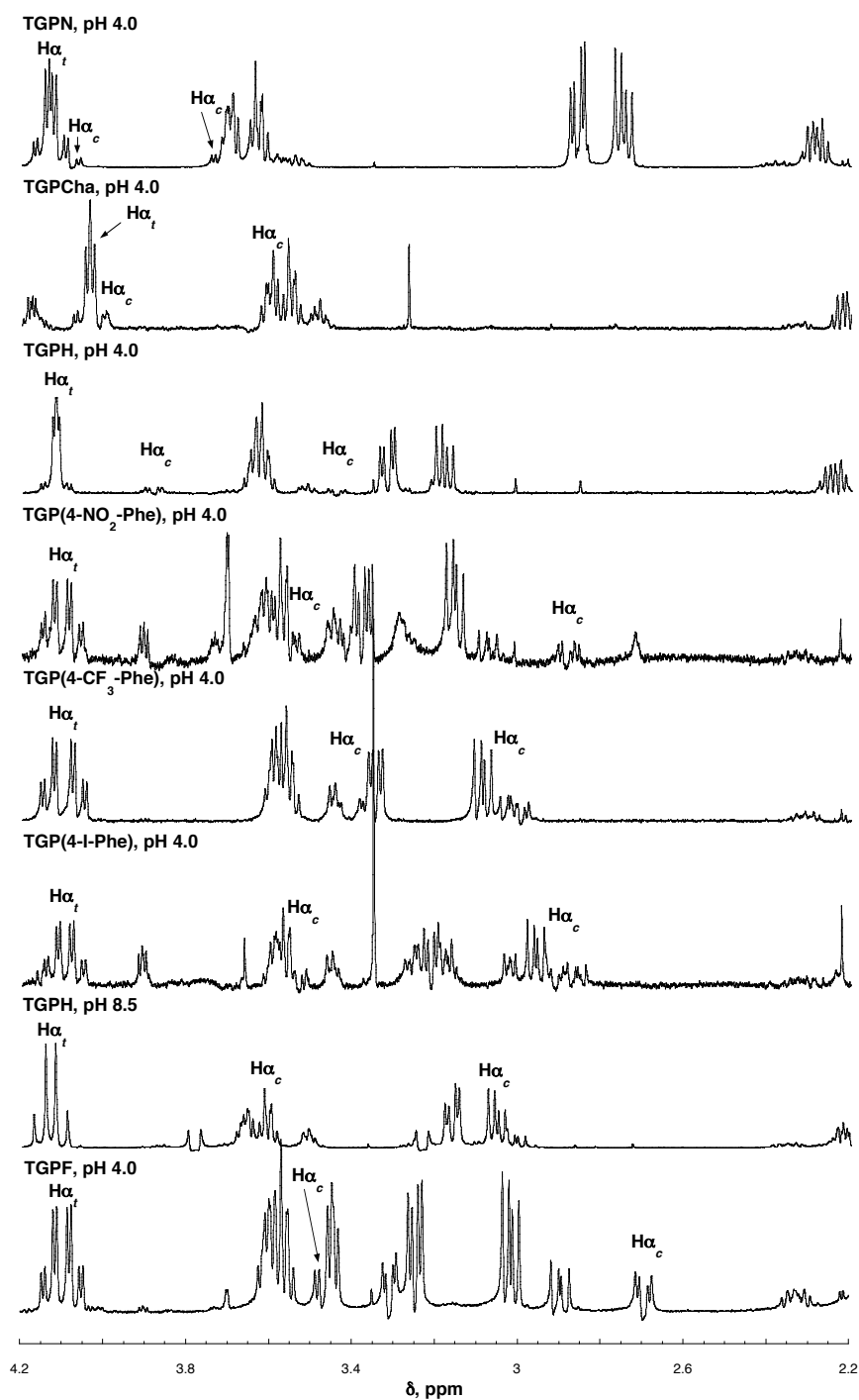


**Figure 3.4:** The <sup>1</sup>H NMR spectra of H $\alpha$  region of Ac-TGPX-NH<sub>2</sub>: X = Phe, His (pH 8.5), 4-I-Phe, 4-CF<sub>3</sub>-Phe, 4-NO<sub>2</sub>-Phe, His (pH 4). Peptides were dissolved in 5 mM phosphate buffer (pH as indicated) containing 25 mM NaCl in 90% H<sub>2</sub>O/10% D<sub>2</sub>O. Data were collected at 298 K.

### Structural implications of pThr<sub>403</sub>/pSer<sub>404</sub> and R406W on *tau* peptides

Substitution of serine for glycine allows the direct comparison between Ac-TGPX-NH<sub>2</sub> and *tau*<sub>403-406</sub> Ac-TSPX-NH<sub>2</sub> model peptides. Peptides were synthesized and analyzed by NMR with all combinations of modifications (phosphorylation versus unmodified) at Thr<sub>403</sub> and/or Ser<sub>404</sub> with both Arg<sub>406</sub> or Trp<sub>406</sub>. In addition, a control peptide was synthesized and analyzed with Asn<sub>406</sub> to directly compare the effects of glycine to serine substitution on model peptides Ac-TXPN-NH<sub>2</sub> (Table 3.2). Substitution of Gly of Ser destabilized the *cis* isomer by 0.21 kcal/mol. Within model peptides, Basu found substitution of Ser for Gly lead to destabilization of the *cis* isomer by 0.25 kcal/mol (Ac-XPA-NH<sub>2</sub>) and 0.19 kcal/mol (Ac-XPY-NH<sub>2</sub>), consistent with our observations.<sup>80</sup> These results are consistent with smaller entropic and steric penalties upon forming the *cis* isomer associated with glycine, which lacks a side chain. Within *tau* R406W is known to lead to increased rates of AD formation in animal models. Substitution of R406W in Ac-TSPX-NH<sub>2</sub> stabilized the *cis* isomer by -0.17 kcal/mol. These results are consistent with Basu's observations that substitution of Tyr for Ala in Ac-SPX-NH<sub>2</sub> stabilized the *cis* isomer by -0.19 kcal/mol.<sup>80</sup> Within *tau*, phosphorylation of Ser<sub>404</sub> is also associated with the onset of AD. To determine the structural effects of Ser<sub>404</sub> phosphorylation, peptides Ac-TSPR-NH<sub>2</sub> and Ac-TSPW-NH<sub>2</sub> with phosphorylation at Ser<sub>404</sub> (pSer) and/or Thr<sub>403</sub> (pThr) were examined by NMR.

Tau<sub>403-406</sub>-derived peptides containing phosphorylated residues were examined at both pH 6.5 and 7.2 (typical pK<sub>a</sub> = ~5.5-6.0) to determine the electronic contribution of the phosphate on structure. Furthermore, it is important to study these effects at physiological pH (~ 7.2). Differences in structure due to both states may be directly

correlated to interactions involving the phosphate. Surprisingly, phosphorylation of Ser<sub>404</sub> led to an increase in the cis amide population for both peptide TpSPR ( $K_{trans/cis} = 5.1$  at pH 7.2,  $K_{trans/cis} = 5.5$  at pH 6.5) and TpSPW ( $K_{trans/cis} = 3.2$  at pH 7.2,  $K_{trans/cis} = 3.5$  at pH 6.5). Interestingly, greater cis population was observed for the dianionic phosphate (data at pH 7.2) due to the dianionic phosphate carrying a more negative charge. Surprisingly, phosphorylation of Thr<sub>403</sub> increased the cis population of pTSPR ( $K_{trans/cis} = 8.0$  at pH 7.2,  $K_{trans/cis} = 9.6$  at pH 6.5), yet decreased the cis population of pTSPW ( $K_{trans/cis} = 12.3$  at pH 7.2,  $K_{trans/cis} = 12.0$  at pH 6.5) relative to unmodified peptides. Destabilization observed for TSPW peptides could be due to repulsive effects between the indole ring and the phosphate group while in the cis conformation.<sup>88, 89</sup> Overall the structural effects of pThr<sub>403</sub> were different in Ac-pTSPR-NH<sub>2</sub> and Ac-pTSPW-NH<sub>2</sub> peptides. Interestingly, *tau* is also known to be phosphorylated at both Thr<sub>403</sub> and Ser<sub>404</sub>.<sup>90</sup>

To determine the structural effects of both pThr<sub>403</sub> and pSer<sub>404</sub>, double-phosphorylated *tau*<sub>403-406</sub> Ac-pTpSPR/W-NH<sub>2</sub> peptides were synthesized and analyzed by NMR. Double-phosphorylated peptides pTpSPR ( $K_{trans/cis} = 4.4$  at pH 7.2,  $K_{trans/cis} = 5.6$  at pH 6.5) and pTpSPW ( $K_{trans/cis} = 4.7$  at pH 7.2,  $K_{trans/cis} = 4.3$  at pH 6.5) exhibited values of  $K_{trans/cis}$  comparable to that of the mono-phosphorylated Ser<sub>404</sub> peptides. Interestingly, double-phosphorylated pTpSPR stabilized the *cis* isomer by -0.08 kcal/mol (pH 7.2 for pTpSPR) more than phosphorylation of serine alone, consistent with both phosphorylation events stabilizing the cis-Pro amide bond in TSPR peptides. In contrast to TSPR, double phosphorylation of TSPW destabilized the *cis* isomer by 0.23 kcal/mol relative to TpSPW. Inversely, phosphorylation of serine stabilized pTSPW *cis* isomer by -0.57 kcal/mol. Furthermore, the destabilization observed for pTpSPW was greater at pH 7.2 than 6.5, suggesting

phosphate electrostatics play a direct role in cis-destabilization. These data are consistent with a cis-destabilizing interaction involving phosphorylation of threonine and R406W. Alternatively, these data may be explained by a trans-favoring interaction involving phosphorylation of threonine and R406W, although this was not observed in TSPR peptides. Additional NMR experiments were performed to identify specific interactions due to both Ser<sub>404</sub> phosphorylation and R<sub>406</sub>W substitution.

	$K_{\text{trans/cis}}$ pH 7.2	$\Delta G_{\text{trans/cis}}$ kcal mol <sup>-1</sup> pH 7.2	$K_{\text{trans/cis}}$ pH 6.5	$\Delta G_{\text{trans/cis}}$ kcal mol <sup>-1</sup> pH 6.5	$K_{\text{trans/cis}}$ pH 4.0	$\Delta G_{\text{trans/cis}}$ kcal mol <sup>-1</sup> pH 4.0
<b>TSPN</b>	n.a.	n.a.	n.a.	n.a.	10.4	-1.39
<b>TSPR</b>	n.a.	n.a.	n.a.	n.a.	11.4	-1.44
<b>TpSPR</b>	5.1	-0.96	5.5	-1.01	n.a.	n.a.
<b>pTSPR</b>	8.0	-1.23	9.6	-1.34	n.a.	n.a.
<b>pTpSPR</b>	4.4	-0.88	5.6	-1.02	n.a.	n.a.
<b>TSPW</b>	n.a.	n.a.	n.a.	n.a.	7.9	-1.22
<b>TpSPW</b>	3.2	-0.69	3.5	-0.74	n.a.	n.a.
<b>pTSPW</b>	12.3	-1.49	12.0	-1.47	n.a.	n.a.
<b>pTpSPW</b>	4.7	-0.92	4.3	-0.86	n.a.	n.a.

**Table 3.2:** NMR-derived data for *tau*<sub>403-406</sub> Ac-TSPX-NH<sub>2</sub> peptides.  $\Delta G = -RT \ln K_{\text{trans/cis}}$ . Peptides were dissolved in 5 mM phosphate buffer (pH 4.0, 6.5, or 7.2) containing 25 mM NaCl in 90% H<sub>2</sub>O/10% D<sub>2</sub>O. Data were collected at 298 K. pS = phosphorylated serine residue, pT = phosphorylated threonine residue.

Previous work has demonstrated that phosphorylation of serine and threonine residues leads to an intra-residue phosphate-amide hydrogen bond.<sup>91-95</sup> NMR experiments performed on *tau*<sub>403-406</sub> peptides revealed a downfield chemical shift of the amide proton of the phosphorylated residue in all peptides (Table 3.3). Both TSPR and TSPW sequences had similar chemical shifts for Thr (8.22 ppm, 8.19

ppm) and Ser (8.41 ppm, 8.40 ppm). Phosphorylation of Ser<sub>404</sub> led to a downfield chemical shift of Ser in both TpSPR (8.71 ppm at pH 7.2 and 8.69 ppm at pH 6.5) and TpSPW (8.78 ppm at pH 7.2 and 8.70 ppm at pH 6.5) peptides. The NMR data also reveals a decrease in  $^3J_{\alpha N}$  for all phosphorylated residues, which directly correlates to the  $\phi$  torsion angle and is consistent with serine and threonine adopting a more compact conformation (ordering of structure) upon both phosphorylation.

Phosphorylation led to a decrease in  $^3J_{\alpha N}$  for Ser<sub>404</sub> in TSPW, from 6.7 Hz at pH 7.2 and 6.1 Hz at pH 6.5. Phosphorylation of Thr<sub>403</sub> led to a downfield chemical shift in both threonine residues in pTSPR (8.75 ppm at pH 7.2 and 8.61 ppm at pH 6.5) and pTSPW (8.84 ppm at pH 7.2 and 8.66 ppm at pH 6.5) peptides.

Phosphorylation also led to a decrease in  $^3J_{\alpha N}$  for Thr<sub>403</sub> in TSPR peptides; from 8.1 Hz (unmodified threonine) to 6.1 Hz (pThr, pH 7.2) and 6.6 Hz (pThr, pH 6.5).

Similar effects were observed due to phosphorylation of Thr<sub>403</sub> in TSPW peptides; from 8.0 Hz (unmodified threonine) to 5.8 Hz (pThr, pH 7.2) and 6.5 Hz (pThr, pH 6.5).

Double-phosphorylated peptides exhibited similar chemical shifts of the phosphorylated serine residues (8.89 ppm pTpSPR (pH 7.2) and 8.75 ppm for dianionic pTpSPW (pH 7.2) peptides) to the monophosphorylated TpSPX peptides.

The  $^3J_{\alpha N}$  coupling constant of phosphoserine (4.4 Hz for pTpSPR (pH 7.2) and 5.7 Hz for pTpSPW (pH 7.2)) was similar to TpSPX peptides. Together, these data are consistent with organization occurring within both serine and threonine residues upon phosphorylation.

The downfield chemical shift and decrease in  $^3J_{\alpha N}$  observed for phosphorylated residues are consistent with an intra-residue phosphate amide hydrogen bond.<sup>91-95</sup>

Consistent with other work, phosphorylation of threonine in TSPW peptides led to an overall greater decrease in  $^3J_{\alpha N}$  values than serine phosphorylation.<sup>81, 94, 91</sup> On the N-

terminus of  $\alpha$ -helices and within Ac-KXPP-NH<sub>2</sub> peptides, threonine phosphorylation led to an overall greater decrease in  $^3J_{\alpha N}$  than serine phosphorylation. The  $^3J_{\alpha N}$  directly correlates to the phi torsion angle within peptide and protein structure.  $\alpha$ -Helices and polyproline helices (PPII) are highly ordered and are characterized by phi torsion angles of approximately  $-57^\circ$  for  $\alpha$ -helices and  $-75^\circ$  for PPII. The observed increase in cis population for peptides containing phosphoserine may be due to the formation of this intra-residue phosphate amide hydrogen bond, suggested by both the downfield chemical shift of the phosphorylated residue amide hydrogen and a decrease in the phi torsion angle. In all cases, phosphorylation of serine and threonine within peptides led to conformational restriction, and effects only differed in magnitude. The observed increase in cis population for peptides containing phosphoserine may be due to the formation of this intra-residue phosphate amide hydrogen bond. The alpha protons of serine were further examined to determine effects of both phosphorylation of serine and R406W.

Peptide	Residue	(pH ≤ 6.5)	(pH ≤ 6.5)	(pH 7.2)	(pH 7.2)
		$^3J_{\alpha N}$ (Hz)	$\delta$ , H <sup>N</sup> (ppm)	$^3J_{\alpha N}$ (Hz)	$\delta$ , H <sup>N</sup> (ppm)
<b>TSPR</b>	Thr	8.1	8.22	n.a.	n.a.
	Ser	n.d.	8.41	n.a.	n.a.
<b>TPSPR</b>	pSer	5.6	8.69	4.4	8.71
<b>pTSPR</b>	pThr	6.6	8.61	6.1	8.75
<b>pTpSPR</b>	pThr	7.0	8.59	5.3	8.91
	pSer	5.8	8.75	4.4	8.89
<b>TSPW</b>	Thr	8.0	8.19	n.a.	n.a.
	Ser	6.7	8.40	n.a.	n.a.
<b>TPSPW</b>	pSer	6.1	8.70	5.3	8.78
<b>pTSPW</b>	pThr	6.5	8.66	5.8	8.84
<b>pTpSPW</b>	pThr	6.9	8.58	5.9	8.84
	pSer	6.0	8.72	5.7	8.89
<b>TSPN</b>	Thr	8.0	8.22	n.a.	n.a.
	Ser	6.8	8.45	n.a.	n.a.

**Table 3.3:** NMR-derived data for *tau*<sub>403-406</sub> Ac-TSPX-NH<sub>2</sub> peptides. Peptides were dissolved in 5 mM phosphate buffer (pH 4.0 or 8.5) containing 25 mM NaCl in 90% H<sub>2</sub>O/10% D<sub>2</sub>O. Data were collected at 298 K. n.d. = no data due to spectral overlap. n.a. = not applicable.

Further examination of serine and phosphoserine alpha hydrogens revealed an upfield chemical shift of all serine alpha protons in the *cis* conformation relative to the *trans* conformation (Table 3.4). The magnitude of this upfield shift ranged between -0.19 ppm (pTS(H $\alpha$ )PR) to -0.20 ppm (TS(H $\alpha$ )PR) for all TSPR peptides, consistent with phosphorylation having no effect on the chemical shift of the serine alpha proton (table). Furthermore, the control peptide TSPN exhibited a -0.23 ppm shift in the serine alpha proton from *trans* to *cis* states, consistent with that of TSPR peptides. Substitution of Trp for Arg led to a -0.40 ppm upfield chemical shift of the serine alpha proton from *trans* to *cis* states, twice the magnitude of that observed

for TSPR and consistent with a favorable CH/ $\pi$  interaction in Trp-containing peptides. This observation is consistent with R406W leading to an increased cis population due to a favorable CH/ $\pi$  interaction. These observations are also consistent with the observed upfield chemical shifts of glycine alpha protons for both TGPY (-1.07 ppm and -0.42 ppm) and TGPW (-1.52 ppm and -0.71 ppm) peptides when in a cis conformation. Again, no difference in serine alpha proton chemical shifts were observed due to phosphorylation alone, with overall Ser H $\alpha$  changes from trans to cis states of TpSPW being identical to that of TSPW. Furthermore, no differences were observed in phosphoserine alpha proton chemical shift due to differences in pH. Together, these data are consistent with phosphorylation having no direct effects on the serine H $\alpha$  chemical shift, consistent with previous observations in  $\alpha$ -helices.<sup>91</sup> Interestingly, pTSPW exhibited the smallest upfield chemical shift in the serine alpha hydrogen in the *cis* versus *trans* conformation (-0.05 ppm), suggesting potentially an interaction involving phosphothreonine and tryptophan that is destabilizing to the observed CH/ $\pi$  interaction observed within other peptides. Phosphorylation of serine to form pTpSPW led to an upfield chemical shift in the serine alpha proton in the cis state relative to trans. The observed upfield chemical shift is greater at pH 6.5 (-0.30 ppm) than at pH 7.2 (-0.22 ppm). Serine phosphorylation in all cases led to an increase in cis population but only led to an upfield chemical shift in cis serine alpha protons for pTpSPW. These data are consistent with the presence of a serine H $\alpha$ (*i*-2)-cis-Pro-aromatic(*i*) interaction stabilizing the cis state. Phosphorylation of Thr<sub>403</sub> destabilizes this interaction leading to an increase in trans population. The source of this destabilization is most likely due to anion/ $\pi$  repulsion.<sup>88, 89</sup> Although these effects may be general for tetra-peptides, they may deviate in larger *tau* segments due to the formation of secondary structures.

Peptide	pH	$\delta$ , $H\alpha_{trans}$ (ppm)	$\delta$ , $H\alpha_{cis}$ (ppm)	$\Delta\delta$ , $H\alpha_{cis}-H\alpha_{trans}$ (ppm)
TGPY	4.0	4.01	3.59, 2.94	-1.07, -0.42
TGPW	4.0	4.00, 3.90	3.19, 2.48	-1.52, -0.71
TSPN	4.0	4.80	4.57	-0.23
TSPR	4.0	4.79	4.59	-0.20
TpSPR	6.5	4.86	4.68	-0.18
	7.2	4.81	4.65	-0.16
pTSPR	6.5	4.78	4.60	-0.18
	7.2	4.80	4.61	-0.19
pTpSPR	6.5	4.85	n.d.	n.d.
	7.2	4.81	n.d.	n.d.
TSPW	4.0	4.72	4.32	-0.40
TpSPW	6.5	4.74	4.35	-0.39
	7.2	4.69	4.30	-0.39
pTSPW	6.5	4.68	4.63	-0.05
	7.2	4.68	4.63	-0.05
pTpSPW	6.5	4.72	4.42	-0.30
	7.2	4.70	4.48	-0.22

**Table 3.4:** NMR-derived Ser  $H\alpha$  data for  $\tau_{403-406}$  Ac-TSPX-NH<sub>2</sub> and Gly  $H\alpha$  data for Ac-TGPX-NH<sub>2</sub> peptides. Peptides were dissolved in 5 mM phosphate buffer (pH 4.0, 6.5, or 7.2) containing 25 mM NaCl in 90% H<sub>2</sub>O/10% D<sub>2</sub>O. Data were collected at 298 K. n.d. = no data due to peak resolution.

To determine the generality of these effects, larger  $\tau_{395-411}$  peptides were synthesized and analyzed via NMR containing unmodified and phosphorylated Ser<sub>404</sub> both with either Arg<sub>406</sub> or Trp<sub>406</sub> (Table 3.5). The unmodified  $\tau_{395-411}$  was observed to have a  $K_{trans/cis}$  of 10.8 at pH 6.5, similar to that of the tetra-peptide TSPR ( $K_{trans/cis}$  = 11.4). Phosphorylation of Ser<sub>404</sub> led to a slight increase in the cis population ( $K_{trans/cis}$  = 9.1) greatly favoring the *trans* isomer relative to TpSPR ( $K_{trans/cis}$  = 5.1). Although no data were obtained for  $\tau_{395-411}$  R406W, the combined effects of Ser<sub>404</sub> phosphorylation and R406W substitution led to a significant increase in the cis

population ( $K_{trans/cis} = 6.0$ ) for the mixed mono/dianionic phosphate (pH 6.5). The tetra-peptide data would suggest that greater cis populations would be observed at the more physiologically relevant pH 7.2. Overall, phosphorylation of Ser<sub>404</sub> and R406W each led independently to an increase in cis population in *tau*<sub>395-411</sub> peptides.

Peptide	$K_{trans/cis}$ pH 7.2	$K_{trans/cis}$ pH 6.5	$K_{trans/cis}$ pH 4.0	Ser/pSer (pH ≤ 6.5)		pSer (pH ≥ 7.2)	
				$^3J_{\alpha N}$ (Hz)	$\delta H^N$ (ppm)	$^3J_{\alpha N}$ (Hz)	$\delta H^N$ (ppm)
<b><i>tau</i><sub>395-411</sub></b>	n.a.	10.8	n.a.	n.d.	n.d.	n.a.	n.a.
<b><i>tau</i><sub>395-411</sub> pS<sub>404</sub></b>	9.1	8.8	n.a.	5.5	8.61	4.5	8.67
<b><i>tau</i><sub>395-411</sub> R406W</b>	n.a.	n.d.	n.a.	n.d.	n.d.	n.a.	n.a.
<b><i>tau</i><sub>395-411</sub> R406W</b>	n.d.	6.0	n.a.	5.8	8.76	5.4	8.82

**Table 3.5:** NMR-derived data for *tau*<sub>395-411</sub> peptides. Peptides were dissolved in 5 mM phosphate buffer (pH 4.0 or 8.5) containing 25 mM NaCl in 90% H<sub>2</sub>O/10% D<sub>2</sub>O. Data were collected at 298 K. n.d. = no data due to spectral overlap. n.a. = not applicable.

## Discussion

Herein, I have conducted a preliminary examination focusing on the effects of R406W mutation and phosphorylation events that may impact cis-trans isomerism of the prolyl amide bond within model peptides Ac-TGPX-NH<sub>2</sub>, Ac-TSPR/W-NH<sub>2</sub>, and *tau*<sub>395-411</sub> variants. To examine the relationships between the electronic identity of the aromatic amino acid, the H $\alpha(i-2)$ -cis-Pro-aromatic(*i*) CH/ $\pi$  interaction, and cis-trans isomerism, peptides of the sequence Ac-TGPX-NH<sub>2</sub> were analyzed by NMR, differing in *tau*<sub>403-406</sub> by one residue, incorporating both natural (His, Trp, Tyr, Phe, and Asn) and unnatural amino-acids (4-NO<sub>2</sub>-Phe, 4-CF<sub>3</sub>-Phe, 4-I-

Phe, and Cha) at residue 4. I have also conducted the first study on the effects of phosphorylation on cis-trans isomerism of Ser-cis-Pro-Xxx motifs; *tau*<sub>403-406</sub>-derived peptides Ac-TSPR/W-NH<sub>2</sub>, serine analogues of Ac-TGPX-NH<sub>2</sub>, were analyzed by NMR, focusing on the structural implications of threonine and serine phosphorylation events in both the presence and absence of R406W, and their role in cis-trans isomerism within *tau*<sub>403-406</sub>. These studies were expanded to *tau*<sub>395-411</sub> to examine the effects of Ser<sub>404</sub> phosphorylation and R406W mutation, and their structural roles in a larger *tau* context.

All TGPX peptides containing an aromatic residue, with the exception of TGPH at pH 4.0 (His(H<sup>+</sup>)), exhibited higher cis populations than the control peptides TGPN and TGPC<sub>h</sub>a. Interestingly, canonical aromatic residues (except for His) followed the opposite of the expected trend based solely on electronics of the aromatic group of  $K_{trans/cis}$  as a function of aromatic electronics: His(H<sup>+</sup>) (10.0) > His (4.0) > Trp (3.7) > Tyr (3.0) > Phe (2.5). Work performed on Ac-GXPG-NH<sub>2</sub> sequences, an analogue of Ac-TGPX-NH<sub>2</sub>, demonstrated an expected trend based solely on aromatic electronics: Phe ( $K_{trans/cis} = 4.9$ ) > Tyr ( $K_{trans/cis} = 4.0$ ) > Trp ( $K_{trans/cis} = 3.0$ ).<sup>50</sup> Interestingly, these results are similar to work performed by Meng et al. on Ac-TYPX-NH<sub>2</sub> peptides. They, and others, found that Ac-TY<sub>1</sub>PF-NH<sub>2</sub> stabilized the cis-Pro amide bond by -0.15 kcal/mol more than Ac-TYPW-NH<sub>2</sub>.<sup>54, 60</sup> Unlike aromatic-cis-Pro and cis-Pro-aromatic interactions on the restriction of two amino acids, H $\alpha$ (*i*-2)-cis-Pro-Aromatic interactions involve the rotational restriction of three residues including an interaction with a non-proline residue (CH/ $\pi$  interactions involving proline are less disfavorable in entropy due to the already restricted side chain), leading to greater entropic penalties associated with formation of the cis amide bond and subsequent, and enthalpically favorable, CH/ $\pi$  interaction. Basu analyzed Ac-PPX-NH<sub>2</sub> models to

reveal tyrosine and tryptophan both had unfavorable entropic values of approximately -5 cal/deg/mol (Trp exhibited slightly more unfavorable entropy than Tyr), yet had favorable enthalpic values of -1.7 kcal/mol (Trp) and -1.1 kcal/mol (Tyr), with a *cis*-favoring trend of Tyr > Phe > Trp > His.<sup>55, 76</sup> Further work revealed an entropic cost of -9.8 cal/mol/deg and a favorable enthalpy of -2.4 kcal/mol associated with Ac-GPY-NH<sub>2</sub> forming the *cis* conformation, greater than all other amino acids at residue 1.<sup>77</sup> These findings rationalize the peptide Ac-TGPW-NH<sub>2</sub> exhibiting the largest upfield chemical shift in Gly alpha protons (*trans* = 4.00 ppm, 3.90 ppm; *cis* = 3.19 ppm, 2.48 ppm) relative to Ac-TGPY-NH<sub>2</sub> (*trans* = 4.01 ppm; *cis* = 3.59 ppm, 2.94 ppm), yet due to entropic penalties the Tyr variant maintains a higher *cis* population than Trp. Based solely on aryl electronics, the trend in  $K_{trans/cis}$  of Ac-TGPH-NH<sub>2</sub> is consistent with a *cis* stabilizing H $\alpha$ (*i*-2)-*cis*-Pro-Aromatic interaction. Protonated His pH 4.0 is electron deficient compared to neutral His at pH 8.0, yet are entropically identical. If the observed interaction is enthalpically based on aromatic electronics, then we would expect a higher *cis* population for neutral His versus His(H<sup>+</sup>).

In contrast to canonical aromatic amino acids, all TGPX peptides containing phenylalanine derivatives did follow an expected trend in  $K_{trans/cis}$  relative to the electronic nature of the aromatic: 4-NO<sub>2</sub>-Phe ( $K_{trans/cis}$  = 3.6) > 4-CF<sub>3</sub>-Phe ( $K_{trans/cis}$  = 3.5) > Tyr ( $K_{trans/cis}$  = 3.0) > 4-I-Phe ( $K_{trans/cis}$  = 2.5) = Phe ( $K_{trans/cis}$  = 2.5). The functional groups contribute minimally to the entropic cost of the *cis* isomer, allowing an expected trend in  $K_{trans/cis}$  based on aryl electronics. Further temperature dependent NMR and subsequent van't Hoff analysis would be necessary to support these proposed models. Entropic penalties of forming the *cis* isomer, the  $K_{trans/cis}$  values, and the dramatic upfield chemical shift in *cis* Gly alpha hydrogens for TGPW and TGPY peptides, are all consistent with the presence of a *cis*-stabilizing H $\alpha$ (*i*-2)-*cis*-Pro-

Aromatic interaction within all peptides containing aromatic amino acids. Substitution of serine for glycine allows direct correlation between TGPX and both unmodified and phosphorylated  $\tau_{403-406}$  (Ac-TSPR/W-NH<sub>2</sub>) variants.

Single point substitution allowed for direct comparison of results between Ac-TGPX-NH<sub>2</sub> peptides and  $\tau_{403-406}$  derived peptides Ac-TSPR/W/N-NH<sub>2</sub>. Control peptide Ac-TSPN-NH<sub>2</sub> exhibited a  $K_{trans/cis}$  of 10.4, comparable to that of Ac-TSPR-NH<sub>2</sub> ( $K_{trans/cis} = 11.4$ ) and less than that of Ac-TGPN-NH<sub>2</sub> ( $K_{trans/cis} = 7.4$ ). The decrease in *cis* population due to Gly/Ser substitution is most likely due to increased steric and entropic penalties associated with forming the *cis* isomer.<sup>54, 77</sup> Substitution of R406W led to an increase in the amount of *cis* amide bond ( $K_{trans/cis} = 7.9$ ) and an upfield chemical shift in Ser<sub>404</sub> alpha proton of -0.40 ppm. These data are consistent with H $\alpha$ (*i*-2)-*cis*-Pro-Aromatic interactions present for *cis* isomers of both TGPX and  $\tau_{403-406}$  R406W peptides. Smaller upfield chemical shifts between -0.19 ppm and -0.23 ppm were observed for all TSPR peptides due to formation of the *cis* isomer, an effect observed by others.<sup>50, 52, 76, 77</sup> Within  $\tau$ , phosphorylation of Ser<sub>404</sub> is directly correlated with the onset of AD. To explore the effects of Ser<sub>404</sub> phosphorylation, both  $\tau_{403-406}$  derived peptides with Arg<sub>406</sub> and Trp<sub>406</sub> were analyzed with pSer<sub>404</sub>.

To our knowledge, there are no examples of phosphorylation significantly affecting *cis*-*trans* isomerism of Ser-*cis*-Pro-Xxx motifs. Surprisingly, phosphorylation of Ser<sub>404</sub> stabilized the *cis* isomer by -0.48 kcal/mol (pH 7.2) and -0.43 kcal/mol (pH 6.5) in TpSPR peptides. Phosphorylation of Ser<sub>404</sub> in TpSPW stabilized the *cis* isomer by -0.53 kcal/mol (pH 7.2) and -0.48 kcal/mol (pH 6.5). Variations in stability between the different protonation states indicate that the negative charge carried by the phosphate correlates to stability of the *cis* amide bond. In addition to an increase in *cis*-Pro amide bond, phosphorylated serine residues within both peptides exhibited a

downfield chemical shift in the amide proton of the phosphorylated residue along with a decrease in  $^3J_{\alpha N}$ , consistent with significant ordering within the phosphorylated residue. The magnitudes of both the downfield chemical shift and decrease in  $^3J_{\alpha N}$  are lesser than those observed in  $\alpha$ -helices and polyproline structures, and consistent with a weaker phosphate-amide intra-residue hydrogen bond.<sup>87-91</sup> Interestingly, phosphorylation of Ser<sub>404</sub> and no impact on the chemical shift of phosphoserine alpha protons, consistent with observed results of serine phosphorylation on the N-terminus of  $\alpha$ -helices, and in contrast to the mean downfield chemical shift of 0.13 ppm (dianionic phosphate) observed due to phosphorylation of serine residues within the proline-rich domain of *tau*.<sup>90, 91</sup> Further temperature-dependent NMR studies performed by Ganguly have suggested a hydrogen bond between the serine amide and the carboxy-amide terminus that stabilized the *trans* isomer. Phosphorylation may eliminate this interaction via the intra-residue phosphate-amide hydrogen bond. These data are consistent with Ser<sub>404</sub> phosphorylation and R406W have unique and additive mechanisms of *cis*-Pro stabilization within *tau*<sub>403-406</sub> model peptides. These data also suggest that within full-length *tau*, both phosphorylation of Ser<sub>404</sub> and R406W mutation may lead to an increase in *cis*-Pro bond population.

Interestingly, Thr<sub>403</sub> has also been found to be phosphorylated in *tau* from AD brains.<sup>91</sup> The effects of Thr<sub>403</sub> phosphorylation were investigated on peptides with Arg<sub>406</sub> or Thr<sub>406</sub>. Surprisingly, phosphorylation of Thr<sub>403</sub> in pTSPR led to stabilization of the *cis* isomer by -0.21 kcal/mol at pH 7.2 and -0.10 kcal/mol at pH 6.5. In contrast, phosphorylation of Thr<sub>403</sub> in pTSPW led to stabilization of the *trans* isomer by -0.27 kcal/mol at pH 7.2 and -0.25 kcal/mol at pH 6.5. Again, a downfield chemical shift in the amide proton of the phosphorylated residue of 0.39 ppm (pTSPR pH 7.2) and 0.47 ppm (pTSPW pH 7.2), along with a decrease in  $^3J_{\alpha N}$  of 1.5 Hz for pTSPR (pH 7.2) and

1.5 Hz for pTSPR (pH 7.2), indicate of ordering within the phosphothreonine residue. The magnitudes of both the downfield chemical shifts and decreases in  $^3J_{\alpha N}$  are less than those observed in  $\alpha$ -helices and polyproline structures, and consistent with a weaker phosphate-amide intra-residue hydrogen bond. As expected, threonine phosphorylation in Arg-containing peptides had no effect on the chemical shift of *cis* serine alpha proton. Surprisingly, threonine phosphorylation in Trp peptides had a dramatic effect on the chemical shift of only *cis* serine alpha protons, leading to a 0.05 ppm upfield chemical shift from *trans* to *cis* isomers and a downfield chemical shift of 0.31 ppm from Thr-Ser-*cis*-Pro-Trp to pThr-Ser-*cis*-Pro-Trp. These data are consistent with Thr<sub>403</sub> phosphorylation destabilizing the H $\alpha$ (*i*-2)-*cis*-Pro-Aromatic interaction between the aromatic face of Trp<sub>406</sub> and Ser<sub>404</sub> alpha proton. The source of the *cis*-Pro destabilization is most likely due to enthalpically unfavorable anion/ $\pi$  interaction between the phosphate on Thr<sub>403</sub> and the aromatic face of Trp<sub>403</sub>, present through space during a H $\alpha$ (*i*-2)-*cis*-Pro-Aromatic interaction. Alternatively, there may be an enthalpically favorable *trans*-Pro stabilizing interaction involving phosphorylated threonine and an unidentified interaction. The later is less likely and is in stark contrast to the observed pTSPR peptide data. These data suggest that phosphorylation of Thr<sub>403</sub> maybe be a mechanism by which R406W *tau* mutants may be stabilized by favoring the *trans* isomer. Interestingly, both Thr<sub>403</sub> and Ser<sub>404</sub> have been found to be phosphorylated within AD brains.<sup>91</sup>

To investigate the effects of phosphorylation of both Thr<sub>403</sub> and Ser<sub>404</sub>, peptides were analyzed with both phosphorylated residues and Arg<sub>406</sub> or Trp<sub>406</sub>. Interestingly, double-phosphorylated peptides stabilized the *cis*-Pro amide bonds for pTpSPR peptides by -0.56 kcal/mol at pH 7.2 and -0.42 kcal/mol at pH 6.5. Again, a downfield chemical shift was observed for the amide protons of both dianionic

phosphorylated residues (0.34 ppm for pSer and 0.37 ppm for pThr), along with a decrease in  $^3J_{\alpha N}$  of 1.1 Hz for pThr. Consistent with pThr/Trp *cis*-Pro destabilization, Thr<sub>403</sub> phosphorylation of TpSPW (pTpSPW) destabilized the *cis*-Pro amide bond by 0.23 kcal/mol at pH 7.2 and 0.12 kcal/mol at pH 6.5. Interestingly, threonine phosphorylation of TpSPR led to a downfield chemical shift in the *cis* phosphoserine amide proton of 0.17 ppm for the dianionic phosphate and 0.09 ppm for the monoanionic phosphate. In all, the *cis* conformations of both peptides are stabilized by double phosphorylation relative to the unmodified peptides.

Together, these data present a unique and novel switch to tune *cis*-Pro amide bonds. Data from TGPX series, along with data from others, have demonstrated that H $\alpha$ (*i*-2)-*cis*-Pro-Aromatic interactions suffer from entropic penalties associated with side chain and main chain restrictions. For these reasons, proline and glycine residues are observed to have the highest population of *cis* amide bonds within Xxx-*cis*-Pro-aromatic sequence contexts due to the interaction of the *i*-1 residue H $\alpha$  with the *i*+1 aromatic face.<sup>54, 77</sup> Formation of the *cis*-Pro isomer for TSPX sequences may require conformational restraint on both serine and threonine side chains. Data herein are consistent in every phosphorylated peptide with phosphorylation leading to a phosphate-amide intra-residue hydrogen bond. The formation of this hydrogen bond is enthalpically favorable and may counter the entropically unfavorable formation of the *cis* isomer. Phosphothreonine and phosphoserine residues may act as proline analogues in a structurally similar yet functionally distinct manner than proposed for  $\alpha$ -helices.<sup>91</sup> Supporting this hypothesis would require temperature-dependent NMR studies to establish the entropic contribution of the phosphate amide hydrogen bond. To confirm the generality of the observations within *tau*<sub>403-406</sub>, analysis of larger *tau* segments is required.

Four larger  $\tau_{395-411}$  analogues were synthesized and analyzed via NMR containing unmodified and phosphorylated Ser<sub>404</sub> along with Arg<sub>406</sub> or Trp<sub>406</sub>. The native and unmodified  $\tau_{395-411}$  was observed to have a  $K_{trans/cis}$  of 10.8 at pH 6.5, similar to that of Ac-TSPR-NH<sub>2</sub> ( $K_{trans/cis} = 11.4$ ). Consistent with phosphorylation of Ser<sub>404</sub> in tetra-peptides, phosphorylation of Ser<sub>404</sub> in  $\tau_{395-411}$  led to decrease in  $K_{trans/cis} = 8.8$ , and a downfield chemical shift in the phosphorylated amide proton. Interestingly, R406W mutation with phosphorylated pSer<sub>404</sub> in  $\tau_{395-411}$  led to a substantial increase in cis-Pro population ( $K_{trans/cis} = 6.0$ ) and a downfield chemical shift in pSer<sub>404</sub> amide proton. These findings are suggestive of a H $\alpha(i-2)$ -cis-Pro-Aromatic interaction in addition to pSer-cis-Pro stabilization within  $\tau_{395-411}$  R406W. The observed values and changes in  $K_{trans/cis}$  observed in  $\tau_{395-411}$  are consistent with  $\tau_{403-406}$  tetrapeptides.

Together, these data suggest a general mode in which phosphorylation of Ser or Thr residues preceding Pro-aromatic sequences may function to stabilize the cis-Pro amide bond, via distinct yet cooperative mechanisms. The data herein are consistent with an enthalpically favorable H $\alpha(i-2)$ -cis-Pro-Aromatic interaction present in TGPX, TSPW, and  $\tau_{395-411}$  R406W peptides stabilizing the cis-Pro isomer. The role of Ser<sub>404</sub> phosphorylation is less clear. Given that Thr<sub>403</sub> phosphorylation stabilizes TSPR cis-Pro amide bonds proximally, and that both phosphorylation events stabilize TSPR, phosphorylation of Ser<sub>404</sub> may be a mechanism by which the enthalpically favorable intra-residue phosphate amide hydrogen bond locks the side chain of serine, removing entropic penalties associated with H $\alpha(i-2)$ -cis-Pro-Aromatic interactions.

Current models of AD suggest that phosphorylation of Ser<sub>404</sub> on the C-terminal tail of  $\tau$  leads to disassociation of the C-terminus with the repeat region and subsequent aggregation through  $\tau$ - $\tau$  interactions.<sup>27, 28</sup> PP2A is responsible for

dephosphorylating exclusively *trans* pThr/pSer-Pro motifs and is assisted by the prolyl isomerase Pin1, which is found to be downregulated and/or inhibited by oxidation within patients with AD.<sup>78, 79</sup> The data herein suggest that both pSer<sub>404</sub> and R406W in full-length *tau* may lead to an increase in phosphoserine-cis-Pro amide bonds, preventing dephosphorylation by PP2A, leading to dissociation of the C-terminal tail from the repeat region. Phosphorylation of Ser<sub>404</sub> also leads to phosphorylation of Ser<sub>400</sub> and Ser<sub>396</sub> through processive phosphorylation by GSK-3 $\beta$ . Thus, increased *cis* amide bond at pSer<sub>404</sub>-Pro<sub>405</sub> also leads to increased phosphorylation at Ser<sub>396</sub> and Ser<sub>400</sub>. Dissociation of the C-terminal tail due to phosphorylation exposes the repeat region for *tau-tau* aggregation and subsequent onset of AD (Figure 3.5). To confirm the findings herein, further kinetic studies involving PP2A and GSK-3 $\beta$  must be conducted on *tau*<sub>395-411</sub>. Although these studies have been directed at *tau*, these data suggest that pSer-Pro and possibly pThr-Pro sequences may be widespread in nature as method for tuning *cis/trans* isomerism within proteins.

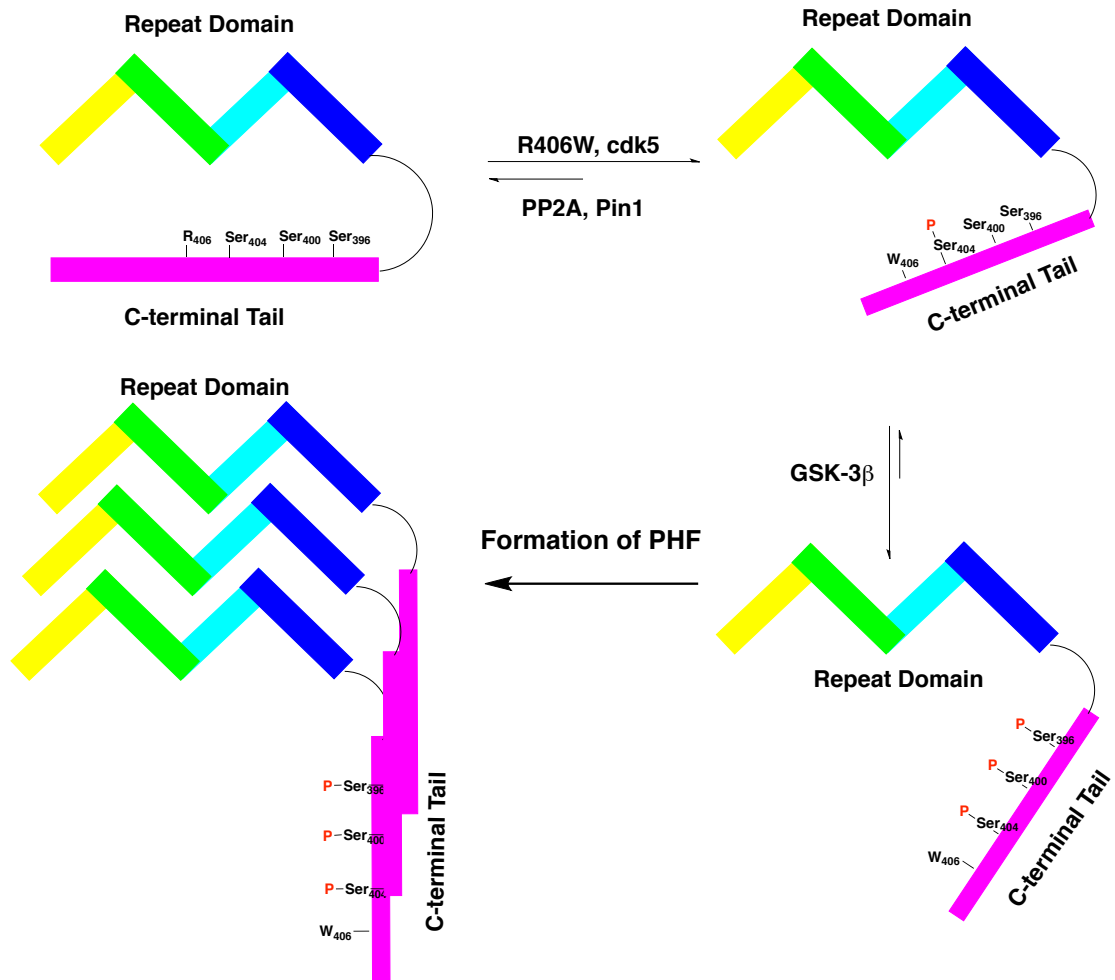


**Figure 3.5:** Schematic representation of the kinetic formation of paired helical filament formation promoted by both R406W mutation and phosphorylation of Ser<sub>404</sub>.

## Experimental

### Materials

Fmoc-L-amino acids were purchased from Chem-Impex (Wood Dale, IL) or Novabiochem (San Diego, CA). O-(1H-Benzotriazol-1-yl)-1,1,3,3-tetramethyluronium hexafluorophosphate (HBTU), O-(7-azabenzotriazol-1-yl)-1,1,3,3-tetramethyluronium hexafluorophosphate (HATU), Rink amide resin (loading capacity of 0.37 mmol/g), and diisopropylethylamine (DIPEA) were purchased from Chem-Impex. 1,2-Ethanedithiol (EDT) was purchased from TCI America (Portland, OR). Trifluoroacetic acid (TFA), triethylsilane (TES), phenol, thioanisole, and tetrazole were purchased from Acros. Piperidine was purchased from Aldrich. Acetonitrile (MeCN), methylene chloride (CH<sub>2</sub>Cl<sub>2</sub>), methanol (MeOH), chloroform (CHCl<sub>3</sub>), tetrahydrofuran (THF), dimethylformamide (DMF), pyridine, diethyl ether (Et<sub>2</sub>O), sodium chloride, acetic acid, and acetic anhydride were purchased from Fischer. 2,2,2-trifluoroethanol (TFE), and *O,O'*-dibenzyl-*N,N*-diisopropylphosphoramidite was purchased from Alfa Aesar. Deionized water was purified by a Milipore Synergy 185 water purification system with a Simpак2 cartridge.

### Phosphorylation of serine/threonine on peptides on solid phase

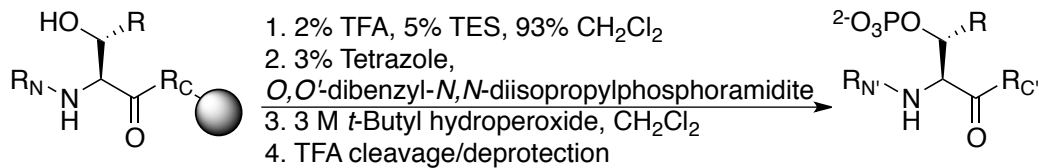


**Figure 3.6:** Scheme for the chemical phosphorylation of peptides on resin and subsequent cleavage/deprotection. R = CH<sub>3</sub> (Thr) or R = H (Ser).

Trityl-protected serine/threonine residues were incorporated at intended sites of chemical phosphorylation to allow for selective modification of the peptides on resin. The resin was swelled in CH<sub>2</sub>Cl in a fritted reaction vessel for 45 minutes. Trityl deprotection was effected using a solution of 2% TFA, 5% TES, and 93% CH<sub>2</sub>Cl<sub>2</sub> (3×3 mL, 1 minute each), followed by washing of the resin with CH<sub>2</sub>Cl<sub>2</sub>. To the resin was added 3 mL of 3% tetrazole solution in MeCN (1.35 mmol) and 500 μL of *O,O'*-dibenzyl-*N,N*-diisopropylphosphoramidite (1.52 mmol). The phosphitylation reaction was allowed to mix for 6 hours. The resin was then washed with DMF (3×3 mL) and CH<sub>2</sub>Cl<sub>2</sub> (3×3 mL). The resin was then treated with 4 mL of 3 M *tert*-butyl hydroperoxide in CH<sub>2</sub>Cl<sub>2</sub> for 1 hour, after which it was washed with DMF (3×3 mL), MeOH (3×3 mL), and CH<sub>2</sub>Cl<sub>2</sub> (3×3 mL). The resin was dried after washing with diethyl ether. The phosphorylated peptide was then subjected to cleavage from the resin and deprotection using reagent K (84% TFA and 4% each of H<sub>2</sub>O/phenol/thioanisole/ethanedithiol) or 92.5% TFA/5% TES/2.5% H<sub>2</sub>O for 3 hours.

### Synthesis and characterization data for all peptides

Peptides were synthesized on a Rainin PS3 peptide synthesizer or manually on Rink amide resin via standard Fmoc solid phase peptide synthesis using HBTU as a coupling reagent for all amino acids. 60 minute couplings were performed with 4 equivalents of canonical amino acids or 3 equivalents of unnatural amino acids. All peptides were acetylated on the N-terminus using 5% acetic anhydride in pyridine. All peptides were subjected to cleavage from resin and deprotection for 3 hours using reagent K (84% TFA and 4% each of H<sub>2</sub>O/phenol/thioanisole/ethanedithiol) or a solution of 92.5% TFA, 5% TES, and 2.5% H<sub>2</sub>O. TFA was removed by evaporation. Peptides were precipitated with cold ether and the precipitate was dried.

Resin containing Ac-TSPR peptide was swelled in CH<sub>2</sub>Cl<sub>2</sub> for 1 hour then rinsed (3 × 5 min) with a solution containing 5% TES, 2% TFA, and 93% CH<sub>2</sub>Cl<sub>2</sub> (to remove trityl protection groups on serine and threonine residues) then washed with CH<sub>2</sub>Cl<sub>2</sub>. The resin was then washed with 10 mL of a solution containing 5% TES, 10% TFA, and 85% CH<sub>2</sub>Cl<sub>2</sub> to selectively cleave the Pbf protected peptide from resin. The elution was collected in a 10 mL solution of H<sub>2</sub>O/MeCN (1:1) and subjected to reduced pressure to remove TFA and CH<sub>2</sub>Cl<sub>2</sub>. The solution was then lyophilized and purified via HPLC. The purified Ac-TSPR(Pbf)-NH<sub>2</sub> peptide was then deprotection for 2 hours using reagent K (84% TFA and 4% each of H<sub>2</sub>O/phenol/thioanisole/ethanedithiol). The TFA was removed by evaporation. Peptides were precipitated with cold ether and the precipitate was dried.

Resin containing Ac-T(OPO(OBn)<sub>2</sub>S(OPO(OBn)<sub>2</sub>PR(Pbf)) was swelled in CH<sub>2</sub>Cl<sub>2</sub> for 1 hour then washed with 10 mL of a solution containing 5% TES, 10% TFA, and 85% CH<sub>2</sub>Cl<sub>2</sub> (to selectively cleave the protected peptide). The elution was collected in a 10 mL solution of H<sub>2</sub>O/MeCN (1:1) and subjected to reduced pressure to

remove TFA and  $\text{CH}_2\text{Cl}_2$ . The solution was then lyophilized and purified via HPLC. The purified peptide  $\text{Ac-T(OPO(OBn)}_2\text{S(OPO(OBn)}_2\text{PR(Pbf)-NH}_2$  was then deprotection for 2 hours using reagent K (84% TFA and 4% each of  $\text{H}_2\text{O}$ /phenol/thioanisole/ethanedithiol). The TFA was removed by evaporation. Peptides were precipitated with cold ether and the precipitate was dried.

All dried peptides were dissolved in water, then filtered through a  $0.45\ \mu\text{m}$  syringe filter. All peptides were purified using reverse phase HPLC on a Vydac C18 semi-preparative column ( $250 \times 10\ \text{mm}$ ,  $5\text{-}10\ \mu\text{m}$  particle,  $300\ \text{\AA}$  pore) or on a Varian Microsorb MV C18 analytical column ( $250 \times 4.6\ \text{mm}$ ,  $3\text{-}5\ \mu\text{m}$  particle,  $100\ \text{\AA}$  pore) using a linear gradient of buffer B (20% water, 80% MeCN, and 0.05% TFA) in buffer A (98% water, 2% MeCN, and 0.06% TFA). Peptides were characterized by ESI-MS (positive ion mode) on an LCQ Advantage (Finnigan) or Shimadzu mass spectrometer.

**Table 3.6:** Purification procedure for synthetic peptides.

Peptide sequence	Peptide purification	$t_R$
Ac-TGPN-NH <sub>2</sub>	Isocratic 100% buffer A over 30 minutes	7.8 min
Ac-TGPCha-NH <sub>2</sub>	0-25% buffer B in buffer A over 60 minutes	53.1 min
Ac-TGPH-NH <sub>2</sub>	Isocratic 100% buffer A over 10 minutes followed by a linear gradient of 0-10% buffer B in buffer A over an additional 20 minutes	15.2 min
Ac-TGP(4-NO <sub>2</sub> -Phe)-NH <sub>2</sub>	0-25% buffer B in buffer A over 60 minutes	48.4 min
Ac-TGP(4-CF <sub>3</sub> -Phe)-NH <sub>2</sub>	0-35% buffer B in buffer A over 60 minutes	51.0 min
Ac-TGP(4-I-Phe)-NH <sub>2</sub>	0-30% buffer B in buffer A over 60 minutes	55.1 min
Ac-TGPF-NH <sub>2</sub>	0-15% buffer B in buffer A over 60 minutes	50.4 min
Ac-TGPY-NH <sub>2</sub>	Isocratic 100% buffer A over 10 minutes followed by a linear gradient of 0-10% buffer B in buffer A over an additional 50 minutes	42.9 min
Ac-TGPW-NH <sub>2</sub>	0-15% buffer B in buffer A over 60 minutes	52.6 min
Ac-TSPN-NH <sub>2</sub>	Isocratic 100% buffer A over 30 minutes	7.4 min
Ac-TSPR(Pbf)-NH <sub>2</sub>	0-45% buffer B in buffer A over 60 minutes	47.7 min
Ac-TSPR-NH <sub>2</sub>	Isocratic 100% buffer A over 30 minutes	20.7 min
Ac-TS(OPO <sub>3</sub> <sup>2-</sup> )PR-NH <sub>2</sub>	Isocratic 100% buffer A over 30 minutes	10.3 min
Ac-T(OPO <sub>3</sub> <sup>2-</sup> )SPR-NH <sub>2</sub>	Isocratic 100% buffer A over 30 minutes	7.1 min
Ac-T(OPO(OBn) <sub>2</sub> )-S(OPO(OBn) <sub>2</sub> )-PR(Pbf)-NH <sub>2</sub>	0-100% buffer B in buffer A over 60 minutes	47.0 min
Ac-T(OPO <sub>3</sub> <sup>2-</sup> )S(OPO <sub>3</sub> <sup>2-</sup> )PR-NH <sub>2</sub>	Isocratic 100% buffer A over 30 minutes	5.3 min
Ac-TSPW-NH <sub>2</sub>	0-15% buffer B in buffer A over 60 minutes	53.7 min
Ac-TS(OPO <sub>3</sub> <sup>2-</sup> )PW-NH <sub>2</sub>	Isocratic 100% buffer A over 20 minutes followed by a linear gradient of 0-20% buffer B in buffer A over an additional 40 minutes	46.1 min
Ac-T(OPO <sub>3</sub> <sup>2-</sup> )SPW-NH <sub>2</sub>	0-15% buffer B in buffer A over 60 minutes	43.0 min
Ac-T(OPO <sub>3</sub> <sup>2-</sup> )S(OPO <sub>3</sub> <sup>2-</sup> )PW-NH <sub>2</sub>	Isocratic 100% buffer A over 20 minutes followed by a linear gradient of 0-15% buffer B in buffer A over an additional 40 minutes	44.4 min
Ac-KSPVVSGDTSRHLNSV-NH <sub>2</sub>	0-30% buffer B in buffer A over 60 minutes	48.5 min
Ac-KSPVVSGDTS(OPO <sub>3</sub> <sup>2-</sup> )RHLNSV-NH <sub>2</sub>	0-20% buffer B in buffer A over 60 minutes	50.8 min
Ac-KSPVVSGDTSPWHLNSV-NH <sub>2</sub>	0-25% buffer B in buffer A over 60 minutes	50.0 min
Ac-KSPVVSGDTS(OPO <sub>3</sub> <sup>2-</sup> )PWHLSV-NH <sub>2</sub>	0-30% buffer B in buffer A over 60 minutes	55.4 min

**Table 3.7:** Characterization data for synthetic peptides.

Peptide sequence	Calculated mass	Observed mass
Ac-TGPN-NH <sub>2</sub>	428.2	451.3 (M+Na) <sup>1+</sup>
Ac-TGPCha-NH <sub>2</sub>	467.6	490.3 (M+Na) <sup>1+</sup>
Ac-TGPH-NH <sub>2</sub>	451.2	474.4 (M+Na) <sup>1+</sup>
Ac-TGP(4-NO <sub>2</sub> -Phe)-NH <sub>2</sub>	506.5	529.3 (M+Na) <sup>1+</sup>
Ac-TGP(4-CF <sub>3</sub> -Phe)-NH <sub>2</sub>	529.5	552.3 (M+Na) <sup>1+</sup>
Ac-TGP(4-I-Phe)-NH <sub>2</sub>	587.4	610.2 (M+Na) <sup>1+</sup>
Ac-TGPF-NH <sub>2</sub>	461.2	484.3 (M+Na) <sup>1+</sup>
Ac-TGPY-NH <sub>2</sub>	477.2	500.3 (M+Na) <sup>1+</sup>
Ac-TGPW-NH <sub>2</sub>	500.2	523.4 (M+Na) <sup>1+</sup>
Ac-TSPN-NH <sub>2</sub>	458.5	481.4 (M+Na) <sup>1+</sup>
Ac-TSPR(Pbf)-NH <sub>2</sub>	753.9	775.4 (M+Na) <sup>1+</sup>
Ac-TSPR-NH <sub>2</sub>	500.6	501.3 (M+H) <sup>1+</sup>
Ac-TS(OPO <sub>3</sub> <sup>2-</sup> )PR-NH <sub>2</sub>	580.5	603.3 (M+Na) <sup>1+</sup>
Ac-T(OPO <sub>3</sub> <sup>2-</sup> )SPR-NH <sub>2</sub>	580.5	581.2 (M+H) <sup>1+</sup>
Ac-T(OPO(OBn) <sub>2</sub> )S(OPO(OBn) <sub>2</sub> )PR(Pbf)-NH <sub>2</sub>	1272.5	1273.3 (M+H) <sup>1+</sup>
Ac-T(OPO <sub>3</sub> <sup>2-</sup> )S(OPO <sub>3</sub> <sup>2-</sup> )PR-NH <sub>2</sub>	660.5	683.4 (M+Na) <sup>1+</sup>
Ac-TSPW-NH <sub>2</sub>	531.6	553.3 (M+Na) <sup>1+</sup>
Ac-TS(OPO <sub>3</sub> <sup>2-</sup> )PW-NH <sub>2</sub>	610.5	633.3 (M+Na) <sup>1+</sup>
Ac-T(OPO <sub>3</sub> <sup>2-</sup> )SPW-NH <sub>2</sub>	610.5	633.2 (M+Na) <sup>1+</sup>
Ac-T(OPO <sub>3</sub> <sup>2-</sup> )S(OPO <sub>3</sub> <sup>2-</sup> )PW-NH <sub>2</sub>	690.5	727.4 (M+K) <sup>1+</sup>
Ac-KSPVVSGDTSPRHLSNV-NH <sub>2</sub>	1821.2	911.3 (M+2H) <sup>2+</sup>
Ac-KSPVVSGDTS(OPO <sub>3</sub> <sup>2-</sup> )PRHLSNV-NH <sub>2</sub>	1899.9	951.2 (M+2H) <sup>2+</sup>
Ac-KSPVVSGDTSPWHLSNV-NH <sub>2</sub>	1849.9	927.3 (M+2H) <sup>2+</sup>
Ac-KSPVVSGDTS(OPO <sub>3</sub> <sup>2-</sup> )PWHLSNV-NH <sub>2</sub>	1929.9	966.3 (M+2H) <sup>2+</sup>

### NMR spectroscopy

NMR spectra of peptides were collected at 278 K or 298 K on a Bruker AVX 600 MHz NMR spectrometer equipped with a triple resonance cryoprobe or a TXI probe. Peptides were dissolved in a solution containing 5 mM phosphate buffer (pH 4.0, 7.2, 8.0, or 8.5) and 25 mM NaCl in 90% H<sub>2</sub>O/10% D<sub>2</sub>O. The pH of each individual sample was recorded and adjusted as necessary using dilute HCl or NaOH. All NMR spectra were internally referenced with 100 μM TSP. 1-D NMR spectra were collected with a Watergate pulse sequence and a relaxation delay of 3 s. Coupling constants between the amide and α-protons (<sup>3</sup>J<sub>αN</sub>) were determined directly from the 1-D spectra. Errors in <sup>3</sup>J<sub>αN</sub> are estimated to be ≤ 0.2 Hz. TOCSY NMR

spectra were collected with a Watergate TOCSY pulse sequence, sweep widths of 6009 Hz (7,200 Hz for Trp-containing peptides) in  $t_1$  and  $t_2$ ,  $400 \times 2048$  complex data points, 8 scans per  $t_1$  increment, a relaxation delay of 1.5 s, and a TOCSY mixing time of 60 ms.

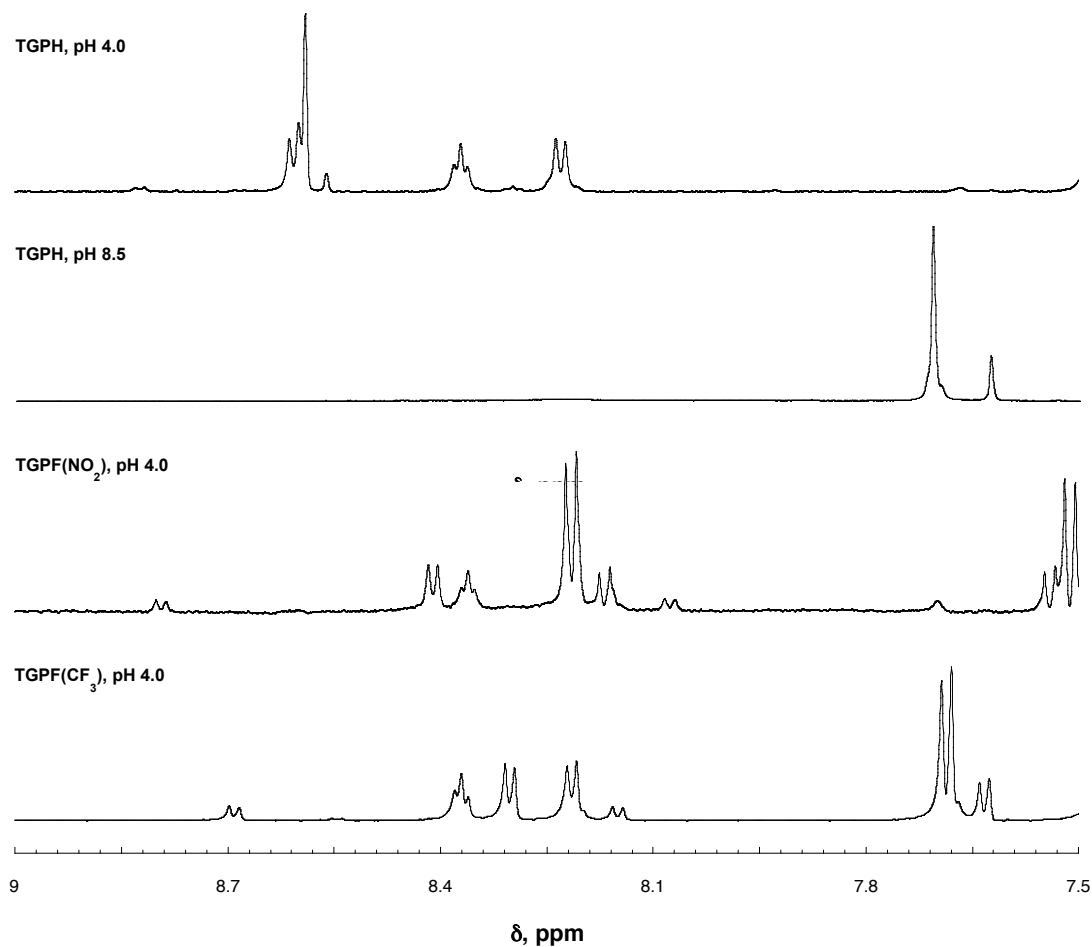


**Figure 3.7:**  $^1\text{H}$  NMR spectra (amide region) of Ac-TGPX-NH<sub>2</sub> peptides. Peptides were dissolved in 5 mM phosphate buffer (pH 4.0 or 8.5) containing 25 mM NaCl in 90% H<sub>2</sub>O/10% D<sub>2</sub>O. Data were collected at 298 K.

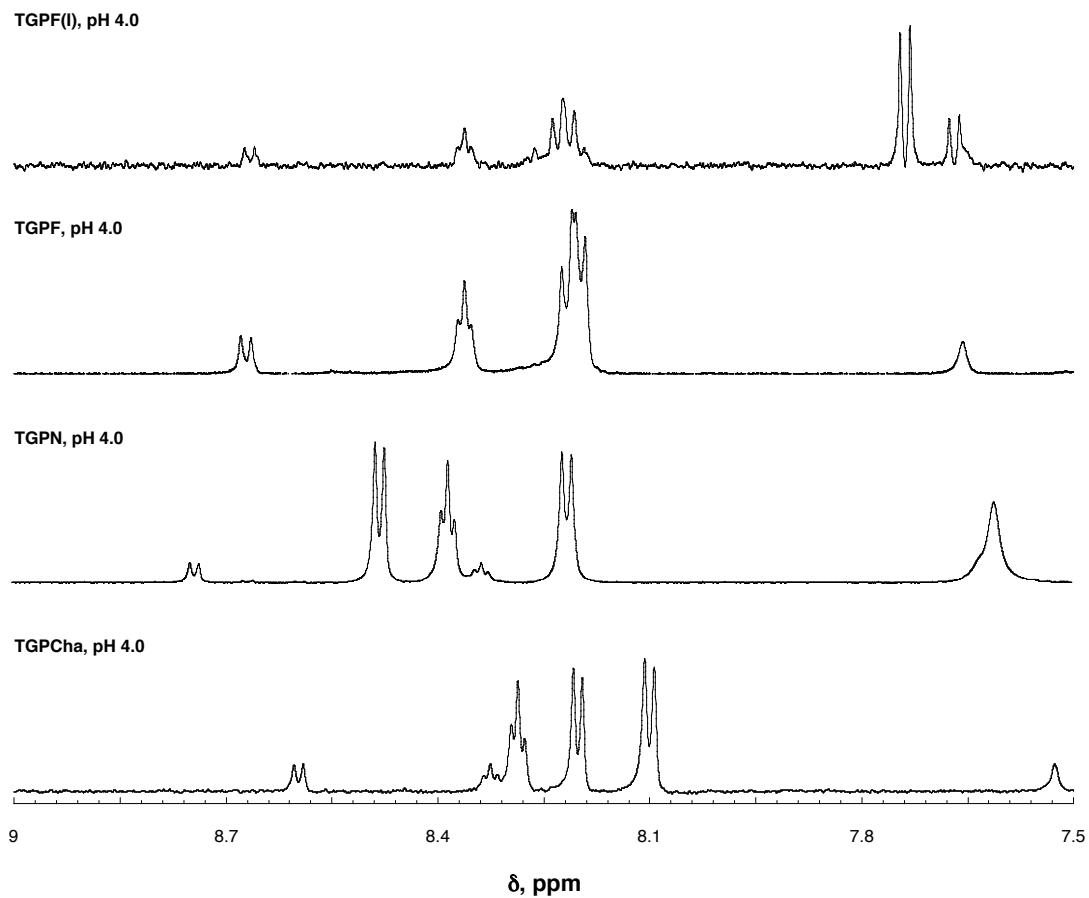


**Figure 3.8:**  $^1\text{H}$  NMR spectra (amide region) of Ac-TGPX-NH<sub>2</sub> peptides. Peptides were dissolved in 5 mM phosphate buffer (pH 4.0 or 8.5) containing 25 mM NaCl in 90% H<sub>2</sub>O/10% D<sub>2</sub>O. Data were collected at 298 K.

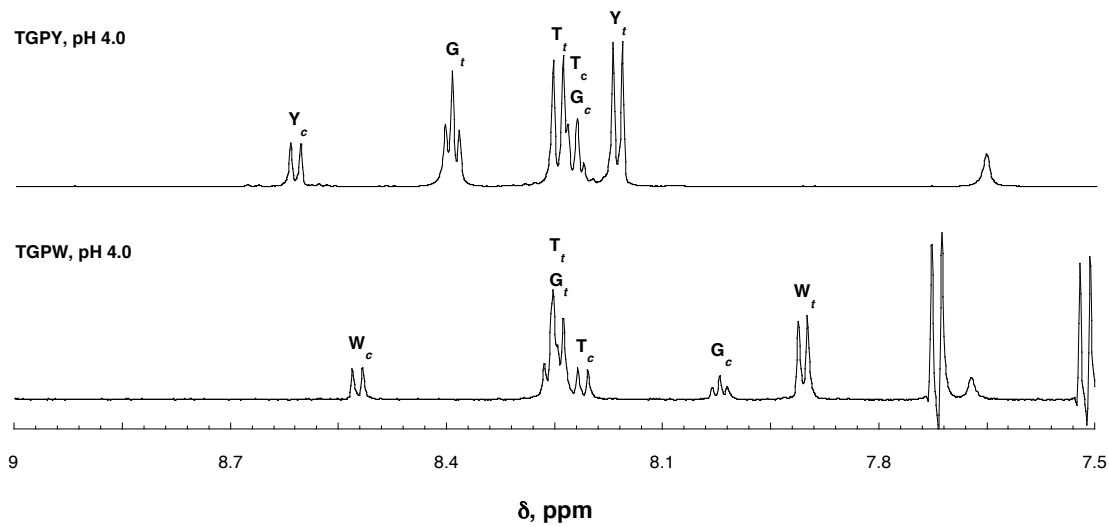


**Figure 3.9:**  $^1\text{H}$  NMR spectra (amide region) of Ac-TGPX-NH<sub>2</sub> peptides. Peptides were dissolved in 5 mM phosphate buffer (pH 4.0 or 8.5) containing 25 mM NaCl in 90% H<sub>2</sub>O/10% D<sub>2</sub>O. Data were collected at 298 K.

Peptide	Isomer	$\delta, H^N$ (ppm)	$^3 J_{\alpha N}$ (Hz)	$\delta, H\alpha$ (ppm)	$\delta, H\beta$ (ppm)	$\delta, H\gamma$ (ppm)	$\delta, H\delta$ (ppm)
<b>TGPY</b>							
Thr	<i>cis</i>	8.22	n.a.	4.41	4.31	1.24	n.a.
	<i>trans</i>	8.24	8.3	4.38	4.27	1.24	n.a.
Gly	<i>cis</i>	8.22	n.d.	3.59, 2.94	n.a.	n.a.	n.a.
	<i>trans</i>	8.40	5.8	4.01	n.a.	n.a.	n.a.
Pro	<i>cis</i>	n.a.	n.a.	4.43	2.33, 2.02	1.87, 1.70	3.48
	<i>trans</i>	n.a.	n.a.	4.35	2.15, 1.94	1.71, 1.63	3.60
Tyr	<i>cis</i>	8.61	8.5	4.71	3.22, 2.84	n.a.	n.a.
	<i>trans</i>	8.16	7.8	4.57	3.17, 2.94	n.a.	n.a.
<b>TGPW</b>							
Thr	<i>cis</i>	8.18	n.d.	4.38	4.29	1.23	n.a.
	<i>trans</i>	8.21	8.5	4.37	4.25	1.22	n.a.
Gly	<i>cis</i>	8.00	6.4	3.19, 2.48	n.a.	n.a.	n.a.
	<i>trans</i>	8.22	n.d.	4.00, 3.90	n.a.	n.a.	n.a.
Pro	<i>cis</i>	n.a.	n.a.	4.30	2.27, 1.98	1.81, 1.60	3.36
	<i>trans</i>	n.a.	n.a.	4.30	2.06, 1.55	2.03	3.45
Trp	<i>cis</i>	8.48	8.4	4.85	3.41, 3.15	n.a.	n.a.
	<i>trans</i>	7.87	7.5	4.67	3.38, 3.25	n.a.	n.a.

**Table 3.8:** Summary of  $^1H$  NMR data. Data were collected in 5 mM phosphate buffer (pH 4.0) containing 25 mM NaCl. Data were collected at 298 K. <sup>a</sup> n.d. = not determined due to spectral overlap. <sup>b</sup> n.a. = not applicable.

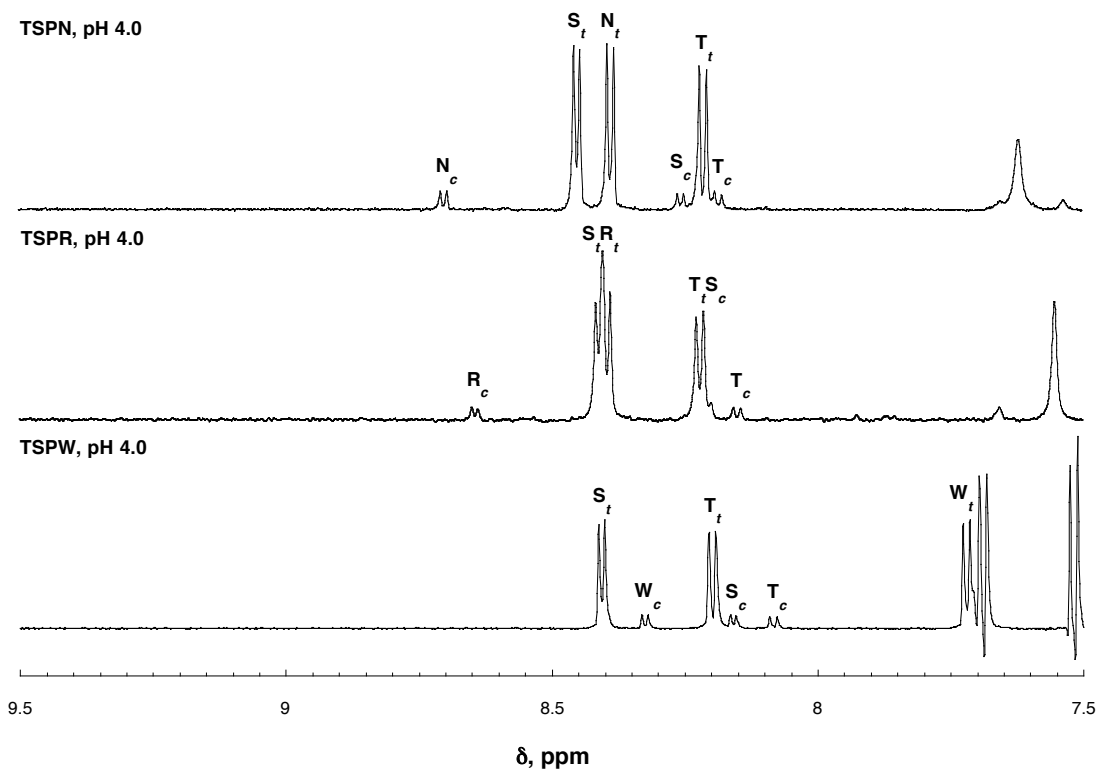


**Figure 3.9:**  $^1\text{H}$  NMR spectra (amide region) of Ac-TSPX-NH<sub>2</sub> peptides. Peptides were dissolved in 5 mM phosphate buffer (pH 4.0 or 8.5) containing 25 mM NaCl in 90% H<sub>2</sub>O/10% D<sub>2</sub>O. Data were collected at 298 K.

Peptide	Isomer	$\delta, H^N$ (ppm)	$^3J_{\alpha N}$ (Hz)	$\delta, H\alpha$ (ppm)	$\delta, H\beta$ (ppm)	$\delta, H\gamma$ (ppm)	$\delta, H\delta$ (ppm)
<b>TSPN</b>							
Ac	<i>cis</i>	n.a.	n.a.	n.a.	n.a.	n.a.	n.a.
	<i>trans</i>	n.a.	n.a.	2.09	n.a.	n.a.	n.a.
Thr	<i>cis</i>	8.18	8.0	4.32	4.16	1.18	n.a.
	<i>trans</i>	8.21	7.6	4.32	4.17	1.18	n.a.
Ser	<i>cis</i>	8.26	7.0	4.57	3.75	n.a.	n.a.
	<i>trans</i>	8.45	6.8	4.80	3.85	n.a.	n.a.
Pro	<i>cis</i>	n.a.	n.a.	n.d.	n.d.	n.d.	n.d.
	<i>trans</i>	n.a.	n.a.	4.45	2.30, 2.03	3.85, 3.77	1.96
Asn	<i>cis</i>	8.70	7.3	4.66	2.84, 2.78	n.a.	n.a.
	<i>trans</i>	8.39	8.1	4.65	2.83, 2.71	n.a.	n.a.
NH <sub>2</sub>	<i>cis</i>	n.a.	n.a.	n.a.	n.a.	n.a.	n.a.
	<i>trans</i>	n.a.	n.a.	n.a.	n.a.	n.a.	n.a.
<b>TSPR</b>							
Ac	<i>cis</i>	n.a.	n.a.	n.d.	n.a.	n.a.	n.a.
	<i>trans</i>	n.a.	n.a.	2.09	n.a.	n.a.	n.a.
Thr	<i>cis</i>	8.15	8.0	4.30	4.18	n.d.	n.a.
	<i>trans</i>	8.22	8.1	4.34	4.20	1.21	n.a.
Ser	<i>cis</i>	8.20	n.d.	4.59	3.75	n.a.	n.a.
	<i>trans</i>	8.41	n.d.	4.79	3.86	n.a.	n.a.
Pro	<i>cis</i>	n.a.	n.a.	n.d.	n.d.	n.d.	n.d.
	<i>trans</i>	n.a.	n.a.	4.45	2.32, 2.03	1.94	3.86, 3.74
Arg	<i>cis</i>	8.63	6.6	4.27	n.d.	n.d.	n.d.
	<i>trans</i>	8.39	n.d.	4.28	1.86, 1.77	1.68	3.22
NH <sub>2</sub>	<i>cis</i>	n.a.	n.a.	7.66, n.d.	n.a.	n.a.	n.a.
	<i>trans</i>	n.a.	n.a.	7.55, 7.15	n.a.	n.a.	n.a.
<b>TSPW</b>							
Ac	<i>cis</i>	n.a.	n.a.	n.d.	n.a.	n.a.	n.a.
	<i>trans</i>	n.a.	n.a.	2.08	n.a.	n.a.	n.a.
Thr	<i>cis</i>	8.08	8.5	4.33	4.16	1.19	n.a.
	<i>trans</i>	8.19	7.9	4.32	4.18	1.18	n.a.
Ser	<i>cis</i>	8.16	6.9	4.32	3.70	n.a.	n.a.
	<i>trans</i>	8.39	6.7	4.72	3.76, 3.69	n.a.	n.a.
Pro	<i>cis</i>	n.a.	n.a.	4.67	2.14, 2.00	1.77	3.38, 3.26
	<i>trans</i>	n.a.	n.a.	4.30	2.12, 1.84	1.61, 1.51	3.70, 3.48
Trp	<i>cis</i>	8.31	6.8	4.65	3.35	n.a.	n.a.
	<i>trans</i>	7.71	7.6	4.70	3.38, 3.21	n.a.	n.a.
NH <sub>2</sub>	<i>cis</i>	7.45, 7.03	n.a.	n.a.	n.a.	n.a.	n.a.
	<i>trans</i>	7.26, 7.12	n.a.	n.a.	n.a.	n.a.	n.a.

**Table 3.9:** Summary of <sup>1</sup>H NMR data for Ac-TSPX-NH<sub>2</sub> peptides. Data were collected in 5 mM phosphate buffer (pH 4.0) containing 25 mM NaCl. Data were collected at 298 K.. <sup>a</sup>n.d. = not determined due to spectral overlap or peak resolution. <sup>b</sup>n.a. = not applicable.

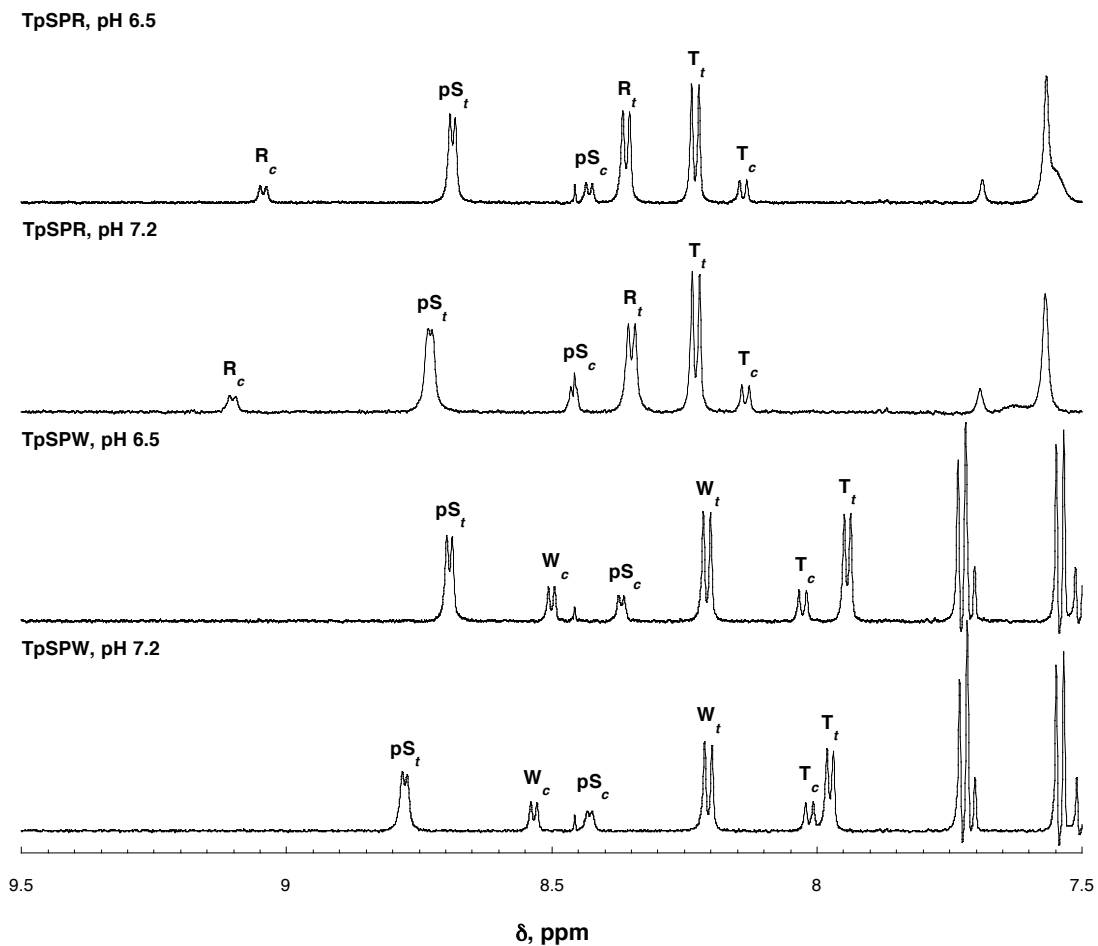


**Figure 3.10:**  $^1\text{H}$  NMR spectra (amide region) of Ac-TpSPX-NH<sub>2</sub> peptides. pS indicates phosphorylated serine residue. Peptides were dissolved in 5 mM phosphate buffer (pH 6.5 or 7.2) containing 25 mM NaCl in 90% H<sub>2</sub>O/10% D<sub>2</sub>O. Data were collected at 298 K.

Peptide	Isomer	$\delta, H^N$ (ppm)	$^3 J_{\alpha N}$ (Hz)	$\delta, H\alpha$ (ppm)	$\delta, H\beta$ (ppm)	$\delta, H\gamma$ (ppm)	$\delta, H\delta$ (ppm)
<b>TpSPR, pH 6.5</b>							
Ac	<i>cis</i>	n.a.	n.a.	n.d.	n.a.	n.a.	n.a.
	<i>trans</i>	n.a.	n.a.	2.12	n.a.	n.a.	n.a.
Thr	<i>cis</i>	8.12	8.4	4.32	4.19	1.22	n.a.
	<i>trans</i>	8.21	8.3	4.37	4.25	1.22	n.a.
pSer	<i>cis</i>	8.42	7.0	4.68	3.95	n.a.	n.a.
	<i>trans</i>	8.69	5.6	4.86	4.10	n.a.	n.a.
Pro	<i>cis</i>	n.a.	n.a.	4.89	2.42, 1.98	2.14	3.60
	<i>trans</i>	n.a.	n.a.	4.44	2.32, 1.96	2.06	3.85
Arg	<i>cis</i>	9.04	7.1	4.31	1.80	1.67	n.d.
	<i>trans</i>	8.34	7.6	4.33	1.85	1.65	3.21
NH <sub>2</sub>	<i>cis</i>	7.69	n.a.	n.a.	n.a.	n.a.	n.a.
	<i>trans</i>	7.57, 7.13	n.a.	n.a.	n.a.	n.a.	n.a.
<b>TpSPR, pH 7.2</b>							
Ac	<i>cis</i>	n.a.	n.a.	n.d.	n.a.	n.a.	n.a.
	<i>trans</i>	n.a.	n.a.	2.11	n.a.	n.a.	n.a.
Thr	<i>cis</i>	8.13	8.3	4.33	4.19	1.22	n.a.
	<i>trans</i>	8.22	8.4	4.37	4.26	1.22	n.a.
pSer	<i>cis</i>	8.45	4.4	4.65	3.95, 3.87	n.d.	n.d.
	<i>trans</i>	8.71	4.8	4.81	4.08, 4.04	n.d.	n.d.
Pro	<i>cis</i>	n.a.	n.a.	n.d.	n.d.	n.d.	n.d.
	<i>trans</i>	n.a.	n.a.	4.44	2.09, 2.05	1.96	3.87
Arg	<i>cis</i>	9.10	6.9	4.32	1.79	n.d.	n.d.
	<i>trans</i>	8.35	7.4	4.34	1.85	1.66	3.21
NH <sub>2</sub>	<i>cis</i>	7.69	n.a.	n.a.	n.a.	n.a.	n.a.
	<i>trans</i>	7.57, 7.13	n.a.	n.a.	n.a.	n.a.	n.a.

**Table 3.10:** Summary of <sup>1</sup>H NMR data for Ac-TpSPR-NH<sub>2</sub> peptide. Data were collected in 5 mM phosphate buffer (pH 6.5 or 7.2) containing 25 mM NaCl. Data were collected at 298 K. <sup>a</sup> n.d. = not determined due to spectral overlap or peak resolution. <sup>b</sup> n.a. = not applicable.

Peptide	Isomer	$\delta$ , H <sup>N</sup> (ppm)	<sup>3</sup> J <sub>dN</sub> (Hz)	$\delta$ , H $\alpha$ (ppm)	$\delta$ , H $\beta$ (ppm)	$\delta$ , H $\gamma$ (ppm)	$\delta$ , H $\delta$ (ppm)
<b>TpSPW, pH 6.5</b>							
Ac	<i>cis</i>	n.a.	n.a.	2.07	n.a.	n.a.	n.a.
	<i>trans</i>	n.a.	n.a.	2.11	n.a.	n.a.	n.a.
Thr	<i>cis</i>	8.02	8.7	4.33	4.17	1.20	n.a.
	<i>trans</i>	8.19	8.2	4.34	4.24	1.22	n.a.
pSer	<i>cis</i>	8.28	6.0	4.35	3.93, 3.89	n.a.	n.a.
	<i>trans</i>	8.59	6.1	4.74	4.02	n.a.	n.a.
Pro	<i>cis</i>	n.a.	n.a.	4.76	n.d.	n.d.	n.d.
	<i>trans</i>	n.a.	n.a.	4.31	2.12	1.90	3.72, 3.55
Trp	<i>cis</i>	8.44	7.0	4.64	3.38, 3.30	n.d.	n.d.
	<i>trans</i>	7.88	7.1	4.68	3.36, 3.30	n.d.	n.d.
NH <sub>2</sub>	<i>cis</i>	7.46, 7.04	n.a.	n.a.	n.a.	n.a.	n.a.
	<i>trans</i>	7.30, 7.07	n.a.	n.a.	n.a.	n.a.	n.a.
<b>TpSPW, pH 7.2</b>							
Ac	<i>cis</i>	n.a.	n.a.	n.d.	n.a.	n.a.	n.a.
	<i>trans</i>	n.a.	n.a.	2.11	n.a.	n.a.	n.a.
Thr	<i>cis</i>	8.00	8.6	4.34	4.19	1.19	n.a.
	<i>trans</i>	8.18	8.3	4.35	4.26	1.20	n.a.
pSer	<i>cis</i>	8.42	5.5	4.30	3.88	n.a.	n.a.
	<i>trans</i>	8.76	5.3	4.69	3.97	n.a.	n.a.
Pro	<i>cis</i>	n.a.	n.a.	n.d.	n.d.	n.d.	n.d.
	<i>trans</i>	n.a.	n.a.	4.31	2.13, 1.91	1.84, 1.62	3.88
Trp	<i>cis</i>	8.51	6.7	4.64	3.39, 3.30	n.a.	n.a.
	<i>trans</i>	7.95	7.2	4.68	3.35, 3.30	n.a.	n.a.
NH <sub>2</sub>	<i>cis</i>	7.48, 7.06	n.a.	n.a.	n.a.	n.a.	n.a.
	<i>trans</i>	7.31, 7.08	n.a.	n.a.	n.a.	n.a.	n.a.

**Table 3.11:** Summary of <sup>1</sup>H NMR data for Ac-TpSPW-NH<sub>2</sub> peptide. Data were collected in 5 mM phosphate buffer (pH 6.5 or 7.2) containing 25 mM NaCl. Data were collected at 298 K. <sup>a</sup> n.d. = not determined due to spectral overlap or peak resolution. <sup>b</sup> n.a. = not applicable.

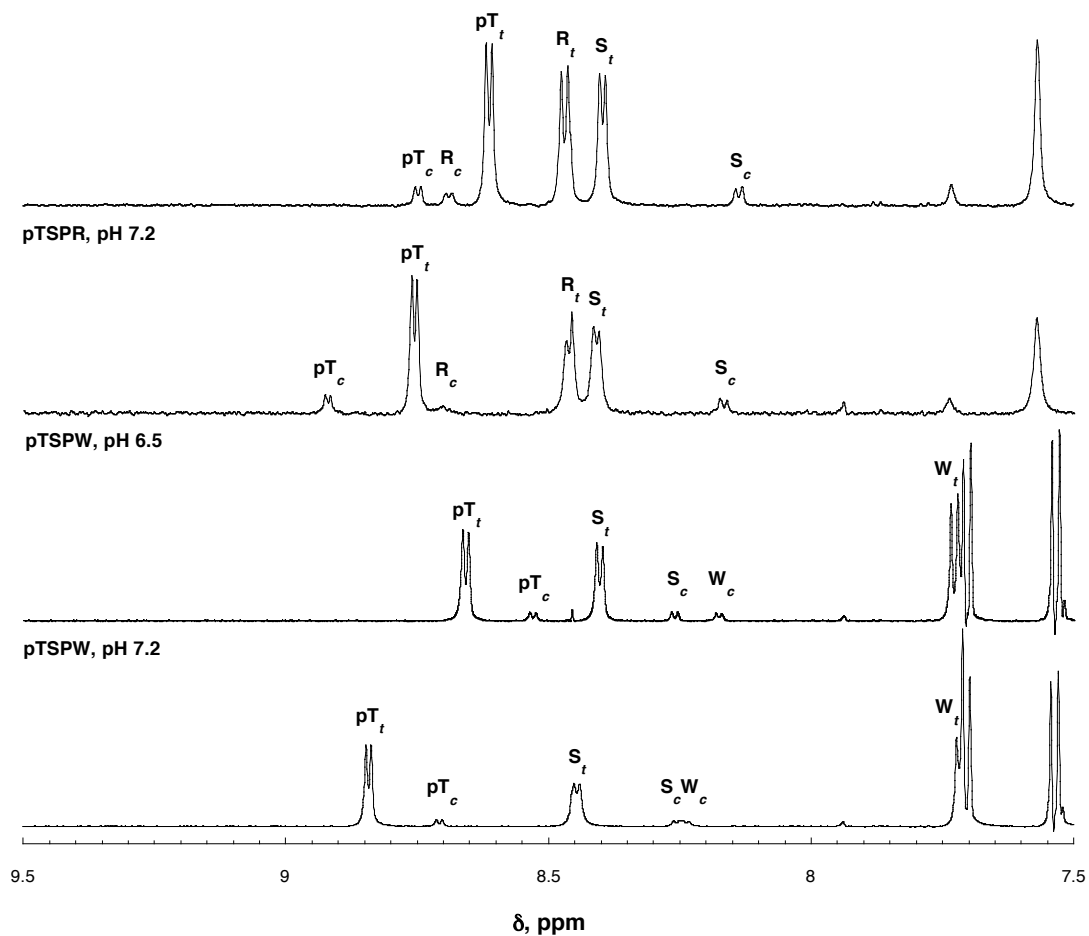


**Figure 3.11:**  $^1\text{H}$  NMR spectra (amide region) of **Ac-pTSPX-NH<sub>2</sub>** peptides. pS indicates phosphorylated serine residue. Peptides were dissolved in 5 mM phosphate buffer (pH 6.5 or 7.2) containing 25 mM NaCl in 90% H<sub>2</sub>O/10% D<sub>2</sub>O. Data were collected at 298 K.

Peptide	Isomer	$\delta$ , H <sup>N</sup> (ppm)	$^3J_{\alpha N}$ (Hz)	$\delta$ , H $\alpha$ (ppm)	$\delta$ , H $\beta$ (ppm)	$\delta$ , H $\gamma$ (ppm)	$\delta$ , H $\delta$ (ppm)
<b>pTSPR, pH 6.5</b>							
Ac	<i>cis</i>	n.a.	n.a.	n.d.	n.a.	n.a.	n.a.
	<i>trans</i>	n.a.	n.a.	2.09	n.a.	n.a.	n.a.
pThr	<i>cis</i>	8.75	6.3	4.16	4.18	1.30	n.a.
	<i>trans</i>	8.61	6.6	4.31	4.51	1.30	n.a.
Ser	<i>cis</i>	8.13	7.7	4.60	3.77	n.a.	n.a.
	<i>trans</i>	8.40	6.5	4.78	3.87	n.a.	n.a.
Pro	<i>cis</i>	n.a.	n.a.	n.d.	n.d.	n.d.	n.d.
	<i>trans</i>	n.a.	n.a.	4.46	2.34	2.06, 1.94	3.87, 3.73
Arg	<i>cis</i>	8.69	6.9	4.29	n.d.	n.d.	n.d.
	<i>trans</i>	8.47	7.5	4.31	1.88	1.75, 1.66	3.21
NH <sub>2</sub>	<i>cis</i>	7.73, 7.12	n.a.	n.a.	n.a.	n.a.	n.a.
	<i>trans</i>	7.57, 7.16	n.a.	n.a.	n.a.	n.a.	n.a.
<b>pTSPR, pH 7.2</b>							
Ac	<i>cis</i>	n.a.	n.a.	n.d.	n.a.	n.a.	n.a.
	<i>trans</i>	n.a.	n.a.	2.08	n.a.	n.a.	n.a.
pThr	<i>cis</i>	8.91	5.6	4.10	4.37	1.30	n.a.
	<i>trans</i>	8.75	6.1	4.24	4.43	1.29	n.a.
Ser	<i>cis</i>	8.16	8.1	4.61	3.76	n.a.	n.a.
	<i>trans</i>	8.41	6.2	4.80	3.87	n.a.	n.a.
Pro	<i>cis</i>	n.a.	n.a.	n.d.	n.d.	n.d.	n.d.
	<i>trans</i>	n.a.	n.a.	4.45	3.87, 3.73	2.34	2.05, 1.93
Arg	<i>cis</i>	8.70	n.d.	n.d.	n.d.	n.d.	n.d.
	<i>trans</i>	8.46	7.5	4.31	1.89	1.76, 1.69	3.23
NH <sub>2</sub>	<i>cis</i>	7.74, 7.12	n.a.	n.a.	n.a.	n.a.	n.a.
	<i>trans</i>	7.57, 7.15	n.a.	n.a.	n.a.	n.a.	n.a.

**Table 3.12:** Summary of <sup>1</sup>H NMR data for Ac-pTSPR-NH<sub>2</sub> peptide. Data were collected in 5 mM phosphate buffer (pH 6.5 or 7.2) containing 25 mM NaCl. Data were collected at 298 K. <sup>a</sup> n.d. = not determined due to spectral overlap or peak resolution. <sup>b</sup> n.a. = not applicable.

Peptide	Isomer	$\delta$ , H <sup>N</sup> (ppm)	<sup>3</sup> J <sub>dN</sub> (Hz)	$\delta$ , H $\alpha$ (ppm)	$\delta$ , H $\beta$ (ppm)	$\delta$ , H $\gamma$ (ppm)	$\delta$ , H $\delta$ (ppm)
<b>pTSPW, pH 6.5</b>							
Ac	<i>cis</i>	n.a.	n.a.	n.d.	n.a.	n.a.	n.a.
	<i>trans</i>	n.a.	n.a.	2.08	n.a.	n.a.	n.a.
pThr	<i>cis</i>	8.53	7.3	4.29	4.49	1.32	n.a.
	<i>trans</i>	8.66	6.5	4.23	4.47	1.28	n.a.
Ser	<i>cis</i>	8.26	6.6	4.63	3.38, 3.32	n.a.	n.a.
	<i>trans</i>	8.40	6.9	4.68	3.75, 3.66	n.a.	n.a.
Pro	<i>cis</i>	n.a.	n.a.	n.d.	n.d.	n.d.	n.d.
	<i>trans</i>	n.a.	n.a.	4.46	2.33	2.05, 1.94	3.87, 3.74
Trp	<i>cis</i>	8.17	6.8	4.34	3.72	n.a.	n.a.
	<i>trans</i>	7.73	7.9	4.69	3.38, 3.19	n.a.	n.a.
NH <sub>2</sub>	<i>cis</i>	7.47, 7.07	n.a.	n.a.	n.a.	n.a.	n.a.
	<i>trans</i>	7.23, 7.15	n.a.	n.a.	n.a.	n.a.	n.a.
<b>pTSPW, pH 7.2</b>							
Ac	<i>cis</i>	n.a.	n.a.	n.d.	n.a.	n.a.	n.a.
	<i>trans</i>	n.a.	n.a.	2.06	n.a.	n.a.	n.a.
pThr	<i>cis</i>	8.7	6.6	4.21	4.42	1.31	n.a.
	<i>trans</i>	8.84	5.8	4.15	4.38	1.27	n.a.
Ser	<i>cis</i>	8.25	n.d.	4.63	3.37, 3.31	n.a.	n.a.
	<i>trans</i>	8.44	6.5	4.68	3.75, 3.68	n.a.	n.a.
Pro	<i>cis</i>	n.a.	n.a.	n.d.	n.d.	n.d.	n.d.
	<i>trans</i>	n.a.	n.a.	4.45	2.33	2.05, 1.94	3.86, 3.73
Trp	<i>cis</i>	8.23	n.d.	4.36	3.74	n.a.	n.a.
	<i>trans</i>	7.72	n.d.	4.68	3.38, 3.20	n.a.	n.a.
NH <sub>2</sub>	<i>cis</i>	7.47, 7.07	n.a.	n.a.	n.a.	n.a.	n.a.
	<i>trans</i>	7.23, 7.16	n.a.	n.a.	n.a.	n.a.	n.a.

**Table 3.13:** Summary of <sup>1</sup>H NMR data for Ac-pTSPW-NH<sub>2</sub> peptide. Data were collected in 5 mM phosphate buffer (pH 6.5 or 7.2) containing 25 mM NaCl. Data were collected at 298 K. <sup>a</sup> n.d. = not determined due to spectral overlap or peak resolution. <sup>b</sup> n.a. = not applicable.

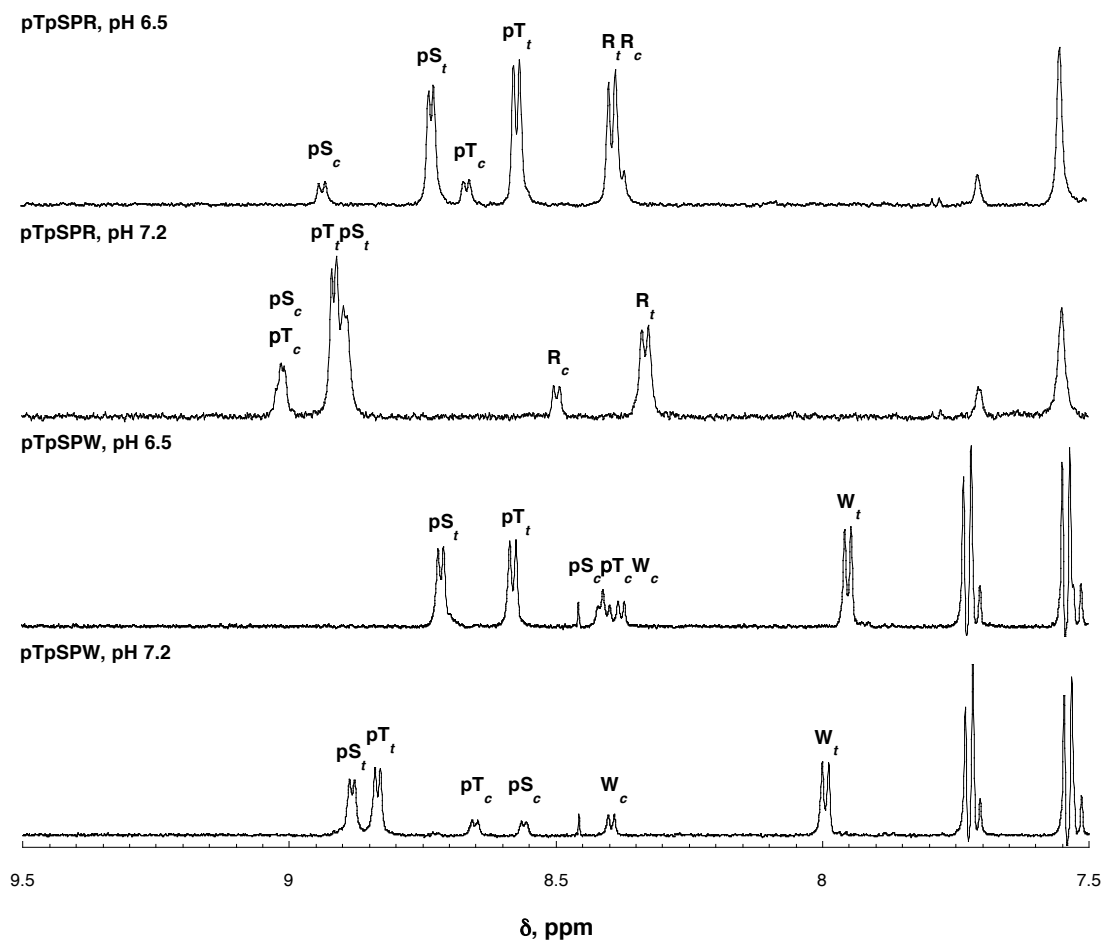


**Figure 3.12:** <sup>1</sup>H NMR spectra (amide region) of Ac-pTpSPX-NH<sub>2</sub> peptides. pS indicates phosphorylated serine residue. Peptides were dissolved in 5 mM phosphate buffer (pH 6.5 or 7.2) containing 25 mM NaCl in 90% H<sub>2</sub>O/10% D<sub>2</sub>O. Data were collected at 298 K.

Peptide	Isomer	$\delta$ , H <sup>N</sup> (ppm)	$^3J_{\alpha N}$ (Hz)	$\delta$ , H $\alpha$ (ppm)	$\delta$ , H $\beta$ (ppm)	$\delta$ , H $\gamma$ (ppm)	$\delta$ , H $\delta$ (ppm)
<b>pTpSPR, pH 6.5</b>							
Ac	<i>cis</i>	n.a.	n.a.	n.d.	n.a.	n.a.	n.a.
	<i>trans</i>	n.a.	n.a.	2.10	n.a.	n.a.	n.a.
pThr	<i>cis</i>	8.66	6.6	4.23	4.44	1.31	n.a.
	<i>trans</i>	8.57	7.0	4.36	4.52	1.31	n.a.
pSer	<i>cis</i>	8.94	7.0	n.d.	3.96	n.a.	n.a.
	<i>trans</i>	8.73	5.5	4.85	4.07	n.a.	n.a.
Pro	<i>cis</i>	n.a.	n.a.	n.d.	2.39, 2.13	1.97	3.60
	<i>trans</i>	n.a.	n.a.	4.45	2.33, 2.09	2.04, 1.96	3.91, 3.83
Arg	<i>cis</i>	8.37	n.d.	4.69	n.d.	n.d.	3.94
	<i>trans</i>	8.39	7.6	4.32	1.89, 1.83	1.68	3.22
NH <sub>2</sub>	<i>cis</i>	7.71, 7.09	n.a.	n.a.	n.a.	n.a.	n.a.
	<i>trans</i>	7.55, 7.12	n.a.	n.a.	n.a.	n.a.	n.a.
<b>pTpSPR, pH 7.2</b>							
Ac	<i>cis</i>	n.a.	n.a.	n.d.	n.a.	n.a.	n.a.
	<i>trans</i>	n.a.	n.a.	2.06	n.a.	n.a.	n.a.
pThr	<i>cis</i>	9.01	n.d.	4.30	4.07	1.31	n.a.
	<i>trans</i>	8.91	5.3	4.19	4.36	1.30	n.a.
pSer	<i>cis</i>	9.01	n.d.	n.d.	4.09	n.a.	n.a.
	<i>trans</i>	8.89	4.5	4.81	4.07, 4.04	n.a.	n.a.
Pro	<i>cis</i>	n.a.	n.a.	4.94	2.41, 2.12	1.99	3.60
	<i>trans</i>	n.a.	n.a.	4.44	2.33, 2.09	2.05, 1.97	3.90, 3.87
Arg	<i>cis</i>	8.50	7.0	4.67	n.d.	n.d.	3.91
	<i>trans</i>	8.33	7.5	4.32	1.86	1.68	3.20
NH <sub>2</sub>	<i>cis</i>	7.70, 7.08	n.a.	n.a.	n.a.	n.a.	n.a.
	<i>trans</i>	7.55, 7.01	n.a.	n.a.	n.a.	n.a.	n.a.

**Table 3.14:** Summary of <sup>1</sup>H NMR data for Ac-pTpSPR-NH<sub>2</sub> peptide. Data were collected in 5 mM phosphate buffer (pH 6.5 or 7.2) containing 25 mM NaCl. Data were collected at 298 K. <sup>a</sup> n.d. = not determined due to spectral overlap or peak resolution. <sup>b</sup> n.a. = not applicable.

Peptide	Isomer	$\delta$ , H <sup>N</sup> (ppm)	<sup>3</sup> J <sub>dN</sub> (Hz)	$\delta$ , H $\alpha$ (ppm)	$\delta$ , H $\beta$ (ppm)	$\delta$ , H $\gamma$ (ppm)	$\delta$ , H $\delta$ (ppm)
<b>pTpSPW, pH 6.5</b>							
Ac	<i>cis</i>	n.a.	n.a.	2.08	n.a.	n.a.	n.a.
	<i>trans</i>	n.a.	n.a.	2.09	n.a.	n.a.	n.a.
pThr	<i>cis</i>	8.40	n.d.	4.33	4.49	1.32	n.a.
	<i>trans</i>	8.57	6.8	4.32	4.53	1.32	n.a.
pSer	<i>cis</i>	8.41	n.d.	4.42	3.93	n.a.	n.a.
	<i>trans</i>	8.71	6.0	4.72	3.99	n.a.	n.a.
Pro	<i>cis</i>	n.a.	n.a.	n.d.	n.d.	1.78	3.18
	<i>trans</i>	n.a.	n.a.	4.33	2.13, 1.92	1.82, 1.61	3.75, 3.58
Trp	<i>cis</i>	8.37	7.3	4.63	3.40, 3.29	n.a.	n.a.
	<i>trans</i>	7.95	7.2	4.65	3.32, 3.30	n.a.	n.a.
NH2	<i>cis</i>	7.46	n.a.	n.a.	n.a.	n.a.	n.a.
	<i>trans</i>	7.31, 7.08	n.d.	n.a.	n.a.	n.a.	n.a.
<b>pTpSPW, pH 7.2</b>							
Ac	<i>cis</i>	n.a.	n.a.	2.06	n.a.	n.a.	n.a.
	<i>trans</i>	n.a.	n.a.	2.07	n.a.	n.a.	n.a.
pThr	<i>cis</i>	8.65	6.9	4.23	4.42	1.32	n.a.
	<i>trans</i>	8.83	5.9	4.20	4.42	1.31	n.a.
pSer	<i>cis</i>	8.56	5.1	4.48	3.89	n.a.	n.a.
	<i>trans</i>	8.88	5.7	4.70	3.97	n.a.	n.a.
Pro	<i>cis</i>	n.a.	n.a.	n.d.	n.d.	1.78, 1.68	3.16
	<i>trans</i>	n.a.	n.a.	4.32	2.13, 1.92	1.83, 1.60	3.77, 3.59
Trp	<i>cis</i>	8.39	7.3	4.63	3.40, 3.29	n.a.	n.a.
	<i>trans</i>	7.99	7.2	4.66	3.32	n.a.	n.a.
NH2	<i>cis</i>	7.43, n.d.	n.a.	n.a.	n.a.	n.a.	n.a.
	<i>trans</i>	7.31, 7.06	n.a.	n.a.	n.a.	n.a.	n.a.

**Table 3.15:** Summary of <sup>1</sup>H NMR data for Ac-pTpSPW-NH<sub>2</sub> peptides. Data were collected in 5 mM phosphate buffer (pH 6.5 or 7.2) containing 25 mM NaCl. Data were collected at 298 K. <sup>a</sup>n.d. = not determined due to spectral overlap or peak resolution. <sup>b</sup>n.a. = not applicable.

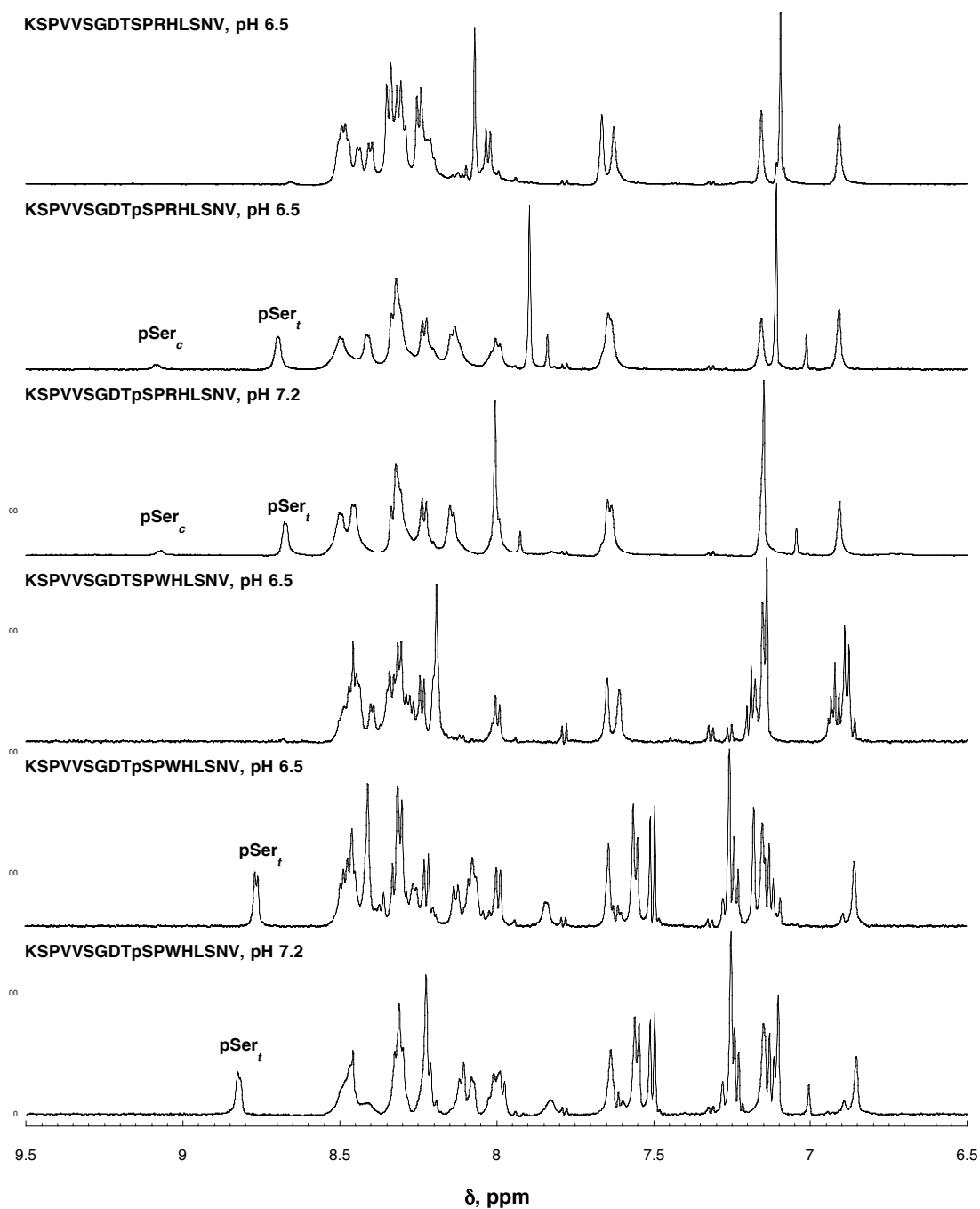


**Figure 3.13:**  $^1\text{H}$  NMR spectra (amide region) of Ac-KSPVVSGDTxSPXHLSNV-NH<sub>2</sub> peptides. pS indicates phosphorylated serine residue. Peptides were dissolved in 5 mM phosphate buffer (pH 6.5 or 7.2) containing 25 mM NaCl in 90% H<sub>2</sub>O/10% D<sub>2</sub>O. Data were collected at 298 K.

## Full TOCSY Spectra of all Peptides

Ac-TGPY-NH<sub>2</sub> (pH 4.0, 298 K)

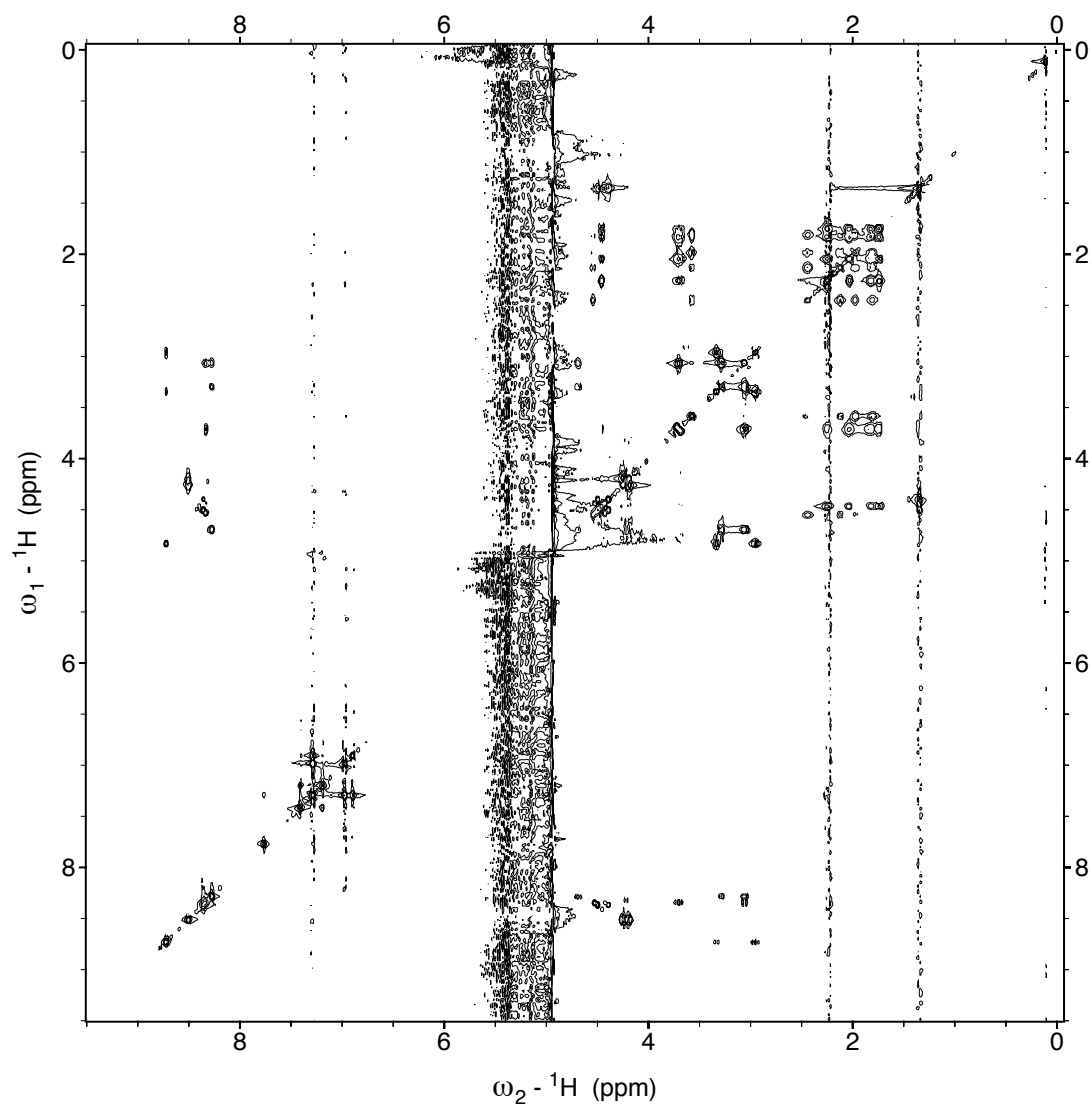


**Figure 3.14:** Full TOCSY spectra of Ac-TGPY-NH<sub>2</sub> (pH 4.0, 298 K). Peptide was dissolved in 5 mM phosphate buffer containing 25 mM NaCl in 90% H<sub>2</sub>O/10% D<sub>2</sub>O. Data were collected at 298 K.

Ac-TGPW-NH<sub>2</sub> (pH 4.0, 298 K)

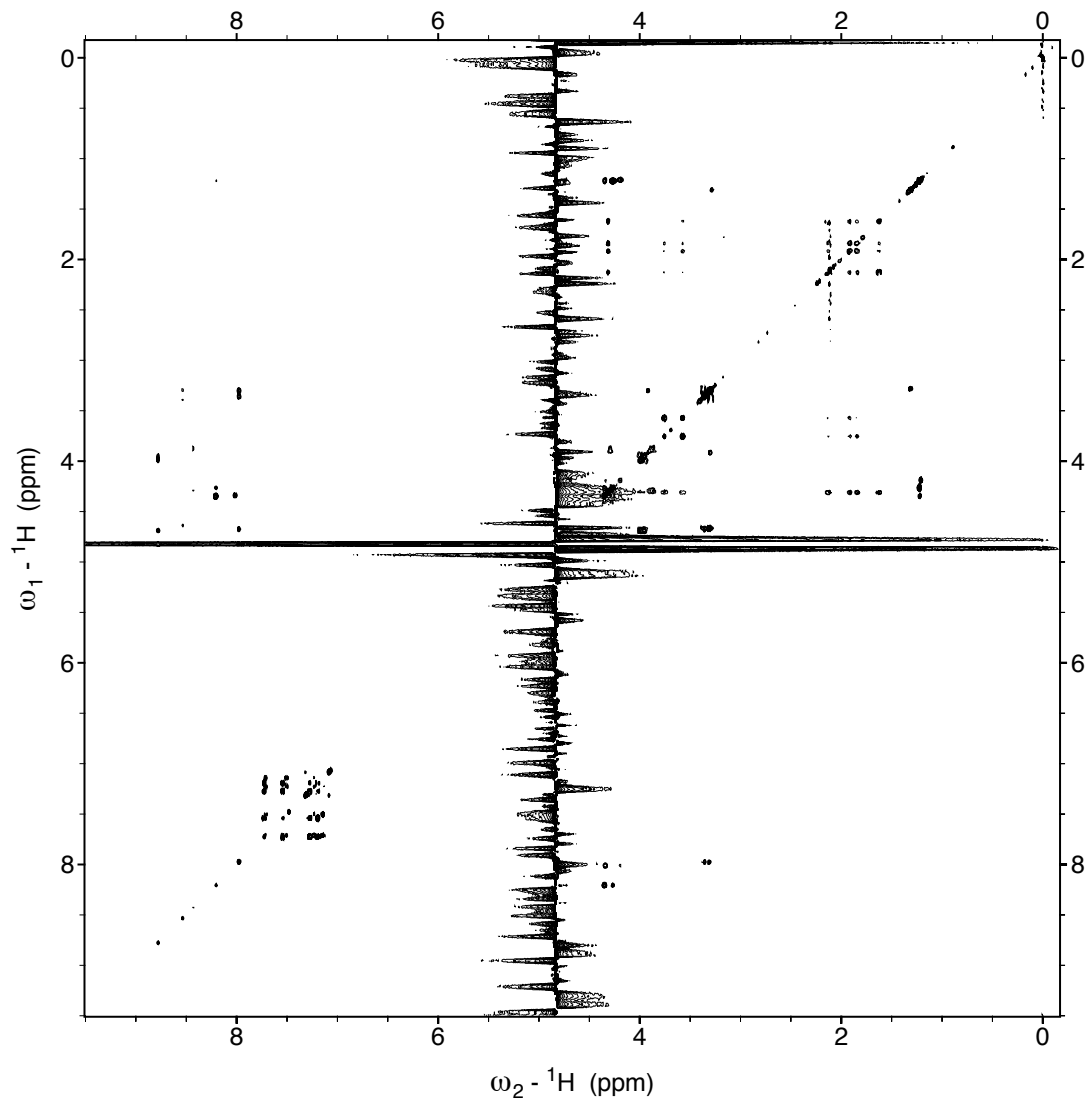


**Figure 3.15:** Full TOCSY spectra of Ac-TGPW-NH<sub>2</sub> (pH 4.0, 298 K). Peptide was dissolved in 5 mM phosphate buffer containing 25 mM NaCl in 90% H<sub>2</sub>O/10% D<sub>2</sub>O. Data were collected at 298 K.

Ac-TSPN-NH<sub>2</sub> (pH 4.0, 298 K)

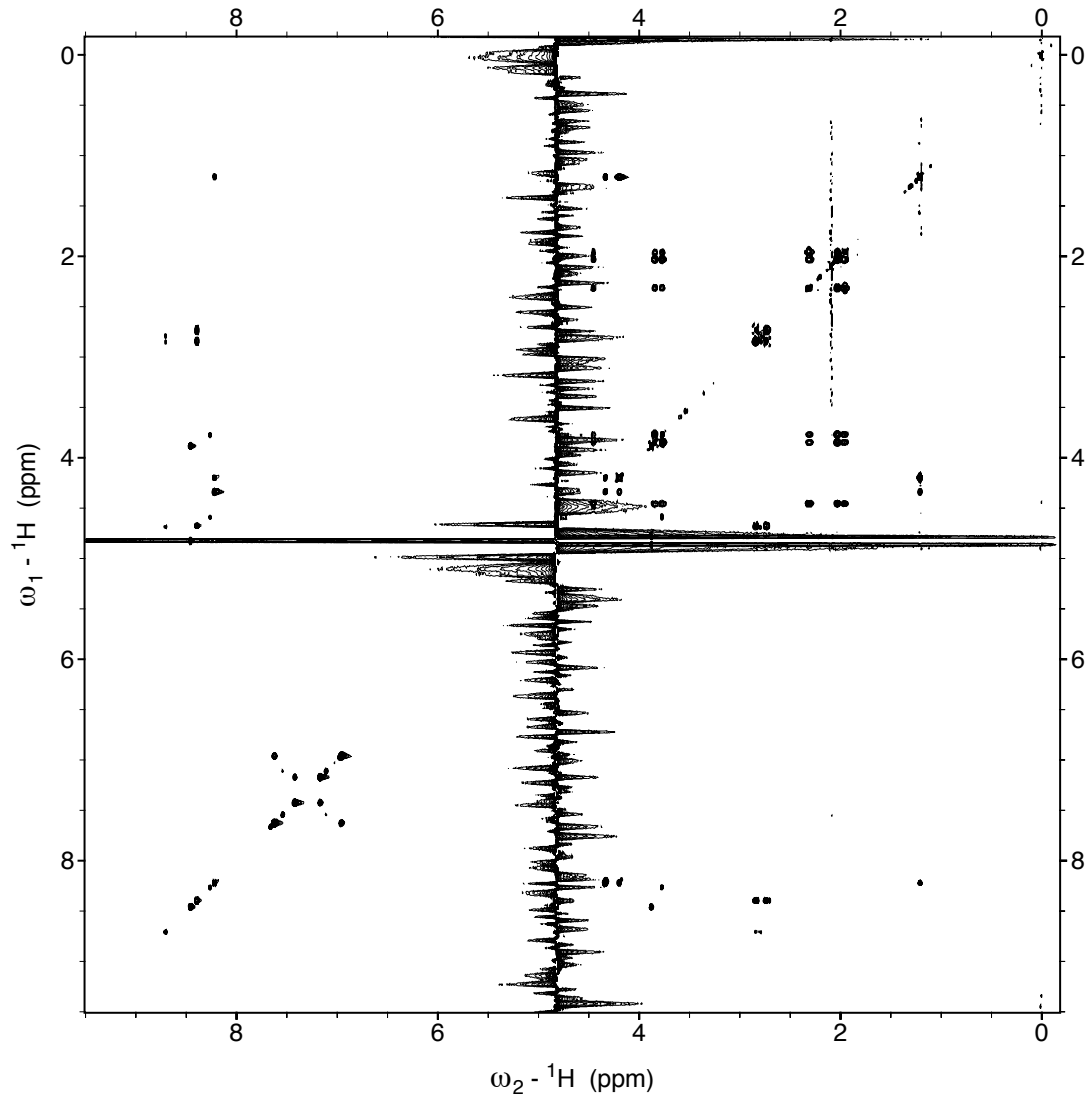


**Figure 3.16:** Full TOCSY spectra of Ac-TSPN-NH<sub>2</sub> (pH 4.0, 298 K). Peptide was dissolved in 5 mM phosphate buffer containing 25 mM NaCl in 90% H<sub>2</sub>O/10% D<sub>2</sub>O. Data were collected at 298 K.

Ac-TSPR-NH<sub>2</sub> (pH 4.0, 298 K)

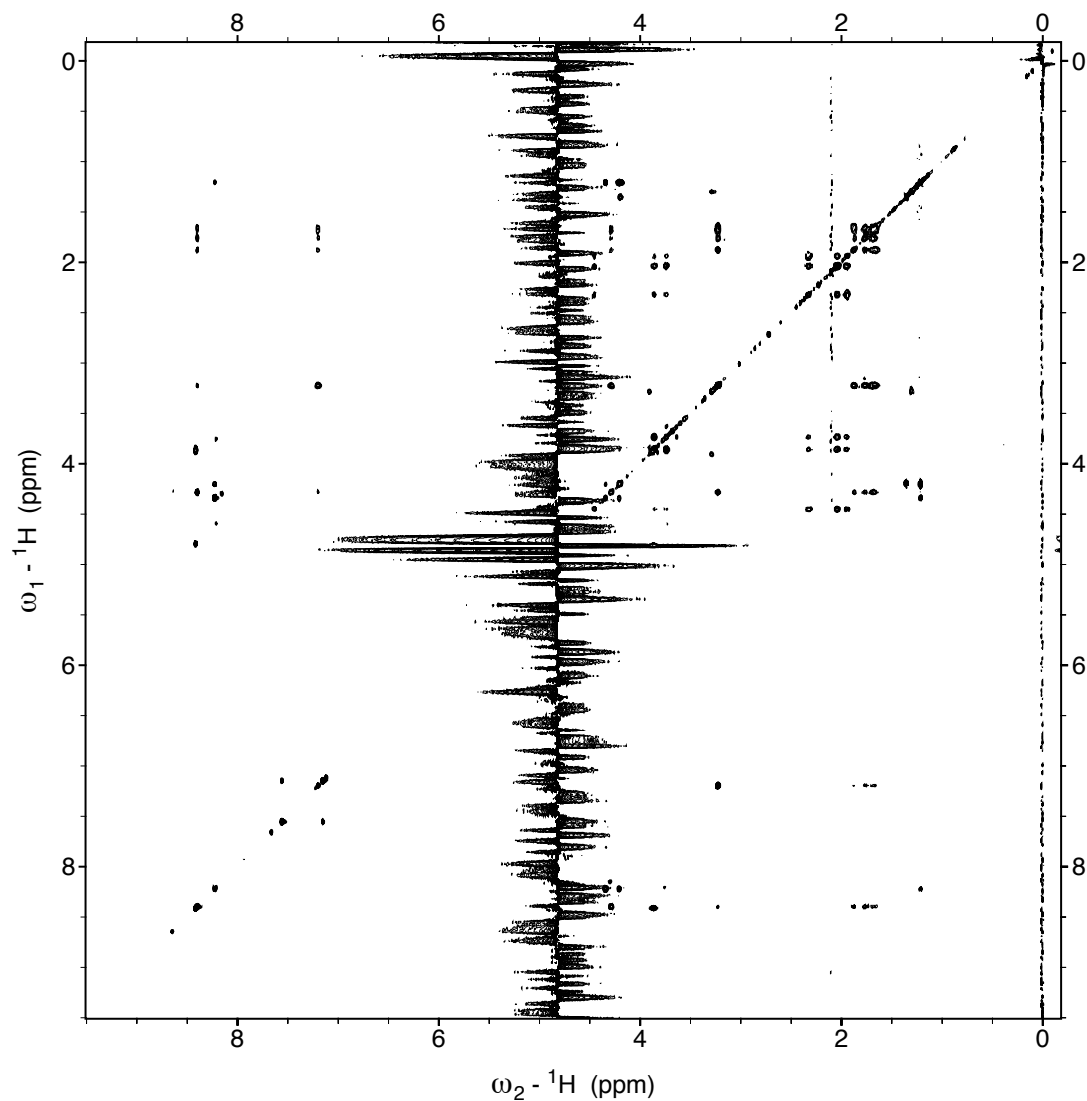


**Figure 3.17:** Full TOCSY spectra of Ac-TSPR-NH<sub>2</sub> (pH 4.0, 298 K). Peptide was dissolved in 5 mM phosphate buffer containing 25 mM NaCl in 90% H<sub>2</sub>O/10% D<sub>2</sub>O. Data were collected at 298 K.

Ac-TSPW-NH<sub>2</sub> (pH 4.0, 298 K)

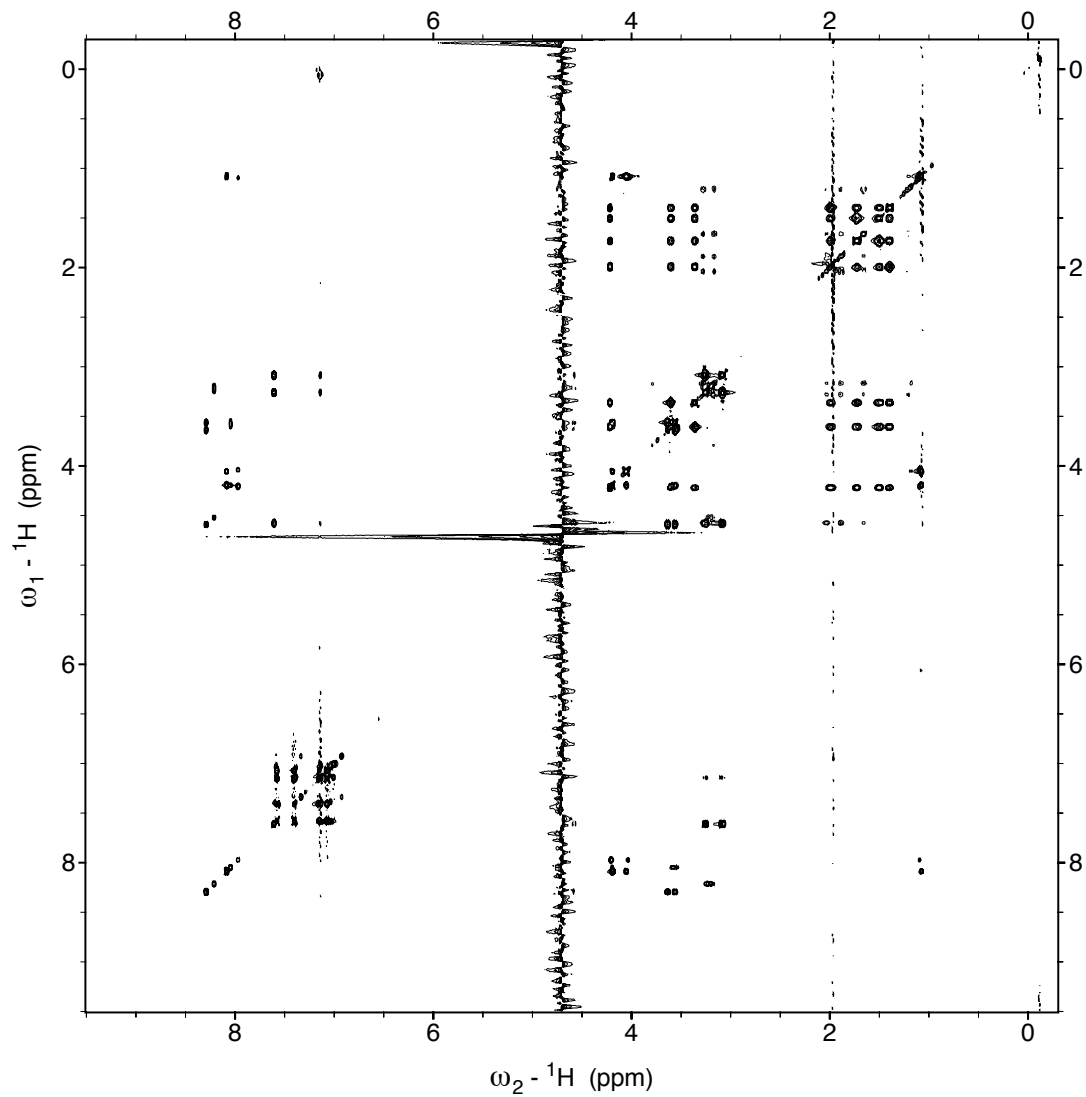


**Figure 3.18:** Full TOCSY spectra of Ac-TSPW-NH<sub>2</sub> (pH 4.0, 298 K). Peptide was dissolved in 5 mM phosphate buffer containing 25 mM NaCl in 90% H<sub>2</sub>O/10% D<sub>2</sub>O. Data were collected at 298 K.

Ac-TpSPR-NH<sub>2</sub> (pH 6.5, 298 K)

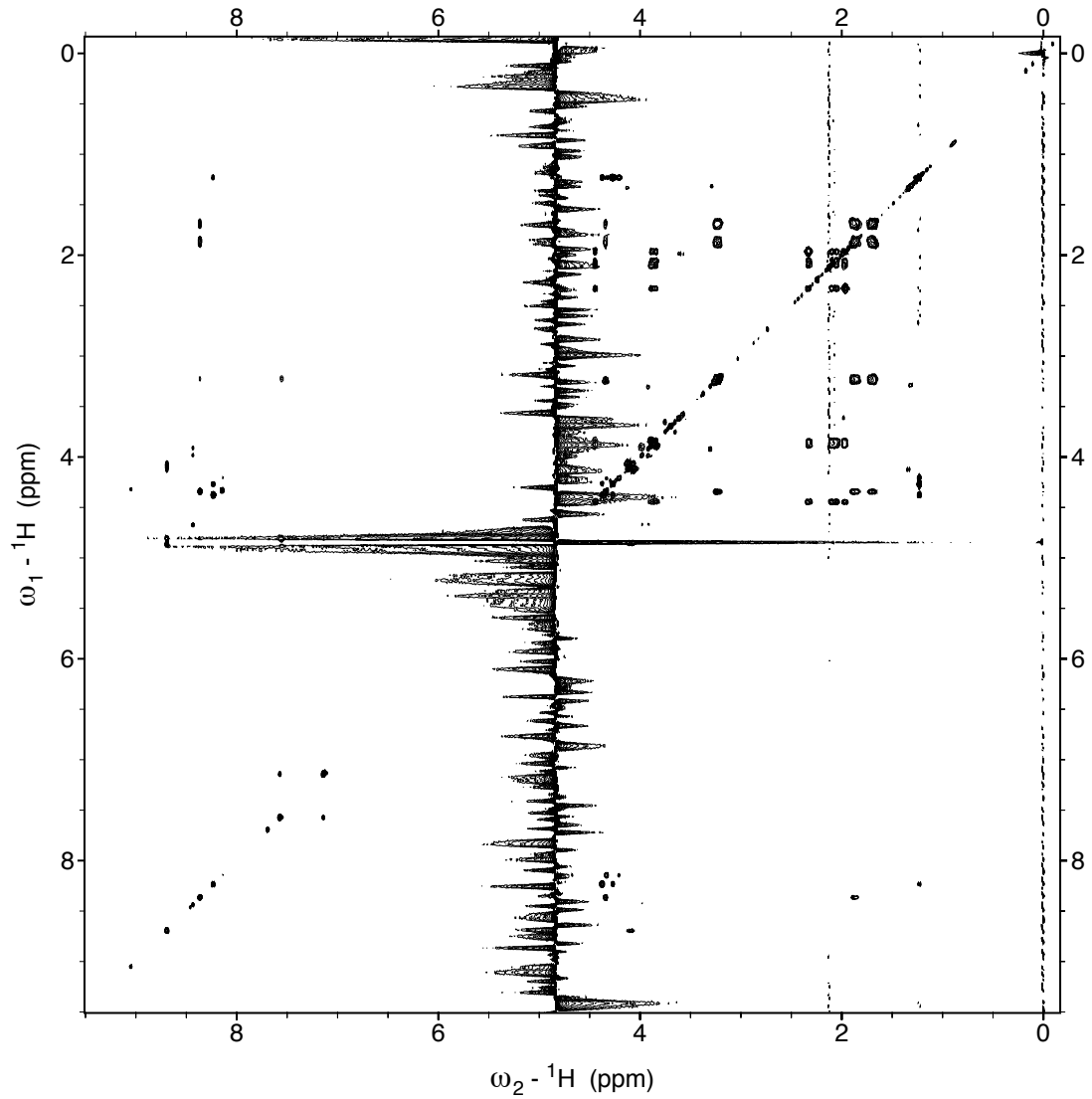


**Figure 3.19:** Full TOCSY spectra of Ac-TpSPR-NH<sub>2</sub> (pH 6.5, 298 K). Peptide was dissolved in 5 mM phosphate buffer containing 25 mM NaCl in 90% H<sub>2</sub>O/10% D<sub>2</sub>O. Data were collected at 298 K.

Ac-TpSPR-NH<sub>2</sub> (pH 7.2, 298 K)

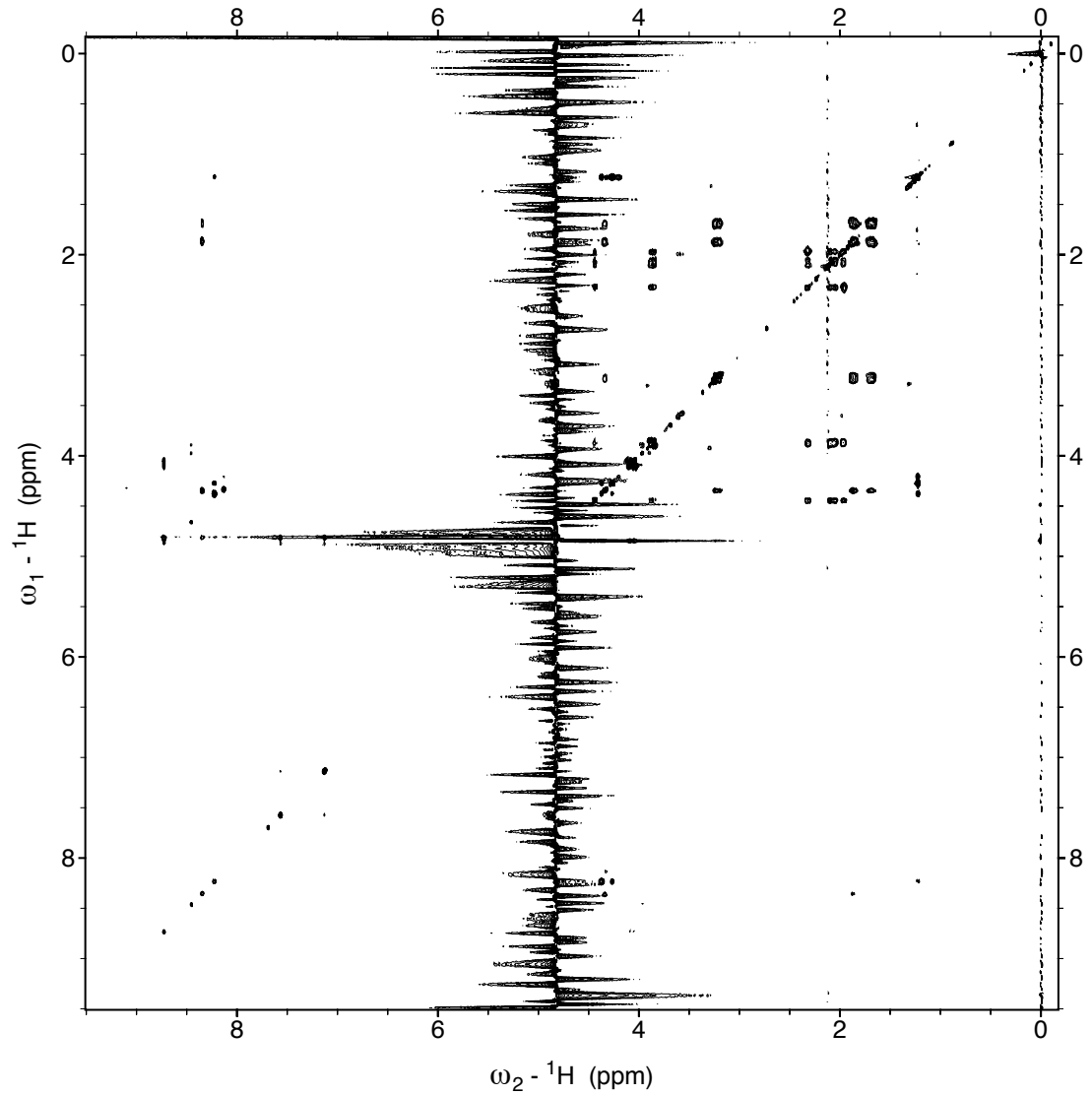


**Figure 3.20:** Full TOCSY spectra of Ac-TpSPR-NH<sub>2</sub> (pH 7.2, 298 K). Peptide was dissolved in 5 mM phosphate buffer containing 25 mM NaCl in 90% H<sub>2</sub>O/10% D<sub>2</sub>O. Data were collected at 298 K.

Ac-TpSPW-NH<sub>2</sub> (pH 6.5, 298 K)

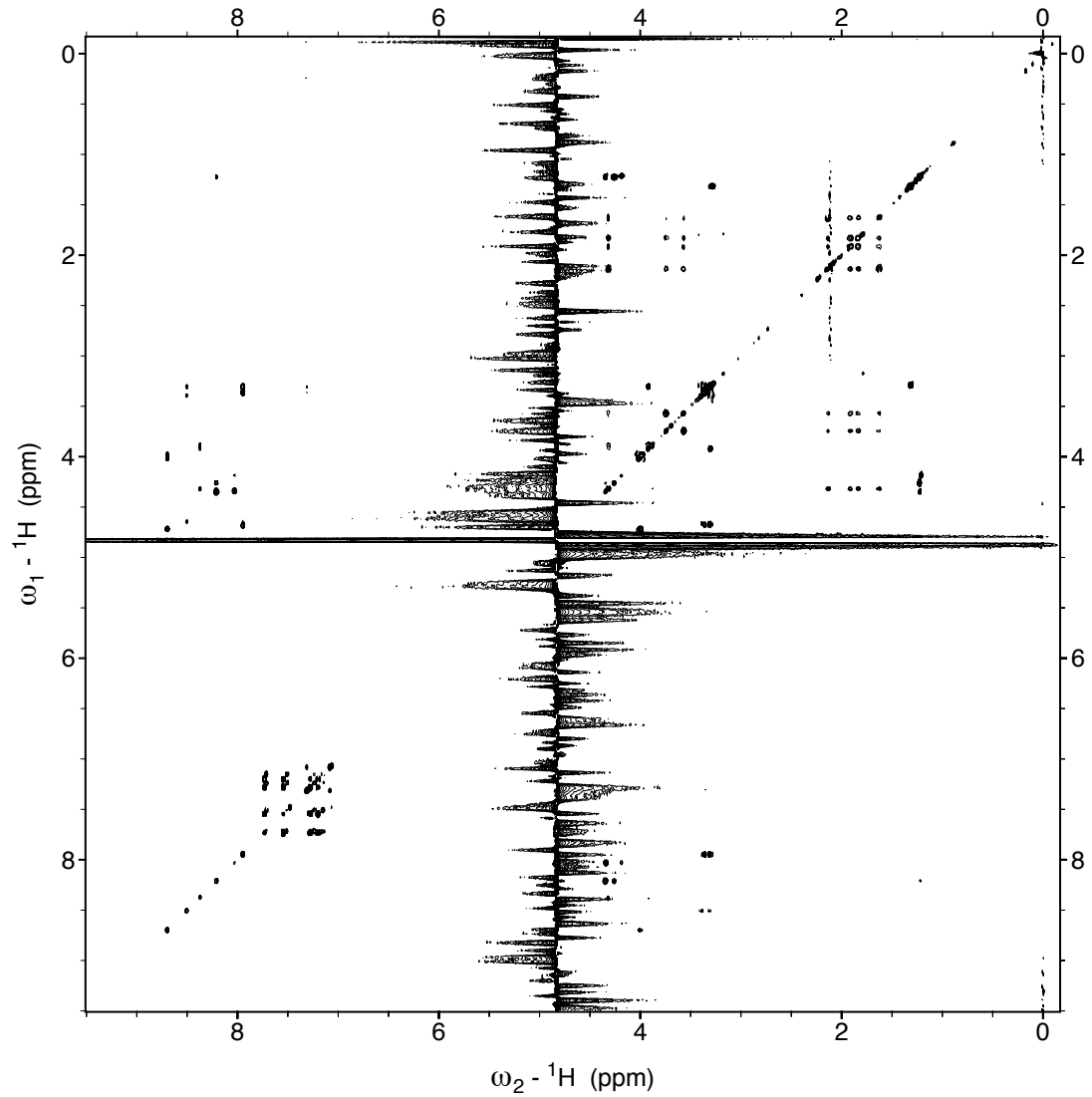


**Figure 3.21:** Full TOCSY spectra of Ac-TpSPW-NH<sub>2</sub> (pH 6.5, 298 K). Peptide was dissolved in 5 mM phosphate buffer containing 25 mM NaCl in 90% H<sub>2</sub>O/10% D<sub>2</sub>O. Data were collected at 298 K.

Ac-TpSPW-NH<sub>2</sub> (pH 7.2, 298 K)

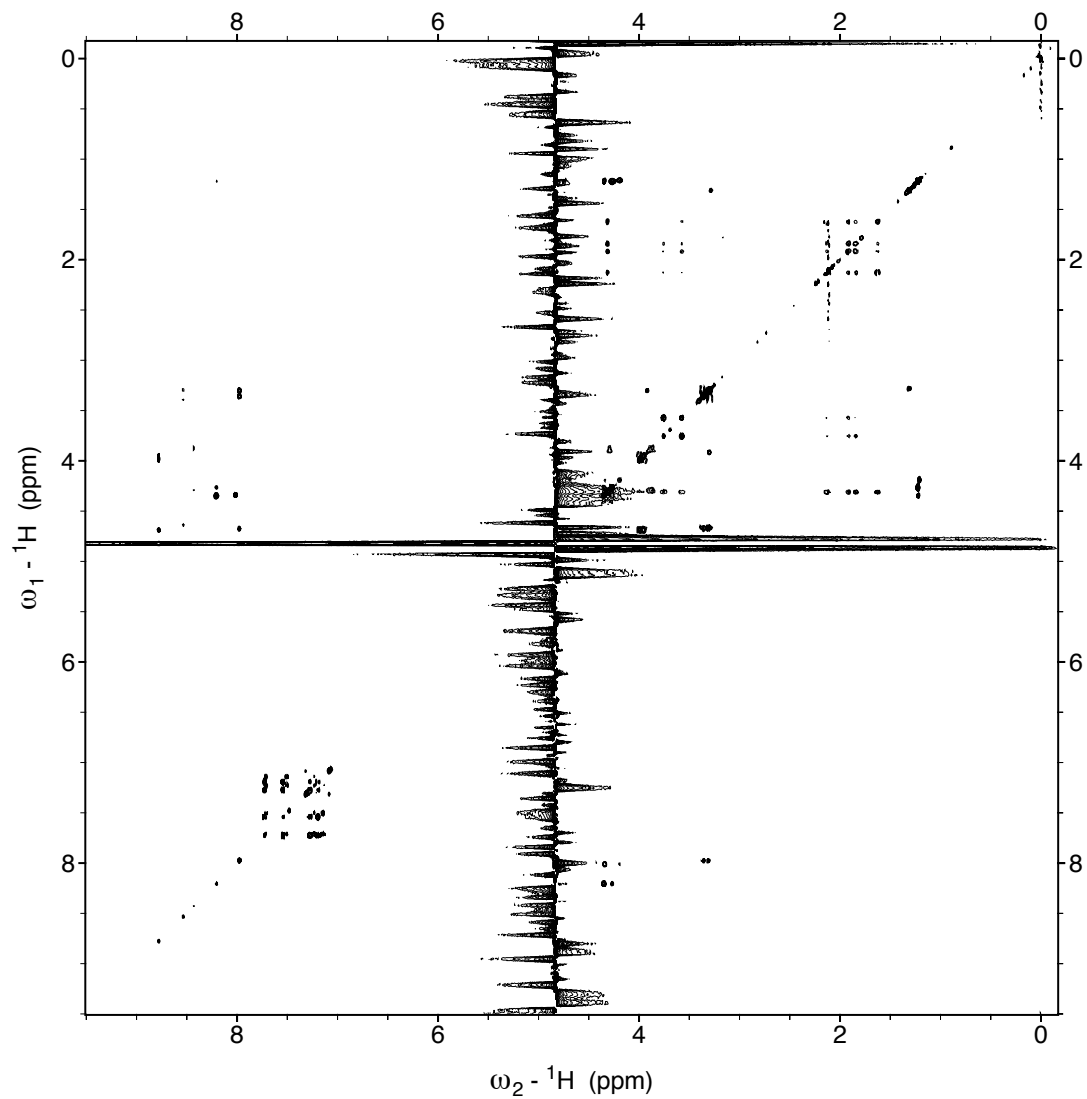


**Figure 3.22:** Full TOCSY spectra of Ac-TpSPW-NH<sub>2</sub> (pH 7.2, 298 K). Peptide was dissolved in 5 mM phosphate buffer containing 25 mM NaCl in 90% H<sub>2</sub>O/10% D<sub>2</sub>O. Data were collected at 298 K.

Ac-pTSPR-NH<sub>2</sub> (pH 6.5, 298 K)

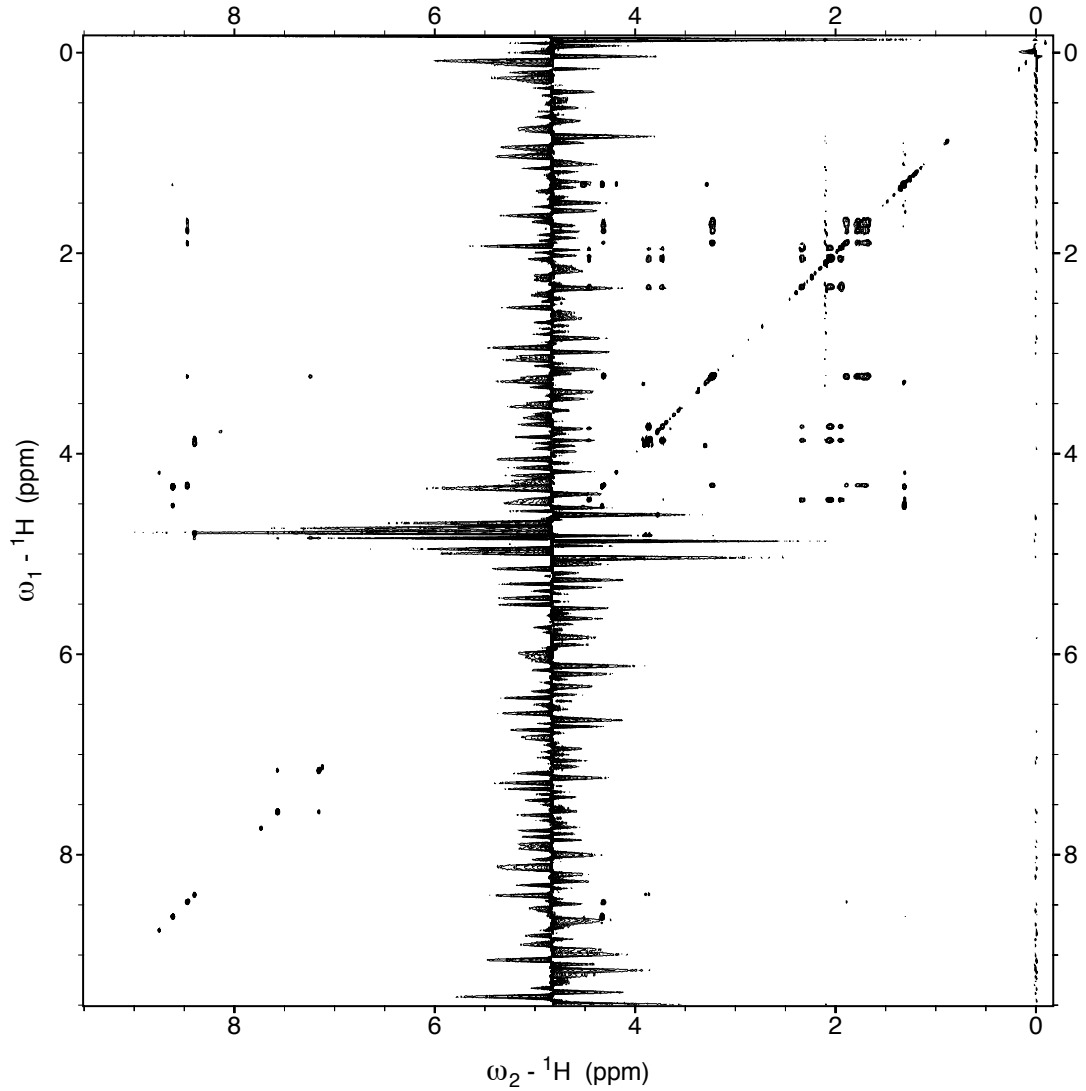


**Figure 3.23:** Full TOCSY spectra of Ac-pTSPR-NH<sub>2</sub> (pH 6.5, 298 K). Peptide was dissolved in 5 mM phosphate buffer containing 25 mM NaCl in 90% H<sub>2</sub>O/10% D<sub>2</sub>O. Data were collected at 298 K.

Ac-pTSPR-NH<sub>2</sub> (pH 7.2, 298 K)

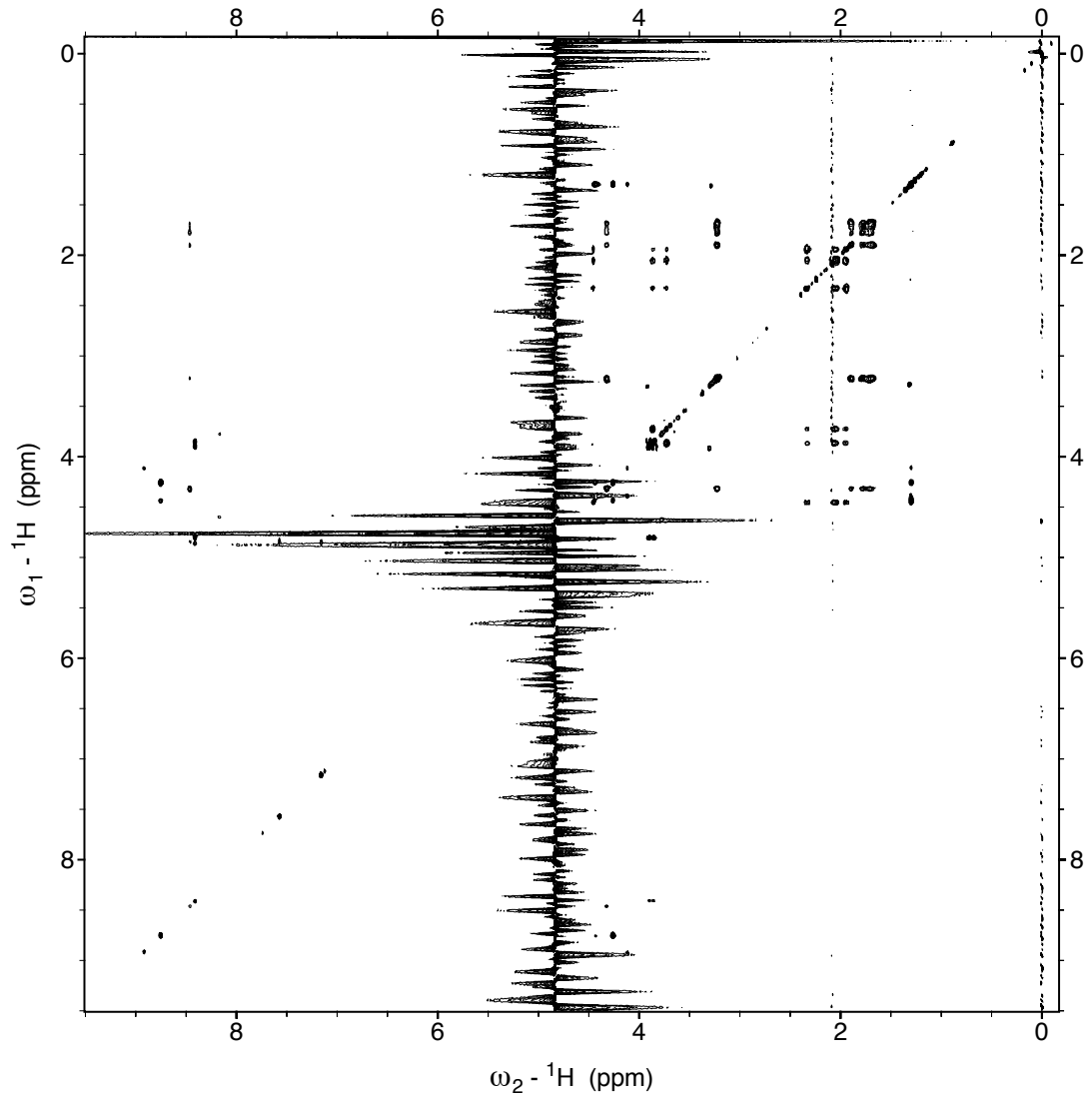


**Figure 3.24:** Full TOCSY spectra of Ac-pTSPR-NH<sub>2</sub> (pH 7.2, 298 K). Peptide was dissolved in 5 mM phosphate buffer containing 25 mM NaCl in 90% H<sub>2</sub>O/10% D<sub>2</sub>O. Data were collected at 298 K.

Ac-pTSPW-NH<sub>2</sub> (pH 6.5, 298 K)

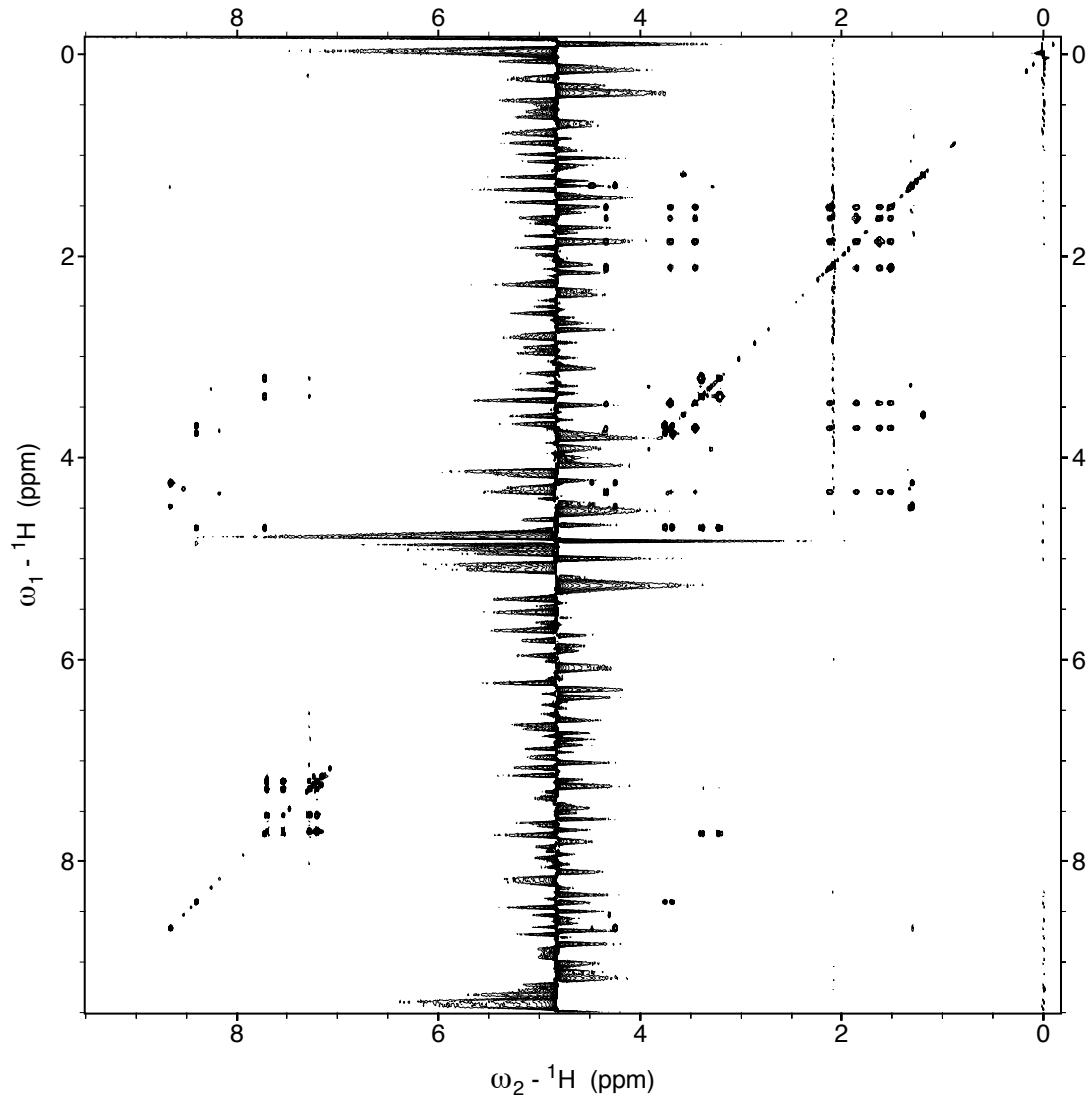


**Figure 3.25:** Full TOCSY spectra of Ac-pTSPW-NH<sub>2</sub> (pH 6.5, 298 K). Peptide was dissolved in 5 mM phosphate buffer containing 25 mM NaCl in 90% H<sub>2</sub>O/10% D<sub>2</sub>O. Data were collected at 298 K.

Ac-pTSPW-NH<sub>2</sub> (pH 7.2, 298 K)

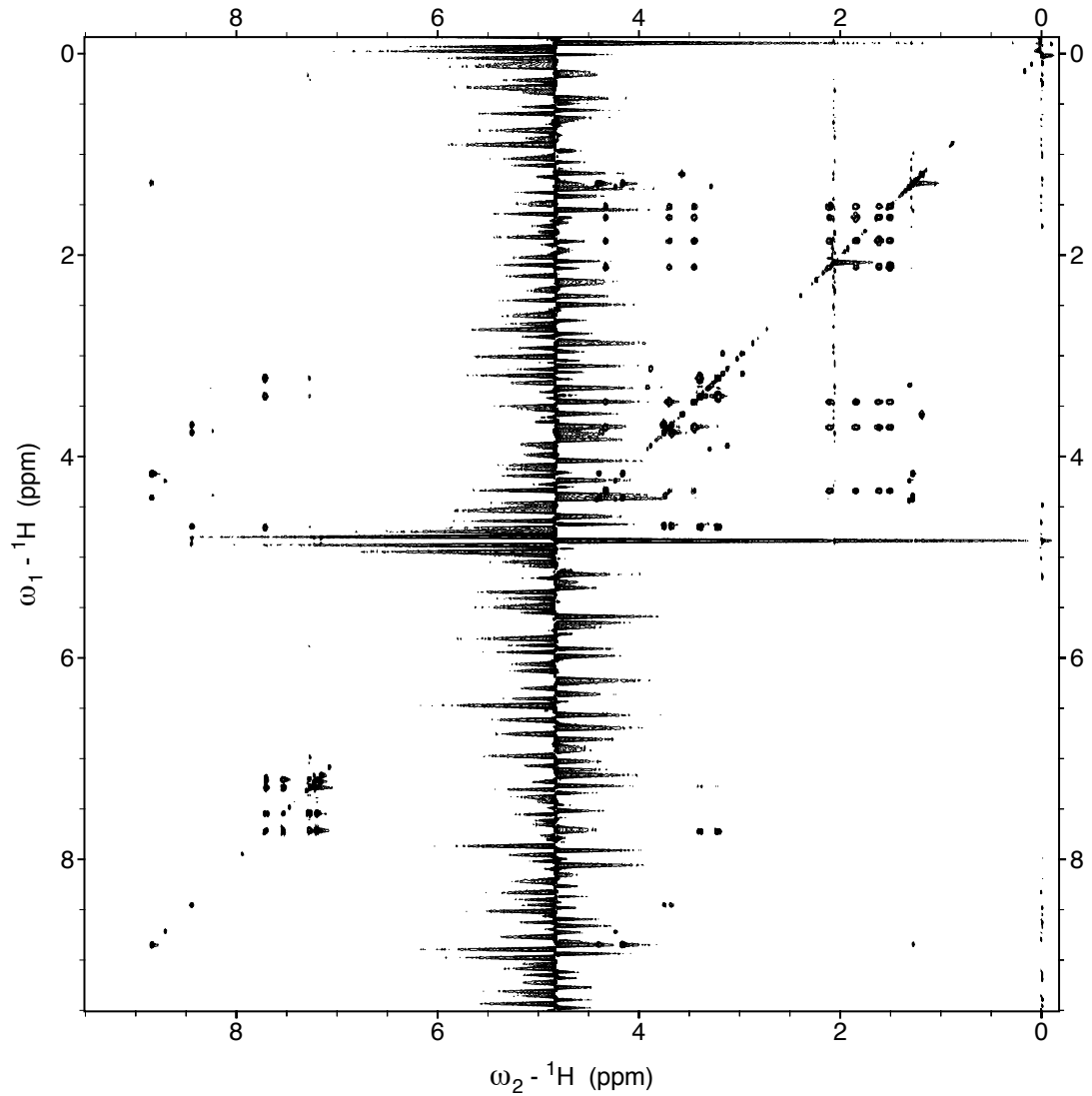


**Figure 3.26:** Full TOCSY spectra of Ac-pTSPW-NH<sub>2</sub> (pH 7.2, 298 K). Peptide was dissolved in 5 mM phosphate buffer containing 25 mM NaCl in 90% H<sub>2</sub>O/10% D<sub>2</sub>O. Data were collected at 298 K.

Ac-pTpSPR-NH<sub>2</sub> (pH 6.5, 298 K)

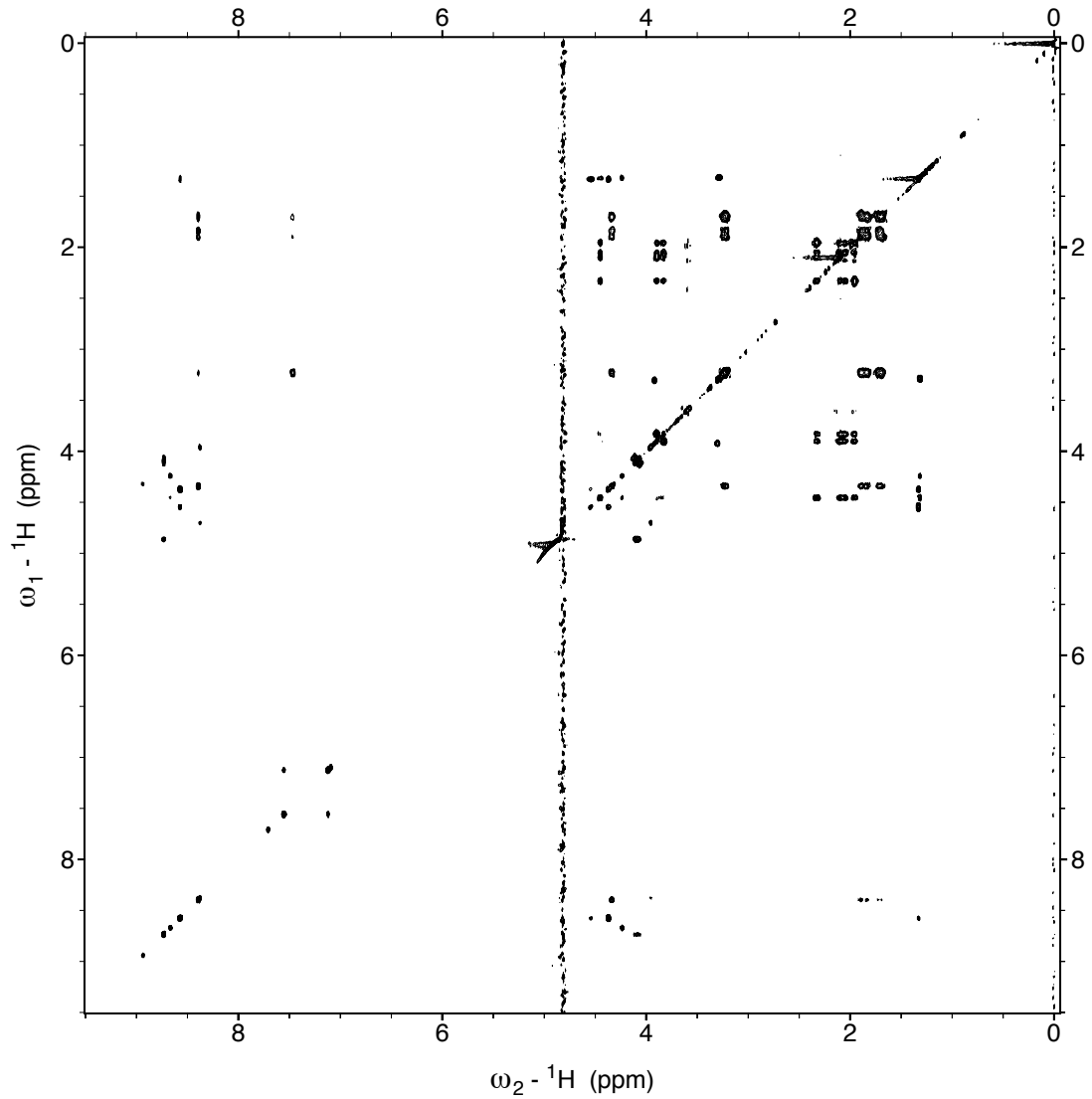


**Figure 3.27:** Full TOCSY spectra of Ac-pTpSPR-NH<sub>2</sub> (pH 6.5, 298 K). Peptide was dissolved in 5 mM phosphate buffer containing 25 mM NaCl in 90% H<sub>2</sub>O/10% D<sub>2</sub>O. Data were collected at 298 K.

Ac-pTpSPR-NH<sub>2</sub> (pH 7.2, 298 K)

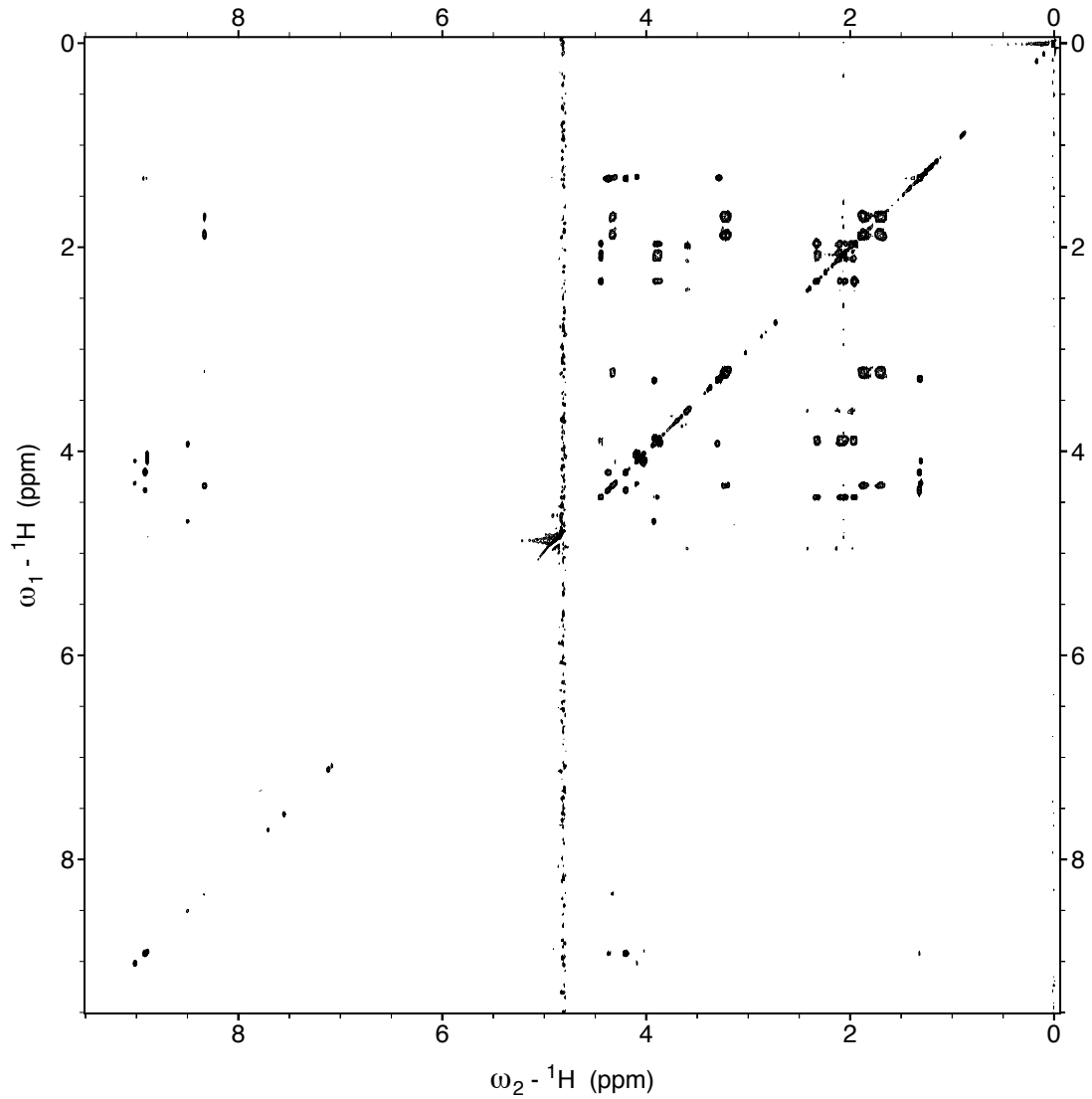


**Figure 3.28:** Full TOCSY spectra of Ac-pTpSPR-NH<sub>2</sub> (pH 7.2, 298 K). Peptide was dissolved in 5 mM phosphate buffer containing 25 mM NaCl in 90% H<sub>2</sub>O/10% D<sub>2</sub>O. Data were collected at 298 K.

Ac-pTpSPW-NH<sub>2</sub> (pH 6.5, 298 K)

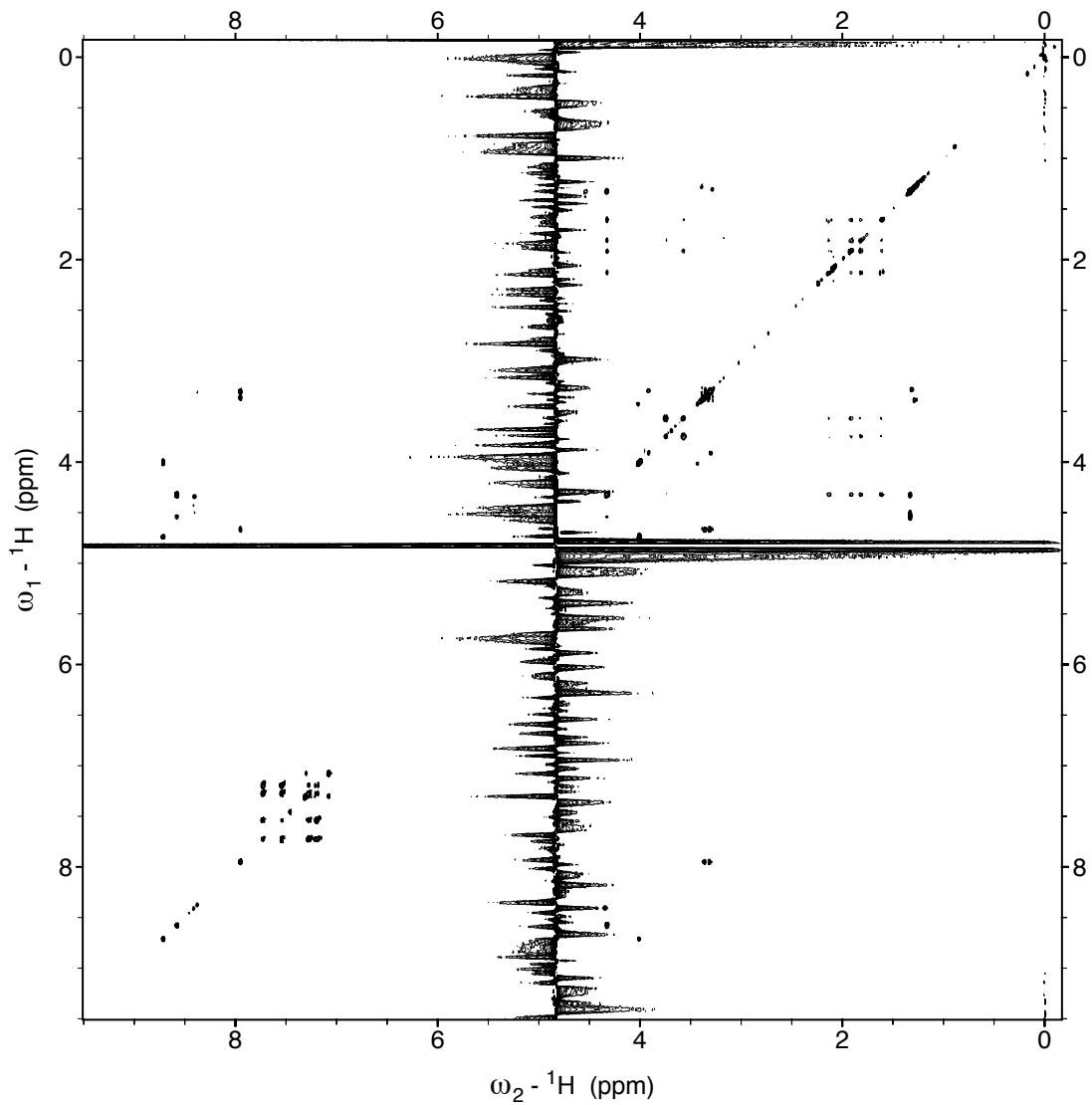


**Figure 3.29:** Full TOCSY spectra of Ac-pTpSPW-NH<sub>2</sub> (pH 6.5, 298 K). Peptide was dissolved in 5 mM phosphate buffer containing 25 mM NaCl in 90% H<sub>2</sub>O/10% D<sub>2</sub>O. Data were collected at 298 K.

Ac-pTpSPW-NH<sub>2</sub> (pH 7.2, 298 K)

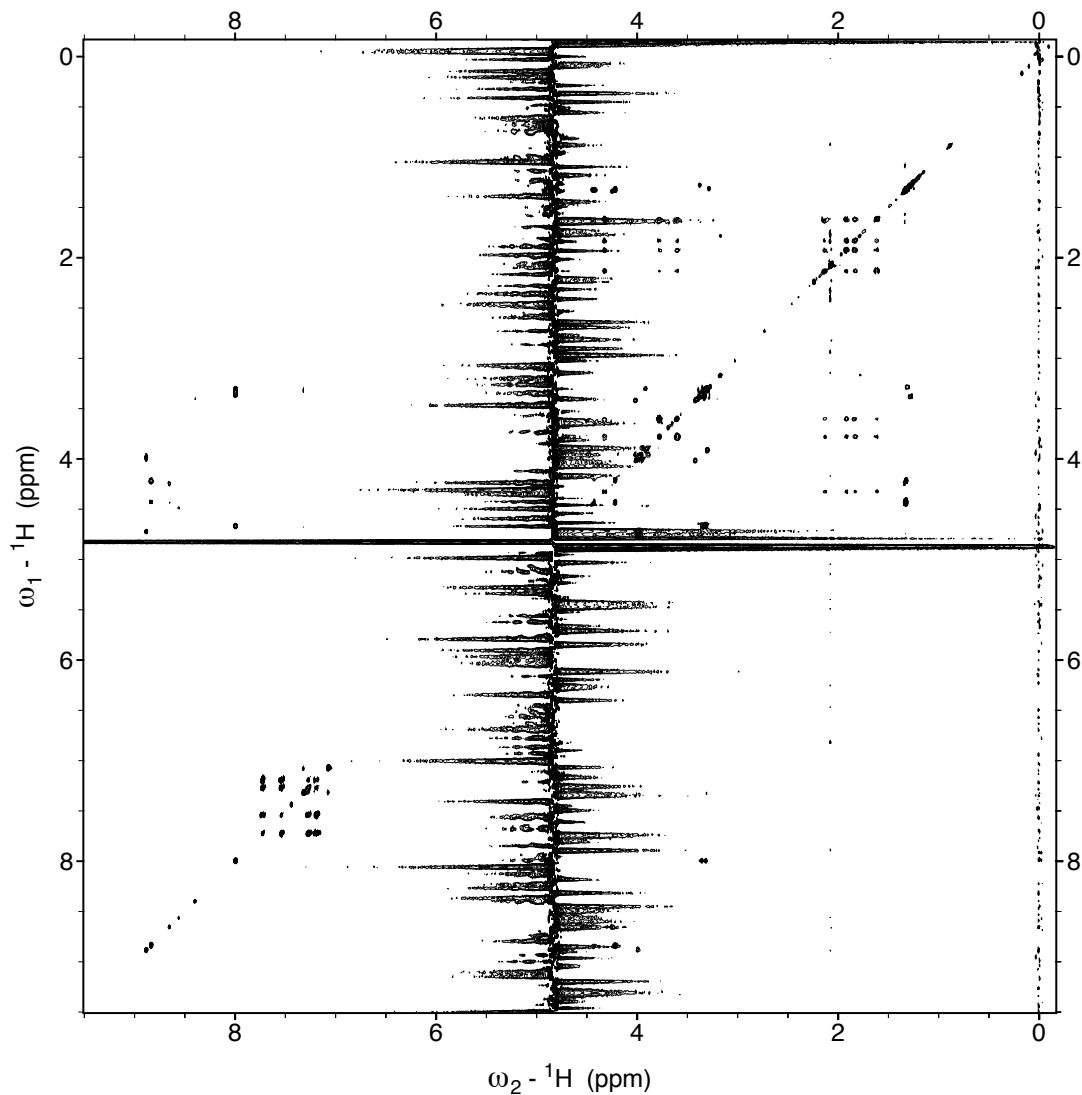


**Figure 3.30:** Full TOCSY spectra of Ac-pTpSPW-NH<sub>2</sub> (pH 7.2, 298 K). Peptide was dissolved in 5 mM phosphate buffer containing 25 mM NaCl in 90% H<sub>2</sub>O/10% D<sub>2</sub>O. Data were collected at 298 K.

Ac-KSPVVSGDTSPRHLSNV-NH<sub>2</sub> (pH 6.5, 298 K)

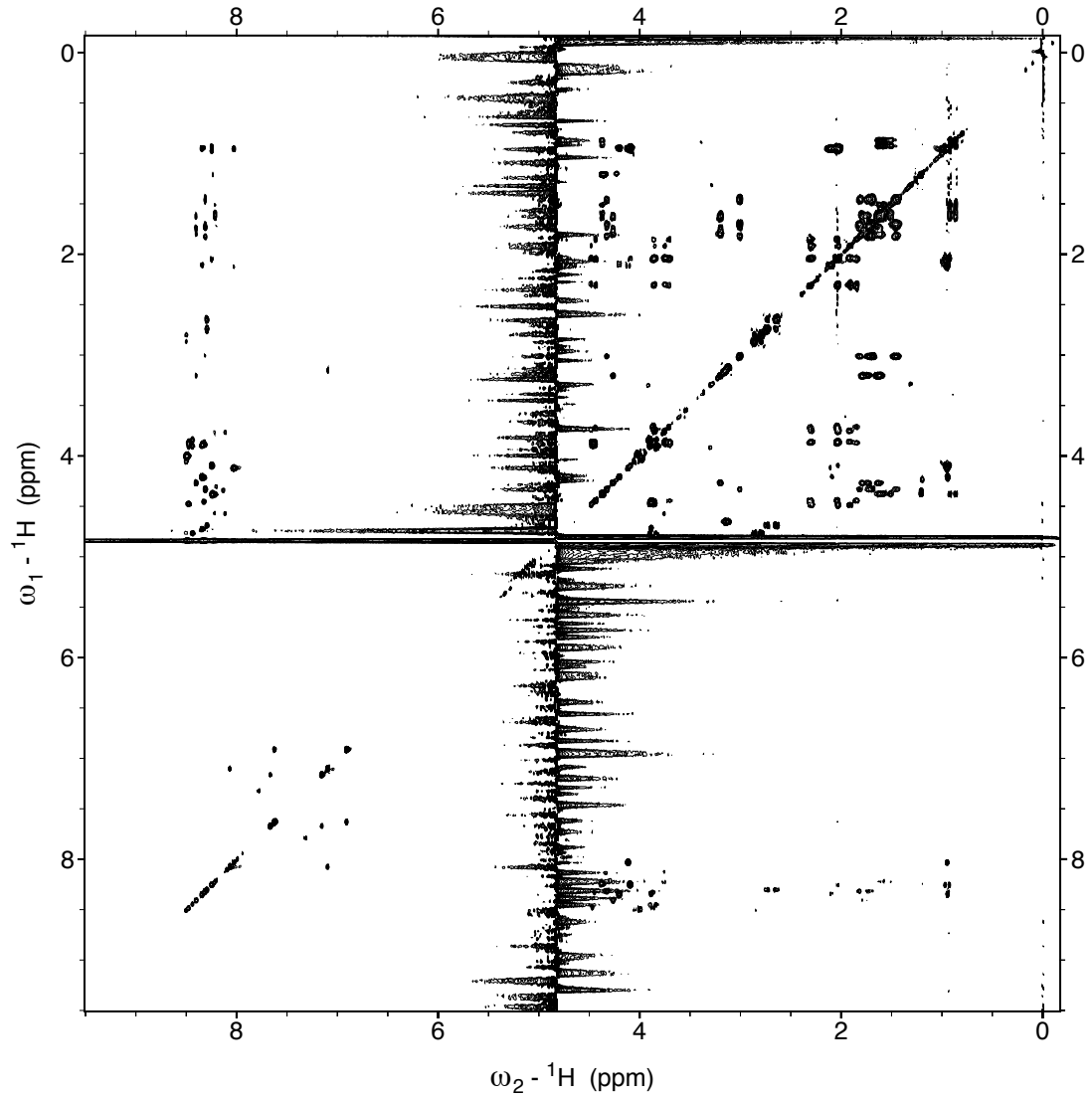


**Figure 3.31:** Full TOCSY spectra of *tau*<sub>395-411</sub> (pH 6.5, 298 K). Peptide was dissolved in 5 mM phosphate buffer containing 25 mM NaCl in 90% H<sub>2</sub>O/10% D<sub>2</sub>O. Data were collected at 298 K.

Ac-KSPVVSGDTSPWHLNV-NH<sub>2</sub> (pH 6.5, 298 K)

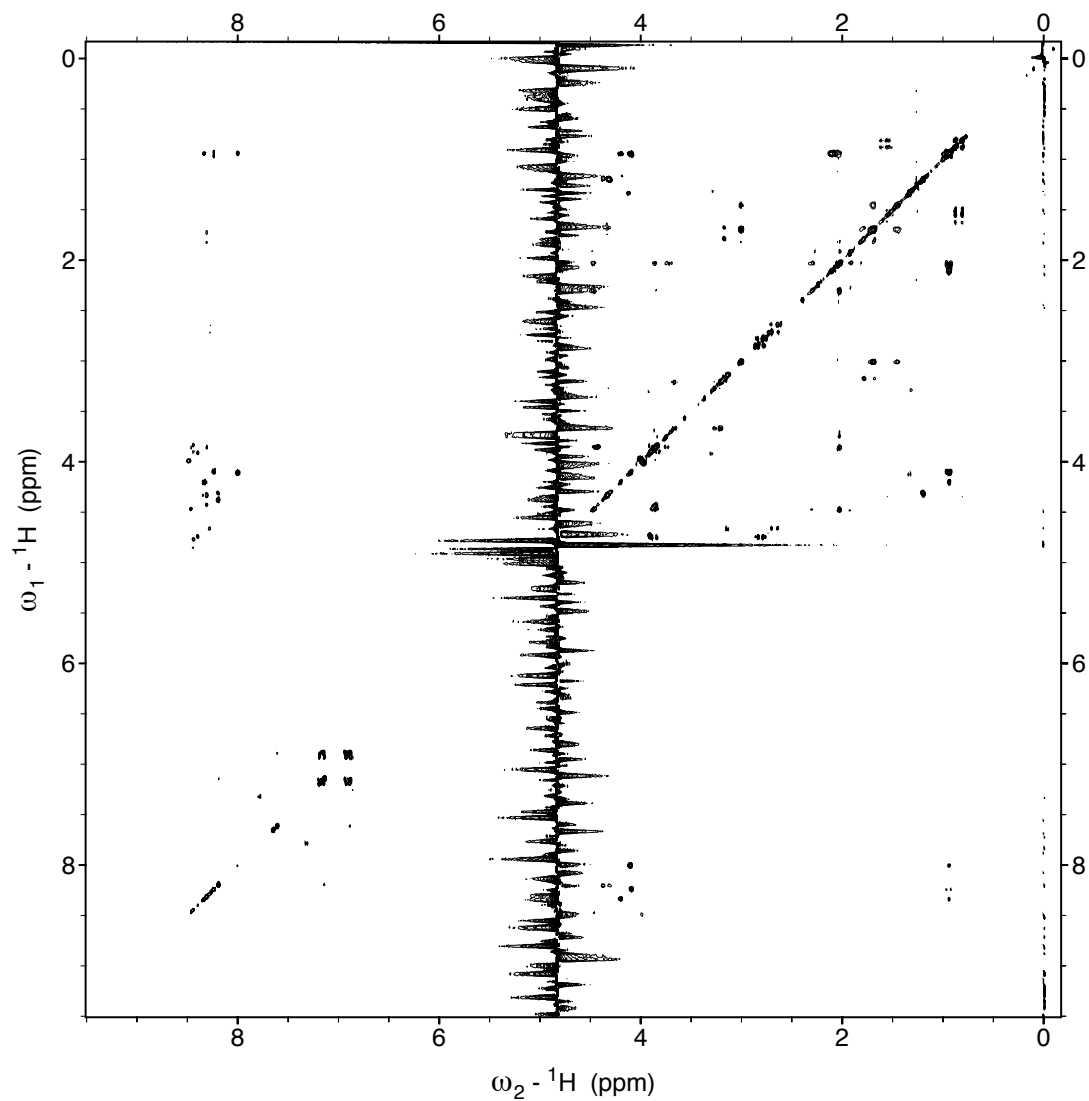


**Figure 3.32:** Full TOCSY spectra of *tau*<sub>395-411</sub> R406W (pH 6.5, 298 K). Peptide was dissolved in 5 mM phosphate buffer containing 25 mM NaCl in 90% H<sub>2</sub>O/10% D<sub>2</sub>O. Data were collected at 298 K.

Ac-KSPVVSGDTpSPRHLSNV-NH<sub>2</sub> (pH 6.5, 298 K)

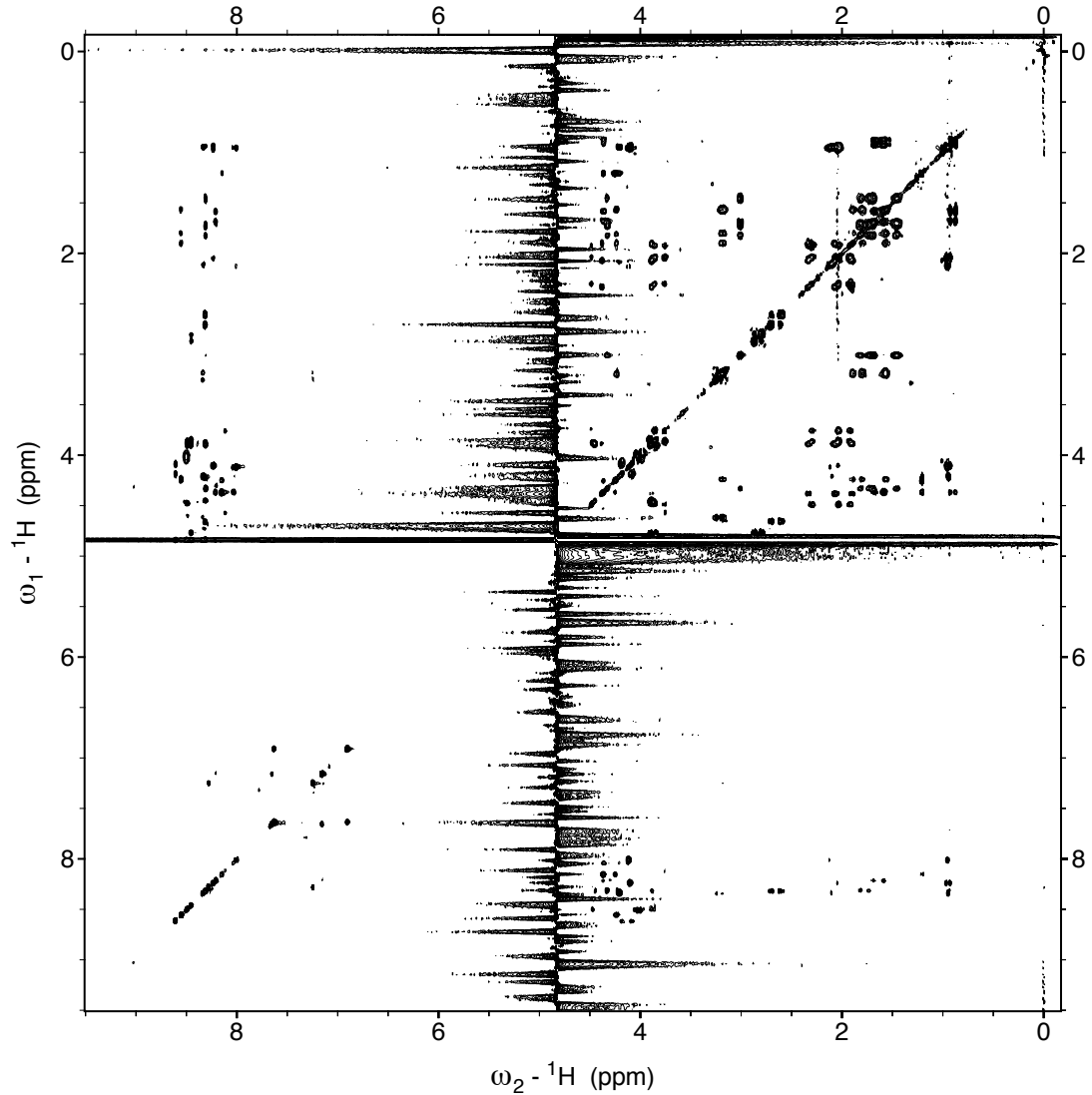


**Figure 3.33:** Full TOCSY spectra of *tau*<sub>395-411</sub> pSer<sub>404</sub> (pH 6.5, 298 K). Peptide was dissolved in 5 mM phosphate buffer containing 25 mM NaCl in 90% H<sub>2</sub>O/10% D<sub>2</sub>O. Data were collected at 298 K.

Ac-KSPVVSGDTpSPRHLSNV-NH<sub>2</sub> (pH 7.2, 298 K)

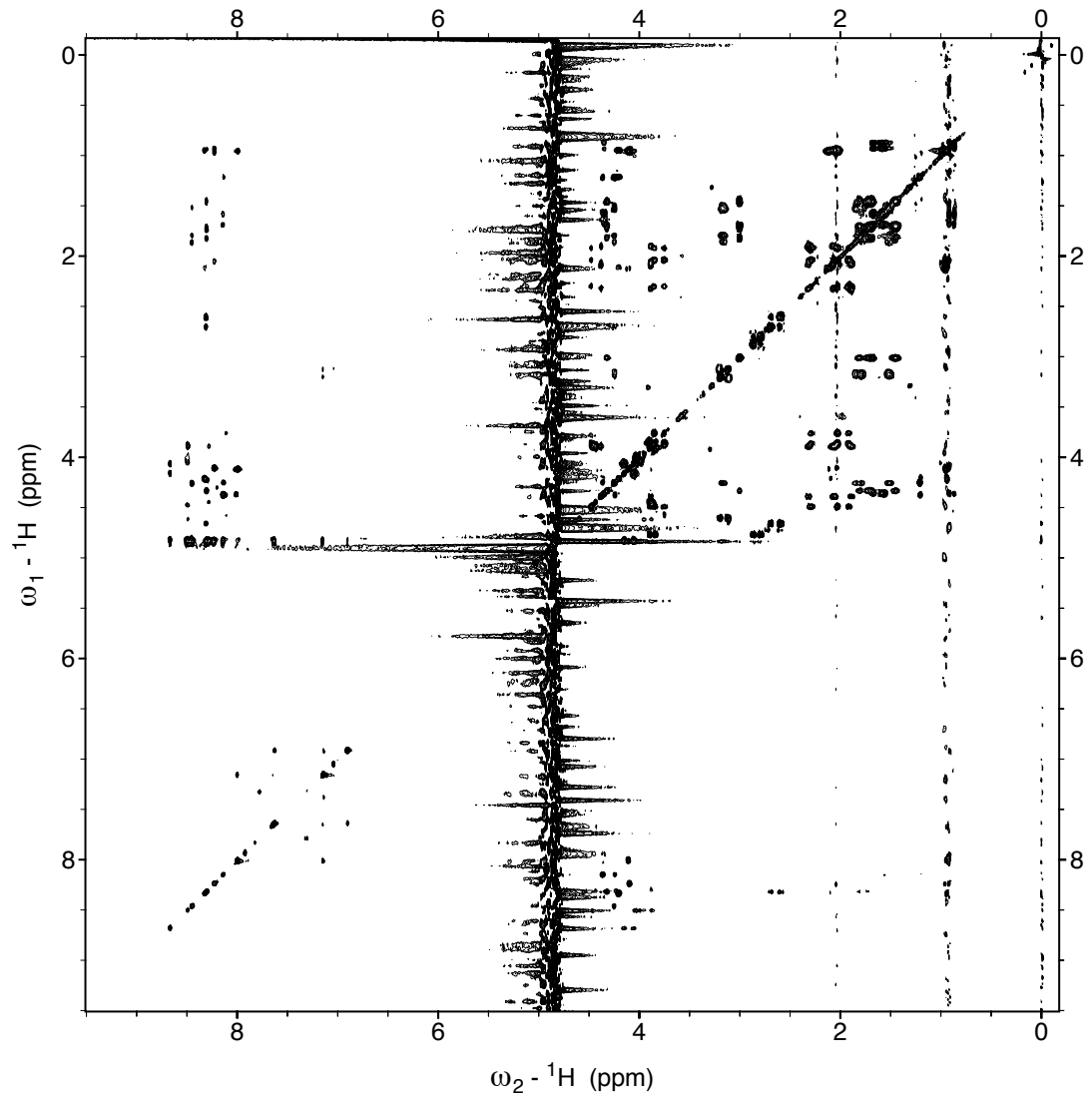


**Figure 3.34:** Full TOCSY spectra of *tau*<sub>395-411</sub> pSer<sub>404</sub> (pH 7.2, 298 K). Peptide was dissolved in 5 mM phosphate buffer containing 25 mM NaCl in 90% H<sub>2</sub>O/10% D<sub>2</sub>O. Data were collected at 298 K.

Ac-KSPVVSGDTpSPWHLSNV-NH<sub>2</sub> (pH 6.5, 298 K)

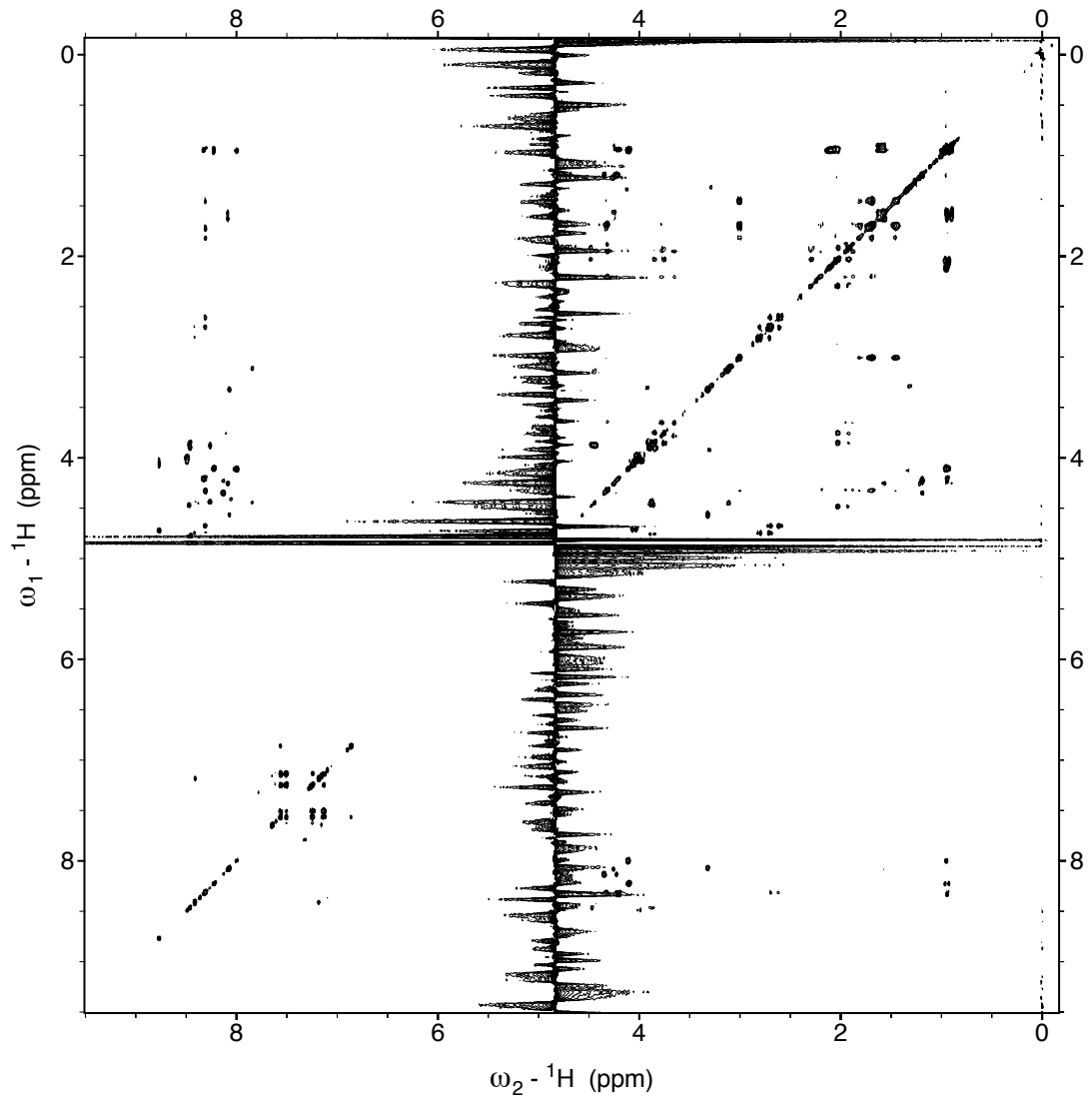


**Figure 3.35:** Full TOCSY spectra of *tau*<sub>395-411</sub> pSer<sub>404</sub> R406W (pH 6.5, 298 K). Peptide was dissolved in 5 mM phosphate buffer containing 25 mM NaCl in 90% H<sub>2</sub>O/10% D<sub>2</sub>O. Data were collected at 298 K.

Ac-KSPVVSGDTpSPWHLSNV-NH<sub>2</sub> (pH 7.2, 298 K)

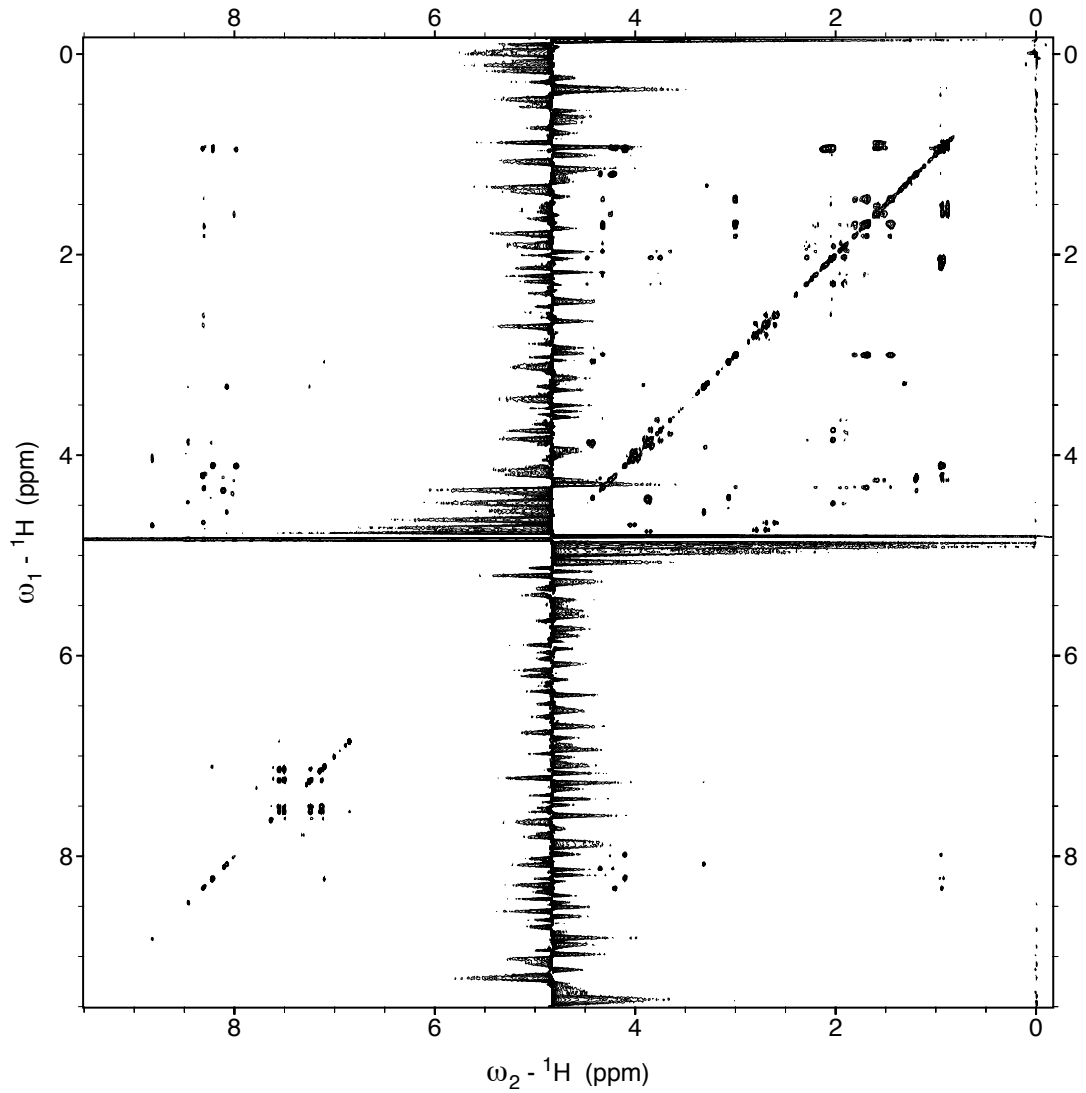


**Figure 3.36:** Full TOCSY spectra of *tau*<sub>395-411</sub> pSer<sub>404</sub> R406W (pH 7.2, 298 K). Peptide was dissolved in 5 mM phosphate buffer containing 25 mM NaCl in 90% H<sub>2</sub>O/10% D<sub>2</sub>O. Data were collected at 298 K.

## REFERENCES

1. [http://www.alz.org/alzheimers\\_disease\\_facts\\_and\\_figures.asp](http://www.alz.org/alzheimers_disease_facts_and_figures.asp)
2. Wong, C. W., Quaranta, V., Glenner, G. G. *Proc. Natl. Acad. Sci. U.S.A.* **1985**, *82*, 8729-8732.
3. Master, C. L., Simms, G., Weinman, N. A., Multhau, G., McDonald, B. L., Beyreuther. *Proc. Natl. Acad. Sci. U.S.A.* **1985**, *82*, 4245-4249.
4. Kan, J., Lemaire, H.-G., Unterbeck, A., Salbaum, J. M., Masters, C. L., Grzeschik, K.-H., Multhaup, G., Beyreuther, K., Muller-Hill, B. *Nature*, **1987**, *245*, 733-736.
5. Sisodia, S. S., Koo, E. H., Beyreuther, K., Unterbeck, A., Price, D. L. *Science*, **1990**, *248*, 492-495.
6. Kelly, J. W. *Curr. Opin. Struct. Biol.* **1998**, *8*, 101-106.
7. Gong, C.-X., Liu, F., Grundke-Iqbal, I., Iqbal, K. *J. Neural. Transm.* **2005**, *112*, 813-838.
8. Grundke-Iqbal, I., Iqbal, K., Quinlan, M., Tung, Y. C., Zaidi, M. S., Wisniewski, H. M. *J. Biol. Chem.* **1986**, *261*, 6084-6089.
9. Iqbal, K., Grundke-Iqbal, I., Smith, A. J., George, L., Tung, Y. C., Zaidi, T. *Proc. Natl. Acad. Sci.* **1989**, *86*, 5646-5650.
10. Lee, V. M., Balin, B. J., Otvos, L., Trojanowski, J. Q. *Science*, **1991**, *251*, 675-678.
11. Kopke, E., Tung, Y. C., Shaikh, S., Alonso, A. C., Iqbal, K., Grundke-Iqbal, I. *J. Biol. Chem.* **1993**, *268*, 24374-24384.
12. Cleveland, D. W., Hwo, S. Y., Kirschner, M. W. *J. Mol. Biol.* **1977**, *116*, 227-247.
13. Wille, H., Drewes, G., Biernat, J., Mandelkow, E. M., Mandelkow, E. J. *Cell Biol.* **1992**, *118*, 573-584.

14. Schweers, O., Schonbrunn-Hanebeck, E., Marx, A., Mandelkow, E. *J. Biol. Chem.* **1994**, *269*, 24290-24297.
15. Von Bergen, M., Friedhoff, P., Biernat, J., Heberle, J., Mandelkow, E. M., Mandelkow, E. *Proc. Natl. Acad. Sci. U.S.A.* **2000**, *97*, 5129-5134.
16. Barghorn, S., Mandelkow, E. *Biochemistry*, **2002**, *41*, 14885-14896.
17. Jeganathan, S., von Bergen, M., Mandelkow, E. M., Mandelkow, E. *Biochemistry*, **2008**, *47*, 10526-10539.
18. Littauer, U. Z., Giveon, D., Thierauf, M., Ginzburg, I., Ponstingl, H. *Proc. Natl. Acad. Sci. U.S.A.* **1986**, *83*, 7162-7166.
19. Butner, K. A., Kirschner, M. W. *J. Cell Biol.* **1991**, *115*, 717-730.
20. Gustke, N., Trinczek, B., Biernat, J., Mandelkow, E. M., Mandelkow, E. *Biochemistry*, **1994**, *33*, 9511-9522.
21. Goode, B. L., Denis, P. E., Panda, D., Radeke, M. J., Miller, H. P., Wilson, L., Feinstein, S. C. *Mol. Biol. Cell.* **1997**, *8*, 353-365.
22. Jeganathan, S., von Bergen, M., Brutlach, H., Steinhoff, H.-J., Mandelkow, E. *Biochemistry*, **2006**, *45*, 2283-2293.
23. Wischik, C. M., Novak, M., Edwards, P. C., Klug, A., Tichelaar, W., Crowther, R. A. *Proc. Natl. Acad. Sci. U.S.A.* **1988**, *85*, 4884-4888.
24. Jakes, R., Novak, M., Davison, M., Wischik, C. M. *EMBO J.* **1991**, *10*, 2725-2729.
25. Friedhoff, P., Schneider, A., Mandelkow, E. M., Mandelkow, E. *Biochemistry*, **1998**, *37*, 10223-10230.
26. Novak, M., Kabat, J., Wischik, C. M. *EMBO J.* **1993**, *12*, 365-370.
27. Rissman, R. A., Poon, W. W., Blurton-Jones, M., Oddo, S., Torp, R., Vitek, M. P., LaFerla, F. M., Rohn, T. T., Cotman, C. W. *J. Clin. Invest.* **2004**, *114*, 121-130.
28. Gamblin, T. C., Chen, F., Zambrano, A., Abraha, A., Lagalwar, S., Guillozet, A. L., Lu, M., Fu, T., Garcia-Sierra, F., LaPointe, N., Miller, R., Berry, R. W., Binder, L. I., Cryns, V. L. *Proc. Natl. Acad. Sci. U.S.A.* **2003**, *100*, 10032-10037.

29. Goedert, M., Jakes, R., Spillantini, M. G., Hasegawa, M., Smith, M. J., Crowther, R. A. *Nature*, **1996**, 383, 550-553.
30. Kampers, T., Friedhoff, P., Biernat, J., Mandelkow, E. M., Mandelkow, E. *FEBS Lett.* **1996**, 399, 344-349.
31. Berry, R. W., Abraha, A., Lagalwar, S., LaPointe, N., Gamblin, T. C., Cryns, V. L., Binder, L. I. *Biochemistry*, **2003**, 42, 8325-8331.
32. Abraha, A., Ghoshal, N., Gamblin, T. C., Cryns, V., Berry, R. W., Kuret, J., Binder, L. I. *J. Cell Sci.* **2000**, 113, 3737-3745.
33. Alonso, A. del C., Mederlyova, A., Novak, M., Grundke-Iqbal, I., Khalid, I. *J. Biol. Chem.* **2004**, 279, 34873-34881.
34. Sibille, N., Sillen, A., Leroy, A., Wieruszeski, J.-M., Mulloy, B., Landrieu, I., Lippens, G. *Biochemistry*, **2006**, 45, 12560-12572.
35. Morishima-Kawashima, M., Hasegawa, M., Takio, K., Suzuki, M., Yoshida, H., Watanabe, A., Titani, K., Ihara, Y. *Neurobiol. Aging*. **1995**, 16, 365-371.
36. Gong, C.-X., Liu, F., Grundke-Iqbal, I., Iqbal, K. *J. Neural. Transm.* **2005**, 112, 813-838.
37. Iqbal, K., Alonso, A. C., Chen, S., Chohan, M. O., El-Akkad, E., Gong, C.-X., Khatoon, S., Li, B., Liu, F., Rahman, A., Tanimukai, H., Grundke-Iqbal, I. *Biochim. Biophys. Acta.* **2005**, 1739, 198-210.
38. Hanger, D. P., Byers, H. L., Wray, S., Leung, K.-Y., Saxton, M. J., Seereeram, A., Reynolds, C. H., Ward, M. A., Anderton, B. H. *J. Biol. Chem.* **2007**, 282, 23645-23654.
39. Evans, D. B., Rank, K. B., Bhattacharya, K., Thomsen, D. R., Gurney, M. E., Sharma, S. K. *J. Biol. Chem.* **2000**, 275, 24977-24983.
40. Imahori, K., Uchida, T. *J. Biochem.* **1997**, 121, 179-188.
41. Mandelkow, E.-M., Drewes, G., Biernat, J., Gustke, N., Lint, J. V., Vandenheede, J. R., Mandelkow, E. *FEBS*, **1992**, 314, 315-321.
42. Singh, T. J., Zaidi, T., Grundke-Iqbal, I., Iqbal, K. *FEBS. Lett.* **1995**, 358, 4-8.

43. Tatebayashi, Y., Miyasaka, T., Chui, D.-H., Akagi, T., Mishima, K., Iwasaki, K., Fujiwara, M., Tanemura, K., Murayama, M., Ishiguro, K., Planel, E., Sato, S., Hashikawa, T., Takashima, A. *Proc. Natl. Acad. Sci.* **2002**, *99*, 13896-13901.
44. Buee, L., Bussiere, T., Buee-Scherrer, V., Delacourte, A., Hof, P. R. *Brain. Res. Rev.* **2000**, *33*, 95-130.
45. Gotz, J., Ittner, L. M. *Nature*, **2008**, *9*, 532-544.
46. Stewart, D. E., Sarkar, A., Wampler, J. E. *J. Mol. Biol.* **1990**, *214*, 253-260.
47. Ramachandran, G. N., Mitra, A. K. *J. Mol. Biol.* **1976**, *107*, 85-92.
48. Radzicka, A., Pedersen, L., Wolfenden, R. *Biochemistry*, **1988**, *27*, 4538-4541.
49. MacArthur, M. W., Thornton, J. M. *J. Mol. Biol.* **1991**, *218*, 397-412.
50. Weiss, M. S., Jabs, A., Hilgenfeld, R. *Nat. Struct. Biol.* **1998**, *5*, 676.
51. Jabs, A., Weiss, M. S., Hilgenfeld, R. *J. Mol. Biol.* **1999**, *286*, 291-304.
52. Pal, D., Chakrabarti, P. *J. Mol. Biol.* **1999**, *294*, 271-288.
53. Kemmink, J., Creighton, T. E. *J. Mol. Biol.* **1993**, *234*, 861-878.
54. Yao, J., Feher, V. A., Espejo, B. F., Reymond, M. T., Wright, P. E., Dyson, H. J. *J. Mol. Biol.* **1994**, *243*, 736-753.
55. Yao, J., Dyson, H. J., Wright, P. E. *J. Mol. Biol.* **1994**, *243*, 754-766.
56. Kemmink, J., Creighton, T. E. *J. Mol. Biol.* **1995**, *245*, 251-260.
57. Reimer, U., Scherer, G., Drewello, M., Kruber, S., Schutkowski, M., Fischer, G. *J. Mol. Biol.* **1998**, *279*, 449-460.
58. Wu, W.-J., Raleigh, D. P. *Biopolymers*. **1998**, *45*, 381-394.
59. Nardi, F., Kemmink, J., Sattler, M., Wade, R. C. *J. Biomol. NMR.* **2000**, *17*, 63-77.
60. Meng, H. Y., Thomas, K. M., Lee, A. E., Zondlo, N. J. *Biopolymers*. **2006**, *84*, 192-204.
61. Brown, A. M., Zondlo, N. J. *Biochemistry*. **2012**, *51*, 5041-5051.

62. Zondlo, N. J. *Acc. Chem. Res.* **2013**, *46*, 1039-1049.
63. Dasgupta, B., Chakrabarti, P., Basu G. *FEBS*, **2007**, *581*, 4529-4532.
64. Umezawa, Y., Tsuboyama, S., Takahashi, H., Uzawa, J., Nishio, M. *Bioorg. Med. Chem.* **1999**, *282*, 2021-2026.
65. Brandl, M., Weiss, M. S., Jabs, A., Suhnel, J., Hilgenfeld, R. *J. Mol. Biol.* **2001**, *307*, 357-377.
66. Silva, M. M., Poland, B. W., Hoffman, C. R., Fromm, H. J., Honzatko. *J. Mol. Biol.* **1995**, *254*, 431-446.
67. Toth, G., Murphy, R. F., Lovas, S. *Protein. Eng.* **2001**, *14*, 543-547.
68. Bhattacharyya, R., Chakrabarti, P. *J. Mol. Biol.* **2003**, *331*, 925-940.
69. Satoh, T., Cowieson, N. P., Hakamata, W., Ideo, H., Fukushima, K., Kurihara, M., Kato, R., Yamashita, K., Wakatsuki, S. *J. Biol. Chem.* **2007**, *282*, 28246-28255.
70. Pandey, A. K., Naduthambi, D., Thomas, K. M., Zondlo, N. J. *J. Am. Chem. Soc.* **2013**, *135*, 4333-4363.
71. Pandey, A. K., Thomas, K. M., Forbes, C. R., Zondlo, N. J. *Biochemistry*, **2014**, (just accepted).
72. Thomas, K. M., Naduthambi, D., Tririyaa, G., Zondlo, N. J. *Org. Lett.* **2005**, *7*, 2397-2400.
73. Thomas, K. M., Naduthambi, D., Zondlo, N. J. *J. Am. Chem. Soc.* **2006**, *128*, 2216-2217.
74. Forbes, C. R., Zondlo, N. J. *Org. Lett.* **2012**, *14*, 464-467.
75. Pandey, A. K., Naduthambi, D., Thomas, K. M., Zondlo, N. J. *J. Am. Chem. Soc.* **2013**, *135*, 4333-4363.
76. Zondlo, N. J. *Nat. Chem. Biol.* **2010**, *6*, 567-568.
77. Newberry, R. W., VanVeller, B., Guzei, I. A., Raines, R. T. *J. Am. Chem. Soc.* **2013**, *135*, 7843-7846.
78. Bartlett, G. J., Newberry, R. W., VanVeller, B., Raines, R. T., Woolfson, D. N. *J. Am. Chem. Soc.* **2013**, *135*, 18682-18688.

79. Ganguly, H. K., Majumder, B., Chattopadhyay, S., Chakrabarti, P., Basu, G. *J. Am. Chem. Soc.* **2012**, *134*, 4661-4669.
80. Ganguly, H. K., Kaur, H., Basu, G. *Biochemistry.* **2013**, *52*, 6348-6357.
81. Zhou, X. Z., Kops, O., Werner, A., Lu, P.-J., Shen, M., Stoller, G., Kullertz, G., Stark, M., Fischer, G., Lu, P. K. *Mol. Cell.* **2000**, *6*, 873-883.
82. Lim, J., Lu, K. P. *Biochim. Biophys. Acta.* **2005**, *1739*, 311-322.
83. Pastorino, L., Sun, A., Lu, P.-J., Zhou, X. Z., Balastik, M., Finn, G., Wulf, G., Lim, J., Li, S.-H., Li, X., Xia, W., Nicholson, L. K., Lu, K. P. *Nature*, **2006**, *440*, 528-534.
84. Butterfield, D. A., Abdul, H. M., Opii, W., Newman, S. F., Joshi, G., Ansari, M. A., Sultana, R. *J. Neurosci.* **2006**, *98*, 1697-1706.
85. Butterfield, D. A., Poon, H. F., St. Clair, D., Keller, J. N., Pierce, W. M., Klein, J. B., Markesbery, W. R. *Neurobiology of Disease.* **2006**, *22*, 223-232.
86. Laughrey, Z. R., Kiehna, S. E., Riemen, A. J., Waters, M. L. *J. Am. Chem. Soc.* **2008**, *130*, 14625-14633.
87. Pople, J. A. *J. Chem. Phys.* **1956**, *24*, 1111.
88. Riemen, A. J., Waters, M. L. *J. Am. Chem. Soc.* **2009**, *131*, 14081-14087.
89. Riemen, A. J., Waters, M. L. *J. Am. Chem. Soc.* **2010**, *132*, 9007-9013.
90. Tholey, A., Lindemann, A., Kinzel, V., Reed, J. *Biophysical J.* **1999**, *76*, 76-87.
91. Wang, J.-Z., Xia, Y.-Y., Grundke-Iqbal, I., Iqbal, K. *J. Alzheimers. Dis.* **2013**, *33*, S123-S139.
92. Bienkiewicz, E. A., Lumb, K. J. *J. Biomol. NMR.* **1999**, *15*, 203-206.
93. Landrieu, I., Lacosse, L., Leroy, A., Wieruszkeski, J.-M., Trivelli, X., Sillen, A., Sibille, N., Schwalbe, H., Saxena, K., Langer, T., Lippens, G. *J. Am. Chem. Soc.* **2006**, *128*, 3575-3583.
94. Brister, M. A., Pandey, A. K., Bielska, A. A., and Zondlo, N. J. *J. Am. Chem. Soc.* **2014**, *136*, 3803-3816.

95. Elbaum, M. B., Zondlo, N. J. *Biochemistry*. **2014**, *53*, 2242-2260.